eman ta zabal zazu

Universidad del País Vasco

Euskal Herriko Unibertsitatea

Morphofunctional changes in a rat model of Parkinson's disease - Effects of neurotrophic factors administration

DOCTORAL THESIS

Catalina Requejo Rodríguez

Leioa, 2015

eman ta zabal zazu

Universidad del País Vasco
Euskal Herriko Unibertsitatea

NEUROZIENTZIEN SAILA
DEPARTAMENTO DE NEUROCIENCIAS

MEDIKUNTZA ETA ODONTOLOGIA FAKULTATEA
FACULTAD DE MEDICINA Y ODONTOLOGÍA

Morphofunctional changes in a rat model of Parkinson's disease - Effects of neurotrophic factors administration

DOCTORAL THESIS

Catalina Requejo Rodríguez

Leioa, 2015

This Doctoral Thesis has been carried out thanks to the economic support of the University of the Basque Country (UPV/EHU), (UFI: Eldunanotek), the Basque Government (Saiotek program and GIC 794/13, LaNCE) and SGIker (UPV/EHU). It was also possible thanks to the collaboration with the NanoBioCel Group (UPV/EHU) and the group for Neuropharmacology (UPV/EHU). C. Requejo has held a predoctoral fellowship for the training of Research Personnel (Formación de Personal Investigador) for the period 2011-2015.

AGRADECIMIENTOS (Acknowledgements)

Cómo resumir en pocas palabras todo lo que tengo que agradecer…

En primer lugar, a mi director de Tesis Doctoral, José Vicente Lafuente, por haberme dado la oportunidad de pertenecer a su grupo de investigación, por enseñarme a dudar, por hacerme reflexionar sobre aquello que da lugar a duda, en resumen, por haberme enseñado lo que realmente significa investigar. Pero, ¿Qué es un grupo, sin un grupo? Por ello, también tengo que agradecer toda la ayuda que mis compañeros me han dado a lo largo de estos años. A mi gran compañero de Tesis, Álvaro: muchas gracias Alvarillo por todo, por haberme acogido desde el principio, porque habéis pasado Esti y tú de ser compañeros a grandes amigos. A Harkaitz, quién me introdujo en el apasionante mundo del "Mercator", y que siempre está dispuesto a echar una mano, y sabes que con él unas risas nunca van a faltar. A Naiara, por ser de esas personas, que siempre te apoyan. A Hodei, por sus conocimientos informáticos y por toda la ayuda recibida en las jaulas de entorno enriquecido. A Susana, con esa risa contagiosa y a Iran, por haberme aguantado tantos años en el "cubículo".

También quería agradecer al Departamento de Neurociencias, y a su director, Pedro Grandes, por permitirme formar parte del mismo y por facilitarme siempre todas las gestiones.

Por otro lado, quería agredecer a todas las personas, cuya colaboración ha sido fundamental en el desarrollo de esta Tesis. Muy especialmente quería dar las gracias a la Dra. Luisa Ugedo del Departamento de Farmacología de la UPV/EHU en Leioa, por toda la ayuda recibida y por todos sus consejos y dedicación, y a todo su grupo de Neurofarmacología. Especialmente al Dr. José Ángel Ruiz, por haber llevado a cabo y haberme enseñado los procedimientos estereotáxicos y por toda su ayuda en los test de comportamiento. Gracias José Ángel por toda tu paciencia y por todo el tiempo que me has dedicado.

También quería agredecer a la Dra. Rosa Hernández y a todo su grupo de NanoBioCel del Departamento de Farmacología de la UPV/EHU en Vitoria, en especial a Enara, por realizar la caracterización de las microesferas y de las nanoesferas de PLGA *in*

vitro y la encapsulación de los factores neurotróficos, así como los ensayos de bioactividad en cultivos celulares, tras la encapsulación.

Al personal del animalario de la UPV/EHU, siempre tan atentos y trabajando tan duro para que a los animales no les falte de nada.

I am deeply indebted to Professor Dafin F. Muresanu (Cluj-Napoca, Romania) and Dr. Herbert Mössler (Oberburgau, Austria) for introducing me with cerebrolsyin and Dr. Z. Ryan Tian and Asya Ozkizilcik (Fayetteville, AR, USA) for helping in nanowiring of Cerebrolysin used in this study.

I would also want to thank to Matt Lavoie for accepting me in his prestigious laboratory at Harvard Institute of Medicine (HIM) and introducing me into the LRKK2 and alpha-synuclein world. Thanks also to all the people from Lavoie's Lab, especially to John, I am very grateful for your time and patience, for making me feel like one more and teaching the techniques to characterization of the endocytic pathways involved in the microglial uptake of α-synuclein, such as transient transfection, cell culture maintenance and western blot, among others. Thanks too much, I appreciate everything you have done for me. All of you made my internship in Boston very pleasant and unforgettable.

A todos mis compañeros del labo: a "las luisas" (Belén, Bárbara, Fátima, Laura, Ianis…), a los "Matutes" (Anita, Ane, Esti, Mónica, Silvia, Manu, Asier, Saioa, Tania, Andrea, Alazne, Hazel…), al laboratorio de "Pedro" (Iani, Ana, Sara, Josune, Juan…), por tantos momentos vividos. Por lo mucho que hemos disfrutado investigando, por todos los congresos que hemos asistido, y quería agradeceros también, el apoyo y la ayuda que siempre me habéis dado, incluso en mis momentos de más frustración.

Muchas gracias Anita por haberme dado tantos ánimos y por haber estado siempre tan presente. Cómo hubiera hecho yo el western blot sin ti. A Iani, por estar siempre tan pendiente y por su admirable espíritu de superación. A Ane, por esa felicidad que siempre le acompaña y por todo su apoyo en la recta final de esta Tesis. A Belén, una de las mejores personas que he conocido, gracias por todo, nunca he

conocido a nadie con tantas ganas de ayudar a los demás y siempre con una sonrisa, capaz de quedarse hasta las tantas en el labo por ayudarte. Por esos cafés con sus "pitis", por esas quedadas fuera del labo, en pocas palabras chicas, por todo el tiempo que hemos compartido.

A Luis Martínez, que con su humor inteligente siempre ha sido capaz de arrancarme una sonrisa en mis momentos de máximo agobio. Muchas gracias por tu ejemplo de dedicación a la ciencia.

Agradecer también al Departamento de "BioCel" (Maitane, Patri, María,…) por todos esos momentos en el refugio y por toda vuestra ayuda y consejos.

A mis amigas de Valladolid: Ana, tu siempre tan orgullosa de mis logros, muchas gracias Anuski. A mis amigas del colegio ("las Martas" y Leti), por haber estado siempre pendientes. A Carmen, por su interés constante.

A mi cuadrilla de Bilbao (Cris Gar, Marta, Ledes, Bego, Ángela, Txatxe, Esti, Elena, Anius, Ana, Vicky, López, Miriam, Inés, Laly y Laú) por todas sus muestras de ánimo.

Quería agradecer especialmente también, a mi gran amiga Mercedes. Gracias Mer por todo, por haber aguantado todas mis "crisis" y animarme cuando todo lo veía negro. A Vicky, una de esas amigas, que son capaces de ir a tu casa para llevarte chocolates y hacerte sonreír.

Y cómo no a mis amigas de la Uni: Maitane, Rocío, Erika, Marta y Arantza. Que juntas nos iniciamos en el mundo de la Biología y juntas nos doctoramos. Por todos esos cafés en "el refugio", en los que nos animábamos mutuamente. Por esos momentos de desesperación que sólo nosotras conocemos… Gracias chicas por todo.

Maitane y Hugo, quería agradeceros toda vuestra disposición y ayuda en la maquetación de esta Tesis. Gracias por vuestra paciencia, dedicación y sobre todo por ser tan buenos amigos.

Y llegando al final, quería agradecer a mi familia, que gracias a la confianza que siempre han depositado en mí, he podido llegar hasta aquí. Especialmente, a mi Tía Paz,

por estar siempre animándome y mostrándome todo su orgullo. A mi hermana, que aunque discutamos a veces, siempre me ha demostrado toda su admiración y respeto. A mis padres, a los que les debo todo, por haber confiado siempre en mí, dándome todo su cariño y apoyo, haciéndome ver que siempre hay luz al final del túnel. Esta Tesis es en parte también vuestra.

Por último, no quiero olvidarme de mis ratas, las principales protagonistas de esta Tesis, con las que he compartido tantas y tantas horas, las que me han acompañado en este tiempo y que sin ellas nada de esto hubiera sido posible.

Dedicated to my family

“El cerebro no es un vaso para llenar, sino una lámpara por encender”

Plutarco

“Observar sin pensar es tan peligroso como pensar sin observar”

Ramón y Cajal

INDEX

ABBREVIATIONS

6-OHDA	6-hydroxydopamine
AC	Anterior commissure
Acb	Accumbens nucleus
ADN	Axodendritic network
ARTN	Artemin
BBB	Blood-brain barrier
BDNF	Brain derived neurotrophic factor
BrdU	BromodeoxyUridine
CBL	Cerebrolysin
CDNF	Cerebral dopaminergic neurotrophic factor
CL	Contralateral
CPC	Caudate putamen complex
CNS	Central nervous system
DA	Dopamine
DAB	3,3 diaminobenzidine
DBS-STN	Deep brain stimulation of the subthalamic nucleus
DCX	Doublecortin
DTT	Dithiothreitol
DNA	Deoxyribonucleic acid
EE	Enriched environment

EP	Entopeduncular nucleus
e-SN	External substantia nigra
FDA	Food and Drug Administration
bFGF	Basic fibroblast growth factor
G-CSF	Granulocyte colony stimulating factor
GDNF	Glial cell line-derived neurotrophic factor
GFLs	Glial cell line-derived neurotrophic factor family ligands
GFAP	Glial fibrillary acidic protein
GP	Globus pallidus
GPe	External segment of the globus pallidus
GPi	Internal segment of the globus pallidus
HGF	hepatocyte growth factor
IHC	Immunohistochemistry
IL	Ipsilateral
IGF	Insulin-like growth factors
IOD	Integrated optical density
I.p.	Intraperitoneal
KPBS	Potassium phosphate-buffered saline
L-DOPA	L-3,4-dihydroxyphenylalanine
LB	Lewy bodies

LC	Locus coeruleus
LEA	*Lycopersycum esculentum agglutinin*
LRRK2	Leucine-rich repeat kinase 2
MANF	Mesencephalic astrocyte-derived neurotrophic factor
MFB	Medial forebrain bundle
MTC	Medullary thyroid cancer
MS	Microspheres
MPTP	1-methyl-4-phenyl- 1,2,3,6-tetrahydropyridine
NGS	Normal goat serum
NMDA	*N*-methyl-D-aspartic acid
NRTN	Neurturin
NS	Nanospheres
NT-3	Neurotrophin-3
NTF	Neurotrophic factor
PB	Phosphate buffer
PBS	Phosphate buffered saline
PDGF-CC	Platelet derived growth factor
PFA	Paraformaldehyde
PI3K	Phosphatidylinositol 3-kinase
PLGA	Poly(lactic-co-glycolic acid)

PD	Parkinson's disease
PVDZ	Polyvinylidene difluoride
RNA	Ribonucleic acid
ROS	Reactive oxygen species
RT	Room temperature
RTK	Receptor tyrosine kinase
SE	Standard error
SPS	Sodium dodecyl sulfate
SN	Substantia nigra
SNc	Substantia nigra compacta
SNr	Substantia nigra reticulata
SNl	Substantia nigra lateralis
STN	Subthalamic nucleus
SVZ	Subventricular zone
TH	Tyrosine hydroxylase
TH-ir	Tyrosine hydroxylase immunoreactive
TK	Tyrosine kinase
TKI	Tyrosine kinase inhibitor
TMB	Tris maleate buffer
TPM	Turns per minute

VEGF	Vascular endothelial factor
VTA	Ventral tegmental area

ABSTRACT

Abstract

Parkinson's disease (PD) is the second most common neurodegenerative disorder in the world. PD is characterized pathologically by the degeneration and loss of the dopaminergic neurons in the substantia nigra (SN). Numerous works have been proposed for the study of the neuronal degeneration in PD using different animal's models, although none of them have been exact to understand the pathogenesis of PD. Therefore, the mechanism by which tyrosine hydroxylase activity may be enhanced or how it may affect dopamine tissue content in either striatum or SN in PD is unknown. The 6-hydroxydopamine (6-OHDA)-induced model is one of the most extensively used model in rats for reproducing the loss of dopaminergic neurons in the substantia nigra compacta (SNc). Additionally, the topological distribution of changes in the dopaminergic system is a factor to take into account to describe the morphological changes occurred in this model.

Current therapies available for PD are not effective in the long-term and cannot repair the already damaged area. That is why, current research efforts are being focused in new neuroprotective and neuroregenerative strategies that will halt the neurodegenerative process.

The aim of the present research was to study the morphological changes occurring in different rat models of PD induced by 6-OHDA injection and to verify the usefulness of the proposed approach to characterize different models and its suitability for elucidating the benefits of therapeutic strategies such as the administration of neurotrophic factors (vascular endothelial growth factor [VEGF] and glial cell line-derived neurotrophic factor [GDNF]) or nanowired Cerebrolysin (CBL) or the housing in enriched environment (EE). Likewise, the effects of administering a selective tyrosine kinase inhibitor (vandetanib) which blocks the VEGFR2 and RET receptors in a Preclinical model of PD were also assessed to elucidate molecular pathways involved in this model.

Three different models were characterized according to the site of 6-OHDA injection and the time of evolution in order to describe the model and the different therapeutic strategies. Firstly, a Severe model, injecting 6-OHDA into the medial

forebrain bundle (MFB); then a Partial model was assessed by the injection of 6-OHDA into the striatum, for 3 weeks, and finally we carried out a Prodromal or Preclinical model by injecting 6-OHDA into the striatum with a short time of evolution where motor symptoms were scarcely apparent.

Regarding treatments, striatal implantation of PLGA-microspheres (MS) or nanospheres (NS) loaded with VEGF and GDNF were administered in the Severe and Partial models respectively for 14 weeks to test the synergistic effect of combining both neurotrophic factors. In the Preclinical model, we evaluated the neuroprotective effects after housing rats in EE and the intraperitoneal administration for a week of nanowired CBL. On the other hand, in this Preclinical model we also administered orally vandetanib (the tyrosine kinase inhibitor).

In vivo effects of the treatments were assessed using amphetamine induced rotational behavioral test. Morphological analysis was carried out by histology, histochemistry, immunohistochemistry and stereology. Biochemical analysis was also performed using western blot in the Preclinical model to elucidate the molecular pathways involved in this process.

Our results are promising, showing that the 6-OHDA induced model provides the possibility to assess three different severity grades of PD. Moreover, it was suitable to assess the morphological consequences of the lesion and the effects of different treatments.

Following anatomical and topological distribution in the Partial model we paid attention to changes arising in SN. We identified a sector of SN more sensitive for morphological changes, the “external SN” (e-SN), which included one third of the SN-reticulata (SNr) and the lateral half of the SNc. The measurements carried out on the e-SN –topographically related to the lesioned area of the striatum- reach more specific and significant results than those carried out using the entire SN, emerging as a promising region for further studies.

Abstract

Rostro-caudal gradients of morphological changes exhibited in the striatum and in the SN, in addition to the specific anatomic distribution of the dopaminergic system, were indicative of a differential selective vulnerability of this system. A deeper knowledge of this distribution could be useful in order to assess the lesion, as well as the administration and diffusion of treatments.

Functional improvement and morphological recovery after VEGF and GDNF implantation in the Severe and Partial model is related to the preservation of the TH-positive volume in the striatum and of the cell number and axodentritic network in the SN. In addition, these findings support the neurorestorative role of VEGF+GDNF in the dopaminergic system and the synergistic effect between both factors.

The combination of CBL and EE had effects which were indicative of protective mechanisms by which these strategies can promote functional and morphological improvement by activation of survival signaling pathways after dopamine depletion in a preclinical rat model of PD, supporting the synergism of both strategies.

We also demonstrate for the first time the deleterious effect of inhibiting VEGFR2 and RET on the dopaminergic system, confirming the beneficial and synergistic effect exhibited by neurotrophic factors in PD.

In conclusion, our findings suggest protective and/or restorative mechanisms mobilized by neurotrophic factors, CBL and EE, which significantly reduced 6-OHDA degeneration of dopaminergic neurons in the SN of adult rats, preserved nigrostriatal projections, and improved dopaminergic function, showing selective vulnerability along the rostro-caudal axis in the dopaminergic system.

I. INTRODUCTION

1. Parkinson's disease

Parkinson's disease (PD) is the second most common neurodegenerative disorder in the world after Alzheimer disease (Feng et al., 2010). It was initially described by James Parkinson in 1817, who published "an assay on the shaking palsy" where first described the clinical syndrome, as a neurological disorder, consisting of resting tremor and a peculiar form of progressive motor disability (Samii et al., 2004) that was later to bear his name (Parkinson, 2002). Previously referred to as paralysis agitans, Charcot later in the 19th century gave credit to Parkinson by referring to the disease as "maladie de Parkinson" or Parkinson's disease (Kempster et al., 2007). Nowadays, PD is described as a progressive neurodegenerative disease with motor, non-motor, and behavioral dysfunction.

Due to the current high life expectancy of our society, the number of cases of PD is increasing, and this disease is becoming a serious public health problem. In fact, today PD affects approximately 0.1% of the world population and occurs most frequently in people over 80 years old, with a prevalence of 1–3%. However, a younger onset of PD is also possible, it was published that incidence rates increase after the age of 50, with a prevalence of 0.5–1% in people between 65 and 69 years of age, and rapidly increase over the age of 75 (Nussbaum & Ellis, 2003; de Lau et al., 2004). On the other hand, according to studies of death rates and prevalence, male sex seems to be the sex more susceptible to suffer PD. Men have on average a 2-fold higher incidence of developing PD and 1.3–3.7-fold higher prevalence of PD compared to women, at all ages and for all nationalities studied (Baldereschi et al., 2000; Van Den Eeden et al., 2003; Wooten et al., 2004; Haaxma et al., 2007). In fact, studies from human and animal models of PD indicate that the male bias in PD may be explained by sex differences in nigral gene expression (Loke et al., 2015). Thus, estrogens may exert some form of neuroprotection in the preclinical stage of PD, or may even postpone the beginning of the degenerative

process, but fail once symptoms have become clinically apparent (Haaxma et al,. 2007).

Among the factors implied in neurodegeneration, a decrease in energetic cellular efficiency together with the synthesis and activity of neurotrophic factors (NTFs) play a crucial role. Both are involved in regional vulnerability (Obeso et al., 2010).

At the present, despite of the efforts to find some therapy to prevent PD, it has only been possible to proof the existence of some neuroprotective substances, such as caffeine and nicotine, or risk factors as aging and genetic (Figure 1).

1.1. Clinical signs, symptoms and diagnosis

PD is generally defined as an idiopathic or sporadic disease characterized pathologically by the degeneration and loss of the dopaminergic neurons in the substantia nigra (SN) and the presence of Lewy pathology (Olanow & Obeso, 2012). Additionally, during the early stages of the disease, called the presymptomatic phase, PD patients develop non-motor deficits including olfaction impairment, vagal dysfunction and sleep disorders (Angot & Brundin, 2009), indicating that other neurotransmitter systems (e.g. cholinergic, adrenergic, serotoninergic) also degenerated and cell loss is also seen in other brain areas (Schapira, 2009). In fact, the lack of motor symptoms during the early disease stage may be due to “neuronal reserve” or active compensatory mechanism(s), such as collateral axonal sprouting from surviving dopaminergic neurons (Arkadir et al., 2014). The typical motor symptoms appear when there is 50–60% of dopaminergic neuron loss and 70–80% of dopamine (DA) depletion (Schapira, 2009; Sato et al., 2013). The cognitive functions decline at more advanced stages (Angot & Brundin, 2009). Thus, there are motor and non-motor symptoms associated to PD:

- **Motor symptoms:** The cardinal features of PD are mainly motor symptoms and include tremor at rest, rigidity and bradykinesia. In addition, flexed posture and freezing (motor blocks) have been also included as feature of Parkinsonism. Tremor and rigidity are considered as "positive" phenomena, while bradykinesia together with postural reflex abolition and the freezing are considered as "negative" phenomena.
- **Non-motor symptoms:** Non-motor extra SN symptoms are common and often underappreciated and can be as disabling as motor symptoms (Sullivan et al., 2007). These include, cognitive and psychiatric changes, autonomic dysfunction and sleep disturbances. In fact, the presence of cognitive impairment or dementia in patients with PD is associated with loss of independence, a lower quality of life and a reduction in survival time (Irwin et al., 2013). Interestingly, other symptoms such as hypotension, sweating, sphincter and erectile dysfunction have been described (Jankovic, 2008). In addition, it has even been proposed that the non-nigral pathology dominates the earlier and later stages of PD (Del Tredici et al., 2002; Braak et al., 2004, 2006).

On the other hand, the types of symptoms present and their severity depend significantly on the length of time since onset, the rapidity of functional decline, and whether the patient received medication (Deumens et al., 2002).

As a result of these clinical symptoms, PD is now recognized as a complex clinicopathological entity. The majority of PD cases are sporadic (Feng et al., 2010) and the etiology and pathogenesis remain enigmatic (Brundin et al., 2008). However, parkinsonian disorders can be classified as four types: primary (idiopathic) Parkinsonism, secondary (acquired, symptomatic) Parkinsonism, heredo-degenerative Parkinsonism and multiple system degeneration (Parkinsonism plus syndromes). Several features, such as tremor, early gait abnormality (e.g., freezing), postural instability, pyramidal tract findings and

response to levodopa, can be used to differentiate PD from other parkinsonian disorders (Jankovic, 2008).

The diagnosis of PD relies mainly on the clinical detection of the motor symptoms, physical examination, and improvement of symptoms and signs with dopaminergic treatment (Samii et al., 2004). Thus, as illustrated in Figure 1 according to Miller and O'Callaghan in 2015, since the clinical diagnosis of PD usually occurs only after a substantial number of SN neurons have degenerated, there is a need for PD biomarkers that include (Miller & O'Callaghan, 2015):

- **Prodromal, preclinical or premotor stage biomarkers**
- **Biomarkers of risk or susceptibility**
- **Motor stage biomarkers**

The unilateral or asymmetric onset of a bradykinetic rigid syndrome with resting tremor is a subsequent good response to an adequate dose of a dopaminergic agent given for a sufficient period. Indeed, when there is doubt about the diagnosis related to the distinction of PD from essential or dystonic tremor, or postsynaptic forms of Parkinsonism, functional imaging of the dopamine pathways can be helpful.

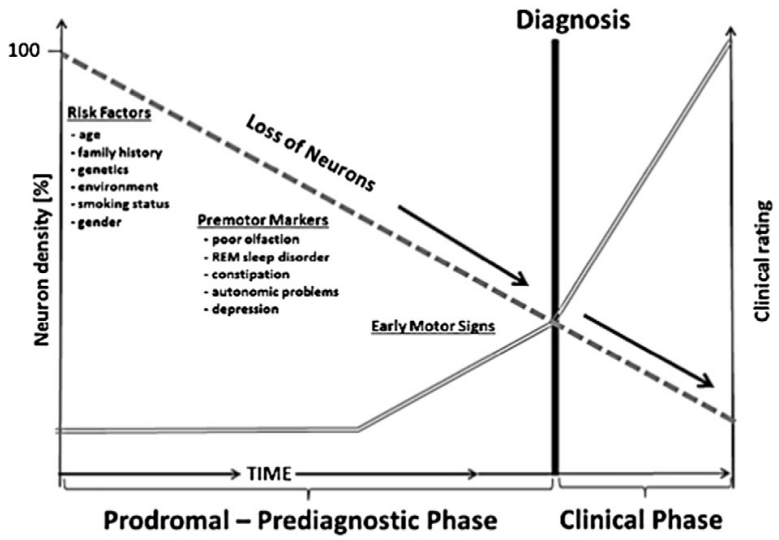

Figure 1. Schematic representation of factors and premotor markers associated with loss of neurons (————) **prior to onset of motor signs and clinical diagnosis** (====) (Miller and O'Callaghan, 2015).

Unfortunately, there is no definitive diagnostic test, because symptoms used in the clinical diagnosis of PD also occur in other disorder, but not all these clinical "looka-likes" have a neurodegenerative component (Miller & O'Callaghan, 2015). Therefore, the criterion for definitive diagnosis of PD is confirmed by the histopathological analysis obtained at autopsy.

1.2. Pathogenesis of Parkinson's disease

The pathological hallmark of PD is the degeneration of dopaminergic neurons in the substantia nigra compacta (SNc) of the midbrain and the presence of Lewy bodies (LB). Despite the number of pathogenic mechanisms, that has been suggested to be involved in PD, such as oxidative stress, mitochondria defects, protein mishandling/or-and misfolding and inflammation, the original causative factor is unknown yet. Therefore, it is essential to have a precise understanding on the complexity and topology of the connections and projections along the nigrostriatal dopaminergic system, about the cellular and molecular heterogeneity of the caudate putamen complex (CPC) and SN in order to elucidate about the

pathogenesis, the search of new treatment strategies and their correct application. On the other hand, the interaction of all pathological mechanisms involved in PD could be a requisite to take into account in order to elucidate about the causative factor of PD (Figure 2).

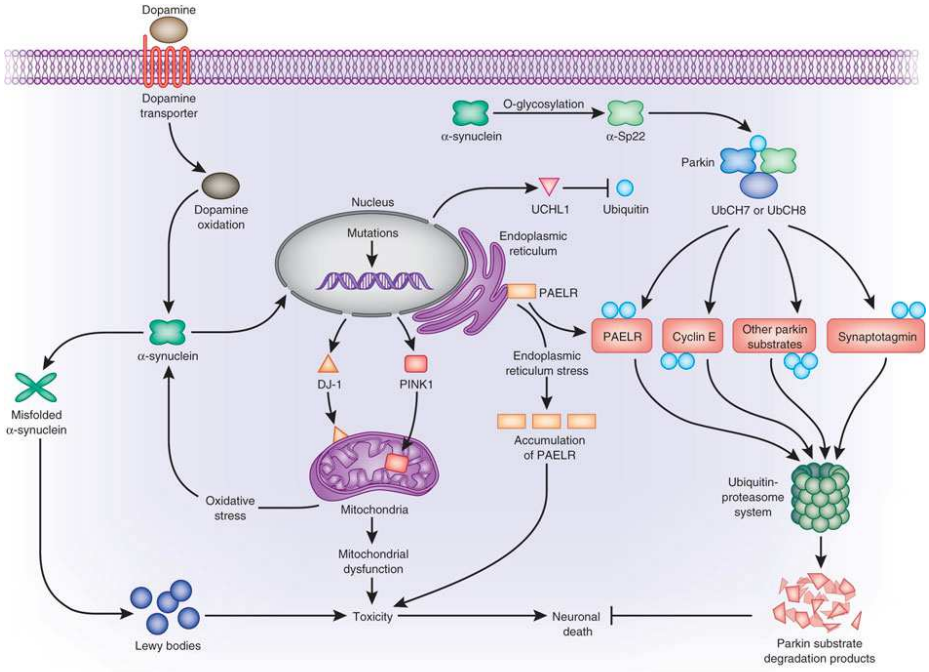

Figure 2. Schematic summary of etiopathogenic mechanisms and interactions in the dopaminergic cells of the substantia nigra in Parkinson's disease (Obeso et al., 2010). Cell death may be caused by the toxicity due to α-synuclein aggregation and Lewy body formation, proteosomal system dysfunction, reduced mitochondrial activity and subsequent oxidative stress, among others. Gene mutations are associated with impairment of one or several of these mechanisms, being also responsible for cell death.

1.2.1. Degeneration of nigrostriatal dopaminergic system

One of the major pathological hallmark of PD is the selective degeneration of nigrostriatal dopaminergic pathway (Figure 3a,b) (Greenamyre et al., 2003). This neural pathway provides a connection between SN and striatum and has an important role in controlling motor activities (Greenamyre et al., 2003; Uversky, 2004). The cell bodies of dopaminergic neurons in this pathway are located in SNc and their axons project into striatum (Bové et al., 2005). Progressive

neurodegeneration of these dopaminergic neurons located in ventrolateral and caudal portion of the SNc in PD (Fearnley & Lees, 1991) results in a profound depletion of DA in the striatum, being most affected the lateral SN projections to putamen (Kish et al., 1988) (Figure 3b).

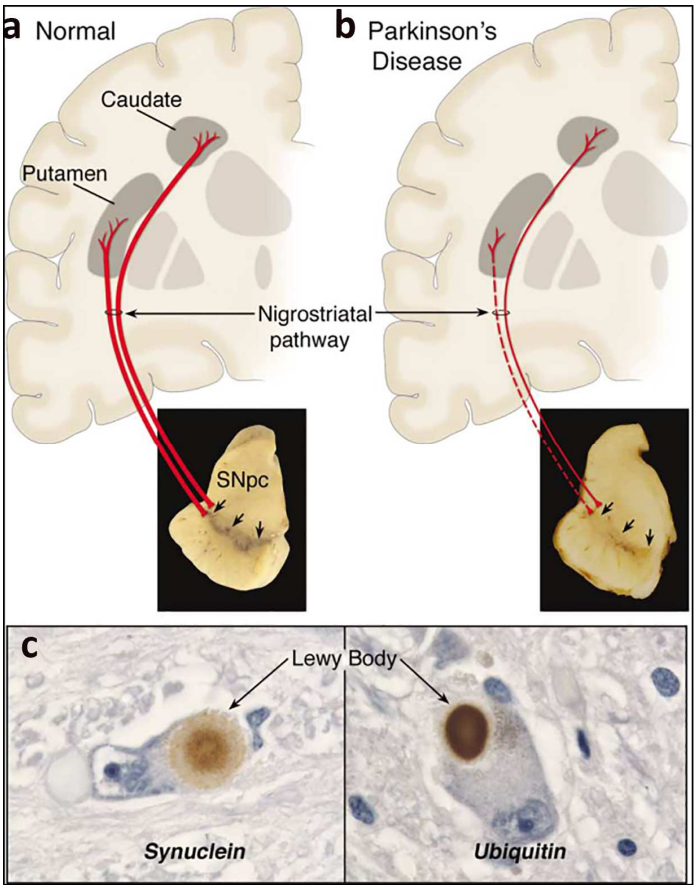

Figure 3. Schematic representation of the normal nigrostriatal pathway (a) and after dopaminergic degeneration (b) and Lewy body formation (c) in Parkinson's disease in humans (Dauer & Przedborski, 2003).

However, SN damage is always accompanied by extensive extranigral pathology, including noradrenergic neurons of the locus coeruleus (LC) and dorsal vagal nucleus, serotonergic neurons of the dorsal raphe and cholinergic neurons within the substantia innominata (particularly in the nucleus basalis of Meynert) and in the pedunculopontine nucleus (Jellinger, 1990). Thus, apart from nigrostriatal dopaminergic system other neurotransmitter systems are involved,

such as the glutamatergic, cholinergic, adrenergic or serotoninergic (Hornykiewicz, 1998; Schapira, 2009). Damage to these important neuronal systems may play a significant role in some of the non-movement-related aspects of PD such as cognition and depression (Deumens et al., 2002).

1.2.2. Lewy body formation

Lewy bodies, the other pathological hallmark of PD, represent a cytoplasmic eosinophilic proteinaceous inclusion within the neurons (Figure 3c). They are formed by more than 25 compounds, principally α-synuclein and ubiquitin with a diameter of 8-30 µm (Samii et al., 2004). Lewy bodies are commonly located in the dopaminergic neurons of SN, locus coeruleus, the dorsal motor nucleus of the vagus, and the nucleus basalis of Meynert, but also other pigmented brainstem and subcortical nuclei, such as the anterior cingulate and the association neocortex also show these inclusions (Jellinger, 2001).

1.2.3. Mitochondrial dysfunction and oxidative stress

Mitochondria are highly dynamic organelles essential for a range of cellular processes including ATP production, reactive oxygen species (ROS) management, calcium homeostasis, and control of apoptosis.

Oxidative stress defines the disequilibrium between the levels ROS produced and the ability of a biological system to detoxify the reactive intermediates, creating a perilous state contributing to cellular damage (Dias et al., 2013).

Since mitochondria play a dual function as source and target of ROS, compelling evidence suggests that mitochondrial dysregulation plays a critical role in the pathogenesis of PD. Furthermore, impairment of mitochondrial function leads to cellular damage and is related to neurodegeneration (Zhu & Chu, 2010).

Particularly, a systemic decrease in the complex I activity of the mitochondrial electron transfer chain was reported in the tissues of brain, skeletal muscle, and platelets of PD patients (Sherer et al., 2003; Greenamyre et al., 2003; Alam et al., 2004).

The extensive production of ROS in the brain may provide an explanation for the magnitude of the role that the reactive molecules in PD. In fact, it has been observed damage in nigral neurons of patients with PD caused by free radicals like ROS and peroxynitrite.

On the other hand, the link between oxidative stress and dopaminergic neuronal degeneration is further supported by modeling the motor aspects of PD in animals with toxins that cause oxidative stress including 1-methyl-4-phenyl-1,2,3,6-tetrahydropyridine (MPTP), rotenone, 1,1'-dimethyl-4,4'-bipyridinium dichloride (paraquat), and 6-hydroxydopamine (6-OHDA) (Fukushima et al., 1997; Perier et al., 2003; Callio et al., 2005; Richardson et al., 2005).

Interestingly, the discovery of genes linked to familial forms of PD, such as alpha-synuclein, parkin, DJ-1, PINK-1 and Leucine-rich repeat kinase 2 (LRRK2) has yielded important insights into the molecular pathways in the disease pathogenesis and highlighted previously unknown mechanisms by which oxidative stress contributes to the disease (Figure 2). Some of these mechanisms are complex, involve various cell biologic processes, and are modulated by several of these proteins. These discoveries are also beginning to help to interpret some of the biochemical defects in the PD brain (Dias et al.,2013). In fact, it has been indicated that there are certain polymorphisms in the genes of complex I and mutations in some nuclear genes like PINK1 and DJ-1, which are encoding mitochondrial proteins, in developing familial PD (Figure 2) (Greenamyre et al. 2003; Schapira, 2002). Furthermore, it has been shown recently that oxidative stress promotes the uptake of α-synuclein by various cell types resulting in

mitochondrial inhibition (Figure 2) (Luk et al. 2012; Pukass & Richter-Landsberg, 2014).

1.2.4. Failure of protein degradation systems

The two major degradation systems are the ubiquitin-proteasome system and the autophagy–lysosome system. These degradation systems are involved in the clearance of defective cellular structures such as misfolded or damaged proteins, and dysfunctional organelles such as defective mitochondria. However, genetic and pathological evidence strongly indicate the involvement of defective clearance systems in PD (Figure 2) (Martinez-Vicente et al., 2008; Harris & Rubinsztein, 2012; Nalls et al.,2011).

Normally, misfolded proteins are first sent to chaperons and if they still lack a proper folding they are sent to proteasomes for degradation through several pathways such as ubiquitination. The formation of Lewy bodies in PD brains has revealed the question of whether there is a relationship between these cytoplasmic protein aggregates and proteasome activity, since high amounts of ubiquitin are found in Lewy bodies deposits (Dauer & Przedborski, 2003; Greenamyre et al., 2003). Also, the mutations of some proteins normally involving in proteasome ubiquitination system are observed in the familial PD (Figure 2). Likewise, there are studies that inhibition of proteasome activity cause neuronal loss in SN. All the studies so far support the important role of proteasomal activity in PD. However, the exact relationship between proteasome and α-synuclein aggregation is still unknown (Greenamyre et al., 2003).

While this evidence demonstrates the involvement of cellular clearance mechanisms in PD, it is unclear whether that involvement is primarily beneficial or detrimental. It has been argued that exaggerated clearance activity may contribute to neuronal injury (Chu, 2006; Xu & Zhang, 2011). The predominant view, however,

is that the removal of abnormal proteins and organelles is neuroprotective (Fujita et al., 2014).

1.2.5. Neuroinflammation

Interactions between neurons and non-neuronal cells also participate in the cascade of events leading to neurodegeneration in PD (Hirsch et al., 2013). Indeed, astrocytosis, microgliosis, and even lymphocyte infiltration are found in the substantia nigra in postmortem studies in PD (Przedborski, 2007; Hirsch & Hunot, 2009).

Numerous evidences supported that neuroinflammation in PD is mediated mainly by activated microglia (Block et al., 2007). Microglia are phagocytic cells, components of the innate immune system of the central nervous system, that usually have a resting phenotype but become activated upon brain injury or immune challenge. In fact, microglia can enter an overactivated state as response to environmental toxins and release ROS that produce neurotoxicity. Thus activation of microglia may contribute to the oxidative damage through ROS. They can also promote neurodegeneration by producing other potentially toxic agents such as glutamate and tumor necrosis factor-alpha (Block et al., 2007; Chéret et al., 2008; Ceulemans et al., 2010; Dumont and Beal. 2011). In addition, a local microglial activation could be found within the SN, along a global astrogliosis (Mallajosyula et al., 2008).

On the other hand, microglial cells also produce anti-inflammatory cytokines and exert phagocytic activities that could prevent the extension of neuronal degeneration. In this context, trying to switch the phenotype of microglial cells from a proinflammatory M1 to an immunomodulatory M2 phenotype might represent an interesting therapeutic strategy (Benner et al., 2004).

However, the postmortem studies do not allow the determination of whether neuroinflammation participates in neuronal degeneration or merely represents a consequence of it. To address this issue, changes occurring in animal models of PD have been investigated along with the effects of interfering with such mechanisms on the extent and time course of neuronal loss.

1.3. Etiology

Although the cause of PD remains unknown, PD is likely a result of multiple factors, including normal aging, genetic predisposition and environmental exposures (Figure 4).

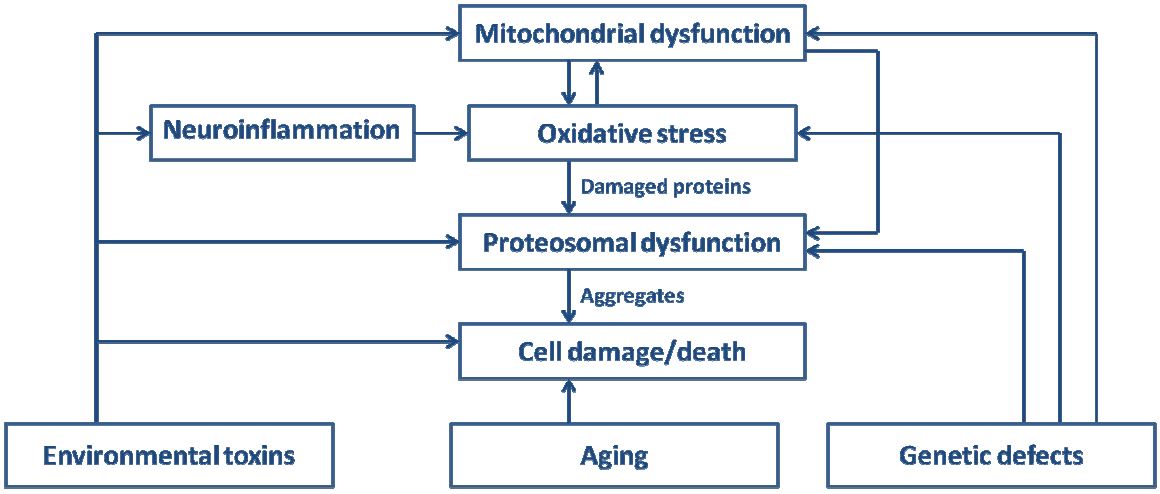

Figure 4. A summary of the etiopathogenic interface between environmental, aging and genetic forms of parkinsonism (Adapted from Schapira, 2009)

1.3.1. Environmental factors

Exposure to various toxins like MPTP or pesticides like rotenone or paraquat used in agriculture may be a secondary etiology of PD (Langston et al., 1983; Betarbet et al., 2000; Thiruchelvam et al., 2000). In fact, chronic exposure to a common pesticide can reproduce the anatomical, neurochemical, behavioral and neuropathological features of PD (Figure 4) (Betarbet et al., 2000).

Thus, a rural residency and exposure to pesticides appear to increase the risk of the development of PD, particularly young-onset PD (Rajput et al., 1986; Rajput and Uitti, 1988; Semchuk et al., 1992; Schapira, 2006). Although an environmental contribution to the cause of PD seems likely, no specific agent has been clearly identified as causative (Schapira, 2009).

1.3.2. Aging

Aging is often though that may be critical for PD. In fact, the different agents involved in the etiology of PD are also involved in aging (Rodriguez et al., 2015). The vulnerability of dopaminergic neurons increases with the age and because of that these neurons are more susceptible to silent toxics (Going et al., 2002; Takubo et al., 2002; Jeyapalan and Sedivy, 2008; de Cabo et al., 2014). Although aging may be the only factor implied in sporadic PD, since both prevalence and incidence increase with age (Tanner, 2003), aging itself is not the main factor in the neurodegeneration of the nigrostriatal dopaminergic pathway.

1.3.3. Genetic factors in Parkinson's disease

Genetic factors have a substantial impact on the phenotypic variance of PD status, and they are responsible for some familiar forms of PD, with recent heritability estimates near approximately 60% (Lill et al., 2015). In fact, α-synuclein has been the most widely investigated genetic determinant for pathogenesis of PD (Polymeropoulos et al., 1997). However, apart from α-synuclein, several other familial PD-linked genes were subsequently identified, which includes Parkin/PARK2, UCHL1, DJ-1/PARK7, PINK1 and leucine-rich repeat kinase 2 (LRRK2) (Tan and Skipper, 2007; Kulkarni et al., 2015). Interestingly, LRRK2, PINK1, and DJ-1, which are present in mitochondrial membranes, have been suggested to play a role in ROS production by a defective maintenance of the mitochondrial membrane potential (Knott et al., 2008; Wang et al., 2011).

Patients with these genetic mutations only account for about 5-15% of all PD cases, while the majority of cases belong to idiopathic or sporadic PD, whose causes are largely unknown.

1.4. Parkinson's disease treatment

It is not known how long SN degeneration begins before the onset of PD symptoms and before the diagnosis is made. Clues from clinical, pathological and imaging studies suggest this period could be 6–8 years (Schapira & Obeso, 2006), although this is likely to be much longer in patients with genetic causes of PD. Thus, there is a long latency between onset and the eventual 50–60% nigral loss and 70–80% dopamine depletion that is estimated to induce clinical features. This concept now underlies the move towards earlier rather than later introduction of symptomatic treatment for PD. In fact, the basis for early treatment is reinforced by the rapid progression of PD in the early phase after diagnosis.

Although PD is a major priority for health care systems, dopaminergic therapies are the most used, e.g. the current pharmacological treatment with L-3,4-dihydroxyphenylalanine (L-DOPA), which focuses on modifying motor symptoms without treating the neurodegenerative process, without providing neuroprotection to the surviving dopaminergic neurons and without any attempt to repair the underlying disease. On the other hand, invasive ways for delivering more continuous dopaminergic therapy, such as apomorphine pumps and DuiDopa®, as well as neurosurgical interventions, such as brain stimulation, are necessary in case of complication, intolerance or side effects to the medication (Wijeyekoon & Barker, 2009).

In this context, current research efforts are focused on halting neuro-degeneration using promising alternatives such as antioxidants, antiapoptotic agents, cell-based therapies, and neuroprotective agents (Herrán et al., 2013).

1.4.1. Pharmacological treatment

L-DOPA is considered the standard/essential drug for treatment of PD. It is the precursor of dopamine (Figure 5) that cross the blood-brain barrier (BBB) through a large amino acid transporter (Kageyama et al., 2000) and its administration is an attempt to replace exogenously the characteristic deficit of dopamine in PD. L-DOPA alleviates bradykinesia, the increase in muscle tone and tremor, but does not reduce non-motor symptoms (Mercuri and Bernardi, 2005). DA agonists, COMT, and MAO-B inhibitors are also used as adjunctive treatment to L-DOPA (Schapira, 2009; Tarazi et al., 2014). However, the efficiency of L-DOPA decreases over time and many patients develop motor fluctuations (wearing-off and on–off phenomena), dyskinesias and behavioral abnormalities (Mercuri and Bernardi 2005; Obeso et al., 2010).

Figure 5. Conversion of L-DOPA to dopamine catalyzed by DOPA decarboxylase.

1.4.2. Surgical treatment

Surgical treatment is an alternative for PD, especially when the pharmacological treatment is not able to improve the symptoms or when the prolonged use of L-DOPA causes complications. The surgical procedure includes the ablation or lesion and the neurostimulation of the subthalamic nucleus (STN) or the globus pallidus (GP), which are considered the most adequate for stimulation. Nowadays, the stimulation is the election surgical procedure, due to the reversibility of its effects, the low morbid-mortality, the possibility to remove it

in case of any problem, such as impulse control disorders or psychosis, or the apparition of better treatments, and the possibility to adjust the parameters in each patient (Starr et al., 1998; Benabid et al., 2003; Nilsson et al., 2005). In this context, deep brain stimulation of the subthalamic nucleus (STN-DBS) is an evidence based treatment in advanced stages of PD as it has been shown to improve motor fluctuations, dyskinesia and quality of life better than medication (Voon et al., 2009). Furthermore, a recent study has shown that medication can be significantly reduced following STN-DBS and prospective controlled studies establishing an evidence-based co-medication of STN-DBS in patients are needed (Alexoudi et al., 2015).

However, stimulation has also some problems or limitations, such as fragility of the electrode system, susceptibility to injections, elevated economic cost, difficulty in adjusting the parameters, or the replacement of the batteries after a period of time (Oh and Chase, 2002; Doshi et al., 2002).

1.4.3. Other treatments

Other treatments have been proposed to treat PD, although none of them have provided remarkable therapeutic benefits.

a) **Cell transplant:** Though the invasive ways can be very competent in providing symptomatic relief, but without any considerable effort to reinstate the root cause of the disease. Thus, the restorative approaches, using cell therapy and neurotrophic support, for dopaminergic nigrostriatal tract may serve very practical (Kulkarni et al., 2015). In fact, cell therapies in PD have been a major research interest for the last 30 years with the main focus being on using them for replacement of the degenerating (and lost) dopaminergic neuronal innervation of the striatum from the SN (Wijeyekoon & Barker, 2009).

b) **Genetic treatment:** These strategies are based on restoring the lost brain functions by substitution of enzymes critical for the synthesis of neurotransmitters or neurotrophic factors (NTFs) in order to increase the functions of remaining dopaminergic neurons in the brain and find new target for the treatment (Björklund & Kirik, 2009). To achieve this purpose and obtain a correct transference of the gene, virus (Kang and Nakamura, 2003; Carlsson et al., 2005), fibroblasts (Fisher et al., 1991) or astrocytes (Lundberg et al., 1996) have been used.

c) **Neuroprotection:** Neuroprotection-based therapies may be a useful treatment to reduce or stop the progression of PD. Several works have been developed to study the efficacy of using neuroprotective mechanisms. One of these mechanism could be the transference of genes that codify for antioxidants in dopaminergic cells, which may protect SNc from cell loss (Kang and Nakamura, 2003). Other neuroprotective and neurorestorative approach is the utilization of NTFs or growth factors, which could prevent or stop the neuronal death. In addition, the inactivation of STN could be also considered as a neuroprotective strategy (Maesawa et al., 2004).

1.4.4. Future strategies: Neurotrophic factors administration

Current research is focused on the development of therapeutic strategies that will halt the neurodegenerative process, rather than simply treat the clinical symptoms. Thus, an interesting and promising approach to this challenge is the use of NTFs. NTFs are proteins that act as growth factors and play an important role in the maintenance, survival, specification and maturation of specific neuronal populations (Figure 6) (Siegel & Chauhan, 2000; Sullivan & Toulouse, 2011).

Administration of NTFs can be by different means and by different presentations, in this context we focused on the following strategies:

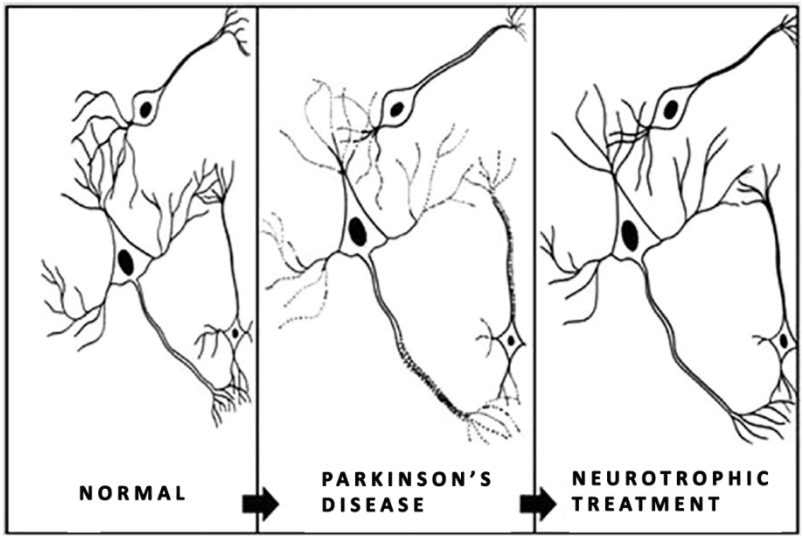

Figure 6. Diagrammatic representation of the contact between two neurons developed under normal and pathological conditions. Neurotrophic factor therapy for neurodegenerative conditions is anticipated to prevent cell body and synaptic atrophy, to stimulate the synthesis of proteins necessary for transmitter release machinery, and under special conditions, to reinstate lost synaptic contacts (Adapted from Kordower & Bjorklund, 2013).

- **Poly(lactic-co-glycolic acid) (PLGA) microspheres (MS) or nanospheres (NS)**

The critical problems for the clinical application of NTFs are their rapid degradation rate and their difficulty in crossing the BBB. Thus, different intracranial administration strategies have been used in PD animal models to obtain a continuous and direct release of the factors into the brain (Yasuhara et al., 2004).

Over the past years, one strategy that has gained the attention of the scientific community is the encapsulation of neurotrophic factors into biodegradable and biocompatible **poly(lactic-co-glycolic acid) (PLGA) microspheres (MS) or nanospheres (NS)** (Wong et al., 2012; Herrán et al., 2013, 2014). This approach allows for the intracranial administration of MS or NS by stereotactic techniques, achieving a continuous drug release over time and overcoming the problem of repeated administrations. Several previous studies have demonstrated the efficacy of this technique in improving the motor function and in increasing the fiber density of the striatum (Jollivet, 2004; Garbayo et al.,

2009; Herrán et al., 2014). To evaluate these new therapies, animal models of PD are essential, such as 6-OHDA-lesioned rats.

The local administration of these polymeric microspheres has been found to reduce the possibility of dose dumping, decrease the frequency of drug administration and improve overall systemic effects (Hickey et al., 2002). Regarding polymeric nanospheres, considerable attention has been paid to the improvement of PLGA nanoparticles, making the local delivery of neuroprotective agents into the brain possible. In fact, PLGA-NS can preserve the encapsulated unstable therapeutic drug from enzyme degradation, release the drug in a controlled and continuous manner, enhance its biodistribution, and permit drug targeting (Herrán et al., 2014).

Microspheres had spherical shapes with particle sizes of **16–20 µm** (Herrán et al., 2013). On the other hand, nanospheres are around **250 nm** particle size, which is considered sufficient to form stable dispersions (Herrán et al., 2014). Firstly, microspheres or nanospheres are characterized by *in vitro* MS or NS release study, the biphasic delivery pattern was considered suitable to obtain the desired effect. The initial burst release of a significant amount of the encapsulated factor could help to manage the tissue injury caused by the invasive administration process. However, the constant release profile observed over time may play a key role in restoring the lesion caused by the 6-OHDA injection. However, the microencapsulation process may lead to modifications of the growth factors that could cause the loss of activity. Thus, bioactivity is tested in cell cultures after the factors underwent encapsulation (Herrán et al., 2013).

Once MS or NS are administered, NTFs are released due to diffusion and erosion mechanisms, and, consequently, a constant drug release in therapeutic concentrations in a localized area was obtained, achieving desired effects during the *in vivo* study (Herrán et al., 2013, 2014).

- **Cerebrolysin**

On the other hand, various studies showed that a high concentration of NTFs when given in combination improves motor function and helps in the regeneration of neurons (Sharma et al., 1997; Sharma, 2007b, 2010; Sharma and Johanson, 2007). Therefore, they are administered in high dose exogenously to provide some neuroprotective effects (Winkler *et al.*, 2000; Nyberg & Sharma, 2002). In this context, it has been also proposed other way of administrating various NTFs, which is the intraperitoneal (i.p.) administration of **Cerebrolysin (CBL).** CBL is a mixture of various NTFs, containing active peptide fragments and contains different low-molecular-weight peptides and free amino acids in solution (Menon et al., 2012). The solution is free of proteins, lipids and antigenic properties and each milliliter contains 215.2 mg of the active pharmaceutical ingredient (Plosker, 2009).

Cerebrolysin could exert pleiotropic effects, providing effective neuroprotection, including neurosurvival and neuroplasticity, by its neurotrophic actions and neuroregeneration in different kinds of central nervous system (CNS) injuries (Sharma et al., 2012), like multiple sclerosis, PD, Alzheimer's disease, dementia, and acute or chronic stroke (Muresanu et al., 2010; Sharma, et al., 2010, 2011; Sharma et al., 2010; Sharma et al., 2011).

Despite the promising activity, therapeutic use of Cerebrolysin presents difficulties due to its poor biopharmaceutical properties. In fact, this drug is only partially capable of crossing the BBB since it is formed by 25% of low molecular weight peptides (Hartbauer et al., 2001). Besides, the short half-life and the poor stability in the blood require the administration of high doses. Thus, the bioavailability of Cerebrolysin could be improved through encapsulation in suitable formulations. Among the various colloidal drug delivery systems, polymeric nanoparticles represent a very promising approach to both stabilize and control the delivery of pharmacological agents (Ruozi et al., 2015). Remarkably, delivered

TiO2-nanowired represents a promising strategy as delivery system of Cerebrolysin (Muresanu et al., 2015). In fact, nanowired drugs may penetrate the CNS faster and could reach widespread areas (Tian et al., 2012). TiO2-based (hydrogen titanate) single crystalline ceramic biomaterial with a typical diameter ranging from **50 to 60 nm** and a superb chemical stability that can be used to enhance drug delivery within the CNS (Tian et al., 2012).

2. Anatomical basis of Parkinson's disease: basal ganglia

The basal ganglia are a functional structure in the encephalon formed by several subcortical nuclei and circuits that connects thalamus with the cortex and engaged primarily in motor control, together with a wider variety of roles such as motor learning, executive functions and behavior, and emotions (Lanciego et al., 2012). The principal components of the basal ganglia are the striatum (caudate nucleus and putamen), the external segment of the globus pallidus (GPe), the internal segment of the globus pallidus (GPi, entopeduncular nucleus in rat, EP), the substantia nigra compacta (SNc), the substantia nigra reticulate (SNr) and the subthalamic nucleus (STN) (Figure 7). In fact, PD results from abnormalities of basal ganglia functioning, the degeneration of dopaminergic neurons of the SNc triggers a cascade of functional changes affecting the whole basal ganglia network (Blandini et al., 2000).

The basal ganglia and related nuclei can be broadly categorized as input nuclei, output nuclei and intrinsic nuclei (Lanciego et al., 2012).

- **Input nuclei**: They are structures receiving incoming information from different sources, mainly cortical, thalamic, and nigral in origin. They consist of striatum (caudate nucleus and putamen) and the accumbens nucleus (Acb).
- **Output nuclei**: They are structures that send basal ganglia integrated information to the thalamus and consist of the internal segment of the GPi (EP in rats) and the SNr.
- **Intrinsic nuclei:** These structures, such as GPe, the STN and SNc are located between the input and output nuclei in the relay of information.

Together these interconnected nucleus process and integrate motor, limbic, sensory and associative multifarious inputs coming from areas of the

cerebral cortex and return the processed information to the same cortical region. Thus, different pathways have been described in the basal ganglia (Figure 7):

- **Hyperdirect pathway**: It connects the cortex with the basal ganglia output nuclei (SNr/GPi or EP in rat) through the STN and it is a dynamic's center of voluntary limb movements (Gerfen, 2000).
- **Direct pathway:** It directly connects the striatum and the basal ganglia output nuclei.
- **Indirect pathway:** It connects the striatum and the basal ganglia output nuclei through the GPe and the STN.

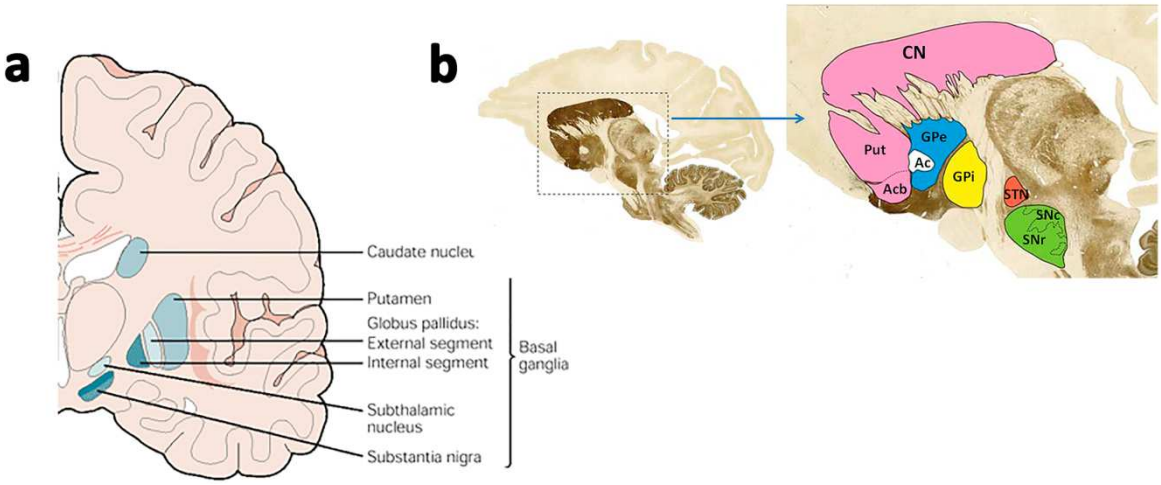

Figure 7. Schematic depiction of the main basal ganglia components. (a) Coronal section of a human brain (Adapted from Nieuwenhuys et al., 2007). **(b)** Parasagittal section of a monkey brain (stained with the acetylcholinesterase method) (Adapted from Lanciego et al., 2012). Abbreviations: CN, caudate nucleus; Put, putamen; GPe, external segment of the globus pallidus.; SNr, substantia nigra reticulate; SNc, substantia nigra compacta; STN, subthalamic nucleus; Acb, accumbens nucleus, GPi, Internal segment of globus pallidus, Ac: anterior commissure.

The requirement for the correct functioning of basal ganglia is the release of dopamine by nigrostriatal neurons at input nuclei. Dopamine binds to the D_1 receptors facilitating the transmission through the direct pathway as well as to the D_2 receptors inhibiting the transmission through the indirect pathway.

2.1. Basal ganglia motor circuit in normal conditions

The basal ganglia motor circuit connects the cerebral cortex to the basal ganglia, and through the thalamus, the basal ganglia to the cerebral cortex. Most of the intrinsic connections of the basal ganglia are GABAergic inhibitory. The only excitatory glutamatergic projection originates in STN (Smith et al., 1998). However, in rats it has been proposed that the EP also receives glutamatergic projections from the GPe (Hazrati et al., 1990). This circuit can be separated in three parts:

- **Afferent projections to the striatum:** These afferents are principally cortical glutamatergic projections and SNc dopaminergic projections.

- **Efferent projections from the striatum:** The striatum presents different types of neurons. According to these neurons types, two pathways have been described within the basal ganglia. The direct pathway which is originated in the striatal GABAergic neurons that express dynorphin (substantia P) and the mRNA of the D_1 receptor. These neurons project directly to the GPi/EP and the SNr. On the other hand, the indirect pathway is originated in the striatal GABAergic neurons that express enkephalin and mRNA of the D_2 receptor. These neurons project to the GPe, later the signal to the STN and from the STN to the GPi/EP in rat and the SNr.

- **Efferent projections from the basal ganglia:** The basal ganglia output nuclei, the GP/EP and the SNr project principally to the thalamus, and in a lower level to the pedunculopontine nucleus and the superior colliculus (Young and Penney, 1984).

Striatum is the main input nuclei of the basal ganglia, in fact the direct and indirect pathways of the basal ganglia motor circuit are initialized by the striatum (Blandini et al., 2000; Zinger et al., 2011) (Figure 8). Activation of the direct pathway, excitatory in its nature, leads to the active inhibition of the GPi/EP

output, thus reducing the thalamus inhibition and facilitating movements. On the opposite sense, the activation of the indirect pathway leads to the inhibition of movements. Both pathways are heavily innervated by the dopaminergic neurons of the SNc (Meredith & Kang, 2006).

2.2. Basal ganglia motor circuit in Parkinson's disease

In PD, because of the degeneration of dopaminergic neurons in SNc, dopaminergic input from SNc into striatum decreases which results in the reduction in direct pathway signal and the subsequent reduction of the inhibition of these striatal neurons over GPi/EP and SNr. On the other hand, there is an increase in the indirect pathway signal. The hyperactivity of the basal ganglia output nuclei lead to the hypoactivity of the thalamic–cortical projections (Figure 8).

Decreased activity in the direct pathway produces a decrease in the disinhibition of the thalamus which in turn prevents certain motor and cognitive functions. Simultaneously, the activity change in the indirect pathway increases inhibition on the thalamic neurons, as a result, motor cortex receives decreased glutamatergic input from the thalamus leading to decrease in movement which in turn results increased muscle tonus, rigidity and bradykinesia in PD patients (Zinger et al., 2011).

In line with these facts, in normal conditions dopamine inhibits the release of acetylcholine in striatum and this inhibition could occur at the level of a common postsynaptic target, most likely the medium spiny projection neurons. Indeed, the imbalance between acetylcholine and dopamine could explain the movement disorder occurred in PD. However, it is necessary to take into account that the release of acetylcholine is also affected by other transmitters, such as the fact that the release of acetylcholine is inhibited by GABA and serotonin but stimulated by glutamate (Parent & Hazrati, 1995). Thus, in rat model, depletion of

DA in striatum leads also to an overall decline in sensorimotor functions including a postural imbalance, deficits in forepaw and digit use, and a complete disruption of syntactic grooming (Meredith & Kang, 2006).

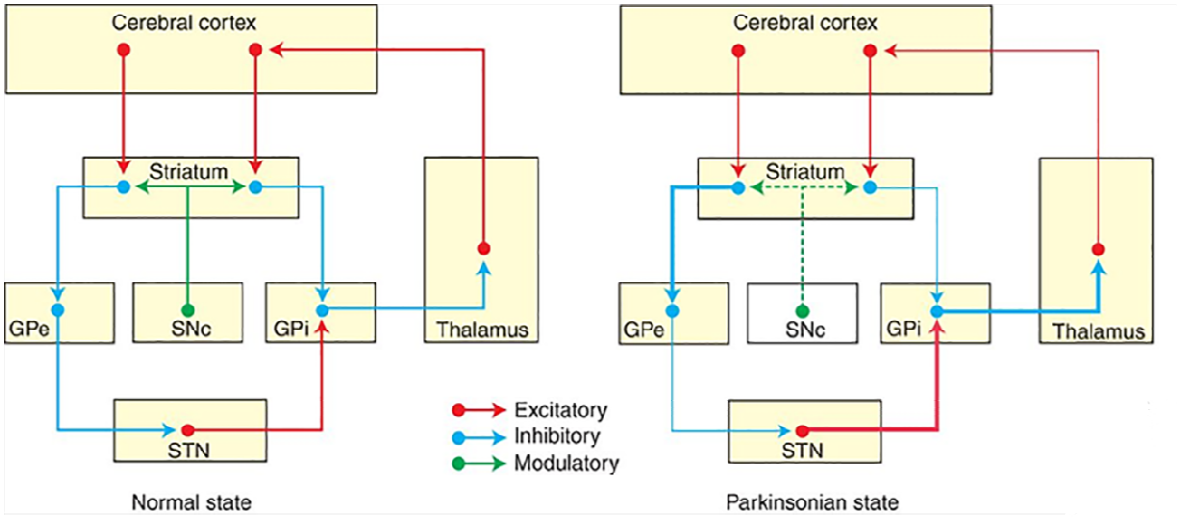

Figure 8. Schematic summary of the basal ganglia motor circuit in normal conditions and in Parkinson's disease (Lanciego et al., 2012). The basal ganglia motor circuit is composed of a corticostriatal projection, consisting of two major striatofugal projection systems which give rise to the direct and indirect pathways, and the efferent pallido–thalamo–cortical projections which close the motor loop. Red arrows indicate excitatory (GABAergic) connections; blue arrows indicate inhibitory (glutamatergic) connections and green arrows indicate modulatory (dopaminergic) connections. The thickness of the arrows represents the functional state of a given circuit. Thicker arrows illustrate hyperactive pathways, whereas thinner ones represent hypoactive circuits.

2.3. Dopaminergic pathways

There are four major dopaminergic pathways in the brain which regulate various central functions and the dysregulation of these dopaminergic systems can lead to impairment in physiological processes, which are observed in neurological pathologies, such as in PD (Loke et al., 2015).

- **Nigrostriatal pathway:** This pathway transmits dopamine from the SNc to the striatum to control voluntary movements (Björklund & Dunnett, 2007; Tsui & Isacson, 2011). In fact, this pathway contains about 75% of the dopamine in the brain and suffers damage in PD. In line with this, it has an important role in the basal ganglia circuit because of belonging to the extrapyramidal motor system.

- **Mesolimbic pathway:** It is formed by dopaminergic projections from ventral tegmental area (VTA) to the limbic system (hypothalamus, hippocampus and amygdala) and this pathway is important for motivation and reward –based learning (Gonzales et al., 2004; Björklund & Dunnett, 2007).

- **Mesocortical pathway:** It is originated from VTA and transmit dopamine to the prefrontal cortex for executive functions such as decision-making, cognitive and social behavior (Robbins, 2000; Björklund & Dunnett, 2007).

- **Tuberoinfundibular pathway.** It is formed by projections from hypothalamus to the pituitary gland. The tuberoinfundibular system is involved in secretion of certain hormones such as prolactin.

2.4. Dopaminergic neurons

Dopaminergic neurons in the mammalian brain are localized in nine major distinctive cell groups (A8-A16) (Figure 9) (Björklund & Dunnett, 2007).

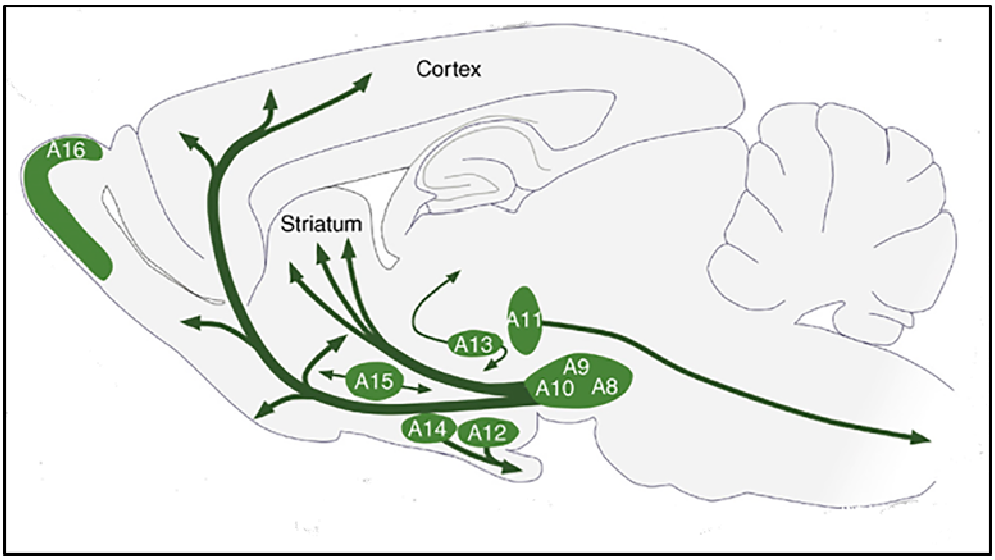

Figure 9. Schematic representation of the distribution of dopaminergic neurons and their projections in a sagittal view of the adult rat brain (Adapted from Björklund & Dunnett, 2007).

Dopaminergic midbrain neurons project widely toward many brain regions (Figure 9), including prominent projections to the frontal cortex and striatum, where through G protein–coupled receptors, dopamine release modulates excitability and synaptic function in target structures. In fact, the midbrain dopaminergic neurons show a complex anatomical organization and projection patterns of the dopaminergic neurons in the A8 (retrorubral area), A9 (SN) and A10 (VTA) cell groups in the mesencephalon (Figure 10). In this context, these neurons can be separated into a dorsal and a ventral tier. The dorsal tier includes cells located in the dorsal aspect of VTA and SN, and the ventral tier comprises a sheet of more densely packed, angular cells located in the ventral parts of VTA and SN (Björklund & Dunnett, 2007). In addition, studies recently showed that some midbrain dopaminergic neurons also release glutamate and GABA, although the behavioral role of co-release is unclear (Stuber et al., 2010; Tritsch et al., 2012).

2.5. Dopaminergic innervation of the basal ganglia: Nigrostriatal projections

The nigrostriatal dopaminergic projections have an essential role in the organization of the basal ganglia; proof of it is that the degeneration of the nigrostriatal pathway leads to a motor deficit and sometimes cognitive decline in PD.

In fact, neuroanatomical studies have indicated that nigrostriatal projections are topographically organized. Dopaminergic projections arise mainly from neurons of the SNc and innervate extensive and heterogeneously in all sub-regions of the striatum (Prensa et al., 1999). Accordingly, neurons from A9, the ventral tier of SN and VTA, innervate the dorsal region of CPC, in contrast to neurons from A10, dorsal part of SN and VTA, that project to ventral striatum and limbic structures and cortical areas (Jungnickel et al., 2011) (Figure 10). Additionally, neurons from A8 nucleus, which form a dorsal and caudal extension of the A9, project to both CPC, limbic structures and cortical areas (Figure 10) (Björklund & Dunnett, 2007). Based on this connectivity, dorsal parts of striatum are involved in motor initiation. In an opposite sense, the ventral, limbic-related part of CPC is implied in complex movements associated to emotions (Jungnickel et al., 2011). Together, there are reciprocal connections to the ventral and dorsal striatum between the mesolimbic and nigrostriatal pathways respectively, which are an integral part of the basal ganglia (Haber et al., 2000).

Some data in monkeys indicate that the rostral two-thirds of the SN are connected with the head of the caudate nucleus, whereas nigral neurons projecting to the putamen are more caudally located, and display a rostro-caudal topography (Smith & Parent, 1986). Although an inverse mediolateral and dorsoventral topography between the SNc and the striatum has also been

proposed in monkeys (Szabo, 1980) led to controversial results regarding the topographic organization of the nigrostriatal projection (Joel & Weiner, 2000).

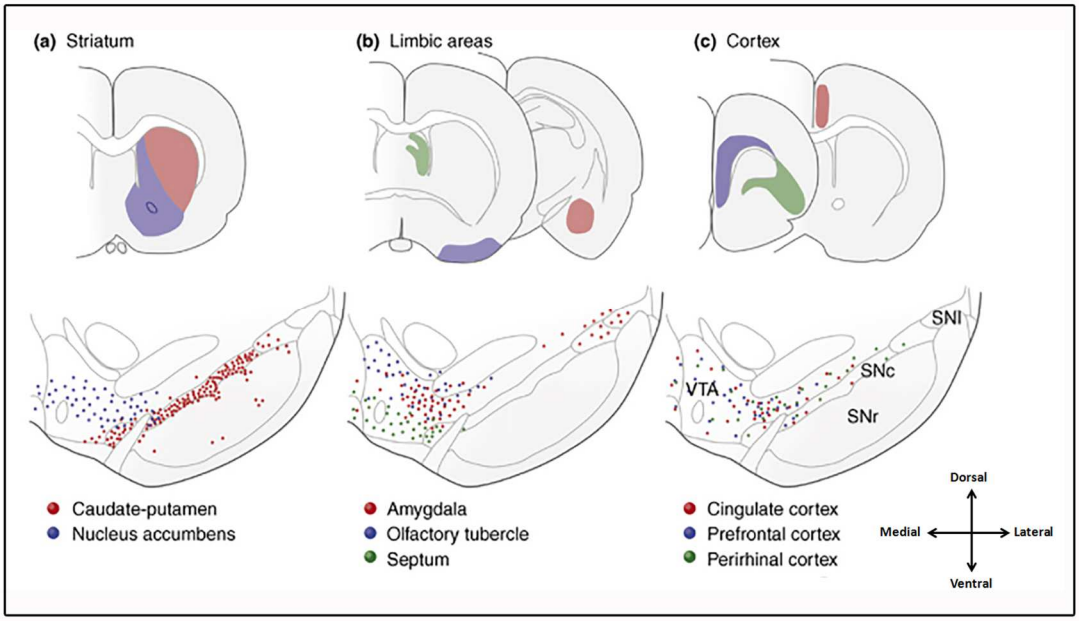

Figure 10. Schematic diagram depict the dopaminergic neurons projections from the mesostriatal, mesolimbic and mesocortical pathways in the rat (Adapted from Björklund and Dunnett, 2007). The dopaminergic neurons in the SN projecting to (**a**) striatal, (**b**) limbic and (**c**) cortical areas are partly intermixed: The cells located in the ventral tier of the SNc [red dots in (**a**)] innervate, probably exclusively, the sensorimotor part of the caudate putamen [red area in the inset in (**a**)], whereas the cells of the dorsal tier comprise neurons that project widely to both limbic and cortical forebrain regions, as illustrated in (**b**) and (**c**), respectively. Abbreviations: SNc, substantia nigra compacta; SNl, substantia nigra lateralis; SNr, substantia nigra reticulata; VTA, ventral tegmental area.

In this context, loss of dopaminergic neurons in SN leads to a denervation of the posterolateral striatum (Franco & Turner, 2012). This happens because nigrostriatal projections are topographically distributed so the oldest neurons, placed on the most lateral SN, project to the posterolateral CPC. Axons of early originated nigral neurons spread via the medial forebrain bundle (MFB) into the ventrolateral part of the CPC (Figure 11) (Bayer, 1984). The chronology of neuronal production is a necessary requisite for the proper anatomical and functional development of the CNS. Accordingly, in the early stage of PD dopaminergic neurons degenerate in the ventrolateral parts of SNc and this degeneration

extends to the other parts of SNc whenever the disease progress (Greffard et al., 2006; Milber et al., 2012).

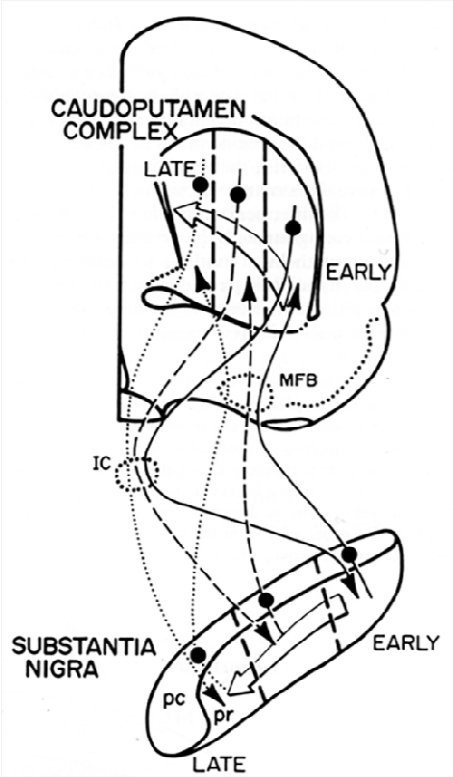

Figure 11. Correlations between neurogenetic gradients and projections of nigrostriatal connections, which are topographical distributed corresponding to older neurons of lateral substantia nigra project to the dorsolateral caudate putamen complex (Bayer, 1984).

3. Experimental animal models of Parkinson's disease

Experimental models of PD are used to reproduce behavioral changes of the human disease in rodents or primates and they are based on the systemic or intracerebral administration of neurotoxins capable of inducing selective degeneration of the nigrostriatal system (Blandini et al,. 2008) (Figure 12). However, the results obtained in animal models have been variable and some of them were contradictory (Israel & Bergman, 2008; Wichmann & DeLong, 2003). On the other hand, the 6-OHDA model has resulted to be the most extensively used model in rats for reproducing the loss of dopaminergic neurons in the SNc occurred in PD (Blandini et al., 2008).

3.1. Neurotoxic models

3.1.1. 6-Hydroxydopamine

6-OHDA model was the first neurotoxin induced animal model of PD causing neurodegeneration of dopaminergic neurons in SNc (Dauer & Przedborski, 2003). It was introduced more than 30 years ago (Ungerstedt, 1968).

Once 6-OHDA enters the neuron, it accumulates in the cytosol and being oxidized leads to increased ROS and quinines production which, in turn, through oxidative stress mechanisms, inactivate biological macromolecules, reduce antioxidant enzyme levels in striatum and increase iron levels in SN (Dauer & Przedborski, 2003; Duty & Jenner, 2011; Tieu, 2011). This elevated iron interacts with the Complex-I and Complex-IV of mitochondria and leads to an inhibition of the respiratory chain and further oxidative stress. These mechanisms of 6-OHDA toxicity are considered as the pathological events of human PD; therefore, it makes the model applicable.

The intracerebral injection of 6-OHDA is still the most frequently used tool for obtaining a controlled nigrostriatal lesion in the animal, due to the relatively low complexity and cost of the procedure (Blandini et al., 2008). The injection is commonly carried out unilaterally, with the contralateral hemisphere serving as control. Bilateral injections are generally avoided, due to the high mortality rate associated with this procedure (Blandini et al., 2008).

This toxin cannot cross the blood brain barrier, because of this it is injected into the SNc, the MFB and the CPC in order to induce a selective differential damage of the nigrostriatal dopaminergic pathway (Deumens et al., 2002). Thus, versatility is another important characteristic of the 6-OHDA model because of depending on the injection site, a complete and immediate or a partial and progressive damage of the SNc can be induced (Blandini et al., 2008). Thus, the site of 6-OHDA administration is critical at determining the extent of the lesion generated and the time course of lesion development:

- **Intrastriatal injection**: Intrastriatal 6-OHDA administration induces a progressive, retrograde degeneration of the nigrostriatal pathway and tends to form a more progressive partial lesion (about 60-80% loss of dopamine in CPC). In fact, a discrete lesion in the ventrolateral CPC would be preferable because this part is thought of as equivalent to the putamen in humans. Thus, it is a good model to study the pathophysiological features in the first stage of development of PD, as well as the effects and neuropathological changes of new therapeutic strategies.

- **Injection into SNc or MFB:** The administration of 6-OHDA into MFB or SNc causes an anterograde degeneration of the nigrostriatal dopaminergic system and trend to form a severe or complete model. Thus, this model allows us to study the advanced stages of PD. The 6-OHDA unilateral lesion in MFB is almost complete eliminating the most of dopaminergic neurons in the ipsilateral SN and resulting in near total depletion of DA in the

ipsilateral striatum. It also results in a denervation supersensitivity of the post-synaptic striatal DA receptors, and a characteristic turning behavior in response to both amphetamine and apomorphine (Ungerstedt, 1968; Dauer & Przedborski, 2003). However, 6-OHDA injections via the MFB may cause additional destruction of the A10 dopaminergic neurons in the VTA, which can complicate experimental analysis (Deumens, 2002). Thus, when compared to MFB lesions (about 97% loss of tyrosine hydroxylase (TH)-immunoreactivity in the SNc), the TH-staining loss in the SNc (about 90% loss of TH-immunoreactivity in the SNc) is somewhat less extensive after SNc lesioning (Deumens et al., 2002).

On the other hand, not only the location of toxin injection, but also the number of injection sites and the concentration of the neurotoxin, it Is important for the model (Kirik et al., 2000). Also, the injection volume is important because of differences in diffusion of the neurotoxin from the injection site to the surrounding brain tissue (Deumens et al., 2002).

A major advantage of the 6-OHDA model is a quantifiable motor deficit (rotation) and its usefulness in the pharmacological screening of agents that have effects on DA and its receptors (Ungerstedt, 1971; Deumens et al., 2002). Typically, two drugs are used for induction of the rotational behaviour in unilaterally lesioned animals: amphetamine and apomorphine. Amphetamine acts as an agonist of dopamine inducing the fast and almost complete release of the neuromediator/neuromodulator dopamine from the presynaptic terminals (Sulzer et al., 2005). Apomorphine, a short-acting dopamine D1 and D2 receptor agonist, functions postsynaptically (Picada et al., 2005).

Nevertheless, It is necessary to take into account that compensatory modulations in dopamine signaling may occur in SN and striatum owing to the existence of basal levels of extracellular DA in SN, which are not affected by 6-OHDA lesion (Sarre et al., 2004).

In addition, although 6-OHDA does not produce or induce proteinaceous aggregates or Lewy-like inclusions like those seen in PD, it has been reported that 6-OHDA does interact with α-synuclein (Blesa et al., 2012).

3.1.2. MPTP

MPTP is a good toxin-based animal model of PD for replicating almost all of these hallmarks except Lewy bodies formation (Halliday et al., 2009). This toxin is highly lipophilic and after systemic administration rapidly crosses the BBB.

It is called protoxin because MPTP needs to be metabolized into 1-methyl-4-phenylpyridinium (MPP+) by the enzyme monoamine oxidase-B (MAO-B) to reveal a toxic effect (Emborg, 2004; Tieu, 2011). This conversion takes place in the astrocytes of SN and striatum and the MPP+ product is taken up by the dopaminergic neurons and terminals in these regions through DA transporter system (Tieu, 2011). Once in the cytoplasm of the neuron, MPP+ leads to ROS production. However, its main toxic effect is based on the accumulation within the mitochondria and inhibiting Complex I of the electron transport chain which causes deficiency in mitochondrial respiration.

Currently, the MPTP model is used in mice and monkeys. Aside from the obvious financial benefits, the mouse model is employed to test theories about cell death in PD, to work out events in the neuronal death process, and to study other pathological effects of PD (Blesa et al., 2012). On the other hand, the MPTP monkey model is mainly used to discern behavioral and symptomatic components of PD, as mice do not develop a level of impairment equal to the human condition. Monkeys also represent the last level of PD treatment research prior to any treatment being administered to humans (Bezard & Przedborski, 2011). However, the data generated by mouse models has led to a better understanding of molecular mechanisms involved in PD, and its utility has proven invaluable. One of the most important aspects of the MPTP mouse model is the possibility to work

with genetically modified mice (Vila et al., 2001; Dauer et al., 2002). In addition, this model can be useful for testing neuroprotective therapies.

3.1.3. Paraquat

Paraquat (N,N_-dimethyl-4-4-4_-bypiridinium) (PQ) is a herbicide widely used in agriculture that exhibits a structural resemblance to MPP+, and, because of this structural similarity, PQ behave like MPTP in exhibiting toxic effects. PQ exerts its deleterious effects through oxidative stress mediated by redox cycling, which generates ROS (Blesa et al.,2012). Recent evidence on the effects of PQ in the nigrostriatal DA system is somewhat ambiguous. Some researchers claim that PQ application in mice exhibit reduced motor activity and a dose-dependent loss of striatal TH-positive striatal fibers and midbrain SNc neurons(Brooks et al., 1999; McCormack et al., 2002), while other affirm that PQ do not display any effect in the nigrostriatal DA system (Thiffault et al., 2000; Thiruchelvam et al., 2000). However, a recent study showed that PQ, in high doses, employs the organic cationic transporter-3 (OCT-3) and the dopamine transporter (DAT) and is toxic to the dopaminergic neurons in the SN (Rappold et al., 2011).

However, the importance of PQ to PD is its ability to induce increases in α-synuclein in individual dopaminergic neurons in the SNc and its ability to induce LB-like structures in dopaminergic neurons of the SNc (Manning-Bog et al., 2002). Thus, the relation of dopaminergic neuron loss with α-synuclein upregulation and aggregation suggests that this model could be valuable for capturing a PD-like pathology.

3.1.4. Rotenone

Rotenone is an herbicide and an insecticide. It is the most potent member of the rotenoid family of neurotoxins found in tropical plants. Rotenone is highly lipophilic and readily crosses the BBB. Chronic exposure to low doses of rotenone

results in inhibition of the mitochondrial electron transport chain in the rat brain. In animals, rotenone has been administered by different routes. Remarkably, intravenous administration is able to cause damage to nigrostriatal DA neurons that is accompanied by α-synuclein aggregation, Lewy-like body formation, oxidative stress, and gastrointestinal problems (Cannon et al., 2009). The most peculiar of this model is that, like paraquat, it seems to replicate almost all of the hallmarks of PD including causing α-synuclein aggregation and Lewy-like body formation (Höglinger et al., 2003; Sherer et al., 2003). Interestingly, a subsequent study has found that rotenone is not specific to the dopaminergic system and has deleterious effects on other neuronal populations. However, there are no documented cases of rotenone induced PD in humans. Thus, it is not clear that this model offers any advantage over other toxic models, such as that of 6-OHDA or MPTP (Blesa et al., 2012).

3.2. Genetic models

The underlying principle for studying genetic mutations of a disease is the belief that the clinical similarities between the inherited and sporadic forms of the disease share a common mechanism that can lead to the identification of molecular and biochemical pathways involved in the disease pathogenesis (Blesa et al., 2012). Animal models of genetic mutations involved in PD (α-synuclein and LRRK2, autosomal dominant PD) and (PINK1/Parkin and DJ-1, autosomal recessive PD) are important as they represent potential therapeutic targets. Overall, these genetic models are able to recapitulate specific aspects of PD.

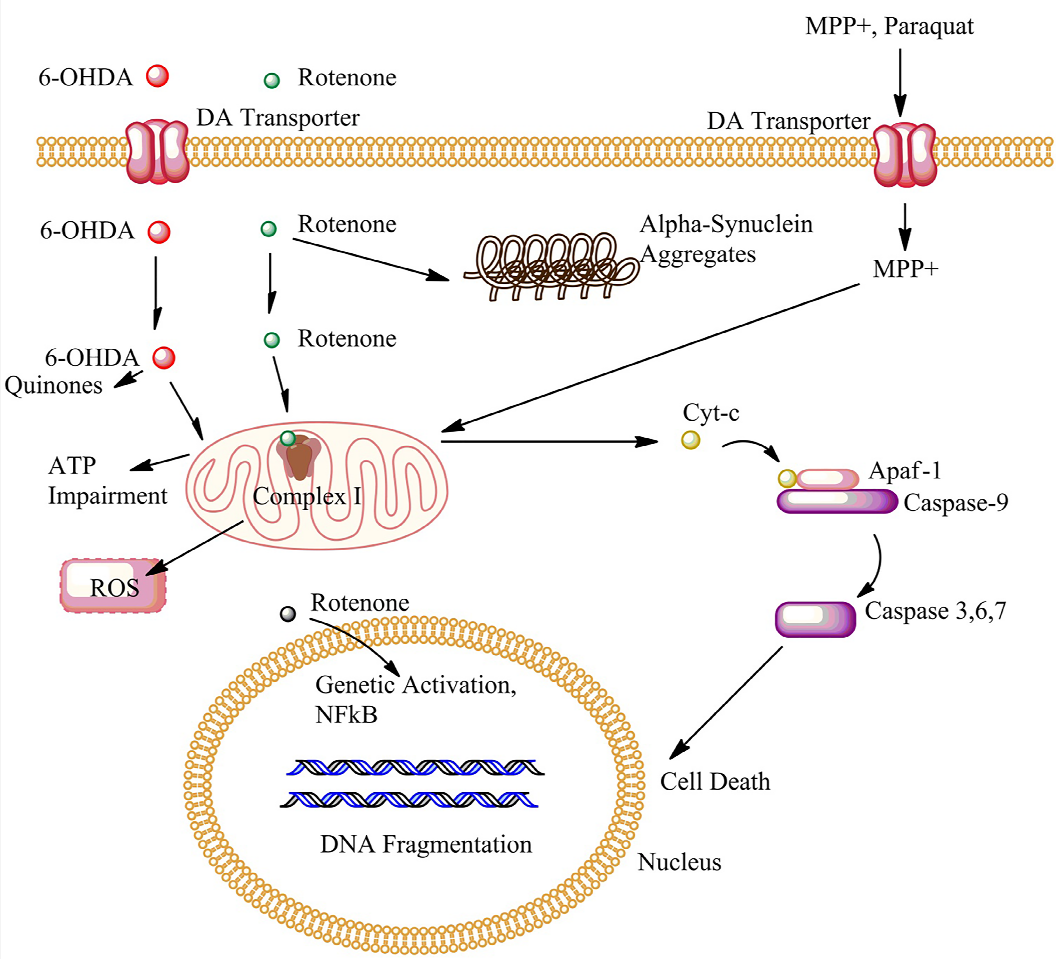

Figure 12. Schematic representation of different action mechanisms for each experimental model of Parkinson's disease (Ricardo Cabezas, 2013).

4. Neurotrophic factors and Parkinson's disease

Neurotrophic factors are a subset of growth factors that play a fundamental role in the regulation of neuronal function, plasticity, development and survival in the developing and adult nervous systems (Yasuda & Mochizuki, 2010).

They are cleaved intracellularly by various enzymes that give rise to the mature protein that are released into the extracellular medium (Lee et al., 2001). Each of these proteins in their mature form (with an approximate molecular weight of 13 kDa) is a protein complex with a mate (dimer), thereby activating specific receptors (Chao, 2003).

In fact, NTFs exert their function mainly mediated by the family of receptor tyrosine kinases (RTKs) (Huang & Reichardt, 2003) and every NTF binds specifically with high affinity to different RTKs (Kaplan & Miller, 2000).

They display effects in proliferation, differentiation, and survival of neurons both during development and in adulthood (Lewin & Barde, 1996). However, their role in regulating synaptic plasticity and in the guidance of axon growth cones has been described (Kaplan & Miller, 2000; Lu et al., 2005; Lafuente et al., 2014), but functions of NTFs and their receptors on non-neuronal cells such as endothelial cells, smooth muscle cells, immune cells and epithelial cells have also been described (Lafuente et al., 2014).

Thus, several neurotrophic and growth factors have been shown to protect dopaminergic neurons and glial cells against induced excitotoxicity by the activation of specific signaling pathways that are responsible for cell survival and axonal sprouting (Ramaswamy & Kordower, 2009; Yasuda & Mochizuki, 2010). Some of them have also been tested in PD clinical trials with some promising results (Ramaswamy & Kordower, 2009; Yasuda & Mochizuki, 2010).

For example, brain derived neurotrophic factor (BDNF) and TNF protect neurons against excitotoxicity through the activation of the transcription factor NF-kB, which induces the expression of antioxidant enzymes such as Mn-SOD and the anti-apoptotic proteins, Bcl-2 and inhibitor of apoptosis proteins IAPs (Mattson, 2008; Lee et al., 2012)). In fact, the endogenous administration of BDNF was shown to protect neurons within the SN from 6-OHDA and MPTP toxicity, both in rat and primate PD models (Ramaswamy & Kordower, 2009).

The family of GDNF includes ligands such as GDNF, neurturin (NRTN), artemin (ARTN) and persephin secreted by astrocytes, it is essential for the survival of dopaminergic neurons (Yasuda & Mochizuki, 2010).

Vascular endothelial growth factor (VEGF) affects to the survival and proliferation of endothelial cells, neurons and astrocytes in the brain, suggesting a potential therapeutic application in PD (Yasuda & Mochizuki, 2010).

Insulin-like growth factors (IGFs) signaling through the phosphatidylinositol 3-kinase (PI3K/Akt) downstream pathway can protect neurons against LPS excitotoxicity in cell culture and *in vivo* (Mattson, 2008; Pang et al., 2010). Furthermore, the activation of this signaling pathway by IGFI can suppress α-synuclein aggregation and toxicity, suggesting a possible therapeutically strategy in PD (Kao, 2009).

Basic fibroblast growth factor (bFGF) protects hippocampal and cortical neurons against glutamate toxicity by changing the expression of *N*-methyl-D-aspartic acid (NMDA) receptors and antioxidant enzymes like superoxide dismutases and glutathione reductase (Mattson, 2008). Furthermore, a co-culture of transgenic overexpressing FGF-2 Schwann cells with dopaminergic neurons improved the survival of dopaminergic neurons and the behavioral outcome in a parkinsonian rat model lesioned with 6-OHDA (Timmer et al., 2004).

There are other NTFs that have shown dopaminergic neuronal protection in Parkinson-like models, including hepatocyte growth factor (HGF), mesencephalic astrocyte-derived neurotrophic factor (MANF), cerebral dopaminergic neurotrophic factor (CDNF), granulocyte colony stimulating factor (G-CSF), and platelet derived growth factor (PDGF-CC) (Ramaswamy & Kordower, 2009; Tang et al., 2010; Yasuda & Mochizuki, 2010; Sullivan & Toulouse, 2011).

Moreover, it is fundamental to take into account that the effects obtained after the injection of NTFs depend on the time, site of administration and the type of lesion used (Kirik et al., 2000).

However, among the NTFs proposed as strategic therapy against PD we have focused our attention on VEGF and GDNF.

4.1. Vacular endothelial growth factor

Vascular endothelial growth factor **(VEGF)** is an endothelial specific growth factor predominantly involved in the formation of new blood vessels (Ferrara and Davis-Smyth, 1997). In addition to its important role in angiogenesis, VEGF also has specific roles in the CNS, stimulating axonal, outgrowth and increasing neuronal survival (Carmeliet & Storkebaum, 2002). VEGF is an important mediator of cell survival, proliferation and angiogenesis (Ferrara, 2009; Shibuya, 2011; Musumeci et al., 2012). It constitutes a family of mammalian homodimeric glycoproteins, comprising VEGF-A, VEGF-B, VEGF-C and VEGF-D and placenta growth factor. VEGF-A is an important and potent mediator of tumour-induced angiogenesis (Ferrara, 2004, 2009). VEGF family members bind to three different VEGF receptors (VEGFR1, VEGFR2 and VEGFR3) with differing selectivity profiles (Ferrara, 2009; Shibuya, 2011).

VEGFR2 is the major regulator of VEGF-driven responses in vascular endothelial cells including permeability, proliferation, invasion and migration. It is

also considered to be a crucial mediator of angiogenesis (Ferrara, 2009; Shibuya, 2011). Its signalling pathways are relatively well understood with tyrosine residues Y1175 and Y1214 in the human VEGFR2 being the main auto-phosphorylation sites activated by VEGF binding and tyrosine kinase (TK) activation. In fact, the neuroprotective role for VEGF which is predominantly mediated via VEGFR-2 has also been described (Storkebaum et al., 2004; Lafuente et al., 2006), which operates via the PI3/Akt and the MEK/ERK pathways (Wick et al., 2002; Kaya et al., 2005).

Multiple studies have argued the potential of VEGF to promote the growth, survival and rescue of dopaminergic neurons *in vitro* (Pitzer et al., 2003; Silverman et al, 1999). It may also protect against 6-OHDA-induced cell death in both a PD rat model and neuronal cultures (Yasuhara et al., 2004).

4.2. Glial cell line-derived neurotrophic factor

Glial cell line-derived neurotrophic factor **(GDNF)** is a NTF that protects catecholaminergic neurons from toxic damage and induces fiber outgrowth (Pascual et al., 2008). This NTF develops an important role in the nigrostriatal system. Thus, removal of GDNF in the adult brain led to more pronounced degeneration (Pascual et al., 2008).

GDNF and three others NTFs form a family of proteins called as GDNF family ligands (GFLs), which includes to neurturin, artemin and persephin. GDNF signals through a receptor complex consisting of a binding component (GFRα1) and a signaling tyrosine kinase, the proto-oncogene RET (Airaksinen & Saarma, 2002). In fact, endogenous RET expression is required for long-term survival of a fraction of nigral dopamine neurons in aged mice (Kramer et al., 2007).Thus, the main signalling pathway of GFLs is mediated by RET-RTK (Sariola & Saarma, 2003).

RET is activated upon binding of GDNF dimer to GFRα1 receptors linked to the plasma membrane via a glycosyl phosphatidylinositol anchor (Airaksinen & Saarma, 2002). Dimerization of RET triggers its autophosphorylation, thus, initiating various intracellular signalling cascades, that regulate cell survival, proliferation, differentiation, neurite outgrowth, synaptic plasticity and morphogenesis (Airaksinen & Saarma, 2002). For example, it has been extensively characterized and is known to activate a number of downstream signaling pathways including Ras/ERK, phosphoinositol-3 kinase (PI3K)/Akt, phospholipase C-gamma (PLCγ), Janus kinase (JAK)/STAT, and ERK5, several of which have pro-survival effects, most notably the PI3K/Akt pathway (Sariola & Saarma, 2003; Pascual et al., 2011).

RET function was found to be important for striatal dopaminergic fiber maintenance, while its role in cell body survival was relatively moderate (Aron et al., 2010).

Thus, GDNF is a potent neuroprotective/neurorestorative factor that has shown effects on dopamine-depleted striatum both *in vitro* (Jakobsen et al., 2005; Zeng et al., 2006; Grandoso et al., 2007) and in experimental animal models of PD (Shingo et al., 2002; Lindvall & Wahlberg, 2008). GDNF has also been shown to induce resprouting of the lesioned nigrostriatal neuron system and thus may have beneficial effects on deafferentiated neurons (Björklund et al., 1997; Love et al., 2005). Fuelled by the encouraging results obtained in animal models, several clinical trials have been carried out to investigate the effectiveness of GDNF in PD patients. Nutt and collaborators administered GDNF intracerebroventricularly but found no significant clinical improvement, and several negative effects were reported (Nutt et al., 2003; Slevin et al., 2007). In addition, a clinical trial conducted by Lang's group was halted after showing no benefit from intraputaminal administration (Lang et al., 2006). The major limiting factor in the above-mentioned trials was suggested to be the suboptimal brain delivery of

GDNF. Thus, new therapeutic approaches need (Piltonen et al., 2011) to be explored to help overcome this limitation.

5. Enriched environment

The study of experience-induced modification of brain morphology has been performed by conducting studies in a laboratory setting where environmental conditions can be modified by enriched environment (EE) in normal and pathological conditions (Markham & Greenough, 2004). From the first studies on environmental modifications, experiments have been performed in the two opposite directions, enrichment and deprivation.

The first approaches to the effects of environment on development can be traced back to the 19th century with Lamarck or Darwin (Lamarck, 1808; Darwin, 1859). The latter reported that rodents raised in nature had bigger brains that caged domestic ones. At the end of the century, both Cajal and Sherrington advanced the effects of learning on synaptic plasticity (Ramón y Cajal, 1894; Foster, 1897).

Although the origin of the studies about effects of EE can be traced back to centuries ago, the first systematic studies can be attributed to Donald Hebb in 1947, when he described how rats taken into his home and cared for as pets performed better on problem solving tests than rats raised in cages (Hebb, 1947). His group of disciples at Berkeley, Rosenzweig, Krech, Bennet and Diamond, defined the concept of environmental enrichment as the combination of complex inanimate and social stimulation (Rosenzweig et al., 1978).

From their first studies, the EE has been constantly implemented with cages bigger than standard ones, full of toys of different colours and shapes, tunnels, material to construct the nest and a shelter, as it has been recently described as compulsory. These objects have been changed (the best schedule has been established as once every two days) and the placement of food has also been changed on a regular basis. Another element that has a substantial influence is social interaction, since wider cages allow rearing a greater number of animals that

interchange social stimulation. Another element of EE is physical exercise, forced or voluntary, that in rodents is commonly implemented by free access to an exercise wheel or by a treadmill (van Praag et al., 2000; Will et al., 2004). Some authors doubt whether physical exercise should be included. However, as physical exercise by itself induces brain changes, most EE paradigms, starting from Hebb, have decided to include it. Recently it has also been reported that physical exercise is required to recover, by EE, from the effects of visual deprivation (Argandoña et al., 2009). In contrast, the role of physical exercise has been depreciated in cognitive models (Pietropaolo et al., 2006).

Rearing in enriched environments induces effects from cellular, molecular or genetic levels up to behavioral ones. Most of the changes at cellular level are in concordance with changes in the expression of genes involved in synaptic function and cell plasticity. Accordingly, the increase in neuronal activity induced by environmental stimuli triggers a series of important events for cortical plasticity, including an increase of the vascular network or an acceleration of visual system development at behavioral, electrophysiological and molecular levels (Cancedda et al., 2004; Sale et al., 2004).

Nevertheless, the effects of rearing in complex environments are not only restricted to neurons. Early studies reported that astrocytic morphology changed due to exposure to enriched environments (Diamond et al., 1964; Szeligo & Leblond, 1977) and later studies showed increased size and density of astrocytes (Sirevaag & Greenough, 1987, 1991). EE also increases vascular density (Black et al., 1987, 1991; Sirevaag et al., 1988; Bengoetxea et al., 2008) and oligodendroglial density (Sirevaag & Greenough, 1987).

Although most morphological studies have been carried out in the visual cortex, (DIAMOND *et al.*, 1964; Diamond *et al.*, 1966; Volkmar & Greenough, 1972), other sensory and non-sensory areas have revealed morphological responses to enriched stimuli, such as the auditory cortex (Greenough et al., 1973),

the somatosensory cortex (Coq & Xerri, 1998), the hippocampus (Rampon et al., 2000), the amygdala (Nikolaev et al., 2002), the basal ganglia (Comery et al., 1995, 1996) and the cerebellar cortex (Greenough et al., 1986).

Thus, EE increases sensory, cognitive and motor stimulation and promotes activation, signaling and neuronal plasticity in all brain areas (Figure 13). An increase in somatosensory or visual stimulus primarily affects these areas, just as an increase of cognitive stimulation affects the hippocampus and motor stimulation affects the motor cortex, striatum or cerebellum. Nevertheless, effects are not so selective, as enrichment produces global effects all over the brain (Nithianantharajah & Hannan, 2006, 2009).

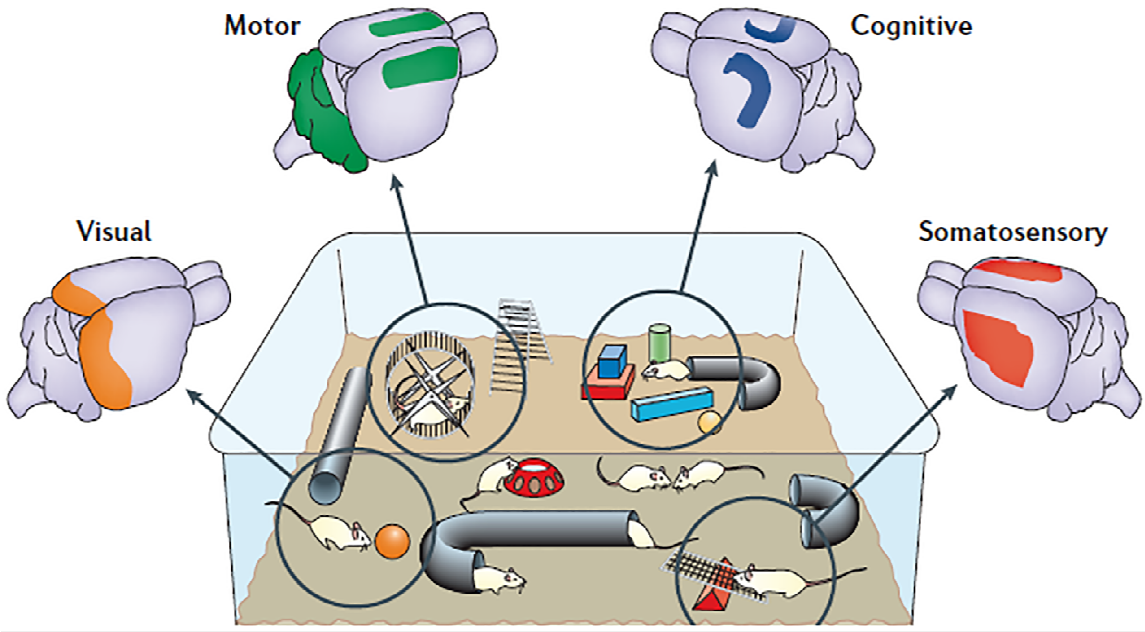

Figure 13. Schematic illustration shows the effects of an enriched environment on different brain areas due to sensorial, cognitive and motor stimulation (Nithianantharajah & Hannan, 2006).

It has been also demonstrated that EE increases the expression of several growth factors, that play an important role in neuronal trophism: nerve growth factor (NGF) (Pham et al., 2002), brain-derived neurotrophic factor (BDNF) (Sale et al., 2004; Franklin et al., 2006), neurotrophin-3 (NT-3) (Ickes et al., 2000), VEGF

that plays a key role in neuronal signaling (Bengoetxea et al., 2008) and although levels of GDNF protein decrease markedly after development, there is evidence that GDNF can increase after EE (Young et al., 1999). At the same time, it increases the expression of synapse proteins and induces changes in the expression of the subunits of the NMDA and AMPA receptors (Naka et al., 2005).

Additionally, the complexity of an animal's environment has been shown to affect not only brain structure and function, but also neurogenesis (van Praag et al., 2000). In line with this, EE is widely proposed as a neuroprotective solution in neurodegenerative diseases (Will et al., 2004; Nithianantharajah & Hannan, 2006; Laviola et al., 2008).

In particular, rat studies showed that a stimulating environment, such as EE, promote neuronal plasticity and glial cell proliferation (Pham et al., 2002; Bezard et al., 2003). The enhanced structural plasticity is accompanied by improvement in motor function, including skilled walking and climbing (Ohlsson & Johansson, 1995; Johansson & Ohlsson, 1996; Risedal *et al.*, 2002) and skilled reaching (Biernaskie & Corbett, 2001).

Recent studies have outlined the importance of the duration of environmental enrichment, as this is relevant to the persistence of its effects on behavior (Amaral et al., 2008).

Due to the beneficial effects of EE on brain development, it is not surprising that it has been postulated as a therapeutic, or at least neuroprotective strategy for most brain diseases, as has been reviewed by Will (2004) and Nithianantharajah (2006) (Will et al., 2004; Nithianantharajah & Hannan, 2006). The concept of Cognitive Brain Reserve postulated by Nithianantharajah and Hannah offers a comprehensive framework for all neurorestorative strategies aimed at CNS diseases (Nithianantharajah & Hannan, 2006).

In studies performed on neurodegenerative diseases, EE has proven a useful tool to prevent the cognitive impairment induced not only by normal aging but also by PD. However, improvements by EE are not only linked to neurodegenerative diseases. In stroke models, stroke motor sequelae are diminished by environmental enrichment (Saucier et al., 2010). EE also enhances transplanted subventricular zone (SVZ) stem cell migration and functional recovery (Hicks et al., 2007), diminishes ischemia-induced amyloidogenesis and enhances functional recovery after stroke (Briones et al., 2009). Finally, EE even has beneficial effects in tumours. It has been recently reported that mice living in an enriched housing environment show reduced tumour growth and increased remission via the BDNF/leptin axis (Cao et al., 2010).

In addition, clinically, physical activity and the experience of novelty have been shown to improve motor and cognitive functions in patients suffering from neurodegenerative disorders in general and PD patients in particular (BILOWIT, 1956; KNOTT, 1957; Hirsch, 2000; Toole et al., 2000).

5.1. Enriched environment and Parkinson's disease

The incidence of PD might be influenced by lifestyle (Olanow & Tatton, 1999; Elbaz & Moisan, 2008) and physical exercise (Chen et al., 2005). Thus, it can be hypothesized that the pathological processes of PD might also be modulated by EE (Jadavji et al., 2006).

Housing in a complex environment with many cage mates and regularly circulated toys, has been reported to be both neuroprotective (Bezard et al., 2003; Faherty et al., 2005) and neurorestorative (Steiner et al., 2006; Goldberg et al., 2012) in models of PD. In healthy animals, an EE can lead to increased growth factor expression in the nigrostriatal pathway (Cohen et al., 2003; Li & Tang, 2005) and hippocampus (Gómez-Pinilla et al., 1997). However, there have also been controversial reports that an EE can stimulate neurogenesis or neural migration

from the SVZ to the SN (Lie et al., 2002; Van Kampen & Robertson, 2005; Shan et al., 2006; Steiner et al., 2006).

Thus, although the mechanism of EE induces neuroprotection and neurorestoration in PD is unknown; numerous data suggest that synthesis and release of NTFs may play a crucial role (Nithianantharajah & Hannan, 2006). EE alters the expression of NTFs and their receptors in several brain areas (Pham et al., 1999; Ickes et al., 2000; van Praag et al., 2000; Gobbo & O'Mara, 2004; Spires et al., 2004) and induces astrogliogenesis (Steiner et al., 2006). In the nigrostriatal system, EE-housed animals show increased BDNF expression in the striatum (Bezard et al., 2003; Turner et al., 2003) and GDNF mRNA in the SN (Faherty et al., 2005).

Abundant experimental evidence shows that EE is beneficial in animal models of PD and studies have shown that EE with physical activity are robust inducers of neuro- and gliogenesis in the adult dental gyrus (Steiner et al., 2006). EE increases resistance to the neurotoxic effect of the Parkinson-inducing drug MPTP and induces a variety of changes in the expression of genes in the striatum against MPTP toxicity to mice (Bezard et al., 2003; Faherty et al., 2005). This is compatible with the dramatic morphological changes induced by EE in the striatum (Bezard et al., 2003; Thiriet et al., 2008). EE also improves motor function after unilateral 6-OHDA injection in rats (Jadavji et al., 2006).

Therefore, these findings suggest that EE might exert neuroprotective and neurorestorative effects on dopaminergic neurons and preserve motor function in rats with dopamine depletion.

6. Tyrosine kinase inhibitors

Tyrosine kinase inhibitors (TKIs) are small organic compounds that affect tyrosine kinase-dependent oncogenic pathways by competing with ATP-binding sites of the tyrosine kinase catalytic domains (Lorusso & Eder, 2008).

Occupation of these sites inhibits autophosphorylation and activation of the tyrosine kinases and prevents the further activation of intracellular signaling pathways. Remarkably, TKIs can be specific to one or several homologous tyrosine kinases.

Because the alterations of protein kinases and their pathways are involved in cancer development, several RTK inhibitors have been tested *in vitro*, preclinical, and clinical studies (Giunti et al., 2013). In this context, several mechanisms have been shown to be involved in the activation of PI3K signaling in medullary thyroid cancer (MTC). In fact, the PI3K/AKT/mTOR pathway was shown to be activated in MTC. Thus, due to increased knowledge of the molecular pathogenesis of MTC, therapeutic agents that target specific altered pathways have been developed. In fact, several multitargeting tyrosine kinase inhibitors, such as vandetanib, that block VEGFR2 and RET, have been performed, but there is not currently available TKI to RET or to VEGFR2. Additionally, it seems that a modest significant association has been observed between VEGFR2 expression and RET mutation status in primary tumors (Rodríguez-Antona et al., 2010). In fact, because of there is considerable cross talk between growth factor pathways, dual inhibition with such agents has become an attractive strategy, in many cancer therapies (Deshpande et al., 2011).

6.1. Vandetanib

Vandetanib (ZD6474), is a reversible orally bioavailable TK-inhibitor, that targets RET, VEGFR2, and VEGFR3, and at higher concentrations to EGFR also (Knight *et al.*, 2010). In fact, as illustrated in figure 14, vandetanib competes with ATP binding in the catalytic domain of several tyrosine kinases, such as VEGFR2 and RET, inhibiting the autophosphorylation. Thus, vandetanib selectively inhibits pathways that are critical for tumor growth and angiogenesis without leading to direct cytotoxic effect on tumor or endothelial cells (Herbst et al., 2007).

It was selected through a subset of compounds after showing the Inhibition of tyrosine kinase activity of the VEGFR-2 receptor *in vitro*. Thus, combining the results *in vitro* with good oral bioavailability and sustained drug levels *in vivo* in plasma, it allows the oral therapy support (Hennequin et al., 2002).

As therapeutic strategy this drug is mainly administered in patients with advanced or metastatic MTC. However, in neurodegenerative disorders vandetanib could not be considered a therapeutical option, but it has been used for elucidating the role of NTF over the signaling pathways.

However, there is no study about the effects of vandetanib in neurodegenerative disorders. Despite vandetanib administration in neurodegenerative disorders could not be considered as a therapeutical strategy, the administration of this drug could use for elucidating the role of NTFs over the signaling pathways.

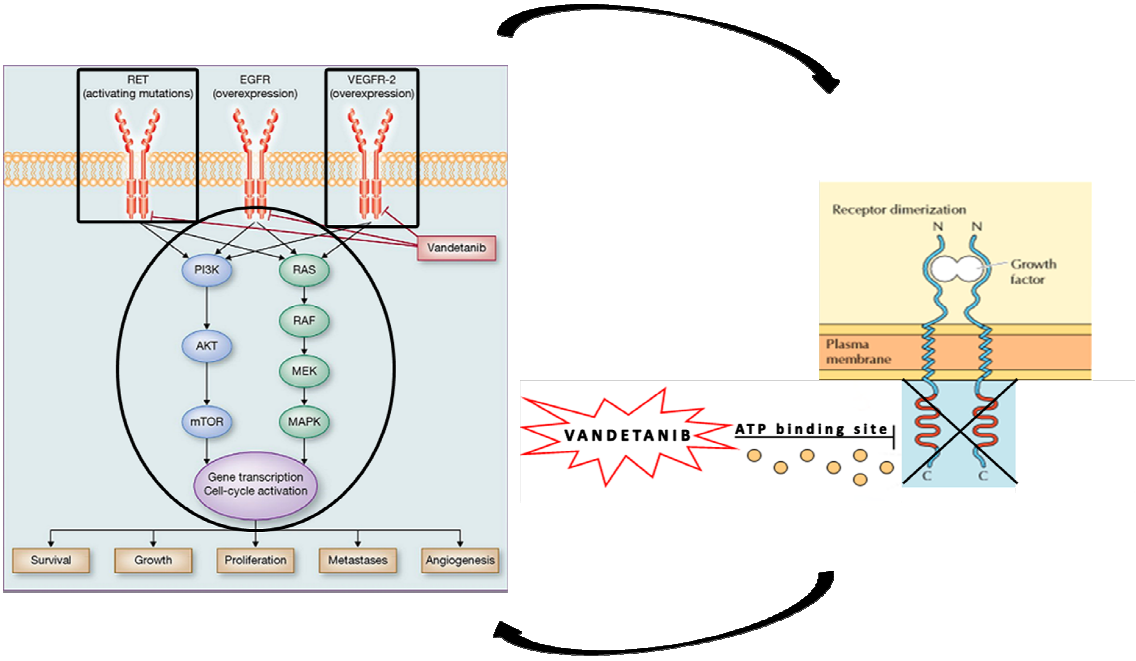

Figure 14. Mechanism of action of vandetanib via VEGFR2 and RET.

II. HYPOTHESIS

Numerous works have been proposed for the study of the neuronal degeneration in PD using different animal's models, although none of them have been exact to understand the pathogenesis of PD. Therefore, the mechanism by which TH activity may be enhanced or how it may affect DA tissue content in either striatum or SN in a progressive PD animal model is unknown. In spite of these considerations, the 6-OHDA-induced model has resulted to be the most extensively used model in rats for reproducing the loss of dopaminergic neurons in the SNc occurred in PD. Additionally, the topological distribution of changes in the dopaminergic system is a factor to take into account to describe the morphological changes occurred in a PD model.

Thus, current therapies presently available for PD are not effective in the long-term and cannot repair the already damaged area. That is why, current research efforts are being focused in new neuroprotective and neuroregenerative strategies that will halt the neurodegenerative process. An interesting approach to raise this challenge is the use of NTFs such as GDNF and VEGF. These proteins play critical roles in the genesis, maturation, survival and protection of developing neurons. However, the critical problems for the clinical application of NTFs are their rapid degradation rate and their difficulty in crossing the BBB. Thus, an alternative to get a continuous drug delivery over time and to allow for the simultaneous administration of different trophic factors is the encapsulation of the NTFs in poly(lactic-co-glycolic acid) (PLGA) compound. Taken together these data, we hypothesize that the characterization of the specific morphological characteristics and the specific organization of the nigrostriatal system may provide information about their physiological functions and responses to 6-OHDA lesion in MFB or striatum. Since changes arising in different sections along the rostro-caudal axis, it could provide the most appropriate parameters to assess the neurorestorative potential of the therapeutic strategies.

On the other hand, we also hypothesize that the following strategies may be a promising treatment to minimize or ameliorate the functional and morphological effects induced by 6-OHDA in different models:

- Brain implantation of biodegradable PLGA nanospheres (NS) or microspheres (MS) loaded with VEGF and GDNF in combination, which could show a synergistic effect on both models.
- Intraperitoneal administration of nanowired Cerebrolysin, which is the only drug whose action is similar to various NTFs, in combination with housing rats in an EE, which could potentiate the expression of NTFs in a Preclinical model.

The crucial role of NTFs in PD, specially VEGF and GDNF, could be supported, among others, by the deleterious effects on the dopaminergic system of vandetanib administration, a selective tyrosine kinase inhibitor blocking signal mediated by VEGFR2 and RET.

III. OBJECTIVES

1. Main objective

The aim of this work was to study the morphological changes occurring in a severe, partial and preclinical rat models of PD induced by 6-OHDA injection and verify the usefulness of the proposed approach to characterize these models and its suitability for elucidating the benefits of therapeutic strategies such as neurotrophic factors (NTFs) administration and housing in enriched environment (EE).

2. Procedural objectives

I. Characterization of the morphological changes in caudate putamen complex (CPC) and substantia nigra (SN) after the administration of 6-hydroxydopamine (6-OHDA) into striatum (Partial model of PD) or medial forebrain bundle (MFB) (Severe model of PD).

II. Analysis of the differential vulnerability of the CPC and SN to the 6-OHDA injection following the rostro-caudal axis of both anatomical structures.

III. Re-evaluation of conventional parameters for determining the progression of the lesion in the model, looking for a more anatomical marker for the stereological studies.

IV. Suitability of the model to test new therapeutic approach.

- **a.** Morphofunctional studies in a Severe model of PD treated with microspheres loaded with NTFs.
- **b.** Morphofunctional studies in a Partial model of PD treated with nanospheres loaded with NTFs.
- **c.** Morphofunctional studies in a Preclinical model of PD treated with nanowired Cerebrolysin compound or housing in an EE alone or with both combined.

V. Study of morphofunctional changes after VEGF-GDNF PLGA microspheres administration in a Severe model of PD in rats.

VI. Evaluation of morphofunctional changes after administration of PLGA-nanospheres loaded with VEGF and GDNF in a Partial model of PD in rats.

VII. Assessment of morphofunctional changes in a Preclinical model of PD in rats, of housing in EE and intraperitoneally nanodelivery of Cerebrolysin in order to elucidate the synergistic potentiating of combining both strategies.

VIII. Elucidate the molecular pathways involved in the Preclinical model of PD analyzing the effects of some therapeutic strategies (Cerebrolysin and EE) over the expression of Akt/p-Akt and caspase-3 in striatum and SN.

IX. To assess the effect after administration of a selective tyrosine kinase inhibitor (vandetanib) blocking the VEGFR2 and RET receptors in the Preclinical model of PD.

IV. MATERIALS AND METHODS

1. Animals

For the present study a total of 40 adult female Sprague-Dawley rats between 150 to 175 g and 74 adult male Sprague-Dawley rats between 275 to 320 g were used: 16 for the characterization of the lesion and 98 for the treatments. Experiments were performed in agreement with the Ethical Committee and Animal Welfare (CEBA) of the University of the Basque Country (CEBA/154/2010//RUIZ ORTEGA), and in accordance with Spanish Royal Decree RD 1201/2005, European Directive 2003/65/EC and the European Recommendation 2007/526/EC on the protection of animals used for scientific purposes.

2. Housing conditions

Rats were housed at standard conditions except to those that were assigned to rise at enrichment environment as treatment after lesioning with 6-OHDA into striatum (Figure 15).

- **Standard conditions (SC):** Rats raised in a standard laboratory cage (500 mm x 280 x 140 mm) at a constant temperature of 22°C, in a 12 hours dark/light cycle and *ad libitum* access to water and food. The maximum number of animals per cage was 4-5.

- **Enriched environment (EE):** Rats raised in a large cage (790 mm x 460 mm x 640 mm) at a constant temperature of 22 °C, in a 12 hours dark/light cycle and *ad libitum* access to water and food. This cage was furnished with colorful toys and differently shaped objects (shelters, tunnels), that were changed every 2 days and the maximum number of animals per cage was 8.

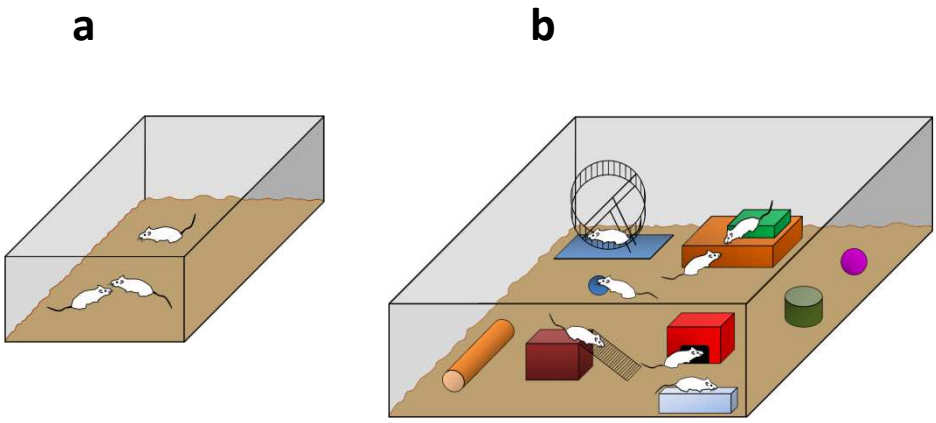

Figure 15. Housing conditions. **(a)** Standard conditions and **(b)** enriched environment

3. Drugs

- **Poly(DL-lactide-co-glycolide) (PLGA)** (Resomer_ RG 752H) with a copolymer ratio of 75:25 (lactic/glycolic%) was acquired from Boehringer Ingelheim (Germany) and **PLGA-microspheres** and **PLGA-nanospheres** were provided by NanoBioCel Group (Laboratory of Pharmaceutics, School of Pharmacy, University of the Basque Country (UPV/EHU), Vitoria, Spain.

- **6-OHDA-HCl**, **desipramine**, **pargyline**, **amphetamine** and **apomorphine** were acquired from Sigma (St. Louis, USA) and were provide by the Department of Pharmacology from the University of the Basque Country (UPV/EHU) (Leioa, Spain).

- **Cerebrolysin (CBL)** was provided by Dr. Hari Shanker Sharma from Uppsala University, University Hospital (Dept. Surgical Sciences), Sweden.

- **Vandetanib** (Ref: V-9402) was acquired to LC Laboratories (USA).

4. Experimental design

The present work was divided into three experimental assays according to the induced model and the treatment used.

Assay I: Morphological characterization of a Severe model of Parkinson's disease and effects of microencapsulated neurotrophic factors

Animals were assigned to describe the model (n=8) or the treatment (n=32).

To characterize the Severe model of PD

a. **6-OHDA group** (n=5 rats): Rats received 6-OHDA into the MFB.

b. **Saline group** (n=3 rats): Rats were injected only with saline solution into MFB (control group).

Animals for the treatment study

Groups consisted of parkinsonized rat groups, which were again anaesthetized 4 weeks after the 6-OHDA injections and MS were implanted into the right striatum. For this purpose rats were divided into 4 groups:

a. **Empty-MS group** (n=5): Rats received empty MS into striatum

b. **VEGF-MS group** (n=9): Rats received MS loaded with VEGF (2.5 µg) into striatum

c. **GDNF-MS group** (n=9): Rats received MS loaded with GDNF (2.5 µg) into striatum

d. **VEGF+GDNF-MS group** (n=9): Rats received MS loaded with VEGF and GDNF (2.5 + 2.5 µg) into striatum

Behavioral evaluations were performed periodically in these groups. Rats were sacrificed three weeks after lesion or 14 weeks after treatment and brains were processed for histology.

Assay II: Morphological characterization of a Partial model of Parkinson's disease and effects of nanoencapsulated neurotrophic factors

As in assay 1, animals were assigned to describe the model (n=8 rats) or the treatment (n=27 rats).

To characterize the Partial model of PD

a. **6-OHDA group** (n=5 rats): Rats received 6-OHDA into the striatum.

b. **Saline group** (n=3 rats): Rats injected only with saline solution into striatum (control group).

Animals for the treatment study

Groups consisted of parkinsonized rats, which were again anaesthetized 3 weeks after the 6-OHDA injections into striatum and NS were implanted into the right striatum using the same stereotaxic coordinates than 6-OHDA. For this purpose rats were divided into 5 groups:

a. **Vehicle-group** (n=5 rats): Rats received only vehicle (phosphate buffered saline [PBS]).

b. **Empty-MS group** (n=5 rats): Rats received empty NS into striatum.

c. **VEGF-NS group** (n=5 rats): Rats received MS loaded with VEGF (2.5 μg) into striatum.

d. **GDNF-NS group** (n=6 rats): Rats received NS loaded with GDNF (2.5 μg) into striatum.

e. **VEGF-NS + GDNF-NS group** (n= 6 rats): Rats received NS loaded with VEGF and GDNF (1.25 μg VEGF + 1.25 μg GDNF) into striatum.

Behavioral evaluations were performed periodically. Rats were sacrificed 3 weeks after lesion or 14 weeks after treatment and brains were processed for histology.

Assay III: Morphofunctional analysis and molecular study after combining therapeutic strategies (Cerebrolysin and enriched environment) and inhibiting VEGFR2 and RET in a Preclinical model of Parkinson's disease.

Rats were partially lesioned with 6-OHDA into the right striatum and 2 weeks after the injection; they were assigned to one of the following experimental groups

a. **6-OHDA group** (n=8 rats): Rats were not treated (control).
b. **Vandetanib group** (n=8 rats): Rats received every day for one week the VEGFR2 inhibitor orally.
c. **EE group** (n=8 rats): Rats housed in EE for one week.
d. **CBL group** (n=8 rats): Rats received nanowired CBL i.p. every day for one week.
e. **CBL + EE group** (n=8 rats): Rats housed in an EE and receiving nanowired CBL i.p. for one week.

Amphetamine motor test was developed at 2 week to assess the lesion and after 3 weeks in order to test the effectiveness of treatment. At 3 week rats were sacrificed and brains were processing for histology (3-4 animals per group) or western blot (4 animals per group).

5. 6-OHDA lesions

Sprague–Dawley rats were anaesthetized with isoflurane inhalation (1.5%–2%; Esteve Química, Barcelona, Spain). Thirty minutes prior to 6-OHDA or saline solution injection; the rats were pre-treated with desipramine (25 mg/kg, i.p.; Sigma-Aldrich, Spain) and pargyline (50 mg/kg, i.p.; Sigma-Aldrich, Spain)(Morera-Herreras et al., 2011)

to protect noradrenergic terminals and to inhibit monoamine oxidase activity, respectively. Once rats were anaesthetized, they were placed on the Kopf stereotaxic instrument (David Kopf Instruments, Tujunga, CA, USA). The head was then firmly positioned within the stereotactic frame by means of ear bars which were placed in the ear canals. Skin covering the skull was longitudinally cut and remaining connective tissue was carefully removed aside by scalpel in order to achieve appropriate visualization of the skull sutures and to define the bregma (a crossing point of parasagittal with coronal sutures) on the surface of the skull as "zero" or "start" point and lambda. After achieving flat positioning of the skull, the coordinates for the injection were calculated related to bregma (Figure 16) as origin from anteroposterior **(AP)** y mediolateral **(ML)** coordinates, and related to dura as origin from dorsoventral **(DV)** coordinates.

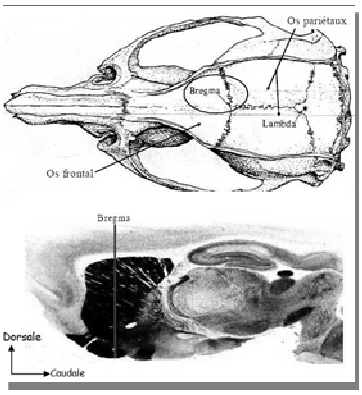

Figure 16. Bregma representation according to Paxinos and Watson (Paxinos & Watson, 2013).

6-OHDA (Sigma, St. Louis, USA) in distilled water containing 1 mg/ml ascorbate was injected into right striatum or MFB according to the model. In both lesions, a Hamilton syringe was used to slowly inject the 6-OHDA at a rate of 1 µl/min for 5 minutes into the right MFB or striatum. Following injection of the neurotoxin, the burr hole was closed using bone wax and standard suturing techniques were used to close the incision.

Depending on the site of unilateral 6-OHDA injection, two different models of PD were described.

5.1. Unilateral 6-OHDA lesion in the medial forebrain bundle (Severe model)

Free base 6-OHDA was unilaterally infused through two injections of 8 and 7 µg performed at two coordinates (Figure 17), relative to the bregma and dura, with the toothbar set at -2.4 and +3.4: 2.5 µl was injected at the first coordinate: **AP** -4.4 mm, **ML** +1.2 mm and **DV** -7.8 mm; and 2 µl was injected into the right nigrostriatal pathway at the second coordinate: **AP** -4.0 mm, **ML** +0.8 mm and **DV** -8.0 mm (Aristieta et al., 2012). According to our established model of PD, this is a severe lesion equivalent to an advanced stage of PD (Miguelez et al., 2011). Saline solution into the right MFB was injected at the same coordinates instead of 6-OHDA for control rats following the same procedure.

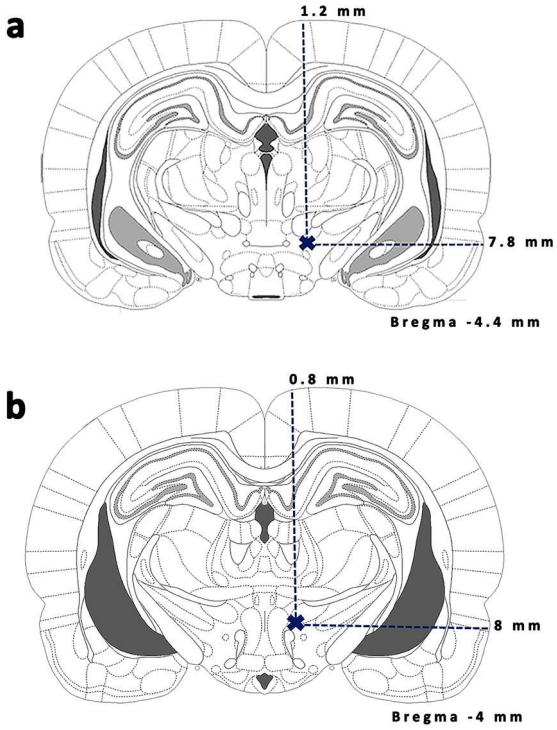

Figure 17. Schematic diagrams of coronal sections illustrating the stereotaxic coordinates corresponding to injections of 6-OHDA in the Severe model. (**a**) First and (**b**) second coordinates are indicated below in mm respect to the bregma. Lines show lateral and dorsoventral coordinates indicating the place of the 6-OHDA injection for each antero-posterior coordinate.

5.2. Unilateral 6-OHDA infusion into the striatum (Partial model)

6-OHDA was unilaterally infused in the right striatum through three different injections (Figure 18). 2.5 µl (7.5 µg) of 6-OHDA were injected in each coordinate: **AP** +1.3 mm **ML** +2.8 mm, and **DV** -4.5 mm; **AP** -0.2 mm, **ML** -3.0 mm, and **DV** -5.0 mm; **AP** -0.6 mm, **ML** -4.0 mm, and **DV** -5.5 mm, relative to bregma and dura with the tooth bar set at -2.4 and +3.4. Taking into account the protocol, this lesion produces a partial degeneration (or parkinsonism) (Björklund et al., 1997). Saline solution into the right striatum was injected at the same coordinates instead of 6-OHDA for control rats following the same procedure.

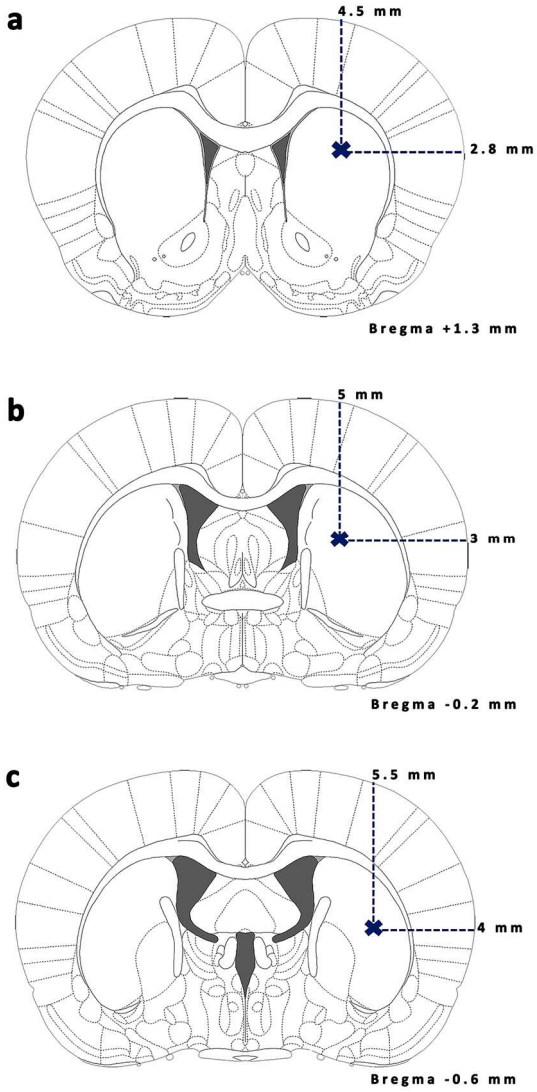

Figure 18. Schematic diagrams of coronal sections illustrating the stereotaxic coordinates corresponding to the striatal injections of 6-OHDA in the Partial model. (**a**) First, (**b**) second and (**c**) third antero-posterior coordinates are indicated below in mm respect to bregma. Lines show lateral and dorsoventral coordinates indicating the place of the 6-OHDA injection for each antero-posterior coordinate.

Two weeks after the 6-OHDA surgery, the rotational behavior was tested with amphetamine administration as a marker of dopaminergic degeneration to determine the grade of the induced lesion. Only rats that rotated more than three full turns per minute (tpm) were included in this study and were randomized divided into different experimental groups previously described.

6. Treatments

6.1. Microsphere implantation

Four weeks after the 6-OHDA lesion was made, the rats were anesthetized by isoflurane inhalation and placed on a stereotactic frame again for poly(lactide-co-glycolide acid) (PLGA)microsphere (MS) implantation.

Microspheres were suspended in PBS (0.1% w/v carboxymethylcellulose, 0.8% w/v Tween and 0.8% w/v mannitol) before administration. Two implantation coordinates were used, relative to the bregma and dura: **AP** +0.5 mm, **ML** -2.5 mm, **DV** -5.0 mm and **AP** -0.5 mm, **ML** -4.2 mm, **DV** -5.0 mm. (Garbayo et al., 2009). Each rat received 2.5 µg of either VEGF or GDNF in a volume of 20 µl or, in the combined group; each rat received a total dose of 2.5 µg of VEGF and 2.5 µg of GDNF in a volume of 40 µl in order to maintain the syringeability and injectability of the formulations.

6.2. Nanosphere implantation

PLGA nanospheres (NS) were implanted 3 weeks after the 6-OHDA injection. Rats were anesthetized with isoflurane (1.5%–2%; Esteve Química) and mounted on a Kopf stereotaxic instrument for NS implantation.

The NS were suspended in 15 µl of PBS (0.1% w/v carboxymethyl cellulose, 0.8% w/v Tween 80 (Ref: P1754; Sigma-Aldrich, Spain) and 0.8% w/v mannitol) before administration. The NS were implanted in the right striatum in three different coordinates: **AP** +1.3 mm, **ML** +2.8 mm, and **DV** -4.5 mm; **AP** -0.2 mm, **ML** +3.0 mm, and **DV** -5.0 mm; **AP** -0.6 mm, **ML** +4.0 mm, and **DV** -5.5 mm, relative to bregma and dura with the tooth bar set at -2.4. Each rat received 2.5 µg of either VEGF or GDNF in a volume of 20 µl or, in the combined group; each rat received a total dose of 1.25 µg of VEGF and 1.25 µg of GDNF in a volume of 20 µl in order to maintain the syringeability and injectability of the formulations.

6.3. Enriched environment

The animals remained in EE after injecting 6-OHDA into striatum for one week prior to sacrifice (Figure 19). Under this condition, as described previously, 8 rats were housed in a large cage (790 mm x 460 mm x 640 mm) consisting of two floors which were connected by a plastic ramp that enabled rats to move from one level to the next and a large external running wheel provided with a device developed by our group to record accurately the amount of turns. It was provided with various enrichment objects, such as tunnels, running wheel, small houses, toys of different shapes, hiding house and tubing that were changed and rearranged frequently to promote exploration and provide to the animals with new sensorial stimulus.

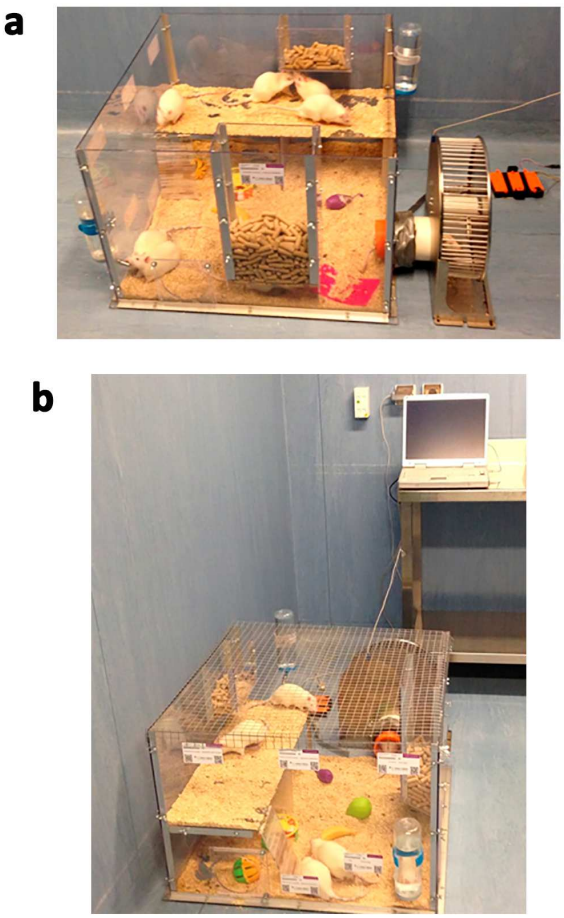

Figure 19. **Pictures of the enriched environment (EE) cage. (a)** Side view of the EE cage with the running wheel incorporated. **(b)** EE cage with the apparatus that registers the movements in the external wheel.

6.4. Cerebrolysin administration

Cerebrolysin (CBL) (Ever NeuroPharma, Austria) is a mixture of various NTFs and active peptide fragments and contains different low-molecular-weight peptides and free amino acids in solution. CBL was administrated through engineered nanowires from TiO2 in the size range of 50-60 nm (obtained from US Wright Patterson Air Force Research Base, Dayton, OH, USA) suspended in 0.05% Tween 80 (Ref: P1754; Sigma-Aldrich). This solution (215.2 mg/ml) was first diluted in distillated water (1:100) and then administrated i.p. (5 mg/kg) once daily for one week.

6.5. Administration of the VEGFR2 and RET inhibitor (Vandetanib)

In order to inhibit the receptor VEGR2 the inhibitor vandetanib was administrated orally for one week every day. In a NaCl solution at 0.9% (Ref: 121659.1211, Panreac Química SA, Barcelona, Spain) with a total volume of 0.15 ml were dissolved:

- 30 mg of **Vandetanib** per Kg of weight of rat.
- **Tween 80** at 1% (Ref: P1754; Sigma-Aldrich, Spain). It is an excipient that is used to stabilize aqueous formulations of oral suspensions, increasing the ability of retaining water.
- **Sucrose** at 5% (Ref: 131621. 1211; Panreac Química SA, Barcelona, Spain). It is a disaccharide combination of the monosaccharides glucose and fructose. It was used to neutralize the bitter flavour produced by the inhibitor due to oral administration.

In order to achieve a homogenous solution, it was mixing during 24 hours at room temperature (RT) before using.

6.6. Combination of enriched environment housing and Cerebrolysin administration

Parkinsonized rats were housed in EE one week receiving CBL i.p. every day. The stress produced by the administration daily of CBL was taken into account.

7. Functional tests

Drug-induced rotational behaviour test is one of the most simple to perform and widely used test for evaluation of the unilateral 6-OHDA lesion (Ungerstedt & Arbuthnott, 1970). Unbalanced dopamine secretion in the brain results in preferable turning of the animal to the side of the lesion. When the rat is challenged with certain drugs such as amphetamine or apomorphine, this rotation tendency increased and leads to a typical “rotational behaviour” ipsilateral or contralateral to the lesion depending on the drug administrated (Figure 20).

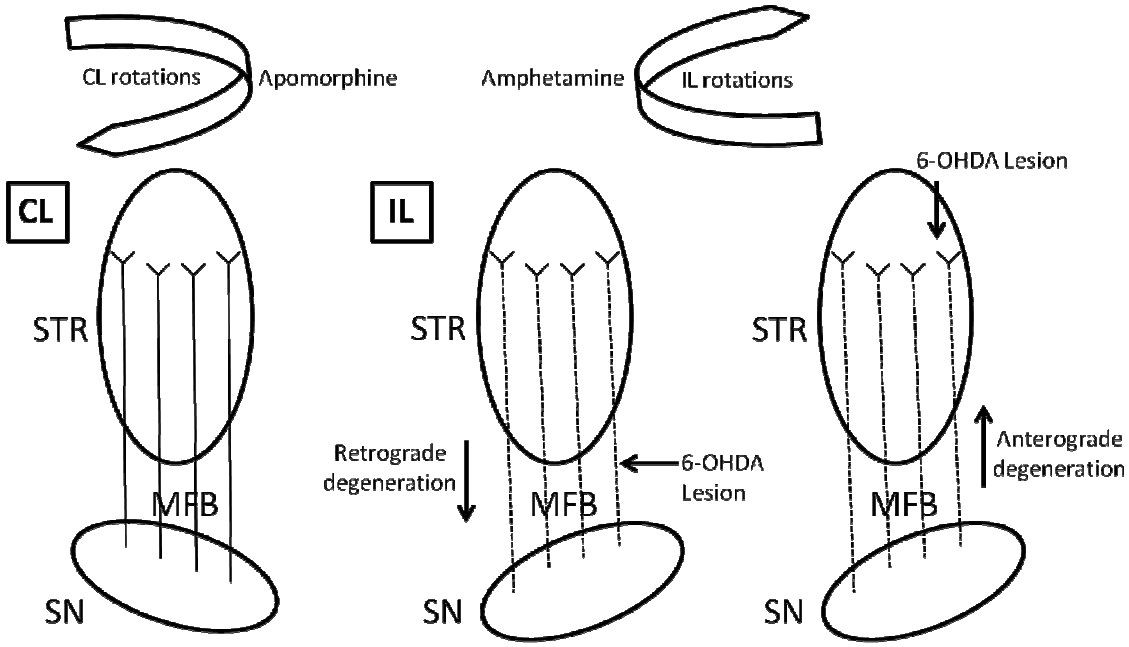

Figure 20. Schematic illustration of the two behavioral tests used in both 6-OHDA induced models of Parkinson's disease (PD). (Adapted from Rodrigues et al., 2003). Abbreviations: STR, striatum; SN: substantia nigra; MFB, medial forebrain bundle; CL, contralateral; IL, ipsilateral.

7.1. Amphetamine-induced rotational test

Two weeks after the lesion with 6-OHDA, animals were injected with D-amphetamine (Sigma-Aldrich, St. Louis, USA) to screen for the severity of the dopaminergic lesion prior to entry into the experimental conditions. After the experimental period, the rats were tested again with the same test of PD motor severity.

After MS or NS implantation, the rats were tested at 2, 4, 6, 8, 10 and 12 weeks by the amphetamine-induced rotational behavior test, as was described by Herrán et al (Herrán et al., 2013, 2014). In the rest of treatments this test was assessed at 1 week after treatment administration prior to sacrifice. Before each behavioral session, animals were weighed and amphetamine (5 mg/kg) was i.p. administered. After 15 minutes of latency, the full ipsilateral rotations were counted for 90 minutes with an automater rotameter (multicounter LE3806; Harvard Apparatus, Holliston, MA, USA). Data were expressed as the number of full tpm. In the assay 3, it was also calculated the rotations

every 5 minutes for 90 minutes, and data were expressed as the number of full turns per 5 minutes.

7.2. Apomorphine-induced rotational test

The rotational behavior was tested with apomorphine to test contralateral rotation behavior at 14 week after MS or NS implantation. The apomorphine (a dopaminergic agonist) was used as a DA degeneration indicator because it induces contralateral turning behavior after dopaminergic denervation. Thus, before each behavioral session, animals were weighed and apomorphine (0.5 mg/kg) was subcutaneously administrated. After 5 minutes of latency, the full contralateral rotations were measured for 50 minutes with an automated rotameter (Harvard Apparatus multicounter LE3806). Data were expressed as the number of full turns per 5 minutes.

8. Proliferation assay

BromodeoxyUridine (BrdU) was used to study the cell proliferation after MS or NS administration. Different dose of BrdU (Ref: B5002; Sigma-Aldrich) administration and timing was developed according to the treatment and model.

- In rats treated with MS (2 rats per group) **80 mg/kg** body weight of BrdU diluted in NaCl at 0.9%, was injected i.p. **three times at intervals of three hours**. One hour after the last injection, animals were sacrificed.

- In rats treated with NS (5 vehicle rats, 5 rats treated with empty MS and 5 rats treated with VEGF and GDNF in combination) **200 mg/kg** body weight of BrdU diluted in NaCl at 0.9%, was i.p. administered **five days before sacrifice.**

9. Morphological analysis

After the survival period (3 weeks for rats used to describe the models and 14 weeks for rats treated with microspheres or nanospheres), the rats were i.p. anaesthetized with chloral hydrate at 20% (Ref: 141975, Panreac Química SA, Barcelona, Spain) and transcardially perfused with 0.9% NaCl solution in order to remove blood cells from brain. When blood has been cleared from body, NaCl was replaced by 4% paraformaldehyde (PFA) (Ref: 141541.1211, Panreac) in 0,1 M PBS (pH 7.4) for tissue fixation. Fixation preserves the ultrastructure, stabilizes protein and peptide conformation so that antibodies can bind to antigen sites.

Afterwards, the rats were decapitated and the brain carefully removed from the skull and placed into 4% PFA solution overnight at 4 °C for post-fixation. The next day, brains were transferred to a 30% sucrose solution in 0.1M PBS, for cryoprotection. After 1–3 days (when brain sank), fixed brains were photographed in order to assess macroscopically the lesion induced in the right hemisphere by surgery.

Then, two coronal blocks containing the entire SN and the entire striatum, were dissected using a Rodent Brain matrix (ASI Instruments, USA). For this purpose, brains were cut transversally at different levels in order to obtain the striatal and nigral block tissue. Firstly, brains were cut transversally at the level of olfactory bulb (Figure 21b1), optic chiasm (Figure 21b2), stalk pituitary (Figure 21b3) and body trapezoid (Figure 20b4) Striatum block included from the level of optic chiasm to the level of stalk pituitary, and nigral block included from the level of stalk pituitary to the level of body trapezoid (Figure 21). The rest of blocks were removed.

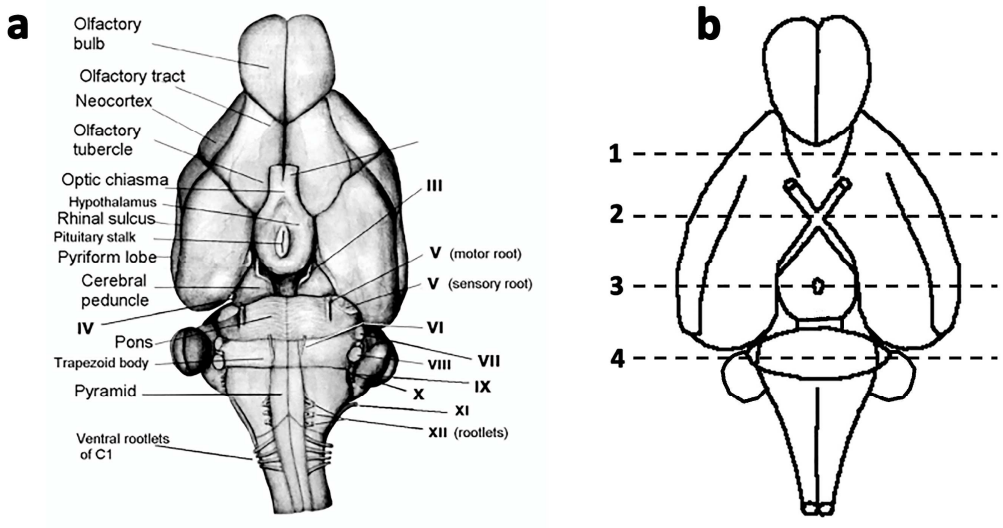

Figure 21. Dissection of the caudate putamen complex and substantia nigra. (a) Ventral view of the rat brain includes labels which indicate each anatomical structure **(b)** Schematic representation of the ventral rat brain. The brain was firstly cut transversally at the level of the olfactory bulb (**b**1) and the optic chiasm **(b2).** The striatum block was dissected with two horizontal **(b2, b3)** cuts at the level of the optic chiasm and pituitary stalk. The nigral block was also dissected with two horizontal cuts **(b3, b4)** at the level of the pituitary stalk and trapezoid body.

The block containing striatum and the block containing SN, were embedded in Tissue-Tek OCT compound (Electron Microscopy Sciences, USA), frozen and coronally sectioned with a freezing microtome (Ref: 1325, Leica Instruments, Germany). Serial 50 µm thick coronal sections in series were obtained. Between levels +1.6 to -1-6 respect to bregma were defined the sections for striatum and between levels from -4.52 to -6-3 the sections for SN, as defined in the rat brain atlas of Paxinos and Watson (Paxinos & Watson, 2013). Serial coronal sections were collected in free-floating with 0.1 M PBS containing 0.6% sodium azide (Ref: S-2002, Sigma-Aldrich) for storage.

9.1. Histological analysis

Histology is the ability to visualize or differentially identify microscopic structures and it is frequently enhanced through the use of histological stains. There are many staining techniques that have been used to selectively stain cells and cellular components.

Thus, in order to assess structural changes after lesion and treatments in striatum and SN, Nissl staining was developed.

9.1.1. Nissl staining

Nissl staining is a classic nucleic acid staining method traditionally used on nervous tissue sections. A basic dye, in this case toluidine blue binds to negatively charged nucleic acids like ribonucleic acid (RNA) and deoxyribonucleic acid (DNA). Nissl staining typically marks the endoplasmic reticulum due to ribosomal RNA, as well as the nucleus and other accumulations of nucleic acid.

Sections for Nissl staining were mounted on gelatin coated slides, hydrated through a battery of alcohols with decreased graduation, incubated in 1% toluidine blue (pH 4.1) solution in distilled water for 1 minute. Then, sections were washed with distilled water and dehydrated through a battery of alcohols with increased graduation, and coverslipped and mounted in DPX mounting medium (Sigma-Aldrich, Germany).

9.2. Histochemistry

Histochemistry refers to the use of chemical reactions between chemicals and components within tissue. In this study, butyrylcholinesterase and lectin histochemistry were developed on 50 µm thick free-floating sections in parallel to visualize the microvascular changes after injecting 6-OHDA and after MS or NS implantation.

9.2.1. Butyrilcholinesterase histochemistry

Sections were histochemically processed for butyrylcholinesterase to visualize the vascular pattern following the method referred by Argandoña and Lafuente, 1996. Sections were washed twice in 0.1 M Tris Maleate Buffer (TMB) (pH 6), acetylcholinesterase was inhibited with BW284CS1 (1,5-bis(4-allyldimethylammoniumphenyl)-pentan-3-one dibromide) (Ref: A-9013, Sigma–Aldrich,

Spain) 0.05 M for 20 minutes, then bath and sections were incubated overnight at RT in dark conditions with the following incubation solution: butyrylthiocholine iodide (Ref: 108150250, Acros Organics, Barcelona, Spain) 1 mg/ml, 5% sodium citrate 0.1 M (Ref: 6448, Merck, Germany), 10% copper sulphate 30 mM (Ref: 1596, Sigma-Aldrich, Spain), 10% BW284CS1 0.05 mM, 10% potassium ferricyanide 5 mM Ref: 141503, Panreac Química SA, Barcelona, Spain) and 65% TMB 0.1 M. The next day, sections were washed in TMB, mounted on gelatin-coated slides, dehydrated and covered.

9.2.2. Lectin histochemistry

Lectins are vegetal glycoproteins with the capacity to bind selectively to foreign glycoconjugates. Many lectins have demonstrated their utility as markers of the vascular wall. For this study we have used the tomato Lectin (*Lycopersycum esculentum agglutinin,* LEA).

This histochemistry was performed on sections with FITC-conjugated *Lectin lycopersycum* (Ref: L0401; Sigma-Aldrich; 1:100). The entire histochemistry is carried out in dark conditions, because the LEA primary antibody is attached to a green fluorescent molecule. Firstly, the sections were washed twice with PBS 0.1 M, then, the sections were placed in a blocking solution of PBS 0.1 M+ bovine serum albumin (BSA) 5% (Ref: A7906, Sigma-Aldrich) + Triton X-100 (Ref: T-6878, Sigma-Aldrich) 0.5% for 2 hours. Primary antibodies diluted in the blocking solution like previously stated, was incubate overnight at 4 ºC. After washing three times with PBS 0.1 M, sections were incubated for 5 minutes with Hoechst 33258 (Sigma-Aldrich) 5µg/ml in PBS 0.1 M. After rinsing three times with PBS 0.1 M, coronal slices were mounted in gelatinised slides and cover with Vectashield (Ref: x-0517, Vector laboratories, USA) and cover-slides.

Fluorescence images were acquired with an Olympus Fluoview FV500 confocal microscope using sequential acquisition to avoid overlapping of fluorescent emission spectra. The images have been treated with FV 10-ASW 1.6 Viewer and Adobe Creative Suite 4.

9.3. Immunohistochemistry

Immunohistochemistry (IHC) combines anatomical, immunological and biochemical techniques to identify discrete tissue components by the interaction of target antigens with specific antibodies tagged with a visible label. In this study, IHC was carried out by an enzymatic system, which uses the endogenous peroxidase activity of the tissue and can be detected by reacting fixed tissue sections with the chromogenic diaminobenzidine (DAB) substrate. Results were visualized by optical microscopy (Ref: BH-2, Olympus Optical SA, Spain).

On the other hand, when the stain is a fluorescent molecule, it is named as immunofluorescence. To visualize the results, images were acquired with an Olympus Fluoview FV500 confocal microscope using sequential acquisition to avoid overlapping of fluorescent emission spectra. The images have been treated with FV 10-ASW 1.6 Viewer and Adobe Creative Suite 4.

For immunohistochemistry and immunofluorescence parallel sections were developed in free-floating.

9.3.1. Immunohistochemistry for tyrosine hydroxylase and glial fibrillary acidic protein

Tyrosine hydroxylase (TH) is the rate-limiting enzyme in the biosynthesis of dopamine. Therefore, it is a useful marker of DA neurons and projections and allows their localization in different areas of the brain. Thus, TH immunostaining is the key to assess the nigrostriatal degeneration induced by 6-OHDA injection or examine the effects of the treatments on this system.

Glial fibrillary acidic protein (GFAP) is expressed in the central nervous system in astrocyte cells. It is involved in many important CNS processes, such as the cell-communication, and it has been shown as also been shown to be important in repair

after CNS injury. For this purpose, this marker is useful to study the glial scar and the activation of astrocytes produced by the lesion after injecting the toxin, the control and the treatments.

For TH and GFAP immunochemistry, endogenous peroxidases were neutralized with a solution of 3% hydrogen peroxide (H_2O_2), 10% methanol in potassium phosphate-buffered saline (KPBS) (0.02 M, pH 7.1) for TH immunochemistry or PBS for GFAP immunochemistry, during 30 minutes at RT. For TH immunostaining, cerebral slices were preincubated with 5% normal goat serum (NGS) (Ref: S-1000, Vector Laboratories, USA) and 1% Triton X-100 in KPBS (KPBS-T) for 1 hour and then incubated overnight with rabbit polyclonal anti-tyrosine hydroxylase (Ref: AB-152, Millipore; 1:1000) in 5% NGS KPBS/T at 4 ºC. For GFAP immunostaining, coronal slices were preincubated with 5% BSA and 0.05% Triton X-100 in 0.1 M PBS for 2 hours and after that these slices were incubated with monoclonal mouse anti-GFAP (Ref: G-3893, Sigma-Aldrich; 1:400) overnight at 4 ºC. Sections incubated with anti-TH, after rinsing twice with KPBS and once with 2.5% NGS KPBS-T, were exposed to 2 hours with a secondary biotinylated goat anti-rabbit IgG (Ref: BA1000, Vector Laboratories; 1:200) in KPBS-T containing 2.5% NGS. Sections incubated with anti-GFAP were rinsed three times with PBS and exposed to biotinylated anti-mouse secondary antibody (Elite ABC kit, Vector Laboratories) for 2 hours at RT. All slices were processed with avidin-biotin-peroxidase complex (Elite ABC kit, Vector Laboratories, Inc., Burlingame, CA, USA) for 1 h and 3,3 diaminobenzidine (DAB) (Ref: 8001, Sigma-Aldrich) as chromogen. Finally, slices were mounted, dehydrated and coverslipped with DPX medium (Ref: 06522, Sigma-Aldrich, Spain).

9.3.2. Immunofluorescence for VEGF and OX-42

For immunofluorescence, parallel sections were incubated with the following primary antibodies: rabbit polyclonal anti-VEGF (Ref: sc-152; Santa Cruz Biotechnology, Inc., USA, 1:200) and monoclonal anti-OX-42 (Ref: MCA275G Serotec; 1:200) to study angiogenesis and inflammation in both 6-OHDA induced PD models. Firstly, sections were rinsed with 0.1 M PBS (pH 7.4), preincubated for 1 hour with the blocking solution

(5% BSA and 0.05% Triton X-100 in 0.1 M PBS) and these sections were incubated overnight at 4 ºC with the correspondent primary antibodies. The next day, section were washed followed by the incubation with a secondary antibody conjugated with a fluorochrome for 1 hour in the darkness and at RT: Alexa 568 conjugate goat anti-rabbit IgG (Ref: A11036 Invitrogen; 1:400) or Alexa 488 conjugate goat anti-mouse IgG (Ref: A11029 Invitrogen; 1:400), respectively. After rinses, Hoechst 33258 was added to counterstain the nuclei for 10 minutes. Slices were washed, mounted and coverslipped with medium Vectashield (Vector laboratories).

9.3.3. Immunofluorescence for BromodeoxyUridine

For the detection of bromodeoxyUridine (BrdU) immunostaining free-floating sections were rinsed with 0.1 M PBS and preincubated with the blocking solution PBS 0.1 M+BSA 5% (Sigma-Aldrich; ref: A7906) + Triton X-100 (Sigma-Aldrich ref: T-6878) 0.5% for 2 hours. Then, sections were incubated in HCl (Ref: 131020.1611; Panreac Química) 2 N at 37 ºC for DNA denaturalization for 30 minutes followed by a 10-minutes rinsed in tetraborate sodium decahydrate (Ref: B9876; Sigma-Aldrich) 0,1 M at pH 8.5 for 10 minutes. Afterwards, coronal sections were incubated with the monoclonal primary antibody anti-BrdU (Ref: sc-51514; Santa Cruz Biotechnology; 1:200) overnight at 4 ºC. After washes with PBS 0.1 M, sections were incubated with the secondary fluorescent-dye-conjugated antibody Alexa 488 conjugate anti-mouse IgG (Ref: A11029; Invitrogen; 1:400) diluted in the blocking solution, for 1 hour at RT. After rinsing with PBS 0.1 M, Hoechst 33258 (Sigma-Aldrich) 5 µg/ml in PBS 0.1M, was added to counterstain the nuclei for 10 minutes. The slices were washed with PBS 0.1 M, mounted and coverslipped with medium Vectashield (Ref: x-0517; Vector laboratories).

The visualisation was made with a fluorescent microscope (Olympus Optical SA: ref BX-41).

9.3.4. Double immunofluorescence for BromodeoxyUridine and doublecortin

To detect BrdU and doublecortin (DCX), a double immunostaining was carried out in order to assess the neurogenesis and differentiation respectively after administration of NS loaded with VEGF and GDNF. Briefly, free-floating sections were incubated overnight with goat polyclonal anti-DCX (Ref: sc-8066; Santa Cruz Biotechnology; 1:200) at 4 ºC and later visualized with an Alexa 633 conjugated donkey anti-goat IgG (Ref: A-21082; Invitrogen; 1:400) for 1 hour at RT. After several washes, sections were denatured with 2 N HCl for 30 minutes and incubated overnight with the primary antibody anti-BrdU at 4 ºC, followed by incubation with a secondary Alexa 488 conjugated goat anti-mouse IgG (Ref: A11029; Invitrogen; 1:400) antibody. After rinsing, Hoechst 33258 was added to counterstain the nuclei for 10 minutes. The slices were washed, mounted and coverslipped with medium Vectashield (Ref: x-0517; Vector laboratories, USA).

First antibody	Secondary antibody
Rabbit anti-TH; 1:1000 (Ref: AB-152, Millipore, USA)	Biotinylated goat anti-rabbit IgG; 1:2000 (Ref: BA1000, Vector Laboratories)
Mouse anti-GFAP; 1:400 (Ref: G-3893, Sigma-Aldrich; 1:400)	Biotinylated Anti-mouse Ig G; 1:200 (Ref: PK-6102, Vectastain ABC Kit, Vector Laboratories)
Rabbit anti-VEGF; 1:200 (Ref: sc-152; Santa Cruz Biotechnology, Inc., USA)	Alexa 568 conjugate goat anti-rabbit IgG; 1:400 (Ref: A11036 Invitrogen)
Mouse anti-OX-42 ; 1:200 (Ref: MCA275G, Serotec)	Alexa 488 conjugate goat anti-mouse IgG; 1:400 (Ref: A11029 Invitrogen)
Mouse anti-BrdU; 1:200 (Ref: sc-51514; Santa Cruz Biotechnology)	Alexa 488 conjugate goat anti-mouse IgG; 1:400 (Ref: A11029 Invitrogen)
Goat anti-DCX; 1:200 (Ref: sc-8066; Santa Cruz Biotechnology)	Alexa 633 conjugated donkey anti-goat IgG; 1:400 (Ref: A-21082; Invitrogen)

Table 1. Primary and secondary antibodies used for immunohistochemistry and immunofluorescence.

10. Quantitative analysis

10.1. Quantification of BrdU-positive cells

To calculate the number of positive-BrdU cells, two sections per rat were counted at high magnification (×40). The cells in the subventricular zone (SVZ) have been counted taking into consideration all the cells of the subependymal zone and all the cells 25 µm close to the most external lateral wall of the ventricle. The migratory cells have been counted within an area as long as the lateral ventricular wall and 250 µm wide within the caudate putamen. All the counting has been made by the same person in a "blind" way.

10.2. Stereological analysis

Stereology estimates quantities as a number, length, surface or volume. It gives a set of convenient, unbiased and efficient tools and methods for quantification of multi-dimensional characteristics of tissues. With the correct sampling strategy, and depending on the orientation of the tissue to be analyzed, this add-on gives the access to a large palette of stereological tools.

A total of 8 sections, one from every 8 sections of striatum and SN were measured per brain for the animals involved in this study. All the measurements were evaluated using a computerized image analysis system (Mercator Image Analysis system; Explora Nova, La Rochelle, France) (Figure 22). After having defined the outlines of regions of interest at x4 magnification, the estimation of cell numbers and prolongations of the coronal sections were quantified at x40 magnification in the previously drawn regions by using optical fractionator method. Volume data is also required for the estimation of the number, because of that it is also implemented by this system.

Sum up, optical fractionator method uses thick sections and estimates the total number of cells from the number of cells sampled with a Systematic Randomly Sampled

(SRS) set of unbiased virtual counting spaces covering the entire region of interest with uniform distance between unbiased virtual counting spaces in directions X, Y and Z. Another method calculates the mean cell density (Nv) within the unbiased virtual counting spaces by dividing the number of cells counted within all counting spaces by the number of investigated counting spaces and their uniform volume. When multiplying this average density with the volume of the investigated region of interest, one obtains an unbiased estimate of the total number of cells in the region of interest.

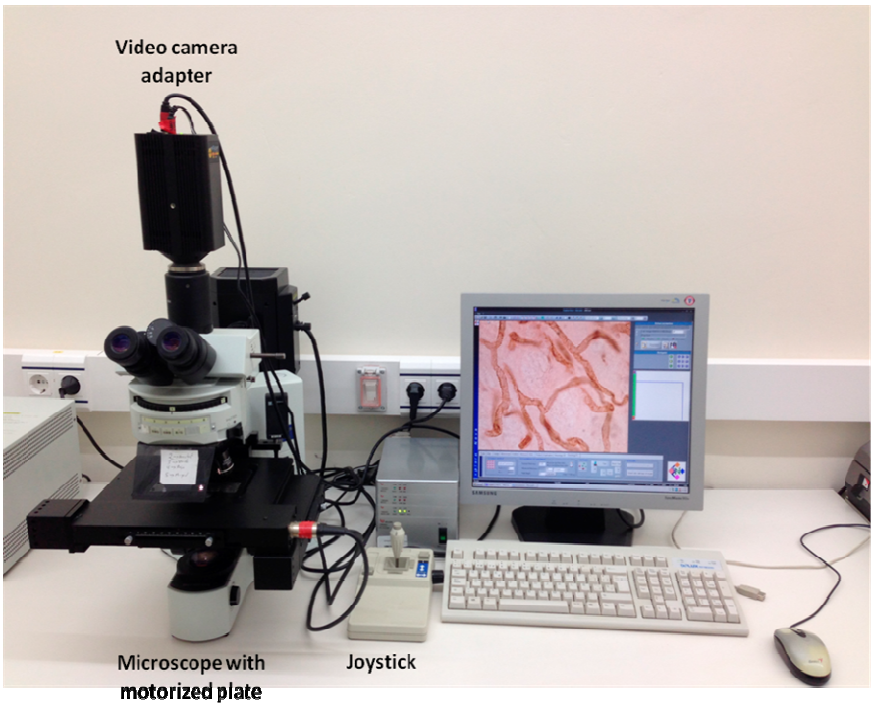

Figure 22 . Morphometric equipment used for the stereological analysis.

10.2.1. Integrated optical density

Digitalized images from coronal sections corresponding on rats treated with NS and vehicle in the Partial model of PD were taken with a 1,200 dpi resolution digital scanner (Epson, Suwa, Japan). The integrated optical density (IOD) reading was corrected for background staining (subtracting the values of a region outside of the tissue). For each animal, the IOD was estimated at two middle–caudal levels along the

basal ganglia according to Paxinos and Watson (Paxinos & Watson, 2013) placing a square of 900 μm^2 on the most degenerated lateral region: **1) middle striatum** (bregma -0.24 mm); **2) caudal striatum** (bregma -0.60 mm). Optical density values are given as percentage of ipsilateral striatum versus the contralateral non-lesioned striatum, which was considered as 100% (Figure 23).

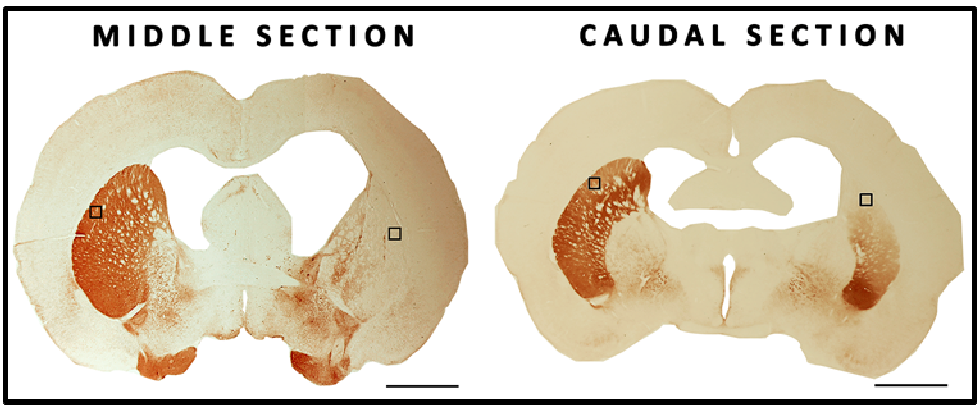

Figure 23. The images show the middle and caudal sections of the caudate putamen complex for TH immunohistochemistry. Squares placed on the lesioned and non-lesioned hemispheres delimit the surfaces in which integrated optical density was measured. Scale bar = 2 mm.

10.2.2. Volume of affected striatum

On each experimental group, the TH-negative volume of the CPC was calculated in order to find an alternative histological marker to the IOD for evaluation of the lesion and its recovery after 6-OHDA administration.

To achieve this aim, the TH-negative volume of the ipsilateral CPC and its entire volume were both measured (Figure 24). Values were expressed as a percentage of the TH-negative volume versus the entire volume of the ipsilateral CPC.

For each animal, the TH-negative volume was estimated at a whole CPC and at three representative CPC levels according to Paxinos and Watson's Atlas (Paxinos & Watson, 2013): **rostral** (bregma +0.70 mm), **middle** (bregma -0.26 mm) and **caudal** (bregma -0.80 mm) sections.

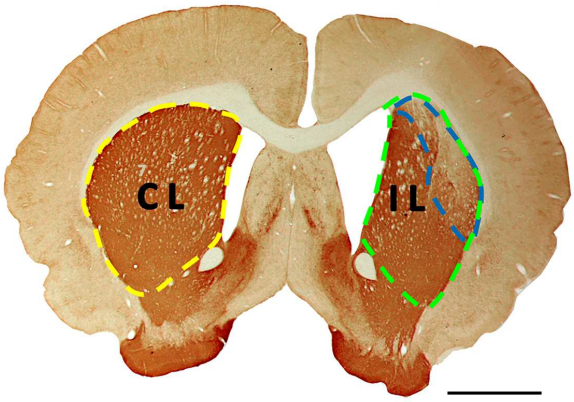

Figure 24. Measurements of TH-negative volume in coronal striatal sections. CL and IL hemispheres are delimited in yellow and green respectively to measure the TH volume. In blue the TH-negative volume in IL hemisphere is also outlined to measure the TH-negative volume. All measurements are carried out by the computerized image analysis system (Mercator Image Analysis system, Explora Nova, La Rochelle, France). Results are expressed as the percentage of the TH-negative volume versus the entire volume of the ipsilateral CPC. Scale bar = 2 mm. Abbreviations: CL, contralateral; IL, ipsilateral; TH, tyrosine hydroxylase.

10.2.3. Tissue retraction of the caudate putamen complex

Tissue retraction of the CPC was calculated by measuring the volume occupied by the ipsilateral CPC with respect to the contralateral one, on TH-immunostained sections. The volume of both striata was calculated integrating all measurements of the CPC sections.

For each animal, the tissue retraction was estimated at a whole CPC and at three representative CPC levels according to Paxinos and Watson's Atlas (Paxinos and Watson, 1997): **rostral** (bregma +0.70 mm), **middle** (bregma -0.26 mm) and **caudal** (bregma -0.80 mm) sections.

10.2.4. Neuron density and axodendritic network in substantia nigra

TH-immunoreactive (TH-ir) neurons and the axodendritic network (ADN) were measured using optical fractionators method provided by the computerized image analysis system (Mercator Image Analysis system, Explora Nova, La Rochelle, France),

previously described. Probes of 50×50 µm separated by 100 µm were launched into the entire SN and also into a delimited region, including SN-Lateral (SNl), one third of SN-reticulata (SNr) and the lateral half of SN-compacta, which we named "external-SN "(e-SN) and where the most prominent changes were observed (Figure 25). Subsequently, ADN density only was analyzed in this e-SN in the Partial model.

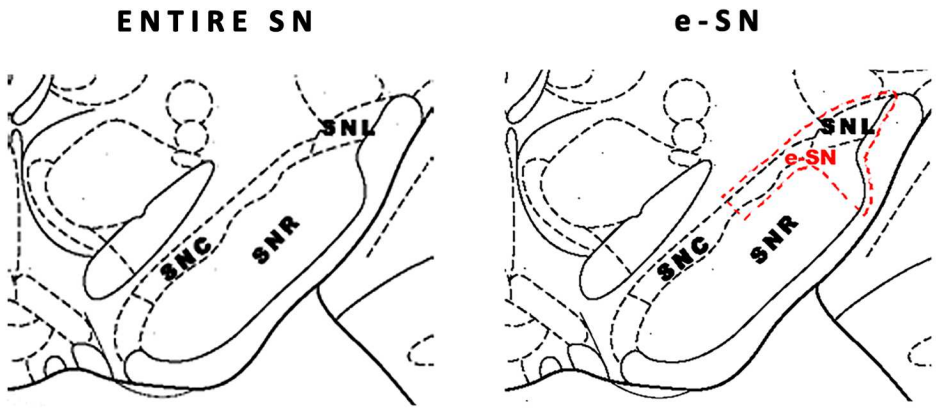

Figure 25. Pictures of the entire substantia nigra (SN) and the delimited external-SN (e-SN,) which includes the SN par lateralis (SNl), one third of the SN reticulata (SNr) and the lateral half of the SN compacta (SNc).

Immunopositive neurons and ADN inside the probe, or crossing the right side of the X–Y axis, were counted (Figure 26). TH-ir neurons and ADN were calculated per section and per animal considering all the SN slices and considering only three representative rostro-caudal levels, according to Paxinos & Watson's Atlas (Paxinos & Watson, 2013): **rostral SN** (bregma, -5.20 mm), **middle SN** (bregma, -5.60) and c**audal SN** (bregma, -6.04) sections. Data were expressed as a percentage of the neurons or ADN present on the lesioned side versus the non-lesioned hemisphere.

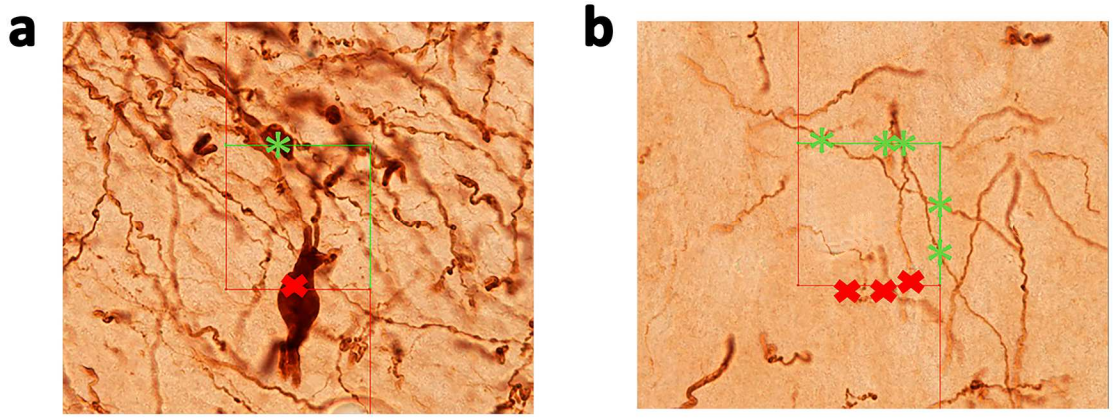

Figure 26. Computerized images represent the launched probes inside the delimited region. (**a**) Neurons inside or crossing the sides of the probe. (**b**) Axodendritic network (ADN) crossing the sides of the probe. Red crosses determine neurons and ADN are not taken into account. Green asterisks correspond to the neurons or ADN counted.

10.2.5. Microvascular density

The number of vessels stained with butyrylcholinesterase histochemistry, were measured in the striatum and SN also using the optical fractionator method referred above. In striatum, probes of 50×50 µm separated by 400 µm were launched into the previously delimited striatum. In contrast, probes of 50×50 µm were separated by 150 µm and launched into the previously delimited area corresponding to the entire SN. Only vessels sections or profiles that were inside the probe or crossing on the right side of the X–Y axis were counted (Figure 27).

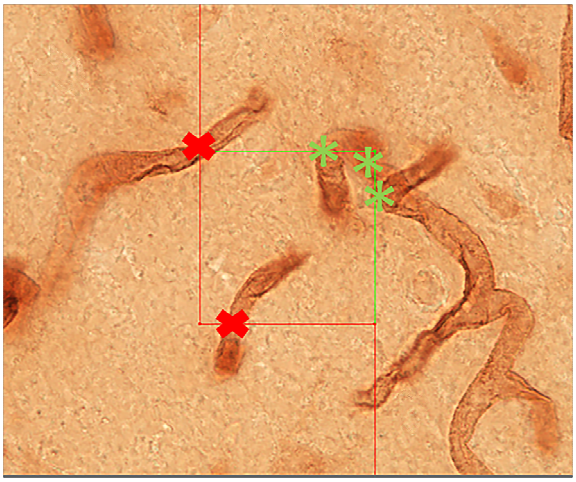

Figure 27. Computerized images represent the microvessels crossing the launched probes in the delimited region. Red crosses determine two axes in which vessels are not taken into account. Green asterisks correspond to microvessels counted in the two green axes.

Vascular density was calculated at all slices of the striatum and SN and also at the three representative sections of striatum and SN, previously described.

11. Biochemical study

In assay 3, rat brains (4 per group) were also processed for western blot after anaesthesia, rats were decapitated in order to study protein expression.

11.1. Microdissection

Rats were anaesthetized by chloral hydrate and decapitated by guillotine to obtain brain in fresh. Brains were removed and placed on a cold metal plate for the microdissection. For this purpose, coronal sections containing the striatum and SN were cut out and subjected to biopsy with a small biopsy needle. Brains were rinsed with PBS to remove any surface blood. Then, in order to examine the differences between the lesioned side and non-lesioned side, striatum and SN were dissected for each hemisphere; taking into account that right hemisphere was the lesioned one. Firstly, cerebellum was separated, and brain was cut bi-half into right and left hemisphere. The

next cut was for removing olfactory bulb in the level of the optic chiasm, and the fourth cut was in the level of pituitary stalk, separating the two coronal slices, one containing striatum and the other the SN. The frontal cortex from the slice contained striatum was removed in the fifth cut, obtaining the striatum (Figure 28). Substantia nigra was collected in the sixth cut, separating the cortex from the slice. Once each specimen was collected, it was quickly frozen on dry ice coronal section containing the striatum and SN for each hemisphere and stored at -80 °C.

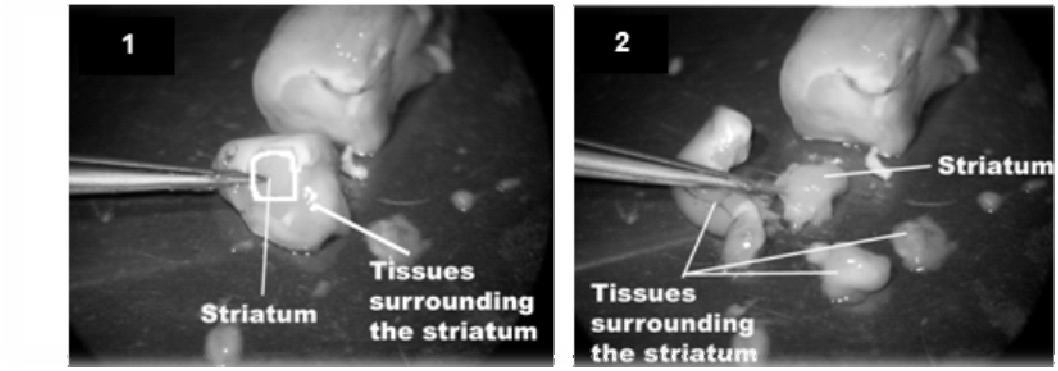

Figure 28. Illustrative representation of the microdissection of the striatum, involving removal of tissue surrounding the striatum.

11.2. Tissue dissection and protein isolation

Brain slices were homogenized (1:20 w/v) in lysis buffer containing 25 µl of protease inhibitor cocktail (Ref: P3840, Sigma-Aldrich, Spain) per ml of lysis buffer.

The lysis buffer was prepared following the next procedure:

- Mix 5 ml of phosphate buffer (PB) + 45 ml of distilled water
- Add to the mix 0.09305 g of ethylenediaminetetraacetic acid (EDTA) (Ref: 1.12029.0100, Merck, Germany), 0.09515 g of ethylene glycol tetraacetic acid (EGTA) (Ref: E4378, Sigma-Aldrich, Spain) and 1 mM dithiothreitol (DTT) (Ref: D5545, Sigma-Aldrich, Spain).

The homogenization was performed by using a plastic homogenizer manually and incubating on ice for 30 minutes. The lysates were then centrifuged (13,000 rpm at 4 ºC for 15 minutes) to remove the insoluble material. Solubilized proteins corresponding to the membrane and cytosolic fractions form each striatum and SN for each hemisphere were recovered in the supernatants after and quantified using the BioRad Protein Assay (USA), based on Bradford's method. This colorimetric assay is based on the absorbance shift in the dye Coomassie induced by protein binding (change from red to blue). The absorbance was read at 595 nm in a fluorometer (Ref: Sinergy HT, BioTek Instruments, Inc.) and the obtained values were plotted to a standard curve made using BSA (Ref: A7906, Sigma-Aldrich).

11.3. Western blot

Western blot is a semiquantitative technique to analyze proteins which combines electrophoresis and immunological detection of proteins by means of antigen-antibody reactions. In a first step, proteins are separated according to their molecular weight in an electric field (electrophoresis). Afterwards, proteins are transferred to a nitrocellulose or polyvinylidene difluoride (PVDF) membrane by means of electric force, in a process known as electrotransfer. Finally, the target proteins are detected by incubation with specific primary antibodies and secondary HRP-conjugated antibodies that ensure the detection of the molecules.

Western blot was carried out in order to assess the survival and apoptotic pathways in striatum and SN after administration of VEGFR2 inhibitor (to demonstrate the neuroprotective role of VEGF on dopaminergic system and examine the effect of inhibiting VEGR2 over the GDNF receptor) and the treatments developed in assay 3 in a Preclinical model of PD. For this purpose, immunoblotting was developed against the following antigens:

- **Phospho-Akt (Ser 473) (60 kDa)**
- **Akt (60 kDa)**
- **Caspase-3 (H-277) (39 kDa)**
- **Tyrosine hydroxylase (TH) (62 kDa)**
- **β-actin (47 kDa)** as loading control

11.3.1. Protein electrophoresis and electrotransfer

Protein electrophoresis was done in denaturing conditions. Thus, disulphur bonds between proteins were broken by boiling them in the presence of DTT. In addition, the differences in charge between proteins were neutralized by a negatively charged anionic detergent such as sodium dodecyl sulfate (SDS) to ensured that proteins were separated along by their molecular weight.

Protein samples were boiled at 95 ºC for 10 minutes in sample buffer 4X containing 200 mM Tris (pH 6.8), 400 mM DTT, 8% SDS (Ref: 1.13760.0100, Merck, Germany), 0.4% Bromophenol blue and 50% glycerol. After that, 20 µg of total protein per sample were loaded into polyacrylamide CRITERION TGX del 12% (Ref: 567-1045, BioRad Laboratories Inc, Spain) gels to separate proteins by molecular weight. A prestained standard molecular weight ruler was included (Ref: 161-0318, BioRad Laboratories Inc, Spain), in order to check the migration and transference of the proteins, as well as to facilitate the detection of the molecular weight of the target protein.

Electrophoresis was carried out in a Criterion Cell cuvette (BioRad, USA) using a running buffer containing 25 mM Tris Base, 200 mM glycine and 0.1% SDS (pH 8.3), at a voltage of 125 V for 15 minutes (to allow the package of the proteins) and at 200 V for the rest of the running phase.

Due to the fact that polyacrylamide gels do not allow antibody access to target proteins, proteins in the gel have to be transferred to a PVDF membrane (Ref: 170-4157, Transfer Pack Trans-Blot Turbo, BioRad Laboratories Inc, Spain) through electric current. In this study, transference was routinely performed in a Trans-Blot Turbo Transfer System (BioRad, USA) for 7 minutes.

11.3.2. Protein immunodetection

Once the proteins were transferred to a membrane all the incubations were made in tris phosphate saline + Tween buffer (TBS-T) (50 mM Tris Base, 200 mM NaCl, 0.05% Tween-20, pH 7.4) at 0.5 %. After blocking the unspecific binding sites with 5% BSA and 1% normal goat serum (NGS) (Ref:S-1000, Vector Laboratories, USA) in TBS-T for 1 hour at RT, membranes were incubated overnight at 4 ºC with the primary antibody in blocking buffer (Table 2). Membranes were subsequently washed 3 times for 10 minutes at RT with TBS-T to eliminate excess of antibody, and incubated for 1 hour at RT with an HRP-conjugated secondary antibody (Table 2). Following 3 washes for 10 minutes with TBS-T and an additional wash in TBS (50 mM Tris Base, 200 mM NaCl, pH 7.4) at RT, antibody labeling was visualized with an enhanced chemiluminescence kit (Ref: RPN 2232, GE Healthcare Life Science, UK). The luminescence of the reaction product was detected in a personal scanner Licor C-DiGit (Li-Cor, Bonsai Advanced Technologies SL, Spain) and visualized with the Image Studio Lite 4.0 software (Li-Cor, Bonsai Advanced Technologies SL, Spain). After developing, membrane was recovered again and incubated with a solution for washing antibodies linked to the membrane (stripping) (Ref: 21059, Thermo Fisher Scientific,USA) for 20 minutes at RT in order to repeat the protein immunodetection with different primary and secondary antibodies performing the same procedure previously described. It was performed for those experiments in which it was necessary to detect several antibodies in the same membrane, such as the detection of phosphorilated isoforms and total levels of one protein (Figure 29).

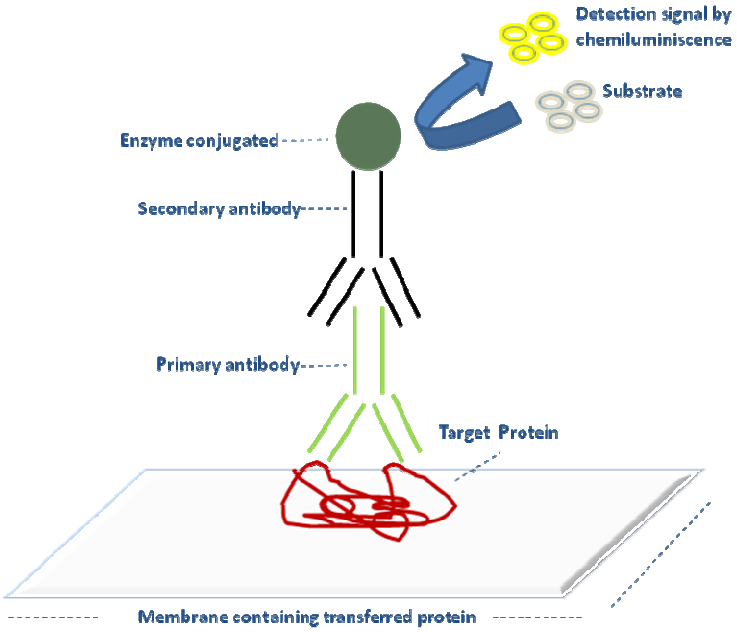

Figure 29. Schematic representation of protein detection by western blot.

The intensity of the obtained band was quantified by densitometry analysis using the Image Studio Lite 4.0 software (Li-Cor, Bonsai Advanced Technologies SL, Spain). Results were normalized to β-actin to correct errors in sample loading and/or protein transfer, except p-Akt which was normalized with Akt.

First antibody	Secondary antibody
Rabbit anti-Phospho-Akt (Ser 473); 1:1000 (Ref: 9271, Cell Signaling Technology Inc, USA)	Anti-rabbit IgG peroxidase conjugate; 1:2000 (Ref: A-6154, Sigma-Aldrich, Spain)
Rabbit anti-Akt; 1:1000 (Ref: 9272, Cell Signaling Technology Inc, USA)	Anti-rabbit IgG peroxidase conjugate; 1:2000 (Ref: A-6154, Sigma-Aldrich, Spain)
Rabbit anti-caspase 3 (H-277); 1:1000 (Ref: sc-7148 ,Santa Cruz Biotechnology Inc, Spain)	Anti-rabbit IgG peroxidase conjugate; 1:2000 (Ref: A-6154, Sigma-Aldrich, Spain)
Rabbit anti-TH; 1:1000 (Ref: AB-152, Millipore, USA)	Anti-rabbit IgG peroxidase conjugate; 1:2000 (Ref: A-6154, Sigma-Aldrich, Spain)
Rabbit anti-Actin; 1:2000 (Ref: A2066, Sigma-Aldrich, Spain)	Anti-rabbit IgG peroxidase conjugate; 1:2000 (Ref: A-6154, Sigma-Aldrich, Spain)

Table 2. Primary and secondary antibodies used for protein detection and quantification.

12. Statistical analysis

All values are expressed as the mean ± SE (standard error). All statistical analysis was performed with GraphPad Prism (v 5; GraphPad Software, Inc., La Jolla, CA, USA) and SPSS Statistics (v 20; IBM Corporation, Armonk, NY, USA). Prior to analysis, the Shapiro–Wilk test was used to assess the normal distribution of samples, and the Levene test was used to determine the homogeneity of variance. One-way analysis of variance (ANOVA) with the Tamhane post hoc test was used to explore differences between groups in multiple comparisons. In the behavioral studies, we used Student's *t*-test to compare intergroup differences and differences between rostro-caudal gradients within each experimental group. Values are considered statistically significant when $p<0.05$.

V. RESULTS

Results were divided into three assays according to the severity of the PD model and the treatments performed. A morphological approach for each model was described. In contrast, functional assessment was only assigned to describe the effects of the treatments.

In addition, all of the rats included in each study gained weight and none of them presented differences in weight gain between the experimental groups at any time point ($p > 0.05$).

1. Assay I: Morphological characterization of a Severe model of Parkinson's disease and effects of microencapsulated neurotrophic factors

Since unilateral 6-OHDA lesion of the nigrostriatal projection was chosen as a possible model for the evaluation of treatment based on MS loaded with NTFs, the criteria for successful surgery and appropriateness of the produced lesion had to be developed first.

In the rat, the most complete unilateral lesions are achieved via injection of the toxin into the MFB where the ascending nigrostriatal pathway is quite compact (Heuer et al., 2012).Thus, we first examined the model assessing the lesion induced by 6-OHDA injection in the MFB and by saline solution as control of lesion, in order to describe morphologically the model. In contrast, functional evaluation was not assessed due to the fact that behavioral test between saline group and 6-OHDA group had not sense.

Then, once the severe lesion induced by 6-OHDA into MFB was morphologically described, we proceed to study the effectiveness of the treatment in this model to test functional and morphologically the suitability of the model. For this purpose rats lesioned with 6-OHDA were used to assess the treatment based on injecting MS loaded with VEGF and GDNF into striatum individually and in combination.

Group	Number (n)	Comments
6-OHDA	5	6-OHDA lesion
Saline	3	Saline solution injection
Empty-MS	5	6-OHDA lesion, striatal administration of empty MS
VEGF-MS	9	6-OHDA lesion, striatal administration of MS loaded with 2.5 µg VEGF
GDNF-MS	9	6-OHDA lesion, striatal administration of MS loaded with 2.5 µg GDNF
VEGF+GDNF-MS	9	6-OHDA lesion, striatal administration of MS loaded with 2.5 µg VEGF and 2.5 µg GDNF

Table 3. Experimental groups from Assay 1 for each condition. Abbreviations: 6-OHDA, 6-hydroxydopamine, MS, microspheres, VEGF, vascular endothelial growth factor, GDNF, glial cell line-derived neurotrophic factor.

Thus, for this study different experimental groups were used. Groups were assigned according to the description of the model or the treatment (Table 3).

The experimental design of assay 1 (Figure 30) runs over almost 5 months demanding weekly hard tasks.

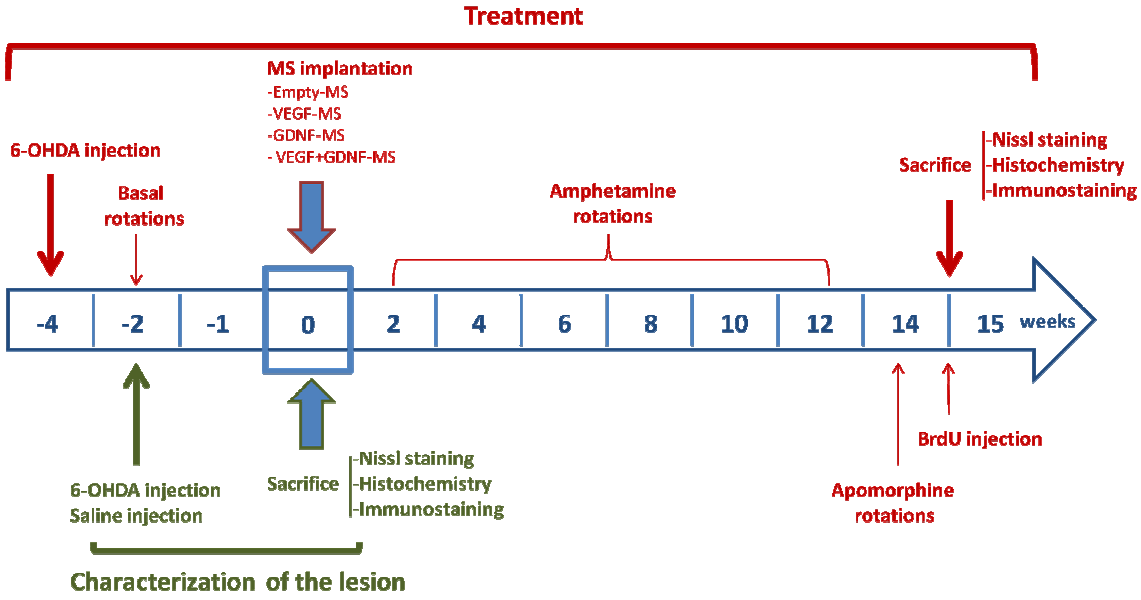

Figure 30. Time course for characterization of the lesion into medial forebrain bundle (green) and for the microsphere treatment (red). Abbreviations: 6-OHDA, 6-hydroxydopamine; MS, microspheres; BrdU: bromodeoxyUridine.

1.1. Morphological features of the Severe model of Parkinson's disease

Sprague Dawley rats were a suited for an effective and reproducible stereotaxic approach to the MFB. The dose of 6-OHDA was used to achieve the complete lesion of the nigrostriatal system, because all rats in this study exhibited more than 3 rotations per minute in the rotational tests.

After three weeks of injecting 6-OHDA or saline solution into MFB, rats were sacrificed by transcardial perfusion, brains were removed and sections from both striatum and SN were collected for morphological evaluation.

Brain surface in the right hemisphere showed the mark of puncture. Both experimental groups did not present any macroscopic difference (Figure 31).

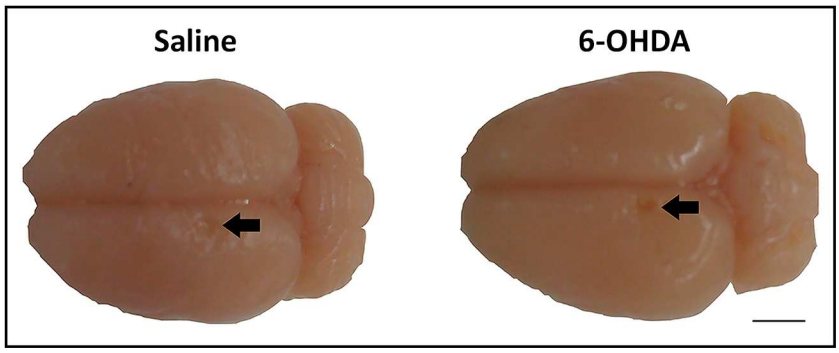

Figure 31. Rat brains representative of each experimental group. Black arrows indicate the puncture scar (lesioned hemisphere) where the 6-OHDA or saline solution was injected into medial forebrain bundle. Scale bar = 2 mm.

Histological changes were evaluated by Nissl staining, TH and GFAP immunostaining and by immunofluorescence for VEGF and OX-42 and histochemistry for LEA in striatum and SN.

To examine morphological changes in the structure, to confirm that the striatum itself was not structurally damaged by the surgical procedure, and to assess the extension of dopamine depletion in striatum and SN after 6-OHDA or saline solution administration, Nissl staining and TH immunostaining was developed in serial coronal sections.

Coronal slices corresponding on Nissl and TH staining respectively from striatum and SN in saline rats did not reveal any morphological change. However, 6-OHDA injection into MFB decreased almost completely the positivity for TH in striatum and SN compared to animals receiving saline alone, confirming the success of the complete MFB lesion (Figure 32). Moreover, macroscopic examination of the Nissl-stained sections showed that rats injected with 6-OHDA had enlargement of the ipsilateral ventricle on the lesioned hemisphere; but comparing ipsi- and contralateral striatum is to be noted the retraction of one (Figure 32e). Nissl-staining for SN in this group also revealed weakly Nissl-stained areas corresponding to the lack of neurons in the ipsilateral region and this is also associated with the loss of positivity observed in TH immunostaining (Figure 32e, f, g, h).

Nevertheless, there were no differences between both groups in terms of injure to other adjacent structures.

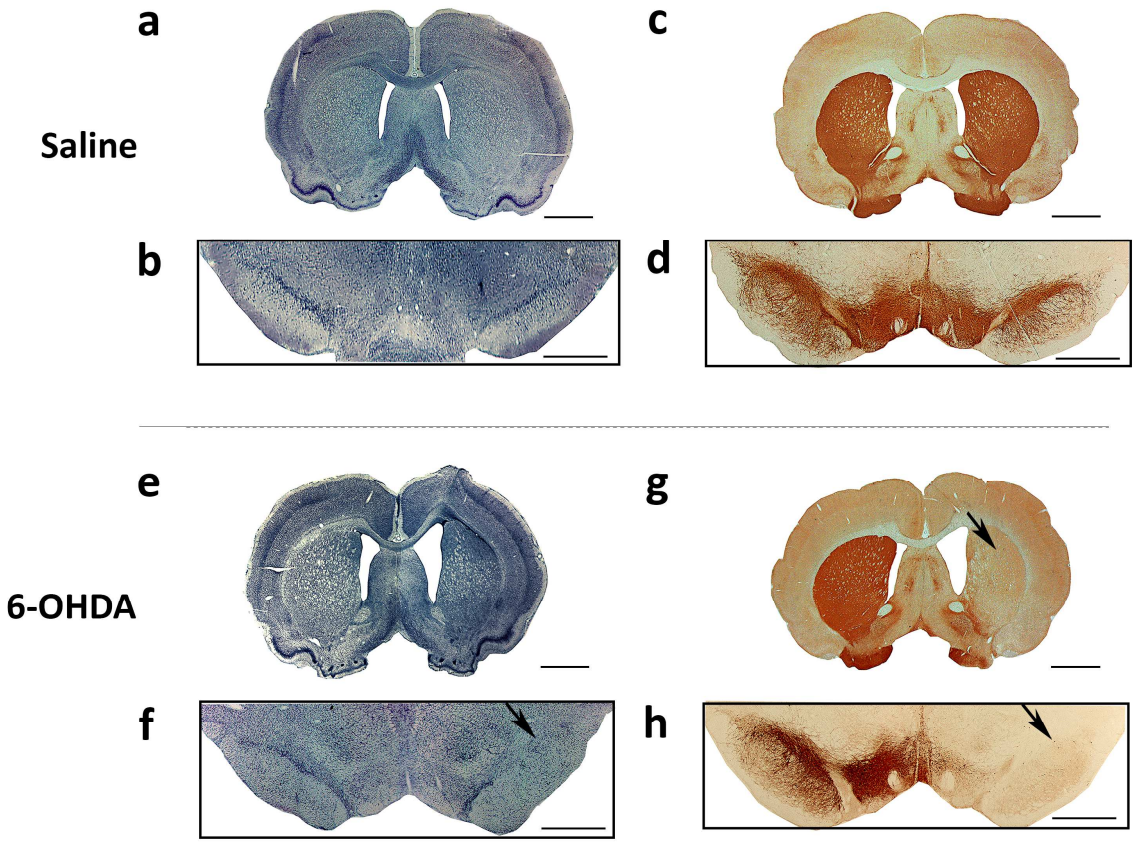

Figure 32. **Loss of staining after 6-OHDA administration**. (**a-d**) Coronal sections from the saline group, stained for Nissl (**a, b**) and tyrosine hydroxylase (TH) immunostaining (**c, d**). (**e-h**) Coronal sections from the 6-OHDA group, stained for Nissl (**e, f**) and TH immunostaining (**g, h**). The black arrow indicates the loss of neuron somata in the substantia nigra (SN) (**f**) and the lack of TH immunoreactivity in the striatum and SN due to 6-OHDA (**g, h**). Scale bar (**b, d, f, h**) = 1 mm; scale bar (**a, c, e, g**) = 2 mm.

We studied astrocytic activation characterized by GFAP upregulation in the Severe model of PD. For that purpose we compared astrocytic activation at ipsilateral and contralateral side to the lesion in striatum and SN in both groups, respectively.

There was no difference in striatum between saline and 6-OHDA group, showing both groups similar GFAP positivity in both hemispheres (Figure 33).

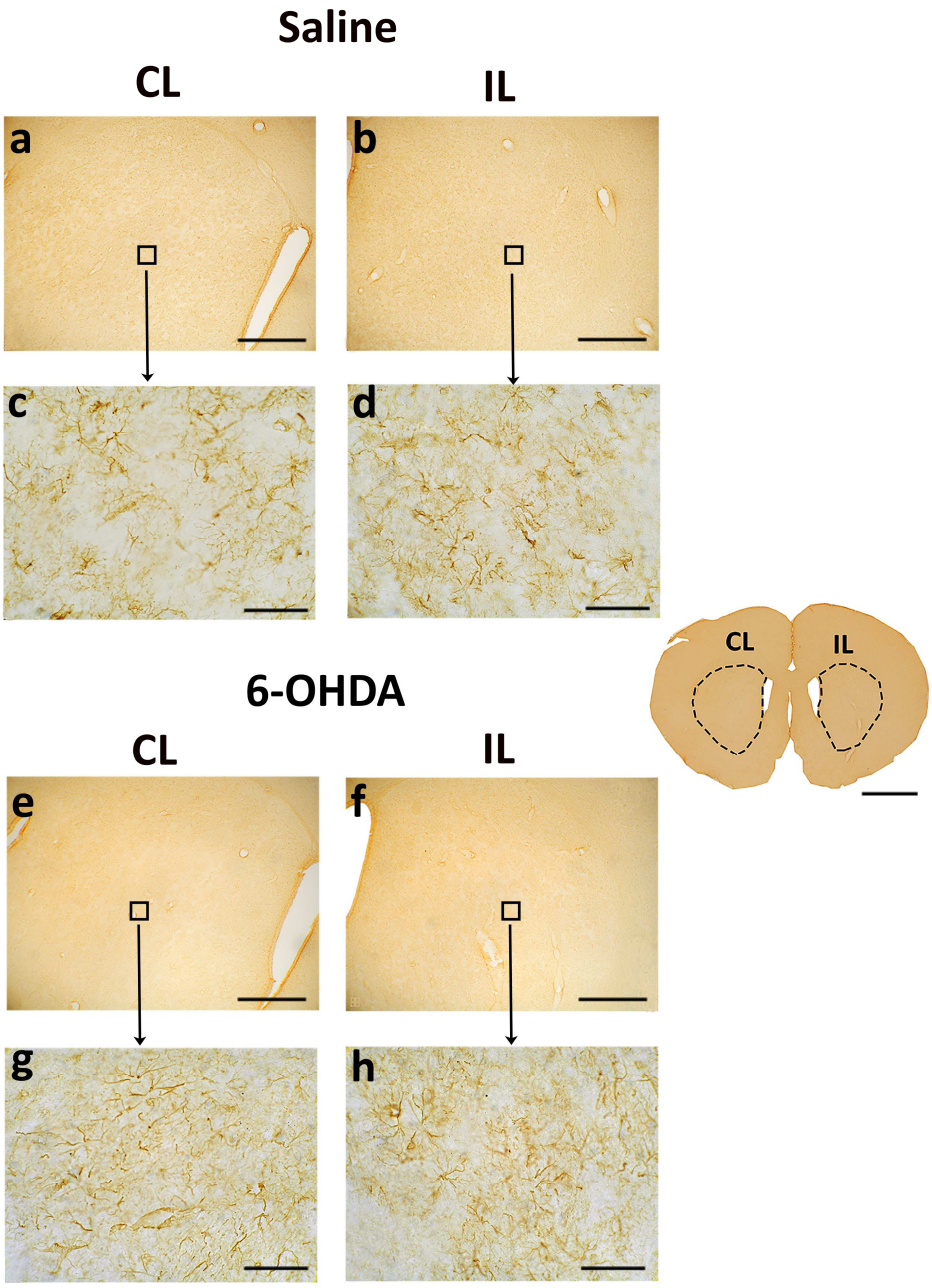

Figure 33. GFAP staining in coronal sections of ipsilateral and contralateral hemispheres of striata from rats injected with 6-OHDA or saline solution into the medial forebrain bundle. Photomicrographs at different magnifications from the striatum of the saline (**a-d**) and 6-OHDA groups (**e-h**). While (**a, b, e, f**) show an overview of these structures, (**c, d, g, h**) show higher magnifications of the area in the rectangle depicted above. In the middle of the figure a representative striatum is represented with delimited contralateral (CL) and ipsilateral (IL) regions, scale bar= 2 mm. Scale bars (**a, b, d, f**) = 500 µm; (**c, d, g, h**) = 50 µm.

In contrast, 6-OHDA group showed in the SN an increase of positivity for GFAP cells in the lesioned side compared to the contralateral hemisphere (Figure 34).

However, this GFAP immunoreactivity seen in the ipsilateral region was not very strong in saline group. The nigrostriatal damage produced by 6-OHDA injection in MFB resulted in apparently more intense staining of astrocytic cell bodies with more branched appearance than the injection of saline solution in the ipsilateral hemisphere of SN (Figure 34h).

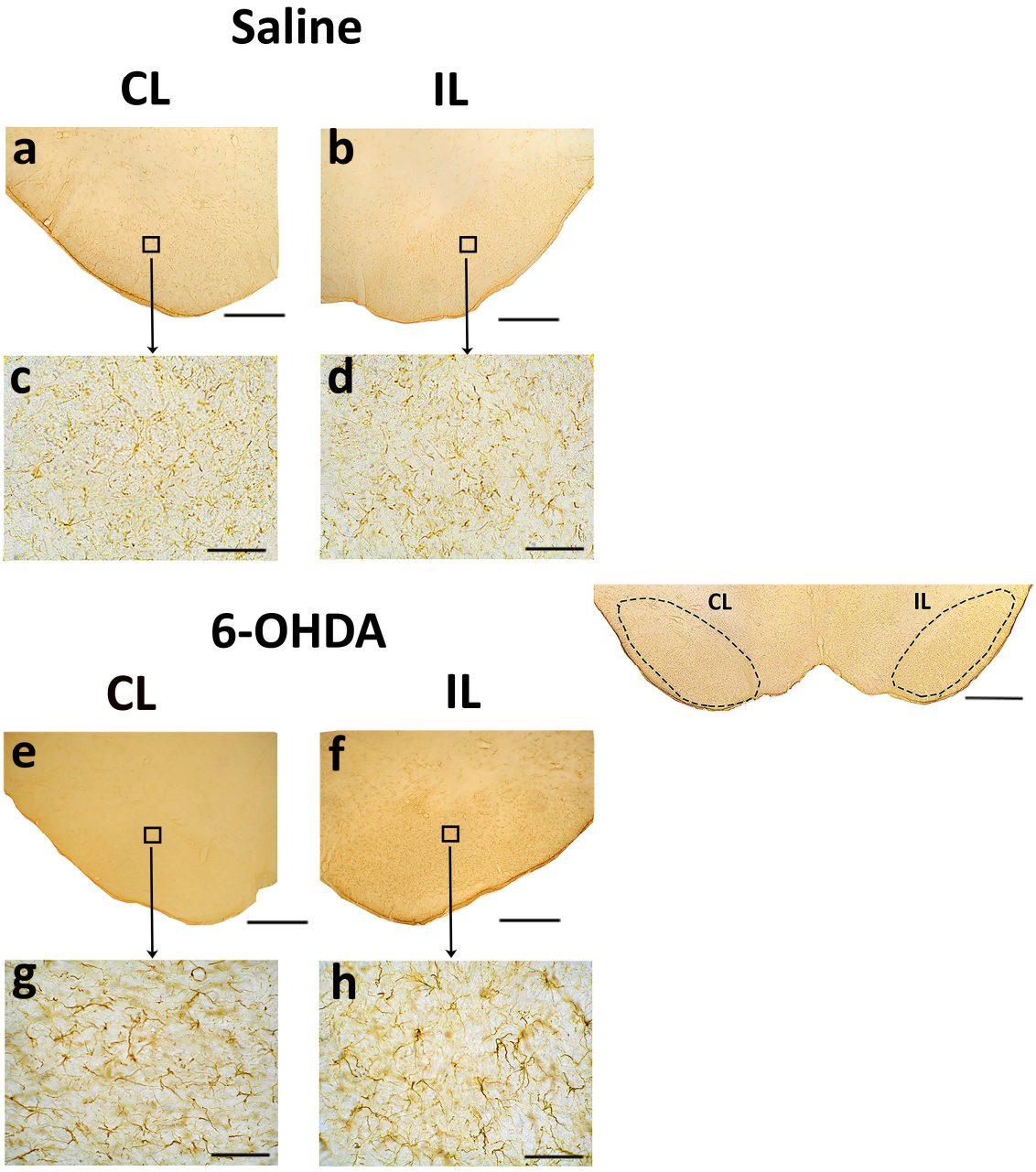

Figure 34. GFAP staining in coronal sections of ipsilateral and contralateral hemispheres of the substantia nigra (SN) of rats injected with 6-OHDA or saline solution into the medial forebrain bundle. Photomicrographs at different magnifications of the SN of the saline group (**a-d**) and 6-OHDA group (**e-h**). While (**a, b, e, f**) show an overview of these structures, (**c, d, g, h**) show higher magnifications of the area in the rectangle depicted above. In the middle of the figure a representative SN is shown with delimited contralateral (CL) and ipsilateral (IL) regions, scale bar= 2 mm. Scale bars: (**a, b, d, f**) = 500 µm; (**c, d, g, h**) = 50 µm.

1.1.1. Quantitative analysis

The effects of 6-OHDA and saline injection into MFB on dopaminergic system were evaluated measuring the TH-ir and the vascular density in striatum and SN by stereology. Measurements were taken place considering the entire structure and three rostro-caudal sections to determine whether 6-OHDA or the simple lesion due to inject saline solution differentially affected to the innervations throughout the striatal complex and to the survival of the neurons in the SN from rostral to caudal levels.

1.1.1.1. Injection of 6-OHDA into the medial forebrain bundle caused a loss of TH-ir and tissue retraction in the injured side of the striatum

To evaluate the TH-ir dopaminergic fibers in striatum, the TH-immunonegative volume of CPC was measured as a histological alternative to IOD. 6-OHDA group decreased almost completely the TH-positivity in the lesioned striatum compared to saline group which did not present loss of the TH-positivity (Figure 35a). The TH-immunonegative volume in rats received 6-OHDA into MFB in the ipsilateral striatum was 3.06±0.16 mm^3, 94.21±2.8 % respect to the contralateral one and in rats injected with saline solution was 0±0 mm^3 and 0±0 % (***p<0.001; Student's *t*-test) (Figure 35a). The intact TH-ir volume observed in saline group showed that the saline administration into MFB did not affect to the TH-positivity in the striatum. In this context, saline and 6-OHDA group did not show a rostro-caudal gradient for the TH-ir in striatum. However, due to the fact that 6-OHDA injection originated an extreme loss of TH-positivity along the rostro-caudal axis, saline and 6-OHDA group showed statistically significant differences in all rostro-caudal sections (***p <0.001; one way ANOVA) (Figure 35b).

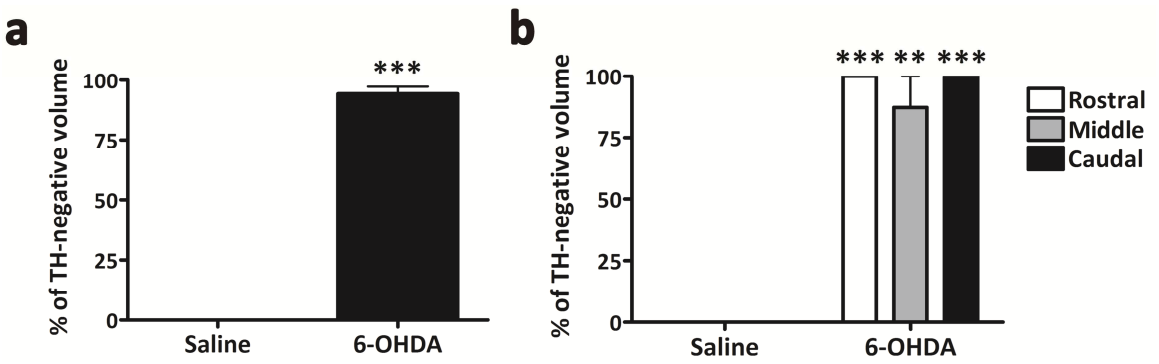

Figure 35. Injection of 6-OHDA into the medial forebrain bundle decreases almost completely the tyrosine hydroxylase (TH)-positive volume in the striatum. (**a**) The % of TH-negative volume in 6-OHDA was close to 100%; in contrast, the saline group did not show loss of TH positivity in the striatum. Significance ***p<0.001 6-OHDA *vs.* saline group. (**b**) There was no rostro-caudal gradient in either group. Data are shown as the mean±SE.

The enlargement of the ipsilateral ventricle in 6-OHDA group described previously in the morphological analysis was quantified. It was probably as a consequence of the tissue retraction produced during the administration of 6-OHDA by the puncture injury. This tissue retraction was measured on TH-immunostained sections in both experimental groups and it was expressed as a percentage of the volume occupied by the injured CPC with respect to the contralateral non-lesioned hemisphere considered as 100%. The volume obtained in the ipsilateral CPC in vehicle group was 3.48±0.14 mm^3 and 3.7±0.16 mm^3 on the contralateral side, showing a 5.4±0.82% of tissue retraction. In rats received 6-OHDA the ipsilateral volume was 3.35±0.13 mm^3 and in contralateral hemisphere the volume was 3.74±0.13 mm^3, showing a 10.21±1.54% of tissue retraction. These results showed that 6-OHDA group increased more the tissue retraction than saline group and these results were statistically significant (**p<0.01; Student's *t*-test) (Figure 36a). On the other hand, these data showed that the lesion into MFB was the responsible for the decrease of 5% in the ipsilateral volume on both groups (Figure 36a). Furthermore, this tissue retraction decreased from rostral to caudal sections in both experimental groups (Figure 36b).

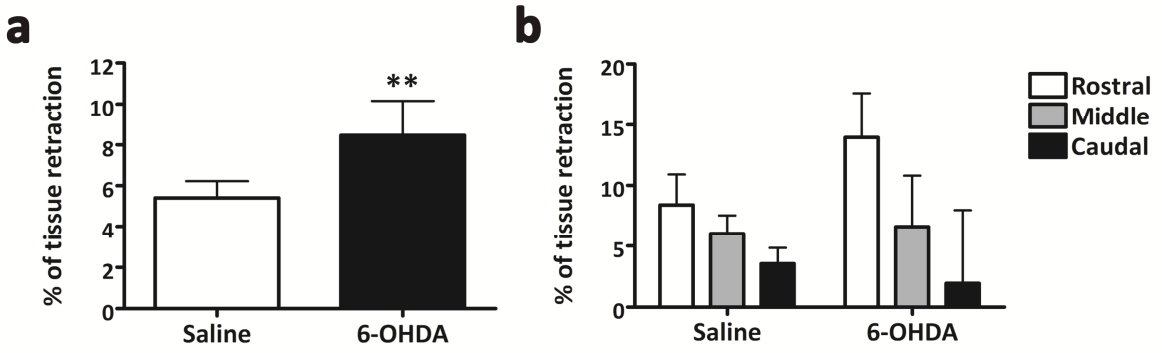

Figure 36. Tissue retraction. The 6-OHDA group showed more tissue retraction than the saline group. (**a**) Significant increase in tissue retraction after 6-OHDA injection. Significance **p<0.01 6-OHDA *vs.* saline. (**b**) There was a tendency towards decreased tissue retraction from rostral to caudal levels in both groups. Data are shown as mean±SE.

1.1.1.2. Gradual loss of TH-ir cells and axodendritic network in the substantia nigra due to the unilateral administration of 6-OHDA into the medial forebrain bundle following a rostro-caudal gradient

TH-immunohistochemical analysis showed a significant depletion in the number of TH-ir neurons and ADN in 6-OHDA group, remaining only 5.54±2.25% of positive neurons and 3.81±0.75% of TH-ir ADN in the ipsilateral side respect to contralateral one. In contrast, the effect of saline solution in the number of neurons and axodendritic network (ADN) was not stronger, remaining 74.96±8.86% of TH-ir neurons and 68.37±2.32% of TH-ir ADN in the lesioned hemisphere respect to the non-lesioned side (Figure 37a, c). Both experimental groups were statistically different regarding the number of TH-ir neurons and ADN density (***p<0.000; Student's *t*-test). Remarkably, the puncture was responsible for the loss of around 30% of TH-ir neurons and ADN respect to the non-lesioned side in saline group (Figure 37a, c).

When rostro-caudal sections of SN were analyzed for neuronal density and ADN density, 6-OHDA group and saline group decreased these values rostro-caudally. However, rats received 6-OHDA presented significantly a lower neuronal density and a lower ADN density at all considered levels than rats injected with saline solution (Figure 37b, d).

Measurements for the percentage of TH-ir neurons in 6-OHDA group were 6.24±3.9% at rostral, 2.31±0.28% at middle, and 0±0% at the caudal sections; and 74.81±7.59% at rostral, 74.44±6.44% at middle, and 53.64±10.03% at the caudal sections for saline group. Saline group and 6-OHDA group were statistically different at all analyzed levels (***p<0.000, for the rostral sections, ***p<0.000, for the middle sections, ***p<0.000 for the caudal sections; Student's *t*-test) (Figure 37b). There was also statistically significant difference between the rostral and the caudal sections within saline group (*p<0.05; ANOVA) (Figure 37b).

Regarding rostral, middle and caudal levels of the SN, the percentage of TH-ir ADN density for the 6-OHDA group was 7.64±3.1%, 3.72±1.15% and 2.87±1.1% for the rostral, middle and caudal sections respectively. In saline group was not found remarkable differences in the three analyzed levels. There were statistically significant differences between both experimental groups at all studied levels (***p<0.000, for the rostral sections, ***p<0.000, for the middle sections, **p<0.01 for the caudal sections; Student's *t*-test) (Figure 37d).

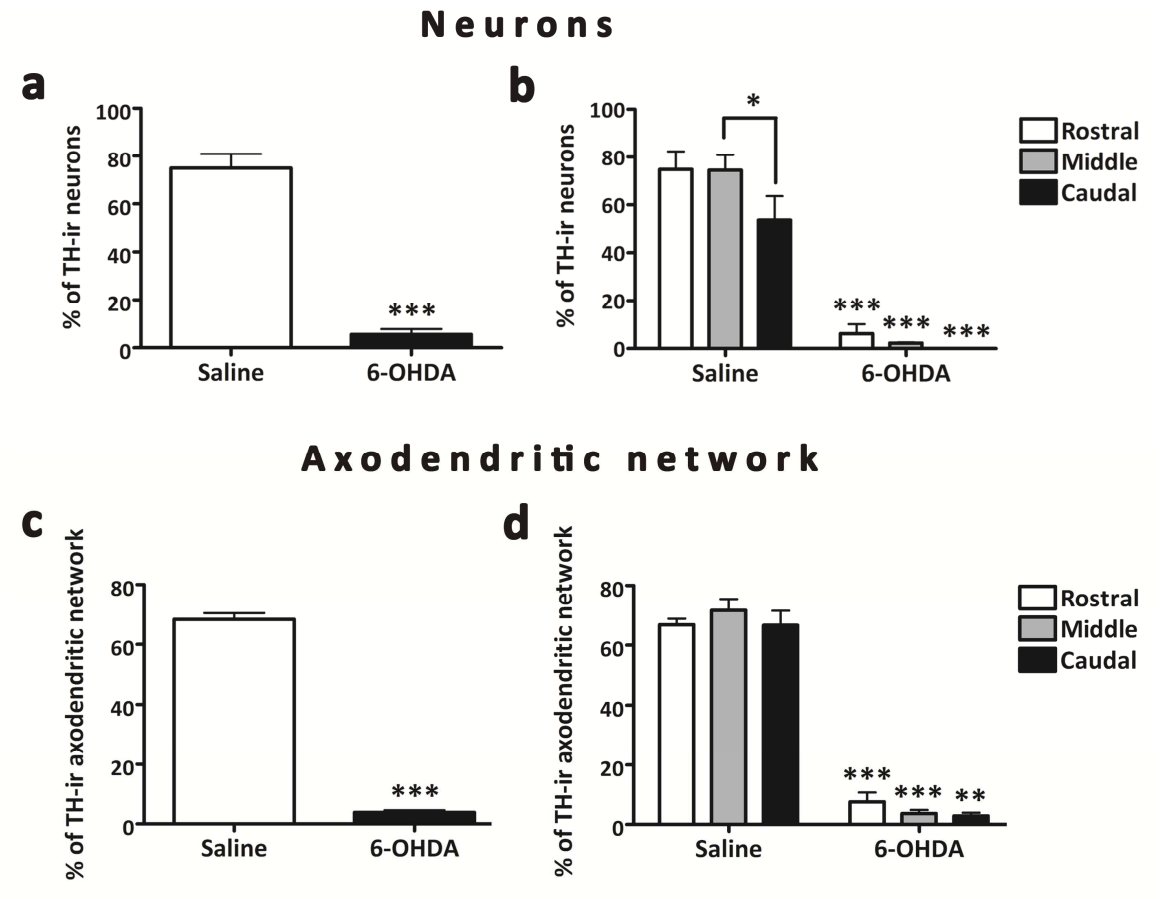

Figure 37. 6-OHDA injection into the medial forebrain bundle induces loss of tyrosine hydroxylase-immunoreactive (TH-ir) neurons in the substantia nigra (SN). (**a**) 6-OHDA administration produced a significant loss of TH-ir neurons in the SN. Significance ***p<0.001 6-OHDA *vs.* saline group. (**b**) Both groups showed a rostro-caudal gradient, which decreased from rostral to caudal levels. Significance ***p<0.001 6-OHDA *vs.* saline group in rostral, middle and caudal sections. * p<0.005 middle section *vs.* caudal section in the saline group. (**c**) The 6-OHDA group presented the most loss of axodendritic network (ADN). Significance ***p<0.001 6-OHDA *vs.* saline group. (**d**) Only the 6-OHDA group showed a rostro-caudal distribution of ADN. Significance ***p<0.001 group in rostral and middle sections. Significance ***p<0.01 6-OHDA *vs.* saline group in caudal sections. Data are shown as the mean±SE.

1.1.1.3. No effect was observed on microvascular density after 6-OHDA or saline solution administration

Microvessels density was measured by butyrylcholinesterase histochemistry, which is a reproducible and reliable method (Argandoña y Lafuente, 1996) that exposes the complete capillary network (vessels between 5-50 µm) homogeneously in every brain areas on a thick section. This method is ideal for the quantification by stereology.

Results showed that the microvessel density was similar in rats receiving 6-OHDA and saline solution in striatum and SN and in both hemispheres. In addition, looking at the rostro-caudal sections in striatum and SN, 6-OHDA and saline rats trended to decrease the vascular density along the rostro-caudal axis in both studied anatomical regions (Figure 38).

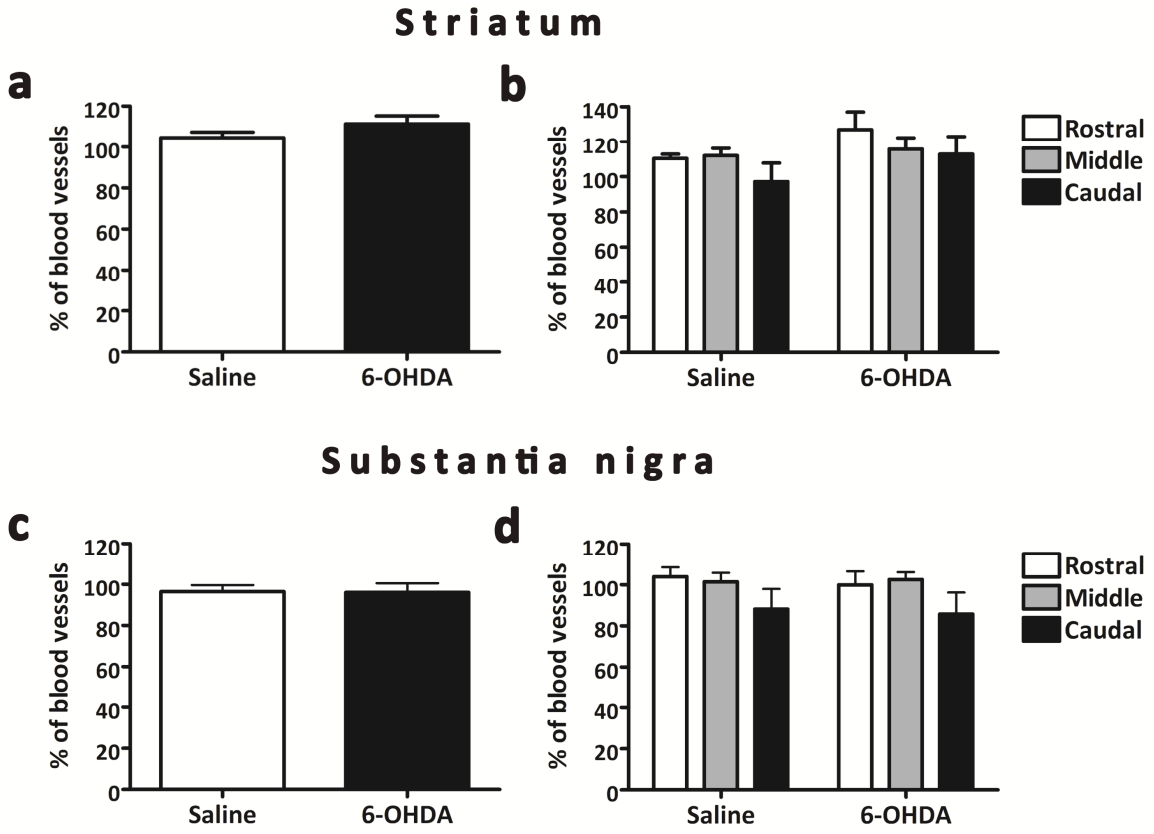

Figure 38. 6-OHDA injected into the medial forebrain bundle did not induce changes in microvascular density. (**a, c**) No changes were found in microvascular density in the striatum and substantia nigra (SN) between both experimental groups. (**b, d**) Both groups showed a tendency to decrease the microvascular density from rostral to caudal sections in striatum and SN. Data are shown as mean±SE.

1.2. Treatment with microencapsulated neurotrophic factors

In order to evaluate the degree of the lesion or recovery after MS implantation rotational behavior test and histological evaluation of the brain slices have been performed after 14 weeks of MS administration in rats lesioned with 6-OHDA after four weeks previously.

All the rats in the study were subjected to the rotational test at 2 weeks after the 6-OHDA lesion to confirm that the lesion was complete and to exclude from the study those rats which exhibited less than 3 rotations per min in order to study the effectiveness of the treatment on the Severe model.

1.2.1. Motor evaluation

The motor function was proved with the amphetamine-induced rotation test. There were no differences in the basal number of rotations between the groups (Figure 39). The evolution in time of the mean number of amphetamine-induced rotations of the control group (empty-MS) showed a tendency to increase from 5.29±1.37 ipsilateral tpm at 0 week to 12.82±0.96 tpm at 12 weeks. Conversely, after GDNF-MS implantation, the number of rotations started to decline at week 4, but the differences between this group and the empty-MS treated group were statistically significant (one-way ANOVA, *$p<0.05$) only at 10 weeks (empty-MS: 14.84±1.399 tpm; GDNF-MS: 5.45±2.50 tpm) and 12 weeks (empty-MS: 12.82±1.45 tpm; GDNF-MS: 3.45±2.33 tpm) after implantation. VEGF-MS administration resulted in lower levels of ipsilateral rotations than those observed for empty-MS (empty-MS: 14.84±1.399 tpm; VEGF-MS: 7.78±1.96 tpm) at week 10. In this group, the number of rotations decreased beginning in week 8, although the decrease was not significant. The tendency of the combined group treated with both VEGF-MS and GDNF-MS (empty-MS: 12.82±1.45 tpm; VEGF+GDNF-MS: 6.37±1.15 tpm) at week 12 (not statistically significant) was similar to that of the GDNF-MS-treated group. The number of rotations began to decline in week 6, but the results were not as

pronounced as those obtained with the dose of GDNF-MS administered alone (Figure 39a).

To confirm the results obtained with amphetamine, rats were subjected to the apomorphine-induced rotational behavior test at week 14. While no statistically significant differences were observed in the number of rotations induced by apomorphine, a tendency was noted that confirms the results obtained in the previous rotational behaviour test. Therefore, Figure 39b showed that the empty-MS-treated group had the highest level of neuronal damage after 3 months of treatment due to its high number of contralateral rotations (Herrán et al., 2013). The GDNF-MS- and VEGF+GDNF-MS-treated groups had the best results with respect to damage area recovery, displaying fewer contralateral rotations (empty-MS: 3.94 ± 1.73 t/5 min; VEGF-MS: 2.69 ± 0.94 t/5 min; GDNF-MS: 1.19 ± 0.46 t/5 min; VEGF+GDNF-MS: 1.17 ± 0.55 t/5 min.

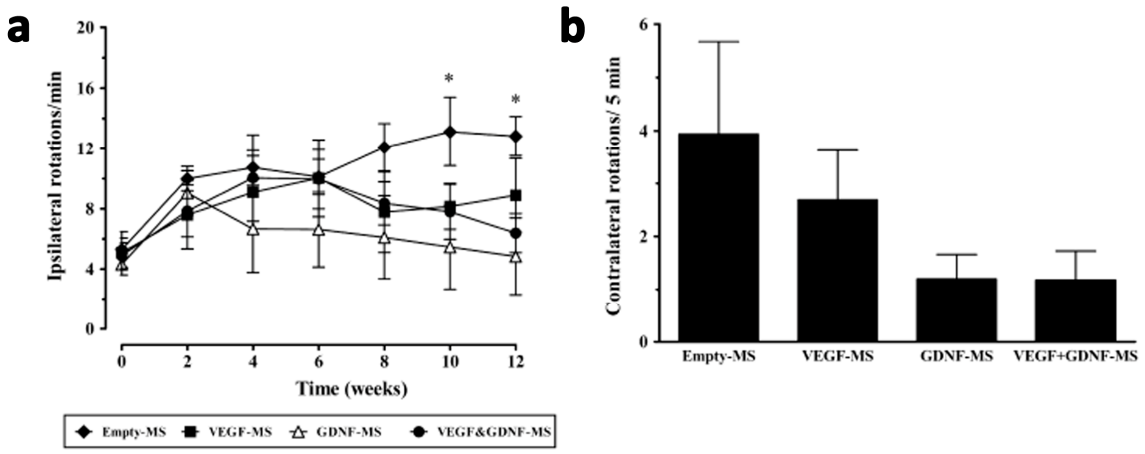

Figure 39. Behavioral tests to assess the functionality after neurotrophic factors administration (Herrán et al., 2013) (**a**) Data obtained from the amphetamine rotational behavior test after microspheres (MS) implantation after 12 weeks: black triangle: empty-MS; black square: VEGF-MS; open triangle: GDNF-MS; black circle: VEGF + GDNF-MS. The empty-MS and GDNF-MS showed statistically significant differences ($p < 0.05$). (**b**) The results obtained from the apomorphine rotational behavior test 14 weeks after implantation. The VEGF + GDNF-MS treated group shows the best recovery of the damaged area. The data are shown as the mean±standard desviation.

1.2.2. Histological changes

Rats were sacrificed after the apomorphine-test evaluation, at 14 week after MS administration. Rat brain surfaces presented macroscopically difference among the experimental groups. Rats received microspheres loaded with VEGF and GDNF had major mark in the right hemisphere than the other studied groups due to the volume of VEGF and GDNF administrated was high (Figure 40).

To examine the morphological changes occurred after MS administration and the effects of combined VEGF and GDNF delivery in striatum; Nissl staining and immunohistochemistry studies were carried out.

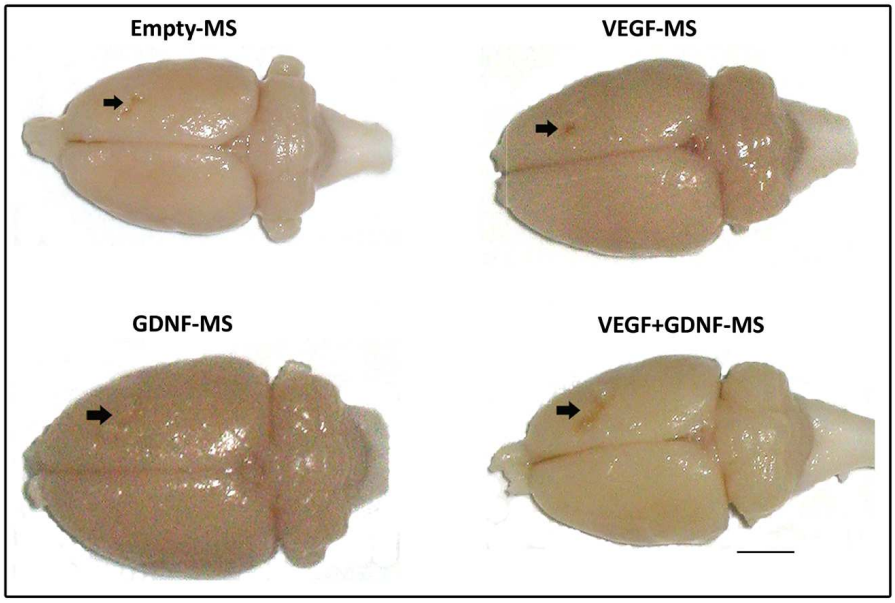

Figure 40. Rat brain surfaces from different groups. The black arrow indicates the puncture scar in the lesioned hemisphere in which the microspheres were injected. Scale bar = 2 mm.

Nissl-stained sections showed a heavily blue area corresponding to the needle track after administration of MS. It was also observed an enlarged ipsilateral ventricle with a contracted striatum on the injured hemisphere due to the subsequent striatal injection of MS and the effect of 6-OHDA lesion (Figure 41). In addition, along the needle

track, it was also possible to observe macrophages and hemosiderin. According to this, rats received VEGF and GDNF had more retracted the striatum than the other groups.

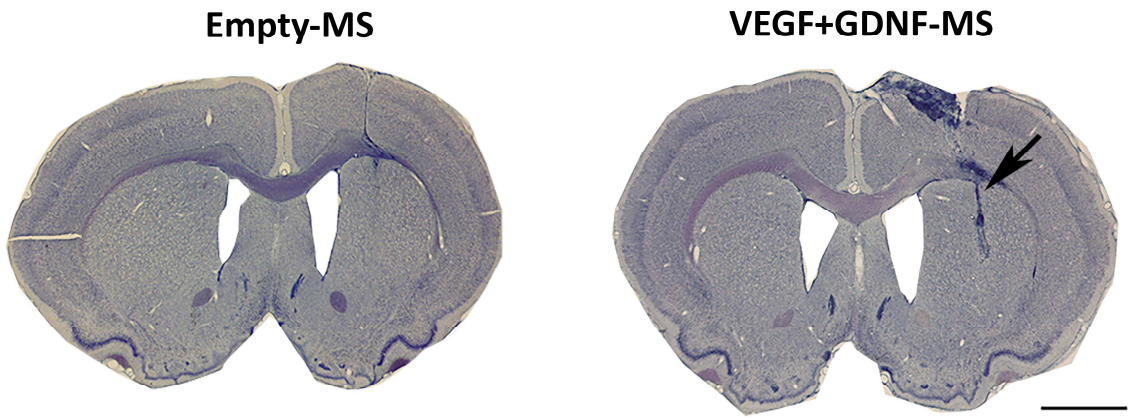

Figure 41 Coronal sections of rats injected with empty microspheres or with microspheres containing VEGF+GDNF at the level of the striatum. The black arrow points to the trajectory of the lesion in the injured hemisphere. Scale bar= 2 mm.

On the other hand, TH-immunostaining sections of striatum and SN revealed more positivity in rats receiving MS loaded with both NTFs than the groups receiving empty MS or the NTF individually (Figure 42).

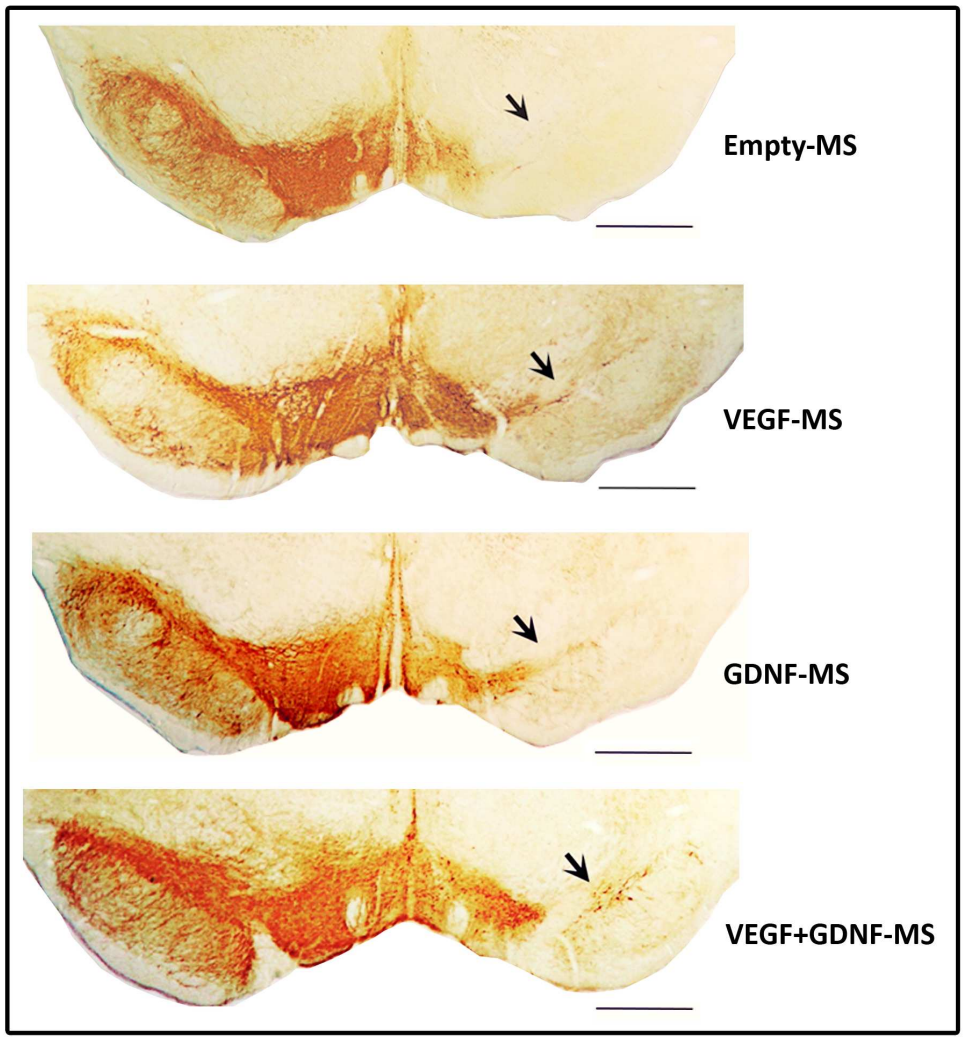

Figure 42. Representative picture of the substantia nigra (SN) after tyrosine hydroxylase (TH)-immunostaining of a control rat implanted with empty microspheres and rats treated with microspheres (MS) loaded with neurotrophic factors individually or in combination. The black arrow points to the SN of the lesioned hemisphere where VEGF+GDNF-MS administration increased regeneration. Scale bar = 1 mm.

Activation of astrocytes after MS implantation was evaluated by GFAP immunostaining. All groups showed increase of GFAP levels in the lesioned side compared to the non-lesioned hemisphere (Figure 43). The implantation of MS induced a remarkable GFAP reaction around the site of the injection (Figure 43b, d, f, h). However, rats receiving both NTFs presented the most expression of GFAP in the injured side of the striatum compared to the rest of studied groups (Figure 43a, b, c, d).

The astrocytes of ipsilateral hemisphere displayed a swollen soma and more branched appearance (Figure 43d, h). These processes suggested an activated state and up-regulation of astrocytes in the lesioned hemisphere.

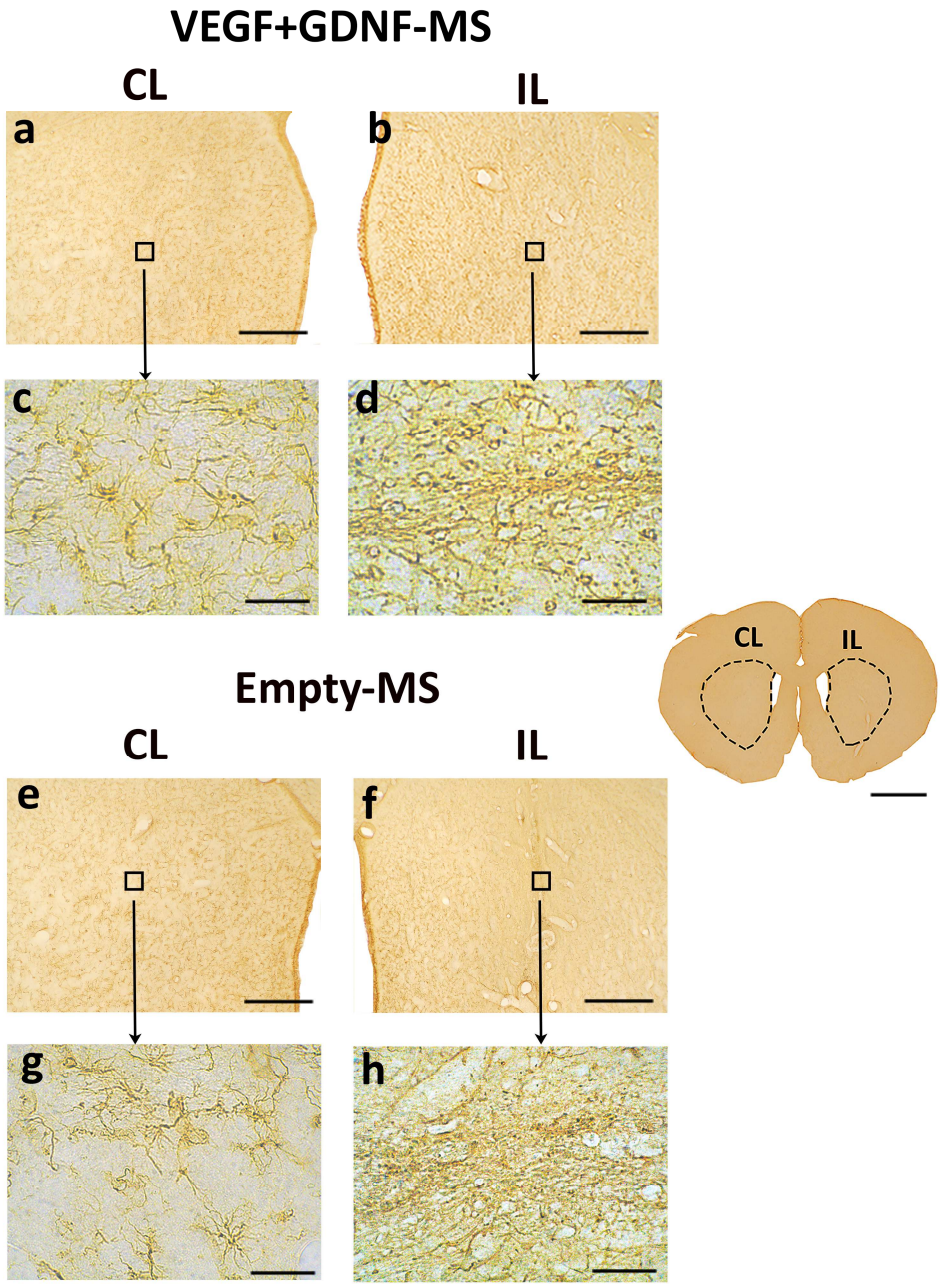

Figure 43. GFAP expression is increased after neurotrophic factors administration into the striatum. (**a-d**) Coronal sections of ipsilateral (IL) and contralateral (CL) hemispheres of the striatum stained with GFAP from lesioned rats treated with microspheres (MS) loaded with VEGF and GDNF. (**e-h**) Photomicrographs from the striatum of lesioned rats treated with empty-MS. While (**a, b, e, f**) show an overview of these structures, (**c, d, g, h**) show higher magnifications of the area in the rectangle depicted above. In the middle of the figure., a representative coronal section is shown with delimited CL and IL regions; scale bar = 2mm. Scale bars: (**a, b, d, f**) = 500 µm; (**c, d, g, h**) = 50 µm.

1.2.3. Proliferative effects of microspheres loaded with neurotrophic factors

To study possible expression of BrdU-positive cells along the SVZ striatum axis in rats treated with NTFs, rats were injected with 3 i.p. injections of BrdU (80 mg/kg) at 3-hour intervals. One hour after the last injection, animals were sacrificed and coronal brain sections were stained for nuclear BrdU incorporation.

Rats received NTFs showed a large number of cells BrdU-positive in the SVZ, indicating a high level of proliferation (Figure 44). In rats received empty-MS the number of BrdU detected in SVZ was decreased in the ipsilateral side respect to the contralateral one (60.16%) compared to the groups treated with NTFs. In fact, the increase in the percentage of BrdU-positive cells of the injured hemisphere respect to the contralateral one, was higher in groups received VEGF individually (286.04%) or combined with GDNF (160.62%) than the group received GDNF individually (95.48%) (Figure 44b). These changes were not statistically significant because BrdU analysis was only developed in two animals per group. Overall, these results highlighted the neurogenic and proliferative effect of VEGF in this model.

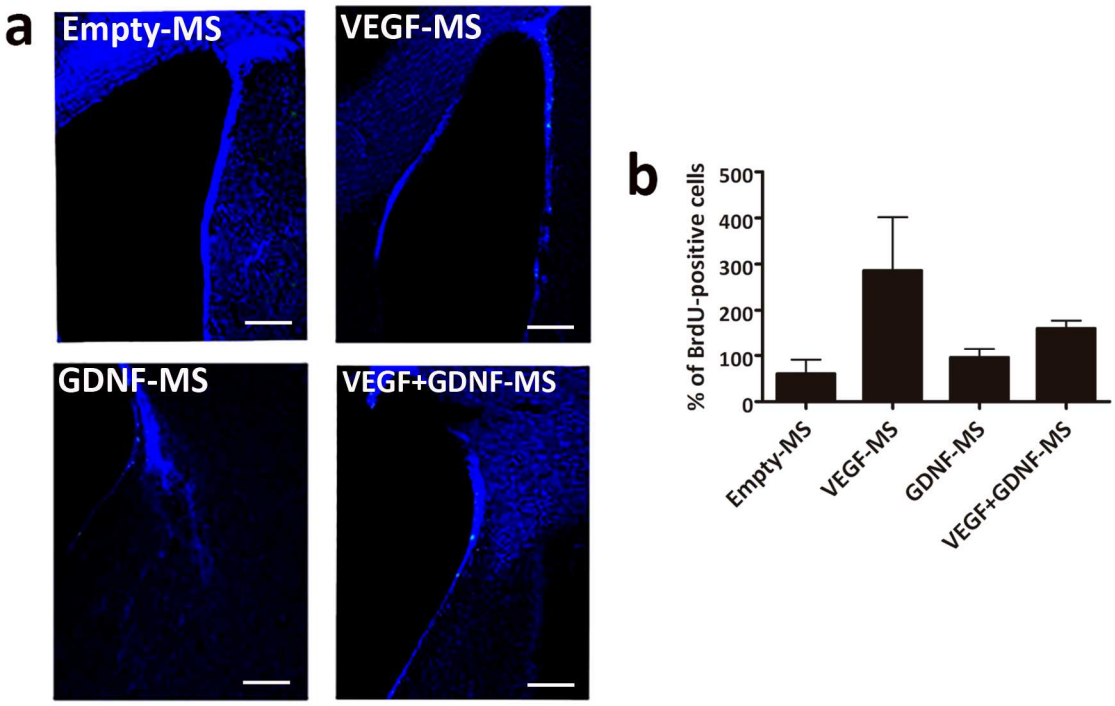

Figure 44. Effect of neurotrophic factors administration on proliferation. (a) Confocal photomicrographs for each experimental group showed the BrdU -positive nucleus in the subventricular zone (SVZ). **(b)** VEGF increased the percentage of BrdU-positive cells, whereas empty microspheres did not exhibit any effect on proliferation. Scale bar = 250 µm. Data are shown as means±SE.

1.2.4. Quantitative analyses

To assess stereological and morphological changes in the striatum and SN induced by the administration of MS into the striatum of 6-OHDA lesioned rats, tissue retraction, process occurred after MS implantation and 6-OHDA lesion, TH-immunoreactive cells and ADN were measured in the whole striatum and SN and along the rostro-caudal axis in both structures in order to evaluate the topological distribution of the dopaminergic system. Quantification of density of vessels was also carried out in order to find modifications related to angiogenesis after NTFs administration.

1.2.4.1. VEGF and GDNF in combination induced tissue retraction

Tissue retraction previously described was measured in order to estimate the morphological effects produced after MS implantation into the striatum of rats. Results showed that groups received MS loaded with GDNF in combination with VEGF or GDNF individually, presented more percentage of tissue retraction (19.13±2.34% and 18.94±1.54% respectively) than those groups received empty-MS (6.07±1.98%) or VEGF individually (10.09±0.98%) (Figure 45a). These differences were statistically significant respect to empty-MS group (**p<0.01, one-way ANOVA), and respect to VEGF-MS group (##p<0.01, one-way ANOVA), suggesting that the volume of both NTFs in MS should have been lower to reduce the damage.

Topological analysis indicated that tissue retraction decreased from rostral to caudal level at all groups considered because of the site of MS injection was closer to the rostral and middle sections (Figure 45b). In rats receiving empty-MS the tissue retraction was lower at all sections studied compared to the other groups. Statistically significant differences were found regarding the rostral and middle sections between empty-MS group (8.17±2.95% at rostral and 3.76±3.37% at middle level) and GDNF-MS group (21.34±3.43% and 16.45±2.89% respectively) (*p<0.05, one-way ANOVA) and regarding middle sections between empty-MS group (3.76±3.37%) and VEGF+GDNF-MS group (20.15±3.5%) (**p<0.01, one-way ANOVA). Differences within GDNF-MS group were also appreciated between rostral (21.34±3.43%) and caudal sections (9.86±4.7%) (*p<0.05, one-way ANOVA).

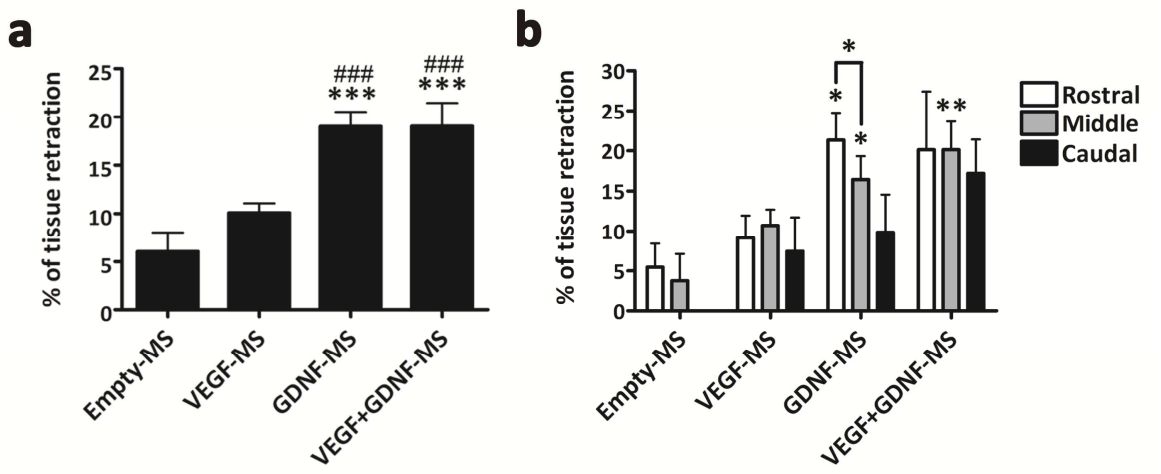

Figure 45. Quantification of tissue retraction in rats treated with microspheres. (**a**) The group treated with GDNF and the group treated with VEGF+GDNF showed a higher percentage of tissue retraction. Significance (***p<0.001, VEGF+GDNF-MS and GDNF-MS group *vs.* empty-MS; ### p<0.001 VEGF-GDNF-MS and GDNF group *vs.* VEGF-MS). (**b**) Tissue retraction decreased from rostral to caudal levels in all experimental groups, being statistically different in rostral and middle sections in the GDNF-group (*p<0.05 rostral *vs.* middle sections from the GDNF group). Statistical differences were also found in the rostral and middle sections of the GDNF-MS group and in the middle sections of the VEGF+GDNF-group with respect to the rostral and middle sections of the empty-MS group (*p<0.05 VEGF+GDNF group and GDNF-MS group *vs.* empty-MS). Data are shown as mean±SE.

1.2.4.2. Positive effects in the substantia nigra after VEGF and GDNF delivery

Measurements obtained after TH-immunostaining were based on changes seen in SN. The decrease in TH-ir caused by 6-OHDA was ameliorated when NTF was administrated individually or in combination (Figure 46). In fact, the number of TH-ir cells was higher in rats receiving VEGF and GDNF (26.71±4.28%), while rats received empty-MS showed an almost depletion of TH-ir cells (5.79±1.88% (Figure 46a). The percentage of TH-ir cells remaining in the injured side was also increased when rats received VEGF (11.88±3.22%) or GDNF (20.47±4.28%) individually in comparison to empty-MS group (5.79±1.88%). Differences were statistically significant between VEGF+GDNF-MS group and empty-MS group (**p<0.01, one-way ANOVA), and between GDNF-MS group and empty-MS group (**p<0.01, one-way ANOVA).

The topographical distribution revealed that the density of TH-ir neurons decreased from rostral to caudal levels at all groups (Figure 46b). Rats received VEGF

and GDNF showed the most recovery at all levels (39.68±4.72% at rostral, 23.74±3% at middle and 15.97±0.82% at caudal section) and differences were statistically significant between rostral and middle level (Figure 46b). Nevertheless, the most statistically significant differences were found at rostral level. Thus, there were statistically significant differences at rostral sections between empty-MS (6.13±3.69%) or VEGF-MS group (11.57±4.71%) respect to VEGF+GDNF-MS group (39.68±4.72%) (**p<0.01, one-way ANOVA). In addition, rats received GDNF also presented more remaining of TH-ir neuron at rostral level (28.62±4.4%) compared to empty-MS group (6.13±3.69%) (#p<0.05, one-way ANOVA) (Figure 46b).

The effect of GDNF administration was appreciated in the sprouting of ADN, which was higher when GDNF was individually administrated (Figure 46c). However, the differences in the percentage of TH-ir ADN remaining in the lesioned hemisphere respect to the contralateral one, between rats received GDNF alone (43.01±2.27%) or in combination (39.23±5.21%) were practically inexistent (Figure 46c). In contrast, the TH-ir density of ADN was statistically lower in rats received empty-MS (24.96±2.78%) or VEGF (27.48±3.27%) compared to rats received GDNF alone (**p<0.01, ## p<0.01; one-way ANOVA).

Distribution from rostral to caudal sections showed an increase in the TH-ir density of ADN on all sections of the GDNF-MS and VEGF+GDNF-MS group. However, no statistic differences were observed either between groups or into themselves (Figure 46d).

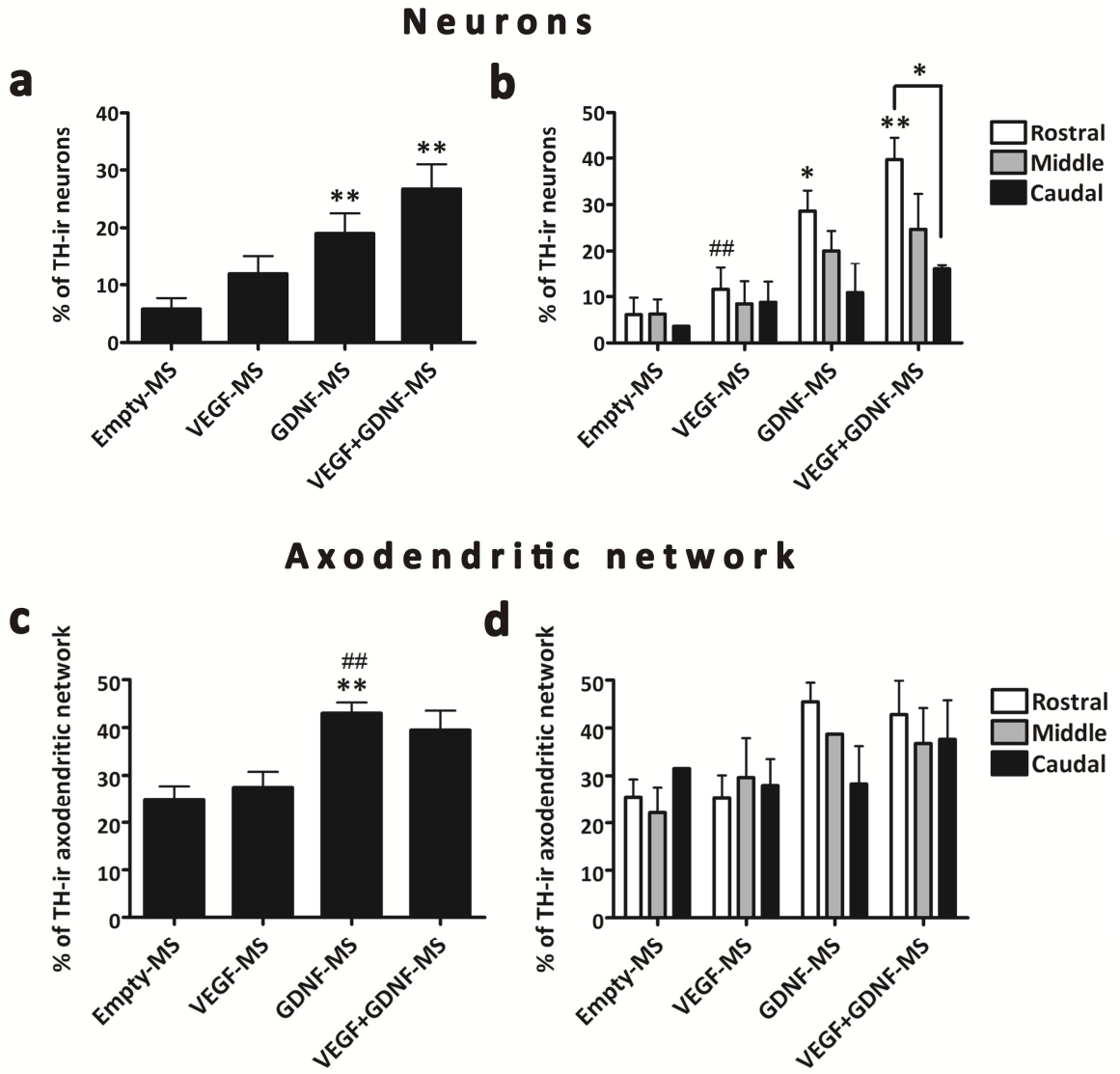

Figure 46. Recovery of neuronal density after VEGF and GDNF administration. (**a**) Rats treated with VEGF and GDNF in combination showed highest neuronal density. Significance (**p<0.01 VEGF+GDNF and GDNF-MS group *vs.* empty-MS). (**b**) Neuronal density decreased from rostral to caudal levels in all experimental groups, being statistically different at rostral and caudal levels in the VEFG+GDNF-MS group (*p<0.05 rostral sections *vs.* caudal sections in VEGF+GDNF-MS group). The highest difference was found at the rostral level between experimental groups (**p<0.01 VEGF+GDNF-MS group and GDNF-MS group *vs.* empty-MS, #p<0.05 VEGF-MS *vs.* VEGF+GDNF-MS group). (**c**) The GDNF-MS group and the VEGF+GDNF-MS group showed the highest percentage of axodendritic network (ADN). Significance (**p<0.01, GDNF-MS group *vs.* empty-MS; ##p <0.01, GDNF-MS group *vs.* VEGF-MS group). (**d**) Rats treated with GDNF individually and with VEGF and GDNF in combination showed a tendency to decrease the density of ADN from rostral to caudal parts. Data are shown as means±SE.

1.2.4.3. GDNF increased the density of microvessels

Microvascular density was measured in the striatum in order to examine changes in angiogenesis as a response of NTF implantation.

Administration of NTFs caused an increase in the density of vessels in comparison to the administration of empty-MS in the striatum (94.63±1.93%) (Figure 47a). Interestingly, when GDNF is injected individually the percentage of blood vessels remaining in the injured hemisphere was higher as compared to the non-lesioned hemisphere, reaching this group the most microvascular density (103.47±·2.23%). In contrast, in the other treated groups the density of vessels trends to be less in the lesioned side than in the contralateral one (Figure 47a). Rats received VEGF alone presented a percentage of microvascular density close to the 100% (99.95±1.51%) and in rats received VEGF and GDNF the density of vessels was a 97.04±2.54%. There were statistically significant differences between GDNF-MS group and empty-MS group (*p<0.05, one-way ANOVA).

Rostro-caudal distribution of vessels in striatum showed that the microvascular density decreased from rostral to caudal sections at all groups, indicating that the effect of NTF and of the lesion in the density of blood vessels was lower the more it was distanced from the site of the injection (Figure 47b). In fact, these differences from rostral to caudal levels were statistically significant in rats received VEGF and GDNF between middle (97.75±4.69%) and caudal levels (88.33±5.47%) respect to the rostral level (115.79±2.73%) (*p<0.05, one-way ANOVA). On the other hand, rats received MS loaded with GDNF presented the most density of vessels at all levels considered (120.41±5.16% at rostral, 104.7±7.16% and 104.7±8.22% at caudal sections). Differences were also statistically significant at rostral level between GDNF-MS group (120.41±5.16%) and empty-MS group (96.17±7.1%) (*p <0.05, one-way ANOVA).

These results showed that the dose used for VEGF in combination with GDNF in microspheres was high, highlighting its neuroprotective effect instead of its angiogenic effect.

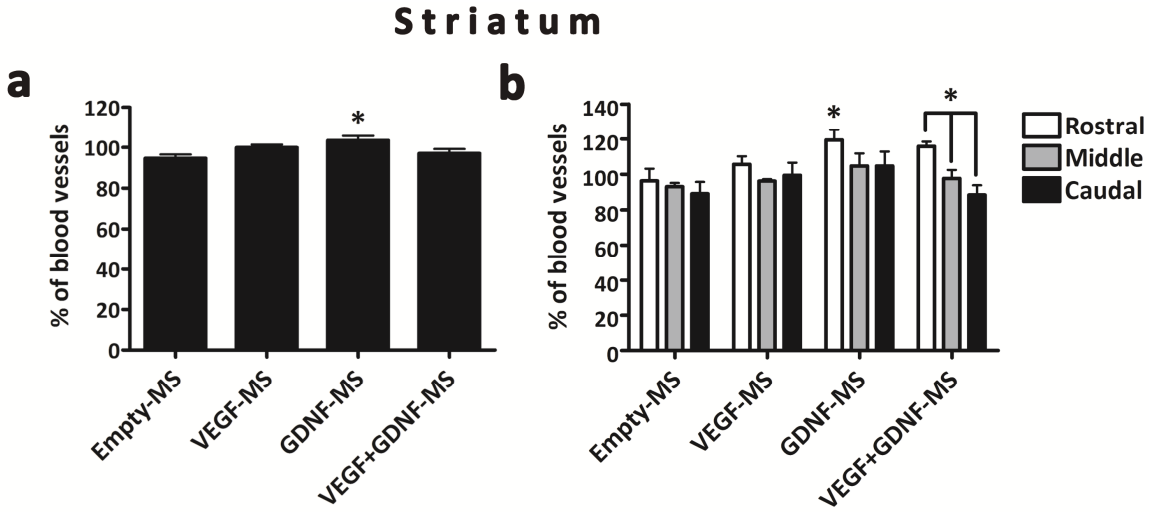

Figure 47 Microvascular density in the striatum of rats treated with microspheres. (**a**) The GDNF-MS group showed the highest microvascular density in the striatum. Significance (*p<0.05 GDNF-MS group *vs.* empty-MS). (**b**) Experimental groups showed a rostro-caudal distribution of microvascular density in the striatum, decreasing from rostral to caudal parts. The VEGF+GDNF-MS group showed statistically significant differences between middle and caudal sections (#p<0.05 middle *vs.* caudal sections from VEGF+GDNF-MS group). Statistically significant differences were also reached in rostral sections between experimental groups (*p<0.05 GDNF-MS group *vs.* empty-MS group). Data are shown as means±SE.

2. Assay II: Morphological characterization of the Partial model of Parkinson's disease and effects of nanoencapsulated neurotrophic factors

Once assessed the Severe model and the treatment based on microspheres to ameliorate the effects of injecting 6-OHDA into MFB, Partial model was also examined in order to achieve rather selective lesion of the CPC. Following the clinical diagram showed in figure 1 this should be a PD model situated at diagnosis time. However, regarding the problems obtained with the size of particles and with the volume administrated of NTFs, in this study we used nanospheres and adjusted the volume of NTFs administrating low doses (half that of individual treatment) of VEGF-loaded PLGA NS and GDNF-loaded PLGA NS in combination to obtain better results.

To reproduce the partial lesion, 6-OHDA was unilaterally administrated and divided over three injection sites in the lateral sector of the striatum, inducing a progressive, retrograde degeneration of the nigrostriatal pathway. Thus, it is a good model to study the pathophysiological features in the first stage of development of PD, as well as the effects and neuropathological changes of new therapeutic strategies like nanoparticles releasing NTFs.

Firstly, we established and assessed morphologically the model, injecting saline solution again as control of lesion into striatum. For this purpose, 6-OHDA and saline rats was processed at 3 weeks postlesion and used to assess the morphological changes of the model.

Then, other 6-OHDA lesioned rats were used for testing the treatment. For that, during and after the nanospheres or vehicle administration the animals were tested for drug-induced rotation test and used to assess the morphological recovery along the nigrostriatal pathway.

Regarding the treatment a new experimental group was also included, the vehicle group to evaluate the lesion produced by injecting twice into striatum. Table 4 showed the different experimental group used in this study following the experimental condition assigned for each one and the time course of the study is illustrated in the Figure 48.

Group	Number (n)	Comments
6-OHDA	5	6-OHDA lesion
Saline	3	Saline solution injection
Vehicle	5	6-OHDA lesion, striatal administration of PBS
Empty-NS	5	6-OHDA lesion, striatal administration of empty NS
VEGF-NS	5	6-OHDA lesion, striatal administration of NS loaded with 2.5 µg VEGF
GDNF-NS	6	6-OHDA lesion, striatal administration of NS loaded with 2.5 µg GDNF
VEGF+GDNF-NS	6	6-OHDA lesion, striatal administration of NS loaded with 1.25 µg VEGF and 1.25 µg GDNF

Table 4. Experimental groups from assay 2 for each condition. Abbreviations: 6-OHDA, 6-hydroxydopamine, NS, nanospheres, VEGF, vascular endothelial growth factor, GDNF, glial cell line-derived neurotrophic factor.

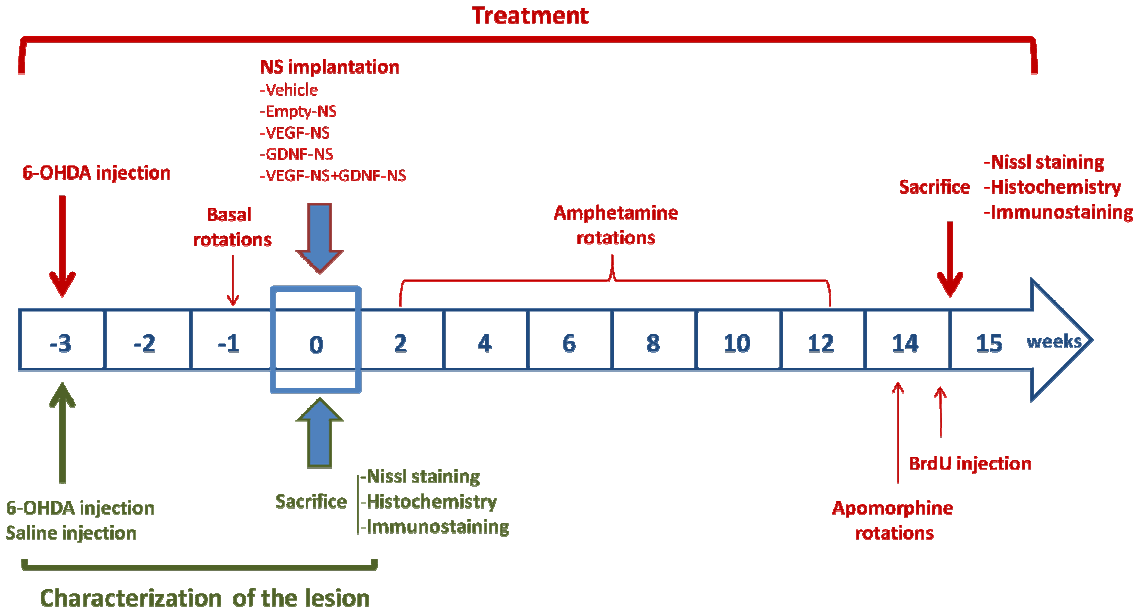

Figure 48. Time course for characterization of the lesion of the striatum (green) and for nanosphere treatment (red). Abbreviations: 6-OHDA, 6-hydroxydopamine; NS, nanospheres; BrdU: bromodeoxyuridine; VEGF, vascular endothelial growth factor; GDNF, glial cell line-derived neurotrophic factor.

2.1. Morphological features of the Partial model of Parkinson's disease

Sprague Dawley rats were also found to be suited for effective and reproducible stereotaxic targeting of the striatum. The effective dose of 6-OHDA was used to achieve the partial lesion of the nigrostriatal system.

Like in assay 1, for the evaluation of the model, after three weeks of injecting 6-OHDA or saline solution into striatum, rats were sacrifice by transcardial perfusion, brains were removed and sections from both the striatum and SN were collected for the morphological evaluation.

Rat brain surfaces showed the three injections marks where either the 6-OHDA or the saline solution was administered. No macroscopically differences were observed between both groups (Figure 49).

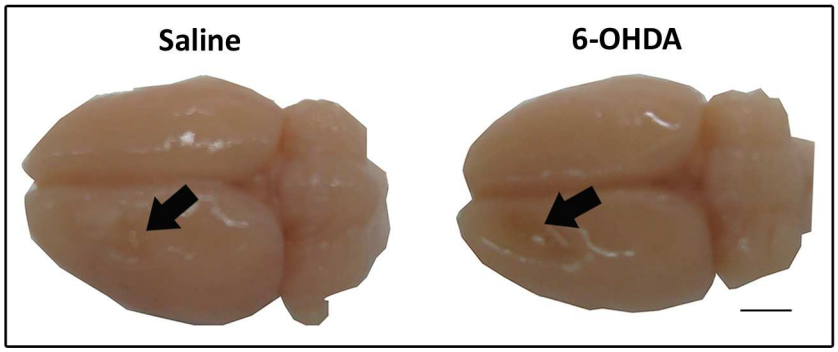

Figure 49. **Rat brain surfaces from rats lesioned in the striatum**. The black arrows indicate the mark of the puncture where 6-OHDA or saline solution was injected. Scale bar = 2 mm.

Coronal sections stained with Nissl showed the needle trajectory into the striatum (Figure 50a), which was almost imperceptible in the TH-immunostaining sections (Figure 50b). On the lesioned side, a slight enlargement of the lateral ventricle was observed, probably due to scar retraction. Rats from the 6-OHDA group showed negativity for TH-immunohistochemistry on the dorsolateral region of the striatum (Figure 50).

In the histopathological analysis, GFAP expression levels were higher on the lesioned sides (Striatum and SN) than on the intact ones. Furthermore, most of the GFAP-positive cells seen in the lesioned side showed a swollen soma. In addition, 6-OHDA rats showed a stronger positivity to GFAP than rats only receiving the saline solution.

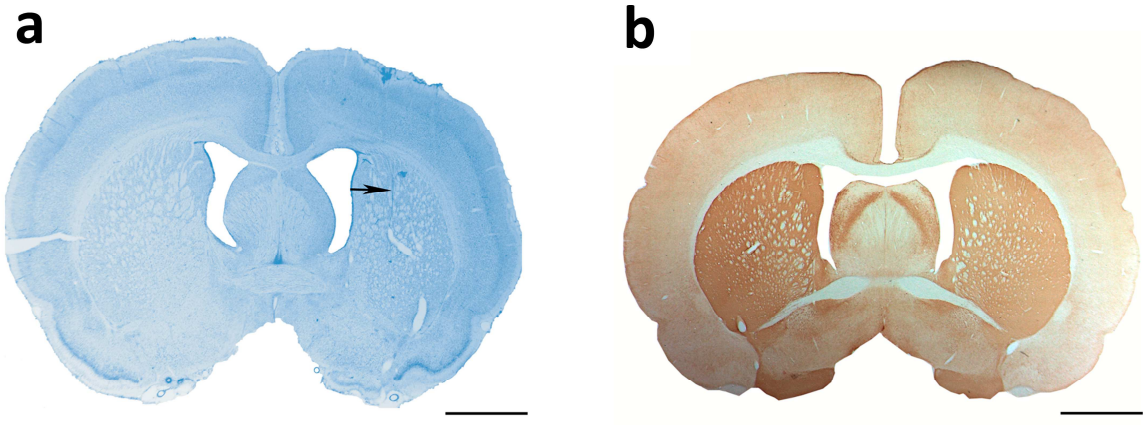

Figure 50. Needle trajectory: Coronal sections from the saline group, Nissl stained (**a**) and tyrosine hydroxylase (TH) immunostained (**b**). The black arrow indicates the needle trajectory in the striatum. Both striata continue to exhibit intense TH-immunoreactivity. Scale bar = 2 mm.

In the SN the main loss of immunoreactivity in 6-OHDA rats was observed in the lateral middle region of the SN, which due to the anatomical distribution allows to identify as ” external SN” (e-SN). e-SN includes SN-Lateral, a part of the SN-reticulata and a half of the SN-compacta. In addition, this new delimited area was topologically related to the lesioned part of striatum (see figure 25).

2.1.1. Immunofluorescence study of VEGF, OX-42 and LEA histochemistry

In order to visualize morphological changes in microglia in striatum and SN, an immunofluorescent staining was performed using OX-42 antibody, a specific microglial marker. Owing to VEGF is a key mediator of angiogenesis, immunofluorescence for VEGF was also carried out to detect VEGF positive cells and a LEA staining to study the morphology of the vessels.

The lesioned striatum and the ipsilateral SN exhibited more intense immunopositivity OX-42, VEGF and LEA immunoreactivity than the control side. Both structures showed a more conspicuous microglial reaction. Meanwhile in healthy side a spotty pattern was found corresponding to ramified microglia, the lesioned one showed a rough pattern of reactive microglia (Figure 51a). Lectin histochemistry for LEA showed

conspicuous microvascular network with abundant amoeboid microglia around the needle trajectory (Figure 51b) and the immunostaining for VEGF displays the microvasculature in the affected CPC.

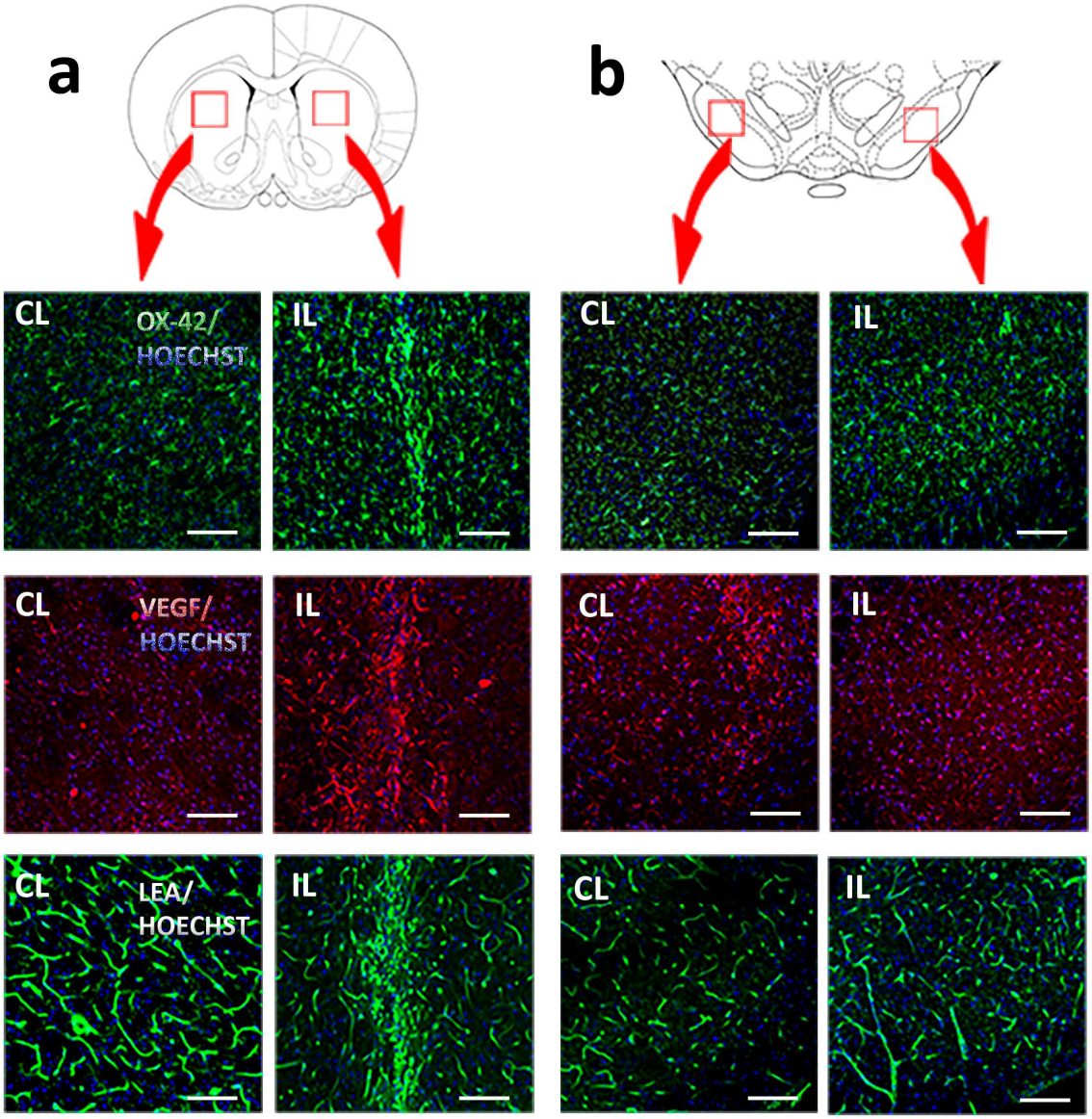

Figure 51. Striatal injection of 6-OHDA increased the expression of OX-42, VEGF and LEA in the ipsilateral hemisphere. Confocal microscopic images of OX42 (green), VEGF (red) and LEA (green) to verify the lesion in the ipsilateral (IL) striatum (**a**) and substantia nigra (**b**) compared to the contralateral (CL) one. Samples were also stained with Hoechst (blue) to visualize nuclei. Scale bar = 275 µm.

2.1.2. Quantitative analysis

The effects of 6-OHDA and saline injection into striatum on dopaminergic system were evaluated measuring the TH-ir and the vascular density in striatum and SN by stereology. Measurements were taken place considering the entire structure and rostro-caudal sections to assess the vulnerability from each region in order to examine the topological distribution of the lesion in both dopaminergic regions of our study.

2.1.2.1. Volume of affected striatum

Degeneration of dopaminergic fibers after the injection of 6-OHDA was evaluated measuring the volume of immunonegative CPC for TH. A significant decrease of the TH-positivity was observed in rats injected with 6-OHDA versus those only injected with the saline solution (Figure 52). The TH-negative volume in 6-OHDA rats was 2.10±0.15mm^3, 65.88±4.59% for the entire ipsilateral striatum and in the saline group was 0.02±0.008mm^3, (0.54±0.34%) (***$p<0.001$; Student's *t*-test) (Figure 52b).

Regarding rostral, middle and caudal levels of the CPC, the percentage of TH-negative volume was 54.49±11.54%, 63.65±11.29% and 84.51±6.73% for the rostral, middle and caudal sections of the 6-OHDA group respectively (Figure 52c). Significant changes were found comparing both groups at these three considered levels (***$p<0.001$, for the rostral sections, ***$p<0.001$, for the middle sections, ***$p<0.001$ for the caudal sections; Student's *t*-test) (Figure 52c). However, no significant differences were found between the different levels within the saline or 6-OHDA groups.

After the histopathological analysis, the previously referred enlargement of the ipsilateral ventricle was appreciated; probably due to tissue retraction caused scarring after the puncture injury. Therefore, a quantification of this tissue retraction was performed and expressed as a percentage of the volume occupied by the ipsilateral CPC with respect to the contralateral one, on TH-immunostained sections. This contralateral

non-lesioned CPC was considered as 100%. The volume was calculated integrating all measurements of the CPC sections using the above referred image analysis system.

The average volume of the entire CPC in the saline group was 2.96±0.23mm^3 on the ipsilateral side and 3.41±0.3mm^3 on the contralateral one (the ipsilateral hemisphere values were found to be 8.65±3.45% lower than those of the contralateral hemisphere). In the 6-OHDA group the average volume for the injured side was 3.19±0.11 mm^3 and 3.65±0.14 mm^3 for the non-injured one (ipsilateral hemisphere values 12.80±1.21% lower than those of the contralateral hemisphere) (Figure 52d). These data show that the puncture is responsible for circa a 10% decrease in tissue volume on both groups, though tissue retraction did not reach any significant differences between the saline and 6-OHDA groups. Moreover, tissue retraction decreased from the rostral to the caudal level in both groups (Figure 52e).

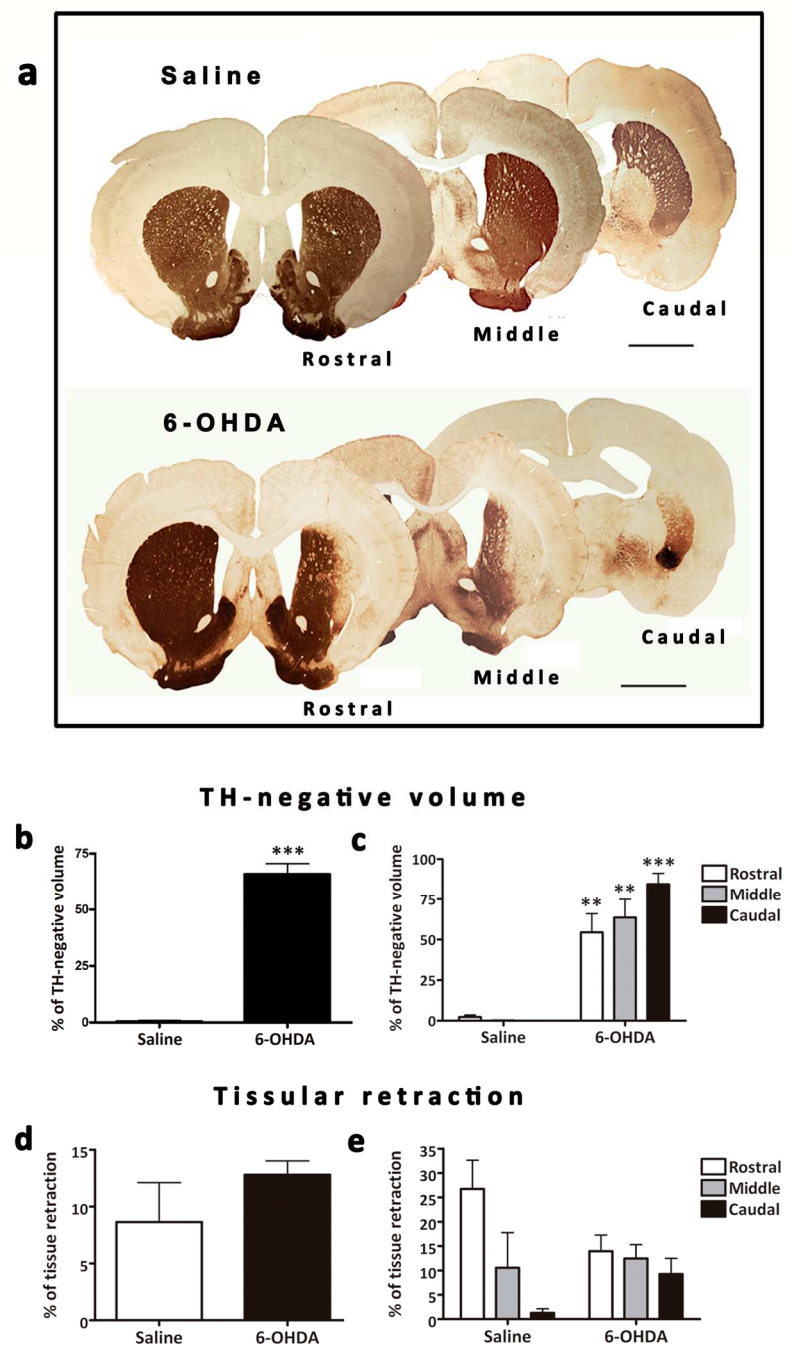

Figure 52. Affected caudate putamen complex (CPC). Series of coronal sections (**a**) show differential tyrosine hydroxylase (TH)-positivity depending on the injected substance and the level considered (rostral, middle and caudal). Scale bar: 2.5 mm. **(b, c**) Loss of TH-positive innervation in the striatum was determined by the percentage of TH-negative volume of the ipsilateral striatum with respect to the total ipsilateral one. Significance ***p<0.001 saline *vs.* 6-OHDA group. (**d, e**) The size of the ipsilateral CPC was assessed by the remaining volume percentage of the ipsilateral *vs.* the contralateral one. Data are shown as mean±SE.

2.1.2.2. Neuron Density and Axodendritic Network in the entire SN and in the "external-SN"

The main neuron loss was observed in the previously defined "external SN" (e-SN) (Figure 53a), where the decrease in TH-ir neurons was comparatively more prominent than in the entire SN.

The number of TH-immunoreactive (TH-ir) cells in SN decreased significantly after the administration of 6-OHDA, with only 20.45±2.33% of positive neurons remaining in the ipsilateral side. The saline group showed minimal variations (85.59±2.20%). There was a highly significant difference between both groups (***p<0.000; Student's *t*-test) (Figure 53b). When rostro-caudal sections of SN were analyzed for neuronal density, a significant reduction in the 6-OHDA group compared to the saline group was found at all levels, being most relevant in the caudal sections (Figure 53c).

Stereological studies showed more significant changes in the e-SN than in the entire SN, indicating that this region is more susceptible to changes using this model. Thus, in rats receiving 6-OHDA, 14.5±2.55% of TH-positive neurons remained, and in the saline group 77.91±4.90% (***p<0.001; Student's *t*-test) (Figure 53d).

Interestingly, the rostro-caudal gradient was much more remarkable in the e-SN than in the entire SN, attaining statistically significant differences between the rostral and caudal sections within the same group (Figure 53e). Measurements for the e-SN were 23.84±1.39% at rostral, 12.9±3.64% at middle, and 6.75±2.53% at the caudal section for the 6-OHDA group; and 90.58±5.97% at rostral, 80.16±5.25% at middle and 62.99±5.56% at the caudal section for the saline group (Figure 53e). In contrast, the entire SN did not show remarkable differences throughout the rostro-caudal axis (21.24±4.15%, 16.93±4.92%, and 21.42±4.85% for the 6-OHDA group; and 86.42±3.95%, 85.42±6.29%, and 79.62±2.3% for the saline group) (Figure 53e).

Owing to the significant changes in neuronal density obtained when analyzing the e-SN, we proceeded to quantify the ADN in this specific region. As expected, 6-OHDA

rats presented a lower ADN density than saline rats (40.45±1.96% *vs.* 81.82±1.96%, ***p<0.001; Student's *t*-test) (Figure 53f).

As for the rostro-caudal distribution, rats receiving 6-OHDA presented a significantly lower ADN density (45.94±3.39% at rostral, 39.9±2.47 at middle, and 37.6±1.3 at the caudal section) than rats receiving just the saline solution (86.62±2.52 at rostral, 94.18±2.34 at middle, and 87.9±2.24 at the caudal section), at all studied sections; however, no trend or differences within the same group were appreciated (***p<0.001 6-OHDA *vs*. saline rats at rostral and middle sections and **p<0.01 at the caudal section; Student's *t*-test) (Figure 53g).

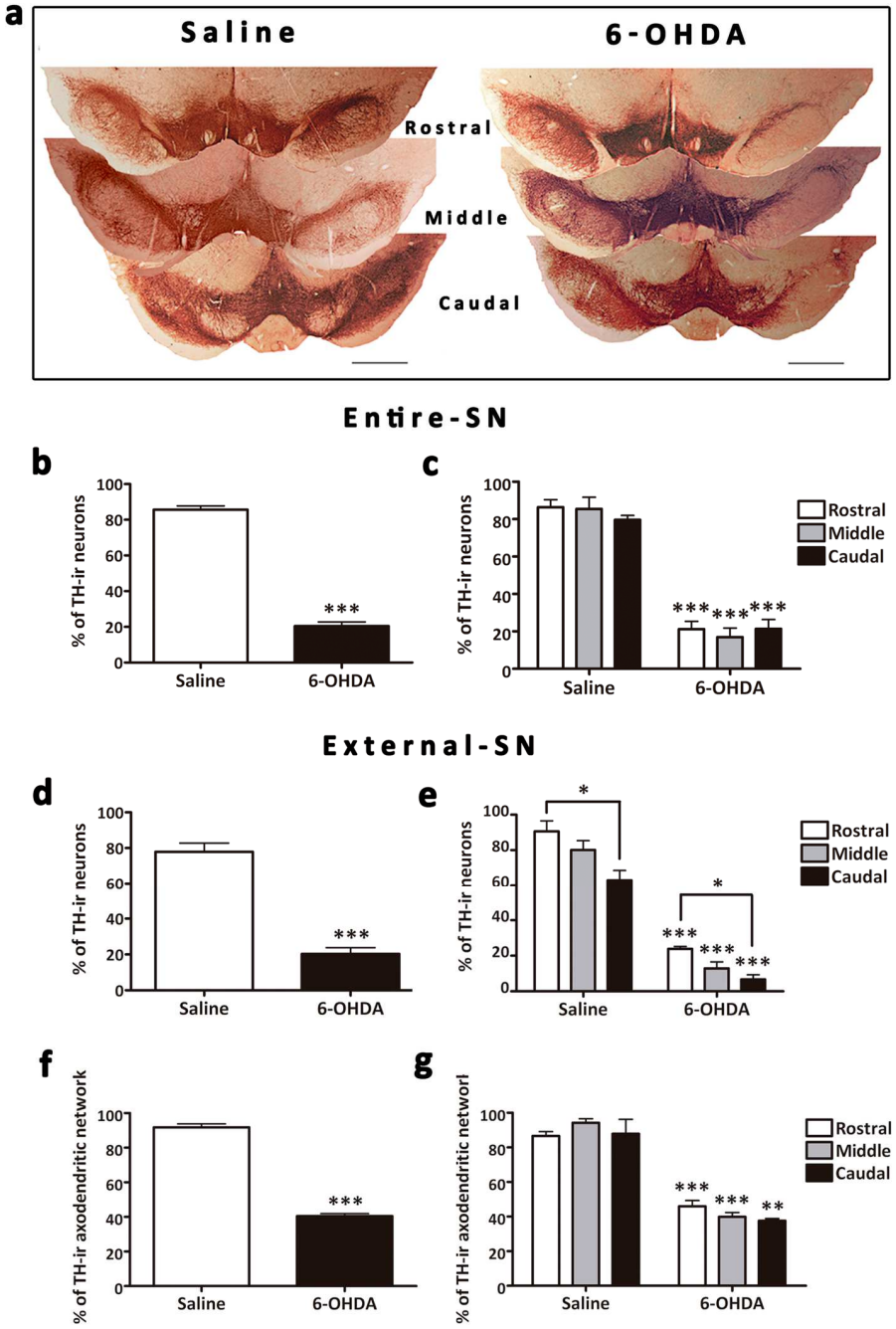

Figure 53. Effects on the substantia nigra (SN). (**a**) Photomicrographs of the rostral, middle and caudal sections of the SN immunostained for tyrosine hydroxylase (TH) in the saline and 6-OHDA groups. Scale bar: 1 mm. (**b, c**) 6-OHDA produced a significant loss of TH-ir neurons in the entire SN and no differences between sections along the rostro-caudal axis were observed. ***p<0.001 saline *vs.* 6-OHDA group. (**d, e**) In the e-SN, the density of neurons decreased in both groups (***p<0.001) and a decreasing rostro-caudal gradient was evident, being significantly different in the rostral and caudal sections (*p<0.05) in both groups. Saline *vs.* 6-OHDA rats presented significant differences in all analyzed sections (***p<0.001). (**f, g**) The density of the axodendritic network (ADN) was measured only in the e-SN. There was a significant difference between both experimental groups (***p<0.001). Analyzed by section, a tendency was only observed in the 6-OHDA group. Data are shown as means ± SE.

2.1.2.3. No change was observed in microvascular density after 6-OHDA into the striatum

Microvessels density was higher in 6-OHDA rats in striatum and SN. However, there was no statistical difference between both groups (Figure 54).

Regarding rostro-caudal sections in striatum, 6-OHDA rats trended to increase the vascular density from rostral to caudal level (Figure 54b). Saline rats did not show changes in the values along this axis (Figure 54b).

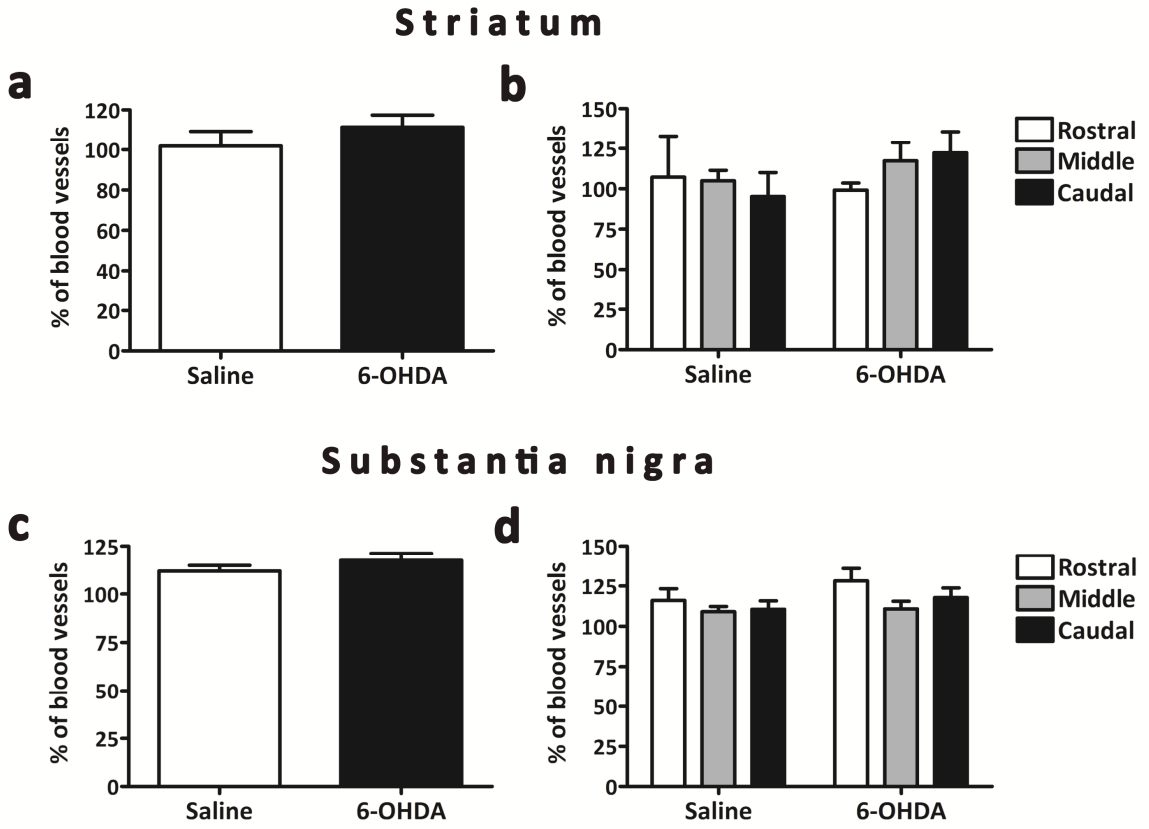

Figure 54. Quantitative analysis of microvascular density in the striatum and substantia nigra (SN) after 6-OHDA injection into the striatum. (**a, c**) Microvascular density was similar in the 6-OHDA and saline groups, in both the striatum and SN. (**b, d**) Graphs show a rostro-caudal distribution of microvessels in the striatum and SN. Saline administration decreases microvascular density from rostral to caudal parts in the striatum and SN. However, 6-OHDA injection increases the microvasculature from rostral to caudal sections in the striatum (**b**), but in the SN this gradient is inverted, with microvessel density decreasing from rostral to caudal sections in this group (**d**). Data are shown as means±SE.

2.2. Treatment with nanoencapsulated neurotrophic factors

In order to analyze the potential of VEGF and GDNF nanoencapsulated in the Partial model, rats were previously parkinsonized and after three weeks NS were implanted. Rotational behavioral tests were developed to assess the functional recovery and morphological evaluation of the brain slices have been performed after 14 weeks of NS administration, when rats were sacrificed.

Only the rats that presented more than three tpm at 2 week after 6-OHDA lesion were included in the study to confirm that the lesion was effective in order to evaluate the effectiveness of the treatment on the Partial model.

2.2.1. Behavioral study: Functional effects of implanted PLGA-nanospheres

In vivo functionality of nanoencapsulated VEGF and GDNF releasing PLGA-NS was assessed by amphetamine-induced rotational test. For that, rats were divided into five experimental groups**: (1) vehicle; (2) empty-NS; (3) VEG- NS (2.5 µg VEGF); (4) GDNF-NS (2.5 µg GDNF)**; and **(5) VEGF-NS** and **GDNF-NS (1.25 µg VEGF and 1.25 µg GDNF).**

In amphetamine-induced experiments, no differences were found in the initial number of rotations between groups, as shown in Figure 55 (Herrán et al., 2014). After a unilateral 6-OHDA lesion, animals receiving only the vehicle administration did not show significant recovery of the rotational behavior at any time (sham: 10.15±2.19 ipsilateral tpm at 0 weeks to 11.57±2.49 tpm at 10 weeks). Rats receiving empty-NS, VEGF-NS, and GDNF-NS treatments showed a slight reduction in rotations at the end of the study (week 10). GDNF-NS implantation, in particular, showed a statistical reduction in the number of rotations when compared with sham group (empty-NS: 9.71±2.92 tpm; VEGF-NS: 6.37±2.11 tpm; GDNF-NS: 4.43±2.75 tpm; $P \leq 0.05$ GDNF NS with respect to sham group, Student's *t*-test). In addition, we observed that striatal implantation of the combined VEGF-NS and GDNF-NS treatment at half the dose of the factors administered individually achieved the best behavioral results and significantly reduced the number of

rotations (VEGF-NS and GDNF-NS: 0.87±0.53 tpm) when compared to the empty NS and sham groups (***p≤0.001 with respect to empty-NS and sham groups, Student's *t*-test (Figure 53a).

Once the amphetamine test was completed, rats were exposed to the apomorphine-induced test. The data obtained from this test confirmed the promising results obtained previously, showing statistically significant changes between the VEGF-NS and GDNF-NS group and sham and empty-NS treatment groups (**p≤0.01 with respect to empty-NS and p≤0.05 with respect to sham group, Student's *t*-test (Figure 53b). As can be seen from Figure 55, the VEGF-NS and GDNF-NS treated group presented the smallest number of contralateral rotations, demonstrating the highest level of behavioral recovery (Herrán et al., 2014).

Assays with NTFs administered alone were not remarkably taken into account because statistically significant differences in functional tests were only to be found where both factors (VEGF+GDNF) were synergistically administrated. Therefore, the advanced stereological study was focused exclusively on this group and the control groups.

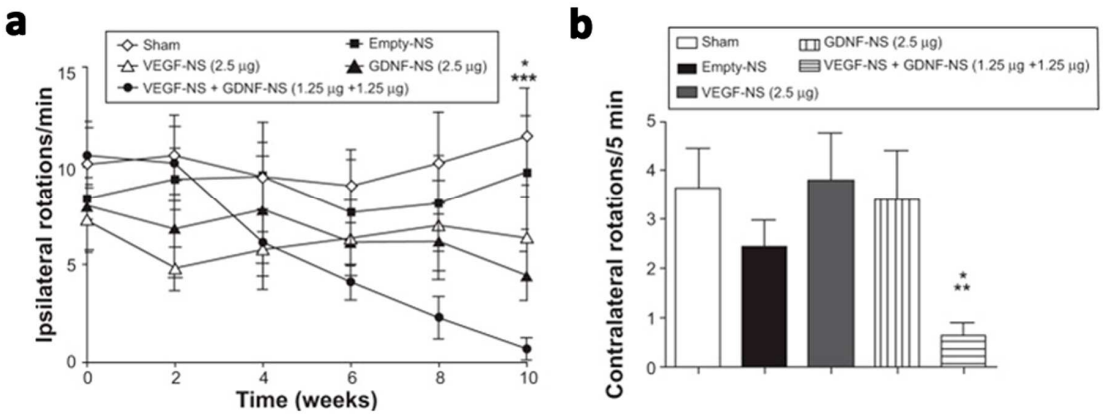

Figure 55 Behavioral study: amphetamine and apomorphine rotational tests. (a) The results obtained from the amphetamine rotational behavior test after nanosphere (NS) administration. The GDNF-NS group *vs.* the sham group showed statistically significant differences (*p≤0.05). The VEGF-NS and GDNF-NS groups *vs.* the sham and empty NS groups showed statistically significant differences (***p<0.001). (**b**) Data obtained from the apomorphine rotational behavior test 14 weeks after NS implantation. The VEGF NS and GDNF NS-treated groups exhibited the best behavioral recovery (*p≤0.05, VEGF-NS and GDNF-NS *vs.* empty-NS; **p<0.01, VEGF-NS and GDNF-NS *vs.* sham). Data are shown as mean ± standard deviation.e data are shown as the mean±standard desviation.

2.2.2. Histological changes after nanospheres implantation

Rats were sacrificed at 14 week after apomorphine-test evaluation. Rat brain surfaces did not present macroscopically difference among the experimental groups. To examine the morphological changes occurred after NS administration and the effects of combined VEGF and GDNF delivery in striatum; Nissl staining and immunohistochemistry studies were carried out.

Some Nissl slices show two trajectories corresponding to the initial administration of 6-OHDA and a subsequent administration due to the treatment (Figure 56a). Tissue around the needle track appeared rarefied with a conspicuous glial reaction and macrophages or hemosiderin are sometimes present along the track. A mild enlargement of the lateral ventricle is frequently appreciated. The astroglial reaction consists of a hypertrophy of cellular processes and up-regulation of GFAP expression. Nanospheres loaded with NTF induced a remarkable glial reaction around the trajectory.

Morphological evidences of tissue damage after NS implantation were undistinguishable to the vehicle, indicating that histological changes around the needle track were induced by the needle itself, and the NS themselves being well tolerated.

Rats receiving 6-OHDA showed an asymmetrical distribution of the toxin effects. These were localized mainly over the dorsolateral region of the striatum. Slices including the needle track frequently displayed an abrupt transition between TH-immunohistochemistry positivity and negativity (Figure 56b).

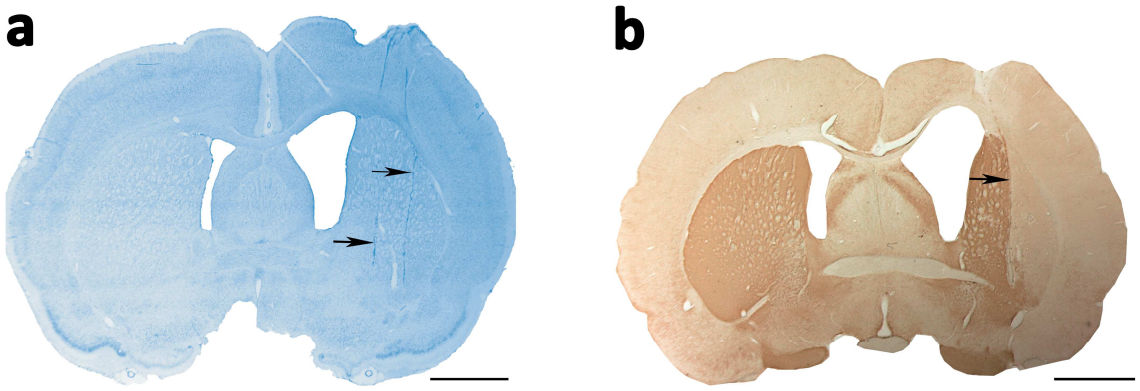

Figure 56. Abrupt limit in the striatum: Coronal sections from the 6-OHDA-treated (vehicle) group, stained for Nissl and tyrosine hydroxylase (TH)-immunohistochemistry (a, b respectively). (**a**) Black arrows mark the trajectory of both surgical procedures (6-OHDA and treatment administration), (**b**) At this level an abrupt limit between TH-positivity and TH-negativity was observed. Scale bar = 2 mm.

2.2.3. Proliferation assay: BrdU/DCX immunofluorescence

Double immunofluorescence for BrdU and DCX was performed to investigate the ability of NTF to promote neurogenesis, cell migration and neuronal differentiation in the SVZ after 6-OHDA lesion. For this reason, striatal tissue sections corresponding on rats treated with vehicle, empty-NS and with NS loaded with VEGF and GDNF in combination were doubly immunostained with BrdU and DCX.

A large amount of cells expressing BrdU-positivity was found in the SVZ and surrounding areas in the group receiving NTFs, which indicates a high level of proliferation. Some of these cells co-expressed DCX (marker of immature neurons) and

were extended all over the SVZ. Some of them were located in areas adjacent to the striatum, suggesting a possible SVZ to striatum migration. In the animals of the vehicle group, the number of BrdU-positive cells was clearly lower and there were no DCX-positive cells (Figure 57), confirming that NTFs induce or maintain neuron differentiation and proliferation levels.

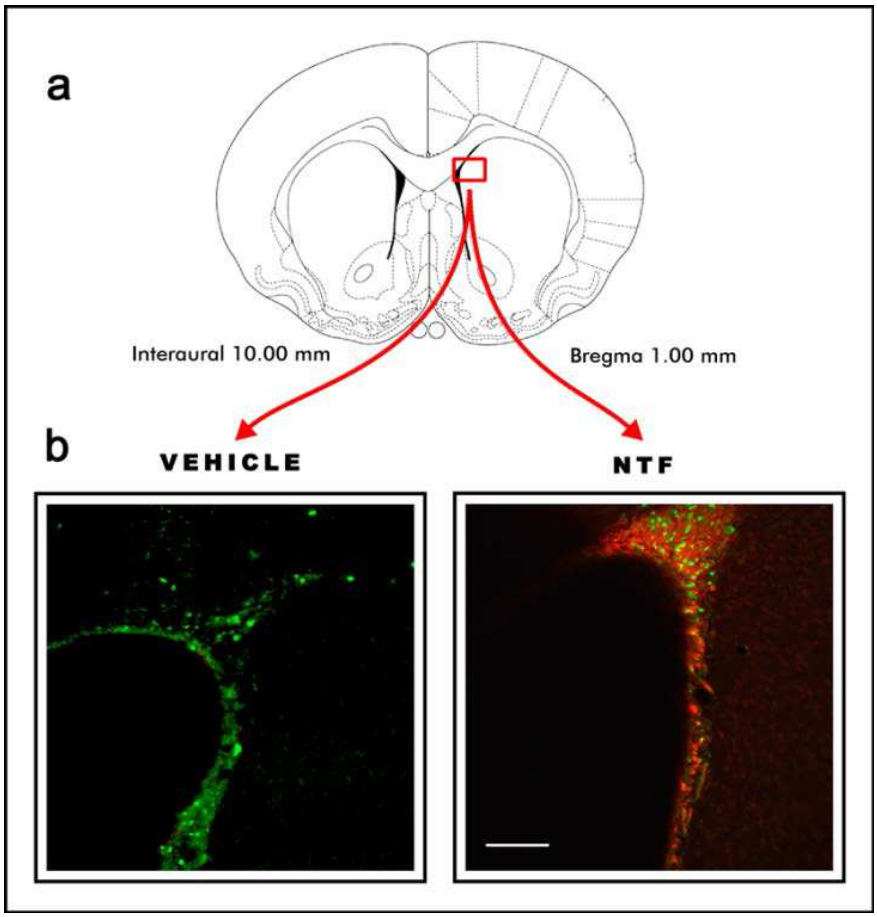

Figure 57. A proliferative and neurogenic effect was observed in the neurotrophic factor (NTF) group: (**a**) Pictures show of the subventricular zone (SVZ) localization, according to the Paxinos and Watson Atlas. (Paxinos & Watson, 2013) (**b**) Confocal micrographies show the BrdU-positive nucleus (green) and the DCX-positive soma (red) in the SVZ and periventricular areas. The NTF group presented more positivity for BrdU and DCX than the vehicle group. In the NTF group, most of the BrdU-positive cells co-expressed DCX. Scale bar = 275 µm.

2.2.4. Quantitative analysis

Stereological analysis was carried out taking into account rats treated with both NTFs, although we also considered all the experimental groups in order to underline the reason of chosen the groups previously mentioned. Thus, the efficacy of each treatment was also analyzed with TH-immunohistochemistry, measuring IOD of TH-positive fibers of the striatum for all experimental groups. However, due to the remarkable differences observed in rats treated with VEGF and GDNF in combination respect to the groups treated with VEGF or GDNF individually, the rest of stereological studies were only focused on rats treated with both NTF in combination.

2.2.4.1. Integrated optical density of striatum

To further investigate the lesioned striatum, we also measured the IOD of TH-positive fibers considering all the experimental groups. To estimate IOD for each animal, we placed a square on the most degenerate region, where we found the significant differences. In addition, IOD was measured at two medial–caudal levels along the basal ganglia according to Paxinos and Watson (Paxinos & Watson, 2013).

The TH+ fiber intensity of the lesioned side expressed as percentage over the control side observed in the striatal area of the VEGF NS and GDNF NS-treated group was 58±4.19%, while that of the vehicle group was 42±2.87%. The combined treatment enhanced the restoration of TH+ fibers and neurons to a greater extent than the treatments with only VEGF or GDNF ($p \leq 0.05$) with respect to the vehicle group, one-way ANOVA. Figure 58 demonstrates enhanced restoration of the lesioned striatum in the VEGF-NS and GDNF-NS group.

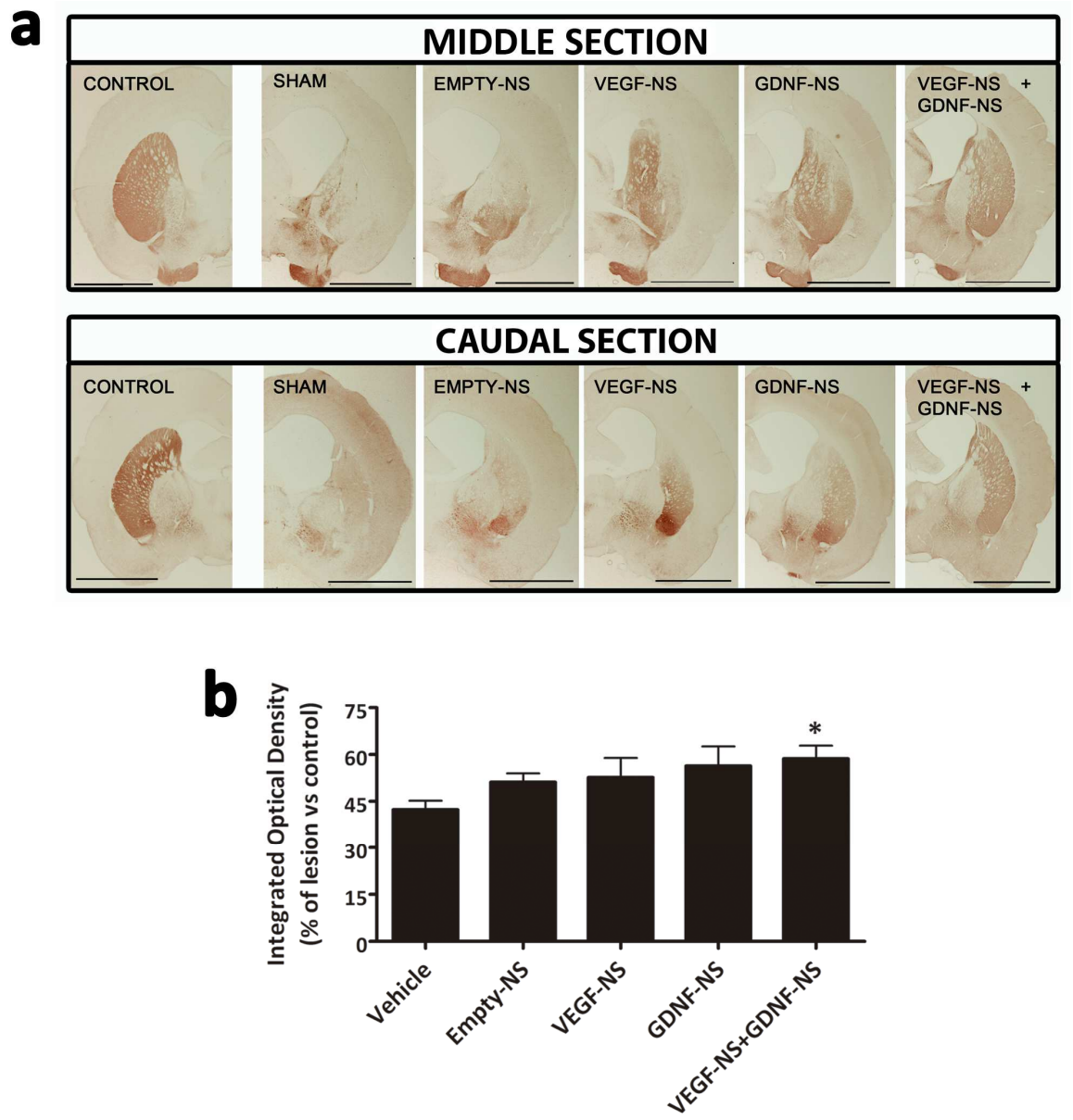

Figure 58. Integrated optical density (IOD) was measured in the striatum. (**a**) The images give an illustrative overview of the medial and caudal sections of the caudate putamen complex for tyrosine hydroxylase immunohistochemistry. Squares placed on lesioned and non-lesioned (control) hemispheres delimit the surfaces where the IOD was measured using a computerized image analysis system. Scale bar = 4 mm. (**b**) The histogram shows the percentage of IOD of the lesioned hemisphere with respect to the non-lesioned hemisphere (control) for each experimental group. Data are shown as the mean ± SE (*p<0.05 VEGF-NS and GDNF-NS group *vs.* vehicle groups.

Owing to groups treated with both NTFs presented the best results, we focused on this group in further studies, as we mentioned previously.

2.2.4.2. Volume of affected striatum

In NTF treated animals, the TH-negative volume of the CPC was 0.94±0.082 mm^3 (41.27±3.21% of the total volume of the ipsilateral CPC). It was less than in the other studied groups (Figure 59) (1.21±0.08 mm^3, 52.92±3.71% in the vehicle group, and 1±0.07 mm^3, 43.74±3.3 % in the empty-NS group). The difference between the NTF and the vehicle group was statistically significant (*$p<0.05$; one way ANOVA) (Figure 59b) and indicated the increased recovery of the treated group.

Distribution from rostral to caudal sections showed a reduction in the TH-negative volume (that is, a TH positivity recovery) on all sections of the NTF group. However, no statistic differences were observed either between groups or into themselves (Figure 59c).

Regarding tissue retraction, measurements did not show significant differences between groups. Owing to the two lesions carried out in these groups, the percentage of tissue retraction was somewhat higher than in the first assay, almost 25%, though, the lowest percentage belonged interestingly to the NTF group (Figure 59d).

The topographical analysis showed that in spite of a lack of statistic differences, the NTF group displayed a gradient showing a remarkable recovery on the rostral sections compared to the control groups (Figure 59e).

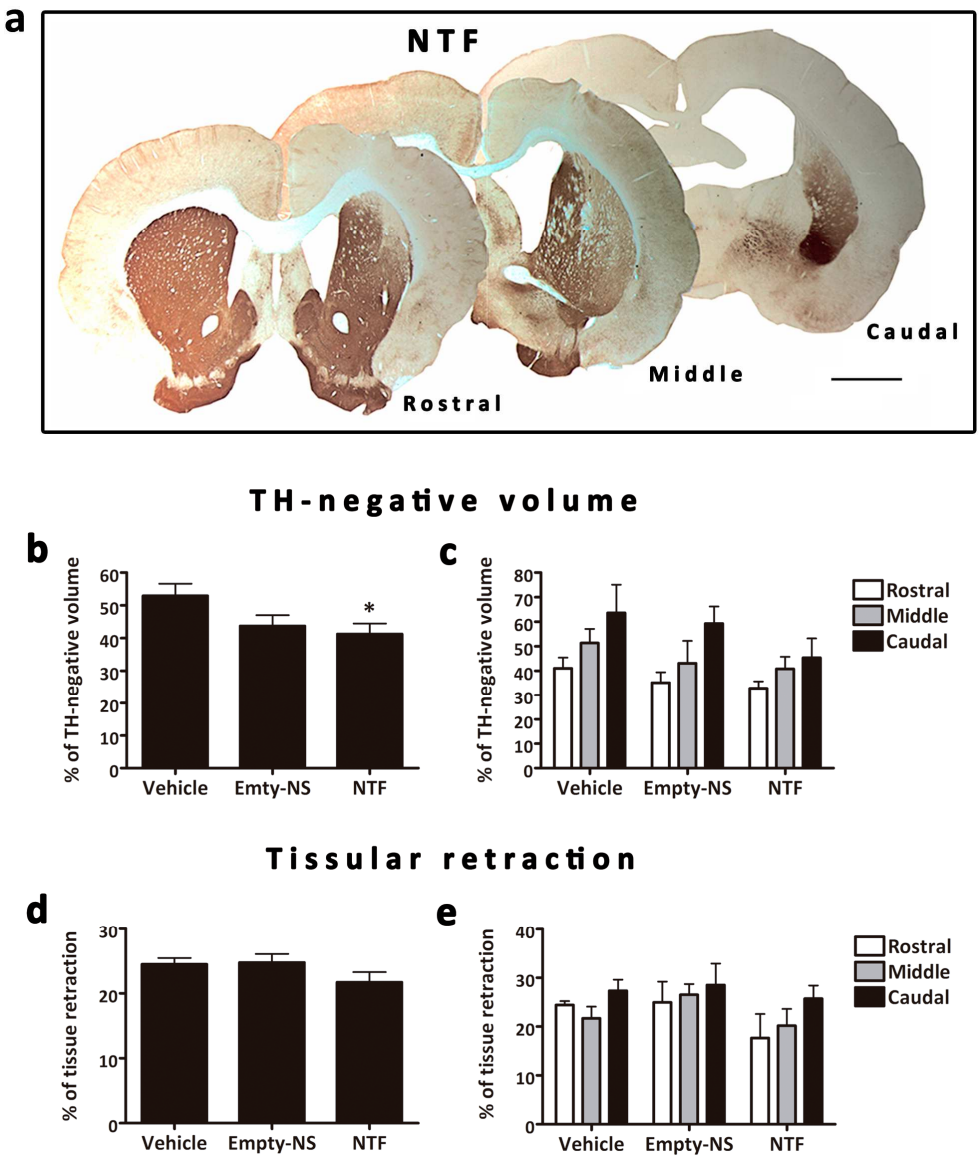

Figure 59. Recovery of tyrosine hydroxylase-immunoreactive (TH-ir) striatal volume. (**a**) Coronal sections from the neurotrophic factor (NTF) group immunostained for TH show a recovery in TH-positive volume at all rostro-caudal levels. Scale bar = 2 mm. (**b**) The % of TH-negative volume is lower in the NTF group with respect to the vehicle and empty-NS groups. Significance (*p<0.05, NTF *vs.* vehicle group). (**c**) TH-negative volume increased from rostral to caudal sections, being lowest in the NTF group. (**d**) Histogram showing tissue retraction. The group receiving NTF showed less tissue retraction than the other groups. (**e**) Tissue retraction increased slightly from rostral to caudal sections, with the decreasing effect of NTF being apparent at all levels studied. Data are shown as means±SE.

2.2.4.3. Neuronal density and axodendritic network in the subtsantia nigra

The SN in the vehicle group and the empty-NS group showed an extreme loss of dopaminergic neurons and fibers, while rats receiving NTFs showed more cells and a TH-positive neuropil (Figure 60). Changes mainly occurred on the external area of SN (e-SN) (Figure 60a), where the most important changes related to neuronal and ADN density were found. This specific region was more affected by the lesion and showed a higher recovery level after NTF administration.

Regarding the entire SN, the number of TH-positive neurons were statistically higher in the NTF group than in the vehicle one (Figure 60b). This increase took place in all sections studied but only achieved significant levels in the rostral section (Figure 60c) (4.23±1.12% *vs*. 19.32±3.22%, *p<0.05, one way ANOVA).

When e-SN was considered, differences were statistically significant and even more marked between the three groups (Figure 60d). The topographical distribution showed that the NTF group increased from rostral to caudal (36.70±10.22%, 44.02±7.19, and 51.11±17.42%) but was only significant *vs*. the vehicle group at the middle level (9.55±4.02% *vs*. 44.02±7.19%, ***p<0.001, one way ANOVA) (Figure 60e).

Stereological studies showed changes in SN regarding neuron density and ADN. These changes were statistically significant (*p<0.05, one way ANOVA) between the three groups considered, and were highly significant (***p<0.001; one way ANOVA) when the e-SN was considered exclusively (Figure 60f).

Evaluations of the ADN in the e-SN revealed that the NTF group presented a higher density of TH-positive ADN (55.7±4.51%) compared to the empty-NS group (45.13±3.97%) or the vehicle group (35.01±3.08%). Differences were statistically significant between the NTF and the vehicle group (***p<0.0001, one way ANOVA) (Figure 60f). Analyzing rostro-caudal sections, its ADN density was statistically significant only at the middle level of these two groups (*p<0.05, one way ANOVA) (Figure 60g).

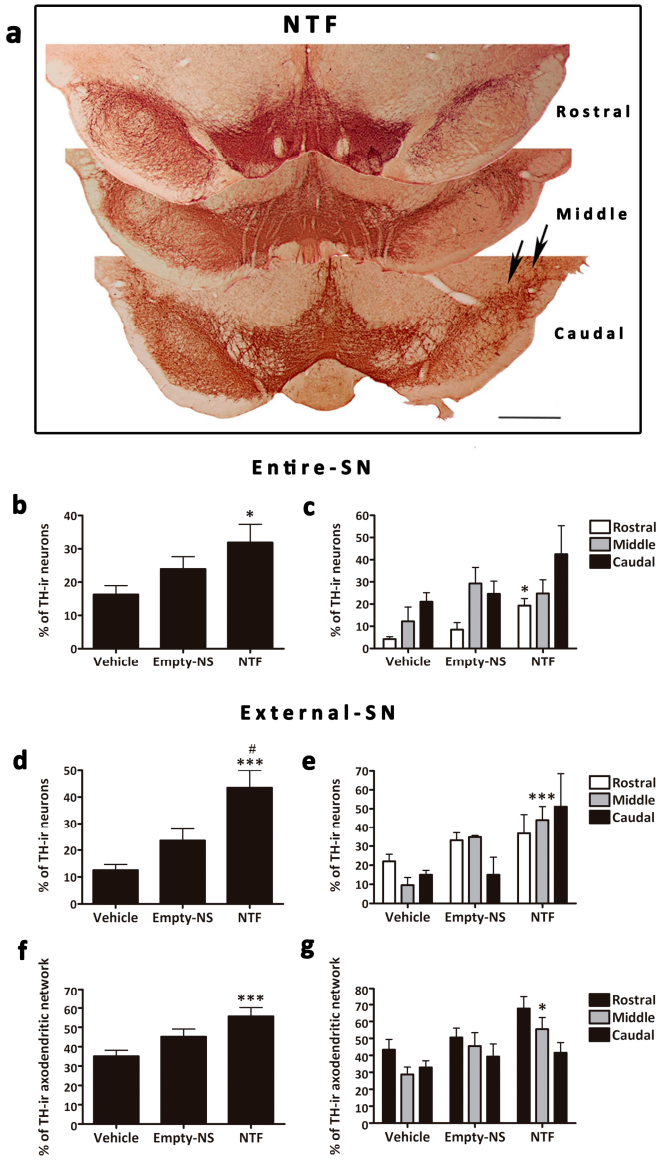

Figure 60. Rescue of tyrosine hydroxylase immunoreactive (TH-ir) neurons and axodendritic network (ADN). (**a**) Photomicrographs of the rostro-caudal sections of TH–immunostained SN from the group receiving neurotrophic factors (NTF). This group showed a significant increase in the number of positive neurons in the ipsilateral hemisphere compared to the control groups. Scale bar = 1 mm. Black arrows point to the e-SN of the lesioned hemisphere, where recovery is more outstanding. (**b**) The histogram shows the percentage of neurons in the entire SN (*p<0.05, NTF *vs.* vehicle group). (**c**) Rostro-caudal distribution is depicted regarding percentage of neurons in the entire SN. There are statistically significant differences at the rostral level between the vehicle and the NTF groups (*p<0.05). (**d**) When the e-SN is considered, more outstanding differences appear between groups (***p<0.001, NTF *vs.* vehicle group; *p<0.05 NTF *vs.* empty-NS group). (**e**) The effect of NTF increased the rostro-caudal percentage of TH-ir neurons in the e-SN. Statistical differences were found between the middle sections of the NTF *vs.* the vehicle group in the e-SN (***p<0.01). (**f**) The ADN in the e-SN was significantly more dense in the NTF group (***p <0.01, NTF *vs.* vehicle group). (**g**) When ADN percentage data in the e-SN are segregated for all rostro-caudal levels, only the middle one presents a mild difference between the NTF and the vehicle group (*p<0.05), and a moderate decreasing rostro-caudal gradient is apparent. Data are shown as means±SE.

2.2.4.4. VEGF and GDNF did not show effecst on microvascular density

Microvascular density in striatum and SN did not reveal statistical differences among experimental groups; although, after a topological analysis a higher density in rostral sections decreasing to caudal ones in striatum, and in the opposite sense for SN was found (Figure 61a).

Rostro-caudal distribution of vessels in striatum and SN was the opposite to the distribution of TH+ fibers in striatum and, neuronal and ADN density in SN, indicating that the lesion increased the vascular density on the dopaminergic system in this model (Figure 61b).

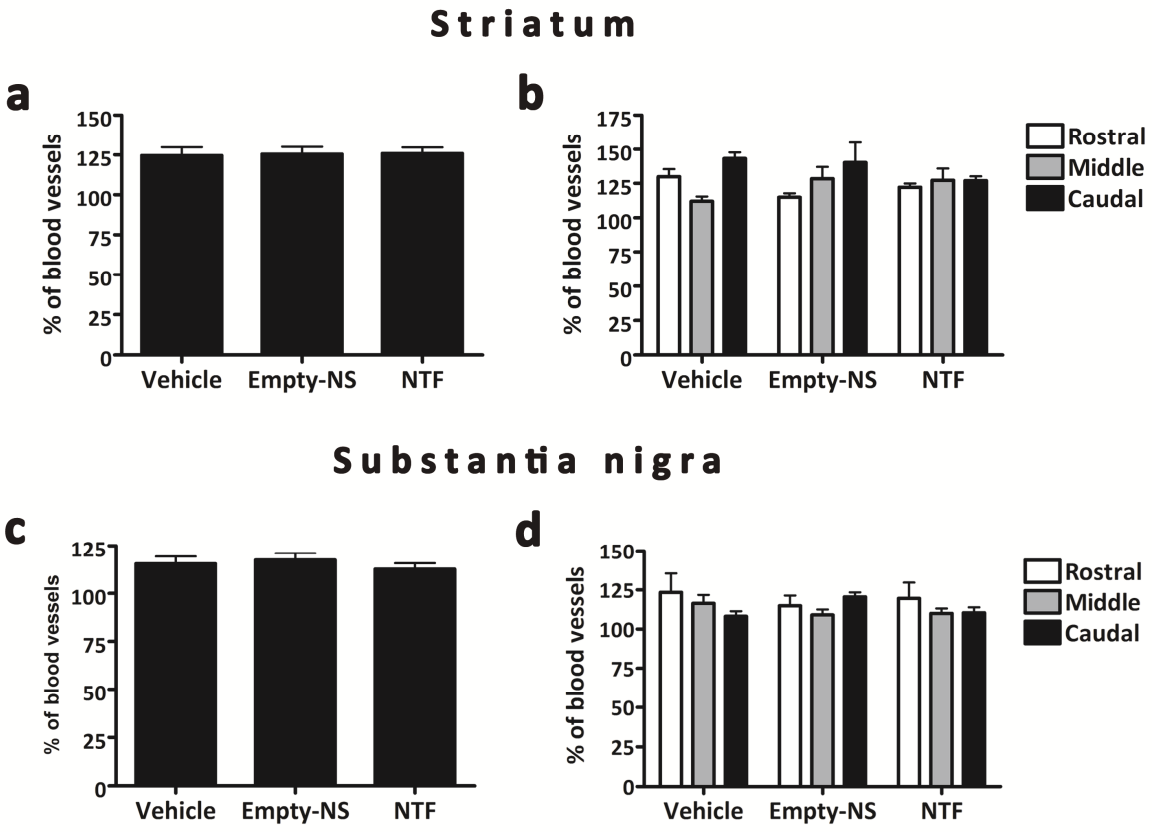

Figure 61. Microvascular density in the striatum and substantia nigra after neurotrophic factors administration. Experimental groups did not show changes in microvascular density in the striatum (**a, c**). There was a tendency towards increased microvascular density from rostral to caudal sections in the striatum (**b**), but this distribution of microvascular density decreased from rostral to caudal levels in the SN (**d**). Data are shown as means ± SE.

3. Assay III: Morphofunctional analysis and molecular study after combining therapeutic strategies (Cerebrolysin and enriched environment) and inhibiting VEGFR2 and RET in a Preclinical model of Parkinson's disease.

For this assay it has been used the Partial model with short time of evolution, the Partial model was described in assay 2, therefore we only focused on the treatments and at the same time we developed an early Partial model, in which motor symptoms were almost undetectable. For this purpose, 6-OHDA was intrastriatally injected in rats, and after 2 weeks with the toxin, treatments were performed during one week prior to be sacrificed.

In this study, regarding the synergistic effect observed in assay 1 and 2 after administering VEGF and GDNF encapsulated and being the Partial model an ideal model to study further therapies and to evaluate mechanism of compensation, we assessed other treatments also based on nanodelivery of NTFs or/and inducing their expression via housing in a EE. In addition, we also wanted to demonstrate the endogenous effect of NTF on this model, for that we also tested the inhibition of VEGFR2 and RET, both are the VEGF and GDNF receptors respectively, in 6-OHDA lesioned rats (Table 5).

Group	Number (n)	Comments
6-OHDA	7	6-OHDA lesion
CBL	8	6-OHDA lesion, 5 mg/kg of CBL i.p. administered
EE	8	6-OHDA lesion, housed in EE
CBL+EE	8	6-OHDA lesion, 5 mg/kg of CBL administered and housed in EE
Vandetanib	8	6-OHDA lesion, VEGFR2 and RET inhibitor (vandetanib 30 mg/kg) orally administered

Table 5. Experimental groups from assay 3. Abbreviations: 6-OHDA: 6-hydroxydopamine; CBL, Cerebrolysin; EE, enriched environment; i.p., intraperitoneal.

The efficacy of the treatments and the detriment of inhibiting VEGFR2 were functionally analyzed with amphetamine-induced rotational behavioral test and morphologically evaluated with TH-immunostaining, measuring the TH+ fibers of the striatum and density of dopaminergic neurons in the SN. Western blot was also carried out in order to assess the survival and apoptotic pathways (Figure 62).

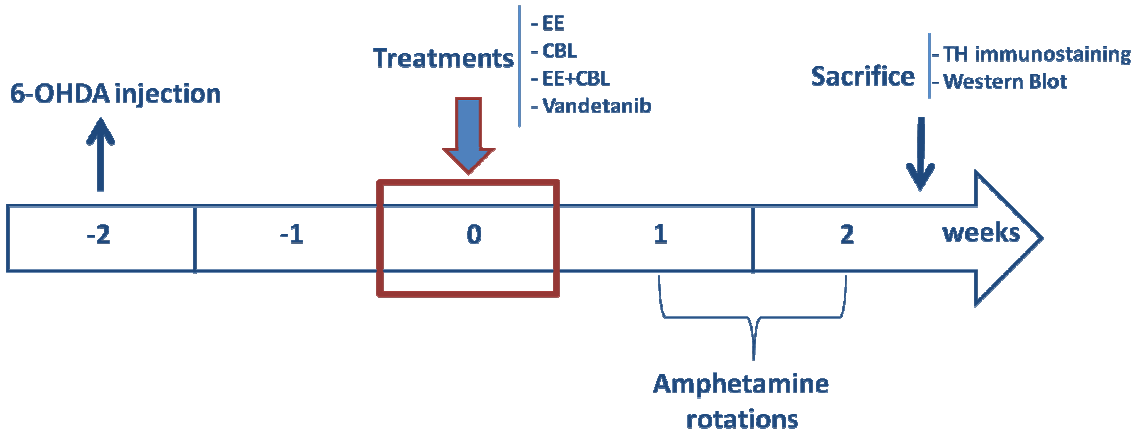

Figure 62. Schematic illustration of the experimental design showing the time course for the assay 3. Abbreviations: EE, enriched environment; CBL, Cerebrolysin; 6-OHDA, 6-hydroxydopamina; TH, tyrosine hydroxylase.

3.1. Improvement of rotational behavior

The behavioral effect after combining or not the administration of CBL and the housing in EE was compared with parkinsonized rats not treated and with those who received the VEGFR2 and RET inhibitor in a unlilateral partial 6-OHDA lesion model.

Amphetamine-induced rotational behavioral test was carried out to corroborate functional deficits due to intrastriatal injection of 6-OHDA at 2 week. There were not differences in the basal number of rotations between animals (Figure 63). Once the motor deficit induced by 6-OHDA was assessed, parkinsonized animals were randomly divided into 5 experimental groups assigned to test each of the conditions under investigation (Table 5). After one week with the treatment or after 3 weeks in case of the group with only toxin, behavioral test was again performed in order to evaluate whether the treatments modified the behavioral dysfunction. Results were expressed as the increase or decrease in the number of rotations before and after treatment. This new strategy for representing the rotations was developed because in this study we only assessed two time points.

However, in this assay no rats turned more than 3 tpm and we represented the results for each experimental group as the total number of rotations in 90 minutes after amphetamine administration. Because of that we considered this assay as a prodromal or preclinical partial 6-OHDA induced model.

Only CBL group (-42.9±12.14 turns) and CBL+EE group (-8.53±5.58 turns) decreased the number of rotations. Rats received vandetanib showed the highest number of ipsilateral rotations (23.29±19.35 turns), even more than the 6-OHDA rats without treating, which were the control group (7.11±14.56 turns) (Figure 63). The improvement seen in rats treated with CBL were statistically significant respect to 6-OHDA rats (*p<0.05, one way ANOVA). In addition, rats treated with CBL and housed in EE showed a tendency to ameliorate the number of rotations (Figure 63).

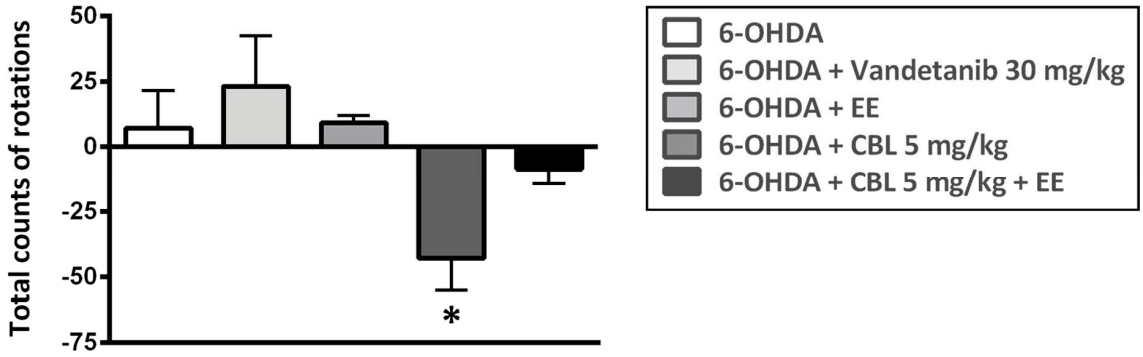

Figure 63. Behavioral effects after treatments. The graph shows the results obtained using the amphetamine-induced behavioral test for 90 minutes. The number of rotations before and after treatment decreased in rats after administering Cerebrolysin (CBL) and CBL combined with housing in an enriched environment (EE) for one week, while rotations in rats treated with vandetanib or housing in EE increased. Results are expressed as the difference in the number of rotations before and after treatments. The CBL group *vs.* the 6-OHDA group show statistically significant differences (*p<0.05). Data are shown as means±SE.

We also assessed the rotations every 5 minutes for 90 minutes in order to elucidate differences in amphetamine metabolism in each experimental group in order to find the time of most activity prior to stabilization. It was also expressed as the increase or decrease in the number of rotations before and after treatment every 5 minutes during 90 minutes (Figure 64). The number of rotations began to decline after

60 minutes, but the results were not as pronounced as those obtained with the CBL administration, which showed the lowest number of rotations in that time (Figure 64). The most relevant decrease in rotation has been achieved by the CBL group although not with differences enough to reach statistical significance.

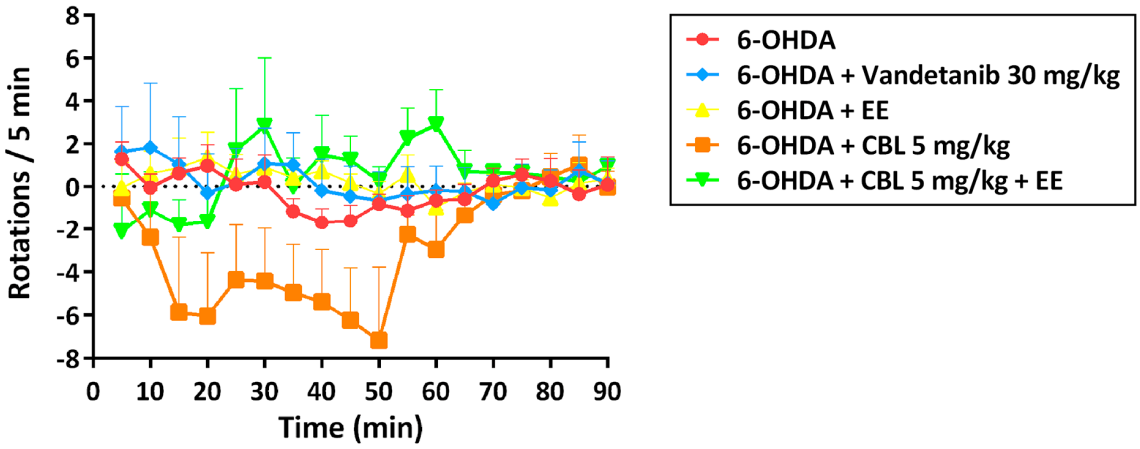

Figure 64. Rotational behavior induced by amphetamine recorded every 5 minutes. 60 minutes after administration, the effects of amphetamine diminished for all experimental groups. Rats treated with Cerebrolysin (CBL) showed the largest difference in metabolizing the amphetamine, whereas the remaining groups did not show differences. Results are expressed as the difference in the number of rotations every 5 minutes before and after treatment. Data are shown as means±SE.

Thus, the results obtained in motor behavioral test support an early partial lesion of the nigro-striatal system induced by intra-striatal injection of 6-OHDA and likely the existence of compensation mechanism following partial dopaminergic lesion.

3.2. Morphological evaluation

Following unilateral injection of 6-OHDA, treatments were administrated and the morphological effects of the treatments on dopaminergic system were examined. Thus, after the last behavioral assessment, rats were sacrificed by transcardial perfusion and brains were removed and processed for TH-immunostaining.

Rat brain surfaces showed the three injections marks where the 6-OHDA was administered. No macroscopically differences were observed between groups.

Macroscopic examination of coronal sections was performed to evaluate structural changes after 6-OHDA injection and TH-ir in the striatum and SN brain regions.

As we described previously, not only the neurotoxicity induced by 6-OHDA but also the neurosurgical procedure itself can lead to an impairment of cerebral structures. Conversely, striatal lesion induced by surgery produced an enlargement of the lateral ventricle in the injured side, which was also assessed and then quantified as tissue retraction. In spite of treatment with neuroprotective substances or conditions, as CBL administration and EE housing, could reduce this side effect; we did not find differences between all the studied groups (Figure 65).

On the other hand, a general reduction in the TH+ staining was seen in many fibers, many of them surrounding the main lesion site in the striatum. Thus, the most loss of TH expression in striatum was located in the middle sections, where the toxin was injected. Indeed, the most caudal sections presented the highest positivity for TH owing to be distant from the lesion (Figure 65). However, as exception, rats received vandetanib showed an intense reduction of TH-positivity in dorsolateral part of striatum, decreased from rostral to caudal sections (Figure 65). This fact indicated that this treatment affected negativity to the dopaminergic fibers in the striatum and showing the same tendency to decrease the positivity for TH than the rest of the partially lesioned groups previously studied in the other study.

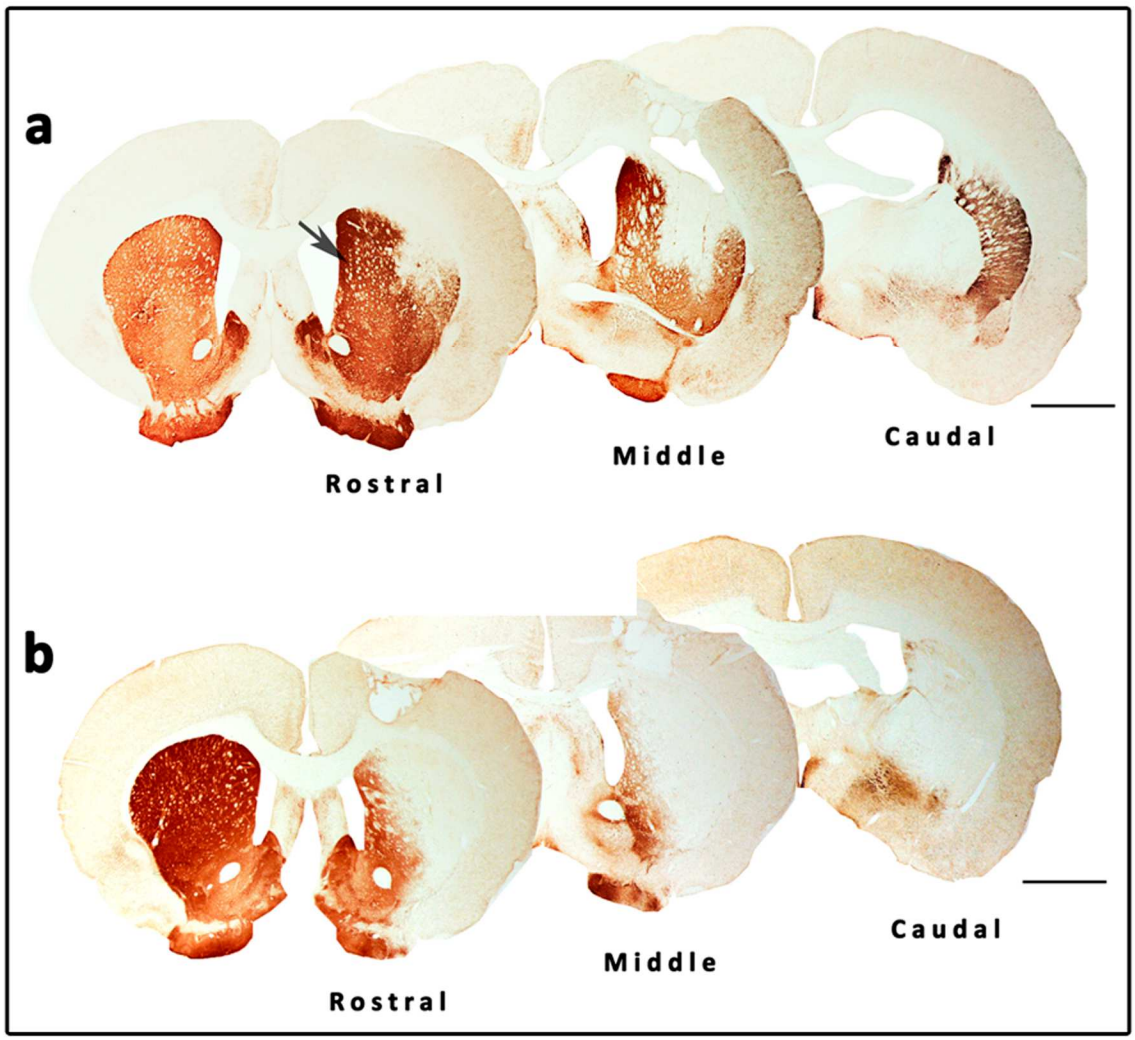

Figure 65. Rostro-caudal distribution after 6-OHDA injection. The loss of tyrosine hydroxylase (TH)-positivity in the striatum was different along the rostro-caudal axis and this topological distribution was different in 6-OHDA, CBL, EE and CBL+EE groups with respect to the vandetanib group. (**a**) Photomicrographs of the rostral, middle and caudal sections of the striatum from the 6-OHDA group. The arrow indicates the enlarged ventricle in the lesioned hemisphere due to scar retraction after 6-OHDA injection. In contrast, (**b**) the vandetanib group showed a decrease in TH-positivity from rostral to caudal sections. Scale bar = 2 mm.

Regarding SN, the loss of positivity for TH was focused on the previous region delimited and described as external SN. Interestingly, we observed changes in TH expression, showing rats received CBL and were housed in EE the most positivity for TH. In contrast, rats only received 6-OHDA and rats administered with vandetanib presented the lossest in positivity for TH, indicating that vandetanib induced degeneration. In addition, only group received vandetanib presented a topological distribution for TH-

positivity, decreasing the positivity from rostral to caudal sections, like in striatum. In the rest of the experimental groups these differences were undetectable.

3.2.1. Quantitative analysis

Stereological analysis was carried out in order to assess the ability of CBL and EE housing to restore in striatum and SN the level of TH following unilateral injection of 6-OHDA. For this purpose, we measured the affected volume and the tissue retraction in striatum and the density of dopaminergic neurons in SN. However, changes did not occur along the rostro-caudal axis in the SN, since the differences were not found to be statistically significant.

3.2.2.1. Vandetanib increased the loss of TH-positive terminals in the striatum after 6-OHDA injection

As we previously describe, two stereological approaches have been used to evaluate the structural injury induced by 6-OHDA in the striatum. The administration of vandetanib dramatically increases the volume of CPC negative for TH-immunoreaction (Figure 66a). In fact, in the vandetanib group the TH-negative volume was 2.09±0.13 mm^3 (showed 72.28±3.64% of the total volume of the ipsilateral CPC). This group presented more affected volume than the other experimental groups (1.18±0.13 mm^3, 33.9±2.58% in the 6-OHDA group, 1.31±0.2 mm^3, 42.05±2.18% in the CBL group, 1.36±0.11 mm^3, 40.39±2.27% in the EE group and, 1.33±0.15 mm^3, 44.06±2.67% in the CBL+EE group). Only rats received vandetanib presented statistically significant differences respect to the other groups (***$p<0.001$; one way ANOVA) (Figure 66a). Thus, rats lesioned with 6-OHDA without any additional treatment did not show differences respect to rats received NTF and/or rats housed in EE.

Concerning to tissue retraction, measurements did not show significant differences between groups. However, owing to the lesion induced by the striatal 6-OHDA administration, the percentage of tissue retraction was around 10-15% in all

groups (Figure 66b). Remarkably, 6-OHDA group showed the most tissue retraction 15.08%.

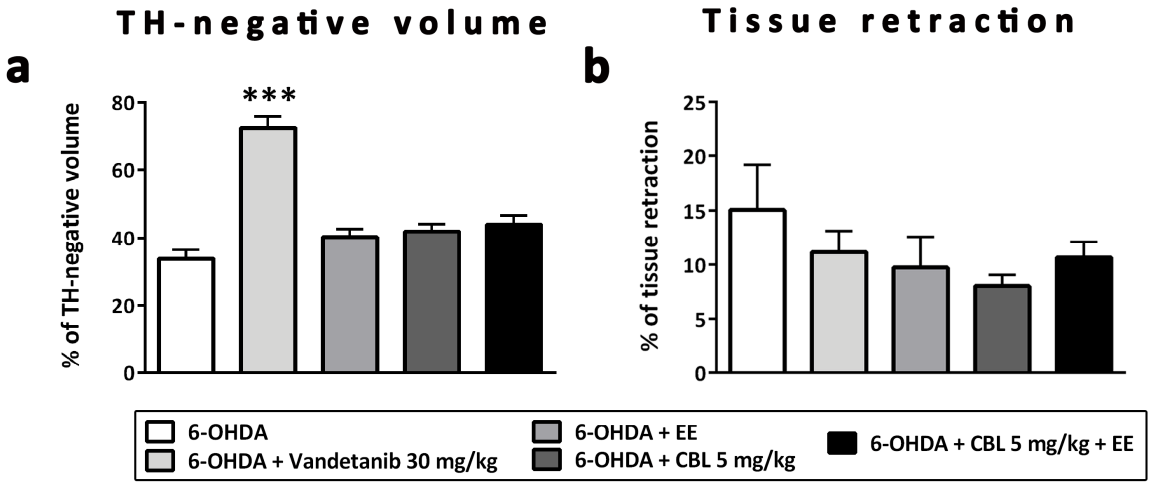

Figure 66. Quantitative analysis in the striatum. (**a**) The graph shows the results obtained after measuring TH-negative volume. The vandetanib group showed the highest percentage of TH-negativity with respect to the other groups and these differences were statistically different. Significance ***p<0.01 vandetanib *vs.* 6-OHDA groups. Results are expressed as the percentage of TH-negative volume of the ipsilateral striatum with respect to the total ipsilateral one. (**b**) The percentage of tissue retraction. Results are expressed as the total volume of the percentage of the ipsilateral striatum *vs.* the contralateral one. Data are shown as means±SE.

Moreover, when comparing topological distribution of vandetanib treated animals, quantitative analysis revealed that the most abundant denervation (% of TH-negative volume) was found within caudal levels of the striatum and significant differences were noticed between rostral (57.61±7.68%) and middle section (66.71±10.13) respect to the caudal one (84.95±5.45%) within this group (***p<0.001 for rostral sections and *p<0.05 for middle sections; one way ANOVA). In contrast, in the rest of the animals, including those only treated with the toxin, the highest percentage of TH-negative volume was found in the middle level, which corresponded to the levels located closer to the 6-OHDA injection sites. However, statistically significant differences between groups were only found in caudal levels comparing vandetanib group respect to the other groups. Remarkably, we also found statistically significant differences within

6-OHDA group between middle and caudal sections (44.33±1.75% and 21.52±4.18% respectively) (*p<0.05; one way ANOVA).

3.2.2.2. Combination of Cerebrolysin and enriched environment housing promoted neurorestorative effects in the SN

In spite of CBL administration and EE housing did not show any protective effect on dopaminergic fibers in striatum, a neurorestorative effect was appreciated combining both strategies in SN. Vandetanib administration also presented the highest loss of dopaminergic neurons in SN in agreement with the results showed in the striatum.

TH-ir neurons were counted in the entire SN and in the external SN; this specific region was more affected by vandetanib administration, although showed more recover after CBL administration and after housing in EE than in the entire SN (Figure 67).

Regarding the entire SN, the density of dopaminergic neurons was statistically higher in the group combining both strategies (CBL administration and housing in EE), with respect to the 6-OHDA and vandetanib groups (51.55±4.55% *vs.* 28.72±3.17% and 26.53±2.64%) (***p<0.001 respect to vandetanib group and ###p<0.001 respect to 6-OHDA group; one way ANOVA) (Figure 67a). On the other hand, rats only administered with CBL or only housing in EE also presented statistically significant differences respect to 6-OHDA rats and vandetanib group (43.77±2.87% and 42.13±3.41% *vs*. 28.72±3.17% and 26.53±2.64%), although these differences were not as remarkably as combining both strategies (**p<0.01 respect to vandetanib group and ##p< 0.01 respect to 6-OHDA group; one way ANOVA).

However, when the e-SN was considered statistically significant differences were only found for CBL and EE groups respect to rats treated with vandetanib (56.44±8.425% and 54.34±7.65% *vs.* 22.80±4.33%) (#p<0.05; one way ANOVA) (Figure 67b). Remarkably, rats combining both strategies also presented the most statistically significant differences respect to vandetanib group (66.61±13.37% *vs.* 22.80±4.33%) (##p<0.01; one way ANOVA).

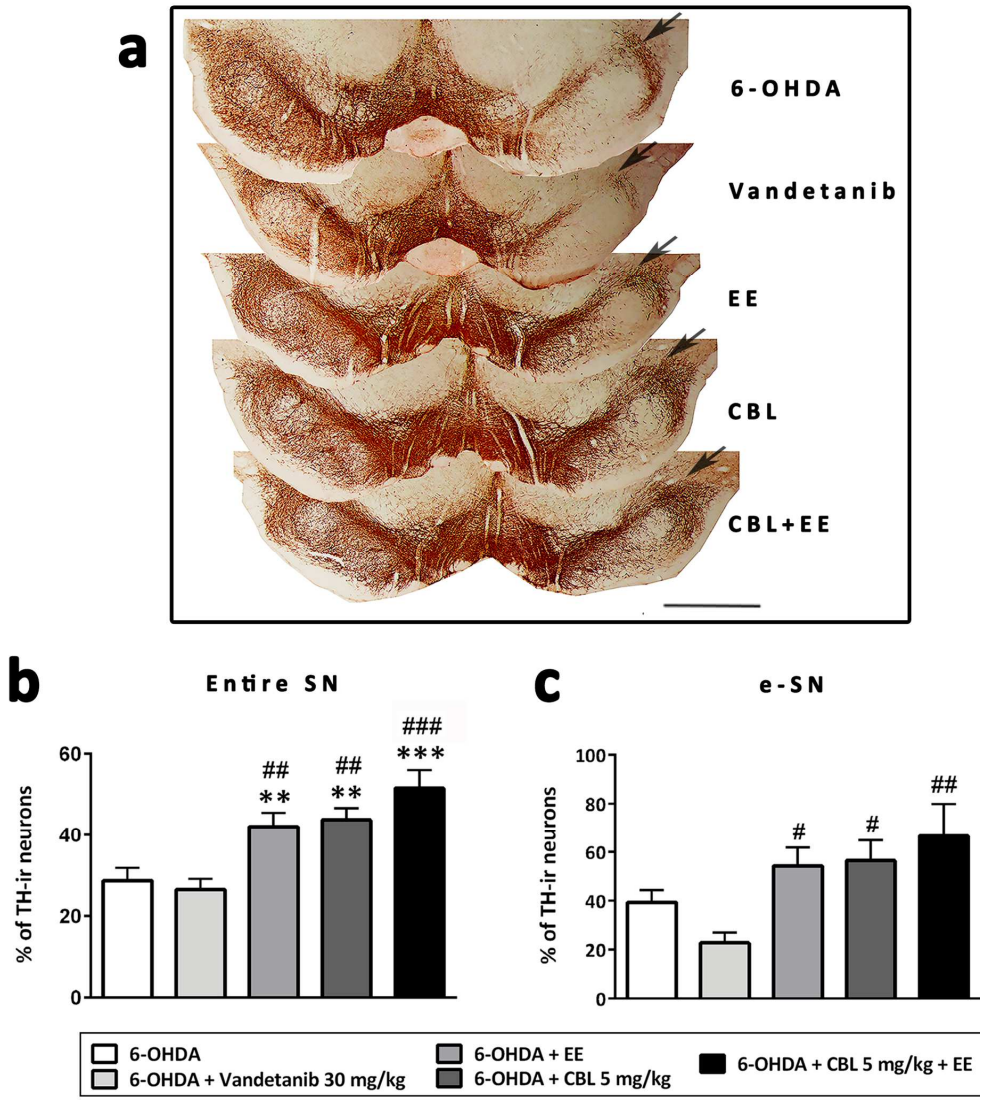

Figure 67. The density of TH-positive neurons in the substantia nigra (SN) increased in the CBL+EE group. (**a**) Photomicrographs of the TH-immunostained SN for every group. Scale bar = 1 mm. **(a-b)** Graphs show the density of neurons in the SN. Results are expressed as the percentage of the ipsilateral SN *vs.* the contralateral one. (**b**) Regarding the entire SN, the CBL+EE group showed the highest neuronal density (***p<0.001, CBL+EE *vs.* 6-OHDA group and ###p<0.001, CBL+EE group *vs.* vandetanib group). (**c**) The CBL+EE group also showed the highest increase in neuronal density in the external SN (##p<0.01, CBL+EE group *vs.* vandetanib group). Data are shown as means±SE.

These data suggested that the i.p. administration of a NTF mixture (as Cerebrolysin) resulted in a neurorestorative effect as well as preservation of functional behavior in rats partially lesioned (allowing the development of a Preclinical model). However, results also supported a synergistic effect of combining drug administration

with EE housing. All of it resulted the highest significant neuronal density accompanied by a tendency of functional recovering.

Overall, results showed that 6-OHDA injection into the striatum in this study only induced a partial and moderate lesion of dopamine cells in the SN. Thus, we also suggested in this assay an early partial lesion, which could correspond to the preclinical state.

3.3. Effects of the treatments on the signaling pathways

Biochemical study was carried out in order to assess signaling pathways related to survival and apoptotic mechanisms by western blot. In addition, TH was also analyzed by western blot to corroborate results obtained by immunohistochemical analysis. For that, rats were sacrificed by decapitation and the brains were then removed, ipsilateral and contralateral striatum and SN were dissected and processed.

Thus, western blot was used as a technique to evaluate the markers of dopaminergic neurons (TH), apoptotic process (cleaved caspase-3) and survival mechanism (p-Akt/Akt) in striatum and SN. ß-actin was used as loading control for caspase-3 and TH expressing the results as the percentage of caspase-3/ ß-actin and TH/ ß-actin ratios of the lesioned hemisphere respect to the non lesioned one set as 100%. In contrast, p-Akt was normalized by total Akt levels and the activation of Akt was evaluated as the percentage of p-Akt respect to Akt in ipsilateral hemisphere respect to contralateral one set as 100%.

3.3.1. Analysis of TH by western blot in the striatum and substantia nigra

TH protein level was also determined by western blot analysis in striatum and SN. Remarkably, no statistically significant differences were found between experimental groups. Consistent with the results in TH-immunostaining, the CBL and CBL+EE group showed a tendency to restore the TH levels compared to 6-OHDA group and vandetanib group in SN (85.75±4.21% and 77.33±10.53% *vs.* 52.75±11.06% and 70±3.51%, respectively).

3.3.2. Combination of Cerebrolysin and enriched environment housing induced an increase in Akt signaling

To elucidate further any role of an intracellular-signaling pathways in cell survival that lead to neuroprotection and neuroregeneration induced by CBL administration or/and EE housing in SN, the activation of protein kinase Akt was evaluated. In fact, Akt can be activated after the binding of growth factors on many specific cell-surface receptors. Thus, Akt could be also a potential down-stream target of VEGFR2 and RET in order to also study the effects of vandetanib administration.

Combining strategies, rearing in EE and nanodelivery of CBL, induced phosphorylation of Akt by 129.7±27.61% in striatum and by 155±29.67% in SN, showing more phosphorylation of Akt in SN.

a) Striatum

CBL+EE group in striatum increased the protein expression of p-Akt/Akt against 6-OHDA toxicity compared to the other groups (129.7±27.61% in CBL+EE group *vs.* 97.67±10.17% in 6-OHDA group, 102±7.95% in vandetanib group, 111.3±13.88% in EE group and 106.5±11.5% in CBL group) (Figure 68). In spite of presenting the most percentage of Akt activation respect to the other groups, 6-OHDA lesioned rats treated

with CBL and housing in EE did not present statistically significant differences respect to the 6-OHDA group.

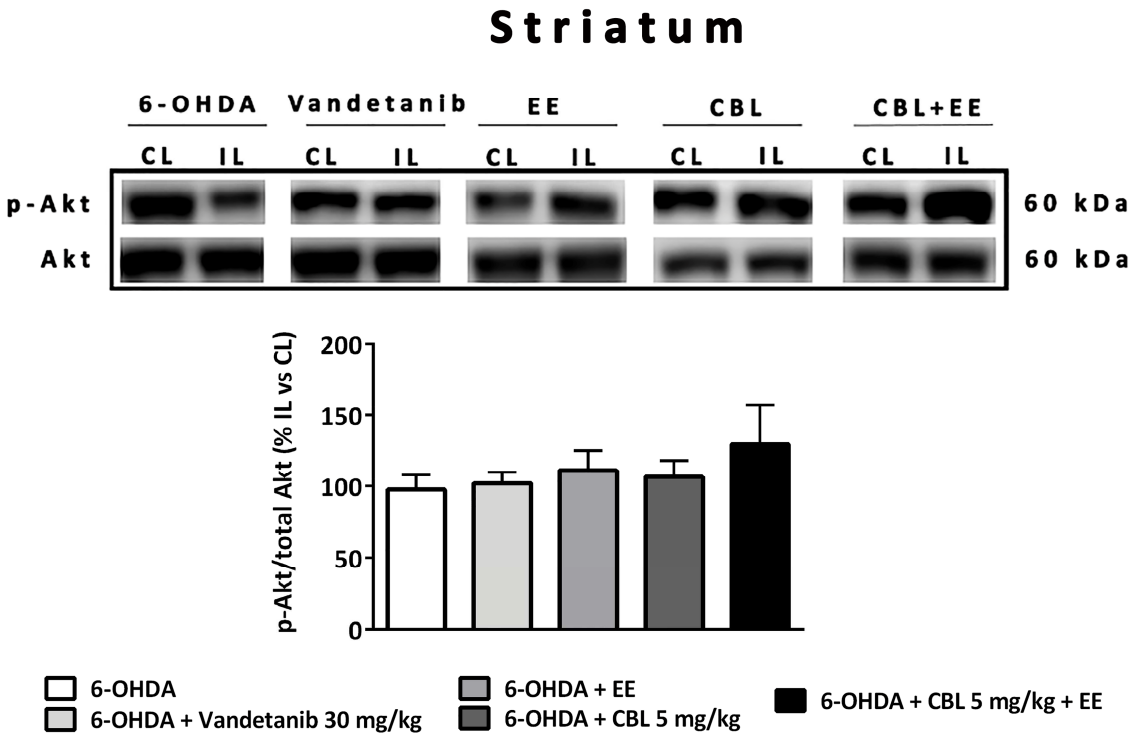

Figure 68. p-Akt protein expression in the striatum. Western blot (upper panel) of p-Akt and Akt protein expression in the contralateral (CL) and ipsilateral (IL) caudate putamen complex for each experimental group; quantification (lower panel) of band density. Results are expressed as the percentage of the p-Akt/Akt ratio in the lesioned hemisphere with respect to the non-lesioned one. The ratio of p-Akt/Akt in the CL hemisphere was set as 100%. Differences were not statistically significant, although the p-Akt/Akt ratio showed the highest increase in the CBL+EE group.

b) Substantia nigra

When the SN was analyzed, the activation of Akt was only found in CBL+EE group, showing statistically significant differences respect to the other experimental groups, even respect to rats only treated with CBL or only housing in EE (155±29.67% in CBL+EE group *vs*. 69±7.37% in EE group, 76.5±4.5% in CBL group, 82.67±6.49% in 6-OHDA group and 81.67±7.45% in vandetanib group) (*$p<0.05$; one way ANOVA) (Figure 69).

As expected, data also showed that vandetanib administration did not induce activation of Akt in SN, indicating that inhibition of VEGFR2 and RET produced negative effects on cellular survival.

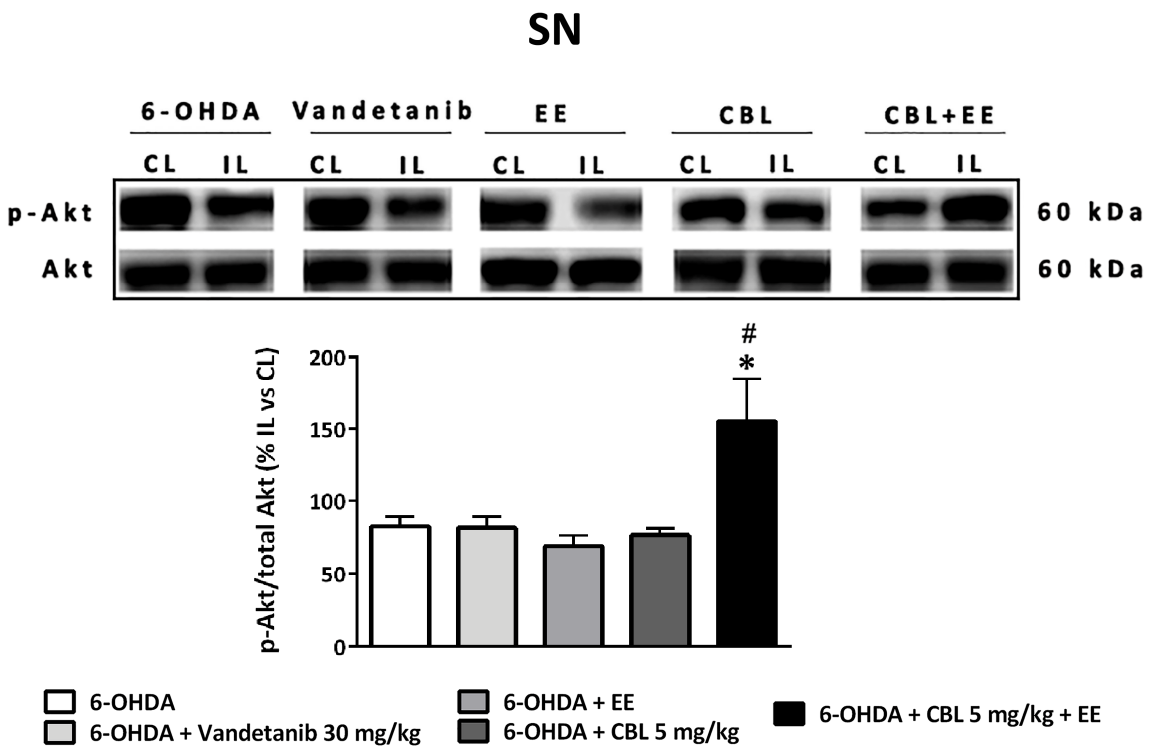

Figure 69. p-Akt protein expression in the substantia nigra. Western blots (upper panel) and quantification (lower panel) of p-Akt/Akt ratios. Results are expressed as the percentage of the p-Akt/Akt ratio in the lesioned hemisphere (IL) with respect to the non-lesioned one (CL). The CBL+EE group showed a significant increase in p-Akt expression compared to the other experimental groups (*p<0.05, CBL+EE group *vs.* 6-OHDA group; #p<0.05, CBL+EE group *vs.* vandetanib group).

3.3.3. Vandetanib increased caspase-3 expression

To verify that vandetanib is involved in neuronal cell death in the context of PD, apoptotic-related protein was evaluated by examining the expression levels of caspase-3 in every treatment.

Interestingly, the evaluation of the expression of casapase-3 levels followed the same tendency in striatum and SN for every experimental group, increasing this expression in vandetanib group and decreasing in CBL+EE group.

a) Striatum

In the striatum, statistically significant differences were found in CBL+EE and vandetanib groups respect to 6-OHDA group (68±3.61% and 134.3±14.19% *vs*. 102±6 %) (*p<0.05, CBL+EE and vandetanib group *vs*. 6-OHDA group; one way ANOVA). Interestingly, the most differences in caspase-3 expression were differences in CBL+EE and vandetanib groups (##p<0.01, CBL+EE *vs*. vandetanib group; one way ANOVA) (Figure 80).

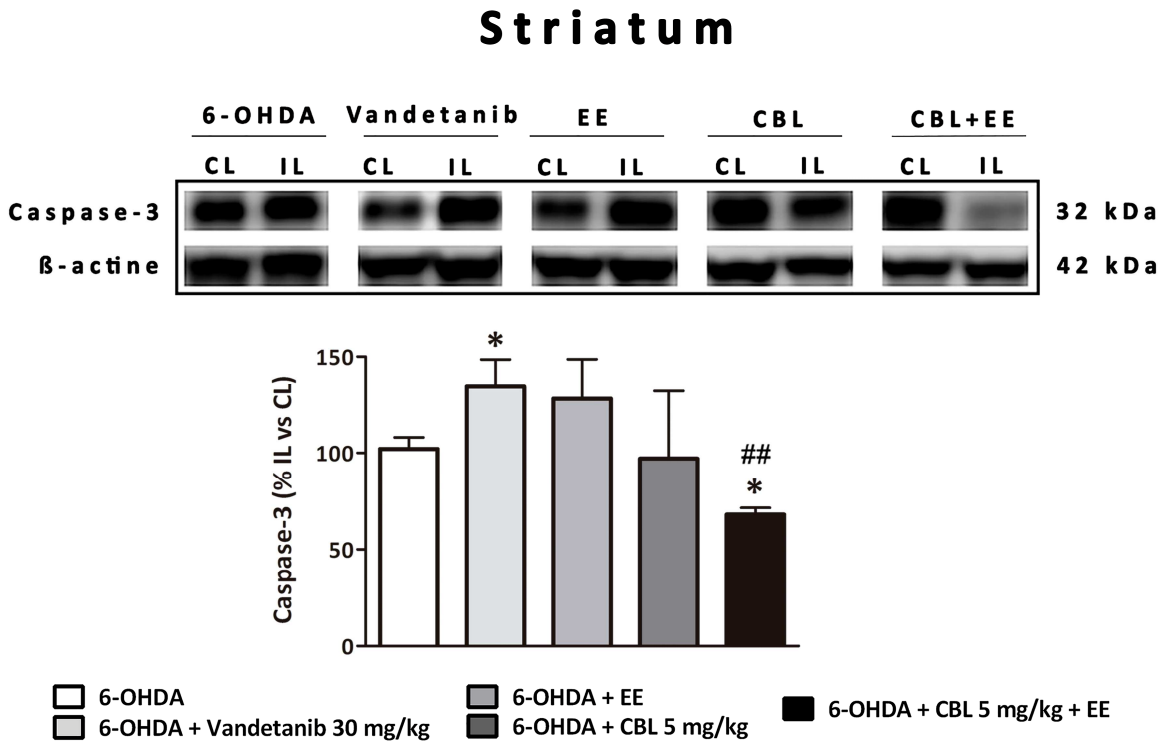

Figure 70. Caspase-3 expression in the striatum. Western blots (upper panel) and quantification (lower panel) of caspase-3 protein expression. Data were normalized to ß-actin protein levels and are presented as the percentage of the caspase-3/actin ratio in the lesioned hemisphere (IL) *vs.* the non-lesioned one (CL). Caspase-3 levels were significantly increased in the vandetanib group and significantly decreased in the CBL+EE group (*p≤0.05, CBL+EE group and vandetanib group *vs.* 6-OHDA group, #p≤0.05, CBL+EE group *vs.* vandetanib group).

b) Substantia nigra

The vandetanib group showed the highest expression of caspase-3 (144.7±10.9%) and rats treated with CBL and housing in EE exhibited the lowest levels of expression (96±19.04%), but the differences in the SN were not statistically different (Figure 71).

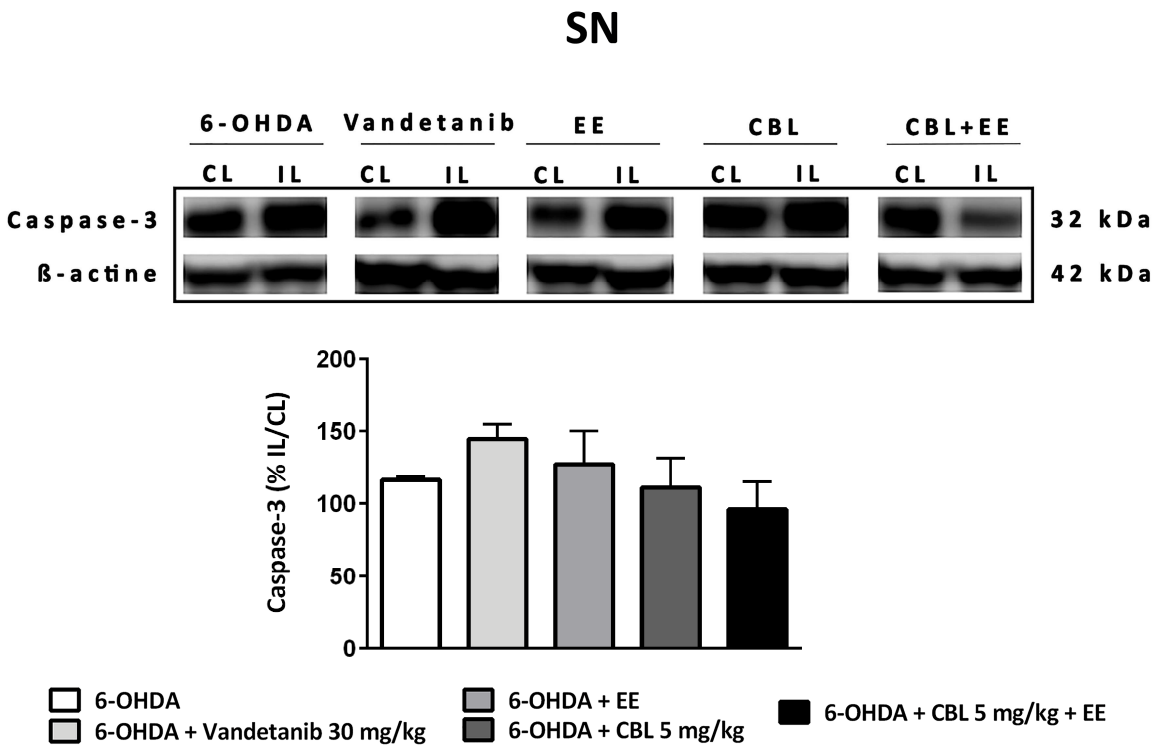

Figure 71. Caspase-3 expression in the substantia nigra. Western blots (upper panel) and quantification (lower panel) of caspase-3 protein expression. Results were normalized to ß-actin protein expression and are expressed as the percentage of the caspase-3/actin ratio in the lesioned hemisphere (IL) with respect to the non-lesioned one (CL). There were no significant differences between groups. The vandetanib group showed a tendency to increase the caspase-3 levels, whereas caspase-3 expression decreased in the CBL+EE group.

These data indicated that the cotreatment with CBL administration and housing in EE could prevent and reverse 6-OHDA-induced cell death in this model, inducing antiapoptotic effect on this model. On the other hand, inhibition of VEGFR2 and RET remarkably increased apoptotic effect induced by 6-OHDA.

VI. DISCUSSION

The classical method of intracerebral injection of 6-OHDA depending on the site of injection, involving different degrees of nigrostriatal dopaminergic neurons and it is largely used to investigate motor, morphological and biochemical dysfunctions in PD. In fact, in this study, 6-OHDA induced model provides the assessment of three different severity grades of PD and it was suitable to test the lesion morphologically and the effects of different treatments. We also propose innovated stereological procedures to assess the striatum and SN involvement in these models.

NTFs are considered a hopeful treatment for PD (Krakora et al., 2013), demonstrating positive effects in rodent and primates models. There are few works about the therapeutic effectiveness of using NTFs in combination as treatment of various neurodegenerative disorders (Herrán et al., 2013, 2014; Krakora et al., 2013; Requejo et al., 2015). Our results are promising, although it should be essential to adjust the dose of both NTFs in the severe model in order to reduce the tissue damage in further studies.

Rostro-caudal gradients of the morphological changes exhibited in the striatum and in the SN, in addition to the specific anatomic distribution of the dopaminergic system, suggest a differential selective vulnerability of this system. A deeper knowledge of this distribution could be useful in order to assess the lesion, as well as the administration and diffusion of treatments. The measurements carried out on the e-SN – topographically related to the lesioned area of the striatum- reach more specific and significant results than those carried out in the entire SN, emerging as a promising region for further studies.

Functional improvement and morphological recovery after VEGF and GDNF implantation is related to the preservation of the TH-positive volume, cells and ADN in the striatum and SN. In addition, these findings support the neurorestorative role of VEGF+GDNF on the dopaminergic system and the synergistic effect between both factors.

Partial model exhibited the best option to assess the treatment, because of that the intrastriatal injection of 6-OHDA in adult rats with more weight, provided us the insight to assess a Preclinical model. This model was presymptomatic, because no rat showed 3 tpm, although molecular mechanisms were activated in these rats leading to assess molecular changes after the treatments. Thus, this model was suitable to test neuroprotective strategies and clues to develop future treatments against PD. In this context, targeting of neuroprotective treatments should focus on the midbrain and in the restoration of DA levels in the striatum will also be required in order to achieve functional behavioral outcomes.

1. Morphological changes in the caudate putamen complex and substantia nigra after 6-OHDA administration into the medial forebrain bundle

It is well known that the unilateral injection of 6-OHDA into MFB is the most widely used model of PD in rats (Deumens et al., 2002) because the lesion results in an extensive depletion of dopaminergic fibers in the striatum as well as cells in the SN, leading to the motor impairments. In fact, it is necessary approximately the 80% of loss in DA levels of striatum in order to manifest the symptoms (Deumens et al., 2002). Therefore, this model is very useful to mimic behavioral, biochemical, and histopathological abnormalities observed in advanced stages of patients with PD (Henderson et al., 2003). On the other hand, oxidative stress, which is considered an important pathogenic factor in PD because it could affect the survival of dopaminergic neurons, displays a pivotal role in the neurotoxicity induced by 6-OHDA (Baluchnejadmojarad et al., 2010; Tapias et al., 2014).

Morphological changes induced by injection of 6-OHDA into MFB were observed. To assess the degeneration in striatum and SN produced by the administration of 6-OHDA into the MFB, we developed different morphological approaches.

Examination of coronal sections after 6-OHDA or saline solution administration into MFB revealed an enlarged homolateral ventricle with a retracted striatum on the injured hemisphere, which was more remarkable in 6-OHDA rats. It was also observed in works carried out in a Partial model of PD, where 6-OHDA was injected into striatum (Przedborski et al., 1995). Therefore, in rats treated with MS injected into striatum this homolateral enlargement of the ventricle was more pronounced.

Nissl-staining did not reveal any significant change in the striatum of the 6-OHDA or saline-treated rats. However, in rats in which microspheres had been implanted into the striatum, striatal sections stained with Nissl showed and hypocromic areas corresponding to the needle track. Accordingly, it has been reported that Nissl staining correlated well in the striatal model, but there was a discrepancy between measures obtained in the MFB-lesioned animals (Yuan et al., 2005). Nevertheless, Nissl staining could be useful for getting a better estimation of the size and trajectory of the lesion when administrating some treatment in the striatum in this model.

It has been reported an evaluation of the loss of dopaminergic neurons requires concomitant loss of a DA marker, such as the TH-ir, and loss of a general neuronal marker, such as staining for Nissl staining (Sauer & Oertel, 1994; Przedborski et al., 1995). However, we have to take into account that Nissl staining considers all neuronal populations existent in the SN, i.e. dopaminergic neurons and non-dopaminergic neurons.

In order to protect against the toxicity produced by the injection of 6-OHDA into the MFB, we encapsulated VEGF and GDNF, individually and in combination, in biodegradable and biocompatible poly(lactic-co-glycolic) acid (PLGA) polymers for the controlled brain release of NTFs in the brain, using this pharmacological strategy as a possible therapy (Herrán et al., 2013). PLGA-microspheres were well tolerated; they do not present toxic effects and the appearance of an immune response is very unlikely (Herrán et al., 2013, 2014). These treatments were administered into the striatum, according to previous studie, which indicated that in PD the degeneration of

dopaminergic neurons was the consequence of an insult which mainly takes place in the terminals of the striatum (Fearnley & Lees, 1991). In fact, it was reported a protective effect of GDNF on the TH-positive axons terminals in the striatum only when it was administrated into the striatum (Kirik et al., 2000). Thus, the delivery of the treatment into striatum could have more positive effects than injecting into other regions.

1.1. 6-OHDA injection into the medial forebrain bundle increased GFAP expression in the ipsilateral substantia nigra

Injection of 6-OHDA into the MFB increased GFAP levels in the injured SN, while in the striatum there was no difference between the lesioned and non-lesioned striatum. On the other hand, saline injected rats did not show differences between the ipsilateral and contralateral hemispheres in both anatomical structures, suggesting that injury produced by lesioning was not responsible for the gliosis observed in the SN. In contrast, if we had been able to observe the MFB where the saline solution was injected, we would have seen an activated astrocytic response to the insult. This increase in the expression of GFAP in the SN after 6-OHDA injury could be because GFAP plays a supportive and anti-inflammatory role in protecting dopaminergic neurons in the SN in PD models (Jakel et al., 2005, 2007; Burton et al., 2006), because they express dopamine transporters (Karakaya et al., 2007), enabling them to take up 6-OHDA. Astrocytes produce cytokines which modulate inflammation and NTFs, which are involved in the antioxidant pathway in which they control the neurotoxin levels and to cellular homeostasis (Eddleston & Mucke, 1993). In fact, one study carried out by Steiener and collaborators, suggested that the protection induced by EE is mediated by astrocyte activation in the SN (Steiner et al., 2006).

The fact that we observed an increase in GFAP levels in the SN, but not in striatum also corroborates the findings supported by Henning and collaborators, who demonstrated that astrocyte activation could result at sites remote to the lesion in a partial lesion, but not in a severe lesion (Henning et al., 2008). Severe lesion of the MFB

or SN produces anterograde degeneration from the SN to the striatum, with the striatum being distant from the lesion carried out in the MFB in this case. They suggested that astrocytic networks may transmit activation signals to neuronal pathways because they were connected by gap-junctions. This connection could remain if the neuronal pathways degenerate but the total loss of degeneration disrupts glial communication. The present findings support this hypothesis because this increase in GFAP expression observed in the SN was associated with the marked decline of TH+ in the number of neurons in the SN. In addition, these observations corroborated our results showing that the degeneration of neurons and/or their projections induced reactive astrogliosis (Sofroniew, 2005; Wachter et al., 2010). In contrast, other groups have shown a delay in the astrocyte response following 6-OHDA lesion (Walsh et al., 2011; Stott & Barker, 2014), indicating that it is possible that more than 2 weeks is required for astrocyte activation and recruitment to the nigrostriatal structures more distal from the lesion site (Walsh et al., 2011; Stott & Barker, 2014).

These discrepancies related to the lack of GFAP expression in remote sites of the lesion in this model could be because of the use of different rat strains, or varying 6-OHDA doses and injection sites.

2. Morphological changes in the caudate putamen complex after 6-OHDA administration into the striatum

A unilateral infusion of 6-OHDA into the striatum results in several histopathological changes, being the most prominent the loss of TH-ir fibers, terminals and neurons (Gibb, 1997). An analysis of the Nissl staining sections of all experimental groups showed enhanced cellularity around the needle track. The increase of astroglial reaction and reactivity for GFAP is widely used to determine the wound-healing response in SNC (Brodkey et al., 1993). Astrocytes play a major role buffering the environment of neuronal cells (Clarke & Barres, 2013) and, because of this, it would be important to determine which other functions develop in PD, apart from wound healing.

For instance, Fuller and collaborators suggest that astrocytes could increase the viability of endogenous nigrostriatal neurons (Fuller et al., 2014). Rats treated with NTFs showed a potentially regenerative response, increasing their GFAP-positivity compared with the striatum and SN of other treated groups.

Degeneration of nigral dopaminergic neurons in PD is believed to be associated with a glial reaction and inflammatory changes (Barcia et al., 2005). The increased expression of activated microglia, vasculature and VEGF levels showed in the striatum and SN of rats lesioned with 6-OHDA has been also reported in patients with PD (Faucheux et al., 1999). In this context, neuroinflammation mediators are known to be crucial in the progression of PD (Block et al., 2006). In addition, one study developed in monkeys lesioned with MPTP by Barcia et al reported an increase of VEGF expression in non-dopaminergic neurons suggesting that plastic changes also occur in other types of neurons in response to the toxin (Barcia et al., 2005). Therefore, we have corroborated that microglia activation and recruitment of VEGF-positive cells among others are processes implicated in the pathogenesis and progression of PD.

2.1. Remarkable limit inside the striatum

Administration of 6-OHDA into the striatum, rather than a progressive model for PD –as it requires time to check changes after the lesion-, is a suitable model to test neuroprotective and neurotrophic drugs. 6-OHDA produces a selective destruction of the dopaminergic system and provides a suitable model, where it is possible to elucidate the optimal time, in order to initialize the treatment (Agid et al., 1973; Brodkey et al., 1993; Jankovic et al., 1994; Sarre et al., 2004). Intrastriatal administration of 6-OHDA, following the proposed coordinates, induces a lesion in the dorsolateral striatum corresponding to areas with poor expression of calbindin.

Calbindin is a calcium-binding protein that acts as an endogenous calcium buffer (Li et al., 1995). Alterations in the amount of this protein have been found all through the brain in PD patients (Hurley et al., 2013). Stress and neuronal death are mediated by

calcium, and the distribution of calcium-binding proteins is not homogenous in the striatum and in other parts of the brain, being partially responsible for the selective vulnerability of some neuron populations in the CNS (Cervós-Navarro & Lafuente, 1991; Andres-Mateos et al., 2007). Most cases showed a remarkable limit between negative lateral region and positive medial areas. This may probably be a result of the selective vulnerability of these areas to the oxidative stress, previously mentioned, due to lack of calbindin. Neurons require high amounts of energy to maintain their functions, needing an efficient calcium buffering ability (Surmeier et al., 2011).

3. Intratriatal 6-OHDA administration in adult male rats as a Preclinical model

A Preclinical model of Parkinson's disease induced by the intrastriatal administration of 6-OHDA in adult male rats

Models of partial dopaminergic degeneration have been developed with the aim of revealing finer motor deficits (Simola et al., 2013). Regarding this fact, we achieved to get a presymptomatic model to study a podromal stage of PD. Thus, in assay 3, intrastriatal administration of 6-OHDA induced an early Partial model, in which motor symptoms were not appreciated. No rat from assay 3 turned more than 3 tpm after amphetamine behabioral test, before and after treatment. However, morphological assessment revealed DA depletion in striatum and SN in these rats as shown by the TH immunohistochemistry results.

Most studies have examined the behavioral and neurochemical effects of 6-OHDA administration after behavioral deficits first occur, which is typically more than 2 weeks after the injection, even though toxicity to dopaminergic neurons certainly begins almost immediately after the toxin administration (Anastasía et al., 2009). However, we studied the effects after 3 weeks of 6-OHDA injection, without hardly functional amelioration, to assess early changes in dopaminergic system and their

modifications by CBL administration and exposure to EE, and by inhibition of VEGFR2 and RET in this early model.

Athough lesioning conditions were identical in assay 2 and 3, striatal atrophy and neuronal loss was more remarkable in animals from assay 2. In order to the symptoms become apparent, it is thought to be necessary about 80% of DA loss in striatum and the about 70-80% of neuronal loss in SN because of the compensatory mechanisms (Deumens et al., 2002). In fact, before symptoms of PD become apparent, 50–60% of the neurons in the SN and about 20% of the DA innervation in the putamen can still be found (Deumens et al., 2002). In this context, the loss of DA neurons found in this model was around 60-70%. The protection or preservation of neurons seen in this model can be due to alterations in toxin availability, changes in the expression of neuroprotective factors such as the neurotrophins, or interference with activation of the cell death pathways (Faherty et al., 2005). Therefore, we consider this model to be preclinical because there are not motor symptoms or they are scarcely present but it was appreciated an early DA loss. There is growing evidence that a number of symptoms can precede the classical motor features of PD. The period when these symptoms arise can be referred to as the premotor phase of the disease and this notion has been strengthened by recent epidemiological, pathological, and clinical studies which have provided data in favor of the existence of this premotor phase in PD (Tolosa et al., 2007).

Regarding this presymptomatic stage induced in this Preclinical model, we also tested molecular changes, such as marker from survival and apoptotic pathways, and the results obtained showed that in this model 6-OHDA induced an increase in apoptotic pathway and decrease in survival pathways. Thus, we highlight that in the presymptomatic model 6-OHDA was able to activate significantly the neuronal death.

We assessed different treatments in this presymptomatic model, such as i.p. administration of nanowired Cerebrolysin and housing in EE, at 2 week after intrastriatal injection during one week. Effects of inhibiting VEGFR2 and RET were also assessed by administration of vandetanib orally. Neuroprotective effects become apparent after CBL

administration and EE in SN, and the detriment of the inhibition of tyrosine kinase receptors lead to consider this model as appropriate to study molecular changes and to test neuroprotective strategies against degeneration of dopaminergic neurons.

4. Behavioral evaluation

4.1. Recovery after neurotrophic factors administration in a Severe and Partial model

In the **Severe model**, the results of the amphetamine-induced rotation test showed statistically significant differences between the GDNF-MS and empty-MS groups (*$p<0.05$), but no differences (*$p>0.05$) occurred between the empty-MS and VEGF+GDNF-MS groups (Figure 37a). This finding was unexpected, and it suggests that the greater microsphere volume received by the VEGF+GDNF-MS group could complicate the recovery of the damage area (Herrán et al., 2013).

Other research groups have previously shown the abilities of GDNF to improve 6-OHDA-damaged areas (Jollivet et al., 2004; Garbayo et al., 2009). However, it is worth mentioning that these studies used partially lesioned animal models instead of the complete lesions made in the present experiment, which are significantly more difficult to restore. Previous studies have shown that the recovery of the damaged area in this animal model is possible (Grandoso et al., 2007). Instead of this limitation, the results obtained in this behavioral study show that GDNF-MS and VEGF+GDNF-MS are promising treatments for an advanced state of PD.

In a **Partial model**, during the 10 weeks of treatment we corroborated the behavioral benefits generated by VEGF and GDNF administration (Herrán et al., 2014). In the amphetamine-induced rotation test, the results obtained from GDNF treatment were consistent with those of other studies and corroborated the beneficial effects of GDNF in the behavioral recovery. Furthermore, VEGF-NS and GDNF-NS combined treatment presented a lower number of ipsilateral rotations, demonstrating higher

recovery levels when compared with other treatment groups in the lesioned animals. This result was supported by the experimental data obtained from the apomorphine-induced rotation test. Therefore, the positive behavioral results obtained in the combined treatment group suggest that a sufficient recovery in the lesioned brain tissue could have occurred.

4.2. Recovery after Cerebrolysin administration in a Preclinical model

Results obtained after behavioral analysis in the Preclinical model revealed discrete motor changes that were induced by the unilateral nigrostriatal dopamine depletion. In fact, all the 6-OHDA lesioned rats treated or not, did not turn enough compared to the results in the amphetamine-induced rotation test from assay 2 in those rats that were with the toxin for 3 weeks, the same time than these rats. This behavioral improvement could be due to a spontaneous reinnervation from surviving fibers (Jollivet, 2004) because of DA depletion induced by intrastriatal injection of 6-OHDA was not elevated. Accordingly, it was reported that rats are sensitive to changes in motor function associated with neuronal plasticity (Biernaskie & Corbett, 2001), hormonal changes (Metz et al., 2005) and diet.

CBL administration and combination of CBL administration and housing rats in an EE induced a functional recovery, decreasing the number of ipsilateral rotations after the treatment, in comparison with the other groups. In fact, it has been suggested that motor activity induced by EE can reduce the effect of the neurotoxins on the nirgrostriatal dopaminergic system (Tillerson et al., 2001; Cohen et al., 2003) and promote recovery of function (Tillerson et al., 2001). However, in this study the effect of EE individually was not appreciated functionally, because the functional improvement mediated by EE is related to its duration (Jadavji et al., 2006). In this context, while the most studies indicated an exposure to EE for 7 weeks (Jadavji et al., 2006; Steiner et al., 2006), rats in this assay was only exposure to EE during one week. On the other hand, studies have also suggested that the concept of EE mediates compensatory behavior rather than recovery of function (Rose et al., 1993; Johansson et al., 1999).

According to the functional recovery was observed after CBL administration, studies have revealed the effect of CBL administration in functional recovery as consequence of its neuroprotective effect (Masliah & Díez-Tejedor, 2012).

Animals were sacrificed 1 week after treatment in the assay 3 to verify whether the functional improvement seen in rats treated with CBL (CBL group and CBL+EE group) and the behavioral deficit observed after vandetanib administration accomplished the same results morphologically. Remarkably, morphological analysis was also in accordance with functional improvement in rats receiving CBL and housing in EE.

5. An innovative strategy to evaluate striatal degeneration

Striatal degeneration was evaluated taking into account the volume occupied by the TH-negative fibers (Requejo et al., 2015). Degeneration and regeneration are both progressive processes and in order to accurately assess them, the affected surface of the stereological collected sections was delimited, measured and integrated to obtain the exact volume occupied by the TH-negative fibers inside the striatum. Consequently, it is easy to avoid striosomes or vascular sections which might distort conventional IOD measurements. In fact, several works have mentioned the discrepancies in the results of the density measurements due this background (Yuan et al., 2005). Furthermore, positive sprouting of new fibers may be also taken into account.

In fact, we also assessed the IOD in the Partial model after NTF administration (Herrán et al., 2014), but we obtained better results when we assessed the TH-negative volume (Requejo et al., 2015). Due to these artifacts previously described above, we measured the IOD placing an square in the most negative zone from the ipsilateral striatum and in the corresponding region of the contralateral hemisphere following the work carried out by Garbayo et al (Garbayo et al., 2009). These results also showed a significant reinnervation when rats were treated with NS loaded with VEGF and GDNF in combination.

To evaluate the innervations of the striatum after 6-OHDA administration into MFB or striatum we used the innovate procedure previously described; It consisted on measuring the volume occupied by the TH-negative fibers inside the striatum.

In a **Severe model** , animals injected with 6-OHDA into MFB presented around 95% of TH-negative ipsilateral volume of striatum, while rats received saline solution into MFB did not show negativity for TH in striatum. These results showed in saline group indicated that the injury was not involved in the striatal degeneration.

Despite the lesion was not carried out in the striatum, the volume of the injured hemisphere decreased around 10% in 6-OHDA rats and a 5% in saline-rats respect to the contralateral one. Despite values of tissue retraction from rats received saline solution into MFB were lower that obtained when we administered saline solution into striatum, when rats received 6-OHDA into MFB this retraction was similar to rats received the toxin into striatum (Requejo et al., 2015). In addition, there were significant differences between saline and 6-OHDA groups, indicating in this model that not only the scar produced by the lesion, but also the toxin by itself increased this retraction and this injury presented a deleterious effect on SNC.

Remarkably, when rats were treated with MS loaded with NTFs into striatum, presented higher values of tissular retraction than rats only injected with 6-OHDA, which were used for the description of the lesion. However, empty-MS group presented around 6% of tissue retraction in the injured side similar to rats from assay 1 that were only injected with saline solution, despite the fact that the striatum from these rats was injured to administrate the MS. In contrast, the percentage of lesioned volume when MS were loaded with VEGF and GDNF in combination or with GDNF was around 18%, reaching significant differences respect to rats receiving empty MS or MS loaded with VEGF. These results suggested that the volume of NTFs was high and because of this the tissue damage observed bigger. It was in agreement with our previous work also developed in this model and where we showed mild functional recovery probably because of it (Herrán et al., 2013) and according to our previous work, in which we also

suggested that treated groups, which undergo a double injury, present remarkable stereological changes (Cervós-Navarro & Lafuente, 1991; Requejo et al., 2015).

Due to the strong tissue damage produced by the implantation of MS loaded with NTFs and based on the assumption that 6-OHDA induced denervation of the striatum instead of intrastriatal GDNF administration were started 3 weeks postlesion (Rosenblad et al., 2000), we only focused on the SN in order to assess TH-immunostaining in this model.

In the **Partial model**, animals injected with 6-OHDA showed 66% of negative ipsilateral striatum for TH. Rats receiving the saline solution lost only 0.5% of the TH-positive volume. This indicated that the injury was barely involved in the degeneration of TH-positive fibers.

Administration of VEGF and GDNF resulted in a recovery of the TH-positive volume in the CPC, protecting and restoring the dopamine (DA) terminals. Parkinsonized rats treated with both NTFs showed a statistically significant increase in volume (13%) compared to rats treated only with the vehicle.

The functional recovery and increase of TH-positive fibers in the striatum of parkinsonized rats has also been previously reported when rats were treated with GDNF alone (Jollivet, 2004; Garbayo et al., 2009). In fact, previous studies have shown that intrastriatal administration of GDNF stimulates regenerative sprouting from preserved axons (Rosenblad et al., 2000). The TH-positive area recovers out of the remaining cells, showing that the neuroplasticity of axons and dendrites is better preserved than its soma.

The retraction rate of the striatum was evaluated in order to assess the effect of the injury by itself and of recovery after NS implantation in the Partial model.

The volume of the injured hemisphere decreased around 10% in saline and 6-OHDA group, while it was of about 25% for treated groups, which received two striatal lesions, firstly the 6-OHDA injection and then the vehicle or the NS administration. The

lesion by itself produced tissue retraction and, as a side effect, an enlargement of the lateral ventricle, though it did not evidence significant changes between the studied groups of each assay. Only the action of injuring the rats twice clearly increased this retraction (Cervós-Navarro & Lafuente, 1991). Regardless of the administered substance, the injury by itself has a deleterious effect on CNS, and the treated groups, which undergo a double injury, present remarkable stereological changes. Therefore, the effectiveness of therapy must be supposed to be pretty high since a significant functional and morphological recovery was appreciated (Herrán et al., 2014).

On the other hand, in the **Preclinical model** the intrastriatal injection of 6-OHDA did not induce a remarkable loss of positivity for TH. The TH-negative volume was around 1.2-1.3 mm^3 (33-44%) in rats lesioned with 6-OHDA without treatment and in rats treated with CBL and housed in an EE. Thus, there was not significant differences among these experimental groups likely due to the loss of DA was not remarkable to induce changes in these groups. It was in accordance with Yuan and collaborators, who showed that striatal dopaminergic fibers in a Partial model lead to a moderate denervation (55% DA loss) of the striatum after 2 and 5 weeks after lesion (Yuan et al., 2005).

However, vandetanib administration induced a remarkable denervation of striatum similar to rats from assay 2. In fact, rats received the inhibitor of VEGFR2 and RET showed 72% of negative lesioned striatum for TH, presenting statistically significant differences respect to the other groups. These results confirmed the behavioral dysfunction observed in vandetanib group. Thus, the inhibition of VEGFR2 and RET affected negatively to the DA content in the striatum in this Preclinical model, indicating that the inhibition of these TK receptors leads to degeneration of dopaminergic terminals into striatum. In fact, vandetanib group displayed a worse situation that the 6-OHDA group

On the other hand, striatal injection of 6-OHDA in this model induced a retraction of the injured striatal hemisphere similar to rats 6-OHDA rats from assay 1 and 2.

However, this tissue retraction was similar in all groups, showing that the volume of the injured hemisphere decreased around 10-15%. These results indicated that the treatment used in this assay did not induce tissue damage compared to treatment based on striatal injection of MS or NS. Remarkably, rats receiving 6-OHDA showed the most decrease in the lesioned hemisphere (about 15%) confirming the toxic effects of 6-OHDA.

6. Synergistic effects of VEGF and GDNF

Some studies have demonstrated a cooperative crosstalk between VEGF-A and GDNF signalling pathways mediated by VEGFR2 and RET**,** and suggesting a possible feedback loop between these two growth factors (Tufro et al., 2007). However, the molecular link between VEGF and GDNF pathway remains unknown.

Both cytokines bind tyrosine kinase receptors (VEGF-R1 & 2 and GDNF the c-RET), therefore, it is likely that the protective effects of VEGF may be mediated using different signalling cascades in diverse cellular targets compared with GDNF. In fact, we also assessed the effect of inhibiting the VEGFR2 and RET by administrating vandetanib orally in a Partial model carried out in assay 3 in order to determine the effect of these receptors in early states of PD and we obtained interesting results which supported the important effect that these receptors carried out in the nigrostriatal system.

Although neuroprotective effects of VEGF-A overexpression in models of PD were reported (Yasuhara et al., 2004), detrimental vascular effects, such as edema and disruption of the blood-brain barrier, occurred (Harrigan et al., 2003; Rite et al., 2007). These negative side effects have not been observed in our assays , despite VEGF-A binds to the neuroprotective VEGFR1 and, in addition, to VEGFR2, and the receptor is thought to mediate in angiogenic effects (Olsson et al., 2006; Falk et al., 2010).

On the other hand, studies have shown an neuroprotective effect after sustained VEGF-B delivery into a rodent brain (Poesen et al., 2008) or genetic VEGF-B

overexpression (Dhondt et al., 2011; Yue et al., 2014), which is not surprising given that VEGF-B only binds to the protective VEGFR-1, whereas VEGF-A binds to both VEGFR-1 and VEGFR-2, the receptor thought to mediate the angiogenic effects (Olsson et al., 2006; Falk et al., 2010). VEGFR-1 on the other hand is tied to protective effects in many organs, including the brain. However, in dopaminergic neurons the pathways for VEGF-B have not yet been elucidated. There is a work that evidences the effectiveness of the treatment with VEGF-B and GDNF in a preclinical *in vivo* model of PD (Yue et al., 2014). The role of VEGFR-1 remains more enigmatic, and its binding to the non-tyrosine kinase receptors NP-1 and NP-2 might be involved in axon guidance (Lafuente et al., 2012). In addition, Huang et al showed that the expression of VEGF was increased in response to GDNF stimulation in several situations (Huang et al., 2014).

VEGF and GDNF induce improvements in behaviour and an enhancement of the surviving neurons, sprouting in order to neurorescue cells and activate neurogenesis. Furthermore, it would be necessary to investigate the signalling pathway of VEGF and GDNF, in order to assess the possible intracellular interaction.

Taken together, our data suggested that the trophic effects of VEGF and GDNF on nigrostriatal pathways complex likely involves multiple mechanisms and/or mediators. We supported the synergistic effect of combining VEGF and GDNF in the severe and Partial model of PD, these NTFs used different receptors, and both could potentially be additive or even synergistic with each other to produce more profound effects. In fact, GDNF can be considered as the most used growth factor in Preclinical models of PD. However, our data in the complete model showed that VEGF in combination with GDNF was only slightly inferior to GDNF in terms of plasticity in this model. Indeed, administration of VEGF and GDNF produced dopaminergic regeneration and it was supported by increasing of astrocytes, vessels and neurogenesis in the striatum after VEGF and GDNF administration.

Therefore, a major finding in the present work, a part from the differences found in the study of the rostro-caudal topology, is the preservation of the ADN network after

treatment with VEGF and GDNF. Combining both NTFs not only preserves the neuronal bodies, it also has the ability to restore nigrostriatal axons in the severe and Partial models.

6.1. Inhibition of VEGR2 and RET induced a deleterious effect in a Preclinical model

The negative effects by inhibiting VEGFR2 and RET after the administration of the TKI inhibitor vandetanib, lead us to consider VEGF and GDNF as a therapeutic target in PD. Thus, the search of treatments which stimulate or introduce ligands (VEGF and GDNF) of these receptors could be a strategy that opens windows to understand the molecular mechanism of PD.

Motor behavioral deficit and morphological impairment were observed after vandetanib administration, which induced a drastic loss of TH-positive volume in striatum accompanied by a remarkable loss of TH-ir neurons in SN. In fact, vandetanib displayed more injury on the dopaminergic system than the toxicity induced via 6-OHDA by itself.

On the other hand, despite the amount of studies developed about vandetanib in cancer, any study has been developed in order to study the effects of vandetanib administration in neurodegeneration. In fact, vandetanib is used as a therapeutic strategy in several cancers blocking the expression of VEGFR2 and RET, among others (Deshpande et al., 2011).

VEGF and GDNF induce neuroprotection via the PI3K/Akt, pathways downstream of VEGFR2 and RET (Kilic et al., 2006; Pascual et al., 2011). In line with that, it has also been reported that dopamine can function through the Akt/GSK3 signalling cascade (Beaulieu et al., 2007). Because of that we studied the levels of phosphorylated Akt (p-Akt), in order to assess the effects of inhibiting both receptors in this pathway on the

dopaminergic system. We confirmed that vandetanib indeed inhibits p-Akt in SN, showing reduction in the p-Akt/Akt levels, even more than 6-OHDA in striatum and SN.

In contrast, the inhibition of both receptors increased remarkably the expression of caspase-3, inducing apoptosis in striatum and SN. In fact, the expression of caspase-3 was also more remarkable in 6-OHDA rats received vandetanib than rats only receiving 6-OHDA. It is accordance with a study developed in breast and MTC cancer, which indicated that TKI treatment could be effective in increasing apoptosis (Kunnimalaiyaan et al., 2006; Spanheimer et al., 2014). In this context, our results could suggest that inhibition of VEGFR2 and RET lead to DA neuronal loss and DA denervation by activating apoptotic pathways (caspase-3) and inhibiting the survival pathways (p-Akt/total Akt) in striatum and SN.

Thus, the deleterious effect produced by blocking the VEGF and GDNF expression through the inhibition of VEGFR2 and RET, supporting the synergistic effect of VEGF and GDNF, indicating that receptors from both NTF could exhibit their neuroprotective action in PD by Akt signaling cascade, probably activating the PI3K/Akt signaling pathway.

7. Synergistic effect after combining Cerebrolysin and enriched environment housing

We found for the first time that the combination of housing rats in an EE and the i.p. administration of Cerebrolysin resulted in overall nigrostriatal dopaminergic system neuroprotection in a presymptomatic 6-OHDA model. The combination of both strategies lead to the preservation of dopaminergic neurons and their striatal connections, as well as preservation of motor function for one week of treatment. In addition, survival pathway (Akt signaling pathway) was remarkably activated and apoptotic process (caspase-3 activation) reduced in rats treated with both strategies in striatum and SN from 6-OHDA rats. In fact, studies have revealed that the PI3K/Akt

pathway mediates Cerebrolysin-induced progenitor cell proliferation (Zhang et al., 2010) and apoptosis was prevented after CBL administration promoting functional recovery after stroke (Masliah & Díez-Tejedor, 2012). Thus, CBL is a good candidate to protect TH or dopaminergic neurons from apoptosis.

CBL is a mixture of various NTFs, which could contribute to enhanced the neuroregeneration and this preparation has exhibited beneficial effects on neurodegenerative diseases and stroke, enhancing neurogenesis in the dental gyrus, which is the basis for neuronal replacement therapy (Zhang et al., 2010; Masliah & Díez-Tejedor, 2012). In fact, it is the only drug whose action is similar to the various NTFs in combination such as BDNF, GDNF, CNTF and NGF and others (Sharma et al., 2011).

In line with that, one PD study carried out by Lukhanina and collaborators demonstrated that Cerebrolysin may be recommended as an additional neuroprotective drug for brain function improvement in the earlier stages of PD (Lukhanina et al., 2004).

EE increase the expression of NTFs (Bengoetxea et al., 2008). In fact, studies have reported that BDNF (Oliff et al., 1998), VEGF (Ortuzar et al., 2013) and GDNF (Anastasía et al., 2009) are involved in the effects of EE, which expression is increased by exercise (Bezard et al., 2003). Thus, NTFs are upregulated in animals exposed to EE, contributing to the protection against the toxicity of 6-OHDA or MPTP (Bezard et al., 2003). EE imply exercise, in concert with continued mental activity and social interactions, which may provide a non-invasive, non-pharmaceutical mechanism to protect against the onset of parkinsonian symptoms (Faherty et al., 2005).

We corroborate these finding, suggesting that combining CBL administration with EE exhibited functional and morphological improvement after 6-OHDA lesion. In fact, EE is an alternative to invasive treatment.

In spite of a functional improvement was seen by combining these strategies, this functional recovery was not significant. Accordingly, in rats exposed only to EE we did not observe any functional recovery, maybe because the time in which rats remained

under an EE was only for one week. However, we chose this time course in order to check the morphological changes in earlier stage of PD to evaluate the neuroprotective effects of the treatments before the progression of the disease. On the other hand, in a study developed by Jadavji and collaborators indicated a delay in EE animals, beginning at two weeks after lesion (Jadavji et al., 2006). Thus, the mild improvement shown in behavioral results could be related to a late onset of EE exposure starting at two weeks after lesion. In addition, others authors have demonstrated that stress increases motor impairments in the 6-OHDA model (Snyder et al., 1985; Smith et al., 2002). In line with that, although rats exposure to EE and receiving daily i.p. administration of CBL, the possible stress produced by the daily administration of CBL did not affect to increase the vulnerability of dopaminergic neurons to subsequent insult.

Taken together, EE in combination with CBL may provide a neuroprotective therapeutic option in the earlier stage of PD via the stimulation and potentiation of NTFs expression through the activation of signaling pathways implied in survival, supporting a synergistic effect between both strategies. In fact, these strategies are not supposed as invasive effect as intracerebral administration of NTFs.

8. Neurotrophic factors increased GFAP levels in the striatum in the Severe model

Interestingly, the highest GFAP expression was reached in rats treated with VEGF and GDNF in combination, finding the most GFAP expression in the restricted area that demarcated the needle tract, extending to the striatal parenchyma.

In fact, glial proliferation has been described as response to administration of several NTFs *in vitro* (Rabchevsky et al., 1998) and *in vivo* (Krum et al., 2002; Krum & Khaibullina, 2003; Mani et al., 2005). In addition, other study revealed that astrocytes are responsible for VEGF-A and GDNF expressions in the ischemia plus G-cerebrospinal fluid (CSF) condition (Chen et al., 2013). Related to this finding, we could suggest that it

would be possible than the exogenous administration of VEGF and GDNF could activate astrocytes to express these factors endogenously after an insult. Regarding the neuronal loss in SN produced by 6-OHDA; it could be possible that the combination of both factors apart from inducing the activation of astrocytes as an anti-inflammatory mechanism to reduce the damage, they could also induce the transdifferentiation of active astrocytes into mature neurons to restore the loss of dopaminergic neurons. In fact, new neurons are described to originate from cells expressing GFAP (Doetsch, 2003; Kronenberg et al., 2003; Garcia et al., 2004; Kempermann et al., 2004; Burton et al., 2006; Steiner et al., 2006) and a recent results have demonstrated that striatal endogenous reactive astrocytes in response to ischemic injury can transdifferentiation into new neurons (Magnusson et al., 2014). Therefore, the combination of these NTFs could promote the transdiferenciation of these reactive astrocytes into dopaminergic neurons in response to the 6-OHDA lesion. The modulation of reactive microglia and astrocytes may have triggered trophic responses in the lesioned nigrostriatal pathway that may have interfered with the degree of DA lesion. The synthesis of neurotrophic substances is then up-regulated in the reactive astrocytes which via paracrine actions may help maintain lesioned dopamine neurons as well as promote wound/repair (Rodrigues et al., 2003).

Therefore, GFAP expression could display different roles in this model depend on the context and it is supported by other works (Berg et al., 2015). It could act as an anti-inflammatory factor providing neuroprotection/neurorestorative effect by expressing antioxidant enzymes (Makar et al., 1994; Calkins et al., 2009; Coquery et al., 2012; Fernandez-Fernandez et al., 2012) and it could be related to potential GFAP-positive neural precursors. Otherwise, it could act as inflammatory factor due to injure, inducing reactive gliosis in terms of inflammation.

9. Neurogenic effects of VEGF and GDNF

To evaluate whether the NTF group could activate or maintain neuronal proliferation and cellular differentiation so as to support a possible neurogenic effect, we stained cells against BrdU in the Severe model and against BrdU and DCX in the Partial model.

Several studies have described in rats injected with 6-OHDA in the MFB a decrease in cell proliferation in the SVZ (Baker et al., 2004; Höglinger et al., 2004; Winner et al., 2006). In fact, DA depletion is correlated with the decrease in the proliferation and it leads to significantly impaired neurogenesis (Steiner et al., 2006) considering the hypothesis of a direct positive DA regulation of cell proliferation in SVZ region (Höglinger et al., 2004). These suggestions could be reinforced by the lack of TH-ir and neurogenesis found in dopaminergic lesions and besides by the ability of growth factors for promoting the neurogenesis in SVZ.

Accordingly, in the **Severe model**, we used BrdU in order to detect newly-cells formed after NTFs administration. We described an increase in the number of BrdU-positive cells in the SVZ of rats treated with VEGF individually or in combination, showing that VEGF expression promoted the proliferation. VEGF induced proliferation and differentiation of dopaminergic cells *in vivo* (Xiong et al., 2011), it has been implicated in adult neurogenesis (Cao et al., 2004) and increases the neurogenesis after injury (Jin et al., 2000, 2002; Sun et al., 2003; Wang et al., 2009). In addition, one study has recently described that exogenous administration of VEGF increased the neurogenesis in ischemic injured brains (Duan et al., 2015).

Rats treated with GDNF presented less BrdU-positive cells than VEGF-Ms group, because it was reported that GDNF is more involved in the survival and differentiation (Birling & Price, 1995; Schwartz et al., 1997). In addition to this, our results also supported the role of GDNF in promoting plasticity in SN because it was reported that GDNF reduce the degeneration dopamine fibers (McNaught et al., 2002) and induces

sprouting of dopamine axons (Batchelor et al., 2000). Thus, it is important to distinguish between mechanism of cellular plasticity in neurogenic zones and other parts of the adult CNS like the SN, where cellular plasticity, but potentially no neurogenesis takes place (Steiner et al., 2006).

Due to the increase in neurogenesis when we administered MS loaded with VEGF and the intense activation of astrocytes in the striatum of rats treated with VEGF and GDNF, these finding could be in agreement with the recent publication in which they suggest that the VEGF enhance the neurogenesis by the transdifferentiation of astrocytes into mature neurons in injured brains (Duan et al., 2015). We highlight the necessity of further investigation to corroborate if exogenous administration of VEGF due to its neurogenic effect is also able to induce the transdifferentiation of astrocytes into mature dopaminergic neurons in parkinsonized rats.

In **Partial model**, BrdU/DCX double immunofluorescence staining showed an enhanced proliferation near the SVZ in rats treated with VEGF and GDNF.

Correspondingly, the number of BrdU-positive cells from parkinsonized rats treated in the vehicle groups was lower than in the NTF group, and these cells did never co-express with DCX, suggesting that VEGF and GDNF could induce not only an increase but also a differentiation of neurons to migrate towards the injured regions.

Growth factors promote neurogenesis in the SVZ/olfactory bulb (OB)-system while the dopaminergic lesion has the opposite effect. In fact, GDNF is involved in neuronal survival and differentiation during development (Birling & Price, 1995; Schwartz et al., 1997) and VEGF promotes the proliferation and differentiation of dopaminergic cells *in vivo* (Xiong et al., 2011). In addition, it was also reported that growth factors in combination could induce neurogenesis in a synergistic way (Pellegrini et al., 2013; Sopova et al., 2014).

However, it is necessary to difference between proliferation, newly generated cells, and differentiation, in which newly generate cells can take place a new cellular

lineage regarding the requirements. Because of this, new additional experiments would be interesting to carry out with adult neuronal and proliferative markers, such as TH and BrdU in order to corroborate whether the newly cells induced by the administration of VEGF and GDNF, could become dopaminergic neurons to restore the loss induced by the administration of 6-OHDA. Thus, regarding the fact that NTFs are involved in inducing proliferation and differentiation (Requejo et al., 2015). It could be possible that NTFs are able to induce the differentiation of neuroblasts into dopaminergic neurons. In line with this hypothesis, a study developed by Prensa and collaborators, suggested that the primate striatum is able to recruit new neuroblasts as a means to compensate for the lack of DA that characterizes the parkinsonian state would be a major breakthrough in our understanding of the functional organization of the basal ganglia (Prensa et al., 2000).

10. GDNF increased microvascular density in the striatum in the Severe model

Angiogenesis has been reported to be impaired in aging in several tissues including brain (Wang et al., 2004; Iemitsu et al., 2006). In fact, perfusion deficits have also been observed before the onset of clinical symptoms in neurodegenerative disorders, which suggests that the deficits contribute to the pathogenesis of the disease (Carmeliet & Storkebaum, 2002). However, results obtained through measuring microvascular density did not provide any further information neither striatum nor SN between 6-OHDA and saline-group in the **Severe model**, there were not practically difference between them.

On the other hand, in the same model, GDNF administration increased the angiogenesis/ or the microvascular network in the striatum on the lesioned side respect to empty-MS group. Owing to the ability of GDNF to induce sprouting from spared axons near the injection site in the striatum (Jollivet, 2004), it is likely to GDNF is able to induce increase in vessel density, as a plastic response, increasing oxygen and nutrient supply to

the affected brain region. We suggested the increase of microvessel density as a plastic response stimulated by GDNF, because on a cellular level brain plasticity involves functional and structural modifications of synapses, neurons, and non-neuronal cells (Cenci et al., 2009). Due to the fact that an increase in vascular permeability in response to VEGF may result in the release of trophic factors, such as GDNF, which promote dopaminergic neuronal survival (Yasuhara et al., 2004). We also hypothesize that VEGF instead of increasing the microvascular density; it developed its neurogenic effect in order to stimulate GDNF production. Thus, we also suggested that GDNF increased vascular density to induce dopaminergic neuronal survival.

In contrast, results obtained through measuring microvascular density in the **Partial model** did not provide further information neither striatum nor SN in all experimental groups, there were not practically difference between them. However, there was a differential topological distribution of vessels in striatum and SN. It may be relevant because we did not find differences when we studied the microvascular density in the treated rats. It could be because it has been reported that VEGF at low dose induced neuroprotection but did not induce angiogenesis (Yasuhara et al., 2005). Other studies suggest that exercise promoted angiogenesis in the brain of chronic parkinsonian mice (Al-Jarrah et al., 2010). Therefore, whether parkinsonized rats treated with NS had practiced exercise, maybe the microvascular density would have increased in these groups received NTFs.

11. Neuronal rescue and axodendritic sprouting

There is an emerging need for further investigations focusing on the role of compensatory responses after striatal fibers depletion and the decrease of ADN and neurons in SN regarding the pathophysiology of PD. Neurogenesis is a complex process, as it takes a long time for dopaminergic neurons to reach the SN in order to replace neuronal loss due to the lesion. Because of this, the remaining neurons re-innervate this damaged area. Thus, in addition to the cell loss that follows DA denervation (Rosenblad

et al., 2000), it would be essential to examine what occurs upon treatment with VEGF and GDNF on axodendritic sprouting, such as a possible plasticity compensatory response in SN. Synaptic plasticity may contribute to ameliorate brain dysfunction in case of extreme neurodegeneration (Gittis et al., 2011). In fact, authors have showed previously that dopamine plays a key role in cellular plasticity in the SN in PD models (Steiner et al., 2006; Klaissle et al., 2012).

In the **Severe model**, results indicated that this plasticity compensatory response may not be possible in a Severe model of PD due to the high degree of neuronal degeneration. On the other hand, injection of saline solution resulted in a 25% of neuronal and ADN loss, remaining about 75% and 70% of TH-ir neurons and axons respectively in the injured side. These results indicated that ADN and neurons followed the same tendency to decrease after 6-OHDA or saline solution administration.

In contrast, we found differences in terms of neuronal surviving and axonal sprouting when rats were treated with NTFs. Our results showed that ADN was more conserved than neuronal density after MS implantation, highlighting the ability of NTFs in neurons to reach and reinnervate the most vulnerable regions after 6-OHDA lesion.

Therefore, rats receiving VEGF and GDNF showed the highest neuronal density (about 27%), while rats treated with empty MS only about 5% of TH-ir neurons survived. In contrast, regarding axodendritic sprouting a slight difference in rats treated with VEGF and GDNF in combination (about 39%) and in rats treated with GDNF individually (about 43%) was found. Only GDNF-MS group presented statistically significant differences respect to empty-MS (24%) and VEGF-MS group (27%).

In line with these results, it is reported that GDNF induces a sprouting and regrowth of the preserved striatal dopaminergic fibers and stimulates axonal sprouting from the axons of injured dopaminergic neurons (Kirik et al., 2000; Jollivet, 2004).

On the other hand, these newly formed fibers would be the remaining axons of terminals originating from spared or rescued neurons and NTFs could maintenance or

enhanced axodendritic sprouting or regrowth from surviving TH-positive dopaminergic neurons (Rosenblad et al., 2000). Nevertheless, it is necessary to clarify whether these newly formed fibers are originate from spared intact axons or from surviving lesioned axon stumps within the nigrostriatal pathway. In fact, presynaptic plasticity has been long proposed to be one possible mechanism by which locomotor impairment does not manifest until loss of DA exceeds 70% (Bezard et al., 2001; Zigmond et al., 2002), supporting the ability from preexistent neuron to reinnervate the affected regions induced by the effect of NTFs.

In **Partial model**, ADN density decreased less than neuronal density in all groups. This may be due to the compensatory plasticity of pre-existent neurons.

The group receiving NTFs (VEGF and GDNF) showed more significant signs of axodendritic sprouting than the other groups. Hence, a combination of both NTFs not only preserves the neuronal bodies, it also has the ability to restore nigrostriatal axons (Batchelor et al., 2000).

On the other hand, instead of the neuronal loss was not remarkable in the **Preclinical model** compared to the other models, there was significant differences in neuronal preservation in the experimental groups. In fact, optimal protection of TH-ir neurons was found in SN from rats receiving CBL and housing in EE against the toxicity induced by 6-OHDA. CBL+EE group presented the highest neuronal density in SN (about 67%) and showing the most statistically significant differences respect to rats only received 6-OHDA and those administered with the inhibitor of VEGFR2 and RET, which showed the most loss of dopaminergic neurons (about 27-29% of neuronal density, respectively).

Remarkably, although we did not observe a functional improvement in rats only housed in EE, this group showed neuronal recovery. These results were consistent with previously reported EE protection, in which EE housing in 6-OHDA lesioned rats led to preservation of SN cell numbers three weeks post-lesion (Anastasía et al., 2009). Likewise, regarding behavioral improvement after CBL administration was also in

accordance with the neuroprotective effects, because rats received CBL (alone and in combination with EE) showed the most neuronal recovery. In fact, it has been demonstrated that CBL protects the integrity of the neuronal circuits and its administration improved cognitive and behavioral performance (Masliah & Díez-Tejedor, 2012). Additionally, CBL has been found to support the survival of neurons *in vitro* and *in vivo* (Deigner et al., 2000).

Interestingly, we found in the Preclinical model that the dopaminergic neurons are more affected by the 6-OHDA than the DA content in the striatum (58% of positivity for TH in striatum *vs*. 29% of TH-ir neurons in SN in 6-OHDA group). It was in agreement with Kirik and collaborators, who provided the direct demonstration that survival of dopaminergic neurons in SN and preservation of functional striatal denervation were distinctly regulated in the striatal 6-OHDA model (Kirik et al., 2000). On the other hand, our results confirmed that in this Preclinical model the mild functional effects were related to the mild DA loss in striatum. Although we did not observe remarkable changes in motor behavior, the depletion of DA in striatum and the consequent decrease in neuronal density, may be responsible for other non-motor symptoms already described in an early stage of PD, such as negative emotional state (Tadaiesky & Dombrowski, 2008).

Taken together, we highlighted the neuroprotective/neurorestorative effect of treatment based on CBL and EE housing and the deleterious effects of inhibiting VEGFR2 and RET on the neuronal surviving in this Preclinical model.

12. Neuronal density in the substantia nigra in the partial and Preclinical models

Parkinsonized rats showed changes regarding their neuronal density in the entire SN and in e-SN in the **Partial model**. Rats receiving NTFs (VEGF and GDNF) showed a higher neuronal density in the e-SN (about 44%) than in the entire SN (about 32%).

These changes in the distribution of neurons was also found in rats receiving CBL and housed in an EE in **the Preclinical model**, showing more density of neurons in the e-SN (about 63%) than in the entire SN (56%). However, in the Preclinical model, the differences in neuronal density in e-SN were not as remarkable among groups as in rats received VEGF and GDNF in the Partial model. We only found statistically significant differences in treated groups with CBL and housing in EE in e-SN respect to rats received vandetanib, because vandetanib administration induced the most neuronal loss in this region (about 23% of surviving dopaminergic neurons). In fact, the reduction in neuronal density was more remarkable in e-SN in rats treated with the inhibitor of VEGFR2 and RET. On the other hand, the time course for the treatments followed for both assays was different, which could explain the differences found in the e-SN for both assays, owing to rats in the Partial model remained much more time with NTFs before to be sacrificed.

Dopaminergic projections reach the entire striatal complex, following a rostro-caudal topography of the elongated terminals fields. Additional dopaminergic projections reach the amygdala body (Lindvall et al., 1984) and projections to the amygdala arise from the VTA and lateral SNc and SNl (Bayer, 1984). Connected to these topological gradients and taking into account that the topography of SN provides for the organization of the nigrostriatal projection, we identified the "e-SN", which is topologically associated with the dorsolateral region of the CPC, where the 6-OHDA lesion was induced (Deumens et al., 2002). In fact, a significant component of this e-SN is the SNl, which projects to the amygdala. This structure is preserved from the inflicted lesion. Therefore, remaining neurons from the SNl projecting towards the amygdala would be the basis for re-innervation using sprouting mechanisms. These could be reinforced by NTF spreading from CPC areas, making the recovery of functions possible as reported by several authors (Herrán et al., 2014; Yue et al., 2014).

13. Rostro-caudal gradients

We paid attention in the extreme denervation observed in the striatum and the almost depletion of dopaminergic cells reached in SN. Because of that and owing to the results obtained in our recently paper (Requejo et al., 2015), we also studied the degeneration of the striatum and SN considering rostro-caudal levels, in order to search what was the most affected regions after administrating the 6-OHDA and the most susceptible area to be recovered after treatment.

In terms of tissue damage we also examined the topological distribution in striatum according to tissue retraction rate.

In the **Severe model,** parkinsonized rats showed a significant topological distribution along the rostro-caudal axis. Rats decreased tissue retraction rate rostro-caudally, although statistically significant differences only were found in treated rats with MS. Our results indicated that the ipsilateral volume decreased when it was closer the site of injection. It was supported by the fact that GDNF-MS and VEGF+GDNF-MS group presented statistically significant differences respect to empty-MS group, which had the lowest values in tissue retraction rate compared to the others in rostral and middle sections, while caudally these groups did no present statistical differences.

At striatum level, due to the almost complete denervation after 6-OHDA injection, there was not topological distribution of TH-ir fibers. Every striatal section considered presented an intense loss of TH-ir fibers. Thus, in a severe lesion it is not possible to examine the topological distribution of TH-ir fibers into striatum due to the extreme depletion of DA in striatum caused by the 6-OHDA administration into MFB. In addition, no difference was found regarding topological distribution of TH-ir fibers in striatum when saline solution was injected into MFB.

In contrast, we demonstrated a selective vulnerability along the rostro-caudal axis of dopaminergic neurons and ADN to 6-OHDA, revealing very few TH-ir neurons and

ADN remaining in the rostral parts and decreasing from rostral to caudal parts. This topological reduction as a consequence of the toxicity induced by 6-OHDA was also reported by Rosenblad and collaborators (Rosenblad et al., 1999).

These findings were in accordance with other authors that found within SN that neurons of ventrolateral and caudal region were more vulnerability than those in the rostromedial and dorsal region of SN in PD (German et al., 1989; Damier et al., 1999; González-Hernández et al., 2010), progressing the loss of TH+ neurons from lateromedial and rostro-caudal direction (Hernandez-Baltazar et al., 2013).

Saline-group also showed a topological distribution of neuronal density along the rostro-caudal axis, showing differences between middle and caudal sections (74% *vs*. 54%). These results indicated that injure in MFB resulted in a significant reduction of neuronal density at caudal levels, and we suggested a possible anterograde degeneration in SN because of lesioning MFB. This distribution was also demonstrated recently in a Partial model of PD (Requejo et al., 2015). Nevertheless, this group did not present differences in ADN density along the rostro-caudal axis.

Thus, saline group in terms of TH-ir fibers distribution in a Severe model did not show topological distribution neither striatum nor SN.

Interestingly, rats treated with MS also presented this reduction of neuronal density along the rostro-caudal axis. Remarkably, rats receiving VEGF and GDNF presented the highest neuronal density at all levels, showing large differences between rostral and caudal level (40% *vs*. 16%). Rats injected with VEGF and GDNF in combination also showed statistically significant differences at rostral level respect to empty-MS group (6%) and VEGF-MS group (11%). In addition, rats received GDNF individually only presented statistically significant differences at rostral level respect to empty-MS group (29% *vs*. 6%).

On the other hand, this reduction in neuronal density along the rostro-caudal axis was not observed after VEGF and GDNF administration in a Partial model of PD (Requejo

et al., 2015), it was only observed in groups untreated with NTFs. We suggested that these differences found between both PD models regarding the effectiveness of the treatment were originated because neurotoxicity induced by 6-OHDA into MFB was completely different when it was injected into striatum, in which the neuroregeneration could be more effective. Additionally, it was more difficult to restore caudal parts in a Severe model due to the main loss of dopaminergic neurons was focused on this level.

Regarding ADN density, as occurring in 6-OHDA and saline group, rats treated with MS did not show a significant gradient rostro-caudally, it trended to decrease from rostral to caudal levels. Remarkably, groups received VEGF and GDNF presented the most ADN density in caudal parts, instead of GDNF-MS group showed the highest ADN density at rostral and at middle levels. It was relevant, due to the fact that caudal levels were the most affected and VEGF+GDNF-MS group showed the best recovery in terms of surviving cells and ADN sprouting at this level.

Supporting this topological distribution in the dopaminergic system there are developmental studies of the rat nigrostriatal system indicate the rich anatomical interconnections between the striatum and SN in adults are likely to be the outcome of precisely timed developmental events because of pattern of axonal terminations and neurogenetic gradients between them are correlated (Bayer, 1984) (see figure 11). This suggested that due to the fact that rostral levels were less affected by the toxin and more recovery after NTF administration, it would be likely that neurons from rostral part could migrate to caudal levels in long term.

In fact, in a previous study carried out with human embryos implanted after 6-OHDA lesion of the intrinsic mesotelencephalic dopamine pathways, was demonstrated that transplanted nigral neurons placed their natural position within the rostral mesencephalon , extending positive axons on the rostral, but not caudal direction along the myelinated fiber bundles (Lindvall et al., 1984). Other studies carried out in other models of PD have observed this gradient rostro-caudal (Rosenblad et al., 2000).

Anatomical connections could explain that the changes observed in SN were induced by the activity of NTFs in the striatum, i.e. their place of projection (Ortuzar et al., 2013). In addition, previous studies in unilateral 6-OHDA lesion animal model reported that crossed nigrostriatal projections were related to the underlying mechanisms of recovery requiring feedback from behavior activity or the involvement of learning process (Fornaguera et al., 1994; Schwarting & Huston, 1996). Moreover, a recent study revealed that striatal interneurons could develop a role in the compensative response in a 6-OHDA induced model of PD by modulation of dopaminergic projection neurons in the nigrostriatal pathway (Ma et al., 2014).

In addition, topological distribution of microvessels was also observed in striatum and in SN. Saline solution or 6-OHDA administration into MFB trended to decrease from rostral to caudal level in both anatomical parts. This topological distribution was also found in treated rats. In fact, when rats were treated with MS, rats receiving VEGF and GDNF in combination presented statistically significant differences in rostral sections respect to middle and caudal sections (109% *vs*. 86% and 19%). Thus, this increase in microvascular density at rostral levels of striatum could be related to the lesion due to MS administration, enhancing the microvascular density in order to increase oxygen and nutrient supply due to the lesion. Furthermore, this decrease rostro-caudal was in accordance with the loss of dopaminergic neurons and ADN, showing the same pattern the microvascular distribution and the distribution of dopaminergic cells and their prolongations. Accordingly, previous studies have shown relations between changes in the vascularization and neuronal loss in Parkinsonism (Barcia et al., 2005). In addition, we added the possibility of considering the neurovascular coupling to explain this relation.

Taken together, despite the extensive depletion of DA produced by the administration of 6-OHDA into MFB, we can support a topological distribution in the dopaminergic system, showing the same pattern for neurons and vessels. It trend to decrease from rostral to caudal parts, showing a selective vulnerability to 6-OHDA and recovering after the treatment.

In **Partial model**, the quantitative analysis of the rostro-caudal sections of the striatum revealed that rats receiving 6-OHDA presented the highest increase in TH-negative volume at caudal levels, while the saline group did not present any difference throughout the rostro-caudal axis (remaining TH-ir). This supports the special vulnerability of the dorsolateral and caudal regions. Parkinsonized rats also showed a similar distribution in the vehicle group; but rats receiving NTFs showed a significant recovery in TH-positive volume at all levels. However, most of this incipient plasticity consists of wide territories occupied by fine positive fibers. This is a crucial point to reinforce this innovative proposal of using the volume of TH-negative fibers instead the IOD. Areas with positive fibers were usually undervalued when the IOD was measured. These lightly positive areas are the basis for recovery, and these observations are in agreement with other reports concerned with the sprouting of TH-positive fibers in the striatum close to the GDNF injection (Rosenblad et al., 1999, 2000).

A rostro-caudal reduction in the number of neurons was already reported by Rosenblad (Rosenblad et al., 2000), which was attributed to the toxicity of 6-OHDA. However, in the present study a statistically significant difference was also found in the saline group (91% *vs*. 63%).

Interestingly, this rostro-caudal reduction of the neuronal density was observed in rats treated with the vehicle (22% *vs*. 14%) and the empty-NS (33% *vs*. 15%), but not with NTFs. This group showed opposite results like a marked rostro-caudal increase in the number of neurons in the entire SN (19% at the rostral, 25% at the middle, and 43% at caudal section) and in e-SN (37%, 44%, and 51% respectively), which shows a significantly higher density at all levels. This implied a success in the recovery of neurons in the SN, presenting large differences between the rostral and the caudal levels.

ADN density showed a rostro-caudal decrease in all groups of both assays, following the same pattern than the TH-positive fibers in the striatum. This corresponds to the anatomical organization of basal ganglia (García-Amado & Prensa, 2013). The group receiving the NTFs showed a regenerative and plasticity response, the ADN

increasing at all considered levels with respect to the vehicle or the empty-NS group. Anatomical connections could explain that the changes observed in SN were induced by the activity of NTFs in the striatum, i.e. their place of projection (Ortuzar et al., 2013). However, further studies are necessary to assess these effects according to the anatomical connections between the striatum and the SN along the rostro-caudal axis.

Regarding microvascular density, results showed that microvascular density trend to increase from rostral level to caudal level in striatum and to decrease in SN in case of parkinsonized rats and to increase in rats treated. These results obtained in striatum corresponding on opposite sense to the distribution of TH+ fibers or TH+ volume in striatum. Previous studies show relations between changes in the vascularization and neuronal loss in Parkinsonism (Barcia et al., 2005). The results obtained in this model suggest that the increase in microvascular density at caudal levels in striatum could be related to the lesion; because we observed that the most loss of positivity for TH is located in caudal sections. Furthermore, this increase of the microvascular density focused on this part could be in order to increase oxygen and nutrient supply due to the lesion. On the other hand, the gradients shown in SN indicated that the most loss of neurons or ADN corresponding with the reduction of microvascular density in caudal levels. However, when rats were parkinsonized and after that were treated with vehicle or NS, therefore injuring twice at the same coordinates, this gradient was also inverted. It suggested that the passage from the onset of the experiments to sacrifice of the animals could be the explication, because it was different in both experiments.

Topological distribution in the **Preclinical model** was only remarkable when vandetanib was administered, increasing the striatal denervation and nigral loss from rostral to caudal parts. In fact, the denervation and neurodegeneration induced by vandetanib was similar to 6-OHDA in a Partial model, showing the same effect on the nigrostriatal system. Remarkably, 6-OHDA in the Preclinical model induced less degeneration than vandetanib, not showing topological distribution in striatum and SN because of the activation of compensatory changes that may underline the preclinical

stage of this disorder in this model (Zigmond, 1997). Thus, administration of VEGFR2 and RET inhibitor displayed an effect similar to results observed in a Partial model, in which the degeneration was remarkable affecting to the all dopaminergic system (Requejo et al., 2015).

On the other hand, treated groups and 6-OHDA group in this Preclinical model, showed a striatal gradient related to the localization of the lesion (Przedborski et al., 1995). Middle sections showed the most loss of positivity for TH corresponding on with the stereotaxic coordinates of the lesion, while in caudal section the loss of TH-positivity was very low due to these sections was situated farther of the site of 6-OHDA injection. However, the differences were not statistically significant within each one or between groups. Thus, this topological distribution of slight striatal DA depletion found at the middle levels and different to the other models, could be related to the compensation mechanisms by low degeneration induced by 6-OHDA on this early stage of the disease.

14. Changes in protein expression involved in survival and apoptosis

We carried out a systematic characterization by western blot of the molecular changes induced by 6-OHDA in a Preclinical model in order to assess the whether neuroprotective effects of the different treatments in the morphological recovery was due to changes on survival and apoptotic pathways. For this purpose, we assessed p-Akt and caspase-3 activation within striatum and SN. Results showed the same tendency in the expression of both markers in striatum and SN for all experimental groups.

In addition, we also assessed TH expression in striatum and SN by western blot. Our results showed the same tendency between groups than in immunohistochemical study.

Although the pathways involved in cell death are now understood at the molecular level, the precise nature of the role that plays in PD remains unknown (Burke,

2010). In fact, Burke and collaborators suggested that an early molecular event in PD may be the loss of survival signalling provided by phosphorylated Akt (Burke, 2010). In fact, activation of PI3K/Akt signaling pathway has been shown to be linked to cell survival (Dudek et al., 1997; Kauffmann-Zeh et al., 1997). In line with that, due to PI3K/Akt pathway has been reported to be neuroprotective for the dopaminergic neurons of the SNc in rats model of PD (Quesada et al., 2008), the activation of protein kinase Akt was evaluated to elucidate any role of cellular-signalling in neuroprotection seen previously by the morphological analysis upon treatment with CBL and EE in combination. Our findings showed that the combination of both strategies prevented the activation of caspase-3 and induced significantly activation of p-Akt in the lesioned SN. In ipsilateral striatum, we also observed increase of p-Akt, compared to the other groups, but was not significant. Remarkably, only combination of EE and CBL induced the activation of p-Akt in SN.

Thus, regarding the possible intracellular signaling pathways implicated in the neuroprotective mechanism related to CBL and EE, our results indicated that Akt signaling cascade plays a key role. In fact, p-Akt expression may be the way in which NTF induces neuroprotection, by increasing the survival of dopaminergic neurons.

On the other hand, our data strongly suggest the participation of caspase-3 in vandetanib and 6-OHDA group in neuronal degeneration in striatum and SN, activating the enzyme responsible for apoptotic DNA fragmentation. It was in agreement with previous studies, which have revealed that apoptosis plays a major role in neuronal degeneration (Hartmann et al., 2001; Cheng et al., 2007) and that activation of caspase-3, plays a crucial role in the 6-OHDA-activated apoptosis of dopaminergic cells (Hernandez-Baltazar et al., 2013). Furthermore, neurotoxins commonly used to induce experimental PD, such as 6-OHDA and MPTP, have been shown to exert their pro-apoptotic actions via the activation of caspase-3 (Wang et al., 2005) which is believed to be the final executor of apoptotic DNA damage.

Thus, the 6-OHDA-caused neurodegeneration in a Preclinical model was supported by the results of western blot, suggesting the activation of caspase-3 and inhibition of Akt activation, as a mechanism by which 6-OHDA and vandetanib induced the dopaminergic cell death. Results were in accordance with a study in which showed that 6-OHDA injected into the striatum leads to a progressive apoptosis of nigral dopaminergic neurons and activation of caspase-3 (Hernandez-Baltazar et al., 2013).

Therefore, this analysis not also provides a detailed description of changing in protein expression within striatum and SN after 6-OHDA lesion in a Preclinical model, but also could reveal the mechanisms, by which the different strategies used in this study could display their effect.

15. Future perspectives

It is relevant that the morphological and functional results obtained after NTFs administration were consistent. In the Severe model, we obtained better functional results after GDNF-MS and VEGF+GDNF–MS administration. In contrast, the same groups increased tissue retraction in striatum, but reached the most relevant results in the SN, because we found in this model that the dose used of VEGF and GDNF in combination was not as effective in improving the outcome of this model as the lower dose we used in treated rats with both NTFs in a Partial model of PD (Herrán et al., 2014; Requejo et al., 2015). Therefore, regardless of the dose used, VEGF and GDNF seem to be unable to preserve the tissue against the lesion made directly by their administration, suppressing part of the VEGF+GDNF effects.

Thus, instead of these groups developing tissue damage after implantation in the striatum, they are able to induce positive effects, such as restoring the dopaminergic degeneration and developing other important morphological benefits. Therefore, it is especially important to highlight the possible synergistic effect in the Severe model. Regarding the effects of NS loaded with VEGF and GDNF in combination reducing the dose by half in the Partial model, it would be interesting to test this strategy in the

Severe model in order to reduce the tissue damage and enhance the synergistic effect of both NTFs.

We also wanted to highlight the importance of including saline-injected rats as a control because it is a good way to discriminate between the host's response to the surgery and the response induced by the neurotoxin. It is important to have knowledge about the host brain's normal physiological response to injury in order to assess in detail whether injuring is able to produce a significant insult, which could indicate whether the model is suitable for the pathology studies and further treatments.

On the other hand, alterations in cells size, dendrite length and gene expression have been observed in 6-OHDA models (Stott & Barker, 2014). Thus, it would be interesting to analyze these morphological patterns after administration of VEGF and GDNF, to assess whether these NTFs in combination, apart from restoring the loss of dopaminergic neurons are able to revert to the normal cellular morphology and dendrite length. Furthermore, to study the cellular morphology, genetic expression of dopaminergic markers and dendritic size following a rostro-caudal distribution along the nigrostriatal system could reveal differences along this gradient which should be taken into account in order to determine what part is more vulnerable or recovers more easily after a lesion to study in future clinical trials. It is fundamental to keep in mind that when we study one system like unique, we pay no heed to the changes that are occurring in each part.

Concerning to the results obtained in rats housed in EE, it would be necessary to increase the time in EE conditions in order to improve the functional and morphological effects. Studies have demonstrated the effectiveness of the housing in EE as a neuroprotective strategy against PD, and in these studies the time in which rats remained under EE conditions was about 7 weeks (Steiner et al., 2006). Thus, regarding the synergistic effect observed combining CBL administration and EE, if we had increased the remaining of rats in EE, clearer results might have been. Because VEGF and GDNF in combination induced neurogenesis in SVZ after a 6-OHDA lesion it was also

reported that neurogenesis and gliogenesis in neurogenic zones are robustly stimulated by physiological stimuli, physical activity and an EE, respectively (Steiner et al., 2006).Thus, housing rats in an EE together with the i.p. administration of CBL could be a strategy to increase neurogenic effects.

Diagnosis of a presymptomatic stage is a useful strategy to ameliorate the effects of DA decline in the progression of PD. Therefore, it could be interesting in further studies to test the emotional and cognitive deficits associated with premotor behavioral signs through behavioral tests that assess a variety of psychological functions, including locomotor activity, emotional reactivity and depression, anxiety and memory in the rat model of early phase PD and to assess the effects of the treatments proposed in this study (VEGF-NS+GDNF-NS, CBL and housing in EE). In fact, it is known that 6-OHDA in rats is able to induce premotor behavioral signs similar to a preclinical stage of the disease (Tadaiesky et al., 2008). Cognitive impairments are also common in PD. Between 15% and 20% of PD patients develop a frank dementia, and less severe cognitive impairment is a well recognized feature early in the disease that has been shown to be an important predictor of future quality of life (Schrag et al., 2000). On the other hand, to assess the administration of vandetanib using these tests could give us information about the effects of inhibiting the VEGF2 and RET in the processing of memory.

Accordingly, related to the e-SN, where we observed a recovery after NTFs administration and at the same time this region of the SN was more vulnerable to 6-OHDA and vandetanib administration. This region is associated with the dorsolateral striatum, which is involved in learning and memory processes. Furthermore, neurons from e-SN also project to the amygdala. Because of that the evaluation of the cognitive and emotional effects after 6-OHDA and after NTFs administration could support the importance of focusing on this region in future studies in order to consider e-SN as a promising region to test the neuroprotective and neuroregenerative treatments against PD. In addition, to assess fluorogold retrograde labeling of neurons in this e-SN could demonstrate the integrity of the axonal projections in this region along the nigrostriatal and mesolimbic pathways.

VII. CONCLUSIONS

Conclusions

1. The 6-OHDA model is a very suitable model to correlate morphological and functional changes with molecular ones.

2. A Preclinical model allows an assessment of the presymptomatic state of Parkinson's disease in which morphological and molecular changes are present in order to test strategies to protect against neurodegeneration.

3. Stereological quantification of delimited tyrosine hydroxylase negative volume of the caudate putamen complex seems to be more accurate than the integrated optical density estimation; this parameter is more affected by the heterogeneous distribution of striosomes and sections of striatal blood vessels. In addition the new proposed marker is sensitive to mild changes in the axodendritic network due to neuroplasticity.

4. The different rostro-caudal gradients exhibited in the striatum and substantia nigra after 6-OHDA injection and VEGF and GDNF administration, suggest a specific anatomical distribution of dopaminergic neurons and terminals in the rostro-caudal axis, which could be useful in order to assess the lesion, administration and diffusion of treatments.

5. Measurements focused on the "external substantia nigra", which are topographically related to the lesioned area of the striatum, achieve more specific and significant results than when the whole substantia nigra is measured.

6. Functional improvement and morphological recovery after implantation of nano/microspheres loaded with VEGF and GDNF is associated with the preservation of tyrosine hydroxylase positive cells and the axodendritic network in the striatum and substantia nigra.

7. Mild evidence of lesion recovery after combination of VEGF and GDNF in the Severe model points to the necessity for further studies, such as investigating this

recovery in a Partial Parkinson's disease model in which the plasticity potential is better conserved.

8. The combination of VEGF-nanospheres and GDNF-nanospheres at half the dose of their individual administration could represent a suitable and promising treatment for neuron regeneration and protection in the Partial model of Parkinson's disease.

9. The combination of Cerebrolysin and enriched environment provided evidence of protective mechanisms by which this combined strategy promoteed functional and morphological improvement by activation of survival signaling pathways after dopamine depletion in a preclinical rat model of Parkinson's disease.

10. Inhibition of VEGFR2 and RET by the oral administration of vandetanib produced deleterious effects on the dopaminergic system, supporting the potent and synergistic effects exerted by VEGF and GDNF in Parkinson's disease.

11. These findings support the neurorestorative role of VEGF+GDNF on the dopaminergic system and the synergistic effect between both factors. Similar beneficial effects were also found with the combination of Cerebrolysin and enriched environment.

In summary, intracerebral injections of 6-OHDA can produce selective DA depletion in the striatum and destruction of dopaminergic neurons in the SN, allowing the study of different degrees of severity of PD and the synergistic effects of different therapeutic strategies. Our findings suggest protective and/or restorative mechanisms mobilized by NTFs, CBL and EE, which significantly reduced 6-OHDA degeneration of dopaminergic neurons in the SN of adult rats, preserved nigrostriatal projections, and improved dopaminergic function, showing selective vulnerability along the rostro-caudal axis in the dopaminergic system. We also demonstrate for the first time the deleterious effect of inhibiting VEGFR2 and RET on the dopaminergic system, confirming the beneficial and synergistic effect exhibited by NTFs in PD.

VIII. REFERENCES

Agid, Y., Javoy, F., & Glowinski, J. (1973) Hyperactivity of remaining dopaminergic neurones after partial destruction of the nigro-striatal dopaminergic system in the rat. *Nat New Biol*, **245**, 150–151.

Airaksinen, M.S. & Saarma, M. (2002) The GDNF family: signalling, biological functions and therapeutic value. *Nat Rev Neurosci*, **3**, 383–394.

Alam, M., Mayerhofer, A., & Schmidt, W.J. (2004) The neurobehavioral changes induced by bilateral rotenone lesion in medial forebrain bundle of rats are reversed by L-DOPA. *Behav Brain Res*, **151**, 117–124.

Alexoudi, A., Shalash, A., Knudsen, K., Witt, K., Mehdorn, M., Volkmann, J., & Deuschl, G. (2015) The medical treatment of patients with Parkinson's disease receiving subthalamic neurostimulation. *Parkinsonism Relat Disord*, **21**, 555–560; discussion 555.

Al-Jarrah, M., Jamous, M., Al Zailaey, K., & Bweir, S.O. (2010) Endurance exercise training promotes angiogenesis in the brain of chronic/progressive mouse model of Parkinson's Disease. *NeuroRehabilitation*, **26**, 369–373.

Amaral, O.B., Vargas, R.S., Hansel, G., Izquierdo, I., & Souza, D.O. (2008) Duration of environmental enrichment influences the magnitude and persistence of its behavioral effects on mice. *Physiol Behav*, **93**, 388–394.

Anastasía, A., Torre, L., de Erausquin, G.A., & Mascó, D.H. (2009) Enriched environment protects the nigrostriatal dopaminergic system and induces astroglial reaction in the 6-OHDA rat model of Parkinson's disease. *J Neurochem*, **109**, 755–765.

Andres-Mateos, E., Perier, C., Zhang, L., Blanchard-Fillion, B., Greco, T.M., Thomas, B., Ko, H.S., Sasaki, M., Ischiropoulos, H., Przedborski, S., Dawson, T.M., & Dawson, V.L. (2007) DJ-1 gene deletion reveals that DJ-1 is an atypical peroxiredoxin-like peroxidase. *Proc Natl Acad Sci U S A*, **104**, 14807–14812.

Angot, E. & Brundin, P. (2009) Dissecting the potential molecular mechanisms underlying alpha-synuclein cell-to-cell transfer in Parkinson's disease. *Parkinsonism Relat Disord*, **15 Suppl 3**, S143–S147.

Argandoña, E.G., Bengoetxea, H., & Lafuente, J. V (2009) Physical exercise is required for environmental enrichment to offset the quantitative effects of dark-rearing on the S-100beta astrocytic density in the rat visual cortex. *J Anat*, **215**, 132–140.

Aristieta, A., Azkona, G., Sagarduy, A., Miguelez, C., Ruiz-Ortega, J.Á., Sanchez-Pernaute, R., & Ugedo, L. (2012) The role of the subthalamic nucleus in L-DOPA induced dyskinesia in 6-hydroxydopamine lesioned rats. *PLoS One*, **7**, e42652.

Arkadir, D., Bergman, H., & Fahn, S. (2014) Redundant dopaminergic activity may enable compensatory axonal sprouting in Parkinson disease. *Neurology*, **82**, 1093–1098.

Aron, L., Klein, P., Pham, T.-T., Kramer, E.R., Wurst, W., & Klein, R. (2010) Pro-survival role for Parkinson's associated gene DJ-1 revealed in trophically impaired dopaminergic neurons. *PLoS Biol*, **8**, e1000349.

Baker, S.A., Baker, K.A., & Hagg, T. (2004) Dopaminergic nigrostriatal projections regulate neural precursor proliferation in the adult mouse subventricular zone. *Eur J Neurosci*, **20**, 575–579.

Baldereschi, M., Di Carlo, A., Rocca, W.A., Vanni, P., Maggi, S., Perissinotto, E., Grigoletto, F., Amaducci, L., & Inzitari, D. (2000) Parkinson's disease and parkinsonism in a longitudinal study: two-fold higher incidence in men. ILSA Working Group. Italian Longitudinal Study on Aging. *Neurology*, **55**, 1358–1363.

Baluchnejadmojarad, T., Roghani, M., & Mafakheri, M. (2010) Neuroprotective effect of silymarin in 6-hydroxydopamine hemi-parkinsonian rat: involvement of estrogen receptors and oxidative stress. *Neurosci Lett*, **480**, 206–210.

Barcia, C., Bautista, V., Sánchez-Bahillo, A., Fernández-Villalba, E., Faucheux, B., Poza y Poza, M., Fernandez Barreiro, A., Hirsch, E.C., & Herrero, M.-T. (2005) Changes in vascularization in substantia nigra pars compacta of monkeys rendered parkinsonian. *J Neural Transm*, **112**, 1237–1248.

Batchelor, P.E., Liberatore, G.T., Porritt, M.J., Donnan, G.A., & Howells, D.W. (2000) Inhibition of brain-derived neurotrophic factor and glial cell line-derived neurotrophic factor expression reduces dopaminergic sprouting in the injured striatum. *Eur J Neurosci*, **12**, 3462–3468.

Bayer, S.A. (1984) Neurogenesis in the rat neostriatum. *Int J Dev Neurosci*, **2**, 163–175.

Beaulieu, J.-M., Gainetdinov, R.R., & Caron, M.G. (2007) The Akt-GSK-3 signaling cascade in the actions of dopamine. *Trends Pharmacol Sci*, **28**, 166–172.

Benabid, A.L., Le Bas, J.F., & Pollak, P. (2003) Therapeutic and physiopathological contribution of electric stimulation of deep brain structures in Parkinson's disease. *Bull Acad Natl Med*, **187**, 305–319; discussion 319–322.

Bengoetxea, H., Argandon, E.G., Lafuente, V., Neuroscience, E., Sarriena, B., & Sarriena, B. (2008) Effects of Visual Experience on Vascular Endothelial Growth Factor Expression during the Postnatal Development of the Rat Visual Cortex. *Cereb Cortex*, **18**, 1630-9.

Benner, E.J., Mosley, R.L., Destache, C.J., Lewis, T.B., Jackson-Lewis, V., Gorantla, S., Nemachek, C., Green, S.R., Przedborski, S., & Gendelman, H.E. (2004) Therapeutic immunization protects dopaminergic neurons in a mouse model of Parkinson's disease. *Proc Natl Acad Sci U S A*, **101**, 9435–9440.

Berg, J., Roch, M., Altschüler, J., Winter, C., Schwerk, A., Kurtz, A., & Steiner, B. (2015) Human adipose-derived mesenchymal stem cells improve motor functions and are neuroprotective in the 6-hydroxydopamine-rat model for Parkinson's disease when cultured in monolayer cultures but suppress hippocampal neurogenesis and hippocampal memory functi. *Stem Cell Rev*, **11**, 133–149.

Betarbet, R., Sherer, T.B., MacKenzie, G., Garcia-Osuna, M., Panov, A. V, & Greenamyre, J.T. (2000) Chronic systemic pesticide exposure reproduces features of Parkinson's disease. *Nat Neurosci*, **3**, 1301–1306.

Bezard, E., Crossman, A.R., Gross, C.E., & Brotchie, J.M. (2001) Structures outside the basal ganglia may compensate for dopamine loss in the presymptomatic stages of Parkinson's disease. *FASEB J*, **15**, 1092–1094.

Bezard, E., Dovero, S., Belin, D., Duconger, S., Jackson-Lewis, V., Przedborski, S., Piazza, P.V., Gross, C.E., & Jaber, M. (2003) Enriched environment confers resistance to 1-methyl-4-phenyl-1,2,3,6-tetrahydropyridine and cocaine: involvement of dopamine transporter and trophic factors. *J Neurosci*, **23**, 10999–11007.

Bezard, E. & Przedborski, S. (2011) A tale on animal models of Parkinson's disease. *Mov Disord*, **26**, 993–1002.

Biernaskie, J. & Corbett, D. (2001) Enriched rehabilitative training promotes improved forelimb motor function and enhanced dendritic growth after focal ischemic injury. *J Neurosci*, **21**, 5272–5280.

Bilowit, D.S. (1956) Establishing physical objectives in the rehabilitation of patients with Parkinson's disease; gymnasium activities. *Phys Ther Rev*, **36**, 176–178.

Birling, M.C. & Price, J. (1995) Influence of growth factors on neuronal differentiation. *Curr Opin Cell Biol*, **7**, 878–884.

Björklund, A. & Dunnett, S.B. (2007) Dopamine neuron systems in the brain: an update. *Trends Neurosci*, **30**, 194–202.

Björklund, A., Rosenblad, C., Winkler, C., & Kirik, D. (1997) Studies on neuroprotective and regenerative effects of GDNF in a partial lesion model of Parkinson's disease. *Neurobiol Dis*, **4**, 186–200.

Björklund, T. & Kirik, D. (2009) Scientific rationale for the development of gene therapy strategies for Parkinson's disease. *Biochim Biophys Acta*, **1792**, 703–713.

Black, J.E., Sirevaag, A.M., & Greenough, W.T. (1987) Complex experience promotes capillary formation in young rat visual cortex. *Neurosci Lett*, **83**, 351–355.

Black, J.E., Zelazny, A.M., & Greenough, W.T. (1991) Capillary and mitochondrial support of neural plasticity in adult rat visual cortex. *Exp Neurol*, **111**, 204–209.

Blandini, F., Armentero, M.-T., & Martignoni, E. (2008) The 6-hydroxydopamine model: news from the past. *Parkinsonism Relat Disord*, **14 Suppl 2**, S124–S129.

Blandini, F., Nappi, G., Tassorelli, C., & Martignoni, E. (2000) Functional changes of the basal ganglia circuitry in Parkinson's disease. *Prog Neurobiol*, **62**, 63–88.

Blesa, J., Phani, S., Jackson-Lewis, V., & Przedborski, S. (2012) Classic and new animal models of Parkinson's disease. *J Biomed Biotechnol*. DOI: 10.1155/2012/845618

Block, M.L., Li, G., Qin, L., Wu, X., Pei, Z., Wang, T., Wilson, B., Yang, J., & Hong, J.S. (2006) Potent regulation of microglia-derived oxidative stress and dopaminergic neuron survival: substance P vs. dynorphin. *FASEB J*, **20**, 251–258.

Block, M.L., Zecca, L., & Hong, J.-S. (2007) Microglia-mediated neurotoxicity: uncovering the molecular mechanisms. *Nat Rev Neurosci*, **8**, 57–69.

Bové, J., Prou, D., Perier, C., & Przedborski, S. (2005) Toxin-induced models of Parkinson's disease. *NeuroRx*, **2**, 484–494.

Braak, H., Bohl, J.R., Müller, C.M., Rüb, U., de Vos, R.A.I., & Del Tredici, K. (2006) Stanley Fahn Lecture 2005: The staging procedure for the inclusion body pathology associated with sporadic Parkinson's disease reconsidered. *Mov Disord*, **21**, 2042–2051.

Braak, H., Ghebremedhin, E., Rüb, U., Bratzke, H., & Del Tredici, K. (2004) Stages in the development of Parkinson's disease-related pathology. *Cell Tissue Res*, **318**, 121–134.

Briones, T.L., Rogozinska, M., & Woods, J. (2009) Environmental experience modulates ischemia-induced amyloidogenesis and enhances functional recovery. *J Neurotrauma*, **26**, 613–625.

Brodkey, J.A., Gates, M.A., Laywell, E.D., & Steindler, D.A. (1993) The complex nature of interactive neuroregeneration-related molecules. *Exp Neurol*, **123**, 251–270.

Brooks, A.I., Chadwick, C.A., Gelbard, H.A., Cory-Slechta, D.A., & Federoff, H.J. (1999) Paraquat elicited neurobehavioral syndrome caused by dopaminergic neuron loss. *Brain Res*, **823**, 1–10.

Brundin, P., Li, J.-Y., Holton, J.L., Lindvall, O., & Revesz, T. (2008) Research in motion: the enigma of Parkinson's disease pathology spread. *Nat Rev Neurosci*, **9**, 741–745.

Burke, R.E. (2010) Intra cellular signalling pathways in dopamine cell death and axonal degeneration. *Prog Brain Res*, **183**, 79-97.

Burton, N.C., Kensler, T.W., & Guilarte, T.R. (2006) In vivo modulation of the Parkinsonian phenotype by Nrf2. *Neurotoxicology*, **27**, 1094–1100.

Calkins, M.J., Johnson, D.A., Townsend, J.A., Vargas, M.R., Dowell, J.A., Williamson, T.P., Kraft, A.D., Lee, J.-M., Li, J., & Johnson, J.A. (2009) The Nrf2/ARE pathway as a potential therapeutic target in neurodegenerative disease. *Antioxid Redox Signal*, **11**, 497–508.

Callio, J., Oury, T.D., & Chu, C.T. (2005) Manganese superoxide dismutase protects against 6-hydroxydopamine injury in mouse brains. *J Biol Chem*, **280**, 18536–18542.

Cancedda, L., Putignano, E., Sale, A., Viegi, A., Berardi, N., & Maffei, L. (2004) Acceleration of visual system development by environmental enrichment. *J Neurosci*, **24**, 4840–4848.

Cannon, J.R., Tapias, V., Na, H.M., Honick, A.S., Drolet, R.E., & Greenamyre, J.T. (2009) A highly reproducible rotenone model of Parkinson's disease. *Neurobiol Dis*, **34**, 279–290.

Cao, L., Jiao, X., Zuzga, D.S., Liu, Y., Fong, D.M., Young, D., & During, M.J. (2004) VEGF links hippocampal activity with neurogenesis, learning and memory. *Nat Genet*, **36**, 827–835.

Cao, L., Liu, X., Lin, E.-J.D., Wang, C., Choi, E.Y., Riban, V., Lin, B., & During, M.J. (2010) Environmental and genetic activation of a brain-adipocyte BDNF/leptin axis causes cancer remission and inhibition. *Cell*, **142**, 52–64.

Carlsson, T., Winkler, C., Burger, C., Muzyczka, N., Mandel, R.J., Cenci, A., Björklund, A., & Kirik, D. (2005) Reversal of dyskinesias in an animal model of Parkinson's disease by continuous L-DOPA delivery using rAAV vectors. *Brain*, **128**, 559–569.

Carmeliet, P. & Storkebaum, E. (2002) Vascular and neuronal effects of VEGF in the nervous system: implications for neurological disorders. *Semin Cell Dev Biol*, **13**, 39–53.

Cenci, M.A., Ohlin, K.E., & Rylander, D. (2009) Parkinsonism and Related Disorders Plastic effects of L-DOPA treatment in the basal ganglia and their relevance to the development of dyskinesia. *Park Realt Disord*, **15**, S59–S63.

Cervós-Navarro, J. & Lafuente, J. V (1991) Traumatic brain injuries: structural changes. *J Neurol Sci*, **103 Suppl**, S3–S14.

Ceulemans, A.-G., Zgavc, T., Kooijman, R., Hachimi-Idrissi, S., Sarre, S., & Michotte, Y. (2010) The dual role of the neuroinflammatory response after ischemic stroke: modulatory effects of hypothermia. *J Neuroinflammation*, **7**, 74.

Chao, M. V (2003) Neurotrophins and their receptors: a convergence point for many signalling pathways. *Nat Rev Neurosci*, **4**, 299–309.

Chen, C.-H., Huang, S.-Y., Chen, N.-F., Feng, C.-W., Hung, H.-C., Sung, C.-S., Jean, Y.-H., Wen, Z.-H., & Chen, W.-F. (2013) Intrathecal granulocyte colony-stimulating factor modulate glial cell line-derived neurotrophic factor and vascular endothelial growth factor A expression in glial cells after experimental spinal cord ischemia. *Neuroscience*, **242**, 39–52.

Chen, H., Zhang, S.M., Schwarzschild, M.A., Hernán, M.A., & Ascherio, A. (2005) Physical activity and the risk of Parkinson disease. *Neurology*, **64**, 664–669.

Cheng, B., Yang, X., Hou, Z., Lin, X., Meng, H., Li, Z., & Liu, S. (2007) D-beta-hydroxybutyrate inhibits the apoptosis of PC12 cells induced by 6-OHDA in relation to up-regulating the ratio of Bcl-2/Bax mRNA. *Auton Neurosci*, **134**, 38–44.

Chéret, C., Gervais, A., Lelli, A., Colin, C., Amar, L., Ravassard, P., Mallet, J., Cumano, A., Krause, K.-H., & Mallat, M. (2008) Neurotoxic activation of microglia is promoted by a nox1-dependent NADPH oxidase. *J Neurosci*, **28**, 12039–12051.

Chu, C.T. (2006) Autophagic stress in neuronal injury and disease. *J Neuropathol Exp Neurol*, **65**, 423–432.

Clarke, L.E. & Barres, B.A. (2013) Emerging roles of astrocytes in neural circuit development. *Nat Rev Neurosci*, **14**, 311–321.

Cohen, A.D., Tillerson, J.L., Smith, A.D., Schallert, T., & Zigmond, M.J. (2003) Neuroprotective effects of prior limb use in 6-hydroxydopamine-treated rats: possible role of GDNF. *J Neurochem*, **85**, 299–305.

Comery, T.A., Shah, R., & Greenough, W.T. (1995) Differential rearing alters spine density on medium-sized spiny neurons in the rat corpus striatum: evidence for association of morphological plasticity with early response gene expression. *Neurobiol Learn Mem*, **63**, 217–219.

Comery, T.A., Stamoudis, C.X., Irwin, S.A., & Greenough, W.T. (1996) Increased density of multiple-head dendritic spines on medium-sized spiny neurons of the striatum in rats reared in a complex environment. *Neurobiol Learn Mem*, **66**, 93–96.

Coq, J.O. & Xerri, C. (1998) Environmental enrichment alters organizational features of the forepaw representation in the primary somatosensory cortex of adult rats. *Exp brain Res*, **121**, 191–204.

Coquery, N., Blesch, A., Stroh, A., Fernández-Klett, F., Klein, J., Winter, C., & Priller, J. (2012) Intrahippocampal transplantation of mesenchymal stromal cells promotes neuroplasticity. *Cytotherapy*, **14**, 1041–1053.

Damier, P., Hirsch, E.C., Agid, Y., & Graybiel, A.M. (1999) The substantia nigra of the human brain. II. Patterns of loss of dopamine-containing neurons in Parkinson's disease. *Brain*, **122 (Pt 8**, 1437–1448.

Dauer, W., Kholodilov, N., Vila, M., Trillat, A.-C., Goodchild, R., Larsen, K.E., Staal, R., Tieu, K., Schmitz, Y., Yuan, C.A., Rocha, M., Jackson-Lewis, V., Hersch, S., Sulzer, D., Przedborski, S., Burke, R., & Hen, R. (2002) Resistance of alpha -synuclein null mice to the parkinsonian neurotoxin MPTP. *Proc Natl Acad Sci U S A*, **99**, 14524–14529.

Dauer, W. & Przedborski, S. (2003) Parkinson's Disease. *Neuron*, **39**, 889–909.

De Lau, L.M.L., Giesbergen, P.C.L.M., de Rijk, M.C., Hofman, A., Koudstaal, P.J., & Breteler, M.M.B. (2004) Incidence of parkinsonism and Parkinson disease in a general population: the Rotterdam Study. *Neurology*, **63**, 1240–1244.

de Cabo, R., Carmona-Gutierrez, D., Bernier, M., Hall, M.N., & Madeo, F. (2014) The Search for Antiaging Interventions: From Elixirs to Fasting Regimens. *Cell*, **157**, 1515–1526.

Deigner, H.P., Haberkorn, U., & Kinscherf, R. (2000) Apoptosis modulators in the therapy of neurodegenerative diseases. *Expert Opin Investig Drugs*, **9**, 747–764.

Del Tredici, K., Rüb, U., De Vos, R.A.I., Bohl, J.R.E., & Braak, H. (2002) Where does parkinson disease pathology begin in the brain? *J Neuropathol Exp Neurol*, **61**, 413–426.

Deshpande, H., Roman, S., Thumar, J., & Sosa, J.A. (2011) Vandetanib (ZD6474) in the Treatment of Medullary Thyroid Cancer. *Clin Med Insights Oncol*, **5**, 213–221.

Deumens, R., Blokland, A., & Prickaerts, J. (2002) Modeling Parkinson's disease in rats: an evaluation of 6-OHDA lesions of the nigrostriatal pathway. *Exp Neurol*, **175**, 303–317.

Dhondt, J., Peeraer, E., Verheyen, A., Nuydens, R., Buysschaert, I., Poesen, K., Van Geyte, K., Beerens, M., Shibuya, M., Haigh, J.J., Meert, T., Carmeliet, P., & Lambrechts, D. (2011) Neuronal FLT1 receptor and its selective ligand VEGF-B protect against retrograde degeneration of sensory neurons. *FASEB J*, **25**, 1461–1473.

Diamond, M.C., Krech, D., & Rosenzweig, M.R. (1964) The effects of an enriched environment on the histology of the rat cerebral cortex. *J Comp Neurol*, **123**, 111–120.

Diamond, M.C., Law, F., Rhodes, H., Lindner, B., Rosenzweig, M.R., Krech, D., & Bennett, E.L. (1966) Increases in cortical depth and glia numbers in rats subjected to enriched environment. *J Comp Neurol*, **128**, 117–126.

Dias, V., Junn, E., & Mouradian, M.M. (2013) The role of oxidative stress in Parkinson's disease. *J Parkinsons Dis*, **3**, 461–491.

Doetsch, F. (2003) The glial identity of neural stem cells. *Nat Neurosci*, **6**, 1127–1134.

Doshi, P.K., Chhaya, N., & Bhatt, M.H. (2002) Depression leading to attempted suicide after bilateral subthalamic nucleus stimulation for Parkinson's disease. *Mov Disord*, **17**, 1084–1085.

Duan, C.-L., Liu, C.-W., Shen, S.-W., Yu, Z., Mo, J.-L., Chen, X.-H., & Sun, F.-Y. (2015) Striatal astrocytes transdifferentiate into functional mature neurons following ischemic brain injury. *Glia*, **63**, 1660–1670.

Dudek, H., Datta, S.R., Franke, T.F., Birnbaum, M.J., Yao, R., Cooper, G.M., Segal, R.A., Kaplan, D.R., & Greenberg, M.E. (1997) Regulation of neuronal survival by the serine-threonine protein kinase Akt. *Science*, **275**, 661–665.

Dumont, M. & Beal, M.F. (2011) Neuroprotective strategies involving ROS in Alzheimer disease. *Free Radic Biol Med*, **51**, 1014–1026.

Duty, S. & Jenner, P. (2011) Animal models of Parkinson's disease: a source of novel treatments and clues to the cause of the disease. *Br J Pharmacol*, **164**, 1357–1391.

Eddleston, M. & Mucke, L. (1993) Molecular profile of reactive astrocytes--implications for their role in neurologic disease. *Neuroscience*, **54**, 15–36.

Elbaz, A. & Moisan, F. (2008) Update in the epidemiology of Parkinson's disease. *Curr Opin Neurol*, **21**, 454–460.

Emborg, M.E. (2004) Evaluation of animal models of Parkinson's disease for neuroprotective strategies. *J Neurosci Methods*, **139**, 121–143.

Faherty, C.J., Shepherd, K.R., Herasimtschuk, A., & Smeyne, R.J. (2005) Environmental enrichment in adulthood eliminates neuronal death in experimental Parkinsonism. *Mol Brain Res*, **134**, 170–179.

Falk, T., Gonzalez, R.T., & Sherman, S.J. (2010) The yin and yang of VEGF and PEDF: multifaceted neurotrophic factors and their potential in the treatment of Parkinson's Disease. *Int J Mol Sci*, **11**, 2875–2900.

Faucheux, B.A., Bonnet, A.M., Agid, Y., & Hirsch, E.C. (1999) Blood vessels change in the mesencephalon of patients with Parkinson's disease. *Lancet (London, England)*, **353**, 981–982.

Fearnley, J.M. & Lees, A.J. (1991) Ageing and Parkinson's disease: substantia nigra regional selectivity. *Brain*, **114 (Pt 5**, 2283–2301.

Feng, L.R., Federoff, H.J., Vicini, S., & Maguire-Zeiss, K.A. (2010) Alpha-synuclein mediates alterations in membrane conductance: a potential role for alpha-synuclein oligomers in cell vulnerability. *Eur J Neurosci*, **32**, 10–17.

Fernandez-Fernandez, S., Almeida, A., & Bolaños, J.P. (2012) Antioxidant and bioenergetic coupling between neurons and astrocytes. *Biochem J*, **443**, 3–11.

Ferrara, N. & Davis-Smyth, T. (1997) The Biology of Vascular Endothelial Growth Factor. *Endocr Rev*, **18**, 14-25.

Ferrara, N. (2004) Vascular endothelial growth factor as a target for anticancer therapy. *Oncologist*, **9 Suppl 1**, 2–10.

Ferrara, N. (2009) Vascular endothelial growth factor. *Arterioscler Thromb Vasc Biol*, **29**, 789–791.

Fisher, L.J., Jinnah, H.A., Kale, L.C., Higgins, G.A., & Gage, F.H. (1991) Survival and function of intrastriatally grafted primary fibroblasts genetically modified to produce L-dopa. *Neuron*, **6**, 371–380.

Fornaguera, J., Carey, R.J., Huston, J.P., & Schwarting, R.K. (1994) Behavioral asymmetries and recovery in rats with different degrees of unilateral striatal dopamine depletion. *Brain Res*, **664**, 178–188.

Franco, V. & Turner, R.S. (2012) Testing the contributions of striatal dopamine loss to the genesis of parkinsonian signs. *Neurobiol Dis*, **47**, 114–125.

Franklin, T.B., Murphy, J.A., Myers, T.L., Clarke, D.B., & Currie, R.W. (2006) Enriched environment during adolescence changes brain-derived neurotrophic factor and

TrkB levels in the rat visual system but does not offer neuroprotection to retinal ganglion cells following axotomy. *Brain Res*, **1095**, 1–11.

Fujita, K. a., Ostaszewski, M., Matsuoka, Y., Ghosh, S., Glaab, E., Trefois, C., Crespo, I., Perumal, T.M., Jurkowski, W., Antony, P.M. a, Diederich, N., Buttini, M., Kodama, A., Satagopam, V.P., Eifes, S., Del Sol, A., Schneider, R., Kitano, H., & Balling, R. (2014) Integrating pathways of parkinson's disease in a molecular interaction map. *Mol Neurobiol*, **49**, 88–102.

Fukushima, T., Gao, T., Tawara, T., Hojo, N., Isobe, A., & Yamane, Y. (1997) Inhibitory effect of nicotinamide to paraquat toxicity and the reaction site on complex I. *Arch Toxicol*, **71**, 633–637.

Fuller, H.R., Hurtado, M.L., Wishart, T.M., & Gates, M.A. (2014) The rat striatum responds to nigro-striatal degeneration via the increased expression of proteins associated with growth and regeneration of neuronal circuitry. *Proteome Sci*, **12**, 20.

Garbayo, E., Montero-Menei, C.N., Ansorena, E., Lanciego, J.L., Aymerich, M.S., & Blanco-Prieto, M.J. (2009) Effective GDNF brain delivery using microspheres-A promising strategy for Parkinson's disease. *J Control Release*, **135**, 119–126.

Garcia, A.D.R., Doan, N.B., Imura, T., Bush, T.G., & Sofroniew, M. V (2004) GFAP-expressing progenitors are the principal source of constitutive neurogenesis in adult mouse forebrain. *Nat Neurosci*, **7**, 1233–1241.

García-Amado, M. & Prensa, L. (2013) Distribution of dopamine transporter immunoreactive fibers in the human amygdaloid complex. *Eur J Neurosci*, **38**, 3589–3601.

Gerfen, C.R. (2000) Molecular effects of dopamine on striatal-projection pathways. *Trends Neurosci*, **23**, S64–S70.

German, D.C., Manaye, K., Smith, W.K., Woodward, D.J., & Saper, C.B. (1989) Midbrain dopaminergic cell loss in Parkinson's disease: computer visualization. *Ann Neurol*, **26**, 507–514.

Gibb, W.R. (1997) Functional neuropathology in Parkinson's disease. *Eur Neurol*, **38 Suppl 2**, 21–25.

Gittis, A.H., Hang, G.B., LaDow, E.S., Shoenfeld, L.R., Atallah, B. V, Finkbeiner, S., & Kreitzer, A.C. (2011) Rapid target-specific remodeling of fast-spiking inhibitory circuits after loss of dopamine. *Neuron*, **71**, 858–868.

Giunti, S., Antonelli, A., Amorosi, A., & Santarpia, L. (2013) Cellular signaling pathway alterations and potential targeted therapies for medullary thyroid carcinoma. *Int J Endocrinol*. DOI: 10.1155/2013/803171.

Gobbo, O.L. & O'Mara, S.M. (2004) Impact of enriched-environment housing on brain-derived neurotrophic factor and on cognitive performance after a transient global ischemia. *Behav Brain Res*, **152**, 231–241.

Going, J.J., Stuart, R.C., Downie, M., Fletcher-Monaghan, A.J., & Keith, W.N. (2002) "Senescence-associated" beta-galactosidase activity in the upper gastrointestinal tract. *J Pathol*, **196**, 394–400.

Goldberg, N.R.S., Fields, V., Pflibsen, L., Salvatore, M.F., & Meshul, C.K. (2012) Social enrichment attenuates nigrostriatal lesioning and reverses motor impairment in a progressive 1-methyl-2-phenyl-1,2,3,6-tetrahydropyridine (MPTP) mouse model of Parkinson's disease. *Neurobiol Dis*, **45**, 1051–1067.

Gómez-Pinilla, F., Dao, L., & So, V. (1997) Physical exercise induces FGF-2 and its mRNA in the hippocampus. *Brain Res*, **764**, 1–8.

Gonzales, R.A., Job, M.O., & Doyon, W.M. (2004) The role of mesolimbic dopamine in the development and maintenance of ethanol reinforcement. *Pharmacol Ther*, **103**, 121–146.

González-Hernández, T., Cruz-Muros, I., Afonso-Oramas, D., Salas-Hernandez, J., & Castro-Hernandez, J. (2010) Vulnerability of mesostriatal dopaminergic neurons in Parkinson's disease. *Front Neuroanat*, **4**, 140.

Grandoso, L., Ponce, S., Manuel, I., Arrúe, A., Ruiz-Ortega, J.A., Ulibarri, I., Orive, G., Hernández, R.M., Rodríguez, A., Rodríguez-Puertas, R., Zumárraga, M., Linazasoro, G., Pedraz, J.L., & Ugedo, L. (2007) Long-term survival of encapsulated GDNF secreting cells implanted within the striatum of parkinsonized rats. *Int J Pharm*, **343**, 69–78.

Greenamyre, J.T., Betarbet, R., & Sherer, T.B. (2003) The rotenone model of Parkinson's disease: genes, environment and mitochondria. *Parkinsonism Relat Disord*, **9 Suppl 2**, S59–S64.

Greenough, W.T., McDonald, J.W., Parnisari, R.M., & Camel, J.E. (1986) Environmental conditions modulate degeneration and new dendrite growth in cerebellum of senescent rats. *Brain Res*, **380**, 136–143.

Greenough, W.T., Volkmar, F.R., & Juraska, J.M. (1973) Effects of rearing complexity on dendritic branching in frontolateral and temporal cortex of the rat. *Exp Neurol*, **41**, 371–378.

Greffard, S., Verny, M., Bonnet, A.-M., Beinis, J.-Y., Gallinari, C., Meaume, S., Piette, F., Hauw, J.-J., & Duyckaerts, C. (2006) Motor score of the Unified Parkinson Disease Rating Scale as a good predictor of Lewy body-associated neuronal loss in the substantia nigra. *Arch Neurol*, **63**, 584–588.

Haaxma, C.A., Bloem, B.R., Borm, G.F., Oyen, W.J.G., Leenders, K.L., Eshuis, S., Booij, J., Dluzen, D.E., & Horstink, M.W.I.M. (2007) Gender differences in Parkinson's disease. *J Neurol Neurosurg Psychiatry*, **78**, 819–824.

Haber, S.N., Fudge, J.L., & McFarland, N.R. (2000) Striatonigrostriatal pathways in primates form an ascending spiral from the shell to the dorsolateral striatum. *J Neurosci*, **20**, 2369–2382.

Halliday, G., Herrero, M.T., Murphy, K., McCann, H., Ros-Bernal, F., Barcia, C., Mori, H., Blesa, F.J., & Obeso, J.A. (2009) No Lewy pathology in monkeys with over 10 years of severe MPTP Parkinsonism. *Mov Disord*, **24**, 1519–1523.

Harrigan, M.R., Ennis, S.R., Sullivan, S.E., & Keep, R.F. (2003) Effects of intraventricular infusion of vascular endothelial growth factor on cerebral blood flow, edema, and infarct volume. *Acta Neurochir (Wien)*, **145**, 49–53.

Harris, H. & Rubinsztein, D.C. (2012) Control of autophagy as a therapy for neurodegenerative disease. *Nat Rev Neurol*, **8**, 108–117.

Hartbauer, M., Hutter-Paier, B., Skofitsch, G., & Windisch, M. (2001) Antiapoptotic effects of the peptidergic drug cerebrolysin on primary cultures of embryonic chick cortical neurons. *J Neural Transm*, **108**, 459–473.

Hartmann, A., Michel, P.P., Troadec, J.D., Mouatt-Prigent, A., Faucheux, B.A., Ruberg, M., Agid, Y., & Hirsch, E.C. (2001) Is Bax a mitochondrial mediator in apoptotic death of dopaminergic neurons in Parkinson's disease? *J Neurochem*, **76**, 1785–1793.

Hazrati, L.N., Parent, A., Mitchell, S., & Haber, S.N. (1990) Evidence for interconnections between the two segments of the globus pallidus in primates: a PHA-L anterograde tracing study. *Brain Res*, **533**, 171–175.

Henderson, J.M., Watson, S., Halliday, G.M., Heinemann, T., & Gerlach, M. (2003) Relationships between various behavioural abnormalities and nigrostriatal dopamine depletion in the unilateral 6-OHDA-lesioned rat. *Behav Brain Res*, **139**, 105–113.

Hennequin, L.F., Stokes, E.S.E., Thomas, A.P., Johnstone, C., Plé, P.A., Ogilvie, D.J., Dukes, M., Wedge, S.R., Kendrew, J., & Curwen, J.O. (2002) Novel 4-anilinoquinazolines with C-7 basic side chains: design and structure activity relationship of a series of

potent, orally active, VEGF receptor tyrosine kinase inhibitors. *J Med Chem*, **45**, 1300–1312.

Henning, J., Strauss, U., Wree, A., Gimsa, J., Rolfs, A., Benecke, R., & Gimsa, U. (2008) Differential astroglial activation in 6-hydroxydopamine models of Parkinson's disease. *Neurosci Res*, **62**, 246–253.

Herbst, R.S., Heymach, J. V, O'Reilly, M.S., Onn, A., & Ryan, A.J. (2007) Vandetanib (ZD6474): an orally available receptor tyrosine kinase inhibitor that selectively targets pathways critical for tumor growth and angiogenesis. *Expert Opin Investig Drugs*, **16**, 239–249.

Hernandez-Baltazar, D., Mendoza-Garrido, M.E., & Martinez-Fong, D. (2013) Activation of GSK-3?? and Caspase-3 Occurs in Nigral Dopamine Neurons during the Development of Apoptosis Activated by a Striatal Injection of 6-Hydroxydopamine. *PLoS One*, **8**, 1–13.

Herrán, E., Requejo, C., Ruiz-Ortega, J.A., Aristieta, A., Igartua, M., Bengoetxea, H., Ugedo, L., Pedraz, J.L., Lafuente, J.V., & Hernández, R.M. (2014) Increased antiparkinson efficacy of the combined administration of VEGF- and GDNF-loaded nanospheres in a partial lesion model of Parkinson's disease. *Int J Nanomedicine*, **9**, 2677–2687.

Herrán, E., Ruiz-Ortega, J.Á., Aristieta, A., Igartua, M., Requejo, C., Lafuente, J.V., Ugedo, L., Pedraz, J.L., & Hernández, R.M. (2013) In vivo administration of VEGF- and GDNF-releasing biodegradable polymeric microspheres in a severe lesion model of Parkinson's disease. *Eur J Pharm Biopharm*, **85**, 1183–1190.

Heuer, A., Smith, G. a., Lelos, M.J., Lane, E.L., & Dunnett, S.B. (2012) Unilateral nigrostriatal 6-hydroxydopamine lesions in mice I: Motor impairments identify extent of dopamine depletion at three different lesion sites. *Behav Brain Res*, **228**, 30–43.

Hickey, T., Kreutzer, D., Burgess, D.J., & Moussy, F. (2002) In vivo evaluation of a dexamethasone/PLGA microsphere system designed to suppress the inflammatory tissue response to implantable medical devices. *J Biomed Mater Res*, **61**, 180–187.

Hicks, A.U., Hewlett, K., Windle, V., Chernenko, G., Ploughman, M., Jolkkonen, J., Weiss, S., & Corbett, D. (2007) Enriched environment enhances transplanted subventricular zone stem cell migration and functional recovery after stroke. *Neuroscience*, **146**, 31–40.

Hirsch, E.C. (2000) Nigrostriatal system plasticity in Parkinson's disease: effect of dopaminergic denervation and treatment. *Ann Neurol*, **47**, S115–S120; discussion S120–S121.

Hirsch, E.C. & Hunot, S. (2009) Neuroinflammation in Parkinson's disease: a target for neuroprotection? *Lancet Neurol*, **8**, 382–397.

Hirsch, E.C., Jenner, P., & Przedborski, S. (2013) Pathogenesis of Parkinson's disease. *Mov Disord*, **28**, 24–30.

Höglinger, G.U., Féger, J., Prigent, A., Michel, P.P., Parain, K., Champy, P., Ruberg, M., Oertel, W.H., & Hirsch, E.C. (2003) Chronic systemic complex I inhibition induces a hypokinetic multisystem degeneration in rats. *J Neurochem*, **84**, 491–502.

Höglinger, G.U., Rizk, P., Muriel, M.P., Duyckaerts, C., Oertel, W.H., Caille, I., & Hirsch, E.C. (2004) Dopamine depletion impairs precursor cell proliferation in Parkinson disease. *Nat Neurosci*, **7**, 726–735.

Hornykiewicz, O. (1998) Biochemical aspects of Parkinson's disease. *Neurology*, **51**, S2–S9.

Huang, E.J. & Reichardt, L.F. (2003) Trk receptors: roles in neuronal signal transduction. *Annu Rev Biochem*, **72**, 609–642.

Huang, S.-M., Chen, T.-S., Chiu, C.-M., Chang, L.-K., Liao, K.-F., Tan, H.-M., Yeh, W.-L., Chang, G.R.-L., Wang, M.-Y., & Lu, D.-Y. (2014) GDNF increases cell motility in human colon cancer through VEGF-VEGFR1 interaction. *Endocr Relat Cancer*, **21**, 73–84.

Hurley, M.J., Brandon, B., Gentleman, S.M., & Dexter, D.T. (2013) Parkinson's disease is associated with altered expression of CaV1 channels and calcium-binding proteins. *Brain*, **136**, 2077–2097.

Ickes, B.R., Pham, T.M., Sanders, L.A., Albeck, D.S., Mohammed, A.H., & Granholm, A.C. (2000) Long-term environmental enrichment leads to regional increases in neurotrophin levels in rat brain. *Exp Neurol*, **164**, 45–52.

Iemitsu, M., Maeda, S., Jesmin, S., Otsuki, T., & Miyauchi, T. (2006) Exercise training improves aging-induced downregulation of VEGF angiogenic signaling cascade in hearts. *Am J Physiol Heart Circ Physiol*, **291**, H1290–H1298.

Irwin, D.J., Lee, V.M.-Y., & Trojanowski, J.Q. (2013) Parkinson's disease dementia: convergence of α-synuclein, tau and amyloid-β pathologies. *Nat Rev Neurosci*, **14**, 626–636.

Israel, Z. & Bergman, H. (2008) Pathophysiology of the basal ganglia and movement disorders: from animal models to human clinical applications. *Neurosci Biobehav Rev*, **32**, 367–377.

Jadavji, N.M., Kolb, B., & Metz, G.A. (2006) Enriched environment improves motor function in intact and unilateral dopamine-depleted rats **140**, 1127–1138.

Jakel, R.J., Kern, J.T., Johnson, D.A., & Johnson, J.A. (2005) Induction of the protective antioxidant response element pathway by 6-hydroxydopamine in vivo and in vitro. *Toxicol Sci*, **87**, 176–186.

Jakel, R.J., Townsend, J.A., Kraft, A.D., & Johnson, J.A. (2007) Nrf2-mediated protection against 6-hydroxydopamine. *Brain Res*, **1144**, 192–201.

Jakobsen, B., Gramsbergen, J.B., Møller Dall, A., Rosenblad, C., & Zimmer, J. (2005) Characterization of organotypic ventral mesencephalic cultures from embryonic mice and protection against MPP toxicity by GDNF. *Eur J Neurosci*, **21**, 2939–2948.

Jankovic, J. (2008) Parkinson's disease: clinical features and diagnosis. *J Neurol Neurosurg Psychiatry*, **79**, 368–376.

Jankovic, J., Shoulson, I., & Weiner, W.J. (1994) Early-stage Parkinson's disease: to treat or not to treat. *Neurology*, **44**, S4–S7.

Jellinger, K. (1990) New developments in the pathology of Parkinson's disease. *Adv Neurol*, **53**, 1–16.

Jellinger, K.A. (2001) The pathology of Parkinson's disease. *Adv Neurol*, **86**, 55–72.

Jeyapalan, J.C. & Sedivy, J.M.Cellular senescence and organismal aging. *Mech Ageing Dev*, **129**, 467–474.

Jin, K., Zhu, Y., Sun, Y., Mao, X.O., Xie, L., & Greenberg, D.A. (2002) Vascular endothelial growth factor (VEGF) stimulates neurogenesis in vitro and in vivo. *Proc Natl Acad Sci U S A*, **99**, 11946–11950.

Jin, K.L., Mao, X.O., & Greenberg, D.A. (2000) Vascular endothelial growth factor: direct neuroprotective effect in in vitro ischemia. *Proc Natl Acad Sci U S A*, **97**, 10242–10247.

Joel, D. & Weiner, I. (2000) The connections of the dopaminergic system with the striatum in rats and primates: an analysis with respect to the functional and compartmental organization of the striatum. *Neuroscience*, **96**, 451–474.

Johansson, B.B. & Ohlsson, A.L. (1996) Environment, social interaction, and physical activity as determinants of functional outcome after cerebral infarction in the rat. *Exp Neurol*, **139**, 322–327.

Johansson, B.B., Zhao, L., & Mattsson, B. (1999) Environmental influence on gene expression and recovery from cerebral ischemia. *Acta Neurochir Suppl*, **73**, 51–55.

Jollivet, C. (2004) Striatal implantation of GDNF releasing biodegradable microspheres promotes recovery of motor function in a partial model of Parkinson's disease. *Biomaterials*, **25**, 933–942.

Jollivet, C., Aubert-Pouessel, A., Clavreul, A., Venier-Julienne, M.C., Montero-Menei, C.N., Benoit, J.P., & Menei, P. (2004) Long-term effect of intra-striatal glial cell line-derived neurotrophic factor-releasing microspheres in a partial rat model of Parkinson's disease. *Neurosci Lett*, **356**, 207–210.

Jungnickel, J., Kalve, I., Reimers, L., Nobre, A., Wesemann, M., Ratzka, A., Halfer, N., Lindemann, C., Schwabe, K., Töllner, K., Gernert, M., & Grothe, C. (2011) Topology of intrastriatal dopaminergic grafts determines functional and emotional outcome in neurotoxin-lesioned rats. *Behav Brain Res*, **216**, 129–135.

Kageyama, T., Nakamura, M., Matsuo, A., Yamasaki, Y., Takakura, Y., Hashida, M., Kanai, Y., Naito, M., Tsuruo, T., Minato, N., & Shimohama, S. (2000) The 4F2hc/LAT1 complex transports L-DOPA across the blood-brain barrier. *Brain Res*, **879**, 115–121.

Kang, U.J. & Nakamura, K. (2003) Potential of gene therapy for pediatric neurotransmitter diseases: lessons from Parkinson's disease. *Ann Neurol*, **54 Suppl 6**, S103–S109.

Kao, S.-Y. (2009) Rescue of alpha-synuclein cytotoxicity by insulin-like growth factors. *Biochem Biophys Res Commun*, **385**, 434–438.

Kaplan, D.R. & Miller, F.D. (2000) Neurotrophin signal transduction in the nervous system. *Curr Opin Neurobiol*, **10**, 381–391.

Karakaya, S., Kipp, M., & Beyer, C. (2007) Oestrogen regulates the expression and function of dopamine transporters in astrocytes of the nigrostriatal system. *J Neuroendocrinol*, **19**, 682–690.

Kauffmann-Zeh, A., Rodriguez-Viciana, P., Ulrich, E., Gilbert, C., Coffer, P., Downward, J., & Evan, G. (1997) Suppression of c-Myc-induced apoptosis by Ras signalling through PI(3)K and PKB. *Nature*, **385**, 544–548.

Kaya, D., Gürsoy-Ozdemir, Y., Yemisci, M., Tuncer, N., Aktan, S., & Dalkara, T. (2005) VEGF protects brain against focal ischemia without increasing blood--brain permeability when administered intracerebroventricularly. *J Cereb Blood Flow Metab*, **25**, 1111–1118.

Kempermann, G., Jessberger, S., Steiner, B., & Kronenberg, G. (2004) Milestones of neuronal development in the adult hippocampus. *Trends Neurosci*, **27**, 447–452.

Kempster, P.A., Hurwitz, B., & Lees, A.J. (2007) A new look at James Parkinson's Essay on the Shaking Palsy. *Neurology*, **69**, 482–485.

Kilic, E., Kilic, U., Wang, Y., Bassetti, C.L., Marti, H.H., & Hermann, D.M. (2006) The phosphatidylinositol-3 kinase/Akt pathway mediates VEGF's neuroprotective activity and induces blood brain barrier permeability after focal cerebral ischemia. *FASEB J*, **20**, 1185–1187.

Kirik, D., Rosenblad, C., & Björklund, A. (2000) Preservation of a functional nigrostriatal dopamine pathway by GDNF in the intrastriatal 6-OHDA lesion model depends on the site of administration of the trophic factor. *Eur J Neurosci*, **12**, 3871–3882.

Kish, S.J., Shannak, K., & Hornykiewicz, O. (1988) Uneven pattern of dopamine loss in the striatum of patients with idiopathic Parkinson's disease. Pathophysiologic and clinical implications. *N Engl J Med*, **318**, 876–880.

Klaissle, P., Lesemann, A., Huehnchen, P., Hermann, A., Storch, A., & Steiner, B. (2012) Physical activity and environmental enrichment regulate the generation of neural precursors in the adult mouse substantia nigra in a dopamine-dependent manner. *BMC Neurosci*, **13**, 132.

Knight, Z.A., Lin, H., & Shokat, K.M. (2010) Targeting the cancer kinome through polypharmacology. *Nat Rev Cancer*, **10**, 130–137.

Knott, A.B., Perkins, G., Schwarzenbacher, R., & Bossy-Wetzel, E. (2008) Mitochondrial fragmentation in neurodegeneration. *Nat Rev Neurosci*, **9**, 505–518.

Knott, M. (1957) Report of a case of parkinsonism treated with proprioceptive facilitation technics. *Phys Ther Rev*, **37**, 229.

Kordower, J.H. & Bjorklund, A. (2013) Trophic factor gene therapy for Parkinson's disease. *Mov Disord*, **28**, 96–109.

Krakora, D., Mulcrone, P., Meyer, M., Lewis, C., Bernau, K., Gowing, G., Zimprich, C., Aebischer, P., Svendsen, C.N., & Suzuki, M. (2013) Synergistic effects of GDNF and VEGF on lifespan and disease progression in a familial ALS rat model. *Mol Ther*, **21**, 1602–1610.

Kramer, E.R., Aron, L., Ramakers, G.M.J., Seitz, S., Zhuang, X., Beyer, K., Smidt, M.P., & Klein, R. (2007) Absence of Ret signaling in mice causes progressive and late degeneration of the nigrostriatal system. *PLoS Biol*, **5**, e39.

Kronenberg, G., Reuter, K., Steiner, B., Brandt, M.D., Jessberger, S., Yamaguchi, M., & Kempermann, G. (2003) Subpopulations of proliferating cells of the adult hippocampus respond differently to physiologic neurogenic stimuli. *J Comp Neurol*, **467**, 455–463.

Krum, J.M. & Khaibullina, A. (2003) Inhibition of endogenous VEGF impedes revascularization and astroglial proliferation: roles for VEGF in brain repair. *Exp Neurol*, **181**, 241–257.

Krum, J.M., Mani, N., & Rosenstein, J.M. (2002) Angiogenic and astroglial responses to vascular endothelial growth factor administration in adult rat brain. *Neuroscience*, **110**, 589–604.

Kulkarni, A.D., Vanjari, Y.H., Sancheti, K.H., Belgamwar, V.S., Surana, S.J., & Pardeshi, C. V (2015) Nanotechnology-mediated nose to brain drug delivery for Parkinson's disease: a mini review. *J Drug Target*, 1–14.

Kunnimalaiyaan, M., Ndiaye, M., & Chen, H. (2006) Apoptosis-mediated medullary thyroid cancer growth suppression by the PI3K inhibitor LY294002. *Surgery*, **140**, 1009–1014; discussion 1014–1015.

Lafuente, J.V., Ortuzar, N., Bengoetxea, H., Bulnes, S., & Argandoña, E.G. (2012) Vascular endothelial growth factor and other angioglioneurins: key molecules in brain development and restoration. *Int Rev Neurobiol*, **102**, 317–346.

Lafuente, J.-V., Requejo, C., Bengoetxea, H., Ortuzar, N., & Bulnes, S. (2014) *Neuroprotección en enfermedades neuro y heredo degenerativas*, OmniaScience Monographs. OmniaScience.

Lafuente, J. V, Argandoña, E.G., & Mitre, B. (2006) VEGFR-2 expression in brain injury: its distribution related to brain-blood barrier markers. *J Neural Transm*, **113**, 487–496.

Lanciego, J.L., Luquin, N., & Obeso, J.A. (2012) Functional neuroanatomy of the basal ganglia. *Cold Spring Harb Perspect Med*, **2**, a009621.

Lang, A.E., Gill, S., Patel, N.K., Lozano, A., Nutt, J.G., Penn, R., Brooks, D.J., Hotton, G., Moro, E., Heywood, P., Brodsky, M.A., Burchiel, K., Kelly, P., Dalvi, A., Scott, B., Stacy, M., Turner, D., Wooten, V.G.F., Elias, W.J., Laws, E.R., Dhawan, V., Stoessl, A.J., Matcham, J., Coffey, R.J., & Traub, M. (2006) Randomized controlled trial of intraputamenal glial cell line-derived neurotrophic factor infusion in Parkinson disease. *Ann Neurol*, **59**, 459–466.

Langston, J.W., Ballard, P., Tetrud, J.W., & Irwin, I. (1983) Chronic Parkinsonism in humans due to a product of meperidine-analog synthesis. *Science*, **219**, 979–980.

Laviola, G., Hannan, A.J., Macrì, S., Solinas, M., & Jaber, M. (2008) Effects of enriched environment on animal models of neurodegenerative diseases and psychiatric disorders. *Neurobiol Dis*, **31**, 159–168.

Lee, J., Giordano, S., & Zhang, J. (2012) Autophagy, mitochondria and oxidative stress: cross-talk and redox signalling. *Biochem J*, **441**, 523–540.

Lee, R., Kermani, P., Teng, K.K., & Hempstead, B.L. (2001) Regulation of cell survival by secreted proneurotrophins. *Science*, **294**, 1945–1948.

Lewin, G.R. & Barde, Y.-A. (1996) Physiology of the Neurotrophins. *Annu Rev Neurosci*, **19**, 289–317.

Li, L. & Tang, B.L. (2005) Environmental enrichment and neurodegenerative diseases. *Biochem Biophys Res Commun*, **334**, 293–297.

Li, Z., Decavel, C., & Hatton, G.I. (1995) Calbindin-D28k: role in determining intrinsically generated firing patterns in rat supraoptic neurones. *J Physiol*, **488 (Pt 3**, 601–608.

Lie, D.C., Dziewczapolski, G., Willhoite, A.R., Kaspar, B.K., Shults, C.W., & Gage, F.H. (2002) The adult substantia nigra contains progenitor cells with neurogenic potential. *J Neurosci*, **22**, 6639–6649.

Lill, C.M., Hansen, J., Olsen, J.H., Binder, H., Ritz, B., & Bertram, L. (2015) Impact of Parkinson's disease risk loci on age at onset. *Mov Disord*, **30**, 847–850.

Lindvall, O., Björklund, A., & Skagerberg, G. (1984) Selective histochemical demonstration of dopamine terminal systems in rat di- and telencephalon: new evidence for dopaminergic innervation of hypothalamic neurosecretory nuclei. *Brain Res*, **306**, 19–30.

Lindvall, O. & Wahlberg, L.U. (2008) Encapsulated cell biodelivery of GDNF: a novel clinical strategy for neuroprotection and neuroregeneration in Parkinson's disease? *Exp Neurol*, **209**, 82–88.

Loke, H., Harley, V., & Lee, J. (2015) Biological factors underlying sex differences in neurological disorders. *Int J Biochem Cell Biol*, **65**, 139–150.

Lorusso, P.M. & Eder, J.P. (2008) Therapeutic potential of novel selective-spectrum kinase inhibitors in oncology. *Expert Opin Investig Drugs*, **17**, 1013–1028.

Love, S., Plaha, P., Patel, N.K., Hotton, G.R., Brooks, D.J., & Gill, S.S. (2005) Glial cell line-derived neurotrophic factor induces neuronal sprouting in human brain. *Nat Med*, **11**, 703–704.

Lu, B., Pang, P.T., & Woo, N.H. (2005) The yin and yang of neurotrophin action. *Nat Rev Neurosci*, **6**, 603–614.

Luk, K.C., Kehm, V., Carroll, J., Zhang, B., O'Brien, P., Trojanowski, J.Q., & Lee, V.M.-Y. (2012) Pathological α-synuclein transmission initiates Parkinson-like neurodegeneration in nontransgenic mice. *Science*, **338**, 949–953.

Lukhanina, E.P., Karaban', I.N., Burenok, I.A., Mel'nik, N.A., & Berezetskaia, N.M. (2004) [Effect of cerebrolysin on the electroencephalographic indices of brain activity in Parkinson's disease]. *Zh Nevrol Psikhiatr Im S S Korsakova*, **104**, 54–60.

Lundberg, C., Horellou, P., Mallet, J., & Björklund, A. (1996) Generation of DOPA-producing astrocytes by retroviral transduction of the human tyrosine hydroxylase gene: in vitro characterization and in vivo effects in the rat Parkinson model. *Exp Neurol*, **139**, 39–53.

Ma, Y., Feng, Q., OuYang, L., Mu, S., Liu, B., Li, Y., Chen, S., & Lei, W. (2014) Morphological diversity of GABAergic and cholinergic interneurons in the striatal dorsolateral and ventromedial regions of rats. *Cell Mol Neurobiol*, **34**, 351–359.

Maesawa, S., Kaneoke, Y., Kajita, Y., Usui, N., Misawa, N., Nakayama, A., & Yoshida, J. (2004) Long-term stimulation of the subthalamic nucleus in hemiparkinsonian rats: neuroprotection of dopaminergic neurons. *J Neurosurg*, **100**, 679–687.

Magnusson, J.P., Goritz, C., Tatarishvili, J., Dias, D.O., Smith, E.M.K., Lindvall, O., Kokaia, Z., & Frisen, J. (2014) A latent neurogenic program in astrocytes regulated by Notch signaling in the mouse. *Science (80-)*, **346**, 237–241.

Makar, T.K., Nedergaard, M., Preuss, A., Gelbard, A.S., Perumal, A.S., & Cooper, A.J. (1994) Vitamin E, ascorbate, glutathione, glutathione disulfide, and enzymes of glutathione metabolism in cultures of chick astrocytes and neurons: evidence that astrocytes play an important role in antioxidative processes in the brain. *J Neurochem*, **62**, 45–53.

Mallajosyula, J.K., Kaur, D., Chinta, S.J., Rajagopalan, S., Rane, A., Nicholls, D.G., Di Monte, D.A., Macarthur, H., & Andersen, J.K. (2008) MAO-B elevation in mouse brain astrocytes results in Parkinson's pathology. *PLoS One*, **3**, e1616.

Mani, N., Khaibullina, A., Krum, J.M., & Rosenstein, J.M. (2005) Astrocyte growth effects of vascular endothelial growth factor (VEGF) application to perinatal neocortical explants: receptor mediation and signal transduction pathways. *Exp Neurol*, **192**, 394–406.

Manning-Bog, A.B., McCormack, A.L., Li, J., Uversky, V.N., Fink, A.L., & Di Monte, D.A. (2002) The herbicide paraquat causes up-regulation and aggregation of alpha-synuclein in mice: paraquat and alpha-synuclein. *J Biol Chem*, **277**, 1641–1644.

Markham, J.A. & Greenough, W.T. (2004) Experience-driven brain plasticity: beyond the synapse. *Neuron Glia Biol*, **1**, 351–363.

Martinez-Vicente, M., Talloczy, Z., Kaushik, S., Massey, A.C., Mazzulli, J., Mosharov, E. V, Hodara, R., Fredenburg, R., Wu, D.-C., Follenzi, A., Dauer, W., Przedborski, S., Ischiropoulos, H., Lansbury, P.T., Sulzer, D., & Cuervo, A.M. (2008) Dopamine-modified alpha-synuclein blocks chaperone-mediated autophagy. *J Clin Invest*, **118**, 777–788.

Masliah, E. & Díez-Tejedor, E. (2012) The pharmacology of neurotrophic treatment with Cerebrolysin: brain protection and repair to counteract pathologies of acute and chronic neurological disorders. *Drugs Today (Barc)*, **48 Suppl A**, 3–24.

Mattson, M.P. (2008) Glutamate and neurotrophic factors in neuronal plasticity and disease. *Ann N Y Acad Sci*, **1144**, 97–112.

McCormack, A.L., Thiruchelvam, M., Manning-Bog, A.B., Thiffault, C., Langston, J.W., Cory-Slechta, D.A., & Di Monte, D.A. (2002) Environmental risk factors and Parkinson's disease: selective degeneration of nigral dopaminergic neurons caused by the herbicide paraquat. *Neurobiol Dis*, **10**, 119–127.

McNaught, K.S.P., Björklund, L.M., Belizaire, R., Isacson, O., Jenner, P., & Olanow, C.W. (2002) Proteasome inhibition causes nigral degeneration with inclusion bodies in rats. *Neuroreport*, **13**, 1437–1441.

Menon, P.K., Muresanu, D.F., Sharma, A., Mössler, H., & Sharma, H.S. (2012) Cerebrolysin, a mixture of neurotrophic factors induces marked neuroprotection in spinal cord injury following intoxication of engineered nanoparticles from metals. *CNS Neurol Disord Drug Targets*, **11**, 40–49.

Mercuri, N.B. & Bernardi, G. (2005) The "magic" of L-dopa: why is it the gold standard Parkinson's disease therapy? *Trends Pharmacol Sci*, **26**, 341–344.

Meredith, G.E. & Kang, U.J. (2006) Behavioral models of Parkinson's disease in rodents: a new look at an old problem. *Mov Disord*, **21**, 1595–1606.

Metz, G.A., Tse, A., Ballermann, M., Smith, L.K., & Fouad, K. (2005) The unilateral 6-OHDA rat model of Parkinson's disease revisited: an electromyographic and behavioural analysis. *Eur J Neurosci*, **22**, 735–744.

Miguelez, C., Aristieta, A., Cenci, M.A., & Ugedo, L. (2011) The locus coeruleus is directly implicated in L-DOPA-induced dyskinesia in parkinsonian rats: an electrophysiological and behavioural study. *PLoS One*, **6**, e24679.

Milber, J.M., Noorigian, J. V, Morley, J.F., Petrovitch, H., White, L., Ross, G.W., & Duda, J.E. (2012) Lewy pathology is not the first sign of degeneration in vulnerable neurons in Parkinson disease. *Neurology*, **79**, 2307–2314.

Miller, D.B. & O'Callaghan, J.P. (2015) Biomarkers of Parkinson's disease: Present and future. *Metabolism*, **64**, S40–S46.

Morera-Herreras, T., Ruiz-Ortega, J.A., Linazasoro, G., & Ugedo, L. (2011) Nigrostriatal denervation changes the effect of cannabinoids on subthalamic neuronal activity in rats. *Psychopharmacology (Berl)*, **214**, 379–389.

Muresanu, D.F., Sharma, A., Lafuente, J. V, Patnaik, R., Tian, Z.R., Nyberg, F., & Sharma, H.S. (2015) Nanowired Delivery of Growth Hormone Attenuates Pathophysiology of Spinal Cord Injury and Enhances Insulin-Like Growth Factor-1 Concentration in the Plasma and the Spinal Cord. *Mol Neurobiol*,.

Muresanu, D.F., Zimmermann-Meinzingen, S., & Sharma, H.S. (2010) Chronic hypertension aggravates heat stress-induced brain damage: possible neuroprotection by cerebrolysin. *Acta Neurochir Suppl*, **106**, 327–333.

Musumeci, F., Radi, M., Brullo, C., & Schenone, S. (2012) Vascular endothelial growth factor (VEGF) receptors: drugs and new inhibitors. *J Med Chem*, **55**, 10797–10822.

Naka, F., Narita, N., Okado, N., & Narita, M. (2005) Modification of AMPA receptor properties following environmental enrichment. *Brain Dev*, **27**, 275–278.

Nalls, M.A., Plagnol, V., Hernandez, D.G., Sharma, M., Sheerin, U.-M., Saad, M., Simón-Sánchez, J., Schulte, C., Lesage, S., Sveinbjörnsdóttir, S., Stefánsson, K., Martinez, M., Hardy, J., Heutink, P., Brice, A., Gasser, T., Singleton, A.B., & Wood, N.W. (2011) Imputation of sequence variants for identification of genetic risks for Parkinson's disease: a meta-analysis of genome-wide association studies. *Lancet*, **377**, 641–649.

Nieuwenhuys, R., Voogd, J., & Huijzen, C. van (2007) *The Human Central Nervous System: A Synopsis and Atlas*. *Springer, 4th Edition.*

Nikolaev, E., Kaczmarek, L., Zhu, S.W., Winblad, B., & Mohammed, A.H. (2002) Environmental manipulation differentially alters c-Fos expression in amygdaloid nuclei following aversive conditioning. *Brain Res*, **957**, 91–98.

Nilsson, M.H., Törnqvist, A.L., & Rehncrona, S. (2005) Deep-brain stimulation in the subthalamic nuclei improves balance performance in patients with Parkinson's

disease, when tested without anti-parkinsonian medication. *Acta Neurol Scand*, **111**, 301–308.

Nithianantharajah, J. & Hannan, A.J. (2006) Enriched environments, experience-dependent plasticity and disorders of the nervous system. *Nat Rev Neurosci*, **7**, 697–709.

Nithianantharajah, J. & Hannan, A.J. (2009) The neurobiology of brain and cognitive reserve: mental and physical activity as modulators of brain disorders. *Prog Neurobiol*, **89**, 369–382.

Nussbaum, R.L. & Ellis, C.E. (2003) Alzheimer's disease and Parkinson's disease. *N Engl J Med*, **348**, 1356–1364.

Nutt, J.G., Burchiel, K.J., Comella, C.L., Jankovic, J., Lang, A.E., Laws, E.R., Lozano, A.M., Penn, R.D., Simpson, R.K., Stacy, M., & Wooten, G.F. (2003) Randomized, double-blind trial of glial cell line-derived neurotrophic factor (GDNF) in PD. *Neurology*, **60**, 69–73.

Nyberg, F. & Sharma, H.S. (2002) Repeated topical application of growth hormone attenuates blood-spinal cord barrier permeability and edema formation following spinal cord injury: an experimental study in the rat using Evans blue, ([125])I-sodium and lanthanum tracers. *Amino Acids*, **23**, 231–239.

Obeso, J. a, Rodriguez-Oroz, M.C., Goetz, C.G., Marin, C., Kordower, J.H., Rodriguez, M., Hirsch, E.C., Farrer, M., Schapira, A.H. V, & Halliday, G. (2010a) Missing pieces in the Parkinson's disease puzzle. *Nat Med*, **16**, 653–661.

Obeso, J.A., Rodriguez-Oroz, M.C., Goetz, C.G., Marin, C., Kordower, J.H., Rodriguez, M., Hirsch, E.C., Farrer, M., Schapira, A.H. V, & Halliday, G. (2010b) Missing pieces in the Parkinson's disease puzzle. *Nat Med*, **16**, 653–661.

Oh, J.D. & Chase, T.N. (2002) Glutamate-mediated striatal dysregulation and the pathogenesis of motor response complications in Parkinson's disease. *Amino Acids*, **23**, 133–139.

Ohlsson, A.L. & Johansson, B.B. (1995) Environment influences functional outcome of cerebral infarction in rats. *Stroke*, **26**, 644–649.

Olanow, C.W. & Obeso, J.A. (2012) The significance of defining preclinical or prodromal Parkinson's disease. *Mov Disord*, **27**, 666–669.

Olanow, C.W. & Tatton, W.G. (1999) Etiology and pathogenesis of Parkinson's disease. *Annu Rev Neurosci*, **22**, 123–144.

Oliff, H.S., Berchtold, N.C., Isackson, P., & Cotman, C.W. (1998) Exercise-induced regulation of brain-derived neurotrophic factor (BDNF) transcripts in the rat hippocampus. *Brain Res Mol Brain Res*, **61**, 147–153.

Olsson, A.-K., Dimberg, A., Kreuger, J., & Claesson-Welsh, L. (2006) VEGF receptor signalling - in control of vascular function. *Nat Rev Mol Cell Biol*, **7**, 359–371.

Ortuzar, N., Rico-Barrio, I., Bengoetxea, H., Argandoña, E.G., & Lafuente, J. V. (2013) VEGF reverts the cognitive impairment induced by a focal traumatic brain injury during the development of rats raised under environmental enrichment. *Behav Brain Res*, **246**, 36–46.

Pang, Y., Zheng, B., Campbell, L.R., Fan, L.-W., Cai, Z., & Rhodes, P.G. (2010) IGF-1 can either protect against or increase LPS-induced damage in the developing rat brain. *Pediatr Res*, **67**, 579–584.

Parent, A. & Hazrati, L.N. (1995) Functional anatomy of the basal ganglia. I. The cortico-basal ganglia-thalamo-cortical loop. *Brain Res Brain Res Rev*, **20**, 91–127.

Pascual, A., Hidalgo-Figueroa, M., Gómez-Díaz, R., & López-Barneo, J. (2011) GDNF and protection of adult central catecholaminergic neurons. *J Mol Endocrinol*, **46**, R83–R92.

Pascual, A., Hidalgo-Figueroa, M., Piruat, J.I., Pintado, C.O., Gómez-Díaz, R., & López-Barneo, J. (2008) Absolute requirement of GDNF for adult catecholaminergic neuron survival. *Nat Neurosci*, **11**, 755–761.

Paxinos, G. & Watson, C. (2013) *The Rat Brain in Stereotaxic Coordinates: Hard Cover Edition*. Academic Press.

Pellegrini, L., Bennis, Y., Guillet, B., Velly, L., Garrigue, P., Sabatier, F., Dignat-George, F., Bruder, N., & Pisano, P. (2013) Therapeutic benefit of a combined strategy using erythropoietin and endothelial progenitor cells after transient focal cerebral ischemia in rats. *Neurol Res*, **35**, 937–947.

Perier, C., Bové, J., Vila, M., & Przedborski, S. (2003) The rotenone model of Parkinson's disease. *Trends Neurosci*, **26**, 345–346.

Pham, T.M., Ickes, B., Albeck, D., Söderström, S., Granholm, A.C., & Mohammed, A.H. (1999) Changes in brain nerve growth factor levels and nerve growth factor receptors in rats exposed to environmental enrichment for one year. *Neuroscience*, **94**, 279–286.

Pham, T.M., Winblad, B., Granholm, A.-C., & Mohammed, A.H. (2002) Environmental influences on brain neurotrophins in rats. *Pharmacol Biochem Behav*, **73**, 167–175.

Picada, J.N., Roesler, R., & Henriques, J.A.P. (2005) Genotoxic, neurotoxic and neuroprotective activities of apomorphine and its oxidized derivative 8-oxo-apomorphine. *Braz J Med Biol Res*, **38**, 477–486.

Pietropaolo, S., Feldon, J., Alleva, E., Cirulli, F., & Yee, B.K. (2006) The role of voluntary exercise in enriched rearing: a behavioral analysis. *Behav Neurosci*, **120**, 787–803.

Piltonen, M., Planken, a., Leskelä, O., Myöhänen, T.T., Hänninen, a. L., Auvinen, P., Alitalo, K., Andressoo, J.O., Saarma, M., & Männistö, P.T. (2011) Vascular endothelial growth factor C acts as a neurotrophic factor for dopamine neurons in vitro and in vivo. *Neuroscience*, **192**, 550–563.

Pitzer, M.R., Sortwell, C.E., Daley, B.F., McGuire, S.O., Marchionini, D., Fleming, M., & Collier, T.J. (2003) Angiogenic and neurotrophic effects of vascular endothelial growth factor (VEGF165): studies of grafted and cultured embryonic ventral mesencephalic cells. *Exp Neurol*, **182**, 435–445.

Plosker, G.L. (2009) Eprosartan: a review of its use in hypertension. *Drugs*, **69**, 2477–2499.

Poesen, K., Lambrechts, D., Van Damme, P., Dhondt, J., Bender, F., Frank, N., Bogaert, E., Claes, B., Heylen, L., Verheyen, A., Raes, K., Tjwa, M., Eriksson, U., Shibuya, M., Nuydens, R., Van Den Bosch, L., Meert, T., D'Hooge, R., Sendtner, M., Robberecht, W., & Carmeliet, P. (2008) Novel role for vascular endothelial growth factor (VEGF) receptor-1 and its ligand VEGF-B in motor neuron degeneration. *J Neurosci*, **28**, 10451–10459.

Polymeropoulos, M.H., Lavedan, C., Leroy, E., Ide, S.E., Dehejia, A., Dutra, A., Pike, B., Root, H., Rubenstein, J., Boyer, R., Stenroos, E.S., Chandrasekharappa, S., Athanassiadou, A., Papapetropoulos, T., Johnson, W.G., Lazzarini, A.M., Duvoisin, R.C., Di Iorio, G., Golbe, L.I., & Nussbaum, R.L. (1997) Mutation in the alpha-synuclein gene identified in families with Parkinson's disease. *Science*, **276**, 2045–2047.

Prensa, L., Cossette, M., & Parent, A. (2000) Dopaminergic innervation of human basal ganglia. *J Chem Neuroanat*, **20**, 207–213.

Prensa, L., Parent, A., & Giménez-Amaya, J.M.[Compartmentalized organization of human corpus striatum]. *Rev Neurol*, **28**, 512–519.

Przedborski, S. (2007) Neuroinflammation and Parkinson's disease. *Handb Clin Neurol*, **83**, 535–551.

Przedborski, S., Levivier, M., Jiang, H., Ferreira, M., Jackson-Lewis, V., Donaldson, D., & Togasaki, D.M. (1995) Dose-dependent lesions of the dopaminergic nigrostriatal

pathway induced by intrastriatal injection of 6-hydroxydopamine. *Neuroscience*, **67**, 631–647.

Pukass, K. & Richter-Landsberg, C. (2014) Oxidative stress promotes uptake, accumulation, and oligomerization of extracellular α-synuclein in oligodendrocytes. *J Mol Neurosci*, **52**, 339–352.

Quesada, A., Lee, B.Y., & Micevych, P.E. (2008) PI3 kinase/Akt activation mediates estrogen and IGF-1 nigral DA neuronal neuroprotection against a unilateral rat model of Parkinson's disease. *Dev Neurobiol*, **68**, 632–644.

Rabchevsky, A.G., Weinitz, J.M., Coulpier, M., Fages, C., Tinel, M., & Junier, M.P. (1998) A role for transforming growth factor alpha as an inducer of astrogliosis. *J Neurosci*, **18**, 10541–10552.

Rajput, A.H. & Uitti, R.J. (1988) Neurological disorders and services in Saskatchewan--a report based on provincial health care records. *Neuroepidemiology*, **7**, 145–151.

Rajput, A.H., Uitti, R.J., Stern, W., & Laverty, W. (1986) Early onset Parkinson's disease in Saskatchewan--environmental considerations for etiology. *Can J Neurol Sci*, **13**, 312–316.

Ramaswamy, S. & Kordower, J.H. (2009) Are growth factors the answer? *Parkinsonism Relat Disord*, **15 Suppl 3**, S176–S180.

Rampon, C., Jiang, C.H., Dong, H., Tang, Y.P., Lockhart, D.J., Schultz, P.G., Tsien, J.Z., & Hu, Y. (2000) Effects of environmental enrichment on gene expression in the brain. *Proc Natl Acad Sci U S A*, **97**, 12880–12884.

Rappold, P.M., Cui, M., Chesser, A.S., Tibbett, J., Grima, J.C., Duan, L., Sen, N., Javitch, J.A., & Tieu, K. (2011) Paraquat neurotoxicity is mediated by the dopamine transporter and organic cation transporter-3. *Proc Natl Acad Sci U S A*, **108**, 20766–20771.

Requejo, C., Ruiz-Ortega, J.A., Bengoetxea, H., Garcia-Blanco, A., Herrán, E., Aristieta, A., Igartua, M., Ugedo, L., Pedraz, J.L., Hernández, R.M., & Lafuente, J. V (2015) Topographical Distribution of Morphological Changes in a Partial Model of Parkinson's Disease-Effects of Nanoencapsulated Neurotrophic Factors Administration. *Mol Neurobiol*, **52**, 846-58.

Ricardo Cabezas, Fidel Avila M., Torrente D., Santos El-Bachá R., Morales L., Gonzalez J. & Barreto G.E. (2013) Astrocytes role in Parkinson: A double-edged sword. Neurodegenerative Diseases. *InTech.* DOI: 10.5772/54305.

Richardson, J.R., Quan, Y., Sherer, T.B., Greenamyre, J.T., & Miller, G.W. (2005) Paraquat neurotoxicity is distinct from that of MPTP and rotenone. *Toxicol Sci*, **88**, 193–201.

Risedal, A., Mattsson, B., Dahlqvist, P., Nordborg, C., Olsson, T., & Johansson, B.B. (2002) Environmental influences on functional outcome after a cortical infarct in the rat. *Brain Res Bull*, **58**, 315–321.

Rite, I., Machado, A., Cano, J., & Venero, J.L. (2007) Blood-brain barrier disruption induces in vivo degeneration of nigral dopaminergic neurons. *J Neurochem*, **101**, 1567–1582.

Robbins, T.W. (2000) Chemical neuromodulation of frontal-executive functions in humans and other animals. *Exp brain Res*, **133**, 130–138.

Rodrigues, R.W.P., Gomide, V.C., & Chadi, G. (2003) Striatal injection of 6-hydroxydopamine induces retrograde degeneration and glial activation in the nigrostriatal pathway. *Acta Cir Bras*, **18**, 272–282.

Rodriguez, M., Rodriguez-Sabate, C., Morales, I., Sanchez, A., & Sabate, M. (2015) Parkinson's disease as a result of aging. *Aging Cell*, **14**, 293-308.

Rodríguez-Antona, C., Pallares, J., Montero-Conde, C., Inglada-Pérez, L., Castelblanco, E., Landa, I., Leskelä, S., Leandro-García, L.J., López-Jiménez, E., Letón, R., Cascón, A., Lerma, E., Martin, M.C., Carralero, M.C., Mauricio, D., Cigudosa, J.C., Matias-Guiu, X., & Robledo, M. (2010) Overexpression and activation of EGFR and VEGFR2 in medullary thyroid carcinomas is related to metastasis. *Endocr Relat Cancer*, **17**, 7–16.

Rose, F.D., al-Khamees, K., Davey, M.J., & Attree, E.A. (1993) Environmental enrichment following brain damage: an aid to recovery or compensation? *Behav Brain Res*, **56**, 93–100.

Rosenblad, C., Kirik, D., & Björklund, a (2000) Sequential administration of GDNF into the substantia nigra and striatum promotes dopamine neuron survival and axonal sprouting but not striatal reinnervation or functional recovery in the partial 6-OHDA lesion model. *Exp Neurol*, **161**, 503–516.

Rosenblad, C., Kirik, D., Devaux, B., Moffat, B., Phillips, H.S., & Bjo, A. (1999) Protection and regeneration of nigral dopaminergic neurons by neurturin or GDNF in a partial lesion model of Parkinson ' s disease after administration into the striatum or the lateral ventricle **11**, 1554–1566.

Rosenzweig, M.R., Bennett, E.L., Hebert, M., & Morimoto, H. (1978) Social grouping cannot account for cerebral effects of enriched environments. *Brain Res*, **153**, 563–576.

Ruozi, B., Belletti, D., Sharma, H.S., Sharma, A., Muresanu, D.F., Mössler, H., Forni, F., Vandelli, M.A., & Tosi, G. (2015) PLGA Nanoparticles Loaded Cerebrolysin: Studies on Their Preparation and Investigation of the Effect of Storage and Serum Stability with Reference to Traumatic Brain Injury. *Mol Neurobiol*,.

Sale, A., Putignano, E., Cancedda, L., Landi, S., Cirulli, F., Berardi, N., & Maffei, L. (2004) Enriched environment and acceleration of visual system development. *Neuropharmacology*, **47**, 649–660.

Samii, A., Nutt, J.G., & Ransom, B.R. (2004) Parkinson ' s disease. Lancet, **363**, 1783–1793.

Sariola, H. & Saarma, M. (2003) Novel functions and signalling pathways for GDNF. *J Cell Sci*, **116**, 3855–3862.

Sarre, S., Yuan, H., Jonkers, N., Van Hemelrijck, A., Ebinger, G., & Michotte, Y. (2004) In vivo characterization of somatodendritic dopamine release in the substantia nigra of 6-hydroxydopamine-lesioned rats. *J Neurochem*, **90**, 29–39.

Sato, H., Kato, T., & Arawaka, S. (2013) The role of Ser129 phosphorylation of α-synuclein in neurodegeneration of Parkinson's disease: a review of in vivo models. *Rev Neurosci*, **24**, 115–123.

Saucier, D.M., Yager, J.Y., & Armstrong, E.A. (2010) Housing environment and sex affect behavioral recovery from ischemic brain damage. *Behav Brain Res*, **214**, 48–54.

Sauer, H. & Oertel, W.H. (1994) Progressive degeneration of nigrostriatal dopamine neurons following intrastriatal terminal lesions with 6-hydroxydopamine: a combined retrograde tracing and immunocytochemical study in the rat. *Neuroscience*, **59**, 401–415.

Schapira, A.H. V (2002) Dopamine agonists and neuroprotection in Parkinson's disease. *Eur J Neurol*, **9 Suppl 3**, 7–14.

Schapira, A.H. V (2006) Etiology of Parkinson's disease. *Neurology*, **66**, S10–S23.

Schapira, A.H. V (2009) Neurobiology and treatment of Parkinson's disease. *Trends Pharmacol Sci*, **30**, 41–47.

Schapira, A.H. V & Obeso, J. (2006) Timing of treatment initiation in Parkinson's disease: a need for reappraisal? *Ann Neurol*, **59**, 559–562.

Schrag, A., Jahanshahi, M., & Quinn, N. (2000) What contributes to quality of life in patients with Parkinson's disease? *J Neurol Neurosurg Psychiatry*, **69**, 308–312.

Schwarting, R.K. & Huston, J.P. (1996) The unilateral 6-hydroxydopamine lesion model in behavioral brain research. Analysis of functional deficits, recovery and treatments. *Prog Neurobiol*, **50**, 275–331.

Schwartz, P.M., Borghesani, P.R., Levy, R.L., Pomeroy, S.L., & Segal, R.A. (1997) Abnormal cerebellar development and foliation in BDNF-/- mice reveals a role for neurotrophins in CNS patterning. *Neuron*, **19**, 269–281.

Semchuk, K.M., Love, E.J., & Lee, R.G. (1992) Parkinson's disease and exposure to agricultural work and pesticide chemicals. *Neurology*, **42**, 1328–1335.

Shan, X., Chi, L., Bishop, M., Luo, C., Lien, L., Zhang, Z., & Liu, R. (2006) Enhanced de novo neurogenesis and dopaminergic neurogenesis in the substantia nigra of 1-methyl-4-phenyl-1,2,3,6-tetrahydropyridine-induced Parkinson's disease-like mice. *Stem Cells*, **24**, 1280–1287.

Sharma, A., Muresanu, D.F., Mössler, H., & Sharma, H.S. (2012) Superior neuroprotective effects of cerebrolysin in nanoparticle-induced exacerbation of hyperthermia-induced brain pathology. *CNS Neurol Disord Drug Targets*, **11**, 7–25.

Sharma, H.S. (2007) A select combination of neurotrophins enhances neuroprotection and functional recovery following spinal cord injury. *Ann N Y Acad Sci*, **1122**, 95–111.

Sharma, H.S. (2010) Selected combination of neurotrophins potentiate neuroprotection and functional recovery following spinal cord injury in the rat. *Acta Neurochir Suppl*, **106**, 295–300.

Sharma, H.S., Ali, S.F., Patnaik, R., Zimmermann-Meinzingen, S., Sharma, A., & Muresanu, D.F. (2011) Cerebrolysin Attenuates Heat Shock Protein (HSP 72 KD) Expression in the Rat Spinal Cord Following Morphine Dependence and Withdrawal: Possible New Therapy for Pain Management. *Curr Neuropharmacol*, **9**, 223–235.

Sharma, H.S. & Johanson, C.E. (2007) Intracerebroventricularly administered neurotrophins attenuate blood cerebrospinal fluid barrier breakdown and brain pathology following whole-body hyperthermia: an experimental study in the rat using biochemical and morphological approaches. *Ann N Y Acad Sci*, **1122**, 112–129.

Sharma, H.S., Muresanu, D., Sharma, A., & Zimmermann-Meinzingen, S. (2010) Cerebrolysin treatment attenuates heat shock protein overexpression in the brain following heat stress: an experimental study using immunohistochemistry at light and electron microscopy in the rat. *Ann N Y Acad Sci*, **1199**, 138–148.

Sharma, H.S., Muresanu, D.F., Patnaik, R., Stan, A.D., Vacaras, V., Perju-Dumbrav, L., Alexandru, B., Buzoianu, A., Opincariu, I., Menon, P.K., & Sharma, A. (2011) Superior

neuroprotective effects of cerebrolysin in heat stroke following chronic intoxication of Cu or Ag engineered nanoparticles. A comparative study with other neuroprotective agents using biochemical and morphological approaches in the rat. *J Nanosci Nanotechnol*, **11**, 7549–7569.

Sharma, H.S., Westman, J., Cervós-Navarro, J., Dey, P.K., & Nyberg, F. (1997) Opioid receptor antagonists attenuate heat stress-induced reduction in cerebral blood flow, increased blood-brain barrier permeability, vasogenic edema and cell changes in the rat. *Ann N Y Acad Sci*, **813**, 559–571.

Sharma, H.S., Zimmermann-Meinzingen, S., & Johanson, C.E. (2010) Cerebrolysin reduces blood-cerebrospinal fluid barrier permeability change, brain pathology, and functional deficits following traumatic brain injury in the rat. *Ann N Y Acad Sci*, **1199**, 125–137.

Sherer, T.B., Kim, J.H., Betarbet, R., & Greenamyre, J.T. (2003) Subcutaneous rotenone exposure causes highly selective dopaminergic degeneration and alpha-synuclein aggregation. *Exp Neurol*, **179**, 9–16.

Shibuya, M. (2011) Vascular Endothelial Growth Factor (VEGF) and Its Receptor (VEGFR) Signaling in Angiogenesis: A Crucial Target for Anti- and Pro-Angiogenic Therapies. *Genes Cancer*, **2**, 1097–1105.

Shingo, T., Date, I., Yoshida, H., & Ohmoto, T. (2002) Neuroprotective and restorative effects of intrastriatal grafting of encapsulated GDNF-producing cells in a rat model of Parkinson's disease. *J Neurosci Res*, **69**, 946–954.

Siegel, G.J. & Chauhan, N.B. (2000) Neurotrophic factors in Alzheimer's and Parkinson's disease brain. *Brain Res Brain Res Rev*, **33**, 199–227.

Silverman, W.F., Krum, J.M., Mani, N., & Rosenstein, J.M. (1999) Vascular, glial and neuronal effects of vascular endothelial growth factor in mesencephalic explant cultures. *Neuroscience*, **90**, 1529–1541.

Simola, N., Morelli, M., Frazzitta, G., & Frau, L. (2013) Role of movement in long-term basal ganglia changes: implications for abnormal motor responses. *Front Comput Neurosci*, **7**, 142.

Sirevaag, A.M., Black, J.E., Shafron, D., & Greenough, W.T. (1988) Direct evidence that complex experience increases capillary branching and surface area in visual cortex of young rats. *Brain Res*, **471**, 299–304.

Sirevaag, A.M. & Greenough, W.T. (1987) Differential rearing effects on rat visual cortex synapses. III. Neuronal and glial nuclei, boutons, dendrites, and capillaries. *Brain Res*, **424**, 320–332.

Sirevaag, A.M. & Greenough, W.T. (1991) Plasticity of GFAP-immunoreactive astrocyte size and number in visual cortex of rats reared in complex environments. *Brain Res*, **540**, 273–278.

Slevin, J.T., Gash, D.M., Smith, C.D., Gerhardt, G.A., Kryscio, R., Chebrolu, H., Walton, A., Wagner, R., & Young, A.B. (2007) Unilateral intraputamenal glial cell line-derived neurotrophic factor in patients with Parkinson disease: response to 1 year of treatment and 1 year of withdrawal. *J Neurosurg*, **106**, 614–620.

Smith, A.D., Amalric, M., Koob, G.F., & Zigmond, M.J. (2002) Effect of bilateral 6-hydroxydopamine lesions of the medial forebrain bundle on reaction time. *Neuropsychopharmacology*, **26**, 756–764.

Smith, Y., Bevan, M.D., Shink, E., & Bolam, J.P. (1998) Microcircuitry of the direct and indirect pathways of the basal ganglia. *Neuroscience*, **86**, 353–387.

Smith, Y. & Parent, A. (1986) Differential connections of caudate nucleus and putamen in the squirrel monkey (Saimiri sciureus). *Neuroscience*, **18**, 347–371.

Snyder, A.M., Stricker, E.M., & Zigmond, M.J. (1985) Stress-induced neurological impairments in an animal model of parkinsonism. *Ann Neurol*, **18**, 544–551.

Sofroniew, M. V (2005) Reactive astrocytes in neural repair and protection. *Neuroscientist*, **11**, 400–407.

Sopova, K., Gatsiou, K., Stellos, K., & Laske, C. (2014) Dysregulation of neurotrophic and haematopoietic growth factors in Alzheimer's disease: from pathophysiology to novel treatment strategies. *Curr Alzheimer Res*, **11**, 27–39.

Spanheimer, P.M., Cyr, A.R., Gillum, M.P., Woodfield, G.W., Askeland, R.W., & Weigel, R.J. (2014) Distinct pathways regulated by RET and estrogen receptor in luminal breast cancer demonstrate the biological basis for combination therapy. *Ann Surg*, **259**, 793–799.

Spires, T.L., Grote, H.E., Varshney, N.K., Cordery, P.M., van Dellen, A., Blakemore, C., & Hannan, A.J. (2004) Environmental enrichment rescues protein deficits in a mouse model of Huntington's disease, indicating a possible disease mechanism. *J Neurosci*, **24**, 2270–2276.

Starr, P.A., Vitek, J.L., & Bakay, R.A. (1998) Ablative surgery and deep brain stimulation for Parkinson's disease. *Neurosurgery*, **43**, 989–1013; discussion 1013–1015.

Steiner, B., Winter, C., Hosman, K., Siebert, E., Kempermann, G., Petrus, D.S., & Kupsch, A. (2006) Enriched environment induces cellular plasticity in the adult substantia

nigra and improves motor behavior function in the 6-OHDA rat model of Parkinson's disease. *Exp Neurol*, **199**, 291–300.

Storkebaum, E., Lambrechts, D., & Carmeliet, P. (2004) VEGF: once regarded as a specific angiogenic factor, now implicated in neuroprotection. *Bioessays*, **26**, 943–954.

Stott, S.R.W. & Barker, R.A. (2014) Time course of dopamine neuron loss and glial response in the 6-OHDA striatal mouse model of Parkinson's disease. *Eur J Neurosci*, **39**, 1042–1056.

Stuber, G.D., Hnasko, T.S., Britt, J.P., Edwards, R.H., & Bonci, A. (2010) Dopaminergic terminals in the nucleus accumbens but not the dorsal striatum corelease glutamate. *J Neurosci*, **30**, 8229–8233.

Sullivan, A.M. & Toulouse, A. (2011) Neurotrophic factors for the treatment of Parkinson's disease. *Cytokine Growth Factor Rev*, **22**, 157–165.

Sullivan, K.L., Ward, C.L., Hauser, R.A., & Zesiewicz, T.A. (2007) Prevalence and treatment of non-motor symptoms in Parkinson's disease. *Parkinsonism Relat Disord*, **13**, 545.

Sulzer, D., Sonders, M.S., Poulsen, N.W., & Galli, A. (2005) Mechanisms of neurotransmitter release by amphetamines: a review. *Prog Neurobiol*, **75**, 406–433.

Sun, Y., Jin, K., Xie, L., Childs, J., Mao, X.O., Logvinova, A., & Greenberg, D.A. (2003) VEGF-induced neuroprotection, neurogenesis, and angiogenesis after focal cerebral ischemia. *J Clin Invest*, **111**, 1843–1851.

Surmeier, D.J., Guzman, J.N., Sanchez-Padilla, J., & Goldberg, J.A. (2011) The origins of oxidant stress in Parkinson's disease and therapeutic strategies. *Antioxid Redox Signal*, **14**, 1289–1301.

Szabo, J. (1980) Organization of the ascending striatal afferents in monkeys. *J Comp Neurol*, **189**, 307–321.

Szeligo, F. & Leblond, C.P. (1977) Response of the three main types of glial cells of cortex and corpus callosum in rats handled during suckling or exposed to enriched, control and impoverished environments following weaning. *J Comp Neurol*, **172**, 247–263.

Tadaiesky, M.T. & Dombrowski, P.A. (2008) Emotional , cognitive and neurochemical alterations in a premotor stage model of Parkinson's disease. *Neuroscience*, **156**, 830–840.

Tadaiesky, M.T., Dombrowski, P.A., Figueiredo, C.P., Cargnin-Ferreira, E., Da Cunha, C., & Takahashi, R.N. (2008) Emotional, cognitive and neurochemical alterations in a premotor stage model of Parkinson's disease. *Neuroscience*, **156**, 830–840.

Takubo, K., Izumiyama-Shimomura, N., Honma, N., Sawabe, M., Arai, T., Kato, M., Oshimura, M., & Nakamura, K.-I. (2002) Telomere lengths are characteristic in each human individual. *Exp Gerontol*, **37**, 523–531.

Tan, E.-K. & Skipper, L.M. (2007) Pathogenic mutations in Parkinson disease. *Hum Mutat*, **28**, 641–653.

Tang, Z., Arjunan, P., Lee, C., Li, Y., Kumar, A., Hou, X., Wang, B., Wardega, P., Zhang, F., Dong, L., Zhang, Y., Zhang, S.-Z., Ding, H., Fariss, R.N., Becker, K.G., Lennartsson, J., Nagai, N., Cao, Y., & Li, X. (2010) Survival effect of PDGF-CC rescues neurons from apoptosis in both brain and retina by regulating GSK3beta phosphorylation. *J Exp Med*, **207**, 867–880.

Tanner, C.M. (2003) Is the cause of Parkinson's disease environmental or hereditary? Evidence from twin studies. *Adv Neurol*, **91**, 133–142.

Tapias, V., Cannon, J.R., & Greenamyre, J.T. (2014) Pomegranate juice exacerbates oxidative stress and nigrostriatal degeneration in Parkinson's disease. *Neurobiol Aging*, **35**, 1162–1176.

Thiffault, C., Langston, J.W., & Di Monte, D.A. (2000) Increased striatal dopamine turnover following acute administration of rotenone to mice. *Brain Res*, **885**, 283–288.

Thiriet, N., Amar, L., Toussay, X., Lardeux, V., Ladenheim, B., Becker, K.G., Cadet, J.L., Solinas, M., & Jaber, M. (2008) Environmental enrichment during adolescence regulates gene expression in the striatum of mice. *Brain Res*, **1222**, 31–41.

Thiruchelvam, M., Brockel, B.J., Richfield, E.K., Baggs, R.B., & Cory-Slechta, D.A. (2000) Potentiated and preferential effects of combined paraquat and maneb on nigrostriatal dopamine systems: environmental risk factors for Parkinson's disease? *Brain Res*, **873**, 225–234.

Tian, Z.R., Sharma, A., Nozari, A., Subramaniam, R., Lundstedt, T., & Sharma, H.S. (2012) Nanowired drug delivery to enhance neuroprotection in spinal cord injury. *CNS Neurol Disord Drug Targets*, **11**, 86–95.

Tieu, K. (2011) A guide to neurotoxic animal models of Parkinson's disease. *Cold Spring Harb Perspect Med*, **1**, a009316.

Tillerson, J.L., Cohen, A.D., Philhower, J., Miller, G.W., Zigmond, M.J., & Schallert, T. (2001) Forced limb-use effects on the behavioral and neurochemical effects of 6-hydroxydopamine. *J Neurosci*, **21**, 4427–4435.

Timmer, M., Müller-Ostermeyer, F., Kloth, V., Winkler, C., Grothe, C., & Nikkhah, G. (2004) Enhanced survival, reinnervation, and functional recovery of intrastriatal dopamine grafts co-transplanted with Schwann cells overexpressing high molecular weight FGF-2 isoforms. *Exp Neurol*, **187**, 118–136.

Tolosa, E., Compta, Y., & Gaig, C. (2007) The premotor phase of Parkinson's disease. *Parkinsonism Relat Disord*, **13 Suppl**, S2–S7.

Toole, T., Hirsch, M.A., Forkink, A., Lehman, D.A., & Maitland, C.G. (2000) The effects of a balance and strength training program on equilibrium in Parkinsonism: A preliminary study. *NeuroRehabilitation*, **14**, 165–174.

Tritsch, N.X., Ding, J.B., & Sabatini, B.L. (2012) Dopaminergic neurons inhibit striatal output through non-canonical release of GABA. *Nature*, **490**, 262–266.

Tsui, A. & Isacson, O. (2011) Functions of the nigrostriatal dopaminergic synapse and the use of neurotransplantation in Parkinson's disease. *J Neurol*, **258**, 1393–1405.

Tufro, A., Teichman, J., Banu, N., & Villegas, G. (2007) Crosstalk between VEGF-A/VEGFR2 and GDNF/RET signaling pathways. *Biochem Biophys Res Commun*, **358**, 410–416.

Turner, C.A., Lewis, M.H., & King, M.A. (2003) Environmental enrichment: effects on stereotyped behavior and dendritic morphology. *Dev Psychobiol*, **43**, 20–27.

Ungerstedt, U. (1968) 6-Hydroxy-dopamine induced degeneration of central monoamine neurons. *Eur J Pharmacol*, **5**, 107–110.

Ungerstedt, U. (1971) Striatal dopamine release after amphetamine or nerve degeneration revealed by rotational behaviour. *Acta Physiol Scand Suppl*, **367**, 49–68.

Ungerstedt, U. & Arbuthnott, G.W. (1970) Quantitative recording of rotational behavior in rats after 6-hydroxy-dopamine lesions of the nigrostriatal dopamine system. *Brain Res*, **24**, 485–493.

Uversky, V.N. (2004) Neurotoxicant-induced animal models of Parkinson's disease: understanding the role of rotenone, maneb and paraquat in neurodegeneration. *Cell Tissue Res*, **318**, 225–241.

Van Den Eeden, S.K., Tanner, C.M., Bernstein, A.L., Fross, R.D., Leimpeter, A., Bloch, D.A., & Nelson, L.M. (2003) Incidence of Parkinson's disease: variation by age, gender, and race/ethnicity. *Am J Epidemiol*, **157**, 1015–1022.

Van Kampen, J.M. & Robertson, H.A. (2005) A possible role for dopamine D3 receptor stimulation in the induction of neurogenesis in the adult rat substantia nigra. *Neuroscience*, **136**, 381–386.

Van Praag, H., Kempermann, G., & Gage, F.H. (2000) Neural consequences of environmental enrichment. *Nat Rev Neurosci*, **1**, 191–198.

Vila, M., Jackson-Lewis, V., Vukosavic, S., Djaldetti, R., Liberatore, G., Offen, D., Korsmeyer, S.J., & Przedborski, S. (2001) Bax ablation prevents dopaminergic neurodegeneration in the 1-methyl- 4-phenyl-1,2,3,6-tetrahydropyridine mouse model of Parkinson's disease. *Proc Natl Acad Sci U S A*, **98**, 2837–2842.

Volkmar, F.R. & Greenough, W.T. (1972) Rearing complexity affects branching of dendrites in the visual cortex of the rat. *Science*, **176**, 1445–1447.

Voon, V., Fernagut, P.-O., Wickens, J., Baunez, C., Rodriguez, M., Pavon, N., Juncos, J.L., Obeso, J.A., & Bezard, E. (2009) Chronic dopaminergic stimulation in Parkinson's disease: from dyskinesias to impulse control disorders. *Lancet Neurol*, **8**, 1140–1149.

Wachter, B., Schürger, S., Rolinger, J., von Ameln-Mayerhofer, A., Berg, D., Wagner, H.-J., & Kueppers, E. (2010) Effect of 6-hydroxydopamine (6-OHDA) on proliferation of glial cells in the rat cortex and striatum: evidence for de-differentiation of resident astrocytes. *Cell Tissue Res*, **342**, 147–160.

Walsh, S., Finn, D.P., & Dowd, E. (2011) Time-course of nigrostriatal neurodegeneration and neuroinflammation in the 6-hydroxydopamine-induced axonal and terminal lesion models of Parkinson's disease in the rat. *Neuroscience*, **175**, 251–261.

Wang, H., Keiser, J.A., Olszewski, B., Rosebury, W., Robertson, A., Kovesdi, I., & Gordon, D. (2004) Delayed angiogenesis in aging rats and therapeutic effect of adenoviral gene transfer of VEGF. *Int J Mol Med*, **13**, 581–587.

Wang, H.-L., Chou, A.-H., Wu, A.-S., Chen, S.-Y., Weng, Y.-H., Kao, Y.-C., Yeh, T.-H., Chu, P.-J., & Lu, C.-S. (2011) PARK6 PINK1 mutants are defective in maintaining mitochondrial membrane potential and inhibiting ROS formation of substantia nigra dopaminergic neurons. *Biochim Biophys Acta*, **1812**, 674–684.

Wang, X., Chen, S., Ma, G., Ye, M., & Lu, G. (2005) Involvement of proinflammatory factors, apoptosis, caspase-3 activation and Ca2+ disturbance in microglia activation-mediated dopaminergic cell degeneration. *Mech Ageing Dev*, **126**, 1241–1254.

Wang, Y.-Q., Cui, H.-R., Yang, S.-Z., Sun, H.-P., Qiu, M.-H., Feng, X.-Y., & Sun, F.-Y. (2009) VEGF enhance cortical newborn neurons and their neurite development in adult rat brain after cerebral ischemia. *Neurochem Int*, **55**, 629–636.

Wichmann, T. & DeLong, M.R. (2003) Pathophysiology of Parkinson's disease: the MPTP primate model of the human disorder. *Ann N Y Acad Sci*, **991**, 199–213.

Wick, A., Wick, W., Waltenberger, J., Weller, M., Dichgans, J., & Schulz, J.B. (2002) Neuroprotection by hypoxic preconditioning requires sequential activation of vascular endothelial growth factor receptor and Akt. *J Neurosci*, **22**, 6401–6407.

Wijeyekoon, R. & Barker, R.A. (2009) Cell replacement therapy for Parkinson's disease. *Biochim Biophys Acta*, **1792**, 688–702.

Will, B., Galani, R., Kelche, C., & Rosenzweig, M.R. (2004) Recovery from brain injury in animals: relative efficacy of environmental enrichment, physical exercise or formal training (1990-2002). *Prog Neurobiol*, **72**, 167–182.

Winkler, T., Sharma, H.S., Stålberg, E., Badgaiyan, R.D., Westman, J., & Nyberg, F. (2000) Growth hormone attenuates alterations in spinal cord evoked potentials and cell injury following trauma to the rat spinal cord. An experimental study using topical application of rat growth hormone. *Amino Acids*, **19**, 363–371.

Winner, B., Geyer, M., Couillard-Despres, S., Aigner, R., Bogdahn, U., Aigner, L., Kuhn, G., & Winkler, J. (2006) Striatal deafferentation increases dopaminergic neurogenesis in the adult olfactory bulb. *Exp Neurol*, **197**, 113–121.

Wong, H.L., Wu, X.Y., & Bendayan, R. (2012) Nanotechnological advances for the delivery of CNS therapeutics. *Adv Drug Deliv Rev*, **64**, 686–700.

Wooten, G.F., Currie, L.J., Bovbjerg, V.E., Lee, J.K., & Patrie, J. (2004) Are men at greater risk for Parkinson's disease than women? *J Neurol Neurosurg Psychiatry*, **75**, 637–639.

Xiong, N., Zhang, Z., Huang, J., Chen, C., Jia, M., Xiong, J., Liu, X., Wang, F., Cao, X., Liang, Z., Sun, S., Lin, Z., & Wang, T. (2011) VEGF-expressing human umbilical cord mesenchymal stem cells, an improved therapy strategy for Parkinson's disease. *Gene Ther*, **18**, 394–402.

Xu, M. & Zhang, H. (2011) Death and survival of neuronal and astrocytic cells in ischemic brain injury: a role of autophagy. *Acta Pharmacol Sin*, **32**, 1089–1099.

Yasuda, T. & Mochizuki, H. (2010) Use of growth factors for the treatment of Parkinson's disease. *Expert Rev Neurother*, **10**, 915–924.

Yasuhara, T., Shingo, T., Kobayashi, K., Takeuchi, A., Yano, A., Muraoka, K., Matsui, T., Miyoshi, Y., Hamada, H., & Date, I. (2004) Neuroprotective effects of vascular endothelial growth factor (VEGF) upon dopaminergic neurons in a rat model of Parkinson's disease. *Eur J Neurosci*, **19**, 1494–1504.

Yasuhara, T., Shingo, T., Muraoka, K., & Kameda, M. (2005) The differences between high and low-dose administration of VEGF to dopaminergic neurons of in vitro and in vivo Parkinson's disease model. *Brain Res*, **1038**, 1–10.

Young, A.B. & Penney, J.B. (1984) Neurochemical anatomy of movement disorders. *Neurol Clin*, **2**, 417–433.

Young, D., Lawlor, P.A., Leone, P., Dragunow, M., & During, M.J. (1999) Environmental enrichment inhibits spontaneous apoptosis, prevents seizures and is neuroprotective. *Nat Med*, **5**, 448–453.

Yuan, H., Sarre, S., Ebinger, G., & Michotte, Y. (2005) Histological, behavioural and neurochemical evaluation of medial forebrain bundle and striatal 6-OHDA lesions as rat models of Parkinson's disease. *J Neurosci Methods*, **144**, 35–45.

Yue, X., Hariri, D.J., Caballero, B., Zhang, S., Bartlett, M.J., Kaut, O., Mount, D.W., Wüllner, U., Sherman, S.J., & Falk, T. (2014) Comparative study of the neurotrophic effects elicited by VEGF-B and GDNF in preclinical in vivo models of Parkinson's disease. *Neuroscience*, **258**, 385–400.

Zeng, X., Chen, J., Deng, X., Liu, Y., Rao, M.S., Cadet, J.-L., & Freed, W.J. (2006) An in vitro model of human dopaminergic neurons derived from embryonic stem cells: MPP+ toxicity and GDNF neuroprotection. *Neuropsychopharmacology*, **31**, 2708–2715.

Zhang, C., Chopp, M., Cui, Y., Wang, L., Zhang, R., Zhang, L., Lu, M., Szalad, A., Doppler, E., Hitzl, M., & Zhang, Z.G. (2010) Cerebrolysin enhances neurogenesis in the ischemic brain and improves functional outcome after stroke. *J Neurosci Res*, **88**, 3275–3281.

Zhu, J. & Chu, C.T. (2010) Mitochondrial dysfunction in Parkinson's disease. *J Alzheimers Dis*, **20 Suppl 2**, S325–S334.

Zigmond, M.J. (1997) Do compensatory processes underlie the preclinical phase of neurodegenerative disease? Insights from an animal model of parkinsonism. *Neurobiol Dis*, **4**, 247–253.

Zigmond, M.J., Hastings, T.G., & Perez, R.G. (2002) Increased dopamine turnover after partial loss of dopaminergic neurons: compensation or toxicity? *Parkinsonism Relat Disord*, **8**, 389–393.

Zinger, A., Barcia, C., Herrero, M.T., & Guillemin, G.J. (2011) The involvement of neuroinflammation and kynurenine pathway in Parkinson's disease. *Parkinsons Dis*, **2011**, 716859.

IX. APPENDIX

European Journal of Pharmaceutics and Biopharmaceutics 85 (2013) 1183–1190

Contents lists available at SciVerse ScienceDirect

European Journal of Pharmaceutics and Biopharmaceutics

journal homepage: www.elsevier.com/locate/ejpb

Research paper

In vivo administration of VEGF- and GDNF-releasing biodegradable polymeric microspheres in a severe lesion model of Parkinson's disease

Enara Herrán [a,b], José Ángel Ruiz-Ortega [c], Asier Aristieta [c], Manoli Igartua [a,b], Catalina Requejo [d], José Vicente Lafuente [d], Luisa Ugedo [c], José Luis Pedraz [a,b], Rosa María Hernández [a,b,*]

[a] NanoBioCel Group, Laboratory of Pharmaceutics, School of Pharmacy, University of the Basque Country (UPV/EHU), Vitoria, Spain
[b] Biomedical Research Networking Center in Bioengineering, Biomaterials and Nanomedicine (CIBER-BBN), Vitoria, Spain
[c] Dept. Pharmacology, University of the Basque Country (UPV/EHU), Spain
[d] LaNCE, Dept. Neurosciences, University of the Basque Country (UPV/EHU), Spain

ARTICLE INFO

Article history:
Received 10 October 2012
Accepted in revised form 30 March 2013
Available online 30 April 2013

Keywords:
Parkinson's disease
Microparticles
GDNF
VEGF
PLGA
6-OHDA
Growth factors

ABSTRACT

In this work, the neuroregenerative potentials of microencapsulated VEGF, GDNF and their combination on a severely lesioned rat model were compared with the aim of developing a new strategy to treat advanced stages of Parkinson's disease. Both neurotrophic factors were separately encapsulated into polymeric microspheres (MSs) to obtain a continuous drug release over time. The regenerative effects of these growth factors were evaluated using a rotation behaviour test and quantified by the number of surviving TH + cells. The biological activities of encapsulated vascular endothelial growth factor (VEGF) and glial cell line-derived neurotrophic factor (GDNF) were investigated in HUVEC and PC12 cells, respectively. The treatment of 6-OHDA-lesioned rats with GDNF microspheres and with both VEGF and GDNF microspheres resulted in improved results in the rotation behaviour test. Both groups also showed higher levels of neuroregeneration/neuroreparation in the substantia nigra than the control group did. These results were confirmed by the pronounced TH + neuron recovery in the group receiving VEGF + GDNF-MS, demonstrating regenerative effects.

1. Introduction

Parkinson's disease (PD) is the second most common neurodegenerative disorder in the world. Due to the current high life expectancy of our society, the number of cases of PD is increasing, and this disease is becoming a serious public health problem. This disease occurs most frequently in people over 80 years old, with a prevalence of 1–3%. However, a younger onset of PD is also possible, occurring in 0.5–1% of people between 65 and 69 years of age [1].

PD is characterised by the progressive degeneration of the nigrostriatal dopaminergic pathway. This gradual loss of dopaminergic neurons in the substantia nigra pars compacta (SNpc) consequently reduces the dopamine (DA) levels in the striatum [2], which is believed to cause motor function impairments such as rest tremors, rigidity, bradykinesia and postural abnormalities [3]. Current therapies are based on dopamimetic treatments, including the administration of the dopamine precursor levodopa (L-dopa). However, levodopa cannot repair the already damaged area and does not provide neuroprotection to the remaining dopaminergic neurons [4]. Therefore, current research is focused on the development of therapeutic strategies that will halt the neurodegenerative process, rather than simply treat the clinical symptoms. An interesting and promising approach to this challenge is the use of neurotrophic factors (NTFs). NTFs are proteins that act as growth factors and play an important role in the maintenance, survival, specification and maturation of specific neuronal populations [5,6].

Among the NTFs, glial cell line-derived neurotrophic factor (GDNF) is a potent neuroprotective/neurorestorative factor that has shown effects on dopamine-depleted striatum both *in vitro* [7,8] and in experimental animal models of PD [9–12]. Fuelled by the encouraging results obtained in animal models, several clinical trials have been carried out to investigate the effectiveness of GDNF in PD patients. Nutt et al. administered GDNF intracerebroventricularly but found no significant clinical improvement, and several negative effects were reported [13,14]. In addition, a clinical trial conducted by Lang et al. was halted after showing no benefit from intraputamenal administration [15]. The major limiting factor in the above-mentioned trials was suggested to be the suboptimal brain delivery of GDNF. Thus, new therapeutic approaches need to be explored to help overcome this limitation.

Vascular endothelial growth factor (VEGF) is an endothelial-specific growth factor predominantly involved in the formation

* Corresponding author. NanoBioCel Group, Laboratory of Pharmaceutics, School of Pharmacy, University of the Basque Country (UPV/EHU), 01006 Vitoria, Spain. Tel.: +34 945013095; fax: +34 945013040.
E-mail address: rosa.hernandez@ehu.es (R.M. Hernández).

0939-6411/$ - see front matter © 2013 Elsevier B.V. All rights reserved.
http://dx.doi.org/10.1016/j.ejpb.2013.03.034

of new blood vessels [16]. In addition to its important role in angiogenesis, VEGF also has specific roles in the central nervous system, stimulating axonal outgrowth and increasing neuronal survival [17]. Multiple studies have argued the potential of VEGF to promote the growth, survival and rescue of dopaminergic neurons *in vitro* [18,19]. It may also protect against 6-hydroxidopamine (6-OHDA)-induced cell death in both a PD rat model and neuronal cultures [20].

The critical problems for the clinical application of GDNF and VEGF are their rapid degradation rate and their difficulty in crossing the blood–brain barrier. Thus, different intracranial administration strategies have been used in PD animal models to obtain a continuous and direct release of the factors into the brain [21]. Over the past several years, one strategy that has gained the attention of the scientific community is the encapsulation of neurotrophic factors into biodegradable poly(lactic-co-glycolic acid) (PLGA) microspheres (MSs) [22]. This approach allows for the intracranial administration of microspheres by stereotactic techniques, achieving a continuous drug release over time and overcoming the problem of repeated administrations. Several previous studies have demonstrated the efficacy of this technique. Studies carried out by Benoit et al. and Blanco-Prieto et al., in which rats were implanted with GDNF-loaded PLGA microparticles, showed improvements in the amphetamine behavioural assay and increases in the fibre density of the striatum [23,24]. To evaluate these new therapies, animal models of PD are essential. For this purpose, the unilateral 6-OHDA-lesioned rat model has been used more frequently. However, animals in this model can present different severity grades and lesion progressions depending on the location of the 6-OHDA injection. In this work, a middle forebrain bundle injection was performed, inducing a profound and complete lesion and resulting in the loss of more than 90% of nigral cells. This lesion is equivalent to an advanced stage of PD [25,26].

The neurorestorative effects of VEGF and GDNF have been tested separately in previous studies. However, their possible synergistic effects have not yet been evaluated. Thus, the aim of this work was to compare the neuroregenerative potential of VEGF and GDNF PLGA microspheres individually and their combination in a severy lesioned rat model with the aim of developing a new strategy to treat advanced stages of PD.

2. Materials and methods

2.1. Materials

Poly(DL-lactide-co-glycolide) (PLGA) (Resomer® RG 752H) with a copolymer ratio of 75:25 (lactic/glycolic%) was provided by Boehringer Ingelheim (Ingelheim, Germany). Methylene chloride, acetone and poly-ethylene-glycol 400 (PEG 400) were purchased from Panreac (Barcelona, Spain).

Human recombinant VEGF165, murine recombinant GDNF and the Human VEGF ELISA Development Kit were provided by Peprotech EC Ltd., UK. A GDNF E_{max}® ImmunoAssay System was obtained from Promega Corporation (Madison, WI, USA).

Poly(vinyl alcohol) (PVA; average MW = 30,000–70,000), human serum albumin (HSA), poly-L-lysine, 6-OHDA-HCl, desipramine, pargyline, amphetamine, apomorphine and a Cell Counting Kit-8 (CCK-8) were acquired from Sigma (St. Louis, USA).

Pheochromocytoma of adrenal rat gland (PC-12) and human umbilical vein endothelial cells (HUVEC) were obtained from ATCC LGC Standards (Barcelona, Spain). Cell culture reagents were purchased from GIBCO and PromoCell GmbH (Germany).

Antibodies were provided by Pel Freez Biologicals and Vector Laboratories (Burlingame, CA, USA).

2.2. Preparation of microspheres

VEGF- and GDNF-containing PLGA (50:50) microspheres were prepared by modifying a previously described double-emulsion solvent evaporation technique ($W_1/O/W_2$) [27]. The organic phase consisted of 100 mg of PLGA (75:25) dissolved in a 3:1 methylene chloride/acetone mixture. The aqueous solution consisted of 150 μg of either hVEGF or mGDNF, 2.5% poly-ethylene-glycol 400 (PEG 400) and 7% human serum albumin (HSA) dissolved in 150 μl of PBS (pH 7.4). These two phases were sonicated (Branson® sonifier 250) for 15 s at 50 W. The W/O emulsion was added to 30 ml of a 1.5% (w/v) PVA aqueous solution and homogenised at 9500 rpm for 5 min (Ultra Turrax T25, IKA-Labortechnik, Staufen, Germany). The final emulsion thus obtained ($W_1/O/W_2$) was stirred on a magnetic stir plate at room temperature for 3 h to complete the evaporation of the solvent. The resulting microspheres were collected by centrifugation at 10,000*g* (Sigma 3–30 K), washed three times with distilled water and freeze-dried for 24 h (LyoBeta 15, Telstar, Tarrasa, Spain). Empty MSs were prepared using the above-described method but omitting the VEGF or GDNF.

2.3. Characterisation of microspheres: particle size analysis and morphological evaluation

The microsphere morphology and surface characteristics were examined by scanning electron microscopy (SEM, Jeol® JSM-7000F). The mean particle diameter and size distribution were determined by laser diffractometry using a Coulter Counter LS 130 (Amherst, MA, USA). The zeta potential was measured by photon correlation using a Malvern® Zetasizer Nano ZS, Model Zen 3600 (Malvern Instruments Ltd.).

2.4. Encapsulation efficiency (EE) and surface-associated proteins

The microsphere encapsulation efficiency was determined using the Human VEGF ELISA Development Kit and the GDNF E_{max}® ImmunoAssay System after microsphere disruption with dimethyl sulfoxide (DMSO). The surface-associated proteins were assessed by suspending 1.5 mg of microspheres in PBS (pH 7.4) and maintaining an orbital rotation at 37 °C for 30 min. Both supernatants were collected after centrifugation (10,000*g*, 10 min) and measured by ELISA.

2.5. In vitro microsphere release studies

The release profiles of VEGF and GDNF from PLGA microspheres were determined by incubating 1.5 mg of the microspheres in a test tube containing 1 ml of 20 mM PBS (pH 7.4) at 37 ± 0.5 °C and shaking the mixture with a rotator shaker at 25 rpm. At defined time intervals, the release medium was removed by centrifugation (10,000*g*, 10 min) and replaced with 1 ml of fresh buffer. The amounts of VEGF and GDNF in the supernatant were measured by ELISA. This release test was performed in triplicate.

2.6. VEGF and GDNF bioactivity assays

The biological activities of the VEGF and GDNF released from the microspheres were also assessed.

VEGF bioactivity was tested in the HUVEC (human umbilical vein endothelial cells) (PromoCell GmbH, Germany) cells because VEGF induces high proliferation in these cells [28]. HUVEC cells were maintained in endothelial cell growth medium (PromoCell GmbH, Germany) supplemented with a supplement kit and were cultured in special cell culture flasks (Corning® CellBIND® Surface) at 37 °C in humidified air with 5% CO_2. Cells between passages 2 and 3 were seeded into 96-well poly-L-lysine-coated culture plates

at a density of 5×10^3 cells/well. After 24 h, the culture medium was removed, and fresh medium (without the supplement kit) was added and supplemented with one of four options: 1 ng/ml or 10 ng/ml of VEGF released from PLGA microspheres, 1 ng/ml of VEGF solution as a positive control, or the released medium from empty MSs as a negative control. The cells treated with VEGF were incubated for 72 h under standard conditions, and the cell proliferation was measured using a Cell Counting Kit-8 (CCK-8 assay).

The GDNF bioactivity assay was carried out in the PC-12 Adh cell line. This cell line can differentiate in the presence of GDNF to a neuronal phenotype [29], inducing neurite outgrowth. PC12 cells were maintained in F-12K medium supplemented with 15% horse serum, 2.5% foetal bovine serum and 1% penicillin/streptomycin at 37 °C in humidified air with 5% CO_2. Cells between passages 3 and 4 were used for the bioactivity assay. The cells were seeded in culture plates that had previously been coated with an attachment factor (sterile solution containing gelatin at 0.1%). Once the cells were attached, they were treated with 25 ng of GDNF released from MSs. After 7 days in culture, neurite outgrowth was visualised using inverted optical microscopy (microscope model Eclipse TE2000-S Nikon).

2.7. 6-OHDA lesions

Female albino Sprague–Dawley rats (150–175 g) were anaesthetised with isoflurane inhalation and mounted on a Kopf stereotaxic instrument. Thirty minutes prior to 6-OHDA injection; the rats were pre-treated with desipramine (25 mg/kg, i.p.) and pargyline (50 mg/kg, i.p.) [30]. Free base 6-OHDA was unilaterally infused through two injections of 7.5 and 6 μg performed at two coordinates, relative to the bregma and dura, with the toothbar set at −2.4 and +3.4: 2.5 μl was injected at the first coordinate, anteroposterior (AP) −4.4 mm, mediolateral (ML) +1.2 mm and dorsoventral (DV) −7.8 mm; and 2 μl was injected at a rate of 0.5 μl/min into the right nigrostriatal pathway at the second coordinate, AP −4.0 mm, ML +0.8 mm and DV −8.0 mm [31,33]. According to our established model of PD, this is a severe lesion equivalent to an advanced stage of PD [32]. Two weeks after inducing the 6-OHDA lesion, the rats were tested in an amphetamine-induced rotational behaviour test to determine the grade of the induced lesion. Only well-lesioned rats were selected for inclusion in the study (>3 turn/min).

2.8. Microsphere implantation

Four weeks after the 6-OHDA lesion was made, the rats were anesthetised by isoflurane inhalation and placed in a stereotactic frame for microsphere implantation. The rats were divided into four groups of six animals: (1) empty-MS, (2) VEGF-MS, (3) GDNF-MS and (4) VEGF + GDNF-MS. The microspheres were suspended in PBS (0.1% w/v carboxymethylcellulose, 0.8% w/v tween 80 and 0.8% w/v mannitol) before administration. Two implantation coordinates were used, relative to the bregma and dura: AP +0.5 mm, ML −2.5 mm, DV −5.0 mm and AP −0.5 mm, ML −4.2 mm, DV −5.0 mm. [23].

Each rat received 2.5 μg of either VEGF or GDNF in a volume of 20 μl or, in the combined group, each rat received a total dose of 2.5 μg of VEGF and 2.5 μg of GDNF in a volume of 40 μl in order to maintain the syringeability and injectability of the formulations. After microsphere implantation, the rats were housed in standard conditions with a constant temperature of 22 °C, a 12-h dark/light cycle and *ad libitum* access to water and food. All experimental procedures were performed in compliance with the Ethical Committee of Animal Welfare (CEBA) at the University of the Basque Country.

2.9. Behavioural study

After MS implantation, the rats were tested at 2, 4, 6, 8, 10 and 12 weeks by the amphetamine-induced rotational behaviour test, as previously described [32]. Animals were weighed throughout the study before amphetamine administration. Amphetamines were injected intraperitoneally (3 mg/kg) after 15 min of latency, and the total number of full turns in the direction ipsilateral to the lesion was counted for 90 min with an automatised rotameter (Harvard Apparatus multicounter LE3806). The results are expressed as the number of ipsilateral turns per minute.

At week 14, the rotational behaviour was tested with apomorphine to test contralateral rotation behaviour. Apomorphine, a dopaminergic agonist, was injected subcutaneously (0.5 mg/kg) after 5 min of latency, and the total number of full turns in the direction contralateral to the lesion was counted for 50 min. The results are expressed as the number of contralateral turns per 5 min.

2.10. Tyrosine hydroxylase (TH) immunohistochemistry

The rats were transcardially perfused with 0.9% NaCl and ice-cold 4% paraformaldehyde in 0.1 M PBS, pH 7.4. The brains were removed and post-fixed for 48 h in paraformaldehyde and then transferred to a 30% sucrose solution in 0.1 M PBS for cryoprotection. After 1–3 days, brains were sectioned coronally on a freezing microtome (50 μm thick) and collected in PBS containing 0.6% sodium azide for a free-floating TH immunochemistry assay. Tyrosine hydroxylase immunostaining was used to analyse the degree of dopamine denervation in the SN. For TH immunostaining, the endogenous peroxidases were first quenched using 3% H_2O_2 and 10% methanol in potassium phosphate-buffered saline (KPBS) (0.02 M, pH 7.1) for 30 min at room temperature. The brain sections were preincubated with 5% normal goat serum (NGS) and 1% Triton X-100 in KPBS (KPBS/T) for 1 h and then incubated overnight with rabbit polyclonal anti-tyrosine hydroxylase (1:1000) in 5% NGS KPBS/T at 4 °C. After rinsing twice with KPBS and once with KPBS/T, the sections were incubated for 2 h with a secondary biotinylated goat anti-rabbit IgG, which was diluted 1:200 in KPBS/T containing 2.5% NGS. All sections were processed with an avidin–biotin-peroxidase complex (Elite ABC kit, Vector Laboratories) for 1 h, and the reaction was visualised using 3,3′-diaminobenzidine as the chromogen. Finally, the brain sections were mounted, dehydrated and coverslipped with DPX mounting media.

2.11. Integrated optical densitometry (IOD)

The optical density of the substantia nigra TH + dopaminergic structures was measured using a computerised image analysis system (Mercator Image Analysis system, Explora Nova, La Rochelle, France). Fig. 4 shows the delimited area (the entire substantia nigra, SN), where the integrated optical densities were read as grey levels. Images from sections including both SN were taken with a 3200 ppp resolution digital scan (Epson). The IOD reading was corrected for background staining by subtracting the values of an area outside of the SN tissue from the obtained IOD of the SN. Optical density values for the SN on the ipsilateral side were expressed as a percentage of the contralateral non-lesioned side, which was set as 100%.

2.12. Number of neurons and neurite density

Using a stereological tool (optical dissector) provided by the previously referred to Mecator system, probes of 50 × 50 μm separated by 100 μm were launched into the previously delimited area corresponding to the entire substantia nigra (Fig. 4). Positive

cells and neurites that were present inside the probe or crossing on the right side of the *X*–*Y* axis were counted. A minimum of three histological sections per animal and four animals from each experimental group were used. Measurements from each slice were taken, and the mean value per animal was calculated.

2.13. Statistical analysis

Statistical analyses were performed with GraphPad Prism 5. A one-way ANOVA and a post hoc test were used in multiple comparisons. The normal distribution of samples was assessed by the Shapiro–Wilk test, and the homogenity of variance was determined by the Levene test. In the behavioural studies, the Bonferroni post hoc test was applied, and in the histological analyses, intergroup comparisons were assessed for significance using Tamhane post hoc analyses. Values were considered statistically significant when $p < 0.05$.

3. Results

3.1. Microsphere characterisation

The mean particle size of the microspheres was 16.81 ± 0.01 μm for VEGF-MS, 20.08 ± 0.07 μm for GDNF-MS and 17.95 ± 0.01 μm for empty-MS. When observed using scanning electron microscopy (SEM), the microspheres appeared spherical with small pores on the surface (Fig. 1A). These pores were produced by the addition of PEG 400 during microsphere preparation with the aim of achieving a suitable release profile. The EE was 54.14% for VEGF-MS and was slightly lower for GDNF-MS (31.64%). However, in contrast to the difference in EE values, both formulations had similar percentages of surface-associated proteins (approximately 10%) and similar zeta potential values. Table 1 shows the characteristics of the microsphere formulations we prepared.

3.2. In vitro microsphere release study

Fig. 1B shows the release profiles of VEGF and GDNF from the PLGA microspheres. Both formulations had a similar release profile, with an initial burst in the first 24 h and a second constant release rate continuing until the end of the assay. In the first 24 h, 19% of the encapsulated VEGF was released. Between days 2 and 4, VEGF was released at a rate of 3 ng/day/mg from the microspheres. From day 4 until the end of the study, a mean constant release rate of 600 pg/day/mg was observed. Regarding to GDNF, the release of this factor from the microspheres showed a similar profile. In the first day, 19.88% of the encapsulated factor was released. Between days 2 and 4, 5 ng/day/mg and from day 4 until the day 31, a release rate of 800 pg/day/mg was observed.

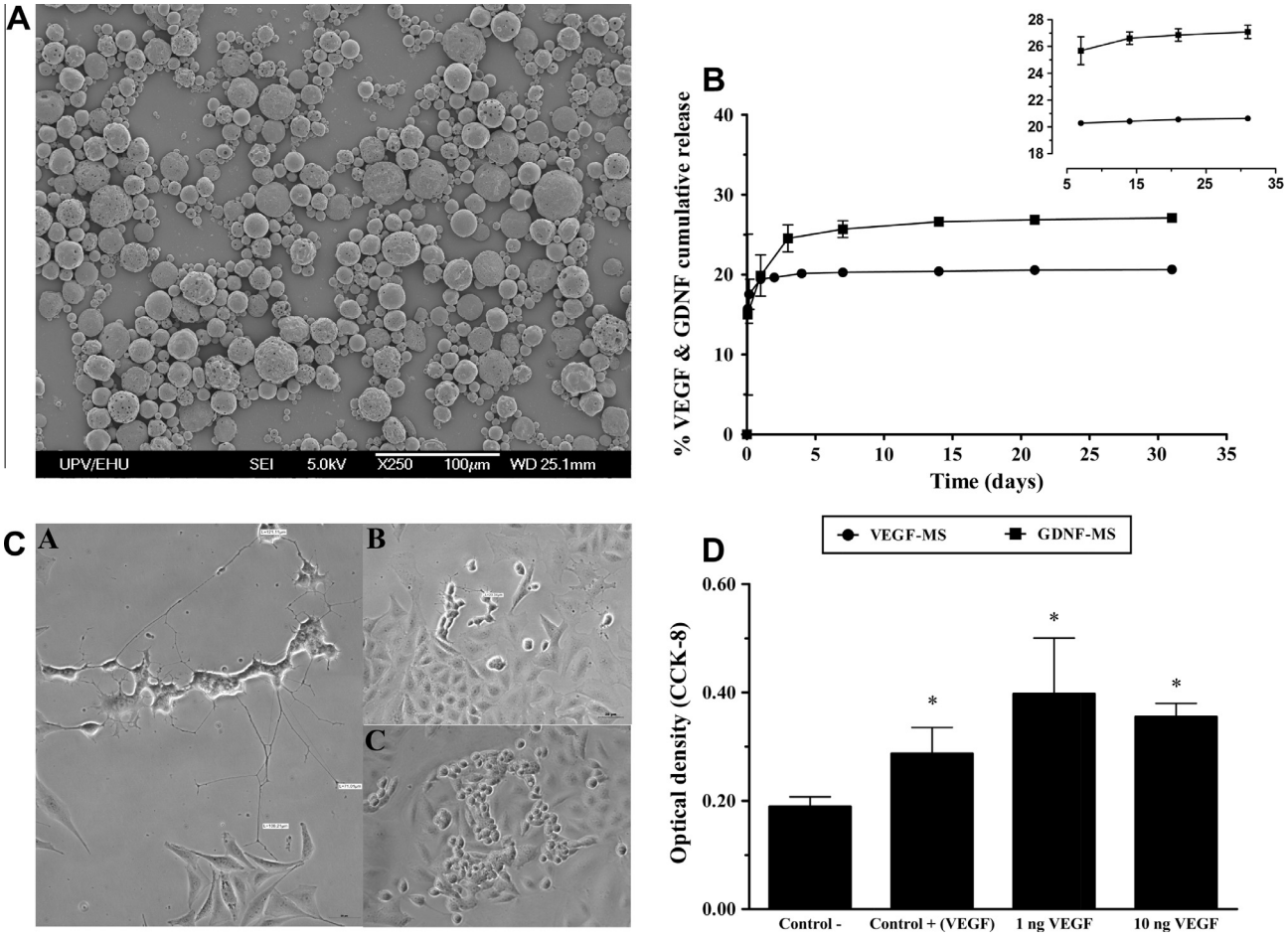

Fig. 1. (A) SEM photomicrograph of the PLGA-MS. The microspheres appear spherical, with small pores on the surface. (B) The *in vitro* GDNF-MS and VEGF-MS release profiles at 37 °C in PBS buffer (pH 7.4). The data are shown as the mean ± SD ($n = 3$). (C) The neurite outgrowth of PC12 cells. (A) GDNF-MS-released medium (25 ng/ml). (B) Empty-MS-released medium. (C) PC12 culture medium. The addition of 25 ng/ml of released GDNF generated high neurite outgrowth. In contrast, groups treated with empty-MS or with culture medium showed no evidence of neurite outgrowth. (D) The viability evaluation of the HUVEC cell line. Treatment with both 1 and 10 ng/ml of VEGF resulted in a significant increase in the proliferation of HUVEC cells with respect to the control ($p < 0.05$, one-way ANOVA). The data are shown as the mean ± SD.

Table 1
Microspheres characterisation. One batch was prepared for each peptide.

Formulation	Size (μm)	Zeta potential (mV)[a]	Encapsulation efficiency (E.E. %)[a]	Surface adsorbed peptide (S.A.P. %)[a]
Empty-MS	17.95 (95% 1.46–33.7)	(−) 15.9 ± 0.25	–	–
VEGF-MS	16.81 (95% 1.21–27.3)	(−) 15.35 ± 0.75	54.14 ± 0.83	10.4 ± 0.84
GDNF-MS	20.08 (95% 1.52–28.5)	(−) 13.05 ± 0.01	31.64 ± 5.93	10.91 ± 1.09

[a] Each batch was measured in triplicate, and results were expressed as mean ± SD.

3.3. VEGF and GDNF bioactivity assays

To confirm the biological activity of VEGF and GDNF after their microencapsulation, bioactivity assays were performed in HUVEC and PC12 cell lines, respectively.

Two different concentrations of VEGF released from MS, a VEGF solution (non-encapsulated) and the empty-MS release medium were added to HUVEC cell cultures. Fig. 1D shows that after 3 days of contact with the VEGF released from MS, cell proliferation increased. No differences were observed among the three VEGF-treated groups (VEGF solution, 1 ng/ml and 10 ng/ml of released VEGF). However, significant differences (one-way ANOVA, $p < 0.05$) were observed when the VEGF groups were compared to the control group (empty-MS-released medium).

When studying GDNF bioactivity, a high neurite outgrowth was observed after adding 25 ng/ml of the GDNF released from MSs to the PC12 cell cultures (Fig. 1C). The images in Fig. 1C illustrate that no neurite outgrowth was detected in the groups treated with either empty-MS-released medium or basic culture medium.

3.4. Behavioural study

The *in vivo* functionality of encapsulated factors was proved with the amphetamine-induced rotation test. For this purpose, the animals were divided into four experimental groups: (1) empty-MS, (2) VEGF-MS, (3) GDNF-MS and (4) VEGF + GDNF-MS.

All of the rats included in the study gained weight and presented no differences in weight gain between the experimental groups at any time point ($p > 0.05$).

As illustrated in Fig. 2A, there were no differences in the basal number of rotations between the groups. The evolution in time of the mean number of amphetamine-induced rotations of the control group (empty-MS) showed a tendency to increase from 5.29 ± 1.37 ipsilateral tpm at 0 week to 12.82 ± 0.96 tpm at 12 weeks. Conversely, after GDNF-MS implantation, the number of rotations started to decline at week 4, but the differences between this group and the empty-MS treated group were statistically significant (one-way ANOVA, $p < 0.05$) only at 10 weeks (empty-MS: 14.84 ± 1.399 tpm; GDNF: 5.45 ± 2.50 tpm) and 12 weeks (empty-MS: 12.82 ± 1.45 tpm; GDNF-MS: 3.45 ± 2.33 tpm) after implantation.

VEGF-MS administration resulted in lower levels of ipsilateral rotations than those observed for empty-MS (empty-MS: 14.84 ± 1.399 tpm; VEGF-MS: 7.78 ± 1.96 tpm) at week 10. In this group, the number of rotations decreased beginning in week 8, although the decrease was not significant.

The tendency of the combined group treated with both VEGF-MS and GDNF-MS (empty-MS: 12.82 ± 1.45 tpm; VEGF + GDNF-MS: 6.37 ± 1.15 tpm) at week 12 (not statistically significant) was similar to that of the GDNF-MS-treated group. The number of rotations began to decline in week 6, but the results were not as pronounced as those obtained with the dose of GDNF-MS administered alone.

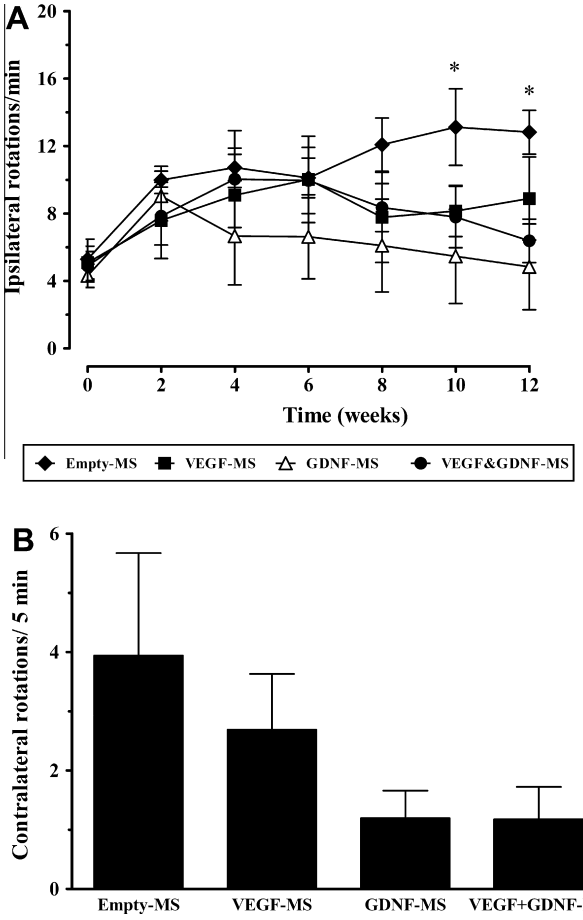

Fig. 2. (A) This graphic illustrates the data obtained from the amphetamine rotational behaviour test after MS implantation after 12 weeks: black triangle: empty-MS; black square: VEGF-MS; open triangle: GDNF-MS; black circle: VEGF + GDNF-MS. The empty-MS and GDNF-MS showed statistically significant differences ($p < 0.05$, one-way ANOVA). (B) The results obtained from the apomorphine rotational behaviour test 14 weeks after implantation. The VEGF + GDNF-MS-treated group shows the best recovery of the damaged area. The data are shown as the mean ± SD ($n = 6$).

To confirm the results obtained with amphetamine, rats were subjected to the apomorphine-induced rotational behaviour test at week 14. While no statistically significant differences were observed in the number of rotations induced by apomorphine, a tendency was noted that confirms the results obtained in the previous rotational behaviour test (Fig. 2B). Therefore, Fig. 2B shows that the empty-MS-treated group had the highest level of neuronal damage after 3 months of treatment due to its high number of contralateral rotations. The GDNF-MS- and VEGF + GDNF-MS-treated groups had the best results with respect to damage area recovery, displaying fewer contralateral rotations (empty-MS: 3.94 ± 1.73 t/5 min; VEGF-MS: 2.69 ± 0.94 t/5 min; GDNF-MS: 1.19 ± 0.46 t/5 min; VEGF + GDNF-MS: 1.17 ± 0.55 t/5 min).

3.5. Immunohistochemical analysis

The TH immunostaining was quantified by measuring the integrated optical density (IOD), the positive neuronal density (ND) and the positive fibre density (FD) by stereology.

Twelve weeks after MS implantation, sections were analysed by TH-immunohistochemistry to examine the presence of dopaminergic structures in the SN.

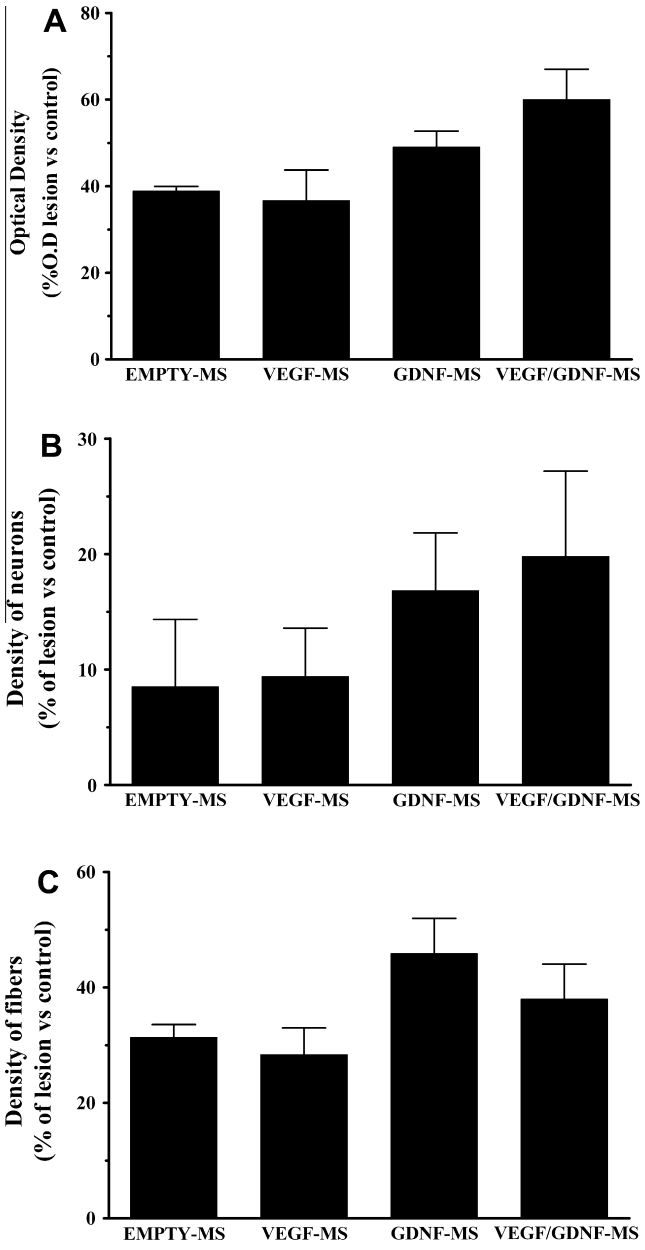

Fig. 3. (A) The optical density (OD) of Th + fibres in the lesioned hemisphere compared to the non-lesioned hemisphere. The OD in the VEGF + GDNF-MS group was greater than that of the remainder of the groups. The results are expressed as a percentage of the intact hemisphere compared to the lesioned side. (B) The density of dopaminergic neurons is expressed as a percentage of the events of the lesioned hemisphere compared to the intact side. The VEGF + GDNF-MS group increased the density of dopaminergic neurons. (C) The density of TH + fibres is expressed as a percentage of the intersections of fibres with the random grid launched inside the delimited SN, and the lesioned hemisphere is compared to the intact one. The GDNF-MS group yielded the best results. The data are shown as the mean ± SEM ($n = 6$).

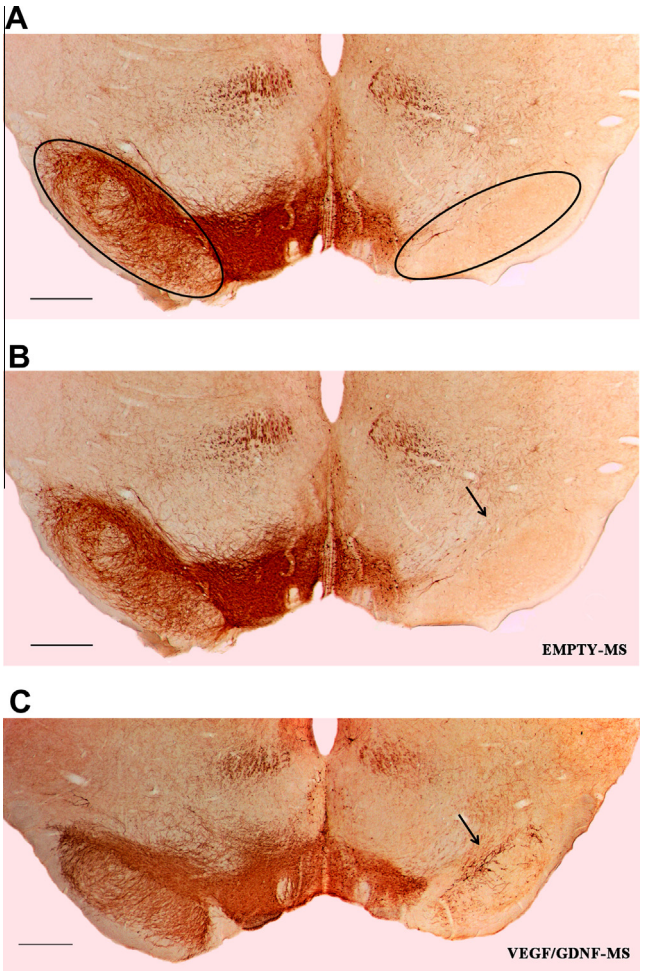

Fig. 4. (A) Photomicrographs showing the extensive loss of TH + cells in the SN (encircled by lines) ipsilateral to the 6-OHDA lesion. All of the 6-OHDA-lesioned rats showed >95% reduction in the optical density of the TH fibre in the lesioned side. The left side corresponds to the intact hemisphere, and the right side corresponds to the lesioned hemisphere. (B) A representative picture of the SN after TH immunostaining of a control rat implanted with empty-MS and VEGF + GDNF-MS. The black arrow points to the SN of the lesioned hemisphere where VEGF + GDNF-MS administration increased regeneration. (For interpretation of the references to colour in this figure legend, the reader is referred to the web version of this article.)

Although the three sets of measured values display no statistically significant differences, a consistent tendency of differences between the sets was observed.

The integrated optical density of the delimited SN in the lesioned hemisphere was compared with that of the non-lesioned area. Fig. 3A shows the percentage of remaining positivity in the ipsilateral hemisphere compared to the non-lesioned half. The optical density in the group receiving both VEGF-MS and GDNF-MS was greater than that of the other groups ($p = 0.06$), suggesting that the combined treatment improved the recovery of TH + structures better than the treatments with only one of the growth factors did (empty-MS: 38.87 ± 1.08; VEGF-MS: 36.68 ± 7.05; GDNF-MS: 49.07 ± 3.67; VEGF + GDNF-MS: 60.01 ± 7.01).

A stereological study showed that the loaded microspheres increased the density of dopaminergic neurons (Fig. 3B). The VEGF + GDNF-MS group showed a 19.79 ± 7.37% increase in the lesioned side with respect to the contralateral side; the empty-MS, VEGF-MS and GDNF-MS groups showed 8.51 ± 5.82%, 9.39 ± 4.18% and 18.83 ± 4.98% increases, respectively.

The density of TH + fibres was strongly reduced in each group after the lesion was made (Fig. 3C). The group given GDNF-MS showed the highest density improvement values (45.85 ± 6.11%). The empty-MS, VEGF-MS and VEGF + GDNF-MS groups showed 31.33 ± 2.23%, 28.36 ± 4.61% and 37.97 ± 6.062% density increases, respectively, in the lesioned side when compared to the contralateral half.

Fig. 4 shows a clear trend of improved recovery of the lesion in the group receiving the combined therapy (VEGF + GDNF-MS) compared to the control group. The black arrow indicates the location of observed neuroregeneration.

4. Discussion

PD is one of the most common progressive neurodegenerative disorders and is characterised by the continuous degeneration of the nigrostriatal dopaminergic pathway. Current therapies in the treatment of PD are not effective long term. Thus, current research focuses on novel neuroprotective and neuroregenerative strategies [6,34]. One of these strategies is the encapsulation of neurotrophic factors such as GDNF and VEGF in biodegradable microspheres. This strategy makes possible the administration of treatments by stereotaxy into the brain, achieving a continuous drug release over time and allowing the simultaneous administration of different trophic factors [23,24].

In the present work, we aimed to address this important issue by designing a novel combined therapy of VEGF and GDNF factors formulated in PLGA microspheres. In this way, we tested whether the joint administration of both factors improves upon the results obtained separately.

To raise this challenge, we designed PLGA microspheres containing either GDNF or VEGF. The local administration of these polymeric microspheres has been found to reduce the possibility of dose dumping, decrease the frequency of drug administration and improve overall systemic effects [35]. Our designed microspheres had spherical shapes with particle sizes of 16–20 μm. In our *in vitro* MS release study, the biphasic delivery pattern was considered suitable to obtain the desired effect. The initial burst release of a significant amount of the encapsulated factor could help to manage the tissue injury caused by the invasive administration process. However, the constant release profile observed over time may play a key role in restoring the lesion caused by the 6-OHDA injection.

The microencapsulation process may lead to modifications of the growth factors that could cause the loss of activity. Thus, VEGF and GDNF bioactivity was tested in cell cultures after the factors underwent encapsulation. The VEGF-MS release medium was added to HUVEC cells, and after 3 days, the cell proliferation was found to be increased (Fig. 1D). In addition, the GDNF-MS release medium was added to PC12 cells, and after 7 days in culture, a high neurite outgrowth was observed (Fig. 1C). The PC12 cell line differentiates to a neuronal phenotype in the presence of neurotrophic factors such a NGF [36,37] and GDNF [29], a change that can be detected when the cells begin to extend their neurites. These results suggest that both VEGF and GDNF maintained their biological activity through the microencapsulation process.

As mentioned above, recent *in vivo* studies have clearly shown that both VEGF and GDNF are able to restore the damaged areas induced in different animal models of PD. However, their possible synergistic effects have not been evaluated in the current literature. Thus, our goal was to investigate the neuroregenerative effects of VEGF and GDNF microencapsulated into PLGA microparticles that were injected into a severely lesioned rat model of PD [26] and to determine whether the combination of these factors led to synergic effects.

The results of the amphetamine-induced rotation test showed statistically significant differences between the GDNF-MS and empty-MS groups ($p < 0.05$), but no differences ($p > 0.05$) occurred between the empty-MS and VEGF + GDNF-MS groups (Fig. 2A). This finding was unexpected, and it suggests that the greater microsphere volume received by the VEGF + GDNF-MS group could complicate the recovery of the damage area.

Other research groups have previously shown the abilities of GDNF and VEGF to improve 6-OHDA-damaged areas [23,38]. However, it is worth mentioning that these studies used partially lesioned animal models instead of the complete lesions made in the present experiment, which are significantly more difficult to restore. Our research group has shown in previous studies that recovery of the damaged area in this animal model is possible [12]. The results obtained in this behavioural study show that GDNF-MS and VEGF + GDNF-MS are promising treatments for an advanced state of PD.

It is interesting to note that the experimental data obtained in the amphetamine test could not be confirmed by the apomorphine-induced rotational behaviour test (Fig. 2B). However, a tendency was observed that was not statistically significant. This lack of significance may be a result of the severity of the model we used, and it suggests that the regeneration that had occurred was not sufficient to alter the results of the apomorphine test [12]. From the data obtained from an immunohistochemical analysis (Figs. 3 and 4), we determined that the association of VEGF and GDNF is more suitable for neuroregeneration. However, the administration of GDNF alone was better for neuroplasticity because the combined administration of both factors inverted the improvement trend. These results may be explained by the larger microsphere volume received by the combined group. Another possible explanation is the concurrent competition of both factors for their main receptors. The crosstalk between these cytokines has been described for the kidney and hypothesised for other organs such as the brain [39]. However, the primary role of VEGF in the neuroplasticity of the hippocampus rather than in influencing the number of neurons has been recently postulated [40].

The mild evidences of lesion recovery found in this paper require greater support, which can be obtained by performing this study in a partial PD model in which the plasticity potential is better conserved.

5. Conclusion

In the present study, both GDNF alone and the combination of GDNF and VEGF microencapsulated into polymeric microsphere demonstrated regenerative effects of in a severely lesioned rat model of PD. Although these results are promising, the volume of microsphere administration and the doses of VEGF and GDNF should be adjusted in the combined group to achieve better results. Such an adjustment would reduce the tissue damage caused during injection and improve the competition of these factors for their receptors.

Acknowledgements

This Project was partially supported by the "Ministerio de Ciencia e Innovación" (SAF2010-20375), the University of the Basque Country (UPV/EHU) (UFI 11/32), the Basque Government (Saiotek SA-2010/00028) and FEDER funds. The authors thank SGIker (UPV/EHU, MICINN, GV/EJ, ESF) for their collaboration. E. Herran thanks the Basque Government for a fellowship grant, and A. Aristieta thanks UPV/EHU for a fellowship grant. We also thank Dr. Ainhoa Murua for her expert comments.

References

[1] R.L. Nussbaum, Alzheimer's disease and Parkinson's disease, The New England Journal of Medicine 348 (2003) 1356–1364.
[2] L. Aron, R. Klein, Repairing the Parkinsonian brain with neurotrophic factors, Trends in Neurosciences 34 (2011) 88–100.
[3] G. Linazasoro, A global view of Parkinson's disease pathogenesis: implications for natural history and neuroprotection, Parkinsonism & Related Disorders 15 (2009) 401–405.
[4] T. Deierborg, D. Soulet, L. Roybon, V. Hall, P. Brundin, Emerging restorative treatments for Parkinson's disease, Progress in Neurobiology 85 (2008) 407–432.
[5] G.J. Siegel, N.B. Chauhan, Neurotrophic factors in Alzheimer's and Parkinson's disease brain, Brain Research Reviews 33 (2000) 199–227.
[6] A.M. Sullivan, A. Toulouse, Neurotrophic factors for the treatment of Parkinson's disease, Cytokine & Growth Factor Reviews 22 (2011) 157–165.

[7] B. Jakobsen, J.B. Gramsbergen, A. Moller Dall, C. Rosenblad, J. Zimmer, Characterization of organotypic ventral mesencephalic cultures from embryonic mice and protection against MPP toxicity by GDNF, European Journal of Neuroscience 21 (2005) 2939–2948.
[8] X. Zeng, J. Chen, X. Deng, Y. Liu, M.S. Rao, J.L. Cadet, W.J. Freed, An in vitro model of human dopaminergic neurons derived from embryonic stem cells: MPP+ toxicity and GDNF neuroprotection, Neuropsychopharmacology 31 (2006) 2708–2715.
[9] O. Lindvall, L.U. Wahlberg, Encapsulated cell biodelivery of GDNF: a novel clinical strategy for neuroprotection and neuroregeneration in Parkinson's disease?, Experimental Neurology 209 (2008) 82–88
[10] T. Shingo, I. Date, H. Yoshida, T. Ohmoto, Neuroprotective and restorative effects of intrastriatal grafting of encapsulated GDNF-producing cells in a rat model of Parkinson's disease, Journal of Neuroscience Research 69 (2002) 946–954.
[11] A. Sajadi, J. Bensadoun, B.L. Schneider, C. Lo Bianco, P. Aebischer, Transient striatal delivery of GDNF via encapsulated cells leads to sustained behavioral improvement in a bilateral model of Parkinson disease, Neurobiology of Diseases 22 (2006) 119–129.
[12] L. Grandoso, S. Ponce, I. Manuel, A. Arrúe, J.A. Ruiz-Ortega, I. Ulibarri, G. Orive, R.M. Hernández, A. Rodríguez, R. Rodríguez-Puertas, M. Zumárraga, G. Linazasoro, J.L. Pedraz, L. Ugedo, Long-term survival of encapsulated GDNF secreting cells implanted within the striatum of Parkinsonized rats, International Journal of Pharmaceutics 343 (2007) 69–78.
[13] J.G. Nutt, K.J. Burchiel, C.L. Comella, J. Jankovic, A.E. Lang, E.R. Laws Jr., A.M. Lozano, R.D. Penn, R.K. Simpson Jr., M. Stacy, G.F. Wooten, ICV GDNF Study Group. Implanted intracerebroventricular. Glial cell line-derived neurotrophic factor, randomized, double-blind trial of glial cell line-derived neurotrophic factor (GDNF) in PD, Neurology 60 (2003) 69–73.
[14] J.T. Slevin, D.M. Gash, C.D. Smith, G.A. Gerhardt, R. Kryscio, H. Chebrolu, A. Walton, R. Wagner, A.B. Young, Unilateral intraputamenal glial cell line-derived neurotrophic factor in patients with Parkinson disease: response to 1 year of treatment and 1 year of withdrawal, Journal of Neurosurgery 106 (2007) 614–620.
[15] A.E. Lang, S. Gill, N.K. Patel, A. Lozano, J.G. Nutt, R. Penn, D.J. Brooks, G. Hotton, E. Moro, P. Heywood, M.A. Brodsky, K. Burchiel, P. Kelly, A. Dalvi, B. Scott, M. Stacy, D. Turner, V.G. Wooten, W.J. Elias, E.R. Laws, V. Dhawan, A.J. Stoessl, J. Matcham, R.J. Coffey, M. Traub, Randomized controlled trial of intraputamenal glial cell line-derived neurotrophic factor infusion in Parkinson disease, Annals of Neurology 59 (2006) 459–466.
[16] N. Ferrara, T. Davis-Smyth, The biology of vascular endothelial growth factor, Endocrine Reviews 18 (1997) 4–25.
[17] P. Carmeliet, E. Storkebaum, Vascular and neuronal effects of VEGF in the nervous system: implications for neurological disorders, Seminars in Cell & Developmental Biology 13 (2002) 39–53.
[18] M.R. Pitzer, C.E. Sortwell, B.F. Daley, S.O. McGuire, D. Marchionini, M. Fleming, T.J. Collier, Angiogenic and neurotrophic effects of vascular endothelial growth factor (VEGF165): studies of grafted and cultured embryonic ventral mesencephalic cells, Experimental Neurology 182 (2003) 435–445.
[19] W.F. Silverman, J.M. Krum, N. Mani, J.M. Rosenstein, Vascular, glial and neuronal effects of vascular endothelial growth factor in mesencephalic explant cultures, Neuroscience 90 (1999) 1529–1541.
[20] T. Yasuhara, T. Shingo, K. Kobayashi, A. Takeuchi, A. Yano, K. Muraoka, T. Matsui, Y. Miyoshi, H. Hamada, I. Date, Neuroprotective effects of vascular endothelial growth factor (VEGF) upon dopaminergic neurons in a rat model of Parkinson's disease, The European Journal of Neuroscience (2004) 1494–1504.
[21] Y. Chen, L. Liu, Modern methods for delivery of drugs across the blood–brain barrier, Advanced Drug Delivery Reviews 64 (2012) 640–665.
[22] H.L. Wong, X.Y. Wu, R. Bendayan, Nanotechnological advances for the delivery of CNS therapeutics, Advanced Drug Delivery Reviews 64 (2012) 686–700.
[23] E. Garbayo, C.N. Montero-Menei, E. Ansorena, J.L. Lanciego, M.S. Aymerich, M.J. Blanco-Prieto, Effective GDNF brain delivery using microspheres – a promising strategy for Parkinson's disease, Journal of Controlled Release 135 (2009) 119–126.
[24] C. Jollivet, A. Aubert-Pouessel, A. Clavreul, M. Venier-Julienne, S. Remy, C.N. Montero-Menei, J. Benoit, P. Menei, Striatal implantation of GDNF releasing biodegradable microspheres promotes recovery of motor function in a partial model of Parkinson's disease, Biomaterials 25 (2004) 933–942.
[25] F. Blandini, M. Armentero, Animal models of Parkinson's disease, FEBS Journal (2012). no–no.
[26] E. Marina E, Evaluation of animal models of Parkinson's disease for neuroprotective strategies, Journal of Neuroscience Methods 139 (2004) 121–143.
[27] I. Gutierro, R.M. Hernández, M. Igartua, A.R. Gascón, J.L. Pedraz, Size dependent immune response after subcutaneous, oral and intranasal administration of BSA loaded nanospheres, Vaccine 21 (2002) 67–77.
[28] S. Singh, B.M. Wu, J.C. Dunn, Delivery of VEGF using collagen-coated polycaprolactone scaffolds stimulates angiogenesis, Journal of Biomedical Materials Research A 100 (2012) 720–727.
[29] E. Garbayo, E. Ansorena, J.L. Lanciego, M.S. Aymerich, M.J. Blanco-Prieto, Purification of bioactive glycosylated recombinant glial cell line-derived neurotrophic factor, International Journal of Pharmaceutics 344 (2007) 9–15.
[30] T. Morera-Herreras, J.A. Ruiz-Ortega, G. Linazasoro, L. Ugedo, Nigrostriatal denervation changes the effect of cannabinoids on subthalamic neuronal activity in rats, Psychopharmacology (Berl) 214 (2011) 379–389.
[31] A. Aristieta, G. Azkona, A. Sagarduy, C. Miguelez, J.A. Ruiz-Ortega, R. Sanchez-Pernaute, L. Ugedo, The role of the subthalamic nucleus in L-DOPA induced dyskinesia in 6-hydroxydopamine lesioned rats, PLoS ONE 7 (2012) e42652.
[32] C. Miguelez, A. Aristieta, M.A. Cenci, L. Ugedo, The locus coeruleus is directly implicated in L-DOPA-induced dyskinesia in parkinsonian rats: an electrophysiological and behavioural study, PLoS ONE 6 (2011) e24679.
[33] G. Paxinos, C. Watson, The Rat Brain in Steretaxic Coordinates, Academic Press, San Diego, 1997.
[34] S.B. Rangasamy, K. Soderstrom, R.A.E. Bakay, J.H. Kordower, Chapter 13 – Neurotrophic factor therapy for Parkinson's disease, Progress in Brain Research 184 (2010) 237–264.
[35] T. Hickey, D. Kreutzer, D.J. Burgess, F. Moussy, In vivo evaluation of a dexamethasone/PLGA microsphere system designed to suppress the inflammatory tissue response to implantable medical devices, Journal of Biomedical Materials Research 61 (2002) 180–187.
[36] X. Cao, M.S. Schoichet, Delivering neuroactive molecules from biodegradable microspheres for application in central nervous system disorders, Biomaterials 20 (1999) 329–339.
[37] T.A. Hadlock, T. Sheahan, M.L. Cheney, J.P. Vacanti, C.A. Sundback, Biologic activity of nerve growth factor slowly released from microspheres, Journal of Reconstructive Microsurgery 19 (2003) 179–184. discussion 185-6.
[38] C. Jollivet, A. Aubert-Pouessel, A. Clavreul, M. Venier-Julienne, C.N. Montero-Menei, J. Benoit, P. Menei, Long-term effect of intra-striatal glial cell line-derived neurotrophic factor-releasing microspheres in a partial rat model of Parkinson's disease, Neuroscience Letters 356 (2004) 207–210.
[39] A. Tufro, J. Teichman, N. Banu, G. Villegas, Crosstalk between VEGF-A/VEGFR2 and GDNF/RET signaling pathways, Biochemical and Biophysical Research Communications 358 (2007) 410–416.
[40] T. Licht, I. Goshen, A. Avital, T. Kreisel, S. Zubedat, R. Eavri, M. Segal, R. Yirmiya, E. Keshet, Reversible modulations of neuronal plasticity by VEGF, Proceedings of the National Academy of Sciences of the United States of America 108 (2011) 5081–5086.

International Journal of Nanomedicine

Dovepress
open access to scientific and medical research

Open Access Full Text Article

ORIGINAL RESEARCH

Increased antiparkinson efficacy of the combined administration of VEGF- and GDNF-loaded nanospheres in a partial lesion model of Parkinson's disease

This article was published in the following Dove Press journal:
International Journal of Nanomedicine
27 May 2014
Number of times this article has been viewed

Enara Herrán[1,2]
Catalina Requejo[3]
Jose Angel Ruiz-Ortega[4]
Asier Aristieta[4]
Manoli Igartua[1,2]
Harkaitz Bengoetxea[3]
Luisa Ugedo[4]
Jose Luis Pedraz[1,2]
Jose Vicente Lafuente[3]
Rosa Maria Hernández[1,2]

[1]NanoBioCel Group, Laboratory of Pharmaceutics, University of the Basque Country (UPV/EHU), School of Pharmacy, Vitoria, Spain; [2]Biomedical Research Networking Center in Bioengineering, Biomaterials and Nanomedicine (CIBER-BBN), Vitoria, Spain; [3]LaNCE, Department of Neurosciences, University of the Basque Country (UPV/EHU), Leioa, Spain; [4]Department of Pharmacology, University of the Basque Country (UPV/EHU), Leioa, Spain

Abstract: Current research efforts are focused on the application of growth factors, such as glial cell line-derived neurotrophic factor (GDNF) and vascular endothelial growth factor (VEGF), as neuroregenerative approaches that will prevent the neurodegenerative process in Parkinson's disease. Continuing a previous work published by our research group, and with the aim to overcome different limitations related to growth factor administration, VEGF and GDNF were encapsulated in poly(lactic-co-glycolic acid) nanospheres (NS). This strategy facilitates the combined administration of the VEGF and GDNF into the brain of 6-hydroxydopamine (6-OHDA) partially lesioned rats, resulting in a continuous and simultaneous drug release. The NS particle size was about 200 nm and the simultaneous addition of VEGF NS and GDNF NS resulted in significant protection of the PC-12 cell line against 6-OHDA in vitro. Once the poly(lactic-co-glycolic acid) NS were implanted into the striatum of 6-OHDA partially lesioned rats, the amphetamine rotation behavior test was carried out over 10 weeks, in order to check for in vivo efficacy. The results showed that VEGF NS and GDNF NS significantly decreased the number of amphetamine-induced rotations at the end of the study. In addition, tyrosine hydroxylase immunohistochemical analysis in the striatum and the external substantia nigra confirmed a significant enhancement of neurons in the VEGF NS and GDNF NS treatment group. The synergistic effect of VEGF NS and GDNF NS allows for a reduction of the dose by half, and may be a valuable neurogenerative/neuroreparative approach for treating Parkinson's disease.

Keywords: nanoparticles, PLGA, 6-OHDA, neuroregeneration, neurotrophic factors, tyrosine hydroxylase

Introduction

In recent years, there has been increasing interest in the struggle against neurodegenerative diseases such as Parkinson's disease (PD). PD is characterized by selective degeneration of the nigrostriatal pathway and a concomitant reduction in the striatal concentration of dopamine, giving rise to motor function impairments such as rigidity, rest tremors, bradykinesia, and postural abnormalities.[1,2]

Although PD is a major priority for health care systems, current dopamimetic therapies, such as L-dopa, focus on modifying motor symptoms without treating the neurodegenerative process and without providing neuroprotection to the surviving dopaminergic neurons.[3] Thus, current research efforts are focused on halting neurodegeneration using promising alternatives such as antioxidants, antiapoptotic agents, cell-based therapies, and neuroprotective agents.[4]

An interesting and promising approach is the use of growth factors (GFs), and specifically the subfamily of the neurotrophic factors (NTFs), which are potentially

Correspondence: Rosa Maria Hernández
NanoBioCel Group, Laboratory of Pharmaceutics, University of the Basque Country (UPV/EHU), School of Pharmacy, Paseo de la Universidad 7, 01006, Vitoria, Spain
Tel +34 945 013 095
Fax +34 945 013 040
Email rosa.hernandez@ehu.es

submit your manuscript | www.dovepress.com
Dovepress
http://dx.doi.org/10.2147/IJN.S61940

major players in therapeutic interventions for neurodegenerative disorders such as PD.[5] NTFs represent one of the most important challenges in the treatment of neurodegenerative diseases due to their roles in the survival and phenotypic differentiation of developing neurons, as well as maintenance and protection of mature and injured neurons.[4,6]

According to the scientific literature, and fueled by the positive results obtained in a previous study published by our group,[7] we decided to continue with the application of NTFs in future works, and, in particular, with the promising combination of glial cell line-derived neurotrophic factor (GDNF) and vascular endothelial growth factor (VEGF). GDNF is a potent factor that is able to act in vitro and in vivo, promoting the survival and differentiation of dopaminergic neurons and protecting these cells from dopaminergic toxins.[8–12] Several clinical trials have been conducted to analyze the potential of GDNF in PD patients; however, in all these studies, intracerebroventricularly or intraputaminally administered GDNF solution presented numerous negative side effects and no significant clinical improvements.[13–15] VEGF has prosurvival effects in neuronal culture and was demonstrated to be protective against 6-hydroxydopamine (6-OHDA) in a PD rat model. In the present study, we used this potent angiogenic growth factor in combination with GDNF, in order to enhance the action of the latter.[16,17]

Major problems for the clinical use of VEGF and GDNF is their rapid degradation rate, their short half-life in vivo, their difficulty in crossing the blood–brain barrier, and, consequently, the need for direct and continuous administration of the factors into the brain.[18,19] One approach that has been examined by our group,[7,20] to overcome these drawbacks is the encapsulation of VEGF and GDNF into biocompatible and biodegradable poly(lactic-co-glycolic acid) (PLGA) microspheres and nanospheres (NS). This strategy permits the intracranial administration of the formulations, allowing for a sustained drug release, with promising results obtained for PD and Alzheimer's disease recovery in preclinical studies.[7,20] The intracranial administration of GDNF-loaded PLGA microspheres has also been demonstrated by other groups to be successful in improving behavioral deficits and reversing anatomical changes.[21,22]

To appraise novel formulations in animal models of PD, various 6-OHDA lesioned rat models have been developed, in which the toxin was injected into different parts of the nigrostriatal pathway. In our previous work,[7] we used a severely lesioned rat model of PD, whereas, in this new study, subregions in the caudoputamen complex were selected as a target for the lesion. This is a partial, more selective damage of the nigrostriatal dopaminergic pathway, which appears to be a particularly effective site in which to assess regeneration accompanied by recovery of motor behavior.[23,24]

Thus, in the present work, we studied the combined potential of low doses (half that of individual treatment) of VEGF-loaded PLGA NS and GDNF-loaded PLGA NS in a partially lesioned PD rat model, with the aim of studying their synergistic effects in neuronal recovery and protection.

Materials and methods

Preparation of NS

Recombinant human VEGF (PeproTech, London, UK) and recombinant murine GDNF (Peprotech) enclosing PLGA (50:50; lactic/glycolic [%]) (Resomer® RG 503; Boehringer Ingelheim, Ingelheim, Germany) NS were prepared as previously described.[20]

Briefly, 133 mg PLGA 50:50 (previously sterilized by gamma radiation) were dissolved in 3.33 mL dichloromethane and emulsified with 200 µL of 0.15% w/v recombinant human VEGF or recombinant murine GDNF aqueous solution (containing 7% [w/v] human serum albumin and 2.5% [w/v] poly-ethylene-glycol 400) by probe sonication for 30 seconds at 50 W (Branson® Sonifier® 250, Biogen, Derio, Spain). The first emulsion was poured into 5% (w/v) polyvinyl alcohol solution and sonicated again for 1 minute, in order to obtain a double emulsion ($w_1/o/w_2$). This emulsion was poured into 2% (v/v) isopropanol solution and stirred at room temperature for 2 hours to promote the removal of the organic solvent. The newly formed NS were separated by centrifugation at 20,000× *g*, resuspended in 2.5% (w/w in respect to PLGA) trehalose aqueous solution and freeze-dried for 24 hours. The entire process of NS preparation was conducted under aseptic conditions. Empty NS (without VEGF or GDNF) were prepared using the same method described above.

Characterization of NS

The mean particle diameter, size distribution, and zeta potential were determined by the Malvern® Zetasizer Nano ZS (model Zen 3600; Malvern Instruments, Malvern, UK). Different surface characteristics of the NS were examined by scanning electron microscopy (JEOL® JSM-7000F; JEOL, Tokyo, Japan).

The encapsulation efficiencies of VEGF and GDNF were determined using a Human VEGF ELISA (enzyme-linked immunosorbent assay) Development Kit (Peprotech) and the GDNF Emax® ImmunoAssay System (Promega Corporation, Fitchburg, WI, USA) after NS disruption with dimethyl sulfoxide. To evaluate the surface-associated protein, 3 mg of NS were suspended in phosphate-buffered saline ([PBS] pH 7.4) and maintained at 37°C

for 30 minutes, under continuous orbital rotation. The resulting supernatant was collected and measured by the corresponding ELISA kit.

Finally, the release profile of VEGF and GDNF from PLGA NS was assessed. Three milligrams of NS was placed in an Eppendorf tube (containing 1 mL of PBS 20 mM [pH 7.4]) at 37°C±0.5°C and shaken with a rotator shaker at 25 rpm. At determined time intervals, the release medium was withdrawn by centrifugation (20,000× *g*, 15 minutes) and replaced with 1 mL of fresh PBS. The amount of VEGF and GDNF in the supernatants was determined by VEGF ELISA and GDNF ELISA kits. The test was carried out in triplicate, representing the obtained results as the percentage of the total amount entrapped in the NS.

Establishment of neurotoxic cell model with 6-OHDA

This assay was conducted in the PC-12 Adh cell line (American Type Culture Collection [ATCC], Manassas, VA, USA), a specific cell lineage of dopaminergic neurons. PC-12 cells were sustained in specific medium (F-12K Gibco®; Thermo Fisher Scientific, Waltham, MA, USA) supplemented with 2.5% fetal bovine serum, 15% horse serum, and 1% penicillin/streptomycin in standard conditions. The culture plates were previously coated with attachment factor (Gibco®) in order to promote the attachment of seeded cells. After 24 hours, freshly prepared 6-OHDA (Sigma-Aldrich, St Louis, MO, USA), at different concentrations (0.05 mM, 0.1 mM, and 0.2 mM), was added into the cell culture. Cell viability was examined at 16 hours after the exposure to 6-OHDA, and CCK-8 (Cell Counting Kit-8 for quantization of viable cell number in proliferation and cytotoxicity assays; Sigma-Aldrich) and 4′,6-diamidino-2-phenylindole (DAPI) immunostaining assays were conducted.

Protective effect of VEGF and GDNF on PC-12 cell cultures

Once the 6-OHDA concentration was selected, VEGF and GDNF protection assays were also conducted in the PC-12 cell line. Cells were seeded in 96-well culture plates at a density of 150×10^3 cells/well, previously treated with an attachment factor, and maintained in standard conditions for 24 hours prior to experimentation. Then, culture medium was replaced, and cells were treated for 16 hours with 6-OHDA (0.1 mM) and 5 ng/mL or 10 ng/mL of the factors released from the NS: 1) 0.1 mM 6-OHDA; 2) 0.1 mM 6-OHDA +10 ng/mL of VEGF; 3) 0.1 mM 6-OHDA +10 ng/mL of GDNF; 4) 0.1 mM 6-OHDA +10 ng/mL VEGF +10 ng/mL GDNF; 5) 0.1 mM 6-OHDA +5 ng/mL VEGF +5 ng/mL GDNF. The bioactivity of the samples was evaluated by measuring cell proliferation by adding 10 µL of CCK-8 to each well.

Animals and 6-OHDA lesion

Thirty minutes before the surgery, male albino Sprague Dawley (150–175 g) rats were pretreated with desipramine (25 mg/kg, intraperitoneally [ip]; Sigma-Aldrich) and pargyline (50 mg/kg, ip; Sigma-Aldrich), to protect noradrenergic terminals and to inhibit monoamine oxidase activity, respectively.[23]

Then, rats were deeply anesthetized with isoflurane (1.5%–2%; Esteve Química, Barcelona, Spain) and placed on a Kopf stereotaxic instrument (David Kopf Instruments, Tujunga, CA, USA). 6-OHDA was unilaterally infused in the right striatum through three different injections. Seven point five micrograms of 6-OHDA were injected in each coordinate: anteroposterior (AP) +1.3 mm, mediolateral (ML) +2.8 mm, and dorsoventral (DV) –4.5 mm; AP –0.2 mm, ML +3.0 mm, and DV –5.0 mm; AP –0.6 mm, ML +4.0 mm, and DV –5.5 mm, relative to bregma and dura with the tooth bar set at –2.4. Taking into account the protocol, this lesion produces a partial degeneration (or parkinsonism).[22]

Two weeks after the 6-OHDA surgery, the rotational behavior was tested with amphetamine administration as a marker of dopaminergic degeneration. Only the rats that rotated more than three full turns/minute were included in this study.

NS implantation surgery

NS were implanted 3 weeks after the 6-OHDA injection. Rats were anesthetized with isoflurane (1.5%–2%; Esteve Química) and mounted on a Kopf stereotaxic instrument for NS implantation. Five different groups of animals were used (six to eight rats per group): 1) vehicle; 2) empty-NS; 3) VEGF NS (2.5 µg VEGF); 4) GDNF NS (2.5 µg GDNF); and 5) VEGF NS and GDNF NS (1.25 µg VEGF and 1.25 µg GDNF). The NS were suspended in 15 µL of PBS (0.1% w/v carboxymethyl cellulose, 0.8% w/v Tween 80 [Sigma-Aldrich] and 0.8% w/v mannitol) before administration.

The NS were implanted in the right striatum in three different coordinates: AP +1.3 mm, ML +2.8 mm, and DV –4.5 mm; AP –0.2 mm, ML +3.0 mm, and DV –5.0 mm; AP –0.6 mm, ML +4.0 mm, and DV –5.5 mm, relative to bregma and dura with the tooth bar set at –2.4.

To carry out this in vivo assay, the rats were housed in usual conditions with a invariable temperature of 22°C, a 12-hour dark/light cycle and ad libitum access to water and food. All experimental methods were carried out in agreement

with the Ethical Committee of Animal Welfare (CEBA) at the University of the Basque Country, Leioa, Spain (CEBA/154/2010//RUIZ ORTEGA).

Behavioral study

Amphetamine-induced turning behavior tests were developed 2, 4, 6, 8, and 10 weeks after the NS implantation, as previously described.[24]

Before each behavioral session, animals were weighed and amphetamine (5 mg/kg) was intraperitoneally administrated. After 15 minutes of latency, the full ipsilateral rotations were counted for 90 minutes with an automatized rotameter (multicounter LE3806; Harvard Apparatus, Holliston, MA, USA). Data were expressed as the number of full turns per minute.

Fourteen weeks after NS implantation, apomorphine-induced rotational behavior was tested. The apomorphine (a dopaminergic agonist) was used as a dopamine (DA) degeneration indicator because it induces contralateral turning behavior after dopaminergic denervation. Thus, before each behavioral session, animals were weighed and apomorphine (0.5 mg/kg) was subcutaneously administrated. After 5 minutes of latency, the full contralateral rotations were measured for 50 minutes with an automatized rotameter (Harvard Apparatus multicounter LE3806). Data were expressed as the number of full turns per 5 minutes.

Figure 1 shows a schematic illustration of the experimental design for the treatments in 6-OHDA lesioned rats.

Tyrosine hydroxylase (TH) immunohistochemistry

Animals underwent transcardial perfusion with saline solution and 4% paraformaldehyde in 0.1 M PBS, pH 7.4. Brains were removed and postfixed for 48 hours in the same fixative solution and then cryopreserved in 30% sucrose diluted in 0.1 M PBS. Three days after, brains were sectioned on a freezing microtome (52 μm thick) and coronal slices collected in PBS containing 0.6% sodium azide. TH immunochemistry assay was performed in free-floating slices and used to evaluate dopamine loss in basal ganglia and substantia nigra (SN). For TH immunostaining, we neutralized endogenous peroxidases with a solution of 3% H_2O_2, 10% methanol in potassium PBS (KPBS) (0.02 M, pH 7.1) for 30 minutes at room temperature. Cerebral slices were preincubated with 5% normal goat serum (NGS) and 1% Triton™ X-100 (Sigma-Aldrich) in KPBS (KPBS/T) for 1 hour and then incubated overnight with rabbit polyclonal anti-TH (1:1000) in 5% NGS KPBS/T at 4°C. After rinsing twice with KPBS and once with 2.5% NGS KPBS/T, slices were incubated for 2 hours with a secondary biotinylated goat anti-rabbit immunoglobulin G (1:200 in KPBS/T containing 2.5% NGS). All slices were processed with avidin–biotin–peroxidase complex (Elite ABC kit; Vector Laboratories, Inc., Burlingame, CA, USA) for 1 hour with 3,3′-diaminobenzidine (DAB) as the chromogen. Finally, slices were mounted, dehydrated, and coverslipped with permanent mounting DPX medium (Sigma-Aldrich).

Integrated optical density (IOD)

The optical density of basal ganglia was evaluated using a computerized image analysis system (Mercator Image Analysis system; Explora Nova, La Rochelle, France). Digitalized images from coronal sections were taken with a 1,200 dpi resolution digital scanner (Epson, Suwa, Japan). The IOD reading was corrected for background staining (subtracting the values of a region outside of the tissue). For each animal, the IOD was estimated at two medial–caudal levels along the basal ganglia according to Paxinos and Watson,[25] placing a square of 900 μm^2 on the most degenerated lateral region: 1) medial striatum (bregma –0.24 mm); 2) caudal striatum

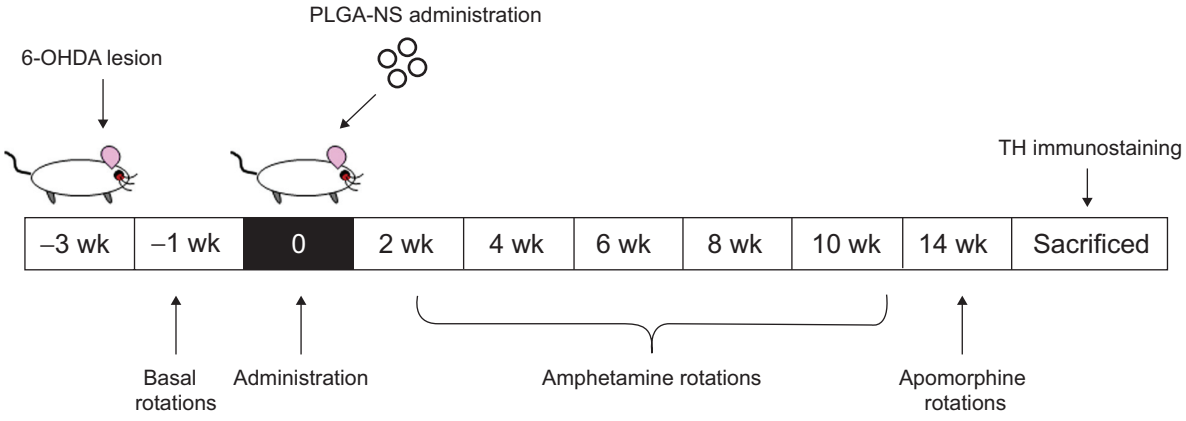

Figure 1 Experimental design for the NS treatments in 6-OHDA lesioned rats.
Abbreviations: 6-OHDA, 6-hydroxydopamine; NS, nanosphere; PLGA, poly(lactic-co-glycolic acid); TH, tyrosine hydroxylase; wk, weeks.

(bregma −0.60 mm). Optical density values are given as percentage of ipsilateral striatum versus the contralateral non-lesioned striatum, which was considered as 100%.

Number of neurons

Immunoreactive neurons were measured using a stereological tool (optical dissector) provided by the computerized image analysis system (Mercator Image Analysis system; Explora Nova, La Rochelle, France). Probes of 50×50 µm separated by 100 µm were launched into the previously delimited region belonging to the lateral region of the SN. This region is topologically related to the dorsolateral caudoputamen complex, where the 6-OHDA lesion was produced.[21,26]

Immunopositive neurons inside the probe or crossing on the right side of the X–Y axis were counted. A minimum of three histological sections per animal and five animals from each experimental group were analyzed. Density of neurons per slice and per animal were calculated.

Statistical analysis

All statistical analysis was performed with GraphPad Prism (v 5; GraphPad Software, Inc., La Jolla, CA, USA) and SPSS Statistics (v 20; IBM Corporation, Armonk, NY, USA). Prior to analysis, the Shapiro–Wilk test was used to assess normal distribution of samples, and Levene's test was used to determine the homogeneity of variance. One-way analysis of variance (ANOVA) with Tamhane's post hoc test was used to explore differences between groups. In the behavioral studies, we used Student's *t*-test to compare intergroup differences. Significance was declared when $P<0.05$.

Results

Characterization of NS

NS presented particle sizes of around 235.6±0.111 nm for VEGF NS, 221.1±0.065 nm for GDNF NS, and 267.00±0.111 nm for empty NS. The zeta potential was similar for all the formulations, around −25 mV. When visualized by scanning electron microscopy, the NS showed a spherical shape without irregularities (Figure 2). The encapsulation efficiency (EE) was 44% for VEGF NS and was higher for GDNF NS, at 74% (Figure 2A and Table 1). Both formulations had similar percentages of surface-associated protein (approximately 23%) and similar in vitro release profiles. Figure 2B shows that VEGF and GDNF released from PLGA NS presented similar release profiles, with an initial burst release of 28%±0.5% of the total loaded protein in the first 24 hours, and a second continuous release rate of 1 ng/day/mg persisting until the end of the assay.

Table 1 Characteristics of the NS

	Empty-NS	GDNF-NS	VEGF-NS
Size (nm)	267.1±0.11	221.1±0.65	235.6±0.11
Zeta potential (mV)	(–) 25.9±4.44	(–) 22.8±6.65	(–) 28.9±6.01
EE %		74.93±4.86	44.06±5.61
SAP %		22.91±6.41	23.28±8.95

Note: The results are presented as the mean ± standard deviation.
Abbreviations: EE, encapsulation efficiency; GDNF, glial cell line-derived neurotrophic factor; NS, nanospheres; SAP, surface associated protein; VEGF, vascular endothelial growth factor.

The combination of VEGF and GDNF released from PLGA NS increases cell viability against 6-OHDA

In this assay, we tested whether VEGF and GDNF released from PLGA NS were able to protect PC-12 cells from 6-OHDA toxicity. As shown in Figure 3A, when the PC-12 cell line was exposed to different 6-OHDA concentrations, the damage to cells was evident under fluorescence microscopy when 0.1 mM and 0.2 mM concentrations were added. These results have been convincingly corroborated by cell viability assay, giving rise to a selection of 0.1 mM 6-OHDA as the ideal dose with which to damage half of the cells (data not shown).

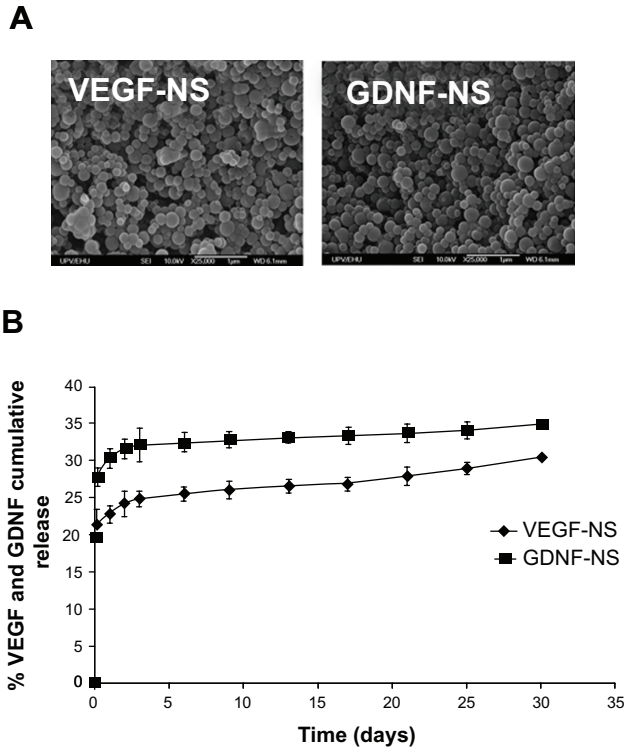

Figure 2 GDNF NS and VEGF NS characterization and in vitro toxicity study.
Notes: (**A**) Scanning electron microscope (SEM) photomicrographs of GDNF NS and VEGF NS. (**B**) The in vitro VEGF NS and GDNF NS release profiles at 37°C in phosphate-buffered saline (pH 7.4). The results are represented as the mean ± standard deviation (n=3).
Abbreviations: GDNF, glial cell line-derived neurotrophic factor; NS, nanospheres; VEGF, vascular endothelial growth factor.

Once the optimal 6-OHDA dose was selected, we found that a combined administration of reduced doses of VEGF and GDNF released from PLGA NS was able to protect dopaminergic cells from 6-OHDA-induced neurotoxicity in vitro. The incubation of PC-12 cells with VEGF (5 ng/mL) and GDNF (5 ng/mL) resulted in a 51% increase in cell viability (negative control: 0.19±0.03; VEGF 5 ng/mL and GDNF 5 ng/mL: 0.29±0.07; $P<0.001$ with respect to control group, one-way ANOVA [Figure 3B]), achieving a synergistic effect when administered together.

Behavioral study: evaluation of in vivo effects of implanted PLGA NS

In vivo functionality of nanoencapsulated VEGF and GDNF releasing PLGA NS was assessed by amphetamine-induced rotation test. Only the rats that presented more than three turns/minute after the 6-OHDA lesion were included in the study, and were divided into five experimental groups: 1) vehicle; 2) empty NS; 3) VEGF NS (2.5 µg VEGF); 4) GDNF NS (2.5 µg GDNF); and 5) VEGF NS and GDNF NS (1.25 µg VEGF and 1.25 µg GDNF). There was no obvious change in the body weight of the rats receiving the different treatments throughout the experiment (data not shown).

In the amphetamine-induced behavioral experiments, no differences were found in the initial number of rotations between groups, as shown in Figure 4A. After a unilateral 6-OHDA lesion, the animals receiving only the vehicle administration did not show significant recovery of the rotational behavior at any time (sham: 10.15±2.19 ipsilateral turns/minute at 0 weeks to 11.57±2.49 turns/minute at 10 weeks). Rats receiving empty NS, VEGF NS, and GDNF NS treatments showed a slight reduction in rotations at the end of the study (week 10). GDNF NS implantation, in particular, showed a statistical reduction in the number of rotations when compared with sham group (empty NS: 9.71±2.92 turns/minute; VEGF NS: 6.37±2.11 turns/minute; GDNF NS: 4.43±2.75 turns/minute; $P<0.05$ GDNF NS with respect to sham group, Student's *t*-test). In addition, we observed that striatal implantation of the combined VEGF NS and GDNF NS treatment at half the dose of the factors administered individually achieved the best behavioral results and significantly reduced the number of rotations (VEGF NS and GDNF NS: 0.87±0.53 turns/minute) when compared to the empty NS and sham groups ($P<0.001$ with respect to empty NS and sham groups, Student's *t*-test [Figure 4A]).

Once the amphetamine test was completed, rats were exposed to the apomorphine-induced test. The data obtained from this test confirmed the promising results obtained previously, showing statistically significant changes between the VEGF NS and GDNF NS group and sham and empty NS treatment groups ($P<0.01$ with respect to empty NS and $P<0.05$ with respect to sham group, Student's *t*-test [Figure 4B]). As can be seen from Figure 4B, the VEGF NS and GDNF NS-treated group presented the smallest number of contralateral rotations, demonstrating the highest level of behavioral recovery.

Histological evaluation of the treatments

The efficacy of the treatment was also analyzed with immunohistochemical techniques, measuring IOD of TH+ fibers of the striatum and density of dopaminergic neurons in the SN (Figure 5A).

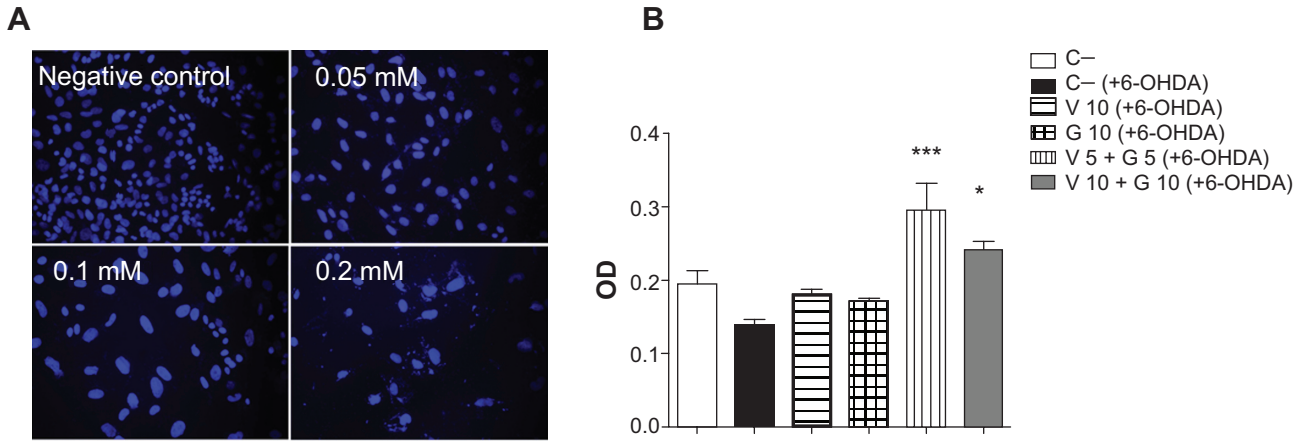

Figure 3 In vitro neurotoxicity assay.
Notes: (**A**) DAPI immunostaining after different 6-OHDA concentration treatments to establish the neurotoxic cell model. (**B**) PC-12 cell viability evaluation after 6-OHDA induced toxicity in vitro. *$P<0.05$, V 10 + G 10 (+6-OHDA) versus C–, and C– (+6-OHDA) groups. ***$P<0.001$, V 5 + G 5 (+6-OHDA) versus C–, and C– (+6-OHDA) groups.
Abbreviations: 6-OHDA, 6-hydroxydopamine; C–, negative control; DAPI, 4′,6-diamidino-2-phenylindole; G 5, GDNF 5 ng/mL; G 10, GDNF 10 ng/mL; GDNF, glial cell line-derived neurotrophic factor; OD, optical density; V 5, VEGF 5 ng/mL; V 10, VEGF 10 ng/mL; VEGF, vascular endothelial growth factor.

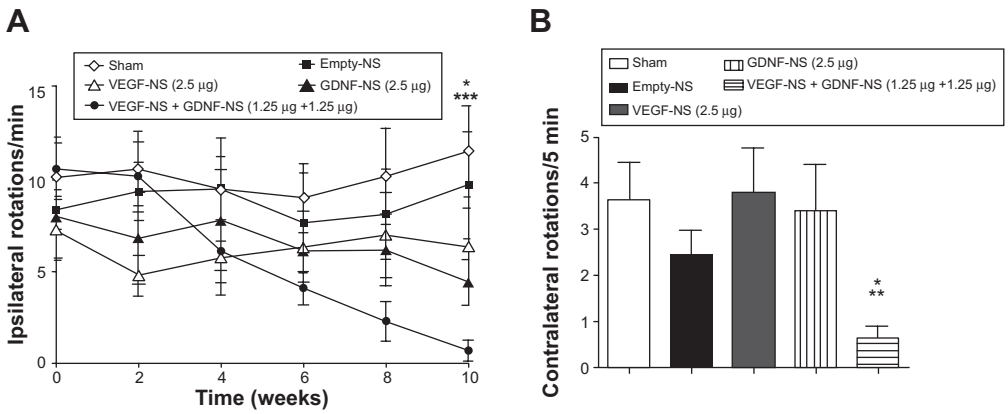

Figure 4 Behavioral study: amphetamine and apomorphine rotational tests.
Notes: (**A**) The results obtained from the amphetamine rotational behavior test after NS administration. GDNF NS group versus sham group show statistically significant differences (*$P<0.05$). The VEGF NS and GDNF NS group versus sham and empty NS groups showed statistically significant differences (***$P<0.001$). (**B**) Data obtained from the apomorphine rotational behavior test 14 weeks after NS implantation. The VEGF NS and GDNF NS-treated group exhibited the best behavioral recovery (*$P<0.05$, VEGF NS and GDNF NS versus empty NS; **$P<0.01$, VEGF NS and GDNF NS versus sham). The data are shown as the mean ± standard deviation (n=6–8).
Abbreviations: GDNF, glial cell line-derived neurotrophic factor; NS, nanospheres; VEGF, vascular endothelial growth factor.

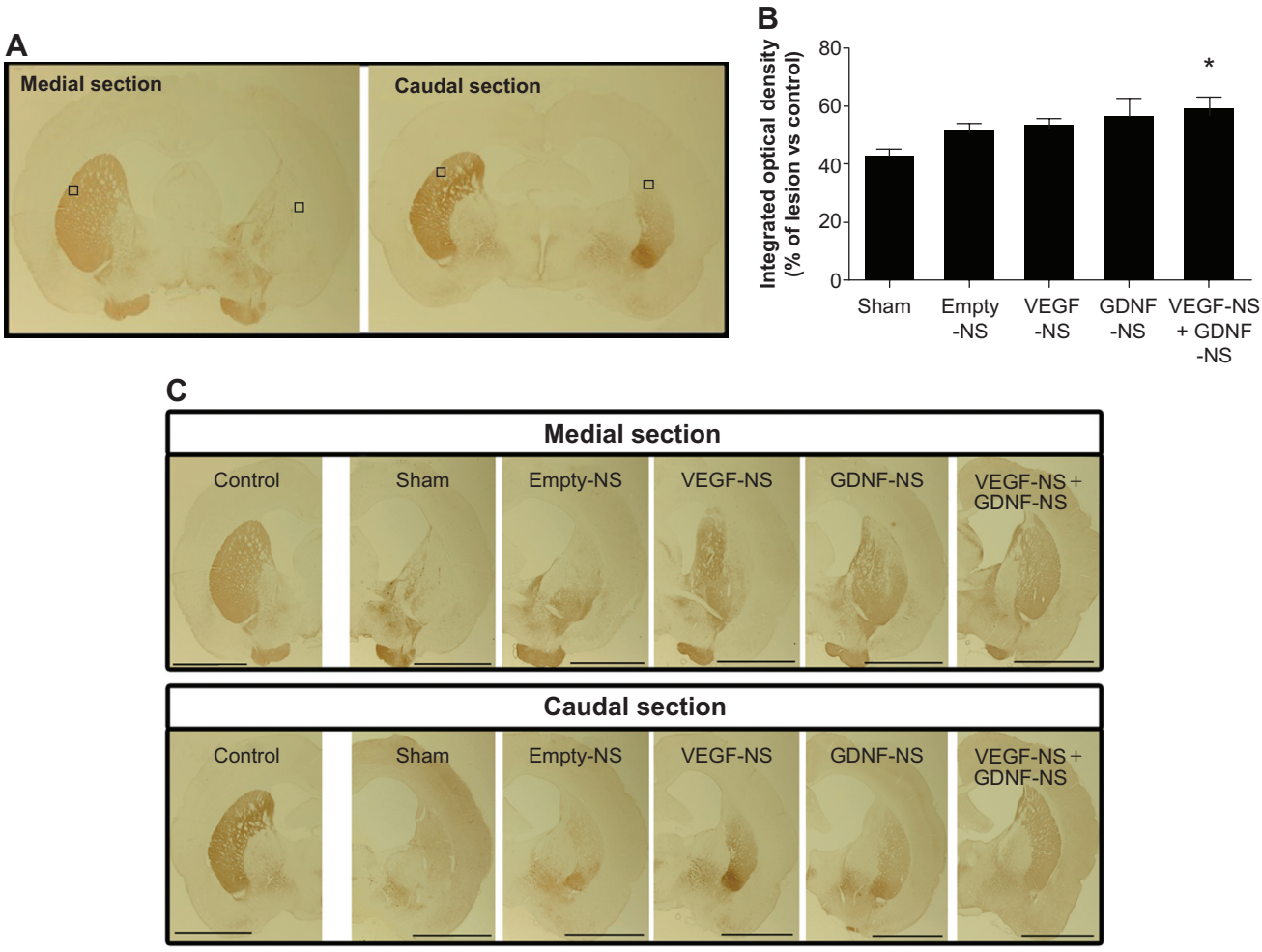

Figure 5 Histological evaluation of the treatments in the striatum.
Notes: (**A**) The images give an illustrative overview of the medial and caudal sections of the caudoputamen complex for TH immunohistochemistry. Squares placed on lesioned and non-lesioned (control) hemispheres delimit the surfaces where the integrated optical density was measured using a computerized image analysis system. Scale bar =2 mm. (**B**) The graphic shows the percentage of integrated optical density of the lesioned hemisphere with respect to the non-lesioned hemisphere (control) for each experimental group. Data are shown as the mean ± standard error of the mean (n=6–8) (*$P<0.05$ VEGF NS and GDNF NS group versus sham group). (**C**) Photomicrographs of striata immunostained for TH from a representative intact hemisphere (control) and 6-OHDA lesioned hemispheres from the different experimental groups.
Abbreviations: 6-OHDA, 6-hydroxydopamine; GDNF, glial cell line-derived neurotrophic factor; NS, nanospheres; TH, tyrosine hydroxylase; VEGF, vascular endothelial growth factor.

From the data shown in Figure 5B, we can see that, 14 weeks after NS implantation, the percentage of TH+ fibers remaining in the ipsilateral hemisphere, in comparison with the non-lesioned half, was greater in the group receiving the combined treatment. The TH+ fiber intensity of the lesioned side expressed as percentage over the control side observed in the striatal area of the VEGF NS and GDNF NS-treated group was 58%, while that of the sham group was 42%. The combined treatment enhanced the restoration of TH+ fibers and neurons to a greater extent than the treatments with only VEGF or GDNF ($P<0.05$ with respect to the sham group, one-way ANOVA [Figure 5B]). Figure 5C demonstrates enhanced restoration of the lesioned striatum in the VEGF NS and GDNF NS group.

Further evidence of this improvement was found when neuron density of the SN was analyzed. Stereological study showed changes in whole SN neuron density, demonstrating that VEGF NS and GDNF NS increased the density of dopaminergic neurons in a satisfactory way. Moreover, these changes were significantly higher among groups when the "external SN" was considered (Figure 6A and B). The results obtained from the analysis of this specific area showed a considerable increase in neuron density in the VEGF NS and GDNF NS-treated group, the neuronal density being 43% of that of the contralateral side, compared to only 11% in the sham cases ($P<0.001$ with respect to sham and empty NS groups, one-way ANOVA [Figure 6C]). This improvement can be clearly observed in the serial pictures of Figure 6D.

Discussion

Extensive work has been carried out in recent years toward PD treatments aiming at reducing or slowing down the progression of neurodegenerative processes. Concerning new treatments, GFs, and especially neurotrophic factors, offer one of the most compelling opportunities for significantly improving the treatment of this serious neurological disorder, treating both the symptoms of the disease as well as its pathogenesis.[27]

In particular, the efficacy of NTFs such as GDNF, or angiogenic factors like VEGF, in the upregulation of essential neurogenic processes makes them ideal candidates for modifying the evolution of this disorder.[4,5,28] Previous studies published by our group, as well as research conducted by numerous other laboratories,[16,29,30] has demonstrated that the administration of VEGF or GDNF improves behavioral deficits as well as decreases neuronal degeneration in different animal models of neurodegenerative disorders.[7,11,20]

Nevertheless, the essential problems for the application of these hydrophilic molecules are their short half-life and rapid degradation rate in vivo. That is why many studies focus on designing different drug delivery systems to enhance the release of these proteins into the brain tissue, either through invasive or noninvasive methods.[31,32]

Considerable attention has been paid to the improvement of PLGA nanoparticles, making the local delivery of neuroprotective agents into the brain possible. In fact, PLGA NS can preserve the encapsulated unstable therapeutic drug from enzyme degradation, release the drug in a controlled and continuous manner, enhance its biodistribution, and permit drug targeting. In addition, numerous studies have demonstrated that PLGA is well tolerated by the brain tissue without toxic effects, with few adverse effects, and in the absence of immune response.[33,34]

Thus, the aim of this study was to administer VEGF-loaded and GDNF-loaded PLGA NS directly into the striatum, and analyze their synergic ability to restore the 6-OHDA-damaged areas, as well as their capability to improve behavioral deficits in a partially lesioned model of PD.

The formulation and characterization of the NS employed in this paper was performed in a similar manner to as reported in our previous work,[20] generating NS of around 250 nm particle size and zeta potential around −30 mV, which is considered sufficient to form stable dispersions. In the current study, the in vitro release experiment conducted with VEGF NS and GDNF NS showed a similar biphasic profile with a sustained VEGF and GDNF release for 30 days. Once NS were administered, VEGF and GDNF were released due to diffusion and erosion mechanisms, and, consequently, a constant drug release in therapeutic concentrations in a localized area was obtained, achieving desired effects during the in vivo study.

As soon as the NS were characterized, and with the goal of defining the doses for the in vivo study in 6-OHDA partially lesioned rats, the efficacy of the combined administration of VEGF NS and GDNF NS in the protection of PC-12 cells from degeneration was assessed in vitro. After establishing an in vitro model of PC-12 cell damage using 6-OHDA toxin, we provided new evidence on the protective effect of the mixed administration of VEGF and GDNF released from NS against 6-OHDA neurotoxicity. In this assay, we demonstrated that the combination of VEGF and GDNF increased the cell viability and attenuated 6-OHDA-induced apoptosis, even when half of the dose of the individual factors was administered, showing the synergistic effects of VEGF and GDNF as suggested by Tufro et al.[35]

After the combined administration was successfully proven to be the most effective in PC-12 cell line cultures, we

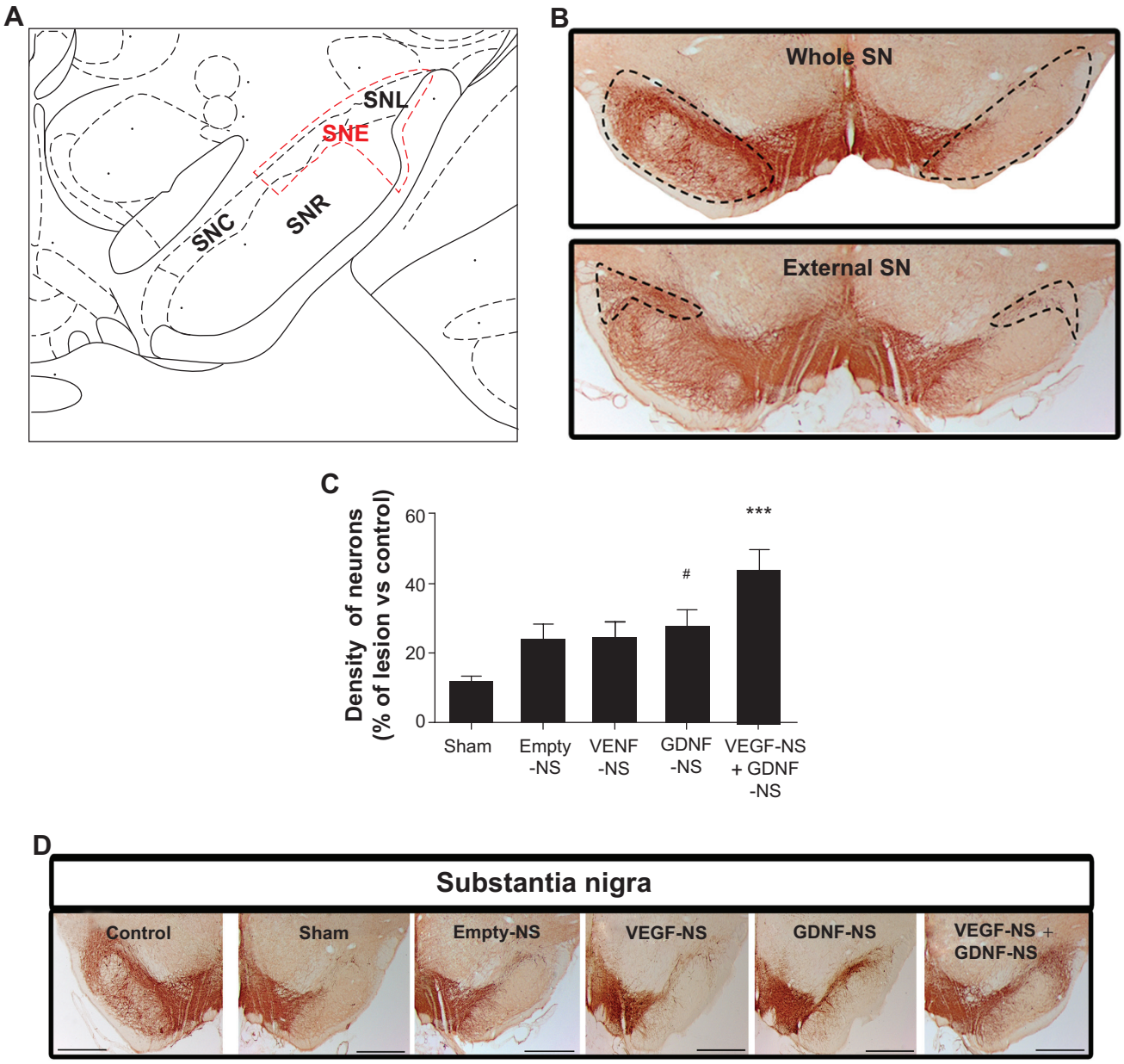

Figure 6 Histological evaluation of the treatments in the SN.
Notes: (**A**) Schematic illustration of the SN with the "external SN" delimited. This area is topologically related to the lesioned area of striatum and includes SNL, a part of the SNR, and half of the SNC. (**B**) Picture of whole SN and delimited "external SN". Scale bar =1 mm. (**C**) Density of dopaminergic neurons in "external SN". The results are expressed as a percentage of lesioned hemisphere compared to the non-lesioned one (control). Data are shown as the mean ± standard error of the mean (n=6–8) (#$P<0.05$ GDNF NS group versus sham group; ***$P<0.001$ VEGF NS and GDNF NS group versus sham and empty NS groups). (**D**) Photomicrographs of SN immunostained for tyrosine hydroxylase from a representative intact hemisphere (control) and 6-OHDA lesioned hemispheres from the different experimental groups. Scale bar =1 mm.
Abbreviations: 6-OHDA, 6-hydroxydopamine; GDNF, glial cell line-derived neurotrophic factor; NS, nanospheres; SN, substantia nigra; SNC, SN pars compacta; SNL, SN lateral; SNR, SN pars reticulata; SNE, SN externa; VEGF, vascular endothelial growth factor.

investigated the in vivo potential of the combined administration at lower doses of VEGF NS and GDNF NS for inducing the restoration of the damage brain areas. The data of this new in vivo study showed improvements on the results obtained in our previous work, carried out in a totally lesioned rat model, using microspheres to administer the factors.[7]

In the present study, we selected a partially lesioned rat model, with the aim of proving the efficacy of our therapy at an incipient stage of PD and with the possibility of comparing with other similar studies published by Garbayo et al and Jollivet et al.[29,30] During the 10 weeks of treatment, we corroborated the behavioral benefits generated by VEGF NS and GDNF NS. In the amphetamine-induced rotation test, the results obtained from GDNF NS treatment were consistent with those of other studies and corroborated the beneficial effects of GDNF in the behavioral recovery. Furthermore,

VEGF NS and GDNF NS combined treatment presented a lower number of ipsilateral rotations, demonstrating higher recovery levels when compared with other treatment groups in the lesioned animals. This result was supported by the experimental data obtained from the apomorphine-induced rotation test. Therefore, the positive behavioral results obtained in the combined treatment group suggest that a sufficient recovery in the lesioned brain tissue could have occurred.

Because the injection of 6-OHDA is directly related to the loss of dopaminergic neurons, and, consequently, is associated with disturbed behavioral function, we investigated the number of TH+ fibers in the striatum of the lesioned rats. The immunohistochemical analysis correlated with the result obtained in the behavioral study, showing increased fiber density in the striatum in the combined treatment group. A particularly interesting finding was the statistically significant changes found in "external SN" dopaminergic neurons after GDNF NS and VEGF NS and GDNF NS treatments. It is well documented that neurons located on the most "external SN" are topologically related to the dorsolateral caudoputamen complex, corresponding to the most lesioned area in this partially lesioned PD rat model. Thus, the restorative changes we observed in SN may be due to the activity of GFs in the striatum.[21,26] These findings support the neurorestorative role of nanoencapsulated VEGF and GDNF on the dopaminergic system, where functional improvement was accompanied with a morphological restoration in a partial-lesion model of PD. The synergistic effects of VEGF NS and GDNF NS allow for a reduction of the dose by half, thus reducing possible side effects, and is a promising neuroregenerative/neuroreparative approach for the treatment of PD.

Conclusion

The data obtained from behavioral studies and immunohistochemical analysis of the striatum and SN confirm that the combination of VEGF NS and GDNF NS at half the dose of their individual administration can be a suitable and promising treatment for neuronal regeneration and protection in a partially lesioned rat model of PD. In addition, the measurements focused on the "external SN" achieve more specific and significant results. Therefore, the administration of VEGF NS and GDNF NS is an interesting potential strategy for the treatment of PD.

Acknowledgments

The "Ministerio de Ciencia e Innovación" (SAF2010-20375), the University of the Basque Country (UPV/EHU) (UFI 11/32), the Basque Government (Saiotek SA-2010/00028), and FEDER funds partially supported this project. The authors are grateful for the cooperation of SGIker (UPV/EHU, MICINN, GV/EJ, ESF). E Herrán appreciates the Basque Government fellowship subvention, and C Requejo and A Aristieta thank UPV/EHU for a fellowship subvention. We thank Dr A Krzyzanowska for the careful revision of the manuscript.

Disclosure

The authors report no conflicts of interest in this work.

References

1. Linazasoro G. A global view of Parkinson's disease pathogenesis: implications for natural history and neuroprotection. *Parkinsonism Relat Disord*. 2009;15(6):401–405.
2. Obeso JA, Rodriguez-Oroz MC, Goetz CG, et al. Missing pieces in the Parkinson's disease puzzle. *Nat Med*. 2010;16(6):653–661.
3. Deierborg T, Soulet D, Roybon L, Hall V, Brundin P. Emerging restorative treatments for Parkinson's disease. *Prog Neurobiol*. 2008;85(4):407–432.
4. Sullivan AM, Toulouse A. Neurotrophic factors for the treatment of Parkinson's disease. *Cytokine Growth Factor Rev*. 2011;22(3):157–165.
5. Ruozi B, Belletti D, Bondioli L, et al. Neurotrophic factors and neurodegenerative diseases: a delivery issue. *Int Rev Neurobiol.* 2012;102:207–247.
6. Siegel GJ, Chauhan NB. Neurotrophic factors in Alzheimer's and Parkinson's disease brain. *Brain Res Brain Res Rev*. 2000;33(2–3):199–227.
7. Herrán E, Ruiz-Ortega JÁ, Aristieta A, et al. In vivo administration of VEGF- and GDNF-releasing biodegradable polymeric microspheres in a severe lesion model of Parkinson's disease. *Eur J Pharm Biopharm*. 2013;85(3 Pt B):1183–1190.
8. Zeng X, Chen J, Deng X, et al. An in vitro model of human dopaminergic neurons derived from embryonic stem cells: MPP+ toxicity and GDNF neuroprotection. *Neuropsychopharmacology*. 2006;31(12):2708–2715.
9. Theofilopoulos S, Goggi J, Riaz SS, Jauniaux E, Stern GM, Bradford HF. Parallel induction of the formation of dopamine and its metabolites with induction of tyrosine hydroxylase expression in foetal rat and human cerebral cortical cells by brain-derived neurotrophic factor and glial-cell derived neurotrophic factor. *Brain Res Dev Brain Res*. 2001;127(2):111–122.
10. Eggert K, Schlegel J, Oertel W, Würz C, Krieg J, Vedder H. Glial cell line-derived neurotrophic factor protects dopaminergic neurons from 6-hydroxydopamine toxicity in vitro. *Neurosci Lett*. 1999;269(3):178–182.
11. Grandoso L, Ponce S, Manuel I, et al. Long-term survival of encapsulated GDNF secreting cells implanted within the striatum of parkinsonized rats. *Int J Pharm*. 2007;343(1–2):69–78.
12. Lindvall O, Wahlberg LU. Encapsulated cell biodelivery of GDNF: a novel clinical strategy for neuroprotection and neuroregeneration in Parkinson's disease? *Exp Neurol*. 2008;209(1):82–88.
13. Nutt JG, Burchiel KJ, Comella CL, et al; ICV GDNF Study Group. Implanted intracerebroventricular. Glial cell line-derived neurotrophic factor. Randomized, double-blind trial of glial cell line-derived neurotrophic factor (GDNF) in PD. *Neurology*. 2003;60(1):69–73.
14. Lang AE, Gill S, Patel NK, et al. Randomized controlled trial of intraputamenal glial cell line-derived neurotrophic factor infusion in Parkinson disease. *Ann Neurol*. 2006;59(3):459–466.
15. Slevin JT, Gash DM, Smith CD, et al. Unilateral intraputamenal glial cell line-derived neurotrophic factor in patients with Parkinson disease: response to 1 year of treatment and 1 year of withdrawal. *J Neurosurg*. 2007;106(4):614–620.

16. Yasuhara T, Shingo T, Kobayashi K, et al. Neuroprotective effects of vascular endothelial growth factor (VEGF) upon dopaminergic neurons in a rat model of Parkinson's disease. *Eur J Neurosci*. 2004;19:1494–1504.
17. Pitzer MR, Sortwell CE, Daley BF, et al. Angiogenic and neurotrophic effects of vascular endothelial growth factor (VEGF165): studies of grafted and cultured embryonic ventral mesencephalic cells. *Exp Neurol*. 2003;182(2):435–445.
18. Talmadge JE. The pharmaceutics and delivery of therapeutic polypeptides and proteins. *Adv Drug Deliv Rev*. 1993;10(2–3):247–299.
19. Chen Y, Liu L. Modern methods for delivery of drugs across the blood–brain barrier. *Adv Drug Deliv Rev*. 2012;64(7):640–665.
20. Herrán E, Pérez-González R, Igartua M, Pedraz JL, Carro E, Hernández RM. VEGF-releasing biodegradable nanospheres administered by craniotomy: a novel therapeutic approach in the APP/Ps1 mouse model of Alzheimer's disease. *J Control Release*. 2013;170(1):111–119.
21. Deumens R, Blokland A, Prickaerts J. Modeling Parkinson's disease in rats: an evaluation of 6-OHDA lesions of the nigrostriatal pathway. *Exp Neurol*. 2002;175(2):303–317.
22. Björklund A, Rosenblad C, Winkler C, Kirik D. Studies on neuroprotective and regenerative effects of GDNF in a partial lesion model of Parkinson's disease. *Neurobiol Dis*. 1997;4(3–4):186–200.
23. Morera-Herreras T, Ruiz-Ortega JA, Linazasoro G, Ugedo L. Nigrostriatal denervation changes the effect of cannabinoids on subthalamic neuronal activity in rats. *Psychopharmacology (Berl)*. 2011;214(2):379–389.
24. Miguelez C, Aristieta A, Cenci MA, Ugedo L. The locus coeruleus is directly implicated in L-DOPA-induced dyskinesia in parkinsonian rats: an electrophysiological and behavioural study. *PLoS One*. 2011;6(9):e24679.
25. Paxinos G, Watson C. *The Rat Brain in Steretaxic Coordinates*. Academic Press, San Diego, CA, USA. 1997.
26. Rosenblad C, Kirik D, Björklund A. Sequential administration of GDNF into the substantia nigra and striatum promotes dopamine neuron survival and axonal sprouting but not striatal reinnervation or functional recovery in the partial 6-OHDA lesion model. *Exp Neurol*. 2000;161(2):503–516.
27. Bartus RT, Baumann TL, Brown L, Kruegel BR, Ostrove JM, Herzog CD. Advancing neurotrophic factors as treatments for age-related neurodegenerative diseases: developing and demonstrating "clinical proof-of-concept" for AAV-neurturin (CERE-120) in Parkinson's disease. *Neurobiol Aging*. 2013;34(1):35–61.
28. Youdim MB, Kupershmidt L, Amit T, Weinreb O. Promises of novel multi-target neuroprotective and neurorestorative drugs for Parkinson's disease. *Parkinsonism Relat Disord*. 2014;20 Suppl 1:S132–S136.
29. Garbayo E, Montero-Menei CN, Ansorena E, Lanciego JL, Aymerich MS, Blanco-Prieto MJ. Effective GDNF brain delivery using microspheres – a promising strategy for Parkinson's disease. *J Control Release*. 2009;135(2):119–126.
30. Jollivet C, Aubert-Pouessel A, Clavreul A, et al. Striatal implantation of GDNF releasing biodegradable microspheres promotes recovery of motor function in a partial model of Parkinson's disease. *Biomaterials*. 2004;25(5):933–942.
31. Garbayo E, Ansorena E, Blanco-Prieto MJ. Drug development in Parkinson's disease: from emerging molecules to innovative drug delivery systems. *Maturitas*. 2013;76(3):272–278.
32. Stockwell J, Abdi N, Lu X, Maheshwari O, Taghibiglou C. Novel central nervous system drug delivery systems. *Chem Biol Drug Des*. 2014;83(5):507–520.
33. Pridgen EM, Langer R, Farokhzad OC. Biodegradable, polymeric nanoparticle delivery systems for cancer therapy. *Nanomedicine (Lond)*. 2007;2(5):669–680.
34. Yamamoto H, Tahara K, Kawashima Y. Nanomedical system for nucleic acid drugs created with the biodegradable nanoparticle platform. *J Microencapsul*. 2012;29(1):54–62.
35. Tufro A, Teichman J, Banu N, Villegas G. Crosstalk between VEGF-A/VEGFR2 and GDNF/RET signaling pathways. *Biochem Biophys Res Commun*. 2007;358(2):410–416.

Mol Neurobiol
DOI 10.1007/s12035-015-9234-y

Topographical Distribution of Morphological Changes in a Partial Model of Parkinson's Disease—Effects of Nanoencapsulated Neurotrophic Factors Administration

C. Requejo[1] · J. A. Ruiz-Ortega[2] · H. Bengoetxea[1] · A. Garcia-Blanco[1] · E. Herrán[3,4] · A. Aristieta[2] · M. Igartua[3,4] · L. Ugedo[2] · J. L. Pedraz[3,4] · R. M. Hernández[3,4] · J. V. Lafuente[1,5]

Received: 25 May 2015

Abstract Administration of various neurotrophic factors is a promising strategy against Parkinson's disease (PD). An intrastriatal infusion of 6-hydroxidopamine (6-OHDA) in rats is a suitable model to study PD. This work aims to describe stereological parameters regarding rostro-caudal gradient, in order to characterize the model and verify its suitability for elucidating the benefits of therapeutic strategies. Administration of 6-OHDA induced a reduction in tyrosine hidroxylase (TH) reactivity in the dorsolateral part of the striatum, being higher in the caudal section than in the rostral one. Loss of TH-positive neurons and axodendritic network was highly significant in the external third of substantia nigra (e-SN) in the 6-OHDA group versus the saline one. After the administration of nanospheres loaded with neurotrophic factors (NTF: vascular endothelial growth factor (VEGF) + glial cell line-derived neurotrophic factor (GDNF)), parkinsonized rats showed more TH-positive fibers than those of control groups; this recovery taking place chiefly in the rostral sections. Neuronal density and axodendritic network in e-SN was more significant than in the entire SN; the topographical analysis showed that the highest difference between NTF versus control group was attained in the middle section. A high number of bromodeoxyuridine (BrdU)-positive cells were found in sub- and periventricular areas in the group receiving NTF, where most of them co-expressed doublecortin. Measurements on the e-SN achieved more specific and significant results than in the entire SN. This difference in rostro-caudal gradients underpins the usefulness of a topological approach to the assessment of the lesion and therapeutic strategies. Findings confirmed the neurorestorative, neurogenic, and synergistic effects of VEGF+GDNF administration.

Keywords Parkinson's disease · Rostro-caudal gradient · VEGF · GDNF · Neuroregeneration · 6-OHDA

✉ C. Requejo
catalina.requejo@ehu.es

[1] Laboratory of Clinical and Experimental Neuroscience (LaNCE), Department of Neuroscience, University of the Basque Country UPV/EHU, Leioa, Vizcaya, Spain

[2] Department of Pharmacology, University of the Basque Country (UPV/EHU), Leioa, Vizcaya, Spain

[3] NanoBioCel Group, Laboratory of Pharmaceutics, School of Pharmacy, University of the Basque Country (UPV/EHU), Vitoria, Alava, Spain

[4] Biomedical Research Networking Center in Bioengineering, Biomaterials and Nanomedicine (CIBER-BBN), Vitoria, Alava, Spain

[5] Group Nanoneurosurgery, Institute of Health Research Biocruces, Barakaldo, Spain

Introduction

Parkinson's disease (PD) is characterized by a selective loss of dopaminergic neurons in the substantia nigra (SN) and a concomitant reduction in the striatal concentration of dopamine. From a clinical point of view, it is associated with motor impairments involving cardinal movement symptoms, resting tremor, muscle rigidity, and postural abnormalities [1, 2].

Among the local factors that may be involved in the motor symptoms of PD, the following have been observed: a degree of dopamine loss, the distribution of changes in the ventral or dorsal parts of SN, an effect on direct and indirect pallidal

Published online: 04 June 2015

pathways, and the topographical representation of the body in the striatum [3].

Administration of 6-hidroxidopamine (6-OHDA) is a suitable model to reproduce PD. In rats, 6-OHDA can be injected into the SN-compacta (SNc), the medial forebrain bundle and the caudate-putamen complex (CPC) in order to induce a selective differential damage of the nigrostriatal dopaminergic pathway. Intrastriatal 6-OHDA administration induces a progressive, retrograde degeneration of the nigrostriatal pathway. Thus, it is a good model to study the pathophysiological features in the first stage of development of Parkinson's disease, as well as the effects and neuropathological changes of new therapeutic strategies like nanoparticles releasing neurotrophic factors (NTF) [4].

Loss of dopaminergic neurons in SN leads to a denervation of the posterolateral striatum [5]. This happens because nigrostriatal projections are topographically distributed so the oldest neurons, placed on the most lateral SN, project to the posterolateral CPC. Axons of early originated nigral neurons spread via the medial forebrain bundle into the ventrolateral part of the CPC [6]. The chronology of neuronal production is a necessary requisite for the proper anatomical and functional development of the central nervous system (CNS). Following anatomical and topological distributions in a partial murine model of PD, we focused our attention on the changes arising in this sector [6].

Among the factors implied in neurodegeneration, a decrease in energetic cellular efficiency together with the synthesis and activity of neurotrophic factors (NTF) play a crucial role. Both are involved in differential regional vulnerability [7]. The neurotoxic effect of 6-OHDA is based on its potent inhibitory effect on the mitochondrial respiratory enzymes (chain complexes I and IV) [8].

Current therapies are not effective in the long term. Therefore, the proposed neurotrophic factor (NTF) alternative, as glial cell line-derived neurotrophic factor (GDNF) and vascular endothelial growth factor (VEGF), provides the opportunity to protect and regenerate the dopaminergic neurons affected in PD. Nevertheless, the clinical application of NTF presents some difficulties, like the cross of the blood–brain barrier (BBB) and a rapid degradation. Brain implantation of biodegradable poly-lactic-co-glycolic acid (PLGA), nanospheres (NS), and microspheres (MS) loaded with NTF is an alternative to attain a continuous drug release over time and to allow for the simultaneous administration of different trophic factors [4, 9].

Regarding the cellular and molecular heterogeneity of the CPC and SN, attention has been paid to changes arising in different sections along the rostro-caudal axis. The aim of this work was to study a set of the morphological changes occurring in a partial murine model of PD and verify the usefulness of the proposed approach, analyzing the findings after the administration of NTF (VEGF and GDNF). The anatomical rostro-caudal distribution of said changes could give us accurate information to assess the reliability of the model and the effectiveness of treatments.

Materials and Methods

For the present study, a total of 24 male Sprague–Dawley rats between 150 and 175 g were used: 8 for the characterization of the lesion and 16 for the treatment assay. Those rats used for the characterization of the lesion were housed in standard conditions, at a constant temperature of 22 °C, in a 12-h dark/light cycle and ad libitum access to water and food. Experiments were performed in agreement with the Ethical Committee and Animal Welfare (CEBA) of the University of the Basque Country (CEBA/154/2010//RUIZ ORTEGA) and in accordance with Spanish Royal Decree RD 1201/2005, European Directive 2003/65/EC, and the European Recommendation 2007/526/EC on the protection of animals used for scientific purposes.

For Assay 1 (characterization of the lesion), the animals were divided into two groups: (a) 6-OHDA group (n=5 rats) receiving 6-OHDA into the striatum and (b) saline group (n=3 rats) injected only with saline solution, and for Assay 2 (the treatment assay), 16 parkinsonized rats were used, coming from a prior study where the functional effectiveness of synergistic administration of VEGF-GDNF was demonstrated [4]. Assay 2 consisted of three previously parkinsonized rat groups, which were again anesthetized 3 weeks after the 6-OHDA injections and NS or vehicle were implanted into the right striatum using the same stereotaxic coordinates: the vehicle rat group (n=5 rats) receiving only the vehicle, the empty-NS rat group (n=5 rats) receiving empty nanospheres, and the neurotrophic factor rat group (n=6 rats) receiving NS loaded with VEGF and GDNF (1.25 μg+1.25 μg). In addition, bromodeoxyuridine (BrdU) was injected (200 mg/kg body weight) into these groups (Ref: B5002; Sigma-Aldrich), dissolved in 1 ml of 0.9 % NaCl and administered intraperitoneally 5 days before sacrifice.

No assays with neurotrophic factors administered alone were taken into account because previous studies have reported that statistically significant differences in functional tests were only to be found where both factors (VEGF+GDNF) [4] were synergistically administrated. Therefore, an advanced stereological study was focused exclusively on this group and the control groups.

Surgical Procedures

Rats were deeply anesthetized with isoflurane (1.5–2 %; Esteve Química, Barcelona, Spain) and placed on a Kopf stereotaxic instrument (David Kopf Instruments, Tujunga, CA, USA). Prior to the injection of 6-OHDA (7.5 micrograms) or

saline (2.5 μl) into the right striatum, the animals were pretreated with desipramine (25 mg/kg, i.p., Sigma, St. Louis, USA) and pargyline (50 mg/kg, i.p., Sigma, St. Louis, USA), to protect the noradrenergic terminals and to inhibit monoamine oxidase activity [10], respectively. The stereotaxic coordinates were established according to Paxinos and Watson atlas [11] in order to get a partial degeneration of the nigrostriatal dopaminergic system [12]: anteroposterior (AP) +1.3 mm, mediolateral (ML) +2.8 mm, and dorsoventral (DV) −4.5 mm; AP −0.2 mm, ML +3.0 mm, and DV −5.0 mm; AP −0.6 mm, ML +4.0 mm, and DV −5.5 mm, relative to the bregma and dura, and with the tooth bar set at −2.4.

Histological and Immunohistochemical Analysis

After the survival period (4 weeks for Assay 1 and 14 for Assay 2), the rats were intraperitoneally anesthetized again and transcardially perfused with 0.9 % NaCl and 4 % paraformaldehyde (PFA) in a 0.1 M phosphate buffer (PBS) with a pH value of 7.4. The brains were removed and post-fixed overnight during 24 h in the same fixative and later transferred to a 30 % sucrose solution in a 0.1 M PBS, for cryoprotection. After 1–3 days (when they sank), coronal sections were obtained with a freezing microtome (50 μm thick) and collected in PBS containing 0.6 % sodium azide for storage.

Nissl Staining

Sections for Nissl staining were mounted on gelatin-coated slides, hydrated through a battery of alcohols with decreased graduation, incubated in toluidine blue (pH 4.1) for 1 min, dehydrated through a battery of alcohols with increased graduation, and coverslipped.

Immunohistochemistry

Tyrosine hydroxylase (TH) and glial fibrillary acidic protein (GFAP) immunochemistry examinations were performed in free-floating slices. Endogenous peroxidases were neutralized with a solution of 3 % H_2O_2, 10 % methanol in potassium phosphate-buffered saline (KPBS) (0.02 M, pH 7.1) for the TH-immunochemistry, and PBS for the GFAP-immunochemistry, during 30 min and at room temperature (RT). For TH immunostaining, cerebral slices were preincubated with 5 % normal goat serum (NGS) and 1 % Triton X-100 in KPBS (KPBS-T) for 1 h, and later incubated overnight with rabbit polyclonal anti-tyrosine hydroxylase (Ref: AB-152; Millipore; 1:1000) in 5 % NGS KPBS/T at 4 °C. For GFAP immunostaining, coronal slices were preincubated with 5 % BSA and 0.05 % Triton X-100 in a 0.1 M PBS for 2 h, and later incubated overnight with monoclonal mouse anti-GFAP (Ref: G-3893; Sigma-Aldrich; 1:400) at 4 °C. Sections incubated with anti-TH, after being rinsed twice with KPBS and once with 2.5 % NGS KPBS/T, were exposed for 2 h to a secondary biotinylated goat anti-rabbit IgG (Ref: BA1000; Vector Laboratories; 1:200) in a KPBS/T containing 2.5 % NGS. Sections incubated with anti-GFAP were rinsed three times with PBS and exposed to biotinylated anti-mouse secondary antibody (Elite ABC kit; Vector Laboratories; USA) for 2 h at RT. All slices were processed for 1 h with avidin-biotin-peroxidase complex (Elite ABC kit; Vector Laboratories; Inc., Burlingame, CA, USA) and 3,3 diaminobenzidine (DAB) as a chromogen. Finally, slices were mounted, dehydrated, and coverslipped with DPX medium (Sigma-Aldrich).

Immunofluorescence for BrdU and doublecortin

To detect BrdU and doublecortin (DCX), a double immunostaining was carried out. Briefly, free-floating sections were incubated overnight with goat polyclonal anti-DCX (Ref: sc-8066 Santa Cruz Biotechnology; 1:200) at 4 °C and later visualized with an Alexa 633 conjugated donkey anti-goat IgG (Ref: A-21082; Invitrogen; 1:400) for 1 h at RT. After several washes, sections were denatured with 2 N HCl for 30 min and incubated overnight with the monoclonal primary antibody anti-BrdU (Ref: sc-51514; Santa Cruz Biotechnology; 1:200) at 4 °C, followed by incubation with a secondary Alexa 488 conjugated goat anti-mouse IgG (Ref: A11029; Invitrogen; 1:400) antibody. After rinsing, Hoechst 33258 was added to counterstain the nuclei for 10 min. The slices were washed, mounted and coverslipped with medium Vectashield (Vector laboratories). To visualize the results, the sections were analyzed with a confocal laser microscope (Olympus Fluoview FV500).

Quantitative Analysis

Volume of Affected Striatum

On each experimental group, the TH-negative volume of the CPC was calculated in order to find an alternative histological marker to the integrated optical density (IOD) for evaluation of the lesion and its recovery after 6-OHDA administration.

To achieve this, the TH-negative volume of the ipsilateral CPC and its entire volume were both measured using a computerized image analysis system (Mercator Image Analysis system, Explora Nova, La Rochelle, France). Values were expressed as a percentage of the TH-negative volume versus the entire volume of the ipsilateral CPC.

For each animal, the TH-negative volume was estimated at a whole CPC and at three representative CPC levels according to Paxinos and Watson atlas [11]: rostral (bregma +0.70 mm), medial (bregma −0.26 mm), and caudal (bregma −0.80 mm) sections.

Neuron Density and Axodendritic Network in SN

TH-immunoreactive (TH-ir) neurons and the axodendritic network (ADN) were measured using a stereological tool (an optical dissector) provided by the computerized image analysis system (Mercator Image Analysis system, Explora Nova, La Rochelle, France). Probes of 50×50 μm separated by 100 μm were launched into the entire SN and also into a delimited region, including SN-lateral (SNl), one third of SN-reticulata (SNr), and the lateral half of SN-compacta, which we named "external-SN" (e-SN) and where the most prominent changes were observed (Fig. 3a). Subsequently, ADN density was only analyzed in this e-SN.

Immunopositive neurons and ADN inside the probe, or crossing the right side of the *X*–*Y*-axis, were counted. TH-ir neurons and ADN were calculated per section and per animal considering all the SN slices and considering only three representative rostro-caudal levels, according to Paxinos and Watson atlas [11]: rostral SN (bregma, −5.20 mm), middle SN (bregma, −5.60), and caudal SN (bregma, −6.04) sections. Data were expressed as a percentage of the neurons or ADN present on the lesioned side versus the non-lesioned hemisphere.

Statistical Analysis

All values are expressed as the mean±S.E. (standard error). Statistical analysis was performed with SPSS Statistics (v 20; IBM Corporation, Armonk, NY, USA). Prior to analysis, the Shapiro–Wilk test was used to assess the normal distribution of samples and Levene's test was used to determine the homogeneity of variance. One-way analysis of variance (ANOVA) with Tamhane's post hoc test was used to explore differences between rostro-caudal gradients within each experimental group. The Student's *t* test was used to compare intergroup differences. Values are considered statistically significant when $p<0.05$.

Results

Assay 1: Characterization of the Lesion

Morphological Study

In the autopsy, rat brain surfaces showed the three injections marks where either the 6-OHDA or the saline solution was administered. No macroscopically differences were observed between both groups.

Coronal sections stained with Nissl showed the needle trajectory into the striatum (Fig. 1a), which was almost imperceptible in the TH immunostaining sections (Fig. 1b). On the lesioned side, a slight enlargement of the lateral ventricle was observed, probably due to scar retraction. Rats from the 6-OHDA group showed negativity for TH immunohistochemistry on the dorso-lateral region of the striatum (Fig. 2a).

In the histopathological analysis, GFAP expression levels were higher on the lesioned sides (striatum and SN) than on the intact ones. Furthermore, most of the GFAP-positive cells seen in the lesioned side showed a swollen soma. In addition, 6-OHDA rats showed a stronger positivity to GFAP than rats only receiving the saline solution.

Quantitative Analysis

Volume of Affected Striatum Degeneration of dopaminergic fibers after the injection of 6-OHDA was evaluated measuring the volume of immunonegative CPC for TH. A significant decrease of the TH positivity was observed in rats injected with 6-OHDA versus those only injected with the saline solution (Fig. 2). The TH-negative volume in 6-OHDA rats was 2.10±0.15 mm^3, 65.88±4.59 % for the entire ipsilateral striatum, and in the saline group was 0.02±0.008 mm^3 (0.54±0.34 %) (***$p<0.000$; Student's *t* test) (Fig. 2b).

Regarding rostral, middle, and caudal levels of the CPC, the percentage of TH-negative volume was 54.49±11.54, 63.65±11.29, and 84.51±6.73 % for the rostral, middle, and caudal sections of the 6-OHDA group, respectively (Fig. 2c). Significant changes were found comparing both groups at these three considered levels (***$p<0.001$, for the rostral sections; ***$p<0.001$, for the middle sections; ***$p<0.001$ for the caudal sections; Student's *t* test) (Fig. 2c). However, no significant differences were found between the different levels within the saline or 6-OHDA groups.

After the histopathological analysis, the previously referred enlargement of the homolateral ventricle was appreciated, probably due to tissue retraction caused scarring after the puncture injury. Therefore, a quantification of this tissue retraction was performed, expressed as a percentage of the volume occupied by the ipsilateral CPC with respect to the contralateral one, on TH-immunostained sections. This contralateral non-lesioned CPC was considered as 100 %. The volume was calculated integrating all measurements of the CPC sections using the above referred image analysis system.

The average volume of the entire CPC in the saline group was 2.96±0.23 mm^3 on the ipsilateral side and 3.41±0.3 mm^3 on the contralateral one (the ipsilateral hemisphere values were found to be 8.65±3.45 % lower than those of the contralateral hemisphere). In the 6-OHDA group, the average volume for the injured side was 3.19±0.11 and 3.65±0.14 mm^3 for the non-injured one (ipsilateral hemisphere values 12.80±1.21 % lower than those of the contralateral hemisphere) (Fig. 2d). These data show that the puncture is responsible for circa a 10 % decrease in tissue volume on both groups, though tissue retraction did not reach any significant

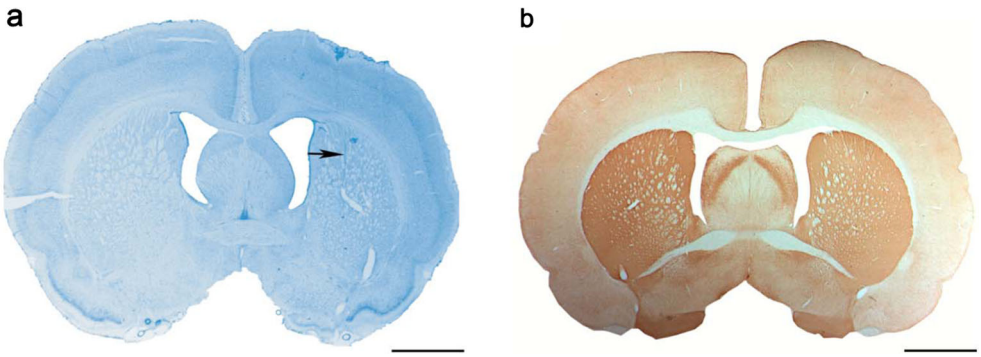

Fig. 1 Needle trajectory: coronal sections from the saline group, stained for Nissl stain (**a**) and TH immunostaining (**b**). *Black arrow* indicates the needle trajectory into the striatum. Both striata remain strong TH-immunopositive. *Scale bar*: 2.5 mm

differences between the saline and 6-OHDA groups. Moreover, tissue retraction decreased from the rostral to the caudal level in both groups (Fig. 2e).

Neuron Density and Axodendritic Network in the Entire SN and in the "External-SN" The main neuron loss was observed in the previously defined "external SN" (e-SN) (Fig. 3a, b), where the decrease in TH-ir neurons was comparatively more prominent than in the entire SN.

The number of TH-immunoreactive (TH-ir) cells in SN decreased significantly after the administration of 6-OHDA, with only 20.45±2.33 % of positive neurons remaining in the ipsilateral side. The saline group showed minimal variations (85.59±2.20 %). There was a highly significant difference between both groups (***$p<0.000$; Student's t test) (Fig. 3c). When rostro-caudal sections of SN were analyzed for neuronal density, a significant reduction in the 6-OHDA group compared to the saline group was found at all levels, being most relevant in the caudal sections (Fig. 3d).

Stereological studies showed more significant changes in the e-SN than in the entire SN, indicating that this region is more susceptible to changes using this model. Thus, in rats receiving 6-OHDA, 14.5±2.55 % of TH-positive neurons remained and in the saline group, 77.91±4.90 % (***$p<0.001$; Student's t test) (Fig. 3e).

Interestingly, the rostro-caudal gradient was much more remarkable in the e-SN than in the entire SN, attaining statistically significant differences between the rostral and caudal sections within the same group (Fig. 3f). Measurements for the e-SN were 23.84±1.39 % at the rostral, 12.9±3.64 % at the middle, and 6.75±2.53 % at the caudal section for the 6-OHDA group and 90.58±5.97 % at the rostral, 80.16±5.25 % at the middle, and 62.99±5.56 % at the caudal section for the saline group (Fig. 3f). By contrast, the entire SN did not show remarkable differences throughout the rostro-caudal axis (21.24±4.15, 16.93±4.92, and 21.42±4.85 % for the 6-OHDA group and 86.42±3.95, 85.42±6.29, and 79.62±2.3 % for the saline group) (Fig. 3d).

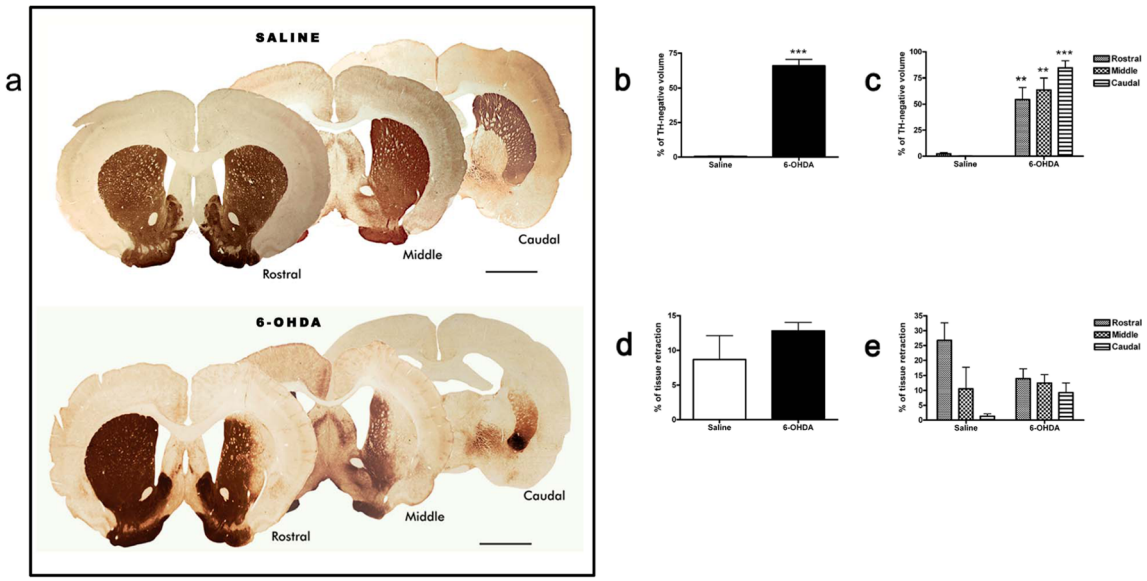

Fig. 2 Affected caudoputamen complex (*CPC*): series of coronal section **a** show differential TH positivity depending on the injected substance and the level considered (rostral, middle, and caudal). *Scale bar*: 2.5 mm. **b**, **c** Loss of TH-positive innervation in the striatum was determined by the percentage of TH-negative volume of the ipsilateral striatum respect to the total ipsilateral one. Significance ***$p<0.001$ saline versus 6-OHDA group. **d**, **e** The size of the ipsilateral CPC was assessed by the remaining volume percentage of the ipsilateral versus the contralateral one

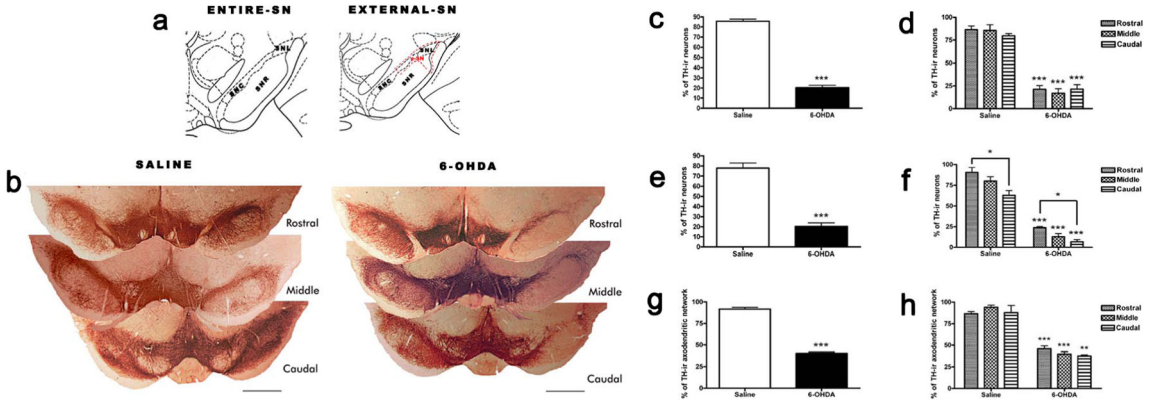

Fig. 3 Effects on substantia nigra (SN). **a** Entire SN and the delimited e-SN. **b** Photomicrographs of the rostral, middle, and caudal sections of SN immunostained for TH in the saline and 6-OHDA groups. *Scale bar*: 1 mm. **c**, **d** 6-OHDA produced a significant loss of TH-ir neurons in the entire SN and no differences between sections along the rostro-caudal axis were observed. ***$p<0.001$ saline versus 6-OHDA group. **e**, **f** In e-SN, the density of neurons decreased in both groups (***$p<0.001$) and a decreasing rostro-caudal gradient was evident, being significantly different at the rostral and caudal sections (*$p<0.05$) in both groups. Saline versus 6-OHDA rats presented significant differences at all analyzed sections (***$p<0.001$). **g**, **h** The density of axodendritic network (ADN) was measured only in the e-SN. There was a significant difference between both experimental groups (***$p<0.001$). Analyzed by section, a tendency was only observed in the 6-OHDA group

Owing to the significant changes in neuronal density obtained when analyzing the e-SN, we proceeded to quantify the axodendritic network (ADN) in this specific region. As expected, 6-OHDA rats presented a lower ADN density than saline rats (40.45±1.96 vs. 81.82±1.96 %, ***$p<0.001$; Student's *t* test) (Fig. 3g).

As for the rostro-caudal distribution, rats receiving 6-OHDA presented a significantly lower ADN density (45.94±3.39 % at the rostral, 39.9±2.47 % at the middle, and 37.6±1.3 % at the caudal section) than rats receiving just the saline solution (86.62±2.52 % at the rostral, 94.18±2.34 % at the middle, and 87.9±2.24 % at the caudal section), at all studied sections; however, no trend or differences within the same group were appreciated (***$p<0.001$ 6-OHDA vs. saline rats at rostral and middle sections and **$p<0.01$ at the caudal section; Student's *t* test) (Fig. 3h).

Assay 2: Treatment with Nanoencapsulated Neurotrophic Factors

Morphological Study

Some Nissl slices show two trajectories corresponding to the initial administration of 6-OHDA and a subsequent administration due to the treatment (Fig. 4a). Tissue around the needle track appears rarefied with a conspicuous glial reaction and macrophages or hemosiderin is sometimes presented along the track. A mild enlargement of the lateral ventricle is frequently appreciated. The astroglial reaction consists of a hypertrophy of cellular processes and up regulation of GFAP expression. Nanospheres loaded with NTF induced a remarkable glial reaction around the trajectory.

Morphological evidences of tissue damage after NS implantation were undistinguishable to the vehicle, indicating that histological changes around the needle track were induced by the needle itself, and the NS themselves being well tolerated.

Rats receiving 6-OHDA showed an asymmetrical distribution of the toxin effects. These were localized mainly over the dorso-lateral region of the striatum. Slices including the needle track frequently displayed an abrupt transition between TH immunohistochemistry positivity and negativity (Fig. 4b).

The TH immunohistochemistry of the striatal sections displays a region showing TH-positive fiber loss which appears to be higher both in the vehicle and empty-NS groups than in the NTF ones. This loss will be quantified.

Proliferation Assay: BrdU/DCX Immunofluorescence

A large amount of cells expressing BrdU positivity was found in the subventricular zone (SVZ) and surrounding areas in the group receiving NTFs, which indicates a high level of proliferation. Some of these cells co-expressed DCX (marker of immature neurons) and were extended all over the SVZ. Some of them were located in areas adjacent to the striatum, suggesting a possible SVZ to striatum migration. In the animals of the vehicle group, the number of BrdU-positive cells was clearly lower and there were no DCX-positive cells (Fig. 5), confirming that NTF induces or maintains neuron differentiation and proliferation levels.

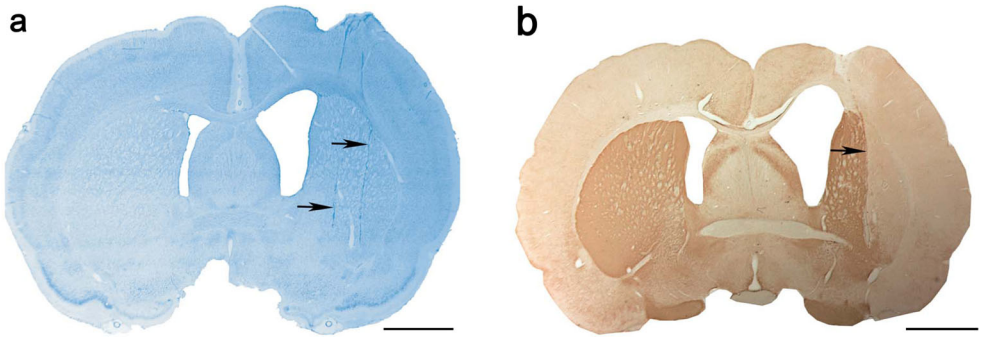

Fig. 4 Abrupt limit in the striatum: coronal sections from the 6-OHDA-treated (vehicle) group, stained for **a** Nissl and **b** TH immunohistochemistry. *Black arrows* in **a** mark the trajectory of both surgical procedures (6-OHDA and treatment administration); in **b,** at this level, an abrupt limit between TH-positivity and TH-negativity was observed. *Scale bar*: 2.5 mm

Quantitative Analysis

Volume of Affected Striatum In NTF-treated animals, the TH-negative volume of the CPC was 0.94±0.082 mm^3 (41.27±3.21 % of the total volume of the ipsilateral CPC). It was less than in the other studied groups (Fig. 6) (1.21± 0.08 mm^3, 52.92±3.71 % in the vehicle group and 1± 0.07 mm^3, 43.74±3.3 % in the empty-NS group). The difference between the NTF and the vehicle group was statistically significant (*$p<0.05$; one-way ANOVA) (Fig. 6b) and indicated the increased recovery of the treated group.

Distribution from rostral to caudal sections showed a reduction in the TH-negative volume (that is, a TH positivity recovery) on all sections of the NTF group. However, no statistic differences were observed either between groups or into themselves (Fig. 6c).

Regarding tissue retraction, measurements did not show any significant difference between groups. Owing to the two lesions carried out in these groups, the percentage of tissue retraction was somewhat higher than in the first assay, almost 25 %, though the lowest percentage belonged interestingly to the NTF group (Fig. 6d).

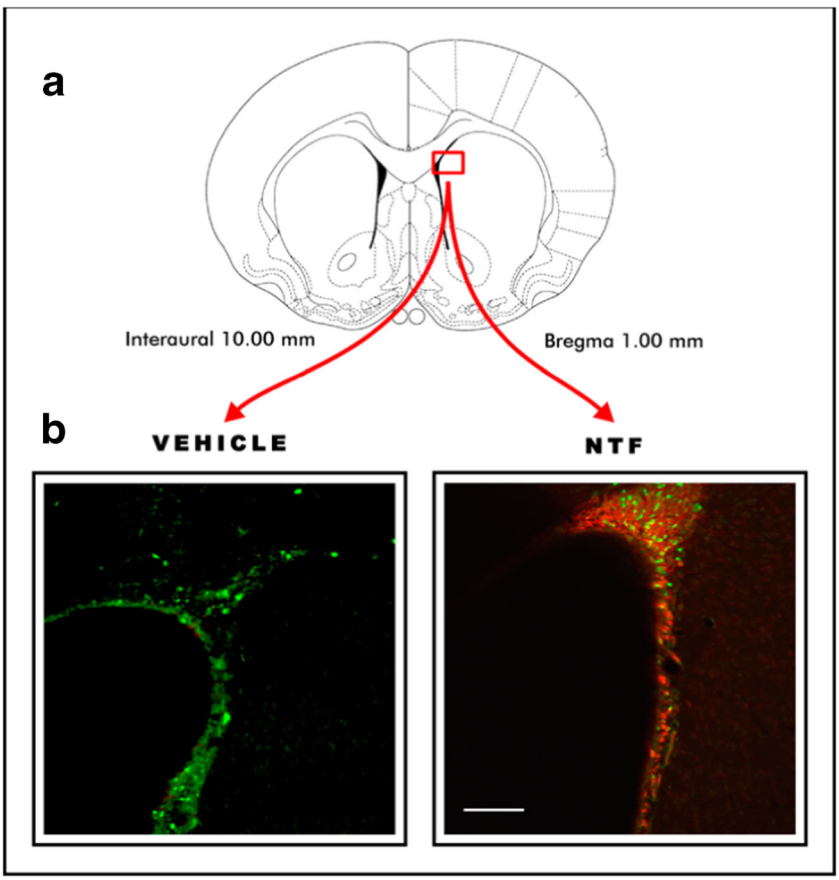

Fig. 5 A proliferative and neurogenic effect is observed in the NTF group: **a** SVZ localization, according to Paxinos and Watson atlas. **b** Confocal micrographs show the BrdU-positive nucleus (*green*) and the DCX-positive soma (*red*) in the SVZ and periventricular areas. The NTF group presents more positivity for BrdU and DCX than the vehicle group. In the NTF group, most of the BrdU-positive cells co-express DCX. *Scale bar*: 275 μm

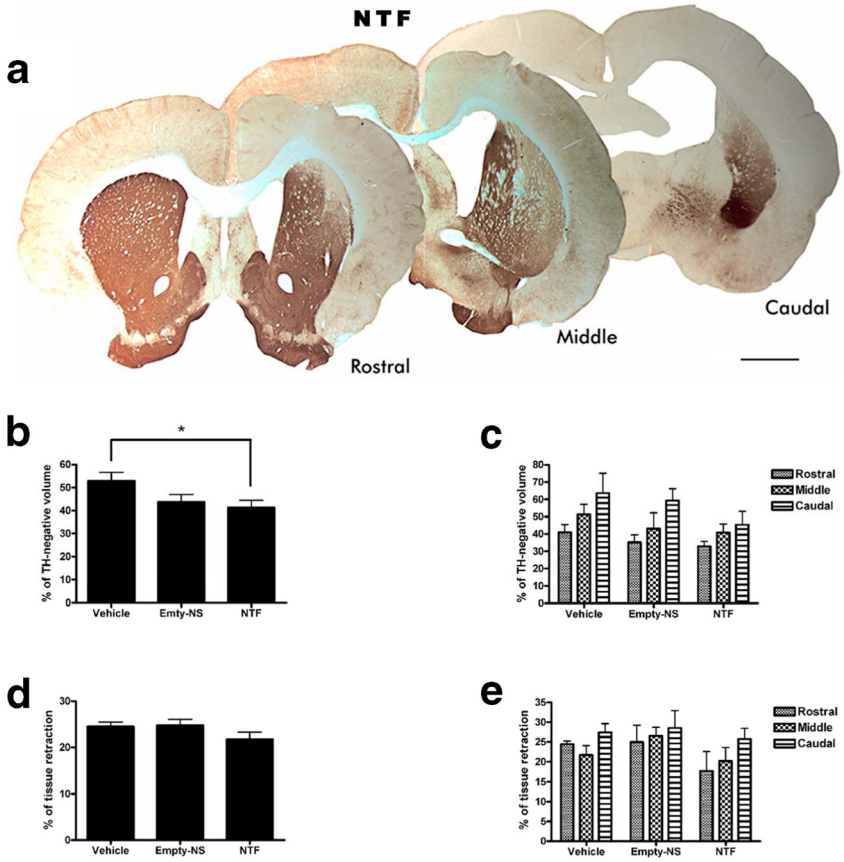

Fig. 6 Recovery of TH-ir striatal volume. **a** Coronal sections from the NTF group immunostained for TH show a recovery in the TH-positive volume at all rostro-caudal levels. *Scale bar*: 2.5 mm. **b** TH-negative volume percentage is lower in the NTF with respect to the vehicle and empty-NS groups. Significance, *$p<0.05$ (NTF vs. vehicle group). **c** The TH-negative volume increases from rostral to caudal sections, being the lowest in the NTF group. **d** Tissue retraction. The group receiving NTF shows lesser tissue retraction than the other groups. **e** Tissue retraction increases slightly from rostral to caudal sections, being the decreasing effect of NTF apparent at all levels studied

The topographical analysis showed that in spite of a lack of statistic differences, the NTF group displayed a gradient showing a remarkable recovery on the rostral sections compared to the control groups (Fig. 6e).

Neuron Density and Axodendritic Network in the Entire SN and in the "External-SN" Substantia nigra from the vehicle group and the empty-NS group showed an extreme loss of dopaminergic neurons and fibers, while rats receiving NTF showed more cells and a TH-positive neuropil (Fig. 7). Changes mainly occurred on the external area of SN (e-SN) (Fig. 7a), where the most important changes related to neuronal and ADN density were found. This specific region was more affected by the lesion and showed a higher recovery level after NTF administration.

Regarding the entire SN, the number of TH-positive neurons was statistically higher in the NTF group than in the vehicle one (Fig. 7b). This increase took place in all sections studied but only achieved significant levels in the rostral section (Fig. 7c) (4.23±1.12 vs. 19.32±3.22 %, *$p<0.05$, one-way ANOVA).

When e-SN was considered, differences were statistically significant and even more marked between the three groups (Fig. 7d). The topographical distribution showed that the NTF group increased from rostral to caudal (36.70±10.22, 44.02±7.19, and 51.11±17.42 %) but was only significant versus the vehicle group at the middle level (9.55±4.02 vs. 44.02±7.19 %, ***$p<0.001$, one-way ANOVA) (Fig. 7e).

Stereological studies showed changes in SN regarding neuron density and ADN. These changes were statistically significant (*$p<0.05$, one-way ANOVA) between the three groups considered and were highly significant (***$p<0.001$; one-way ANOVA) when the e-SN was considered exclusively (Fig. 7f).

Evaluations of the ADN in the e-SN revealed that the NTF group presented a higher density of TH-positive ADN (55.7±4.51 %) compared to the empty-NS group (45.13±3.97 %) or the vehicle group (35.01±3.08 %). Differences were statistically significant between the NTF and the vehicle group (***$p<0.0001$, one-way ANOVA) (Fig. 7f). Analyzing rostro-caudal sections, its ADN density was statistically significant only at the middle level of these two groups (*$p<0.05$, one-way ANOVA) (Fig. 7g).

Discussion

Rostro-caudal gradients of the morphological changes exhibited in the striatum and in the SN, in addition to the specific anatomic distribution of the dopaminergic system, suggest a

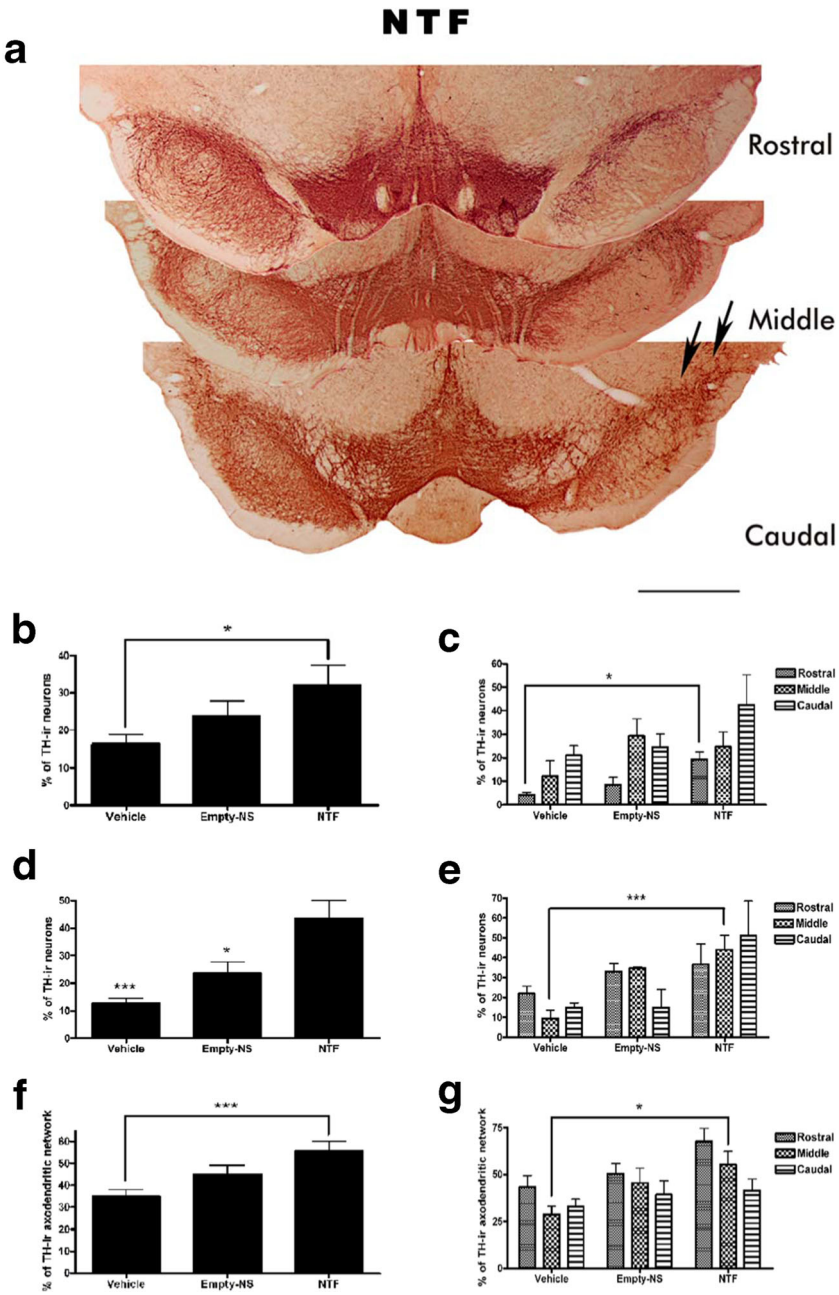

Fig. 7 Rescue of TH-ir neurons and axodendritic network (ADN): **a** photomicrographs of the rostro-caudal sections of TH immunostain SN from the group receiving NTF. This group shows a significant increase of positive neurons in the ipsilateral hemisphere compared to the control groups. *Scale bar*: 1 mm. *Black arrows* point to the e-SN of the lesioned hemisphere, where the recovery is more outstanding. **b** Percentage of neurons in the entire SN (*$p<0.05$, NTF vs. vehicle group). **c** Rostro-caudal distribution is depicted regarding percentage of neurons in the entire SN. There are statistically significant differences at rostral level between the vehicle and the NTF group (*$p<0.05$). **d** When e-SN is considered, more outstanding differences appear between groups (***$p<0.001$, NTF vs. vehicle group; *$p<0.05$ NTF vs. empty-NS group). **e** The effect of NTF increases the rostro-caudal percentage of TH-ir neurons in e-SN. Statistical differences are found between the middle sections of the NTF versus the vehicle group in the e-SN (***$p<0.01$). **f** The axodendritic network in the e-SN is significantly more dense in the NTF group (***$p<0.01$, NTF vs. vehicle group). **g** When ADN percentage data in the e-SN are segregated for all rostro-caudal levels, only the middle one presents a mild difference between the NTF and the vehicle group (*$p<0.05$), and a moderate decreasing rostro-caudal gradient was pointed out

differential selective vulnerability of this system. A deeper knowledge of this distribution could be useful in order to assess the lesion, as well as the administration and diffusion of treatments. The measurements carried out on the e-SN—topographically related to the lesioned area of the striatum—reach more specific and significant results than those carried out in the entire SN, emerging as a promising region for further studies.

Functional improvement and morphological recovery after VEGF and GDNF implantation is related to the preservation of the TH-positive volume, cells, and ADN in the striatum and SN. In addition, these findings support the neurorestorative role of VEGF+GDNF on the dopaminergic system and the synergistic effect between both factors.

Morphological Changes in the CPC and SN

A unilateral infusion of 6-OHDA into the striatum results in several histopathological changes, being the most prominent the loss of TH-ir fibers, terminals, and neurons [13]. An analysis of the Nissl staining sections of all experimental groups showed an enhanced cellularity around the needle track. The increase of astroglial reaction and reactivity for GFAP is widely used to determine the wound-healing response in SNc [14].

Astrocytes play a major role buffering the environment of neuronal cells [15] and, because of this, it would be important to determine which other functions develop in PD, apart from wound healing. For instance, Fuller et al., 2014, suggest that astrocytes could increase the viability of endogenous nigrostriatal neurons [16].

Rats treated with NTF showed a potentially regenerative response, increasing their GFAP positivity compared with the striatum and SN of other treated groups. Degeneration of nigral dopaminergic neurons in PD is also associated with a glial reaction and inflammatory changes [17]. Neuroinflamation mediators are known to be crucial in the progression of PD [18].

Remarkable Limit Inside the Striatum

Administration of 6-OHDA into the striatum, rather than a progressive model for PD—as it requires time to check changes after the lesion—is a suitable model to test neuroprotective and neurotrophic drugs. 6-OHDA produces a selective destruction of the dopaminergic system and provides a suitable model, where it is possible to elucidate the optimal time, in order to initialize the treatment [13, 19–21]. Intrastriatal administration of 6-OHDA, following the proposed coordinates, induces a lesion in the dorso-lateral striatum corresponding to areas with a poor expression of calbindin.

Calbindin is a calcium-binding protein that acts as an endogenous calcium buffer [22] Alterations in the amount of this protein have been found all through the brain in PD patients [23]. Stress and neuronal death are mediated by calcium, and the distribution of calcium-binding proteins is not homogenous in the striatum and in other parts of the brain, being partially responsible for the selective vulnerability of some neuron populations in the central nervous system (CNS) [22, 24]. Most cases showed a remarkable limit between negative lateral region and positive medial areas. This may probably be a result of the selective vulnerability of these areas to the oxidative stress, previously mentioned, due to lack of calbindin. Neurons require high amounts of energy to maintain their functions, needing an efficient calcium buffering ability [25].

An Innovative Strategy to Evaluate Striatal Degeneration

Striatal degeneration was evaluated taking into account the volume occupied by the TH-negative fibers. Degeneration and regeneration are both progressive processes and in order to accurately assess them, the affected surface of the stereological collected sections was delimited, measured, and integrated to obtain the exact volume occupied by the TH-negative fibers inside the striatum. Consequently, it is easy to avoid striosomes or vascular sections which might distort conventional IOD measurements. Furthermore, positive sprouting of new fibers may be also taken into account.

Animals injected with 6-OHDA showed 66 % of negative ipsilateral striatum for TH. Rats receiving the saline solution lost only 0.5 % of the TH-positive volume. This indicated that the injury was barely involved in the degeneration of TH-positive fibers.

Administration of VEGF and GDNF resulted in a recovery of the TH-positive volume in the CPC, protecting and restoring the dopamine (DA) terminals. Parkinsonized rats treated with both NTF showed a statistically significant increase in volume (13 %) compared to rats treated only with the vehicle.

The functional recovery and increase of TH-positive fibers in the striatum of parkinsonized rats has also been previously reported when rats were treated with GDNF alone [26, 27]. In fact, previous studies have shown that intrastrial administration of GDNF stimulates regenerative sprouting from preserved axons [28]. The TH-positive area recovers out of the remaining cells, showing that the neuroplasticity of axons and dendrites is better preserved than its soma.

The retraction rate of the striatum was evaluated in order to assess the effect of the injury by itself and of recovery after NS implantation.

The volume of the injured hemisphere decreased around 10 % in both Assay 1 groups, while it was of about 25 % for Assay 2. The lesion by itself produced tissue retraction and, as a side effect, an enlargement of the lateral ventricle, though it did not evidence significant changes between the studied groups of each assay. Only the action of injuring the rats twice clearly increased this retraction [24]. Regardless of the administered substance, the injury by itself has a deleterious effect on CNS, and the treated groups, which undergo a double injury, present remarkable stereological changes. Therefore, the effectiveness of therapy must be supposed to be pretty high since a significant functional and morphological recovery was appreciated [4].

Suitability of the Model

Synergistic Effect of VEGF and GDNF

Some studies have demonstrated a cooperative crosstalk between VEGF-A and GDNF signaling pathways mediated by VEGFR2 and RET and suggesting a possible feedback loop between these two growth factors [29].

Both cytokines bind tyrosine kinase receptors (VEGF-R1 and 2 and GDNF the c-RET); therefore, it is likely that the protective effects of VEGF may be mediated using different signaling cascades in diverse cellular targets compared with GDNF.

Although neuroprotective effects of VEGF-A overexpression in models of PD were reported [30], detrimental vascular effects, such as edema and disruption of the blood–brain

barrier, occurred [31, 32]. These negative side effects have not been observed in our assays, despite VEGF-A binds to the neuroprotective VEGFR-1 and, in addition, to VEGFR-2, and the receptor is thought to mediate in angiogenic effects [33, 34]. VEGF and GDNF induce improvements in behavior and an enhancement of the surviving neurons, sprouting in order to neurorescue cells and activate neurogenesis. Furthermore, it would be necessary to investigate the signaling pathway of VEGF and GDNF, in order to assess the possible intracellular interaction.

A major finding in the present work, apart from the differences found in the study of the rostro-caudal topology, is the preservation of the ADN network after treatment with VEGF and GDNF. Combining both NTFs not only preserves the neuronal bodies but also has the ability to restore nigrostriatal axons.

Neurogenic Effect of VEGF and GDNF

To evaluate whether the NTF group could activate or maintain neuronal proliferation and cellular differentiation so as to support a possible neurogenic effect, we stained cells against BrdU and DCX. BrdU/DCX double immunofluorescence staining showed an enhanced proliferation near the SVZ in rats treated with VEGF and GDNF.

Correspondingly, the number of BrdU-positive cells from parkinsonized rats treated in the vehicle groups was lower than in the NTF group, and these rats did never co-express with DCX, suggesting that VEGF and GDNF could induce not only an increase but also a differentiation of neurons to migrate towards the injured regions.

Growth factors promote neurogenesis in the SVZ/olfactory bulb (OB)-system while the dopaminergic lesion has the opposite effect. In fact, GDNF is involved in neuronal survival and differentiation during development [35, 36] and VEGF promotes the proliferation and differentiation of dopaminergic cells in vivo [37]. In addition, it was also reported that growth factors in combination could induce neurogenesis in a synergistic way [38, 39].

Axodendritic Sprouting in Substantia Nigra

There is an emerging need for further investigations focusing on the role of compensatory responses after striatal fibers depletion and the decrease of ADN and neurons in SN regarding the pathophysiology of PD. Neurogenesis is a complex process, as it takes a long time for DA neurons to reach the SN in order to replace neuronal loss due to the lesion. Because of this, the remaining neurons re-innervate this damaged area. Thus, in addition to the cell loss that follows DA dennervation [28], it would be essential to examine what occurs upon treatment with VEGF and GDNF on axodendritic sprouting, such as a possible plasticity compensatory response in SN. Synaptic plasticity may contribute to ameliorate brain dysfunction in case of extreme neurodegeneration [40]. ADN density decreased less than neuronal density in all groups. This may be due to the compensatory plasticity of pre-existent neurons.

The group receiving NTF showed more significant signs of axodendritic sprouting than the other groups. Hence, a combination of both NTFs not only preserves the neuronal bodies but also has the ability to restore nigrostriatal axons [41].

Differential Distribution of the Neuronal Density in Substantia Nigra

Parkinsonized rats showed changes regarding their neuronal density in the entire SN and in e-SN. Rats receiving NTF showed a higher neuronal density in the e-SN (about 44 %) than in the entire SN (about 32 %). The time course of the experiments for both assays was different; this could explain the differences found in the e-SN for both assays.

Dopaminergic projections reach the entire striatal complex, following a rostro-caudal topography of the elongated terminal fields. Additional DA projections reach the amygdala body [42], and projections to the amygdala arise from the ventral tegmental area (VTA) and lateral SNc and SNl [6]. Connected to these topological gradients—and taking into account that the topography of SN provides for the organization of the nigrostriatal projection—we identified the "e-SN," which is topologically associated with the dorso-lateral region of the CPC, where the 6-OHDA lesion was induced [43]. A significant component of this e-SN is the SNl, which projects to the amygdala. This structure is preserved from the inflicted lesion. Therefore, remaining neurons from the SNl projecting towards the amygdala would be the basis for re-innervation using sprouting mechanisms. These could be reinforced by NTF spreading from CPC areas, making the recovery of functions possible as reported by several authors [4, 44].

Rostro-Caudal Gradients

A quantitative analysis of the rostro-caudal sections of the striatum revealed that rats receiving 6-OHDA presented the highest increase in TH-negative volume at caudal levels, while the saline group did not present any difference throughout the rostro-caudal axis (remaining TH-ir). This supports the special vulnerability of the dorso-lateral and caudal regions. Parkinsonized rats from Assay 2 also showed a similar distribution in the vehicle group, but rats receiving NTF showed a significant recovery in TH-positive volume at all levels. However, most of this incipient plasticity consists of wide territories occupied by fine positive fibers. This is a crucial point to reinforce this innovative proposal of using the volume of TH-negative fibers instead the IOD. Areas with positive fibers were usually undervalued when the IOD was measured. These

lightly positive areas are the basis for recovery, and these observations are in agreement with other reports concerned with the sprouting of TH-positive fibers in the striatum close to the GDNF injection [28, 45].

A rostro-caudal reduction in the number of neurons was already reported by Rosenblad [28], which was attributed to the toxicity of 6-OHDA. However, in the present study, a statistically significant difference was also found in the saline group (91 vs. 63 %).

Interestingly, this rostro-caudal reduction of the neuronal density was observed in rats treated with the vehicle (22 vs. 14 %) and the empty-NS (33 vs. 15 %), but not with NTF. This group showed opposite results like a marked rostro-caudal increase in the number of neurons in the entire SN (19 % at the rostral, 25 % at the middle, and 43 % at the caudal section) and in e-SN (37, 44, and 51 % respectively), which shows a significantly higher density at all levels. This implied a success in the recovery of neurons in the SN, presenting large differences between the rostral and the caudal levels.

ADN density showed a rostro-caudal decrease in all groups of both assays, following the same pattern than the TH-positive fibers in the striatum. This corresponds to the anatomical organization of basal ganglia [46]. The group receiving the NTF showed a regenerative and plasticity response, the ADN increasing at all considered levels with respect to the vehicle or the empty-NS group. Anatomical connections could explain that the changes observed in SN were induced by the activity of NTF in the striatum, i.e., their place of projection [47]. However, further studies are necessary to assess these effects according to the anatomical connections between the striatum and the SN along the rostro-caudal axis.

Acknowledgments The authors thank the support of the University of the Basque Country (UPV/EHU) (UFI 11/32), the Basque Government (Saiotek SA-2010/00028, GIC 794/13, IT 747/13), "Ministerio de Ciencia e Innovación" (SAF2010-20375), FEDER funds and SGIker (UPV/EHU). C. Requejo appreciates the UPV/EHU for a fellowship subvention.

References

1. Savitt JM, Dawson VL, Dawson TM (2006) Diagnosis and treatment of Parkinson disease: molecules to medicine. J Clin Invest 116:1744–1754
2. Olanow CW, Stern MB, Sethi K (2009) The scientific and clinical basis for the treatment of Parkinson's disease. Neurology 72:1–136
3. Gibb WR (1997) Functional neuropathology in Parkinson's disease. Eur Neurol 38(Suppl 2):21–25
4. Herrán E, Requejo C, Ruiz-Ortega JA, Aristieta A, Igartua M, Bengoetxea H, Ugedo L, Pedraz JL, Lafuente JV, Hernández RM (2014) Increased antiparkinson efficacy of the combined administration of VEGF- and GDNF-loaded nanospheres in a partial lesion model of Parkinson's disease. Int J Nanomedicine 9:2677–2687
5. Franco V, Turner RS (2012) Testing the contributions of striatal dopamine loss to the genesis of parkinsonian signs. Neurobiol Dis 47:114–1125
6. Bayer SA (1984) Neurogenesis in the rat neostriatum. Int J Dev Neurosci 2:163–175
7. Obeso JA, Rodriguez-Oroz MC, Goetz CG, Marin C, Kordower JH, Rodriguez M, Hirsch EC, Farrer M, Schapira AH, Halliday G (2010) Missing pieces in the Parkinson's disease puzzle. Nat Med 16:653–661
8. Glinka Y, Gassen M, Youdim MB (1997) Mechanism of 6-hydroxydopamine neurotoxicity. J Neural Transm Suppl 50:55–66
9. Herrán E, Ruiz-Ortega JÁ, Aristieta A, Igartua M, Requejo C, Lafuente JV, Ugedo L, Pedraz JL, Hernández RM (2013) In vivo administration of VEGF- and GDNF-releasing biodegradable polymeric microspheres in a severe lesion model of Parkinson's disease. Eur J Pharm Biopharm 85:1183–1190
10. Morera-Herreras T, Ruiz-Ortega JA, Linazasoro G, Ugedo L (2011) Nigrostriatal denervation changes the effect of cannabinoids on subthalamic neuronal activity in rats. Psychopharmacol (Berl) 214:379–389
11. Paxinos G, Watson C (1997) The rat brain in steretaxic coordinates. Academic, San Diego
12. Bjorklund A, Winkler C, Rosenblad C, Kirik D (1997) Studies on neuroprotective and regenerative effects of GDNF in a partial lesion model of Parkinson's disease. Neurobiol Dis 4:186–200
13. Przedborski S, Levivier M, Kostic V, Jackson-Lewis V, Dollison A, Gash DM, Fahn S, Cadet JL (1991) Sham transplantation protects against 6-hydroxydopamine-induced dopaminergic toxicity in rats: behavioral and morphological evidence. Brain Res 550:231–238
14. Brodkey JA, Gates MA, Laywell ED, Steindler DA (1993) The complex nature of interactive neuroregeneration-related molecules. Exp Neurol 123:251–270
15. Clarke LE, Barres BA (2013) Emerging roles of astrocytes in neural circuit development. Nat Rev Neurosci 14:311–321
16. Fuller HR, Hurtado ML, Wishart TM, Gates MA (2014) The rat striatum responds to nigro-striatal degeneration via the increased expression of proteins associated with growth and regeneration of neuronal circuitry. Proteome Sci 28;12:20
17. Barcia C, Bautista V, Sánchez-Bahillo A, Fernández-Villalba E, Faucheux B, Poza y Poza M, Fernandez Barreiro A, Hirsch EC, Herrero MT (2005) Changes in vascularization in substantia nigra pars compacta of monkeys rendered parkinsonian. J Neural Transm 112:1237–1248
18. Block ML, Li G, Qin L, Wu X, Pei Z, Wang T (2006) Potent regulation of microglia-derived oxidative stress and dopaminergic neuron survival: substance P vs. dynorphin. FASEB J 20:251–258
19. Sarre S, Yuan H, Jonkers N, Van Hemelrijck A, Ebinger G, Michotte Y (2004) In vivo characterization of somatodendritic dopamine release in the substantia nigra of 6-hydroxydopamine lesioned rats. J Neurochem 90:29–39
20. Agid Y, Javoy F, Glowinski J (1973) Hyperactivity of remaining dopaminergic neurones after partial destruction of the nigro-striatal dopaminergic system in the rat. Nat New Biol 245:150–151
21. Jankovic J, Shoulson I, Weiner WJ (1994) Early-stage Parkinson's disease: to treat or not to treat. Neurology 44(Suppl 1):4–7
22. Li Z, Decavel C, Hatton GI (1995) Calbindin-D28k: role in determining intrinsically generated firing patterns in rat supraoptic neurones. J Physiol 488:601–608
23. Hurley MJ, Brandon B, Gentleman SM, Dexter DT (2013) Parkinson's disease is associated with altered expression of CaV1 channels and calcium-binding proteins. Brain 136:2077–2097
24. Cervós-Navarro J, Lafuente JV (1991) Traumatic brain injuries: structural changes. J Neurol Sci 103:S3–S14
25. Surmeier DJ, Guzman JN, Sanchez-Padilla J, Goldberg JA (2011) The origins of oxidant stress in Parkinson's disease and therapeutic strategies. Antioxid Redox Signal 14:1289–1301
26. Jollivet C, Aubert-Pouessel A, Clavreul A, Venier-Julienne MC, Montero-Menei CN, Benoit JP, Menei P (2004) Long-term effect of intra-striatal glial cell line-derived neurotrophic factor-releasing

microspheres in a partial rat model of Parkinson's disease. Neurosci Lett 356:207–210
27. Garbayo E, Montero-Menei CN, Ansorena E, Lanciego JL, Aymerich MS, Blanco-Prieto MJ (2009) Effective GDNF brain delivery using microspheres—a promising strategy for Parkinson's disease. J Control Release 135:119–126
28. Rosenblad C, Kirik D, Bjorklund A (2000) Sequential administration of GDNF into the substantia nigra and striatum promotes dopamine neuron survival and axonal sprouting but not striatal reinnervation or functional recovery in the partial 6-OHDA lesion model. Exp Neurol 161:503–516
29. Tufro A, Teichman J, Banu N, Villegas G (2007) Crosstalk between VEGF-A/VEGFR2 and GDNF/RET signaling pathways. Biochem Biophys Res Commun 358:410–416
30. Yasuhara T, Shing T, Kobayashi K et al (2004) Neuroprotective effects of vascular endothelial growth factor (VEGF) upon dopaminergic neurons in a rat model of Parkinson's disease. Eur J Neurosci 19:1494–1504
31. Harrigan MR, Ennis SR, Sullivan SE, Keep RF (2003) Effects of intraventricular infusion of vascular endothelial growth factor on cerebral blood flow, edema, and infarct volume. Acta Neurochir (Wien) 145:49–53
32. Rite I, Machado A, Cano J, Venero JL (2007) Blood-brain barrier disruption induces in vivo degeneration of nigral dopaminergic neurons. J Neurochem 101:1567–1582
33. Olsson AK, Dimberg A, Kreuger J, Claesson-Welsh L (2006) VEGF receptor signalling—in control of vascular function. Nat Rev Mol Cell Biol 7:359–371
34. Falk T, Gonzalez RT, Sherman SJ (2010) The yin and yang of VEGF and PEDF: multifaceted neurotrophic factors and their potential in the treatment of Parkinson's disease. Int J Mol Sci 11: 2875–2900
35. Birling MC, Price J (1995) Influence of growth factors on neuronal differentiation. Curr Opin Cell Biol 7:878–847
36. Schwartz PM, Borghesani PR, Levy RL, Pomeroy SL, Segal RA (1997) Abnormal cerebellar development and foliation in BDNF−/− mice reveals a role for neurotrophins in CNS patterning. Neuron 19:269–281
37. Xiong N, Zhang Z, Huang J, Chen C, Zhang Z, Jia M, Xiong J, Liu X, Wang F, Cao X, Liang Z, Sun S, Lin Z, Wang T (2011) VEGF-expressing human umbilical cord mesenchymal stem cells, an improved therapy strategy for Parkinson's disease. Gene Ther 18:394–402
38. Sopova K, Gatsiou K, Stellos K, Laske C (2014) Dysregulation of neurotrophic and haematopoietic growth factors in Alzheimer's disease: from pathophysiology to novel treatment strategies. Curr Alzheimer Res 11:27–39
39. Pellegrini L, Bennis Y, Guillet B, Velly L, Garrigue P, Sabatier F, Dignat-George F, Bruder N, Pisano P (2013) Therapeutic benefit of a combined strategy using erythropoietin and endothelial progenitor cells after transient focal cerebral ischemia in rats. Neurol Res 35: 937–947
40. Gittis AH, Hang GB, LaDow ES, Shoenfeld LR, Atallah BV, Finkbeiner S, Kreitzer AC (2011) Rapid target-specific remodeling of fast-spiking inhibitory circuits after loss of dopamine. Neuron 71:858–868
41. Batchelor PE, Liberatore GT, Porritt MJ, Donnan GA, Howells DW (2000) Inhibition of brain-derived neurotrophic factor and glial cell line-derived neurotrophic factor expression reduces dopaminergic sprouting in the injured striatum. Eur J Neurosci 12:3462–3468
42. Lindvall O, Björklund A, Skagerberg G (1984) Selective histochemical demonstration of dopamine terminal systems in rat di- and telencephalon: new evidence for dopaminergic innervation of hypothalamic neurosecretory nuclei. Brain Res 306:19–30
43. Deumens R, Blokland A, Prickaerts J (2002) Modeling Parkinson's disease in rats: an evaluation of 6-OHDA lesions of the nigrostriatal pathway. Exp Neurol 175:303–317
44. Yue X, Hariri DJ, Caballero B, Zhang S, Bartlett MJ, Kaut O, Mount DW, Wüllner U, Sherman SJ, Falk T (2014) Comparative study of the neurotrophic effects elicited by VEGF-B and GDNF in preclinical in vivo models of Parkinson's disease. Neuroscience 258:385–400
45. Rosenblad C, Kirik D, Devaux B, Moffat B, Phillips HS, Björklund A (1999) Protection and regeneration of nigral dopaminergic neurons by neurturin or GDNF in a partial lesion model of Parkinson's disease after administration into the striatum or the lateral ventricle. Eur J Neurosci 11:1554–1566
46. García-Amado M, Prensa L (2013) Distribution of dopamine transporter immunoreactive fibers in the human amygdaloid complex. Euro J Neurosci 38:3589–3601
47. Ortuzar N, Rico-Barrio I, Bengoetxea H, Argandoña EG, Lafuente JV (2013) VEGF reverts the cognitive impairment induced by a focal traumatic brain injury during the development of rats raised under environmental enrichment. Behav Brain Res 246:36–46

OmniaScience

DOI: *HTTP://DX.DOI.ORG/10.3926/OMS.54*

REFERENCIAR ESTE CAPÍTULO:

Lafuente, J.V., Requejo, C.,Bengoetxea, H.,Ortuzar, N.,Bulnes, S.(2014). Angioglioneurinas y enriquecimiento ambiental: una prometedora alianza para la restauración del cerebro. En García Rodríguez, J.C. (Ed.). Neuroprotección en enfermedades Neuro y Heredo degenerativas. Barcelona, España: OmniaScience; 2014. pp.209-255.

Angioglioneurinas y enriquecimiento ambiental: una prometedora alianza para la restauración del cerebro

José Vicente Lafuente

Catalina Requejo

Harkaitz Bengoetxea

Naiara Ortuzar

Susana Bulnes

LaNCE, Dpto. Neurociencias UPV-EHU, Leioa (Bizkaia), España.

Correspondencia a:
J. V. Lafuente
Departamento de Neurociencias, Laboratorio de Neurociencias Clínicas y Experimentales (LaNCE), Facultad of Medicina y Odontología,
University of the Basque Country UPV/EHU, Barrio Sarriena s/n,
E48940 Leioa, Spain
e-mail: josevicente.lafuente@ehu.es

RESUMEN

El término angioneurinas ha sido propuesto para nombrar moléculas con efectos neuroprotectores, neurogénicos y neurotróficos. Estas moléculas inducen una variedad de respuestas, no sólo en células vasculares y neuronales, también en células gliales. Estas moléculas desempeñan un papel fundamental en el desarrollo del Sistema Nervioso Central (SNC) y en el mantenimiento de las condiciones óptimas para la supervivencia de las células nerviosas en adultos, tomando parte en la protección, división y proliferación de las células neuronales, gliales y endoteliales. Entre las angioneurinas más importantes se encuentran: el factor de crecimiento endotelial vascular (VEGF), el factor derivado del cerebro (BDNF), el factor de crecimiento insulínico tipo-1 (IGF-1) o la eritropoyetina (EPO). Se ha encontrado disminución en la expresión de las angioneurinas en el envejecimiento y en condiciones patológicas, tales como las enfermedades neurodegenerativas o las lesiones cerebrales de origen traumático e isquémico. La administración de estas moléculas actúa como un restaurador del SNC. Dado que sus acciones involucran tanto a las neuronas como a la glía y a los vasos, propusimos el término angioglioneurinas para nombrar a las moléculas que actúan sobre los tres componentes de la unidad neurogliovascular, que la agrupa e identifica como un todo y le confiere además el rango de unidad morfo-funcional del SNC.

El enriquecimiento ambiental ha sido descrito como la combinación de elementos inanimados, la estimulación social, y el ejercicio físico. El enriquecimiento ambiental es la modificación o adición de elementos en el entorno de un animal cautivo de tal manera que con ello se estimulan conductas semejantes a las propias del animal sano en su medio natural. El enriquecimiento pretende estimular comportamientos que satisfagan las necesidades físicas y psicológicas del animal, mejorando con ello las funciones tanto en salud como en la enfermedad, incluyendo cambios morfológicos como fisiológicos. Estos cambios incluyen el aumento de la actividad neuronal y la plasticidad, de la población glial, así como de la remodelación y maduración de la red microvascular. Criarse en ambientes enriquecidos adelanta el inicio del periodo crítico, reduce el deterioro cognitivo fisiológico relacionado con la edad o protege contra disfunciones del comportamiento como por ejemplo las debidas a la adición a drogas.

Entre los efectos beneficiosos de los ambientes enriquecidos en condiciones patológicas se encuentra la recuperación funcional tras procesos traumáticos o isquémicos, la prevención ante las enfermedades neurodegenerativas,

etc. Estos efectos son atribuidos, en parte, a un aumento de la producción de angioglioneurinas.

En conclusión, la exposición a un ambiente enriquecido implica un aumento de la expresión de estas moléculas que podría mejorar la evolución de la mayoría de las enfermedades cerebrales. La combinación de la administración de angioglioneurinas y enriquecimiento ambiental podría ser una estrategia terapéutica prometedora para restaurar el cerebro, si bien hay que conocer mejor algunos efectos secundarios que podría conllevar esta combinación.

1. Introducción

Hay un determinado grupo de citoquinas o factores de crecimiento que debido a su acción tanto sobre neuronas como sobre la microvascularización cerebral han sido denominadas "angioneurinas" [1]. Una angioneurina típica es el factor de crecimiento vascular endotelial (VEGF), otras que se describieron primeramente como neurotrofinas, son por ejemplo el factor neurotrófico derivado del cerebro (BDNF), el factor de crecimiento insulínico tipo 1 (IGF-1) o la eritropoyetina (EPO). Independientemente de su origen, todas estas moléculas actúan sobre la unidad neurovascular [2] y la mayoría de ellas presentan también efectos sobre la neuroglia por ello se propone el término de angliooglioneurina [3, 4].

Entre los mecanismos fundamentales para la supervivencia de las células nerviosas, están las cadenas metabólicas inducidas por las neurotrofinas. Estas desempeñan un papel clave como agentes antiapoptóticos [5]. Las angioglioneurinas pueden llegar a ser un importante recurso terapéutico en la restauración del SNC, especialmente en patologías como apoplejías o lesiones cerebrales traumáticas [4].

El VEGF es un factor angiogénico fundamental durante el desarrollo [6], en la angiogénesis patológica, y como mediador de la permeabilidad vascular [7]. Este factor también presenta propiedades neuroprotectoras, neurotróficas y neurogénicas [8, 9, 10]. La función neuroprotectora del VEGF parece ser debida a una combinación de efectos neuroprotectores directos y a la estimulación de la angiogénesis. En la misma dirección, estudios recientes encontraron, que la neurotrofina BDNF desempeñaba un importante papel en la regulación del desarrollo vascular y en la respuesta a lesiones [11, 12]. Por otra parte, el IGF-1,

además de sus efectos sobre las neuronas, se ha descrito también, como un modulador de la formación de vasos durante el desarrollo del cerebro [13], y como un importante factor promotor en el desarrollo de los vasos [14], y la EPO como la promotora de la angiogénesis [15, 16]. Por tanto, y teniendo en cuenta las funciones previamente descritas, se ha propuesto la administración de angioglioneurinas en modelos de isquemia [17, 18, 19], trauma cerebral [20, 21, 22, 23] y enfermedades neurodegenerativas como el Parkinson, Alzheimer o Esclerosis Multiple [24, 25, 26, 27, 28, 29, 30, 31, 32].

Efectos similares se han descrito para el enriquecimiento ambiental (EA). Numerosos estudios refieren evidencias sobre los cambios inducidos por este paradigma durante el desarrollo del SNC tanto en salud como en enfermedad [33]. El enriquecimiento ambiental tiene importantes efectos sobre la plasticidad de las conexiones nerviosas, especialmente en la corteza visual, donde se ha demostrado que criar desde el nacimiento en un ambiente enriquecido conlleva la aceleración del desarrollo visual [34].

El enriquecimiento ambiental consiste en combinar una serie de elementos y circunstancias que ayudan a estimular conductas semejantes a las propias del animal sano en su medio natural. Así los animales disponen de habitáculos mas amplios, donde se disponen diferentes elementos de variadas formas y colores que son cambiados de posición y sustituidos por otros frecuentemente. En cada ambiente conviven un amplio número de individuos. Todo esto incrementa la estimulación social, visual y el ejercicio físico. Esta asociación induce cambios anatómicos [35], estimula la neurogénesis [36], y es ampliamente propuesta como una medida neuroprotectora en enfermedades neurodegenerativas [37, 38, 39]. Sus efectos han sido estudiados en modelos experimentales de la enfermedad de Alzheimer [40], Parkinson [41], Hungtington [42], lesiones cerebrales traumáticas [43, 44, 45], accidentes cerebrovasculares [46] e incluso tumores [47].

El enriquecimiento ambiental incrementa la expresión de diversos factores de crecimiento que desempeñan un importante papel en el trofismo neuronal, como por ejemplo el factor de crecimiento nervioso (NGF) [48], el factor neurotrófico derivado del cerebro (BDNF) [49, 50], la neurotrofina-3 (NT-3) [51] y el VEGF [52]. El aumento de la actividad neuronal inducida por estímulos ambientales desencadena una serie de eventos importantes para la plasticidad cortical, que incluyen la aceleración del desarrollo del sistema visual a nivel fisiológico, molecular y de comportamiento [34, 49] así como un aumento de la red microvascular [52].

La administración de angioglioneurinas, solas o en combinación con el enriquecimiento ambiental, ha propuesta como una estrategia terapéutica para diversas enfermedades del SNC [3].

En resumen, la exposición a entornos enriquecidos mejora el desarrollo del SNC, con un aumento en la estructura y función de todos los elementos de la unidad neurogliovascular. Por lo tanto, las moléculas que median estas mejoras se podrían denominar angioglioneurinas debido a su triple función.

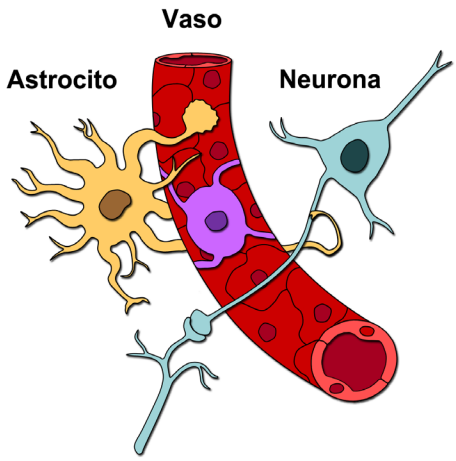

Figura 1. *Representación esquemática de los elementos de la unidad neurogliovascular.*

El objetivo de este capítulo es revisar el potencial neurorestaurador (NRT) del la administración de angioglioneurinas y del enriquecimiento ambiental sobre la corteza cerebral, y las ventajas y desventajas de una estrategia sinérgica basada en su combinación.

2. Angioglioneurinas

2.1. Factor de crecimiento endotelial vascular (VEGF)

Inicialmente fue aislado como factor de permeabilidad vascular (VPF) [53], el gen correspondiente fue clonado en 1989 [54] y posteriormente tras comprobar su participación en los procesos de angiogénesis fue denominado factor de crecimiento endotelial vascular (VEGF) [55]. La familia del VEGF consta de cinco moléculas con un alto grado de homología, VEGF-A, VEGF-B, VEGF-C, VEGF-D

y el factor de crecimiento placentario (PlGF) [56]. El VEGF-A (VEGF) es la forma predominante y es una glicoproteína homodimérica de 45 kDa inducible por hipoxia. De la remodelación alternativa del ARNm del VEGF hay identificadas 7 isoformas, la principal de ellas en el cerebro es el VEGF165, que contiene algunos residuos básicos en parte difusibles y en parte se unen a la matriz extracelular [57].

Parte de la pluripotencialidad del VEGFA165 se debe a la existencia de una variante que se denominó VEGF-A165b [58, 59]. La isoforma 165 y la 165b son generadas por el mismo transcrito, diferenciándose tan solo en los últimos seis amino ácidos codificados por el octavo exón [60]. Esta pequeña variación le confiere dos propiedades que diferencia radicalmente la función de ambas moléculas. Una de esas propiedades es su afinidad por los heparansulfatos de la matriz extracelular, la forma b la pierde, y la otra afecta a su interacción con los receptores de membrana, la forma b dimeriza dos receceptores VEGFR en lugar de un VEGFR con una Neuropilina1 como hace la otra forma, la consecuencia de todo ello es que esta forma b solo media señales de supervivencia en las células. [61]. El VEGF-A165b está altamente expresado en tejidos no angiogénicos [62, 63], y a diferencia del VEGF-A165, está regulado a la baja en tumores y en otras patologías asociadas con una neovascularización anormal [64, 65, 66].

El VEGF es el factor angiogénico más importante en el desarrollo [6], en la angiogénesis patológica [67, 68, 69, 70] y también en la permeabilidad vascular [7]. Pero el papel del VEGF en el tejido nervioso es mucho más extenso adquiriendo cada vez mas relevancia, a medida que se conocen mejor, sus propiedades neuroprotectoras, neurotróficas y neurogénicas [8, 9, 10].

Inicialmente, en el cerebro en desarrollo, el VEGF es producido por neuronas. Mientras que en P13 la expresión neuronal del VEGF comienza a disminuir, la expresión astrocitaria se hace más evidente, hasta que la localización del VEGF cambia, pasa de ser predominantemente neuronal a glial en P24 [52]. Sin embargo, en el cerebro hipóxico, los niveles altos de VEGF neuronal y glial se mantienen hasta P33 [71].

Los principales receptores para el VEGF son los receptores tirosina quinasa VEGFR-1 (Flt-1) y VEGFR-2 (Flk-1/KDR) [6, 72]. El VEGFR-2 desempeña un papel crítico en la correcta diferenciación y organización de las células endoteliales en los lechos vasculares, siendo el mayor mediador de los efectos mitogénicos, angiogénicos y

de aumento de permeabilidad del VEGF [73]. Por otro lado, se cree que el VEGFR-1 regula negativamente la angiogénesis, evitando la unión del VEGF al VEGFR-2 [74]. Se ha descrito también, que el VEGF se une a los receptores no tirosina quinasa, a neuropilina-1 (NP-1) y neuropilina-2 (NP-2), que pueden estar involucrados en la orientación del axón [75]. La coexpresión de los receptores VEGFR-2 y NP-1 aumenta la unión de VEGF a VEGFR-2 y la quimiotáxis mediada por VEGF [76].

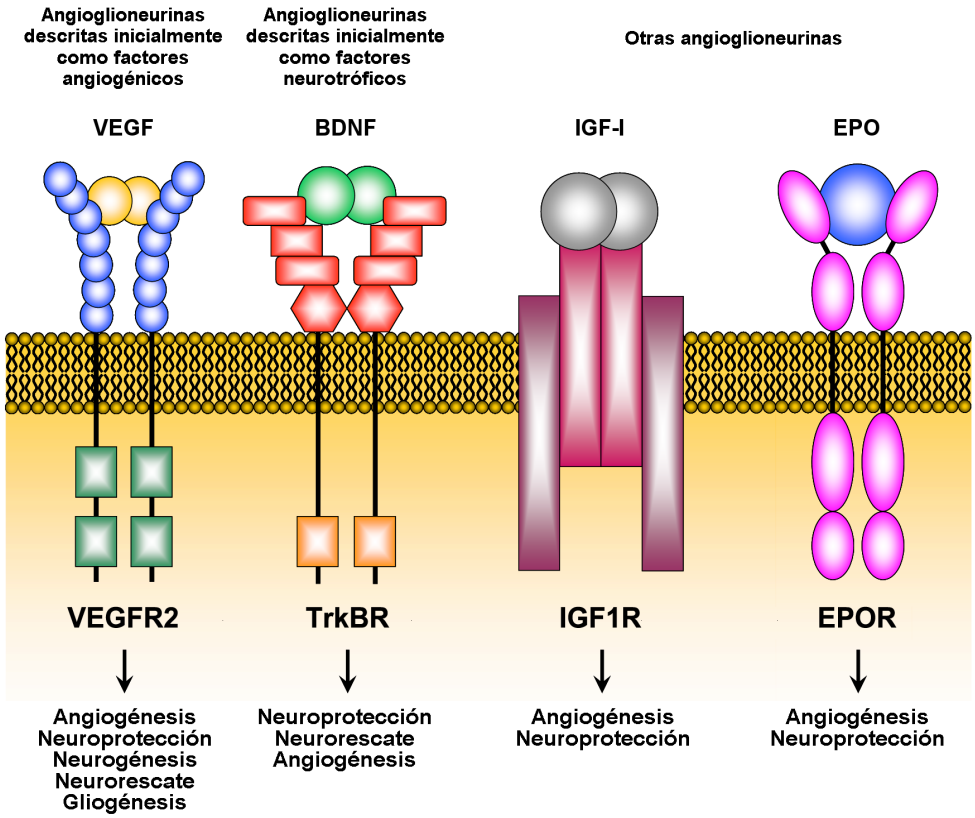

Figura 2. *Representación esquemática de las angiglioneurinas consideradas y sus receptores (modificado de Zacchigna et al., Nat Rev Neurosci; 9(3):169-81. Review).*

En condiciones patológicas, el VEGFR-2 media un efecto antiapoptótico a través de las rutas de señalización dependientes de PI3k que promueve la supervivencia de las células endoteliales inducida por VEGF y se relaciona con la apertura de la BHE en la lesión cerebral [77]. Se ha descrito también, un papel neuroprotector

para el VEGF, que está mediado predominantemente por el VEGFR-2 [5, 78], el cual opera a través de las rutas de PI3/Akt y de MEK/ERK [79, 80]. Estudios recientes han demostrado también que la neuroprotección mediada por el VEGF rescata neuronas colinérgicas de la muerte celular inducida por NMDA *in vivo* [81].

Además de sus propiedades angiogénicas y neuroprotectoras, el VEGFesta implicado en la neurogénesis adulta, promoviendo la proliferación y diferenciación de precursores neuronales [82] o ejerciendo una acción mitógena directa sobre dichos precursores [8, 83, 84]. Además, se ha demostrado que la administración intracerebroventricular del VEGF estimula la neurogénesis en adultos en la zona subventricular y subgranular del giro dentado del hipocampo [8] y promueve el subsiguiente crecimiento de neuritas [85].

Por otro lado, el VEGF media la permeabilidad vascular, induciendo modificaciones en las proteinas transmembrana y en las del citoesqueleto celular que les sirven de anclaje y que constituyen el sustrato morfologico de la barrera hemoencefálica (BHE) [86, 87]. La señalización del VEGF actúa sobre las células endoteliales y también sobre astrocitos y microglía. La astroglía está regulada por varios factores de crecimiento, de hecho, se ha descrito un papel regulador del VEGF sobre el linaje celular astrocitario [88, 89]. Además, se ha demostrado que la infusión exógena de este factor estimula la producción de otros factores astrogliales mitogénicos como el bFGF, potenciando así la acción proliferativa del VEFG [90]. El VEGF-A derivado de astrocitos se ha referido como un importante mediador de la permeabilidad de la barrera hematoencefálica, de la infiltración linfocitaria etc, Estos hallazgos identifican el bloqueo de la señalización del VEGF-A como una vía de protección frente a los trastornos inflamatorios del SNC [91].

En conclusión, en el sistema nervioso el VEGF ejerce efectos pleiotrópicos, influyendo directamente sobre la proliferación, migración y supervivencia de diferentes tipos celulares. Asi en las neuronas actúa sobre el crecimiento axonal y la supervivencia, en las células madre neuronales sobre la proliferación (neurogénesis) y migración, en los astrocitos sobre la proliferación, en las células de Schwann sobre la supervivencia y migración celular y en la microglía sobre la proliferación y migración [92].

2.2. VEGF y enfermedades del sistema nervioso central

El papel terapéutico del VEGF sobre las enfermedades del SNC se ha estudiado en diferentes modelos experimentales. Se ha encontrado que el VEGF y sus receptores están sobreregulados en la isquemia cerebral focal [93, 94, 17, 18]. Experimentos *in vivo* demuestran que los efectos del VEGF en la isquemia cerebral pueden ser tanto beneficiosos como perjudiciales. Mientras que la administración intravenosa temprana del VEGF después de la lesión produce un aumento de permeabilidad de la BHE [95], la administración sistémica, tópica e intracerebral del VEGF ejerce efectos beneficiosos en varios modelos de accidentes cerebrovasculares [93, 80]. La ruta de liberación y el momento de administración del VEGF parece determinar los resultados del tratamiento tras una lesión isquémica [57]. Estos efectos beneficiosos podrían estar relacionados con la angiogénesis estimulada por el VEGF, la permeabilidad vascular modulada, los efectos neuroprotectores directos o bien por la neurogénesis inducida. También hay evidencias de que el VEGF promueve la reparación del nervio después de una lesión de la médula espinal. En estudios llevados a cabo tras la lesión traumática de la medula espinal se encontraba un aumento de la expresión del VEGF y de sus receptores [21] y además la administración local del VEGF mejoró la recuperación [96]. Estos estudios han demostrado que mientras la inhibición del VEGFR-2 extiende el área hemorrágica [96] y aumenta los marcadores de daño neuronal y glial [21], la administración del plásmido del VEGF mejora el resultado de esta lesión [97].

El VEGF también ha sido considerado como protector en las enfermedades neurodegenerativas. Oosthuyse et al (2001) publicaron un estudio que sugiere una relación entre el VEGF y la escleorosis lateral amiotrófica (ELA). Estos autores manipularon el gen del VEGF en ratones, dando lugar a la muerte del 60% de los ratones recién nacidos. El 40% de los ratones que sobrevivieron mostraban síntomas de degeneración de las neuronas motoras a los cinco meses de edad. Además, las neuronas motoras mostraban signos neuropatológicos similares a los de ELA [27]. Niveles reducidos del VEGF también aumentan la gravedad de la degeneración de las neuronas motoras en el modelo estándar de ELA (ratones SOD1G93A) [98]. Se ha sugerido dos posibles mecanismos por los que pueda estar influida la degeneración de las neuronas motoras: la estimulación neurotrófica insuficiente de estas células por parte del VEGF o las anormalidades vasculares debidas a un VEGF insuficiente que pueden poner las neuronas en riesgo por la

aparición de una neurodegeneración tardía provocada por una isquemia crónica [99].

En otros trastornos de las neuronas motoras como la atrofia muscular espinal y bulbar (AMEB) ligada al cromosoma X, los ratones mostraban niveles reducidos de VEGF [100].

La disfunción neurovascular contribuye al deterioro cognitivo y a la neurodegeneración en la enfermedad del Alzheimer (EA). El acoplamiento neurovascular, la inflamación, la regresión de los vasos sanguíneos y la hipoperfusión cerebral podría estar relacionada con los niveles de VEGF, dado los importantes efectos que ejerce sobre las células endoteliales y las neuronas [101, 30, 102]. Se ha propuesto que el aumento de los niveles de expresión del VEGF se produce como una respuesta a la hipoperfusión y a la subsecuente hipoxia tisular relativa que tiene lugar en los cerebro de estos pacientes. Por otro lado en células del sistema inmunes de pacientes con enfermedad de Alzheimer se ha descrito una reducción en la expresión de VEGF, siendo atribuida esta observación a los efectos tóxicos de la β-amiloide sobre dicha expresión [103]. Por todo ello el papel del VEGF en la enfermedad de Alzheimer se considera controvertido y se necesitan más estudios para aclararlo.

In vitro se comporbó que el VEGF protege las neuronas dopaminérgicas mesencefálicas contra la 6-hidroxidopamina (6-OHDA) que induce muerte celular, infiriendo de ello que el VEGF tiene efectos neuroprotectores sobre las neuronas dopaminérgicas, objetivo principal de la neurodegeneración en la enfermedad del Parkinson. Estudios *in vivo* también han puesto de manifiesto efectos beneficiosos sobre el sistema de neuronas dopaminérgicas, tanto a nivel patológico como en estudios de comportamiento. El trasplante de células del riñón de hámster recién nacido (BHK) secretoras de VEGF, en el estriado de ratas, protege contra la administración de 6-OHDA [29]. Estudios recientes sugiere que el trasplante de células madre mesenquimales del cordón umbilical humano (CMCUH) combinado con el VEGF, podría ser una estrategia útil para el tratamiento de la enfermedad del Parkinson, puesto que la expresión del VEGF aumenta significativamente la diferenciación dopaminérgica de las CMCUH *in vivo* [104].

Respecto a enfermedades autoinmunes los niveles de VEGF en suero correlacionan bien con algunas de ellas [105]. Las lesiones en la esclerosis múltiple se asocian con vasos anormales que presentan aumento de la permeabilidad y una alteración de

la perfusión [106, 107]. VEGF puede jugar un papel doble en la esclerosis múltiple, en el modelo de encefalomielitis experimental autoinmune (EAE) en ratas, por un lado la infusión en el estriado empeora la inflamación de la placa y por otro reduce la gravedad de la enfermedad [108].

2.3. Neurotrofinas

Las neurotrofinas son una parte importante de la familia de las angioneurinas, debido a su amplia participación en ambos procesos neuronales y vasculares. Los últimos hallazgos han indicado su implicación en el desarrollo y mantenimiento de los vasos cerebrales, además de su clásico papel en el desarrollo del sistema nervioso [109].

Las neurotrofinas son una familia de proteínas que juegan un papel fundamental en la regulación de la función neuronal, plasticidad, desarrollo y supervivencia [110, 111, 112, 113, 114, 115, 116]. En los mamíferos, las neurotrofinas se componen de cuatro miembros de proteínas relacionadas estructuralmente: el factor de crecimiento nervioso (NGF), el factor neurotrófico derivado del cerebro (BDNF), la neurotrofina-3 (NT-3) y la neurotrofina-4 (NT-4), derivados del mismo gen originario [117]. Inicialmente, las neurotrofinas son sintetizadas como proteínas precursoras (protoneurotrofinas), similares a otros neuropéptidos. Estas protoneurotrofinas son escindidas intracelularmente por varios enzimas que dan lugar a proteínas maduras que son liberadas en el medio extracelular [118]. Cada una de estas proteínas en su forma madura (con un peso molecular aproximado de 13 kDa) es una proteína compleja con una pareja (dímero), activando de este modo a los receptores específicos [119].

Las neurotrofinas ejercen su función mediante dos tipos de receptores transmembrana: la familia de receptores tirosina quinasa (Trk) [120] y el receptor pan-neurotrofina p75NTR (p75 receptor de neurotrofinas). Trk media la proliferación celular, supervivencia y quimiotaxis, y el p75NTR media dos respuestas, por un lado cuando se coexpresan con los receptores Trks, p75NTR mejora la afinidad y la especificidad de las neurotrofinas unidas a Trks, para promover la supervivencia. Por otro lado, la activación de p75NTR por neurotrofinas puede iniciar la apoptosis cuando p75NTR se coexpresa con sortilina, un miembro de la familia del VpS10p [121]. Todas las neurotrofinas se unen con una afinidad similar a p75NTR, pero cada una se une específicamente con elevada afinidad a diferentes receptores Trk [122].

Las neurotrofinas han sido originalmente caracterizadas como factores de crecimiento por sus efectos en la proliferación, diferenciación, y supervivencia de neuronas tanto en el desarrollo como en la edad adulta [111]. Más recientemente, se ha descrito su papel en la regulación de la plasticidad sináptica y en la orientación y guía de los conos de crecimiento axonales [123, 124, 122]; pero las funciones de las neurotrofinas y de sus receptores han sido descritas también en las células no neuronales, tales como las células endoteliales, células musculares lisas, células inmunes y células epiteliales [125, 126, 127, 128, 129, 130].

2.4. Factor neurotrófico derivado del cerebro (BDNF)

El BDNF es un homodímero de 27 Kda que fue identificado por Barde y clonado por Leibrock en los años 80 y es producido por las células gliales principalmente en el cerebro y en la médula espinal [131, 132]. Esta proteína muestra una homología significativa con el factor de crecimiento nervioso (NGF), tanto en sus propiedades bioquímicas (punto isoeléctrico, dimerización y conservación de cisteínas) como en sus propiedades biológicas (supervivencia de neuronas en cultivo).

Los niveles de ARN mitocondrial del BDNF son más abundantes en el cerebro adulto que en el cerebro embrionario [133]. En general, la expresión persistente y transitoria del ARNm se ha demostrado en varias regiones del cerebro de ratas en desarrollo, sugiriendo la existencia de un gradiente rostro-caudal en la expresión de BDNF durante el desarrollo posnatal del cerebro, indicando de este modo su relación con la maduración neuronal [134]. El BDNF muestra un patrón característico de expresión en el hipocampo, mientras que en otras partes tiene una distribución que abarca regiones de la corteza, claustrum, del núcleo endopririforme, de la amígdala y del cerebelo [135, 136, 137, 138].

Desde su descubrimiento, un gran número de evidencias hablan sobre su papel en el desarrollo, fisiología y patología del cerebro. Su importancia se ha demostrado en el desarrollo y supervivencia celular de neuronas corticales y del hipocampo [109]. Además, promueve la diferenciación neuronal de células progenitoras de la pared ventricular del cerebro anterior adulto [139] y tiene un papel esencial en la neuroprotección del SNC. *In vivo*, se ha descrito que el BDNF protege diferentes tipos de neuronas frente a una lesión [140, 141]. Se ha descrito un efecto neuroprotector relevante cuando se administra BDNF por vía intravenosa tras el comienzo de isquemia cerebral focal [141]. Otra serie de experimentos *in vitro* han demos-

trado que el BDNF promueve la supervivencia celular a través de la activación de TrkB, induciendo varias proteínas G pequeñas, así como a través de las rutas reguladas por MAP quinasas (MAPK), PI 3-quinasa (PI3K) y fosfolipasa C [109]. En cultivos de neuronas del hipocampo, el efecto neuroprotector del BDNF fue demostrado contra la toxicidad del glutamato [142]. Algunos resultados confirman que el BDNF junto con el IGF-1 previenen la muerte celular inducida por privación de suero en neuronas del hipocampo[143]. El BDNF también puede promover la supervivencia neuronal en el hipocampo bajo condiciones de defecto de insulina [144].

Evidencias recientes sugieren que el BDNF participa en la regulación de la plasticidad sináptica que surge de la actividad asociada con los procesos de aprendizaje y de memoria [145, 146]. Esta posibilidad es sustentada por varios hallazgos, entre los cuales podemos mencionar que la inducción de la potenciación a largo plazo (LTP) causa aumentos en los niveles del ARNm del BDNF y de su receptor TrkB [147]. Se ha observado también que el BDNF es un mediador critico de plasticidad dependiente de la experiencia en las áreas corticales visuales [148].

A parte de los conocidos efectos sobre las neuronas, estudios recientes han encontrado que el BDNF juega un importante papel en la regulación del desarrollo vascular y en la respuesta a las lesiones. Este factor se expresa de manera específica tanto durante el desarrollo como en la edad adulta [12]. Las células endoteliales de las arterias y capilares del corazón y de los músculos expresan BDNF y TrkB. La falta de BDNF tiene como resultado la disminución de los contactos entre las células endoteliales, y la apoptosis de las mismas. Este factor está implicado en la regulación de los niveles del VEGF en las células del neuroblastoma, indicando que las terapias dirigidas a BDNF/TrkB/PI3K, a las rutas de transducción de señal mTOR y/o a HIF-1alfa tienen el potencial para inhibir la expresión del VEGF y limitar el crecimiento del neuroblastoma [125]. Por otra parte, el BDNF es capaz de inducir neoangiogénesis a través de las células endoteliales del músculo esquelético que expresan TrkB o por reclutamiento de subconjuntos específicos de células hematopoyéticas derivadas de la médula ósea TrkB+, proporcionando un soporte periendotelial para vasos recién formados [149]. La hipoxia crónica subletal, además de alterar la permeabilidad característica de la microvascularización cerebral, produce angiogénesis inducida por un aumento de la secreción de VEGF y BDNF por las células endoteliales y los astrocitos [150].

2.5. BDNF y enfermedades del sistema nervioso central

El BDNF ocupa una posición central en la patología molecular de un gran número de enfermedades cerebrales. El BDNF está implicado en la cascada de cambios electrofisiológicos y de comportamiento que subyacen al estado epiléptico [151]. La epileptogénesis en modelos animales pueden ser inhibida por la infusión de anticuerpos anti-BDNF o usando animales knockout para el BDNF [152, 153]. Los datos electrofisiológicos y de comportamiento demuestran también que la inhibición de la transducción del BDNF inhibe la sensibilización al dolor central [154]. Las enfermedades neurodegenerativas tales como el Alzheimer o el Parkinson muestran una reducción en la expresión del BDNF en el hipocampo o en la substantia nigra [24, 26]. Trastornos de comportamiento como la depresión, también muestran una disminución de los niveles de ARNm del BDNF [155].

2.6. Factor de crecimiento insulínico tipo I (IGF-I)

El IGF-I es una proteína similar a la insulina [156] y es uno de los principales mediadores de la acción de la hormona de crecimiento [157]. El IGF-I es una proteína de cadena sencilla de 70 amino ácidos con tres puentes disulfuro intramoleculares y un peso molecular 7,649 KDa. Se sintetiza principalmente en el hígado (también en riñón) y en los tejidos diana, de una manera autocrina y paracrina. La mayor parte de todo el IGF-I sanguíneo se une a las proteínas transportadoras (BPs). Hay 6 proteínas de unión al IGF (IGF-BPs), lo que aumenta en gran medida la complejidad del sistema IGF [158]. Estos complejos de unión prolongan la vida media del IGF, regulan su distribución en los tejidos y facilitan o bloquean la unión a sus receptores en los tejidos diana [159]. El IGFBP-3 es la proteína más abundante de todas las que se unen al IGF (transportando alrededor del 80% del IGF). El transporte del IGF al sistema nervioso central era un punto controvertido hasta que Nishijima et al. [160], sugirieron que el transporte localizado del IGF através de la barrera hematoencefálica venia posibilitado por el acoplamiento neurovascular que libera una serie de mensajeros que estimulan la acción de la metaloproteinasa-9, que lleva a la escisión de IGFBP-3, permitiendo el paso del IGF sérico al SNC a través de su interacción con el transportador endotelial de lipoproteínas relacionado con el receptor 1. Se tata pues de un proceso posibilitado por la actividad neuronal y la existencia de receptores específicos.

La expresión del IGF-I está restringida en el cerebro a regiones y periodos de desarrollo axonal, maduración dendrítica y sinaptogénesis [161, 162]. El IGF-I actúa principalmente a través de su receptor tirosin quinasa (IGF-1R), que está ampliamente distribuido en el cerebro. La unión de IGF-I a IGF-IR puede activar dos importantes rutas de señalización, las rutas PI3K/Akt y MAPK, estimulando el crecimiento y supervivencia de tipos celulares particulares [156]. El IGF-IR también se entrecruza con la ruta del receptor del factor de crecimiento epidérmico (EGFR) [163, 164], y esta interacción entre las rutas de señalización de EGFR y de IGF-IR puede ocurrir directamente por heterodimerización de los receptores, o indirectamente a través de las moléculas comunes de señalización reguladas a la baja [164]. Una variedad de ensayos *in vitro* e *in vivo* han demostrado que el IGF está involucrado en el desarrollo del sistema nervioso central, durante ambos periodos: prenatal y posnatal. El IGF es un factor de supervivencia para las neuronas sensoriales y motoras [159], actuando como un neuroprotector contra la excitotoxicidad y el estrés oxidativo [165, 166]. Este factor desempeña un papel protector contra la citotoxicidad, para los precursores de los oligodendrocitos [167], y para los oligodendrocitos maduros contra los efectos inducidos por la muerte causada por el factor de necrosis [168]. El IGF ejerce a su vez, efectos sobre la proliferación de los progenitores neurales y de los progenitores de los oligodendrocitos, recuperando así, células de un accidente cerebrovascular isquémico a través de la regeneración, y mejorando la proliferación de progenitores neurales endógenos en ratas [169]. El IGF promueve la sinaptogénesis y la neurogénesis en el giro dentado del hipocampo [170] y modula la plasticidad cerebral a través del crecimiento de las neuritas, de la sinaptogénesis y de la liberación de neurotransmisores [171, 172].

El IGF es importante en el desarrollo de los vasos sanguíneos cerebrales, siendo un factor angiogénico conocido [14]). El IGF-I modula la formación de los vasos durante el desarrollo cerebral [13], modulando también la actividad angiogénica basal y reparando la disminución gradual de la densidad vascular que acompaña al envejecimiento cerebral [173]. La disminución de los niveles del IGF-I en suero inevitablemente se traduciría en la disminución de las capacidades angiogénicas de los cerebros en envejecimiento [174]; pero correspondientemente, los mismos autores afirman que el ejercicio físico promueve la angiogénesis mediada por el IGF-I, ejerciendo un papel neuroprotector y angiogénico. Algunos estudios demuestran que los efectos del ejercicio físico en el cerebro están mediados por IGF-I [175, 176], siendo el IGF-I un importante agente protector fente a la lesión

cerebral [177], isquemia y traumas [178], o cualquier otra patología que requiera la formación de nuevos vasos sanguíneos en el cerebro [179].

2.7. IGF y enfermedades del sistema nerviosos central

La investigación de los niveles de IGF-I se centra específicamente en el envejecimiento y en las enfermedades neurodegenerativas [25], puesto que la edad se asocia con niveles bajos de IGF-I en suero en modelos animales [180] y también en seres humanos [181]. Una serie de patologías cerebrales, que van desde accidentes vasculares hasta la enfermedad del Alzheimer, muestran niveles de IGF-I alterados en suero, pero en este caso hay resultados controvertidos. Ciertas evidencias sugieren que el IGF-I podría ser de utilidad terapéutica en la enfermedad del Alzheimer [182] mientras que otros estudios muestran en cambio que la inhibición del IGF-I, también podría ser beneficioso en dicha enfermedad [183, 184]. Cada vez hay mas evidencias que apoyan el concepto de que la enfermedad del Alzheimer es fundamentalmente una enfermedad metabólica con alteraciones sustanciales y progresivas en la utilización de la glucosa cerebral, y en la capacidad de respuesta a la insulina y a la estimulación de IGF [185].

También hay una relación entre este factor de crecimiento y el cáncer [186]. Los niveles altos de IGF-I circulante y la expresión de IGF-IR están asociados con un mayor riesgo de padecer varios tipos de cánceres comunes. Por ejemplo, en el mieloma múltiple, el IGF-IR es uno de los principales mediadores del crecimiento y de la supervivencia celular [187]. La señalización del IGF-IR es crucial para la transformación tumoral y para la supervivencia de las células malignas, por ello se están desarrollando estrategias terapéuticas dirigidas al desarrollo de antagonistas para el IGF-IR [188].

2.8. Eritropoyetina (EPO)

La eritropoyetina (EPO) es una glicoproteína purificada en 1977 [189] y aislada por [190]. Inicialmente fue descrita como la principal reguladora de eritropoyesis, dado que inhibía la muerte celular programada de los eritrocitos y en consecuencia, permitía su maduración [191]; sin embargo, estudios recientes han demostrado que esta citoquina actúa en diferentes tejidos, incluyendo al sistema nervioso [192]. Si bien se produce en el hígado fetal y en los riñones adultos [193], la EPO y su receptor (EPOR) se han localizado en varias regiones del cerebro de los

mamíferos [194, 195], tanto en las neuronas, como en las células gliales y en las células endoteliales de los capilares del cerebro [196, 197, 192]. Además, la expresión de EPO y EPOR en el cerebro adulto se ve reforzada por la hipoxia [194], y por otros estímulos tales como la hipoglucemia, la insulina y la liberación del factor de crecimiento de la insulina (IGF). Las especies reactivas de oxígeno y la activación del factor inducible por hipoxia (HIF) también llevan a un aumento en la expresión de EPO [198, 199].

La EPO y el EPOR se detectan en el SNC durante el desarrollo fetal [197] y permanecen durante la edad adulta [194]. La expresión de EPOR en la etapa embrionaria sugiere un papel de la EPO en el desarrollo del cerebro y en el mantenimiento de los tejidos [200]. Además, se ha demostrado que la EPO es capaz de inducir diversas respuestas celulares, entre otras se ha descrito como un factor neuroprotector, neurogénico, neurotrófico, angiogénico, antiapoptótico y antiinflamatorio [19, 201].

El papel de EPO en la neuroprotección se ha demostrado a través de la infusión de EPOR soluble en animales sometidos a isquemia leve. La unión competitiva de EPO entre el EPOR endógeno y el soluble causó la muerte neuronal y deterioro de la capacidad de aprendizaje. Ello sugiere que el EPOR endógeno juega un papel crítico en el control de la función neuronal y por lo tanto, tiene un efecto neuroprotector [202]. En cultivo de neuronas, EPO induce neuroprotección a través de la inhibición de la apoptosis y reduciendo el daño en el ADN [203].

Las funciones neurotróficas fueron descritas en primer lugar por [204], tanto *in vitro* como *in vivo*. Los efectos neurotróficos descritos para la EPO incluyen, entre otros, la capacidad para estimular el crecimiento axonal, la formación de neuritas, el crecimiento de nuevas dendritas y la síntesis y liberación de neurotransmisores [205, 206].

Se ha propuesto también, una función neurogénica para EPO. Se ha demostrado que la producción de EPO inducida por hipoxia aparentemente actúa sobre las células madre neuronales en el prosencéfalo, sugiriendo un papel directo de esta citoquina en la neurogénesis [207]. La EPO también induce la expresión del gen de BDNF [208], que está estrechamente racionado con la neurogénesis.

Además de sus efectos sobre las neuronas, la neuroprotección inducida por EPO puede atribuirse a una mejora en la vascularización cerebral, mediante la formación de nuevos vasos. Este efecto angiogénico se observó en diferentes

modelos experimentales, tales como en los arcos aórticos de rata [15] o en el endometrio de ratón [16]. Además, la EPO ayuda en la preservación de la integridad de la barrera hematoencefálica durante una lesión, probablemente restaurando la expresión de las proteínas de las uniones estrechas [209] y reduciendo la inflamación [210] y la expresión de los radicales libres [209].

Los efectos antiapoptóticos de EPO en las células neuronales requieren la activación combinada de rutas de señalización, que incluyen a STAT5, AKT y potencialmente a MAPK, de un modo similar al observado en las células hematopoyéticas [211].

La EPO puede activar las rutas antiinflamatorias y antiapoptóticas, ya sea por la interacción con su clásico receptor EPO-R [212] o por la diana molecular responsable de los efectos de EPO en la protección de los tejidos, el receptor común β (βcR) [213]. El βcR es un dominio de transducción de señal, que está también presente en el complejo del receptor para los factores estimulantes de las colonias de macrófagos y granulocitos, IL-3 e IL-5.

Finalmente, la EPO atenúa la inflamación mediante la reducción de los astrocitos reactivos y la activación de la microglía, y por la inhibición del reclutamiento de las células inmunes en el área lesionada. Por tanto, la EPO tiene un efecto antiinflamatorio que contribuye a sus efectos neuroprotectores directos.

2.9. EPO y enfermedades del sistema nervioso central

Varios estudios se han llevado a cabo para poner a prueba el potencial terapéutico de la EPO en varias enfermedades del SNC.

Diferentes estudios han encontrado que la EPO reducía la producción de mediadores de inflamación, lo que reduce los infartos en la isquemia cerebral [214] y la atenuación de las lesiones en la esclerosis múltiple [215]. Varios modelos animales de accidentes cerebrovasculares han mostrado que la administración de EPO además de reducir el tamaño del infarto [19], reduce del daño histológico y mejora el resultado funcional tras un accidente cerebrovascular experimental [214, 216]. La administración de EPO en modelos experimentales de lesiones cerebrales traumáticas y de la médula espinal, conduce a una recuperación morfológica, funcional y cognitiva [217], aumentando la neurogénesis en el giro dentado [218] y disminuyendo el edema cerebral [22]. La respuesta inflamatoria protege al cerebro y promueve la revascularización para acelerar la recuperación del flujo sanguíneo cerebral [219].

La EPO resultó ser neuropotectora también en modelos de enfermedades neurodegenerativas y neuroinflamatorias. Se ha demostrado en un modelo animal de esclerosis múltiple que el tratamiento con EPO puede retrasar la aparición de la enfermedad y reducir su severidad mediante la administración profiláctica [215]. Por otro lado, la administración de EPO después de la aparición de los signos clínicos de la esclerosis múltiple disminuye el daño del tejido y la respuesta inflamatoria de la médula espinal, y también la permeabilidad de la barrera hematoencefálica [28]. El tratamiento con EPO puede contrarrestar los procesos degenerativos en la enfermedad del Parkinson y en la esclerosis lateral amiotrófica (ELA) por la inhibición de la apoptosis y la estimulación de la regeneración axonal [31]. Otras patologías como la esquizofrenia, la retinopatía o la epilepsia también mostraron mejorías después de la administración de EPO.

3. Enriquecimiento ambiental

El desarrollo postnatal del sistema nervioso central se completa en dos etapas, una genéticamente predeterminada y otra modulada por la experiencia ambiental [220, 221]. Después del nacimiento, la experiencia modula los programas de desarrollo de la arquitectura cortical y de la función [222, 223]. La experiencia media cambios tales como el aumento en el número y tamaño de sinapsis por neurona [224], el aumento de la actividad neuronal [225, 226], el aumento de la demanda metabólica [227, 228] y los cambios de la red vascular [224, 229, 230].

Las primeras aproximaciones a los efectos del ambiente sobre el desarrollo se remontan al siglo XIX con Lamarck y Darwin [231, 232]. Al final de siglo, tanto Cajal y Sherrington adelantaron los efectos del aprendizaje en la plasticidad sináptica [233, 234]. La mayoría de los cambios corticales inducidos por la experiencia se producen durante un periodo temprano de la plasticidad, definido como periodo crítico. Esta ventana de tiempo de la vida postnatal es específica para cada área cerebral, y después de esta reorganización mediada por la experiencia, las funciones sensoriales alcanzan su madurez [235, 236]. El cierre del periodo crítico se completa cuando las redes perineurales se forman alrededor de las neuronas [237].

El estudio de la modificación de la morfología del cerebro inducido por la experiencia se ha realizado mediante estudios de conducta llevados a cabo en un laboratorio, donde las condiciones ambientales se pueden modificar [238]. Desde

los primeros estudios sobre modificaciones ambientales, los experimentos se han realizado en dos direcciones opuestas, el enriquecimiento y la privación.

3.1. Privación sensorial

Aunque la influencia de la experiencia externa tiene lugar en todo el SNC, la mayoría de los estudios de los efectos de los aportes externos se han desarrollado en la corteza visual. El sistema visual tiene una organización jerárquica bien definida que facilita el estudio de sus estructuras a través de la interrupción de las rutas en diferentes etapas o la privación de los aportes utilizando cualquiera de las técnicas invasivas –inyección de tetrodotoxina [239, 148]; cirugía, como la sutura del párpado [240, 241], enucleación bilateral o unilateral [242], la eliminación de la retina [243] – o técnicas no invasivas, tales como la cría en oscuridad [245, 229, 52, 244], o el uso de lentes de contacto opacas [246]. La ausencia de la experiencia visual desde el nacimiento retrasa la maduración normal y mantiene a la corteza visual en un estado inmaduro [241, 247, 248]. En particular, las conexiones visuales no se consolidan, permaneciendo plásticas tras el cierre del periodo crítico fisiológico, y por tanto, la agudeza visual no se desarrolla [237].

Otro sistema sensorial ampliamente utilizado para estudiar los efectos del empobrecimiento ambiental es la corteza somatosensorial, especialmente la región de los "barriles" (barrels) que reciben información sensorial crucial para muchos roedores y felinos procedentes de las vibrisas o pelos del bigote de estos animales [249, 250]. Recortar dichos bigotes empobrece las aferencias sensorial de tal modo que se inducen modificaciones morfológicas y fisiológicas en dicha corteza, máxime cuando la manipulación se desarrolla durante el periodo crítico [251, 252, 253]. Los estudios sobre los efectos de la privación auditiva u olfatoria comparten efectos similares con el sistema visual o con el sistema somatosensorial [254]. Una característica común a toda privación sensorial es la plasticidad compensatoria intermodal que aumenta el rendimiento para los sentidos restantes cuando uno es privado [255, 256].

Probablemente el método más conocido para compensar la deprivación sensorial es por medio del enriquecimiento ambiental, también usado para compensar los efectos de muchas enfermedades cerebrales [257].

3.2. Enriquecimiento sensorial

Los primeros estudios sistemáticos sobre el enriquecimiento ambiental (EA) se pueden atribuir a Donald Hebb en 1947, el cual describió como las ratas cuidadas como animales de compañía, tenian un mejor rendimiento en las pruebas de resolución de problemas, que las ratas criadas en jaulas [258]. Su grupo de discípulos en Berkeley (Rosenzweig, Krech, Bennet y Diamond) definieron el concepto de enriquecimiento ambiental como la combinación de complejos inanimados, la estimulación social y visual y ejercicio físico. Todo ello ejerce una gran variedad de efectos a largo plazo a nivel neuroanatómico, neuroquímico y conductual en varias especies de animales. Desde sus primeros estudios, el enriquecimiento ambiental se ha aplicado utilizando jaulas más grandes que las estándar, llenas de juguetes de diferentes colores y formas (túneles, rampas, refugios, material para construir nidos, etc). Estos objetos y la colocación de los alimentos se cambian de manera periódica. Otro elemento que tiene una influencia sustancial, es la interacción social, jaulas más amplias permiten criar a un mayor número de animales que intercambian estímulos sociales. Otro elemento del enriquecimiento ambiental es el ejercicio físico, forzado o voluntario, que en roedores es comúnmente implementado por el libre acceso a una rueda de ejercicio o por una cinta de caminar [36, 37]. Aunque, algunos autores dudan si el ejercicio físico debería estar incluido, cabe decir que el ejercicio físico por si mismo induce importantes cambios en el cerebro, por ello, la mayoría de los paradigmas sobre el entorno enriquecido, empezando desde Hebb, han decidió incluirlo. Recientemente, se ha puesto también de manifiesto, que el ejercicio físico es requerido para recuperarse de los efectos de la privación visual [259]. Por el contrario, el papel del ejercicio físico se ha despreciado en los modelos cognitivos [24].

Por lo tanto, el enriquecimiento ambiental aumenta la estimulación sensorial, cognitiva, y motora, y promueve la activación, señalización y plasticidad neuronal en todas las áreas del cerebro. Un aumento en el estímulo somatosensorial o visual afecta principalmente a estas áreas, así como un aumento de la estimulación cognitiva afecta al hipocampo y la estimulación motora afecta a la corteza motora, estriado o cerebelo. No obstante, los efectos no son tan selectivos cuando el enriquecimiento produce efectos globales por todo el cerebro [38, 31, 257]. Estos autores usan el término “reserva cognitiva” para referirse al amplio espectro de mecanismos neuroprotectores contra las patologías neurodegenerativas y otras enfermedades cerebrales.

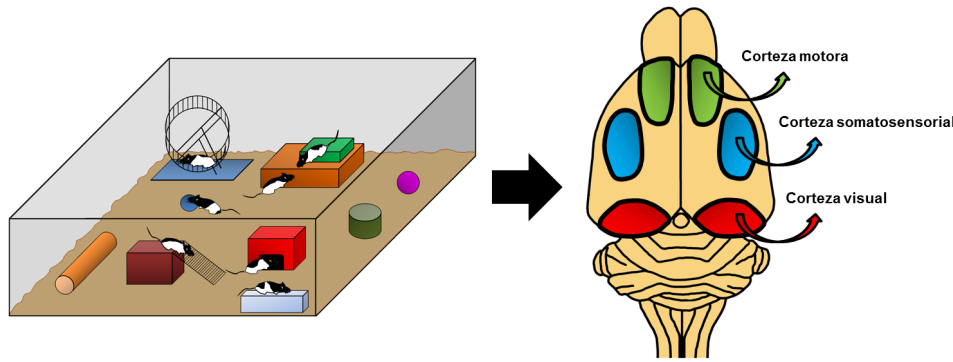

Figura 3. *Representación esquemática de una caja de enriquecimiento ambiental, de mayor tamaño que las estandar, con numerosos objetos de diversos colores y formas, donde conviven un número elevado de individuos. El gráfico de la derecha señala algunas de las áreas donde se pueden encontrar modificaciones debidas a la cría en estas condiciones.*

La cría en ambientes enriquecidos induce efectos desde niveles celulares, moleculares o genéticos hasta niveles de comportamiento. Los estudios del grupo de Berkeley ,demostraban que el enriquecimiento ambiental aumentaba el peso y el grosor cortical [260, 261], y estudios posteriores también describieron un aumento en la ramificación dendrítica y en su longitud, número de espinas dendríticas y en el tamaño de las sinapsis, sobre todo en algunas poblaciones neuronales [262, 263]. El enriquecimiento ambiental y el ejercicio físico tienen importantes efectos sobre la plasticidad de las conexiones neuronales, especialmente en la corteza visual ([34, 49]. El enriquecimiento ambiental también aumenta la neurogénesis en el hipocampo, mediada por VEGF [264]. Aunque, la mayoría de los estudios morfológicos se han llevado a cabo en la corteza visual, como se ha explicado anteriormente [265, 266], otras áreas sensoriales y no sensoriales experimentan cambios morfológicos importantes, asi ocurre por ejemplo en la corteza auditiva [267], la corteza somatosensorial [268], el hipocampo [269], la amígdala [270] o los ganglios basales [271, 272]. No obstante, los efectos de criar en entornos complejos no se limitan solo a las neuronas. Los primeros estudios refirieron que la morfología astrocitaria cambiaba debido a la exposición a entornos enriquecidos [265, 273] y estudios posteriores mostraron un aumento en el tamaño y densidad de los astrocitos [274]. El enriquecimiento ambiental también aumenta la

densidad vascular [227, 52, 224] y la densidad oligodendroglial [274, 275]. Aparte de estos incrementos a nivel tisular, estudios recientes han descrito la aceleración del desarrollo del sistema visual como una consecuencia del enriquecimiento ambiental. La cría de animales en un entorno enriquecido induce la apertura temprana de los ojos y tiene efectos electrofisiológicos, tales como el desarrollo temprano de la agudeza visual [34].

La mayoría de estos cambios a nivel celular están en concordancia con los cambios en la expresión de genes involucrados en la plasticidad sináptica. El enriquecimiento ambiental aumenta los niveles de angioneurinas, tales como el factor de crecimiento nervioso (NGF) [48], el factor neurotrófico derivado del cerebro (BDNF) [49, 50], la neurotrofina-3 (NT-3) [51] y el VEGF que juega un papel clave en la señalización neuronal [52]. Al mismo tiempo, aumenta la expresión de las proteínas sinápticas e induce cambios en la expresión de las subunidades de los receptores NMDA y AMPA [276].

Por último, pero no menos importante, criar en entornos enriquecidos mejora el aprendizaje y la memoria [269, 277, 278], disminuye el deterioro cognitivo debido al envejecimiento [279, 280, 281], disminuye la ansiedad y aumenta la capacidad exploratoria [282]. En modelos experimentales, algunos autores han descrito como la exposición a entornos enriquecidos evita los efectos de criar en oscuridad, en la corteza visual de la rata [283]. Estudios recientes han destacado la importancia de la duración del enriquecimiento ambiental, dado que es relevante para la persistencia de sus efectos sobre el comportamiento [284].

3.3. Enriquecimiento ambiental y enfermedades del sistema nervioso central

Debido a los efectos beneficiosos del enriquecimiento ambiental sobre el desarrollo del cerebro, no es sorprendente que se haya postulado como una terapia, o al menos como una estrategia neuroprotectora para la mayoría de las enfermedades cerebrales [37, 38]. El concepto de "Reserva Cerebral Cognitiva" postulado por Nithianantharajah y Hannah ofrece un marco general para diversas estrategias neurorestauradoras en las enfermedades del SNC.

En los estudios realizados sobre las enfermedades neurodegenerativas, el entorno enriquecido ha demostrado ser una herramienta útil para evitar el deterioro cognitivo inducido no sólo por el envejecimiento normal, sino que también por la enfermedad de Alzheimer. Criar en ambientes complejos mejora las pruebas

cognitivas en modelos de ratones transgénico de la enfermedad del Alzheimer [285], reduce la deposición de ß-amiloide [286] y aumenta la angiogénesis, facilitando la liberación de ß-amiloide [287]. En la enfermedad de Huntington, el enriquecimiento ambiental mejora el déficit cognitivo en un modelo de ratón transgénico [42]. En la enfermedad de Parkinson, el enriquecimiento ambiental aumenta la resistencia al efecto neurotóxico del MPTP, fármaco inductor del Parkinson e induce una variedad de cambios en la expresión de genes en el estriado. Esto es compatible con los drásticos cambios morfológicos inducidos por el enriquecimiento ambiental en el estriado [41, 288]. Las enfermedades genéticas tales como el síndrome de Rett y el síndrome de Down han mejorado las respuestas motoras y de comportamiento cuando los modelos animales son criados en ambientes enriquecidos [288, 290, 291, 292].

Pero las mejoras del enriquecimiento ambiental no sólo están vinculadas a las enfermedades neurodegenerativas. En modelos de accidentes cerebrovasculares, las secuelas motoras de dichos accidentes cerebrovasculares disminuyen con el enriquecimiento ambiental [293].

Los estudios en modelos de traumatismo cráneo-encefálico también han puesto de manifiesto los beneficios que proporciona criar en ambientes enriquecidos. Estos promueven la recuperación de la función cognitiva tras una lesión traumática [43]. También reduce el daño a la BHE inducido por una lesión quirúrgica [45] y disminuye la muerte apoptótica, neuronal además de mejora la vascularización en el mismo modelo [45]. Los estudios en humanos muestran también los beneficios de usar ambientes enriquecidos en la rehabilitación neurofisiológica [294].

Por último, el enriquecimiento ambiental incluso tiene efectos beneficiosos en los tumores. Se ha descrito recientemente que los ratones que viven en un ambiente enriquecido muestran un crecimiento tumoral reducido y una mayor remisión a través del eje BDNF/leptina [47].

3.4. VEGF y enriquecimiento ambiental

Varios estudios han indicado que el enriquecimiento ambiental (EA) aumenta la expresión de algunos factores tróficos, tales como el VEGF o el BDNF [48, 51, 52]. Sin embargo, pocos estudios han probado los efectos de combinar la infusión de VEGF y el EA [45]. Los pocos experimentos realizados han demostrado que la

combinación del VEGF y el EA tienen un efecto sinérgico más fuerte, comparado con la infusión del VEGF solo, tanto a nivel celular como a nivel tisular.

A pesar del aumento de la permeabilidad inducida por la administración del VEGF, la conservación de los tejidos fue mejor cuando la infusión del VEGF se combinó con el EA. Además, parece haber un aumento en las densidades vasculares y neuronales por la aplicación combinada de ambas estrategias [45]. No obstante, se necesitan investigaciones adicionales para evitar los efectos potencialmente negativos, tales como la modificación del periodo crítico [34] o los relacionados con los efectos secundarios del VEGF, como el edema [295].

3.5. BDNF y enriquecimiento ambiental

Numerosos estudios han informado que la exposición a un entorno enriquecido durante el desarrollo y en la edad adulta afecta a la expresión de las neurotrofinas, mediante el aumento en la expresión del NGF [48], del BDNF [49] y de la neurotrofina-3 [51] en áreas cerebrales, tales como el prosencéfado basal, la corteza cerebral, el hipocampo y el cerebelo [296, 51]. Kuzumaki y colaboradores mostraron que un ambiente enriquecido estimula la diferenciación neuronal a partir de precursores en el giro dentado del hipocampo, aumentando la expresión del BDNF con una regulación sostenida de la cromatina en particular. La actividad física también afecta a los niveles de BDNF [297, 298, 299]. Otro estudio informó que la distribución diferencial de los niveles de neurotrofinas en el hipocampo dorsal y ventral puede verse afectado por el enriquecimiento ambiental, que aumenta los niveles de BDNF [300].

El enriquecimiento ambiental en ratones+/- para BDNF esta dirigido por mecanismos distintos en machos y hembras, siendo en los ratones macho, donde el rescate del fenotipo emocional esta relacionado con un aumento en la expresión del BDNF en el hipocampo [301]. Hay un estudio que demuestra como el ejercicio mejora el aprendizaje después de la neurodegeneración inducida en el hipocampo por la administración de ácido kainico lo que se asocia a un aumento de BDNF [302]. En algunos estudios, se ha observado que el ejercicio juega un papel relevante en la modulación de varios factores que inciden en la plasticidad del cerebro, aumentando los niveles de BDNF [299] y en la captación del factor de crecimiento similar a la insulina. Estos factores implican una mejor salud del

animal, una buena protección contra la muerte neuronal [303], y un aumento en la proliferación neuronal [304, 305].

3.6. IGF y enriquecimiento ambiental

Sobre el efecto del enriquecimiento ambiental en la expresión del IGF-I no hay muchos estudios pero si los hay en relación con el ejercicio habiéndose demostrado que el IGF-I media los efectos neuroprotectores debidos a él [303, 306]. El ejercicio aumenta la expresión del IGF en el hipocampo, estando involucrado en la plasticidad del hipocampo, en el aprendizaje y en la memoria [172, 299, 307].

Neutralizando el IGF-I circulante bloquea significativamente la eficacia del EA en la recuperación funcional de la lesión de la médula espinal, apoyando la idea de que el IGF-1 podría ser una posible ayuda terapéutica en la rehabilitación temprana después de una lesión de la médula espinal [306].

Un estudio reciente, ha demostrado que el tratamiento intracortical con IGF-I unido al EA, restablece la plasticidad neuronal en el sistema visual de ratas adultas [308]. Por tanto el IGF-I promueve la plasticidad en el sistema nervioso adulto, pudiendo ser una estrategia para reparar el cerebro en la vida adulta.

Los niveles basales de IGF-I juegan un papel clave en la mediación de los efectos del EA sobre el desarrollo de la retina a través de una acción que requiere el concurso de BDNF [309]. El BDNF está también implicado en las acciones del IGF-I que median los efectos del EA y que podrían ser ejecutados a través de la modulación del circuito inhibitorio intracortical y del desarrollo de las redes perineuronales [310]. Otros trabajo demuestra que los masajes tienen una influencia sobre el desarrollo del cerebro, particularmente sobre el desarrollo visual, y que estos efectos están mediados por el IGF-1 [311]. El EA ejerce efectos sobre el receptor del IGF-I, y se ha demostrado que regula a la alta al gen de dicho receptor en el hipocampo y en la corteza somatosensorial de la rata adulta [312].

3.7. EPO y enriquecimiento ambiental

En experimentos llevados a cabo para establecer los efectos de la administración de EPO en combinación con un ambiente enriquecido [313] observaron que el EA produce un aumento en la expresión del gen de EPO y de EPOR durante la hipoxia. Sin embargo, aún se desconoce si este paradigma podría mejorar los efectos beneficiosos obtenidos por la administración de EPO por sí sola.

4. Observaciones finales

La exposición de pacientes a ambientes enriquecidos juega un importante papel en la restauración del cerebro. Esto implica un aumento de la expresión de las angioglioneurinas que están involucradas en la mejoría observada en varias enfermedades.

Las neurotrofinas son una familia de proteínas que juegan un papel fundamental en la regulación de la función neuronal, plasticidad, desarrollo y supervivencia. Las neurotrofinas se caracterizaron originalmente como factores tróficos por sus efectos en la proliferación, diferenciación y supervivencia de neuronas, tanto durante el desarrollo como en la edad adulta. Más recientemente, se ha descrito su papel en la regulación sináptica y en la orientación de los conos de crecimiento axonales. Se han descrito también, las funciones tanto de las neurotrofinas como de sus receptores sobre las células no neuronales, tales como las células endoteliales, las células musculares lisas, las células inmunes y las células epiteliales. Evidencias sólidas sugieren que el BDNF participa en la regulación de la plasticidad sináptica que surge de la actividad asociada con los procesos de aprendizaje y memoria.

Mientras que la expresión del IGF-I está restringida en el cerebro a las regiones y periodos de crecimiento axonal, maduración dendrítica y sinaptogénesis, desempeñando un papel relevante en el desarrollo de los vasos sanguíneos cerebrales, como factor angiogénico. Algunas patologías cerebrales, como las apoplejías o la enfermedad de Alzheimer, muestran resultados controvertidos con niveles de IGF-I alterados.

Otras de las principales angioglineurinas, la EPO, tiene un efecto antiinflamatorio que contribuye a su efecto neuroprotector directo. Pero una aplicación prolongada podría causar efectos secundarios serios debido a la estimulación de la eritropoyesis. Para este propósito, se han desarrollado citoquinas similares a EPO que carecen del potencial eritropoyético. Los efectos neuroprotectores de los derivados similares a EPO se han estudiado en modelos experimentales de isquemia cerebral y de lesión de la médula espinal [214, 217]. Se han probado los efectos neuroprotectores del VEGF en varios sistemas neuronales, incluyendo el sistema dopaminérgico. El VEGF juega un doble papel en diferentes patologías neurodegenerativas (esclerosis múltiple, enfermedad del Parkinson). Por ejemplo, en el modelo de encefalomielitis experimental autoinmune (EAE) en ratas (remeda

Esclerosis Múltiple), por un lado la infusión en el estriado empeora la inflamación de la placa y por otro reduce la gravedad de la enfermedad.

La combinación de la administración de angioglioneurinas y del enriquecimiento ambiental podría ser una estrategia terapéutica prometedora para solucionar algunos trastornos cerebrales. Sin embargo, se necesitan investigaciones adicionales para establecer el patrón de sincronización óptimo con el fin de garantizar los máximos efectos sinérgicos, evitando al mismo tiempo los potenciales efectos secundarios de esta combinación.

AGRADECIMIENTOS

El trabajo ha sido financado parcialmente por el Grupo de Investigación Consolidado LaNCE (IT 794/13) y el programa Saiotek del Gobierno Vasco y la UFI 11/32 (UPV-EHU).

5. Referencias

1. Zacchigna S, Lambrechts D, Carmeliet P. Neurovascular signalling defects in neurodegeneration. Nat Rev Neurosci 2008; 9:169-181.
• http://dx.doi.org/10.1038/nrn2336

2. Lecrux C, Hamel E. The neurovascular unit in brain function and disease. Acta Physiol (Oxf). 2011 Sep; 203(1):47-59.
• http://dx.doi.org/10.1111/j.1748-1716.2011.02256.x

3. Argando-a EG, Bengoetxea H, Ortuzar N, Bulnes S, Rico-Barrio I, Lafuente JV. Vascular endothelial growth factor: adaptive changes in the neuroglialvascular unit. Curr Neurovasc Res. 2012 Feb; 9 (1):72-81.
• http://dx.doi.org/10.2174/156720212799297119

4. Lafuente JV, Ortuzar N, Bengoetxea H, Bulnes S, Argando-a EG. Vascular endothelial growth factor and other angioglioneurins: key molecules in brain development and restoration. Int Rev Neurobiol. 2012; 102:317-46
• http://dx.doi.org/10.1016/B978-0-12-386986-9.00012-0

5. Storkebaum E, Lambrechts D, Carmeliet P. VEGF: once regarded as a specific angiogenic factor, now implicated in neuroprotection. Bioessays 2004; 26:943-54.
• http://dx.doi.org/10.1002/bies.20092

6. Ferrara N, Gerber HP, LeCouter J. The biology of VEGF and its receptors. Nat Med 2003; 9:669-76.
• http://dx.doi.org/10.1038/nm0603-669

7. Dvorak HF. Discovery of vascular permeability factor (VPF). Exp. Cell Res 2006; 312:522-6.
• http://dx.doi.org/10.1016/j.yexcr.2005.11.026

8. Jin K, Zhu Y, Sun Y, Mao XO, Xie L, Greenberg DA. Vascular endothelial growth factor (VEGF) stimulates neurogenesis *in vitro* and *in vivo*. Proc Natl Acad Sci USA 2002; 99:11946-50.
• http://dx.doi.org/10.1073/pnas.182296499

9. Rosenstein JM, Krum JM. New roles for VEGF in nervous tissue-beyond blood vessels. Exp Neurol 2004; 187:246-53.
• http://dx.doi.org/10.1016/j.expneurol.2004.01.022

10. Storkebaum E, Lambrechts D, Dewerchin M, Moreno-Murciano MP, Appelmans S, Oh H, Van Damme P, Rutten B, Man WY, De Mol M, Wyns S, Manka D, Vermeulen K, Van Den Bosch L, Mertens N, Schmitz C, Robberecht W, Conway EM, Collen D, Moons L, Carmeliet P. Treatment of motoneurons degeneration by intracerebroventriculr delivery of VEGF in a rat model of ALS. Nat Neurosci 2005; 8:85-92.
• http://dx.doi.org/10.1038/nn1360

11. Bozzini S, Gambelli P, Boiocchi C, Schirinzi S, Falcone R, Buzzi P, Storti C, Falcone C. Coronary artery disease and depression: possible role of brain-derived neurotrophic factor and serotonin transporter gene polymorphisms. Int J Mol Med. 2009 Dec;24(6):813-8.
• http://dx.doi.org/10.3892/ijmm_00000297

12. Donovan MJ, Lin MI, Wiegn P, Ringstedt T, Kraemer R, Hahn R, Wang S, Iba-ez CF, Rafii S, Hempstead BL. Brain-derived neurotrophic factor is an endothelial cell survival factor required for intramyocardial vessel stabilization. Development 2000; 127:4531-40.

13. Bar RS, Boes M, Dake BL, Booth BA, Henley SA, Sandra A. Insulin, insulin-like growth factors, and vascular endothelium. Am J Med 1988; 85:59-70.
• http://dx.doi.org/10.1016/0002-9343(88)90398-1

14. Dunn SE. Insulin-like growth factor I stimulates angiogenesis and the production of vascular endothelial growth factor. Growth Horm IGF Res Suppl 2000; A:S41-2.

15. Carlini RG, Reyes AA, Rothstein M. Recombinant human erythropoietin stimulates angiogenesis *in vitro*. Kidney Int 1995; 47:740-5.
• http://dx.doi.org/10.1038/ki.1995.113

16. Yasuda Y, Masuda S, Chikuma M, Inoue K, Nagao M, Sasaki R. Estrogen-dependent production of erythropoietin in uterus and its implication in uterine angiogenesis. J Biol Chem 1998: 273:25381-87.
• http://dx.doi.org/10.1074/jbc.273.39.25381100.
Sopher BL, Thomas PS Jr, LaFevre-Bernt MA, Holm IE, Wilke SA, Ware CB, Jin LW, Libby RT, Ellerby LM, La Spada AR. Androgen receptor YAC transgenic mice recapitulate SBMA motor neuropathy and implicate VEGF164 in the motor neuron degeneration. Neuron 2004; 41:687-99.
• http://dx.doi.org/10.1016/S0896-6273(04)00082-0

17. Plate KH, Beck H, Danner S, Allegrini PR, Wiessner C. Cell type specific upregulation of vascular endothelial growth factor in an MCA-occlusion model of cerebral infarct. J Neuropathol Exp Neurol 1999; 58:654-66.

• http://dx.doi.org/10.1097/00005072-199906000-00010

18. Mu D, Jiang X, Sheldon RA, Fox CK, Hamrick SE, Vexler ZS, Ferriero DM. Regulation of hypoxia-inducible factor 1 alpha and induction of vascular endothelial growth factor in a rat neonatal stroke model. Neurobiol Dis 2003; 14:524-34.
• http://dx.doi.org/10.1016/j.nbd.2003.08.020

19. Brines M, Cerami A. Emerging biological roles for erythropoietin in the nervous system. Nat Rev Neurosci 2005; 6:484-94.
• http://dx.doi.org/10.1038/nrn1687

20. Brines ML, Ghezzi P, Keenan S, Agnello D, de Lanerolle NC, Cerami C, Itri ML, Cerami A. Erythropoietin crosses the blood-brain barrier to protect against experimental brain injury. Proc Natl Acad Sci USA 2001; 97:10526-31.
• http://dx.doi.org/10.1073/pnas.97.19.10526

21. Skold MK, Risling M, Holmin S. Inhibition of vascular endothelial growth factor receptor 2 activity in experimental brain contusions aggravates injury outcome and leads to early increased neuronal and glial degeneration. Eur J Neurosci 2006; 23:21-34.
• http://dx.doi.org/10.1111/j.1460-9568.2005.04527.x

22. Verdonck O, Lahrech H, Francony G, Carle O, Farion R, Van de LY, Remy C, Segebarth C, Payen JF. Erythropoietin protects from post-traumatic edema in the rat brain. J Cereb Blood Flow Metab 2007; 27:1369-76.
• http://dx.doi.org/10.1038/sj.jcbfm.9600443

23. Font MA, Arboix A, Krupinski J. Angiogenesis, neurogenesis and neuroplasticity in ischemic stroke. Curr Cardiol Rev. 2010 Aug;6(3):238-44
• http://dx.doi.org/10.2174/157340310791658802

24. Phillips HS, Hains JM, Armanini M, Laramee GR, Johnson SA, Winslow JW. BDNF mRNA is decreased in the hippocampus of individuals with Alzheimer´s disease. Neuron 1991; 7:695-702.

24. Pietropaolo S, Feldon J, Alleva E, Cirulli F, Yee BK. The role of voluntary exercise in enriched rearing: a behavioral analysis. Behav Neurosci 2006; 120:787-803.
• http://dx.doi.org/10.1037/0735-7044.120.4.787

25. Busiguina S, Fernandez AM, Barrios V, Clark R, Tolbert DL, Berciano J, Torres-Aleman I. Neurodegeneration is associated to changes in serum insulin-like growth factors. Neurobiol Dis 2000; 7:657-65.

26. Howells DW, Porritt MJ, Wong JY, Batchelor PE, Kalnins R, Hughes AJ, Donnan GF. Reduced BDNF mRNA expression in the Parkinson´s disease substantia nigra. Exp Neurol 2000; 166: 127-35.
• http://dx.doi.org/10.1006/exnr.2000.7483

27. Oosthuyse B, Moons L, Storkebaum E, Beck H, Nuyens D, Brusselmans K, Van Dorpe J, Hellings P, Gorselink M, Heymans S, Theilmeier G, Dewerchin M, Laudenbach V, Vermylen P, Raat H, Acker T, Vleminckx V, Van Den Bosch L, Cashman N, Fujisawas H, Drost MR, Sciot R, Bruyninckx F, Hicklin DJ, Ince C, Gressens P, Lupu F, Plate KH, Robberecht W, Herbert JM, Collen D, Carmeliet P. Deletion of the hypoxia-response element in the vascular endothelial growth factor promoter causes motor neuron degeneration. Nat Genet 2001; 28:131-8.
• http://dx.doi.org/10.1038/88842

28. Leist M, Ghezzi P, Grasso G, Bianchi R, Villa P, Fratelli M, Savino C, Bianchi M, Nielsen J, Gerwien J, Kallunki P, Larsen AK, Helboe L, Christensen S, Pedersen LO, Nielsen M, Torup L, Sager T, Sfacteria A, Erbayraktar S, Erbayraktar Z, Gokmen N, Yilmaz O, Cerami-Hand C, Xie QW, Coleman T, Cerami A, Brines M. Derivatives of erythropoietin that are tissue protective but not erythropoietic. Science 2004; 305:239-42.
• http://dx.doi.org/10.1126/science.1098313

29. Yasuhara T, Shingo T, Muraoka K, Kameda M, Agari T, Wen Ji Y, Hayase H, Hamada H, Borlongan CV, Date I. Neurorescue effects of VEGF on rat model of Parkinson´s disease. Brain Res 2005; 1053:10-8.
• http://dx.doi.org/10.1016/j.brainres.2005.05.027

30. Zlokovic BV. Neurovascular mechanisms of Alzheimer´s neurodegeneration. Trends Neurosci 2005; 28:202-
• http://dx.doi.org/10.1016/j.tins.2005.02.001

31. Grunfeld JF, Barhum Y, Blondheim N, Rabey JM, Melamed E; Offen D. Erythropoietin delays disease onset in an amyothropic lateral sclerosis model. Exp Neurol 2007; 204:260-3.
• http://dx.doi.org/10.1016/j.expneurol.2006.11.002

32. Nation DA, Hong S, Jak AJ, Delano-Wood L, Mills PJ, Bondi MW, Dimsdale JE. Stress, exercise, and Alzheimer's disease: a neurovascular pathway. Med Hypotheses. 2011 Jun; 76(6):847-54.
• http://dx.doi.org/10.1016/j.mehy.2011.02.034

33. Nithianantharajah J, Hannan AJ. The neurobiology of brain and cognitive reserve: mental and physical activity as modulators of brain disorders. Prog Neurobiol 2009; 89:369-82.

• http://dx.doi.org/10.1016/j.pneurobio.2009.10.001

34. Cancedda L, Putignano E, Sale A, Viegi A, Berardi N, Maffei L. Acceleration of visual system development by environmental enrichment. J Neurosci 2004; 24:4840-8.
• http://dx.doi.org/10.1523/JNEUROSCI.0845-04.2004

35. Rosenzweig MR, Bennett EL. Psychobiology of plasticity: effects of training and experience on brain and behaviour. Behav Brain Res 1996; 78:57-65.
• http://dx.doi.org/10.1016/0166-4328(95)00216-2

36. van Praag H, Kempermann G, Gage FH. Neural consequences of environmental enrichment. Nature Rev Neurosci 2000; 1:191-8.
• http://dx.doi.org/10.1038/35044558

37. Will B, Galani R, Kelche C, Rosenzweig MR. Recovery from brain injury in animals: relative efficacy of environmental enrichment, physical exercise or formal training (1990-2002). Prog Neurobiol 2004; 72:167-82.
• http://dx.doi.org/10.1016/j.pneurobio.2004.03.001

38. Nithianantharajah J, Hannan AJ. Enriched environments, experience-dependent plasticity and disorders of the nervous system. Nature Rev Neurosci 2006; 7:697-709.
• http://dx.doi.org/10.1038/nrn1970

39. Laviola G, Hannan AJ, Macrì S, Solinas M, Jaber M. Effects of enriched environment on animal models of neurodegenerative diseased and psychiatric disorders. Neurobiol Dis 2008; 31:159-68.
• http://dx.doi.org/10.1016/j.nbd.2008.05.001

40. Jankowsky JL, Melnikova T, Fadale DJ, Xu GM, Slunt HH, Gonzales V, Youkin SG, Borchelt DR, Savonenko AV. Environmental enrichment mitigates cognitive deficits in a mouse model of Alzheimer´s disease. J Neurosci 2005; 25:5217-24.
• http://dx.doi.org/10.1523/JNEUROSCI.5080-04.2005

41. Bezard E, Dovero S, Belin D, Duconger S, Jackson-Lewis V, Przedborski S, Piazza PV, Gross CE, Jaber M. Enriched environment confers resistance to 1-methyl-4-phenyl-1,2,3,6-tetrahydropyridine and cocaine: involvement of dopamine transporter and trophic factors. J Neurosci 2003; 23:10999-1007.

42. Nithianantharajah J, Barkus C, Murphy M, Hannan AJ. Gene-environment interactions modulating cognitive function and molecular correlates of synaptic plasticity in Huntington's disease transgenic mice. Neurobiol Dis 2008; 29:490-504.
• http://dx.doi.org/10.1016/j.nbd.2007.11.006

43. Hamm RJ, Temple MD, O'Dell DM, Pike BR, Lyeth BG. Exposure to environmental complexity promotes recovery of cognitive function after traumatic brain injury. J Neurotrauma 1996; 13:41-7.
• http://dx.doi.org/10.1089/neu.1996.13.41

44. Hoffman AN, Malena RR, Westergom BP, Luthra P, Cheng JP, Aslam HA, Zafonte RD, Kline AE. Environmental enrichment-mediated functional improvement after experimental traumatic brain injury is contingent on task-specific neurobehavioral experience. Neurosci Lett 2008; 431:226-30.
• http://dx.doi.org/10.1016/j.neulet.2007.11.042

45. Ortúzar N, Rico-Barrio I, Bengoetxea H, Argandoña EG, Lafuente JV. VEGF reverts the cognitive impairment induced by a focal traumatic brain injury during the development of rats raised under environmental enrichment. Behavioural Brain Research 2013; 246:36-46.

46. Briones TL, Rogozinska M, Woods J. Environmental experience modulates ischemia-induced amyloidogenesis and enhances functional recovery. Journal Neurotrauma 2009; 26:613-25.
• http://dx.doi.org/10.1089/neu.2008.0707

47. Cao L, Liu X, Lin EJ, Wang C, Choi EY, Riban V, Lin B, During MJ. Environmental and genetic activation of a brain-adipocyte BDNF/leptin axis causes cancer remission and inhibition. Cell. 2010; 142:52-64.
• http://dx.doi.org/10.1016/j.cell.2010.05.029

48. Pham TM, Winblad B, Granholm AC, Mohammed AH. Environmental influences on brain neurotrophins in rats. Pharmacol Biochem Behav 2002; 73:167-75.
• http://dx.doi.org/10.1016/S0091-3057(02)00783-9

49. Sale A, Putignano E, Cancedda L, Landi S, Cirulli F, Berardi N, et al. Enriched environment and acceleration of visual system development. Neuropharmacology 2004; 47:649-60.
• http://dx.doi.org/10.1016/j.neuropharm.2004.07.008

50. Franklin TB, Murphy JA, Myers TL, Clarke DB, Currie RW. Enriched environment during adolescence changes brain-derived neurotrophic factor and TrkB levels in the rat visual system but does not offer neuroprotection to retinal ganglion cells following axotomy. Brain Res 2006; 1095:1-11.
• http://dx.doi.org/10.1016/j.brainres.2006.04.025

51. Ickes BR, Pham TM, Sanders LA, Albeck DS, Mohammed AH, Granholm AC. Long-term environmental enrichment leads to regional increases in neurotrophin levels in rat brain. Exp Neurol 2000; 164:45-52.
• http://dx.doi.org/10.1006/exnr.2000.7415

52. Bengoetxea H, Argando-a EG, Lafuente JV. Effects of visual experience on vascular endothelial growth factor expression during the postnatal development of the rat visual cortex. Cereb Cortex 2008; 18:1630-39.
• http://dx.doi.org/10.1093/cercor/bhm190

53. Senger DR, Galli SJ, Dvorak AM, Perruzzi CA, Harvey VS, Dvorak HF. Tumor cell secrete a vascular permeability factor that promotes accumulation of ascites fluid. Science 1983; 219:983-5.
• http://dx.doi.org/10.1126/science.6823562

54. Ferrara N, Henzel WJ. Pituitary follicular cells secrete a novel heparin-binding growth factor specific for vascular endothelial cells. Biochem Biophys Res Commun 1989; 161:851-8.
• http://dx.doi.org/10.1016/0006-291X(89)92678-8

55. Senger DR, Connolly DT, Van de Water L, Feder J, Dvorak HF. Purification and NH2-terminal amino acid sequence of guinea pig tumor-secreted vascular permeability factor. Cancer Res. 1990 Mar 15; 50(6):1774-8.

56. Ferrara N. Vascular endothelial growth factor: basic science and clinical progress. Endocr Rev 2004; 25:581-611.
• http://dx.doi.org/10.1210/er.2003-0027

57. Ruiz de Almodovar C1, Lambrechts D, Mazzone M, Carmeliet P. Role and therapeutic potential of VEGF in the nervous system. Physiol Rev 2009; 89(2):607-48.

58. Bates DO, Cui TG, Doughty JM, Winkler M, Sugiono M, Shields JD, Peat D, Gillatt D, and Harper SJ. VEGF165b, an inhibitory splice variant of vascular endothelial growth factor, is down-regulated in renal cell carcinoma. Cancer Res 2002; 62: 4123–4131.

59. Cui TG, Foster RR, Saleem M, Mathieson PW, Gillatt DA, Bates DO and Harper SJ. Differentiated human podocytes endogenously express an inhibitory isoform of vascular endothelial growth factor (VEGF165b) mRNA and protein. Am J Physiol Renal Physiol 2004; 286: F767–F773, Darwin C. On the origin of species by means of natural selection, or the preservation of favoured racesin the struggle for life. London. Murray J. 1859.

60. Ladomery MR, Harper SJ, Bates DO. Alternative splicing in angiogenesis: the vascular endothelial growth factor para¬digm. Cancer Lett 2007; 249: 133-142
• http://dx.doi.org/10.1016/j.canlet.2006.08.015

61. Nowak DG, Amin EM, Rennel ES, Hoareau-Aveilla C, Gam¬mons M, Damodoran G, Hagiwara M, Harper SJ, Woolard J, Ladomery MR, Bates DO. Regulation of vascular endothelial growth factor (VEGF) splicing from pro-angiogenic to anti-angiogenic isoforms: a novel therapeutic strategy for angio¬genesis. J Biol Chem 2010; 285: 5532-5540
• http://dx.doi.org/10.1074/jbc.M109.074930

62. Woolard J, Wang WY, Bevan HS, Qiu Y, Morbidelli L, Pritchard-Jones RO, Cui TG, Sugiono M, Waine E, Perrin R, Foster R, Digby-Bell J, Shields JD, Whittles CE, Mushens RE, Gillatt DA, Ziche M, Harper SJ, Bates DO. VEGF165b, an inhibitory vascular endothelial growth factor splice variant: mechanism of action, *in vivo* effect on angiogenesis and endogenous protein expression. Cancer Res 2004; 64:7822-7835
• http://dx.doi.org/10.1158/0008-5472.CAN-04-0934

63. Rennel ES, Varey AH, Churchill AJ, Wheatley ER, Stewart L, Mather S, Bates DO, Harper SJ: VEGF(121)b, a new member of the VEGF(xxx)b family of VEGF-A splice isoforms, inhibits neovascularisation and tumour growth *in vivo*. Br J Cancer 2009; 101:1183-1193.
• http://dx.doi.org/10.1038/sj.bjc.6605249

64. Rennel ES, Hamdollah-Zadeh MA, Wheatley ER, Magnus¬sen A, Schüler Y, Kelly SP, Finucane C, Ellison D, Cebe-Suarez S, Ballmer-Hofer K, Mather S, Stewart L, Bates DO, Harper SJ. Recombinant human VEGF165b protein is an effective anti-cancer agent in mice. Eur J Cancer 2008; 44: 1883-1894
• http://dx.doi.org/10.1016/j.ejca.2008.05.027

65. Tayama M, Furuhata T, Inafuku Y, Okita K, Nishidate T, Mizuguchi T, Kimura Y, Hirata K. Vascular endothelial growth factor 165b expression in stromal cells and colorectal cancer. World J Gastroenterol. 2011; 28;17(44):4867-74.

66. Ehlken C, Rennel ES, Michels D, Grundel B, Pielen A, Junker B, Stahl A, Hansen LL, Feltgen N, Agostini HT, Martin G. Levels of VEGF but not VEGF(165b) are increased in the vitreous of patients with retinal vein occlusion. Am J Ophthalmol. 2011;152(2):298-303.
• http://dx.doi.org/10.1016/j.ajo.2011.01.040

67. Plate KH, Breier G, Weich HA, Risau W. Vascular endothelial growth factor is a potential tumor angiogenesis factor in human gliomas *in vivo*. Nature 1992; 359:845-8.
• http://dx.doi.org/10.1038/359845a0

68. Lafuente JV, Adan B, Alkiza K, Garibi J, Rossi M and Cruz-Sánchez FF Expression of vascular endothelial growth factor (VEGF) and platelet-derived growth factor receptor-b (PDGFR-b) in human gliomas. J Mol Neurosci. 1999; 13 (1-2): 177-185
• http://dx.doi.org/10.1385/JMN:13:1-2:177

69. Marti HJ, Bernaudin M, Bellail A, Schoch H, Euler M, Petit E, Risau W. Hypoxia-induced vascular endothelial growth factor expression precedes neovascularisation after cerebral ischemia. Am J Pathol 2000; 156:965-76.
• http://dx.doi.org/10.1016/S0002-9440(10)64964-4

70. Bulnes S, Lafuente JV. VEGF immunopositivity related to malignancy degree, proliferative activity and angiogenesis in ENU-induced gliomas. J Mol Neurosci 2007; 33:163-72.
• http://dx.doi.org/10.1007/s12031-007-0061-0

71. Ogunshola OO, Stewart WB, Mihalcik V, Solli T, Madri JA, Ment LR. Neuronal VEGF expression correlates with angiogenesis in postnatal developing rat brain. Dev Brain Res 2000; 119:139-53.
• http://dx.doi.org/10.1016/S0165-3806(99)00125-X

72. Xie K, Wei D, Shi Q, Huang S. Constitutive and inducible expression and regulation of vascular endothelial growth factor. Cytokine Growth Factor Rev 2004; 15:297-324.
• http://dx.doi.org/10.1016/j.cytogfr.2004.04.003

73. Shalaby F, Rossant J, Yamaguchi TP, Gertsenstein M, Wu XF, Breitman ML, Schuh AC. Failure of blood-island formation and vasculogenesis in Flk-1-deficient mice. Nature 1995; 376:62-6.
• http://dx.doi.org/10.1038/376062a0

74. Fong GH, Zhang L, Bryce DM, Peng J. Increased hemangioblast commitment, not vascular disorganization, is the primary defect in flt-1 knock-out mice. Development 1999; 126:3015-25.

75. Neufeld G, Cohen T, Shraga N, Lange T, Kessler O, Herzog Y. The neuropilins: multifunctional semaphoring and VEGF receptors that modulate axon guidance and angiogenesis. Trend Cardiovas Med 2002; 12:13-9.
• http://dx.doi.org/10.1016/S1050-1738(01)00140-2

76. Soker S, Takashima S, Miao HQ, Neufeld G, Klagsbrun M. Neuropilin-1 is expressed by endothelial and tumor cells as an isoform-specific receptor for vascular endothelial growth factor. Cell 1998; 92:735-45.
• http://dx.doi.org/10.1016/S0092-8674(00)81402-6

77. Lafuente JV, Argando-a EG, Mitre B. VEGFR-2 expression in brain injury: its distribution related to brain-blood barrier markers. J Neural Trans 2006; 113:487-96.
• http://dx.doi.org/10.1007/s00702-005-0407-0

78. Argando-a EG, Bengoetxea H, Lafuente JV. Effects of intracortical administration and neutralisation of vascular endothelial growth factor in the developing brain. Int J Neuroprot-Neuroregen 2006; 3:45-52.

79. Wick A, Wick W, Waltenberger J, Weller M, Dichgans J, Schulz JB. Neuroprotection by hypoxic preconditioning requires sequential activation of vascular endothelial growth factor receptor and Akt. J Neurosci 2002; 22:6401-7.

80. Kaya D, Gursoy-Ozdemir Y, Yemisci M, Tuncer N, Aktan S, Dalkara T. VEGF protects brain against focal ischemia without increasing blood-brain barrier permeability when administered intracerebroventricularly. J Cereb Blood Flow Metab 2005; 25:1111-8.
• http://dx.doi.org/10.1038/sj.jcbfm.9600109

81. Moser KV and Humpel C. Vascular endothelial growth factor counteracts NMDA-induced cell death of adult cholinergic neurons in rat basal nucleus of Meynert. Brain Res Bull 2005; 65:125-31.
• http://dx.doi.org/10.1016/j.brainresbull.2004.12.005

82. Louissaint A Jr, Raos S, Leventhal C, Goldman SA. Coordinated interaction of neurogenesis and angiogenesis in the adult songbird brain. Nature 2002; 13:945-60.

83. Rosenstein JM, Mani N, Khaibullina A, Krum JM. Neurotrophic effects of vascular endothelial growth factor on organotypic cortical explants and primary cortical neurons. J Neurosci 2003; 23:11036-44.

84. Greenberg DA, Jin K. From angiogenesis to neuropathology. Nature 2005; 438:954-9.
• http://dx.doi.org/10.1038/nature04481

85. Khaibullina AA, Rosenstein JM, Krum JM. Vascular endothelial growth factor promotes neurite maturation in primary CNS neuronal diseases. Dev Brain Res 2004; 148:59-68.
• http://dx.doi.org/10.1016/j.devbrainres.2003.09.022

86. Schoch HJ, Fisher S, Marti HH. Hypoxia-induced vascular endothelial growth factor expression causes vascular leakage in the brain. Brain 2002; 125:2549-57.
• http://dx.doi.org/10.1093/brain/awf257

87. Nordal RA, Wong CS. Molecular targets in radiation-induced blood-brain barrier disruption. Int J Radiat Oncol Biol Phys 2005; 62:279-87.
• http://dx.doi.org/10.1016/j.ijrobp.2005.01.039

88. Rabchevsky AG, Weinitz JM, Coulpier M, Fages C, Tinel M, Junier MP. A role for transforming growth factor alpha as an inducer of astrogliosis. J Neurosci 1998; 18:10541-52.

89. Krum JM, Khaibullina A. Inhibition of endogenous VEGF impedes revascularization and astroglial proliferation: roles for VEGF in brain repair. Exp Neurol 2003; 181:241-57
• http://dx.doi.org/10.1016/S0014-4886(03)00039-6

90. Krum JM, Mani N, Rosenstein JM. Angiogenic and astroglial responses to vascular endothelial growth factor administration in adult rat brain. Neuroscience 2002; 110:589-604.
• http://dx.doi.org/10.1016/S0306-4522(01)00615-7

91. Argaw AT, Asp L, Zhang J, Navrazhina K, Pham T, Mariani JN, Mahase S, Dutta DJ, Seto J, Kramer EG, Ferrara N, Sofroniew MV, John GR. Astrocyte-derived VEGF-A drives blood-brain barrier disruption in CNS inflammatory disease. J Clin Invest. 2012 Jul 2;122(7):2454-68.
• http://dx.doi.org/10.1172/JCI60842

92. Nowacka MM, Obuchowicz E. Vascular endothelial growth factor (VEGF) and its role in the central nervous system: A new element in the neurotrophic hypothesis of antidepressant drug Action. Neuropeptides 2012; 46 (1):1-10
• http://dx.doi.org/10.1016/j.npep.2011.05.005

93. Hayashi T1, Abe K, Suzuki H, Itoyama Y. Rapid induction of vascular endothelial growth factor gene expression after transient middle cerebral artery occlusion in rats. Stroke 1997; 28(10):2039-44.

94. Lafuente JV, Bulnes S, Mitre B and Riese HH. Role of VEGF in an experimental model of cortical micronecrosis. Amino Acids. 2002; 23 (1-3): 241-245
• http://dx.doi.org/10.1007/s00726-001-0135-1

95. Zhang ZG, Zhang L, Jiang Q, Zhang R, Davies K, Powers C, Bruggen N, Chopp M. VEGF enhances angiogenesis and promotes blood-brain barrier leakage in the ischemic brain. J Clin Invest 2000; 106:829-38.
• http://dx.doi.org/10.1172/JCI9369

96. Widenfalk J, Lipson A, Jubran M, Hofstetter C, Ebendal T, Cao Y, Olson L. Vascular endothelial growth factor improves functional outcome and decreases secondary degeneration in experimental spinal cord contusion injury. Neuroscience 2003; 120:951-60.
• http://dx.doi.org/10.1016/S0306-4522(03)00399-3

97. Choi UH, Ha Y, Huang X, Park SR, Chung J, Hyun DK, Park H, Park HC, Kim SW, Lee M. Hypoxia-inducible expression of vascular endothelial growth factor for treatment of spinal cord injury in a rat model. J Neurosurg Spine 2007; 7:54-60.
• http://dx.doi.org/10.3171/SPI-07/07/054

98. Lambrechts D, Storkebaum E, Morimoto M, Del-Favero J, Desmet F, Marklund SL, Wyns S, Thijs V, Andersson J, van Marion I, Al-Chalabi A, Bornes S, Musson R, Hansen V, Beckman L, Adolfsson R, Pall HS, Prats H, Vermeire S, Rutgeerts P, Katayama S, Awata T. Leigh N, Lang-Lazdunski L, Dewerchin M, Shaw C, Moons L, Vlietinck R, Morrison KE, Robberecht W, Van Broeckhoven C, Collen D, Andersen PM, Carmeliet P. VEGF is a modifier of amyotrophic lateral sclerosis in mice and humans and protects motoneurons against ischemic death. Nat Genet 2003; 34:383-94.

99. Sathasivam S. VEGF and ALS. Neurosci Res 2008; 62:71-7.
• http://dx.doi.org/10.1016/j.neures.2008.06.008

101. Tarkowski E, Issa R, Sjogren M, Wallin A, Blennow K, Tarkowski A, Kumer P. Increased intrathecal levels of the angiogenic factors VEGF and TGF-beta in Alzheimer´s disease and vascular dementia. Neurobiol Aging 2002; 23:237-43.
• http://dx.doi.org/10.1016/S0197-4580(01)00285-8

102. Girouard H, Iadecola C. Neurovascular coupling in the normal brain and in hypertension, stroke, and Alzheimer disease. J Appl Physiol 2006; 100:328-35.
• http://dx.doi.org/10.1152/japplphysiol.00966.2005

103. Solerte SB, Ferrari E, Cuzzoni G, Locatelli E, Giustina A, Zamboni M, Schifino N, Rondanelli M, Gazzaruso C, Fioravanti M. Decreased release of the angiogenic peptide vascular endothelial growth factor in Alzheimer´s disease: recovering effect with insulin and DHEA sulfate. Dement Geriatr Cogn Disord 2005; 19:1-10.
• http://dx.doi.org/10.1159/000080963

104. Xiong N, Zhang Z, Huang J, Chen C, Zhang Z, Jia M, Xiong J, Liu X, Wang F, X, Liang Z, Sun S, Lin Z, Wang T. VEGF-expressing human umbilical cord mesenchymal stem cells, an improved therapy strategy for Parkinson's disease. Gene Ther. 2011 Apr;18(4):394-402
• http://dx.doi.org/10.1038/gt.2010.152

105. Carvalho JF, Blank M, Shoenfeld Y. Vascular endothelial growth factor (VEGF) in autoimmune diseases. J Clin Immunol 2007; 27:246-56.
• http://dx.doi.org/10.1007/s10875-007-9083-1

106. Tan IL, Schijndel RA, Pouwels PJ, van WAlderveen MA, Reichenbach JR, Manoliu RA, Barkhof F. MR venography of multiple sclerosis. Am J Neuroradiol 2000; 21:1039-42.

107. Kirk S, Frank JA, Karlik S. Angiogenesis in multiple sclerosis: is it good, bad or an epiphenomenon? J Neurol Sci 2004; 217:125-30.
• http://dx.doi.org/10.1016/j.jns.2003.10.016

108. Proesholdt MA, Jacobson S, Tresser N, Oldfield EH, Merrill MJ. Vascular endothelial growth factor is expressed in multiple sclerosis plaques and can induce inflammatory lesions in experimental allergic encephalomyelitis rats. J Neuropathol Exp Neurol 2002; 61:914-25.

109. Huang EJ, Reichardt LF. Neurotrophins: roles in neuronal development and function. Annu Rev Neurosci 2001; 24:677-736.
• http://dx.doi.org/10.1146/annurev.neuro.24.1.677

110. Korsching S, Thoenen H. Two-site enzyme immunoassay for nerve growth factor. Methods Enzymology 1987; 147:167-85.
• http://dx.doi.org/10.1016/0076-6879(87)47108-5

111. Lewin GR, Barde YA. Physiology of the neurotrophins. Annu Rev Neurosci 1996; 19:289-317.
• http://dx.doi.org/10.1146/annurev.ne.19.030196.001445

112. Segal RA, Greenberg ME. Intracellular signaling pathways activated by neurotrophic factors. Annu Rev Neurosci 1996; 19:463-69.
• http://dx.doi.org/10.1146/annurev.ne.19.030196.002335

113. McAllister AK, Katz LC, Lo DC. Neurotrophins and synaptic plasticity. Annu Rev Neurosci 1999; 22:295-318.
• http://dx.doi.org/10.1146/annurev.neuro.22.1.295

114. Poo MM. Neurotrophins as synaptic modulators. Nat Rev Neurosci 2001; 2:24-32.
• http://dx.doi.org/10.1038/35049004

115. Sofroniew MV, Howe CL, Mobley WC. Nerve growth factor signaling, neuroprotection, and neural repair. Annu Rev Neurosci 2001; 24:1217-81.
• http://dx.doi.org/10.1146/annurev.neuro.24.1.1217

116. Numakawa T, Suzuki S, Kumamaru E, Adachi N, Richards M, Kunugi H. BDNF function and intracellular signaling in neurons. Histol Histopathol 2010; 25:237-58.

117. Hallböök F, Wilson K, Thorndyke M, Olinski RP. Formation and evolution of the chordate neurotrophin and Trk receptor genes. Brain Behav Evol 2006; 68:133-44.
• http://dx.doi.org/10.1159/000094083

118. Lee R, Kermani P, Teng KK, Hempstead BL. Regulation of cell survival by secreted proneurotrophins. Science 2001; 294:1945-8.
• http://dx.doi.org/10.1126/science.1065057

119. Chao MV. Neurotrophins and their receptors: a convergent point for many signaling pathways. Nat Rev Neurosci 2003; 4:299-309.
• http://dx.doi.org/10.1038/nrn1078

120. Huang EJ, Reichardt LF. Trk receptors: roles in neuronal signal transduction. Annu Rev Biochem 2003; 72:609-42.
• http://dx.doi.org/10.1146/annurev.biochem.72.121801.161629

121. Nykjaer A, Lee R, Teng KK, Jansen P, Madsen P, Nielsen MS, Jacobsen C, Kliemannel M, Schwarz E, Willnow TE, Hempstead BL, Petersen CM. Sortilin is essential for proNGF-induced neuronal cell death. Nature 2004; 427:843-8.
• http://dx.doi.org/10.1038/nature02319

122. Kaplan DR, Miller FD. Neurotrophin signal transduction in the nervous system. Curr Opin Neurobiol 2000; 10:381-91.
• http://dx.doi.org/10.1016/S0959-4388(00)00092-1

123. Bibel M, Barde YA. Neurotrophins: key regulators of cell fate and cell shape in the vertebrate nervous system. Genes Dev 2000; 14:2919-37.
• http://dx.doi.org/10.1101/gad.841400

124. Lu B, Pang PT, Woo NH. The yin and yang of neurotrophin action. Nat Rev Neurosci 2005; 6:603-14.
• http://dx.doi.org/10.1038/nrn1726

125. Nakahashi T1, Fujimura H, Altar CA, Li J, Kambayashi J, Tandon NN, Sun B. Vascular endothelial cells synthesize and secrete brain-derived neurotrophic factor. FEBS Lett. 2000 Mar 24;470(2):113-7.

125. Nakamura K, Martin KC, Jackson JK, Beppu K, Woo CW, Thiele CJ. Brain-derived neurotrophic factor activation of TrkB induces vascular endothelial growth factor expression via hypoxia-inducible factor-1 in neuroblastoma cells. Cancer Res 2006; 66:4249-55.
• http://dx.doi.org/10.1158/0008-5472.CAN-05-2789

126. Donovan MJ, Miranda RC, Kraemer R, McCaffrey TA, Tessarollo L, Mahadeo D, Sharif S, Kaplan DR, Tsoulfas P, Parada L, et al. Neurotrophin and neurotrophin receptors in vascular smooth muscle cells. Regulation of expression in response to injury. Am J Pathol. 1995 Aug; 147(2):309-24.

127. Kerschensteiner M, Gallmeier E, Behrens L, Leal VV, Misgeld T, Klinkert WE, Kolbeck R, Hoppe E, Oropeza-Wekerle RL, Bartke I, Stadelmann C, Lassmann H, Wekerle H, Hohlfeld R. 1999. Activated human T cells, B cells, and monocytes produce brain-derived neurotrophic factor *in vitro* and in inflammatory brain lesions: A neuroprotective role of inflammation? J Exp Med 189:865–870.

128. Hahn C, Islamian AP, Renz H, Nockher WA. Airway epithelial cells produce neurotrophins and promote the survival of eosinophils during allergic airway inflammation. J Allergy Clin Immunol. 2006 Apr;117(4):787-94.
• http://dx.doi.org/10.1016/j.jaci.2005.12.1339

129. Tessarollo L. Pleiotrophic functions of neurotrophins in development. Cytokine Growth Factor Rev 1998; 9:125–137

130. Nockher WA, Renz H. Neurotrophins in clinical diagnostics: pathophysiology and laboratory investigation. Clin Chim Acta. 2005 Feb;352(1-2):49-74.
• http://dx.doi.org/10.1016/j.cccn.2004.10.002

131. Barde YA, Edgar D, Thoenen H. Purification of a new neurotrophic factor from mammalian brain. EMBO J 1982; 1:549-53.

132. Leibrock J, Lottspeich F, Hohn A, Hofer M, Hengerer B, Masiakowski P, Thoenen H, Barde YA. Molecular cloning and expression of brain derived neurotrophic factor. Nature 1989; 341:149-52.
• http://dx.doi.org/10.1038/341149a0

133. Maisonpierre PC, Bellucio L, Friedman B, Alderson RF, Wiegand SJ, Furth ME, Lindsay RM, Yancopoulos GD. NT-3, BDNF, and NGF in the developing rat nervous system: Parallel as well as reciprocal patters of expression. Neuron 1990; 5:501-9.
• http://dx.doi.org/10.1016/0896-6273(90)90089-X

134. Friedman WJ, Olson L, Persson H. Cells that express brain-derived neurotrophic factor mRNA in the developing postnatal rat brain. Eur J Neurosci 1991; 3:688-97.
• http://dx.doi.org/10.1111/j.1460-9568.1991.tb00854.x

135. Phillips HS, Hains JM, Armanini M, Laramee GR, Johnson SA, Winslow JW. BDNF mRNA is decreased in the hippocampus of individuals with Alzheimer´s disease. Neuron 1991; 7:695-702.

136. Hofer M, Pagliusi SR, Hohn A, Leibrok J, Barde YA. Regional distribution of brain derived neurotrophic factor mRNA in the adult mouse brain. EMBO J 1990; 9:2459-64.

137. Piriz J, Muller A, Trejo JL, Torres-Aleman I. IGF-I and the aging mammalian brain. Exp Gerontol 2010; doi:10.1016/j.exger.2010.08.022.
• http://dx.doi.org/10.1016/j.exger.2010.08.022

138. Wetmore C, Ernfors P, Persson H, Olson L. Localization of brain derived neurotrophic factor mRNA to neurons in the brain by in situ hybridization. Exp Neurol 1990; 109:141-52.
• http://dx.doi.org/10.1016/0014-4886(90)90068-4

139. Kirschenbaum B, Goldman SA. Brain-derived neurotrophic factor promotes the survival of neurons arising from the adult rat forebrain subependymal zone. Proc Natl Acad Sci U S A 1995; 92:210-4.
• http://dx.doi.org/10.1073/pnas.92.1.210

140. Wu D, Pardridge WM. Neuroprotection with noninvasive neurotrophin delivery to the brain. Proc Natl Acad Sci U S A 1999; 96:254-9.
• http://dx.doi.org/10.1073/pnas.96.1.254

141. Schäbitz WR, Sommer C, Zoder W, Kiessling M, Schwaninger M, Schwab S. Intravenous brain-derived neurotrophic factor reduces infarct size and counterregulates Bax and Bcl-2 expression after temporary focal cerebral ischemia. Stroke 2000; 31:2212-7.
• http://dx.doi.org/10.1161/01.STR.31.9.2212

142. Almeida RD, Manadas BJ, Melo CV, Gomes JR, Mendes CS, Grãos MM, Carvalho RF, Carvalho AP, Duarte CB. Neuroprotection by BDNF against glutamate-induced apoptotic cell death is mediated by ERK and PI3-kinase pathways. Cell Death Differ 2005; 12:1329-43.

143. Zheng WH, Quirion R. Comparative signaling pathways of insulin-like growth factor-1 and brain-derived neurotrophic factor in hippocampal neurons and the role of the PI3 kinase pathway in cell survival. J Neurochem 2004; 89:844-52.
• http://dx.doi.org/10.1111/j.1471-4159.2004.02350.x

144. Johnson-Farley NN, Patel K, Kim D, Cowen DS. Interaction of FGF-2 with IGF-I and BDNF in stimulating Akt, ERK, and neuronal survival in hippocampal cultures. Brain Res 2007; 1154:40-9.
• http://dx.doi.org/10.1016/j.brainres.2007.04.026

145. Pang PT, Teng HK, Zaitsev E, Woo NT, Sakata K, Zhen S, Teng KK, Yung WH, Hempstead BL, Lu B. Cleavage of proBDNF by tPA/plasmin is essential for long-termn hippocampal plasticity. Science 2004; 306:487-91.
• http://dx.doi.org/10.1126/science.1100135

147. Nagappan G, Lu B. Activity-dependent modulation of the BDNF receptor TrkB: mechanisms and implications. Trends Neurosci 2005; 28:464-71.
• http://dx.doi.org/10.1016/j.tins.2005.07.003

148. Caleo M, Maffei L. Neurotrophins and plasticity in the visual cortex. Neuroscientist 2002; 8:52-61.
• http://dx.doi.org/10.1177/1073858402008001l0

149. Kermani P, Rafii D, Jin DK, Whitlock P, Schaffer W, Chiang A, Vincent L, Friedrich M, Shido Keyvani K, Sachser N, Witte OW, Paulus W. Gene expression profiling in the intact and injured brain following environmental enrichment. J Neuropathol Exp Neurol 2004; 63:598-609.

150. Kim H, Li Q, Hempstead BL, Madri JA. Paracrine and autocrine functions of brain-derived neurotrophic factor (BDNF) and nerve growth factor (NGF) in brain-derived endothelial cells. J Biol Chem 2004; 279:33538-46.
• http://dx.doi.org/10.1074/jbc.M404115200

151. Lindvall O, Kokaia Z, Bengzon J, Elmér E, Kokaia M. Neurotrophins and brain insults. Trends Neurosci 1994; 17:490-6.
• http://dx.doi.org/10.1016/0166-2236(94)90139-2

152. Kokaia M, Ernfors P, Kokaia Z, Elmér E, Jaenisch R, Lindvall O. Suppressed epileptogenesis in BDNF mutant mice. Exp Neurol 1995; 133:215-24.
• http://dx.doi.org/10.1006/exnr.1995.1024

153. Binder DK, Routbort MJ, Ryan TE, Yancopoulos GD, McNamara JO. Selective inhibition of kindling development by intraventricular administration of TrkB receptor body. 1999 J Neurosci 19:1424-36.

154. Pezet S, Malcangio M, Lever IJ, Perkinton MS, Thompson SW, Williams RJ, McMahon SB. Noxious stimulation induces Trk receptor and downstream ERK phosphorylation in spinal dorsal horn. Mol Cell Neurosci 2002; 21:684-95.
• http://dx.doi.org/10.1006/mcne.2002.1205

155. Smith MA, Makino S, Kvetnansky R, Post RM. Stress and glucocorticoids affect the expression of brain-derived neurotrophic factor and neurotrophin-3 mRNAs in the hippocampus. J Neurosci 1995; 15:1768-77.

156. Rinderknecht E, Humbel R. The amino acid sequence of human insulin-like growth factor 1 and its structural homology with proinsulin. J Biol Chem. 1978;253:2769–2776

157. Daughaday WH, Rotwein P. Insulin-like growth factors I and II. Peptide, messenger ribonucleic acid and gene structures, serum, and tissue concentrations. Endocr Rev 1989; 10:68-91.
• http://dx.doi.org/10.1210/edrv-10-1-68

158. Jones JI, Clemmons DR. Insulin-like growth factors and their binding proteins: biological actions. Endocr Rev 1995; 16:3-34.

159. Russo VC, Gluckman P, Feldman EL, Werther GA. The insulin-like growth factor system and its pleiotropic functions in the brain. Endocr Rev 2005; 26:916-43.
• http://dx.doi.org/10.1210/er.2004-0024

160. Nishijima T, Piriz J, Duflot S, Fernandez AM, Gaitan G, Gomez-Pinedo U, Verdugo JM, Leroy F, Soya H, Nu-ez A, Torres-Aleman I. Neuronal activity drives localized blood-brain barrier transport of serum insulin-like growth factor-I into the CNS. Neuron 2010; 67:834-46.
• http://dx.doi.org/10.1016/j.neuron.2010.08.007

161. Bondy CA. Transient IGF-I gene expression during the maturation of functionally related central projection neurons. J Neurosci 1991; 11:3442-55.

162. Bondy C, Werner H, Roberts CT Jr, LeRoith D. Cellular pattern of type-I insulin-like growth factor receptor gene expression during maturation of the rat brain: comparison with insulin-like growth factor I and II. Neuroscience 1992; 46:909-23.
• http://dx.doi.org/10.1016/0306-4522(92)90193-6

163. Wheeler DL, Dunn EF, Harari PM, Understanding resistance to EGFR inhibitors-impact on future treatment strategies, Nat. Rev. Clin. Oncol 2010; 493–507

164. van der Veeken J, Oliveira S, Schiffelers RM, Storm G, van Bergen En Henegouwen PM, Roovers RC. Crosstalk between epidermal growth factor receptor- and insulin-like growth factor-1 receptor signaling: implications for cancer therapy. Curr Cancer Drug Targets. 2009 Sep;9(6):748-60.

165. Ernfors P, Wetmore C, Olson L, Persson H. Identification of cells in rat brain and peripheral tissues expressing mRNA for members of the nerve growth factor family. Neuron 1990; 5:511-26.
• http://dx.doi.org/10.1016/0896-6273(90)90090-3

165. Heck S, Lezoualc'h F, Engert S, Behl C. Insulin-like growth factor-1-mediated neuroprotection against oxidative stress is associated with activation of nuclear factor kappaB. J Biol Chem 1999; 274:9828 –35.
• http://dx.doi.org/10.1074/jbc.274.14.9828

166. Vincent AM, Mobley BC, Hiller A, Feldman EL. IGF-I prevents glutamate-induced motor neuron programmed cell death. Neurobiol Dis 2004; 16:407–16.
• http://dx.doi.org/10.1016/j.nbd.2004.03.001

167. Ness JK, Scaduto RC Jr, Wood TL. IGF-I prevents glutamate-mediated bax translocation and cytochrome C release in O4 oligodendrocyte progenitors. Glia 2004; 46:183–94.
• http://dx.doi.org/10.1002/glia.10360

168. Mason JL, Jones JJ, Taniike M, Morell P, Suzuki K, Matsushima GK. Mature oligodendrocyte apoptosis precedes IGF-1 production and oligodendrocyte progenitor accumulation and differentiation during demyelination/remyelination. J Neurosci Res 2000; 61:251-262.
• http://dx.doi.org/10.1002/1097-4547(20000801)61:3<251::AID-JNR3>3.0.CO;2-W

169. Dempsey RJ, Sailor KA, Bowen KK, Tureyen K, Vemuganti R. Stroke induced progenitor cell proliferation in adult spontaneously hypertensive rat brain: effect of exogenous IGF-1 and GDNF. J Neurochem 2003; 87:586-97.
• http://dx.doi.org/10.1046/j.1471-4159.2003.02022.x

170. O'Kusky JR, Ye P, D'Ercole AJ. Insulin-like growth factor-I promotes neurogenesis and synaptogenesis in the hippocampal dentate gyrus during postnatal development. J Neurosci 2000; 20:8435–42.

171. Torres-Aleman I. Insulin-like growth factors as mediators of functional plasticity in the adult brain. Horm Metab Res 1999; 31:114-19.
• http://dx.doi.org/10.1055/s-2007-978707

172. Aberg ND, Brywe KG, Isgaard J. Aspects of growth hormone and insulinlike growth factor-I related to neuroprotection, regeneration, and functional plasticity in the adult brain. Scientific World Journal 2006; 6: 53-80.
• http://dx.doi.org/10.1100/tsw.2006.22

173. Sonntag WE, Lynch CD, Cooney PT, Hutchins PM. Decreases in cerebral microvasculature with age are associated with the decline in growth hormone and insulin-like growth factor I. Endocrinology 1997; 138:3515-20.

174. Lopez-Lopez C, LeRoith D, Torres-Aleman I. Insulin-like growth factor I is required for vessel remodeling in the adult brain. PNAS 2004; 101:9833-38.
• http://dx.doi.org/10.1073/pnas.0400337101

175. Carro E, Nunez A, Busiguina S, Torres-Aleman I. Circulating insulin-like growth factor I mediates effects of exercise on the brain. J Neurosci 2000; 20:2926-33.

176. Trejo JL, Carro E, Torres-Aleman I. Circulating insulin-like growth factor I mediates exercise-induced increases in the number of new neurons in the adult hippocampus. J Neurosci 2001; 21:1628-34.

178. Chavez JC, LaManna JC. Activation of hypoxia-inducible factor-1 in the rat cerebral cortex after transient global ischemia: potential role of insulin-like growth factor-I. J Neurosci 2002; 22:8922-31.

179. Plate KH. Mechanisms of angiogenesis in the brain. J Neuropathol Exp Neurol 1999; 58:313-20.
• http://dx.doi.org/10.1097/00005072-199904000-00001

180. Breese CR, Ingram RL, Sonntag WE. Influence of age and long-term dietary restriction on plasma insulin-like growth factor-1 (IGF-1), IGF-1 gene expression, and IGF-1 binding proteins. J Gerontol 1991; 46:B180-7.
• http://dx.doi.org/10.1093/geronj/46.5.B180

181. Leifke E, Gorenoi V, Wichers C, Von Zur Mühlen A, Von Büren E, Brabant G. Age-related changes of serum sex hormones, insulin-like growth factor-1 and sex-hormone binding globulin levels in men: cross-sectional data from a healthy male cohort. Clin Endocrinol 2000; 53:689-95.
• http://dx.doi.org/10.1046/j.1365-2265.2000.01159.x

182. Carro E, Trejo JL, Gomez-Isla T, LeRoith D, Torres-Aleman I. Serum insulin-like growth factor I regulates brain amyloid-beta levels. Nat Med 2002; 8:1390-7.
• http://dx.doi.org/10.1038/nm1202-793

183. Cohen E, Paulsson JF, Blinder P, Burstyn-Cohen T, Du D, Estepa G, Adame A, Pham HM, Holzenberger M, Kelly JW, Masliah E, Dillin A. Reduced IGF-1 signaling delays age-associated proteotoxicity in mice. Cell 2009; 139:1157-69.
• http://dx.doi.org/10.1016/j.cell.2009.11.014

184. Killick R, Scales G, Leroy K, Causevic M, Hooper C, Irvine EE, Choudhury AI, Drinkwater L, Kerr F, Al-Qassab H, Stephenson J, Yilmaz Z, Giese KP, Brion JP, Withers DJ, Lovestone S. Deletion of Irs2 reduces amyloid deposition and rescues behavioural deficits in APP transgenic mice. Biochem Biophys Res Commun 2009; 386:257-62.
• http://dx.doi.org/10.1016/j.bbrc.2009.06.032

185. de la Monte SM. Brain insulin resistance and deficiency as therapeutic targets in Alzheimer's disease. Curr Alzheimer Res. 2012 Jan;9(1):35-66.
• http://dx.doi.org/10.2174/156720512799015037

186. LeRoith D, Roberts Jr CT. The insulin-like growth factor system and cancer. Cancer Lett 2003; 195:127-37.
• http://dx.doi.org/10.1016/S0304-3835(03)00159-9

187. Jernberg-Wiklund H, Nilsson K. Targeting the IGF-1R signaling and mechanisms for epigenetic gene silencing in human multiple myeloma. Ups J Med Sci. 2012 May;117(2):166-77
• http://dx.doi.org/10.3109/03009734.2012.659293

188. Tao Y, Pinzi V, Bourhis J, Deutsch E. Mechanisms of disease: signaling of the insulin-like growth factor 1 receptor pathway-therapeutic perspectives in cancer. Nat Clin Pract Oncol 2007; 4:591–602.
• http://dx.doi.org/10.1038/ncponc0934

189. Myake T, Kung CK, Goldwasser E. Purification of human erythropoietin. J Biol Chem 1977; 252:5558-64.

190. Lin FK, Suggs S, Lin CH, Browne JK, Smalling R, Egrie JC, Chen KK, Fox GM, Martin F, Stabinsky Z. Cloning and expression of the human erythropoietin gene. Proc Natl Acad Sci USA 1985; 82:7580-4.
• http://dx.doi.org/10.1073/pnas.82.22.7580

191. Jelkmann W. Erythropoietin after a century of research: younger than ever. Eur J Haematol 2007; 78:183-205.
• http://dx.doi.org/10.1111/j.1600-0609.2007.00818.x

192. Nagai A, Nakagawa E, Choi HB, Hatori K, Kobayashi S, Kim SU. Erythropoietin and erythropoietin receptors in human CNS neurons, astrocytes, microglia, and oligodendrocytes grown in culture. J Neuropathol Exp Neurol 2001; 60:386-92.

193. Jelkmann W. Eryhtropoietin: structure, control of production, and function. Physiol Rev 1992; 72:449-89.

194. Marti HH, Wenger RH, Rivas LA, Straumann U, Digicaylioglu M, Henn V, Yonekawa Y, Bauer C, Gassmann M. Erythropoiein gene expresión in human, monkey and murine brain. Eur J Neurosci 1996; 8:666-76.
• http://dx.doi.org/10.1111/j.1460-9568.1996.tb01252.x

195. Harrigan MR, Ennis SR, Sullivan SE, Keep RF. Effects of intraventricular infusion of vascular endothelial growth factor on cerebral blood flow, edema and infarct volume. Acta Neurochir (Wien) 2003; 145:49-53.
• http://dx.doi.org/10.1007/s00701-002-1035-1

196. Digicaylioglu M, Bichet S, Marti HH, Wenger RH, Rivas LA, Bauer C, Gassmann M. Localization of specific erythropoietin binding sites in defined area of the mouse brain. Proc Natl Acad Sci USA1995; 92:3717-20.
• http://dx.doi.org/10.1073/pnas.92.9.3717

197. Juul SE, Anderson DK, Li Y, Christensen RD. Erythropoietin and erythropoietin receptor in the developing human central nervous system. Pediatr Res 1998; 43:40-9.

• http://dx.doi.org/10.1203/00006450-199801000-00007

198. Masuda S, Chikuma M, Sasaki R. Insulin-like growth factors and insulin stimulates erythropoietin production in primary cultures astrocytes. Brain Res 1997; 746:63-70.
• http://dx.doi.org/10.1016/S0006-8993(96)01186-9

199. Chandel NS, Maltepe E, Goldwasser E, Mathieu CE, Simon MC, Schumacker PT. Mitocondrial reactive oxygen species trigger hypoxia-induced transcription. Proc Natl Acad Sci USA 1998; 95:11715-20.
• http://dx.doi.org/10.1073/pnas.95.20.11715

200. Noguchi CT, Asavaritikrai P, Teng R, Jia Y. Role of erythropoietin in the brain. Crit Rev Oncol Hematol 2007; 64:159-71.
• http://dx.doi.org/10.1016/j.critrevonc.2007.03.001

201. Rabie T, Marti HH. Brain protection by erythropoietin: a manifold task. Physiol 2008; 23:263-74.
• http://dx.doi.org/10.1152/physiol.00016.2008

202. Sakanaka M, Wen TC, Matsuda S, Masuda S, Morishita E, Nagao M, Sasaki R. *In vivo* evidence that erythropoietin protects neurons from ischemic damage. Proc Natl Acas Sci USA 1998; 95:4635-40.
• http://dx.doi.org/10.1073/pnas.95.8.4635

203. Digicaylioglu M, Lipton SA. Erythropoietin-mediated neuroprotection involves cross-talk between Jak2 and NF-kappaB signalling cascades. Nature 2001; 412:641-47.
• http://dx.doi.org/10.1038/35088074

204. Konishi Y, Chui DH, Hirose H, Kunishita T, Tabira T. Trophic effect of erythropoietin and other haematopoietic factors on central cholinergic neurons *in vitro* and *in vivo*. Brain Res 1993; 609:29-35.
• http://dx.doi.org/10.1016/0006-8993(93)90850-M

205. Yamamoto M, Koshimura K, Kawaguchi M, Sohmiya M, Murakami Y, Kato Y. Stimulating effect of erythropoietin on the release of dopamine and acetylcholine from the rat brain slice. Neurosci Lett 2000; 292:131-33.
• http://dx.doi.org/10.1016/S0304-3940(00)01441-5

206. Weber A, Maier RF, Hoffmann U, Grips M, Hoppenz M, Aktas AG, Heinemann U, Obiaden M, Schuchmann S. Erythropoietin improves synaptic transmission during and following ischemia in rat hippocampal slice cultures. Brain Res 2002; 958:305-11.
• http://dx.doi.org/10.1016/S0006-8993(02)03604-1

207. Shingo T, Sorokan ST, Shimazaki T, Weiss S. Erythropoietin regulates *in vitro* and *in vivo* production of neuronal progenitors by mammalian forebrain neural stem cells. J Neurosci 2001; 9733-43.

208. Viviani B, Bartesaghi S, Corsini E, Villa P, Ghezzi P, Garau A, Galli CL,Marinovich M. Erythropoietin protects primary hippocampal neurons increasing the expression of brain-derived neurotrophic factor. J Neurochem 2005; 93:412-43.
• http://dx.doi.org/10.1111/j.1471-4159.2005.03033.x

209. Li Y, Lu ZY, Ogle M, Wei L. Erythropoietin prevents blood-brain barrier damage induce by focal cerebral ischemia in mice.Neurochem Res 2007; 32:2132-41.
• http://dx.doi.org/10.1007/s11064-007-9387-9

210. Chen G, Shi JX, Hang CH, Xie W, Liu J, Liu X. Inhibitory effect on cerebral inflammatory agents that accompany traumatic brain injury in a rat model: a potential neuroprotective mechanism of recombinant human erythropoietin (rhEPO). Neurosci Lett 2007; 425:177-82.
• http://dx.doi.org/10.1016/j.neulet.2007.08.022

211. Um M, Lodish HF. Antiapoptotic effects of erythropoietin in differentiated neuroblastoma SH-SY5Y cells require activation of both the STAT5 and AKT signaling pathways. J Biol Chem 2006; 281(9):5648-56.

212. Chateauvieux S, Grigorakaki C, Morceau F, Dicato M, Diederich M. Erythropoietin, erythropoiesis and beyond. Biochem Pharmacol. 2011 Nov 15;82(10):1291-303
• http://dx.doi.org/10.1016/j.bcp.2011.06.045

213. Brines M, Grasso G, Fiordaliso F, Sfacteria A, Ghezzi P, Fratelli M, Latini R, Xie QW, Smart J, Su-Rick CJ, Pobre E, Diaz D, Gomez D, Hand C, Coleman T, Cerami A. Erythropoietin mediates tissue protection through an erythropoietin and common beta-subunit heteroreceptor.Proc Natl Acad Sci U S A. 2004 Oct 12;101(41):14907-12
• http://dx.doi.org/10.1073/pnas.0406491101

214. Villa P, Bigini P, Mennini T, Agnello D, Laragione T, Cagnotto A, Viviani B, Marinovich M, Cerami A, Coleman TR, Brines M; Ghezzi P. Erythropoietin selectively attenuates cytokine production and inflammation in cerebral ischemia by targeting neuronal apoptosis. J Exp Med 2003; 198:971-5.
• http://dx.doi.org/10.1084/jem.20021067

215. Agnello D, Bigini P, Villa P, Mennini T, Cerami A, Brines ML, Ghezzi P. Erythropoietin exerts anti-inflammatory effect on the CNS in a model of experimental autoimmune encephalomyelitis. Brain Res 2002; 952:128-34.

216. Wang Y, Zhang ZG, Rhodes K, Renzi M, Zhang RL, Kapke A, Lu M, Pool C, Heavner G, Choop M. Post-ischemic treatment with erythropoietin or carbamylated erythropoietin reduces infarction and improves neurological outcome in a rat model of focal cerebral ischemia. Br J Pharmacol 2007; 151:1377-84.
• http://dx.doi.org/10.1038/sj.bjp.0707285

217. Yatsiv I, Grigoriadis N, Simeonidou C, Stahel PF, Schmidt OI, Alexandrovitch AG, Tsenter J, Shohami E. Erythropoietin is neuroprotective, improves functional recovery, and reduces neuronal apoptosis and inflammation in a rodent model of experimental closed head injury. FASEB J 2005; 19:1701-03.

218. Lu D, Mahmood A, Qu C, Goussev A, Schallert T, Choop P. Erythropoietin enhances neurogenesis and restores spatial memory in rats after traumatic brain injury. J Neurotrauma 2005; 22:1011-17.
• http://dx.doi.org/10.1089/neu.2005.22.1011

219. Xu F, Yu ZY, Ding L, Zheng SY. Experimental studies of erythropoietin protection following traumatic brain injury in rats. Exp Ther Med. 2012 Dec;4(6):977-982.

220. Mayeux R. Epidemiology of neurodegeneration. Annu Rev Neurosci 2003; 26:81-104.
• http://dx.doi.org/10.1146/annurev.neuro.26.043002.094919

221. Spires TL, Hannan AJ. Nature, nurture and neurology: gene-environment interactions in neurodegenerative disease. FEBS Anniversary Prize Lecture delivered on 27 June 2004 at the 29th FEBS Congress in Warsaw. FEBS J 2005; 272:2347-61.
• http://dx.doi.org/10.1111/j.1742-4658.2005.04677.x

222. Katz LC, Shatz CJ. Synaptic activity and the construction of cortical circuits. Science 1996; 274:1133-8.
• http://dx.doi.org/10.1126/science.274.5290.1133

223. Hensch TK. Critical period regulation. Annu Rev Neurosci 2004; 27:549-79.
• http://dx.doi.org/10.1146/annurev.neuro.27.070203.144327

225. Gilbert CD. Adult cortical dynamics. Physiol Rev 1998; 78:467-85.

226. Yao H, Dan Y. Synaptic learning rules, cortical circuits, and visual function. Neuroscientist 2005; 11:206-16.
• http://dx.doi.org/10.1177/1073858404272404

227. Black JE, Sirevaag AM, Greenough WT. Complex experience promotes capillary formation in young rat visual cortex. Neurosci Lett 1987; 83:351-5.
• http://dx.doi.org/10.1016/0304-3940(87)90113-3

228. Harrison RV, Harel N, Panesar J, Mount RJ. Blood cappilary distribution correlates with hemodynamic-based functional imaging in cerebral cortex. Cereb Cortex 2002; 12:225-33.
• http://dx.doi.org/10.1093/cercor/12.3.225

229. Argando-a EG, Lafuente JV. Effects of dark-rearing on the vascularization of the developmental rat visual cortex. Brain Res 1996; 732:43-51.
• http://dx.doi.org/10.1016/0006-8993(96)00485-4

230. Tieman SB, Mollers S, Tieman DG, White J. The blood supply of the cat's visual cortex and its postnatal development. Brain Res 2004; 998:100-12.
• http://dx.doi.org/10.1016/j.brainres.2003.11.023

231. Lamarck JB. Recherches sur l'organisation des corps vivants. 1808.

232. Darwin C. On the origin of species by means of natural selection, or the preservation of favoured racesin the struggle for life. London. Murray J. 1859.

233. Cajal SRy. Les nouvelles idées sur la structure du système nerveux: chez l'homme et chez les vertébrés. 1894.

234. Foster MSCS. A textbook of Physiology, Part Three: The Central Nervous System. MacMillan & Co. Ltd., London. 1897.

235. Berardi N, Pizzorusso T, Maffei L. Critical periods during sensory development. Curr Opin Neurobiol 2000; 10:138-45.
• http://dx.doi.org/10.1016/S0959-4388(99)00047-1

236. Hensch TK. Critical period plasticity in local cortical circuits. Nature Rev Neurosci 2005; 6:877-88.
• http://dx.doi.org/10.1038/nrn1787

237. Pizzorusso T, Medini P, Berardi N, Chierzi S, Fawcett JW, Maffei L. Reactivation of ocular dominance plasticity in the adult visual cortex. Science 2002; 298:1248-51.
• http://dx.doi.org/10.1126/science.1072699

238. Markham JA, Greenough WT. Experience-driven brain plasticity: beyond the synapse. Neuron glia Biol 2004; 1:351-63.

• http://dx.doi.org/10.1017/S1740925X05000219

239. Riccio RV, Matthews MA. The effect of intraocular injection of tetrodotoxin on fast axonal transport of [3H]proline- and [3H]fucose-labeled materials in the developing rat optic nerve. Neuroscience 1985; 16:1027-39.
• http://dx.doi.org/10.1016/0306-4522(85)90113-7

240. Fifkova E. The effect of unilateral deprivation on visual centers in rats. J Comp Neurol 1970; 140:431-8.
• http://dx.doi.org/10.1002/cne.901400404

241. Fagiolini M, Pizzorusso T, Berardi N, Domenici L, Maffei L. Functional postnatal development of the rat primary visual cortex and the role of visual experience: dark rearing and monocular deprivation. Vision Res 1994; 34:709-20.
• http://dx.doi.org/10.1016/0042-6989(94)90210-0

242. Bedi KS. The combined effects of unilateral enucleation and rearing in a 'dim' red light on synapse-to-neuron ratios in the rat visual cortex. J Anat 1989; 167:71-84.

243. Dehay C, Horsburgh G, Berland M, Killackey H, Kennedy H. Maturation and connectivity of the visual cortex in monkey is altered by prenatal removal of retinal input. Nature 1989; 337:265-7.
• http://dx.doi.org/10.1038/337265a0

244. Cragg BG. Changes in visual cortex on first exposure of rats to light. Effect on synaptic dimensions. Nature 1967; 215:251-3.
• http://dx.doi.org/10.1038/215251a0

244. Sirevaag AM, Black JE, Shafron D, Greenough WT. Direct evidence that complex experience increases capillary branching and surface area in visual cortex of young rats. Brain Res 1988; 471:299-304.
• http://dx.doi.org/10.1016/0165-3806(88)90107-1

245. Borges S, Berry M. The effects of dark rearing on the development of the visual cortex of the rat. J Comp Neurol 1978; 180:277-300.
• http://dx.doi.org/10.1002/cne.901800207

246. Mower GD. The effect of dark rearing on the time course of the critical period in cat visual cortex. Dev Brain Res. 1991; 58151-8.
• 247. Argando-a EG, Rossi ML, Lafuente JV. Visual deprivation effects on the s100beta positive astrocytic population in the developing rat visual cortex: a quantitative study. Dev Brain Res 2003; 141:63-9.
• http://dx.doi.org/10.1016/S0165-3806(02)00643-0

248. Gianfranceschi L, Siciliano R, Walls J, Morales B, Kirkwood A, Huang ZJ, Tonegawa S, Maffei L. Visual cortex is rescued from the effects of dark rearing by overexpression of BDNF. Proc Natl Acad Sci USA 2003; 100:12486-91.
• http://dx.doi.org/10.1073/pnas.1934836100

249. Fox K. Anatomical pathways and molecular mechanisms for plasticity in the barrel cortex. Neuroscience 2002; 111:799-814.
• http://dx.doi.org/10.1016/S0306-4522(02)00027-1

250. Briner A, De Roo M, Dayer A, Muller D, Kiss JZ, Vutskits L. Bilateral whisker trimming during early postnatal life impairs dendritic spine development in the mouse somatosensory barrel cortex. J Comp Neurol 2010; 518:1711-23.
• http://dx.doi.org/10.1002/cne.22297

251. Shoyket M, Land PW, Simons DJ. Whisker trimming begun at birth or on postnatal day 12 affects excitatory and inhibitory receptive fields of layer IV barrel neurons. J Neurophysiol 2005; 94:3987-95.
• http://dx.doi.org/10.1152/jn.00569.2005

252. Foeller E, Celikel T, Feldman DE. Inhibitory sharpening of receptive fields contributes to whisker map plasticity in rat somatosensory cortex. J Neurophysiol 2005; 94:4387-400.
• http://dx.doi.org/10.1152/jn.00553.2005

253. Lee SH, Land PW, Simons DJ. Layer- and cell-type-specific effects of neonatal whisker-trimming in adult rat barrel cortex. J Neurophysiol 2007; 97:4380-5.
• http://dx.doi.org/10.1152/jn.01217.2006

254. Kral A, Eggermont JJ. What's to lose and what's to learn: development under auditory deprivation, cochlear implants and limits of cortical plasticity. Brain Res Rev 2007; 56:259-69.
• http://dx.doi.org/10.1016/j.brainresrev.2007.07.021

255. Rauschecker JP. Compensatory plasticity and sensory substitution in the cerebral cortex. Trends Neurosci 1995; 18:36-43.
• http://dx.doi.org/10.1016/0166-2236(95)93948-W

256. Merabet LB, Pascual-Leone A. Neural reorganization following sensory loss: the opportunity of change. Nature Rev Neurosci 2010; 11:44-52.
• http://dx.doi.org/10.1038/nrn2758

257. Bengoetxea H, Ortúzar N, Rico-Barrio I, Lafuente JV, Argandoña EG. Neither environmental enrichment nor physical exercise alone is enough to recover astrocytic population from dark-rearing. Synergy is required. Front Cell Neurosci, 2013; 7 (170): 1-10 (2013)

258. Hebb DO. The effects of early experience on problem solving at maturity. Am Pscychol 1947; 2:306-7.

259. Argando-a EG, Bengoetxea H, Lafuente JV. Physiscal exercise is required for environmental enrichment to offset the quantitative effects of dark-rearing on the S-100beta astrocytic density in the rat visual cortex. J Anat 2009; 215:132-40.
• http://dx.doi.org/10.1111/j.1469-7580.2009.01103.x

260. Bennett EL, Rosenzweig MR, Diamond MC. Rat brain: effects of environmental enrichment on wet and dry weights. Science 1969; 163:825-6.
• http://dx.doi.org/10.1126/science.163.3869.825

261. Diamond MC, Ingham CA, Johnson RE, Bennett EL, Rosenzweig MR. Effects of environment on morphology of rat cerebral cortex and hippocampus. J Neurobiol 1976; 7:75-85.
• http://dx.doi.org/10.1002/neu.480070108

262. Faherty CJ, Kerley D, Smeyne RJ. A Golgi-Cox morphological analysis of neuronal changes induced by environmental enrichment. Dev Brain Res. 2003; 141:55-61.
• http://dx.doi.org/10.1016/S0165-3806(02)00642-9

263. Leggio MG, Mandolesi L, Federico F, Spirito F, Ricci B, Gelfo F, Petrosini L. Environmental enrichment promotes improved spatial abilities and enhanced dendritic growth in the rat. Behav Brain Res 2005; 163:78-90.
• http://dx.doi.org/10.1016/j.bbr.2005.04.009

264. During MJ, Cao L. VEGF, a mediator of the effect of experience on hippocampal neurogenesis. Curr Alzheimer Res 2006; 3:29-33.
• http://dx.doi.org/10.2174/156720506775697133

265. Diamond MC, Krech D, Rosenzweig MR. The Effects of an Enriched Environment on the Histology of the Rat Cerebral Cortex. J Comp Neurol 1964; 123:111-20.
• http://dx.doi.org/10.1002/cne.901230110

266. Volkmar FR, Greenough WT. Rearing complexity affects branching of dendrites in the visual cortex of the rat. Science 1972; 176:1445-7.
• http://dx.doi.org/10.1126/science.176.4042.1445

267. Greenough WT, Volkmar FR, Juraska JM. Effects of rearing complexity on dendritic branching in frontolateral and temporal cortex of the rat. Exp Neurol 1973; 41:371-8.
• http://dx.doi.org/10.1016/0014-4886(73)90278-1

268. Coq JO, Xerri C. Environmental enrichment alters organizational features of the forepaw representation in the primary somatosensory cortex of adult rats. Exp Brain Res 1998; 121:191-204.
• http://dx.doi.org/10.1007/s002210050452

269. Rampon C, Jiang CH, Dong H, Tang YP, Lockhart DJ, Schultz PG, Tsien JZ, Hu Y. Effects of environmental enrichment on gene expression in the brain. Proc Natl Acad Sci USA 2000; 97:12880-4.
• http://dx.doi.org/10.1073/pnas.97.23.12880

270. Nikolaev E, Kaczmarek L, Zhu SW, Winblad B, Mohammed AH. Environmental manipulation differentially alters c-Fos expression in amygdaloid nuclei following aversive conditioning. Brain Res 2002; 957:91-8.
• http://dx.doi.org/10.1016/S0006-8993(02)03606-5

271. Comery TA, Shah R, Greenough WT. Differential rearing alters spine density on medium-sized spiny neurons in the rat corpus striatum: evidence for association of morphological plasticity with early response gene expression. Neurobiol Learn Mem 1995; 63:217-9.
• http://dx.doi.org/10.1006/nlme.1995.1025

272. Comery TA, Stamoudis CX, Irwin SA, Greenough WT. Increased density of multiple-head dendritic spines on medium-sized spiny neurons of the striatum in rats reared in a complex environment. Neurobiol Learn Mem 1996; 66:93-6.
• http://dx.doi.org/10.1006/nlme.1996.0049

273. Szeligo F, Leblond CP. Response of the three main types of glial cells of cortex and corpus callosum in rats handled during suckling or exposed to enriched, control and impoverished environments following weaning. J Comp Neurol 1977; 172:247-63.

274. Sirevaag AM, Greenough WT. Differential rearing effects on rat visual cortex synapses. III. Neuronal and glial nuclei, boutons, dendrites, and capillaries. Brain Res 1987; 424:320-32.
• http://dx.doi.org/10.1016/0006-8993(87)91477-6

275. Black JE, Zelazny AM, Greenough WT. Capillary and mitochondrial support of neural plasticity in adult rat visual cortex. Exp Neurol 1991; 111:204-9.
• http://dx.doi.org/10.1016/0014-4886(91)90008-Z

276. Naka F, Narita N, Okado N, Narita M. Modification of AMPA receptor properties following environmental enrichment. Brain Dev 2005; 27:275-8.
• http://dx.doi.org/10.1016/j.braindev.2004.07.006

277. Dahlqvist P, Ronnback A, Bergstrom SA, Soderstrom I, Olsson T. Environmental enrichment reverses learning impairment in the Morris water maze after focal cerebral ischemia in rats. Eur J Neurosci 2004; 19:2288-98.
• http://dx.doi.org/10.1111/j.0953-816X.2004.03248.x

278. Dash PK, Orsi SA, Moore AN. Histone deactylase inhibition combined with behavioral therapy enhances learning and memory following traumatic brain injury. Neuroscience 2009; 163:1-8.
• http://dx.doi.org/10.1016/j.neuroscience.2009.06.028

279. Bennett JC, McRae PA, Levy LJ, Frick KM. Long-term continuous, but not daily, environmental enrichment reduces spatial memory decline in aged male mice. Neurobiol Learn and Mem 2006; 85:139-52.
• http://dx.doi.org/10.1016/j.nlm.2005.09.003

280. Mora F, Segovia G, del Arco A. Aging, plasticity and environmental enrichment: structural changes and neurotransmitter dynamics in several areas of the brain. Brain Res Rev 2007;55:78-88.
• http://dx.doi.org/10.1016/j.brainresrev.2007.03.011

281. Segovia G, del Arco A, Mora F. Environmental enrichment, prefrontal cortex, stress, and aging of the brain. J Neural Transm 2009; 116:1007-16.
• http://dx.doi.org/10.1007/s00702-009-0214-0

282. Benaroya-Milshtein N, Hollander N, Apter A, Kukulansky T, Raz N, Wilf A, Yaniv I, Pick CG. Environmental enrichment in mice decreases anxiety, attenuates stress responses and enhances natural killer cell activity. Eur J Neurosci 2004; 20:1341-7.
• http://dx.doi.org/10.1111/j.1460-9568.2004.03587.x

283. Bartoletti A, Medini P, Berardi N, Maffei L. Environmental enrichment prevents effects of dark-rearing in the rat visual cortex. Nat Neurosci 2004; 7:215-6.
• http://dx.doi.org/10.1038/nn1201

284. Amaral OB, Vargas RS, Hansel G, Izquierdo I, Souza DO. Duration of environmental enrichment influences the magnitude and persistence of its behavioral effects on mice. Physiol Behav 2008; 93:388-94.
• http://dx.doi.org/10.1016/j.physbeh.2007.09.009

285. Levi O, Jongen-Relo AL, Feldon J, Roses AD, Michaelson DM. ApoE4 impairs hippocampal plasticity isoform-specifically and blocks the environmental stimulation of synaptogenesis and memory. Neurobiol Dis 2003; 13:273-82.
• http://dx.doi.org/10.1016/S0969-9961(03)00045-7

286. Cracchiolo JR, Mori T, Nazian SJ, Tan J, Potter H, Arendash GW. Enhanced cognitive activity--over and above social or physical activity--is required to protect Alzheimer's mice against cognitive impairment, reduce Abeta deposition, and increase synaptic immunoreactivity. Neurobiol Learn Mem 2007; 88:277-94.
• http://dx.doi.org/10.1016/j.nlm.2007.07.007

287. Herring A, Yasin H, Ambree O, Sachser N, Paulus W, Keyvani K. Environmental enrichment counteracts Alzheimer's neurovascular dysfunction in Tg-CRND8 mice. Brain Pathol 2008; 18:32-9.
• http://dx.doi.org/10.1111/j.1750-3639.2007.00094.x

288. Thiriet N, Amar L, Toussay X, Lardeux V, Ladenheim B, Becker KG, Cadet JL, Solinas M, Jaber M. Environmental enrichment during adolescence regulates gene expression in the striatum of mice. Brain Res 2008; 1222:31-41.
• http://dx.doi.org/10.1016/j.brainres.2008.05.030

289. Martinez-Cue C, Baamonde C, Lumbreras M, Paz J, Davisson MT, Schmidt C, Dierssen M, Florez J. Differential effects of environmental enrichment on behavior and learning of male and female Ts65Dn mice, a model for Down syndrome. Behav Brain Res 2002; 134:185-200.
• http://dx.doi.org/10.1016/S0166-4328(02)00026-8

290. Martinez-Cue C, Rueda N, Garcia E, Davisson MT, Schmidt C, Florez J. Behavioral, cognitive and biochemical responses to different environmental conditions in male Ts65Dn mice, a model of Down syndrome. Behav Brain Res 2005; 163:174-85.
• http://dx.doi.org/10.1016/j.bbr.2005.04.016

291. Dierssen M, Benavides-Piccione R, Martinez-Cue C, Estivill X, Florez J, Elston GN, DeFelipe J. Alterations of neocortical pyramidal cell phenotype in the Ts65Dn mouse model of Down syndrome: effects of environmental enrichment. Cereb Cortex. 2003; 13:758-64.
• http://dx.doi.org/10.1093/cercor/13.7.758

292. Kondo M, Gray LJ, Pelka GJ, Christodoulou J, Tam PP, Hannan AJ. Environmental enrichment ameliorates a motor coordination deficit in a mouse model of Rett syndrome--Mecp2 gene dosage effects and BDNF expression. Eur J Neurosci 2008; 27:3342-50.

• http://dx.doi.org/10.1111/j.1460-9568.2008.06305.x

293. Saucier DM, Yager JY, Armstrong EA. Housing environment and sex affect behavioral recovery from ischemic brain damage. Behav Brain Res 2010; 214:48-54.
• http://dx.doi.org/10.1016/j.bbr.2010.04.039

294. Penn PR, Rose FD, Johnson DA. Virtual enriched environments in paediatric neuropsychological rehabilitation following traumatic brain injury: Feasibility, benefits and challenges. Dev Neurorehabil 2009; 12:32-43.
• http://dx.doi.org/10.1080/17518420902739365

296. Falkenberg T, Mohammed AK, Henriksson B, Persson H, Winblad B, Lindefors N. Increased expression of brain-derived neurotrophic factor mRNA in rat hippocampus is associated with improved sptail memory and enriched environment. Neurosci Lett 1992; 138:153-6.
• http://dx.doi.org/10.1016/0304-3940(92)90494-R

297. Kuzumaki N, Ikegami D, Tamura R, Hareyama N, Imai S, Narita M, Torigoe K, Niikura K, Takeshima H, Ando T, Igarashi K, Kanno J, Ushijima T, Suzuki T, Narita M. Hippocampal epigenetic modification at the brain-derived neurotrophic factor gene induced by an enriched environment. Hippocampus 2010; DOI 10.1002/hipo.20775.
• http://dx.doi.org/10.1002/hipo.20775

298. Widenfalk J, Olson L, Thoren P. Deprived of habitual running, rats downregulate BDNF and TrkB messages in the brain. Neurosci Res 1999; 34:125-32.
• http://dx.doi.org/10.1016/S0168-0102(99)00051-6

299. Cotman CW, Berchtold NC. Exercise: a behavioral intervention to enhance brain health and plasticity. Trends Neurosci 2002; 25:295-301.
• http://dx.doi.org/10.1016/S0166-2236(02)02143-4

300. Zhu SW, Yee BK, Nyffeler M, Winblad B, Feldon J, Mohammed AH. Influence of differential housing on emotional behaviour and neurotrophin levels in mice. Behav Brain Res 2006; 169:10-20.
• http://dx.doi.org/10.1016/j.bbr.2005.11.024

301. Chourbaji S, Hörtnagl H, Molteni R, Riva MA, Gass P, Hellweg R. The impact of environmental enrichment on sex-specific neurochemical circuitries - effects on brain-derived neurotrophic factor and the serotonergic system. Neuroscience. 2012 Sep 18;220:267-76.
• http://dx.doi.org/10.1016/j.neuroscience.2012.06.016

302. Gobbo OL, O'Mara SM. Combining exercise and cyclooxygenase-2 inhibition does not ameliorate learning deficits after brain insult, despite an increase in BDNF levels. Brain Res 2005; 1046:224-9.
• http://dx.doi.org/10.1016/j.brainres.2005.03.046

303. Carro E, Trejo JL, Busiguina S, Torres-Aleman I. Circulating insulin-like growth factor I mediates the protective effects of physical exercise against brain insults of different etiology and anatomy. J Neurosci 2001; 21:5678-84.

304. Cao L, Jiao X, Zuzga DS, Liu Y, Fong DM, Young D, During MJ. VEGF links hippocampal activity with neurogenesis, learning and memory. Nat Genet 2004; 36:827-35.
• http://dx.doi.org/10.1038/ng1395

305. Matsumori Y, Hong SM, Fan Y, Kayama T, Hsu CY, Weinstein PR, Liu J. Enriched environment and spatial learning enhance hippocampal neurogenesis and salvages ischemic penumbra after focal cerebral ischemia. Neurobiol Dis 2006; 22:187-98.
• http://dx.doi.org/10.1016/j.nbd.2005.10.015

306. Koopmans GC, Brans M, Gomez-Pinilla F, Duis S, Gispen WH, Torres-Aleman I, Joosten EA, Hamers FP. Circulating insulin-like growth factor I and functional recovery from spinal cord injury under enriched housing conditions. Eur J Neurosci 2006; 23:1035-46.
• http://dx.doi.org/10.1111/j.1460-9568.2006.04627.x

307. Ding Q, Vaynman S, Akhavan M, Ying Z, Gomez-Pinilla F. Insulin-like growth factor I interfaces with brain-derived neurotrophic factor-mediated synaptic plasticity to modulate aspects of exercise-induced cognitive function. Neuroscience 2006; 140:823-33.
• http://dx.doi.org/10.1016/j.neuroscience.2006.02.084

308. Maya-Vetencourt JF, Baroncelli L, Viegi A, Tiraboschi E, Castren E, Cattaneo A, Maffei L. IGF-1 restores visual cortex plasticity in adult life by reducing local GABA levels. Neural Plast. 2012;2012:250421.
• http://dx.doi.org/10.1155/2012/250421

309. Landi S, Ciucci F, Maffei L, Berardi N, Cenni MC. Setting the pace for retinal development: environmental enrichment acts through insulin-like growth factor 1 and brain-derived neurotrophic factor. J Neurosci 2009; 29:10809-19.
• http://dx.doi.org/10.1523/JNEUROSCI.1857-09.2009

310. Ciucci F, Putignano E, Baroncelli L, Landi S, Berardi N, Maffei L. Insulin-like growth factor 1 (IGF-1) mediates the effects of enriched environment (EE) on visual cortical development. PloS One 2007; 2:e475.
• http://dx.doi.org/10.1371/journal.pone.0000475

311. Guzzetta A, Baldini S, Bancale A, Baroncelli L, Ciucci F, Ghirri P, Putignano E, Sale A, Viegi A, Berardi N, Boldrini A, Cioni G, Maffei L. Massage accelerates brain development and the maturation of visual function. J Neurosci 2009; 29:6042-51.
• http://dx.doi.org/10.1523/JNEUROSCI.5548-08.2009

312. Keyvani K, Sachser N, Witte OW, Paulus W. Gene expression profiling in the intact and injured brain following environmental enrichment. J Neuropathol Exp Neurol 2004; 63:598-609.

313. Sanchez PE, Risso JJ, Bonnet C, Bouvard S, Le-Carvorsin M, Georges B, Moulin C, Belmeguenai A, Bodennec J, Morales A, Pequignot JM, Baulieu EE, Levine RA, Bezin L. Optimal neuroprotection by erythropoietin requires elevated expression of its receptor in neurons. Proc Natl Acad Sci USA 2009; 106:9848-53.